University of Nottingham

UK | CHINA | MALAYSIA

INVESTIGATION OF THE CONTRIBUTION OF VASCULAR ENDOTHELIAL GROWTH FACTOR AND ITS SPLICING AXIS TO JOINT INFLAMMATION AND DAMAGE IN ARTHRITIS

Roheena Sohail

Thesis submitted to the University of Nottingham for the degree of Doctor of Philosophy

March 2024

DECLARATION

I, Roheena Sohail, confirm that the work presented in this thesis was carried out in accordance with the requirements of the University's Regulations and Code of Practice for Research Degree Programs and that it has not been submitted for any other academic award. I confirm that the work and views demonstrated in this thesis are my own. All licensed work (*in vivo*) was done by personal licence holders Drs Nicholas Beazley-Long (mice) and Alexandra Durrant (rats). Where information has been derived from other sources, I confirm this has been indicated in the thesis.

Signed: *Roheena Sohail* Date: 04/03/*2024*

ABSTRACT

Vascular Endothelial Growth Factor-A (VEGF-A) is a key regulator for endothelial cell function, promoting vascular permeability, growth, and angiogenesis. There is an increase in synovial angiogenesis and upregulation of angiogenic growth factors such as VEGF-A during articular joint inflammation in inflammatory arthritis (IA), such as rheumatoid arthritis (RA). This is a major contributor to disease progression.

VEGF-A consists of two splice variant families with each family composed of 9 isoforms of varying length (from 111 – 206 amino acids). The two VEGF-A families, VEGF-A_{xxx}a and VEGF-A_{xxx}b (where xxx denotes the number of amino acids in the isoform) result from the selection of alternative proximal and distal splice sites in exon 8. Selection of the exon 8 proximal splice site results in transcription of pro-angiogenic VEGF-A_{xxx}a and is controlled by the Serine/Arginine Rich Splicing Factor Kinase 1 (SRPK1). When SRPK1 is activated, for example by hypoxia, it phosphorylates Serine/Arginine Rich Splicing Factor 1 (SRSF1) resulting in its nuclear translocation, proximal splice site selection and VEGF-A_{xxx}a production. The CDC-2-dual specificity like protein kinase CLK-1 also contributes to the full activation of SRSF1 and production of VEGF-A_{xxx}a isoforms.

VEGF-A_{xxx}b isoforms predominate in normal tissues with anti-angiogenic functions, whereas VEGF-A_{xxx}a isoforms prevail in pathological angiogenic conditions such as inflammation and solid tumours. The binding of pro-angiogenic VEGF-A_{xxx}a isoforms to endothelial VEGF receptor 2 (VEGFR2) is the main stimulatory signal for angiogenesis. As angiogenesis is a key feature of RA, VEGF-A and its receptors have been suggested as potential therapeutic targets for the condition.

This thesis investigated the effect of systemic inhibition, and endothelial cell-specific genetic knockdown of VEGFR2 on synovitis, cartilage integrity and the expression of two components of the VEGF-A alternative splicing axis, splicing kinase SRPK1 and splice factor SRSF1 in joints, using histology and immunohistochemistry in IA rodent models.

Systemic inhibition of VEGFR2 by PTK787 had no significant effects on inflamed tibio-femoral joint histology in the rat IA model. Inducible endothelial cell-specific genetic VEGFR2 knockdown in mice ($VEGFR2^{ECKO}$) resulted in greater cartilage damage in inflamed mouse tibio-tarsal joints compared to inflamed mice with no $VEGFR2^{ECKO}$. There was no effect of $VEGFR2^{ECKO}$ in un-inflamed mice. The greater cartilage damage in inflamed $VEGFR2^{ECKO}$ mice was associated with significantly reduced vascularity in the most superficial layer of subchondral bone (up to 100μm) and in synovium. The loss of VEGFR2 in endothelial cells and reduced vascularity could result in increased levels of hypoxia and reduced nutrient supply in the joint, contributing to the increased cartilage damage.

SRPK1 and SRSF1 expression was detected in both synovium and cartilage in rodent joints. There were no significant changes in SRPK1 expression in rat or mouse IA models. SRSF1 activation, as measured by number of cells with SRSF1 nuclear localisation (NL), was increased in inflamed synovium in both mouse and rat IA models. The proportion of synovial cells with nuclear localised SRSF1 was not changed. The mouse and rat models therefore had some similarities to but did not recapitulate published observations in human RA synovium, in which proportions of cells with activated SRSF1 were significantly raised.

PTK787 inhibition of VEGFR2 had no significant effect on SRPK1 or SRSF1 expression or activation. SRSF1 NL was significantly lower in $VEGFR2^{ECKO}$ mice that showed increased cartilage damage and reduced vascularity. Synovial proliferation was still seen in the mouse joints. Endothelial VEGFR2 knock down would reduce angiogenesis and increase hypoxia as even if there is upregulation of VEGF-A_{xxx}a expression this cannot exert a pro-angiogenic action. This would lead to greater hypoxia and increased cartilage damage. The reduced SRSF1 NL in synovium of inflamed $VEGFR2^{ECKO}$ mice suggests that genetic knockdown of endothelial VEGFR2 may also affect VEGF-A_{xxx}a production through an, as yet, unknown mechanism.

The effect of novel inhibitors of the splicing kinases SRPK1 and CLK1 were determined in an *in vitro* model of chondrocyte hypertrophy. Exposure of chondrocyte-like ATDC5 cells to ascorbic acid promotes differentiation (day 8-12) when they

express collagen 2A (COL2A1), and transition to a hypertrophic phenotype by day 21 when they express collagen 10A but not COL2A1. Treatment of chondrocyte-like ATDC5 cells *in vitro* with novel SRPK1 or CLK1 inhibitors for 21 days had no effect on mRNA expression of either collagen 2A1 or 10A1. Despite this, the novel CLK1 inhibitor has very similar properties to the experimental drug lorecivivint, so it may still be worth pursuing this compound for effects on cartilage and / or inflammatory joint pain.

In conclusion, the work presented in this thesis shows that targeting VEGFR2 may not be an ideal therapy for IA due to the potential for reduced subchondral vascularity and increased cartilage damage. Human RA synovium has high levels of activated SRSF1, which is partially recapitulated in the rodent CFA IA models. Targeting VEGF-A alternative splicing mechanisms to switch splicing to VEGF-A_{xxx}b isoforms could therefore be considered as a potential therapeutic target in IA. Further work is needed to fully understand how the different VEGF-A splice families contribute to cartilage maintenance in IA or chondrocyte hypertrophy. In addition, selective CLK inhibitors could also be considered as potential novel therapies in OA given their similarities to drugs in late phase clinical trials.

ACKNOWLEDGEMENT

First and foremost I am extremely grateful to my supervisors, Prof. Lucy Donaldson and Prof. David Bates for your invaluable supervision, continuous support, advice, and patience during my PhD. The completion of my Ph.D. would not have been possible without your guidance. I am blessed to have supervisors like you who encouraged and helped me during tense time.

I would I would like to express gratitude to Prof. David Walsh for supporting me using the facilities in his Lab in City Hospital.

Great thanks to Dr. Nick Beazley who trained and help me during start of my PhD and Dr. Dimitrios Amanitis who was always available to help me out.

I would also like to thank Ian Ward for training me for microscopy and Dr. Seyed Shahtaheri for his immense support in my histology work. I would like to thank my friends Dr. Assiya Jaffrani, Dr. Muhammed Tahir for their kind help and support that have made my life in the UK a wonderful time. In addition, I'd like to thank our lab team, Alexandra Durrant, Dr. Matt Swift, Caroline Howells for the invaluable feedback and encouragement greatly influenced how I conducted my experiments and interpreted my findings. I would also like to thank my other lab fellows James, Charles and Ayse for having good time in lab.

Finally, I would like to express my gratitude to my parents and my brothers, their tremendous understanding and encouragement to complete my study.

There must be an extraordinary thank to Punjab Educational Endowment Fund (PEEF)-Pakistan, for the scholarship and believing in me.

Last but not least, I'd like to thank Prof. Lucy Donaldson once again for being the best supervisor and inspiration for me. You are an amazing and a kind hearted person. There is no doubt in saying that I was blessed and honoured to work under your supervision as I couldn't wish for a better supervisor for my PhD.

CONFERENCE ABSTRACTS AND AWARDS

Conference abstract:

NIHR Nottingham BRC Musculoskeletal Theme Virtual Conference Wednesday 27th January 2021 - Investigating the role of blood vessels on cartilage health

Gfvbm/BMVBS conference at Berlin, Germany 2022 - Importance of synovial and subchondral microvessels in maintaining cartilage integrity in inflammatory arthritis

IVBM at Oakland, San Francisco 2022 - Investigating the role of blood vessels and VEGF splicing axis in inflammatory arthritis in mice.

Presentations

SoLS PGR conference 2020 - Investigating the role of blood Vessels and VEGF splicing axis in inflammatory arthritis 2021 (Oral presentation)

Gfvbm/BMVBS conference at Berlin, Germany 2022 - Importance of synovial and subchondral microvessels in maintaining cartilage integrity in inflammatory arthritis (Poster presentation).

IVBM at Oakland, San Francisco 2022 - Investigating the role of blood vessels and VEGF splicing axis in inflammatory arthritis in mice (Poster presentation).

Awards:

Chief Minister Merit PhD Scholarship, Pakistan - 2018

Vice Chancellor PhD scholarship, UK – 2018

COMPARE FUNDING – Travel grant for international conference - Gfvbm/BMVBS conference at Berlin, Germany – 2022

CTTF (Conference, travel, and training fund) award from Research Academy for Gfvbm/BMVBS conference at Berlin, Germany

CTTF (Conference, travel, and training fund) award from Research Academy for IVBM at Oakland, San Francisco – 2022

LIST OF ABBREVIATIONS

Ab	Antibody
ABC	Avidin/Biotin Complex
AC	Articular cartilage
ACR/EULAR	American College of Rheumatology/European League Against Rheumatism
ADAMTS	Metalloproteinase with thrombospondin motifs
ACCP	Anti-cyclic citrullinated peptide antibody
ACPAs	Anti-citrullinated protein antibodies
AIA	Antigen-induced arthritis
Akt/PKB	Protein kinase
AP	Alkaline phosphatase
APCs	Antigen presenting cells
APRs	Acute phase reactants
BCIP	5-bromo-4-chloro-3-indoyl phosphate
Bcl-2	B-cell lymphoma 2
BM	Bone marrow
BMCD	Bone marrow collagen deposition
BSA	Bovine album serum
Cas9	CRISPR-associated protein 9
Cat. No.	Catalogue number
CBD	Cannabidiol
CD	Cytoplasmic domain
CD4	Cluster of differentiation 4
CD31	PECAM-1 Platelet endothelial cell adhesion molecule - 1
CDAI	Clinical Disease Activity Index
cDNA	Complementary DNA
CFA	Complete Freund’s adjuvant
CIA	Collagen induced arthritis
CKD	Cyclin-dependant kinase

cKO	Conditional Knockout
CLK	CDC-like kinases
COL1	Collagen 1
COL10A1	Collagen type X alpha 1
COL2A1	Collagen type II alpha 1
Coll	Collagen fibres
COMP	Cartilage oligomeric matrix protein
Cre	Carbapenem-resistant Enterobacterales
CRISPR	Clustered Regularly Interspaced Short Palindromic Repeats
CRP	C-reactive protein
CTD	carboxy-terminal domain
CTR	Calcitonin receptor
CTLA4	Cytotoxic T-lymphocyte associated protein 4
CVD	Cardiovascular disease
D0	Day 0
D8	Day 8
D12	Day 12
D21	Day 21
DAB	3'3-diaminobenzidine HCl
DAS28	Disease activity score
DEPC	Diethyl pyrocarbonate
dH_2O	Distilled water
DMARD	Disease-modifying antirheumatic drugs
DMEM	Dulbecco's modified minimal essential medium
DNA	Deoxyribonucleic Acid
DNTPs	Deoxyribonucleotide triphosphate
DPX	1,3-diethyl-8-phenylxanthine.
DSS	distal splice site
DYRK	dual-specificity tyrosine-regulated kinases
EC	Endothelial cell
ECKO	Endothelial cells knockout
ECM	Extracellular matrix

EDTA	Ethylenediaminetetraacetic acid
EF5	2-nitroimidazole-based hypoxia marker
EO	Endochondral ossification
ER	Oestrogen receptor
ERK	Extracellular signal-regulated kinase
ESR	Erythrocytes sedimentation rate
Fab	The fragment antigen-binding region
FAK	Focal adhesion kinase
FBS	Foetal bovine serum
Fc	The fragment crystallisable region
FC	Femoral condyle
FGF	fibroblast growth factor
FGFR1	fibroblast growth factor receptor 1
FLS	Fibroblast-like synoviocytes
FVT	Fibrovascular tissue
GAGs	Glycosaminoglycans
GAPDH	Glyceraldehyde 3-phosphate dehydrogenase
GBM	Glioblastoma multiforme
GM-CSF	Granulocyte-macrophage colony-stimulating factor
HA	Hyaluronic acid
H&E	Haematoxylin and eosin
H_2O_2	Hydrogen peroxide
HCQ	hydroxychloroquine
HCs	Hypertrophic chondrocytes
HIER	Heat-induced epitope retrieval
HIF	Hypoxia inducible factor
HLA	human leukocyte antigen
HLA-DRB1	human leukocyte antigen class II histocompatibility - D related beta chain
2-HOBA	2-Hydroxybenzylamine acetate
HRP	Horseradish Peroxide
HSPG	heparin-sulphate proteoglycans

HTNFG	Human tumour necrosis factor gene
ICAM	Intercellular adhesion molecule
i/p	Intraperitoneal
IV	Intravenous
IA	Inflammatory arthritis
IF	Immunofluorescence
IFA	Incomplete Freund’s adjuvant
IFN	Interferon
IgA	Immunoglobulin A
IgD	Immunoglobulin D
IgE	Immunoglobulin E
IGF-1	Insulin-like Growth Factor - 1
IgG	Immunoglobulin G
IgM	Immunoglobulin M
IHC	Immunohistochemistry
IL	Interleukin
IL-1ra	Interleukin-1 receptor antagonist
isoLGs	isolevuglandins
JMD	Juxtamembrane domain
KCl	Potassium chloride
KID	Kinase insert domain
KIT	Receptor tyrosine kinase
KO	Knockout
LHCs	Late hypertrophic chondrocytes
LoxP	Locus of x-over P1
LSAB	Labelled Streptavidin Biotin
Lym	Lymphocytes
MAPK	Mitogen-Activated Protein Kinase
MAPKAPKS	Mitogen-Activated Protein Kinase-Activated Protein Kinases
M.O.M IHC	Mouse on mouse immunohistochemistry
MCSF	Macrophage colony-stimulating factor
MCP-1	Monocyte chemoattractant protein 1

MEK	Mitogen-activated protein kinase
MEM	Minimal Essential Medium
$MgCl_2$	Magnesium chloride
MIP-1α	Macrophage inflammatory protein 1 α
MMLV	Moloney Murine Leukaemia Virus)
MMLV-RT	Moloney Murine Leukaemia Virus - Reverse Transcriptase
MMP	Matrix metalloproteinase
mRNA	Messenger RNA
MTX	Methotrexate
NBT	nitro blue tetrazolium
NCK	Non-catalytic region of tyrosine kinase
NHP	Non-human primates
NF-kB	Nuclear factor kappa B
NHS	Normal horse serum
NICE	UK National institute of Health and Care Excellence
NL	Nuclear localisation
NP-1	Neuropilin-1
NSAIDS	Non-steroidal anti-inflammatory drugs
OA	Osteoarthritis
OC	Osteoclast
OCs	Osteoclasts
OPG	Osteoprotegerin
OPN	Osteopontin
P38	Mitogen-activated protein kinase
PAP	Peroxidase/anti-peroxidase
PBMC	Peripheral blood mononuclear cell
PBS	Phosphate buffered saline
PCLγ	Endothelial phospholipase Cγ
PD1	Programmed cell death protein 1
PDGFRα	Platelet-derived growth factor receptor α
PI3K	Phosphoinositide 3-kinase
PIER	Proteolytic-induced epitope retrieval

PKC	PKC: Protein kinase C
PSS	proximal splice site
PTPN22	Tyrosine-protein phosphatase nonreceptor type 22
PVP	Polyvinylpyrrolidone
RA	Rheumatoid arthritis
RAF	Rapidly Accelerated Fibrosarcoma
RANK	Receptor activator of nuclear factor kappa beta
RANKL	Receptor activator of NFKB ligand
RF	Rheumatoid factor
RNA	Ribonucleic acid
ROI	Regions of interest
RT	Reverse transcriptase
RTK	Tyrosine kinase receptor
RT-PCR	Reverse transcription polymerase chain reaction
RUNX1	Runt-related transcription factor 1
RUNX2	Runt-related transcription factor 2
SCB	Subchondral bone
SF	Splicing factor
SHB	SH2 domain–containing scaffold protein
SIBLINGs	small integrin-binding ligand N-linked glycoproteins
SLE	Systemic lupus erythematosus
SM	Synovial macrophages
snRNPs	Small nuclear ribonucleoprotein particles
SO	Safranin O
SOX	SRY-Box Transcription Factor
SpD	Sprague Dawley
SR	Serine/arginine rich protein
Src	Proto-oncogene tyrosine-protein kinase Src (sarcoma)
SREs	Splicing regulating elements
SRPK1	Serine/arginine-Rich Splicing Factor (SRSF) protein kinase-1
SRSF1	Serine/arginine-rich splicing factor 1
STAT4	Signal transducer and activator of transcription 4

TAE	Tris-acetate-EDTA solution
TB	Trabecular bone
TBS	Tris-buffered saline solution
TBST	Tris-buffered saline solution tween
TGF-ß	Transforming growth factor-β
Tie2	Tyrosine-protein kinase receptor Tie-2
TKD1	Tyrosine kinase domain 1
Th 1	T helper type 1
Th 17	T helper type 17
TIMP	Tissue inhibitor of metalloproteinase
TKIs	Tyrosine kinase inhibitors
TLR	Toll-like receptor
TMD	Transmembrane domain
TNF	Tumour necrosis factor
TRAP	Tartrate-resistant acid phosphatase
TRI	Trizole
Tr-SR	transporting protein
TSAd	TSAd: T cell specific adaptor
Tyr	Tyrosine
UTR	Untranslated region
UV	Ultraviolet
VCAM	Vascular cell adhesion protein
VEGF	Vascular endothelial growth factor
VEGF-A	Vascular endothelial growth factor A
VEGFR1	Vascular endothelial growth factor receptor 1
VEGFR2	Vascular endothelial growth factor receptor 2
VEGFR3	Vascular endothelial growth factor receptor 3
WT1	Wilms tumour suppressor-1

Contents

LIST OF FIGURES

LIST OF TABLES

1. INTRODUCTION

1.1 Inflammatory arthritis

Inflammatory arthritis (IA) is a group of chronic progressive autoimmune diseases caused by multiple factors that result in inflammation. It has three main forms, including axial spondyloarthritis, psoriatic arthritis, and rheumatoid arthritis (RA). Approximately 5% of the population worldwide suffers from chronic IA (Fautrel & Guillemin, 2002) of which the most common form is RA (Karmakar et al., 2010; Pisetsky & Ward, 2012) that primarily affects the lining of the synovial joints and can lead to joint inflammation, cartilage, and bone destruction and results in joint deformity (Aletaha et al., 2010; Arnett et al., 1988; Woolley & Tetlow, 1997). The onset of RA can be at any age - even before the age of 16 (known as juvenile RA) - but usually people develop RA between 30 and 60 (J. Bullock et al., 2019; NHSUK, 2022; VERSUSARTHRITIS, 2023). According to the 2019 "systemic analysis of global burden of disease study", approximately 70% of people affected with RA are women, and 55% are over 55 years (Vos et al., 2020). The symptoms of IA include joint swelling, pain, redness, limited range of motion, stiffness, and can affect other connective tissues such as the heart, skin, lungs, and other organs (Adams et al., 2010).

Global prevalence of RA is approximately 1-2% (Aletaha & Smolen, 2018; Chopra & Abdel-Nasser, 2008; Cross et al., 2014; Gibofsky, 2014). Estimates show around 0.5 to 1% of the population is affected by RA in the United States and northern European countries (Myasoedova et al., 2010). The prevalence in UK is about 1% of the population suffering from RA, which is more than 400,000 people (VERSUSARTHRITIS, 2023).

Rheumatoid arthritis is a growing problem globally that affects quality of life with the possibility of developing long term adverse outcomes including physical and work disability, and increased morbidity and mortality (Y. Cai et al., 2023; Young et al., 2007). It also has a significant impact on both direct and indirect socio-economic costs. Indirect costs often result from lost productivity and work (Van Nies et al., 2014), and

are estimated to be approximately three times more than the costs of treating the disease (Agarwal, 2011). The estimation of daily work-related disability related to RA was about 35% in the US (Allaire et al., 2008).

Early stage treatment, which includes early diagnosis and early referral, with intensive regimens is most effective in the management of RA to prevent longer term disability (Raja et al., 2012; Rudwaleit & Taylor, 2010) and other consequences such as cardiovascular disease (CVD), which is the major cause of death among RA patients with 50% higher risk than the general population (E. Choy et al., 2014). In 2010, both the American College of Rheumatology and the European League Against Rheumatism published the updated classification criteria for RA to facilitate early treatment (Van der Linden et al., 2011) that covers a broader spectrum of early disease features compared to the older criteria sets for RA (Sangha, 2000).

Before moving to more details of RA aetiology, risk factors, pathogenesis, and treatment, I will first briefly discuss the normal structure of synovial joints and tissues.

1.2 Normal synovial joint structure

1.2.1 Structure and composition of normal articular cartilage

Hyaline articular cartilage, in contrast with bone, is an avascular, aneural, and alymphatic structure (Buckwalter & Mankin, 1997). Cartilage is a connective tissue found in synovial joints and is made up of chondrocytes and extracellular matrix (ECM). The chondrocytes, which are the only cells present in cartilage, produce dense and highly organized ECM. Chondrocytes are embedded in the ECM from where they get their nutrition by diffusion. The ECM of cartilage is mainly comprised of a collagenous network containing 10 - 20% type II collagen, proteoglycans (10 – 20%), and glycosaminoglycans (GAGs) (Pap & Korb-Pap, 2015) and 80% water (Maroudas et al., 1991; Sophia Fox et al., 2009; Torzilli, 1985). The ECM provides both structural foundation and a ‘signalling scaffold’ for articular cartilage. This scaffold plays a key role in both the phenotypic stability and site-specific metabolic activities of chondrocytes (Sherwood et al., 2015). It also contributes to cartilage and bone

development during embryogenesis (Chuang et al., 2010; Koziel et al., 2004) by direct interactions with the embedded chondrocytes and retaining their soluble mediators.

There are four zones of cartilage in which different functions, compositions, structures, and chondrocyte anatomy and phenotype vary based on the depth from the cartilage surface, as described below (Figure 1.1).

1.2.1.1 Superficial zone

The superficial zone is the thinnest layer and makes up only 10-20% of the total articular cartilage thickness. This layer is primarily composed of flattened chondrocytes in a high-collagen / low-proteoglycan matrix. It has the highest water content of the four layers, and provides the cartilage with the greatest tensile strength, protecting the deeper layers from shear stresses. Additionally, this zone is in contact with synovial fluid and acts as a filter, preventing infiltration of macromolecules from the synovial tissue and ensuring the cartilage is protected (Bhosale & Richardson, 2008; Sophia Fox et al., 2009).

1.2.1.2 Middle zone

This region makes up 40% to 60% of the entire cartilage volume and serves as a functional and structural connection between the superficial and deep regions. The middle zone consists of chondrocytes with a lower density, randomly arranged collagen fibres, and a higher concentration of proteoglycan. The middle zone acts as the primary defence against compressive forces (Bhosale & Richardson, 2008; Sophia Fox et al., 2009).

1.2.1.3 Deep zone

Cells in the deep zone are spheroidal and arranged perpendicularly to the articular surface. This zone contributes 30% to 40% articular cartilage volume. Moreover, it has the highest proteoglycan concentration as well as largest diameter collagen fibrils with the ability to provide the greatest resistance to compressive forces (Bhosale & Richardson, 2008; Sophia Fox et al., 2009).

1.2.1.4 Calcified cartilage zone

The calcified cartilage zone is mineralised, and anchors the cartilage to bone through collagen fibres. Chondrocytes in this zone are hypertrophic and uniquely produce collagen type X. Collagen X contributes shock absorber functions, together with the subchondral bone. The tidemark differentiates the deep zone from the calcified cartilage with a visible border. The cells in this zone possess very low metabolic activity due to small volume of cells embedded in a calcified matrix. This zone also has high proteoglycan content, and the arrangement of collagen fibrils is the same as in deep zone (Bhosale & Richardson, 2008; Sophia Fox et al., 2009).

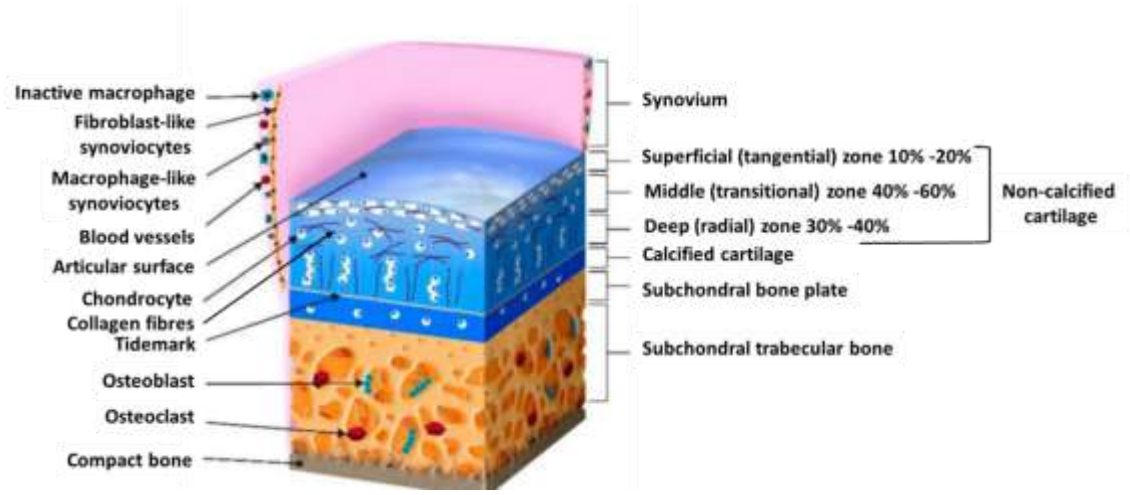

Figure 1.1: Schematic representation of healthy articular cartilage, with cellular organization and contribution percentages of different zones to cartilage volume, (right side), arrangement of collagen fibres from superficial to deep and calcified zones, and the histological state of different cells and tissues (left side) (Kurz et al., 2023).

1.2.2 Synovium

Synovium is the soft tissue lining the diarthrodial joint space. It consists of two layers, the intima and subintima (Figure 1.2). The intima, also known as the synovial membrane, is a continuous layer of 1-2 cell thickness. It comprises type A and type B synoviocytes (Figure 1.5a). Type A synoviocytes are thought to originate from blood monocytes and are similar to macrophages, while type B synoviocytes are locally derived fibroblasts (Malcolm D Smith, 2011; Malcolm D Smith et al., 2003). The intimal layer helps to shape and maintain synovial ECM by the production of matrix

components (e.g. collagens, fibronectin, tenascin, laminin, and proteoglycans) and ECM-degrading enzymes (such as matrix metalloproteinases (MMPs), proteases and cathepsins). Type B synoviocytes produces synovial fluid rich in hyaluronan (hyaluronic acid) and other joint lubricants such as lubricin (Jay et al., 2000; Rhee et al., 2005; Sprott & Fleck, 2023) (Figure 1.5a). Hyaluronic acid (HA) turnover is regulated by the balance between biosynthesis and degradation by hyaluronan synthases and hyaluronidases, respectively (Tobisawa et al., 2021; Valcarcel et al., 2020; G. T. Wu et al., 2023). In addition, MMPs, reactive oxygen species, and other factors present in the extracellular milieu can be involved in HA degradation (Guan et al., 2020).

The synovial fluid acts as a lubricant in addition to being biochemical pool through which regulatory cytokines and nutrients traverse (Castor, 1960). The subintima consists of loose connective tissues, blood and lymphatic vessels, adipose tissue, and infiltrating cells such as macrophages in a collagenous ECM (Malcolm D Smith, 2011). In addition to being a nutrient transport mediator, the subintimal layer also plays an important role in immune modulation and inflammatory responses in the joint (Lyane Haywood & Walsh, 2001). In summary, the synovium plays two crucial roles in maintaining the health of joints. Firstly, it produces lubricants that help cartilage articulate smoothly in a low-friction environment. Secondly, it provides vital nutrients to the cartilage as this tissue lacks its own blood supply.

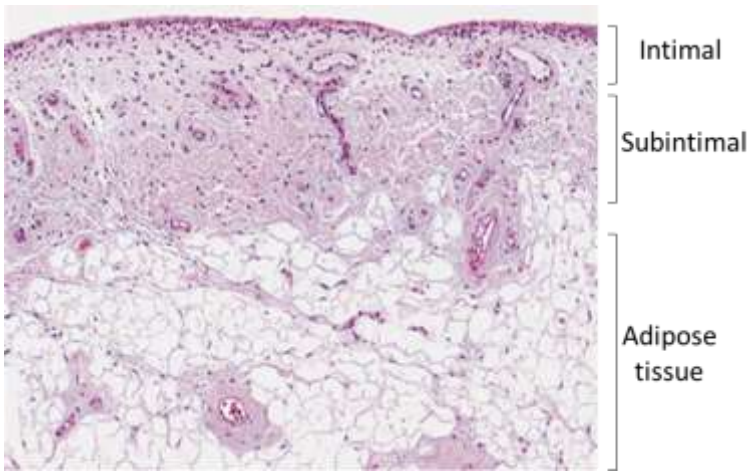

Figure 1.2: Haematoxylin and eosin (H&E) stained normal synovium showing layers and tissue types (Scanzello, 2022).

1.2.3 Subchondral bone

Subchondral bone (SCB) lies immediately beneath the calcified cartilage and tidemark. The tidemark separates calcified from noncalcified cartilage (Lyons et al., 2006), whereas the cement line is the borderline between calcified cartilage and subchondral bone (Imhof et al., 1999). Subchondral bone is divided into the subchondral plate and trabecular bone (Figure 1.3) (M. B. Goldring & Goldring, 2010). Subchondral trabecular bone is relatively porous containing sensory nerves, blood vessels, and bone marrow. It is also metabolically more active than the subchondral bone plate and plays a role in cartilage nutrient supply to the deepest cartilage layers (Suri & Walsh, 2012) as well as exerting important supportive and shock absorbing functions in normal joints (Castaneda et al., 2012). Subchondral bone is actively involved in adapting to the mechanical forces by undergoing modelling and remodelling (S. R. Goldring, 2012). Thus, any change in the microenvironment of SCB may either directly or indirectly affects cartilage metabolism and integrity.

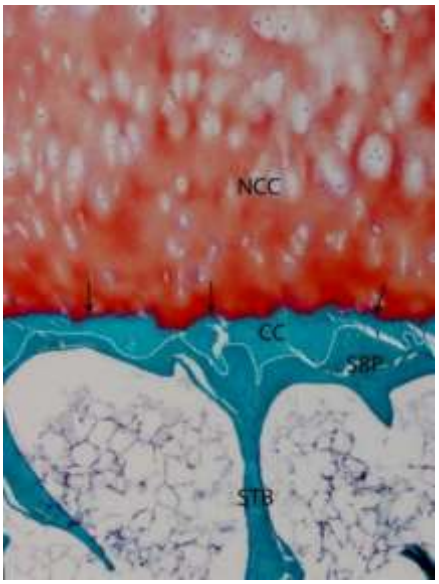

Figure 1.3: Articular cartilage and subchondral bone structure in a normal human joint. CC: calcified cartilage; NCC: noncalcified cartilage; SBP: subchondral bone plate; STB, subchondral trabecular bone. Arrows indicate the tidemark, while the dotted line displays the cement line separating calcified cartilage and subchondral bone (G. Li et al., 2013).

1.3 Pathophysiology of rheumatoid arthritis

Several risk factors contribute to the development of RA (Deane et al., 2017) (discussed in detail see section 1.4, Figure 1.4). Rheumatoid arthritis can be initiated by the complex interaction between environmental factors and the strongest genetic component human leukocyte antigen class II histocompatibility - D related beta chain (HLA-DRB1) (Ishikawa & Terao, 2020; Raychaudhuri et al., 2012; Weyand et al., 1992). During this process, the immune system's tolerance is disrupted, leading to the citrullination of proteins and peptides and the formation of new epitopes. These modified peptides are identified by antigen-presenting cells (APCs) in the adaptive immune system (E. Choy, 2012; Darrah & Andrade, 2018; Willemze et al., 2012). The process of autoimmunity in RA starts with the presentation of autoantigen (neopeptides) to T-cells, which then stimulates B cell differentiation into plasma cells. The plasma cells produce autoantibodies (rheumatoid factor (RF) and anti-citrullinated protein antibodies (ACPA), which further elicit inflammatory responses by recruiting leukocytes into the synovium (Carle et al., 2023; E. Choy, 2012; Volkov et al., 2020; Yap et al., 2018).

In RA leukocytes, such as mast cells, T and B lymphocytes, neutrophils, and monocytes/macrophages, migrate from the bloodstream into synovium through vessel walls. Several cell adhesion molecules including selectins, integrins, and their respective ligands are involved in leukocyte trans-endothelial migration (Agarwal & Brenner, 2006; A. E. Koch, 1998; Szekanecz & Koch, 2008) into the normal synovium. When immune cells infiltrate the normal synovial membrane, it triggers the inflammatory response by releasing pro-inflammatory cytokines like tumour necrosis factor–α (TNF-α), interleukins (IL-1, IL-6, and IL-17), granulocyte–macrophage colony-stimulating factor (GM-CSF), and MMPs. These cytokines then activate other inflammatory cells in the synovium, leading to the release of further cytokines and inflammatory mediators. These local pro-inflammatory mediators include prostaglandins, MMPs, proangiogenic factors (VEGF-A), TNFα, IL-6, and receptor activator of nuclear factor κB ligand (RANKL) (Bartok & Firestein, 2010; Tardito et al., 2019). Eventually synovium becomes hyperplastic (pannus), and the resulting hypoxia stimulates new blood vessel formation (angiogenesis) (Brennan et al., 1989; McInnes

& Schett, 2011; Wallach, 2016). Cytokines such as TNFα, IL1, IL-6, GM-CSF, and interaction of RANK with its ligand cause osteoclast differentiation and activation in the inflamed synovial membrane which leads to cartilage and bone erosion upon pannus invasion into periarticular bone at the cartilage-bone junction (Figure 1.4 & 1.5) (Komatsu & Takayanagi, 2022; Redlich & Smolen, 2012; Wallach, 2016).

Taken together, tissue damage in RA results from dysregulated T and B cell interactions, disrupting immune system balance and producing autoantibodies and cytokines (Catrina et al., 2016; X.-X. Hu et al., 2019; Q. Jiang et al., 2021) (Figure 1.4).

Autoantibodies can develop before the appearance of signs and symptoms and this stage is known as “pre-RA” which can last between as little as a year or persist for more than a decade. The duration of “pre-RA” is linked to the autoantibody profile. Individuals who express RF, ACPAs, and increased levels of C-reactive protein (CRP) develop symptoms within a few months. On the other hand, it may take 5 to 10 years after autoantibody appearance in the individuals who express ACPAs only (Nielen et al., 2004). Patients with "pre-RA" may have only subtle inflammatory changes in the synovium, while established RA may not always show clinical signs and symptoms, despite histologic evidence of inflammation (De Hair et al., 2014). Early signs of RA range from mild arthritis with few involved joints, but no structural damage, to severe polyarticular disease recognised by narrowing of the joint space and erosive disease, which is an indicator of cartilage degradation. Thus, adequate treatment is required to stop RA progression into a more destructive disease.

Apart from the symptoms that affect the joints, many patients also experience extra-articular or systemic manifestations or both (Hochberg et al., 2008). Extra-articular manifestations include vasculitis, rheumatoid nodules, rheumatoid lung, uveitis, pericarditis, and keratoconjunctivitis sicca (Hochberg et al., 2008). Systemic manifestations include CVD, anaemia, osteoporosis, acute-phase protein production, fatigue, and depression (Dayer & Choy, 2010; Pollard et al., 2005).

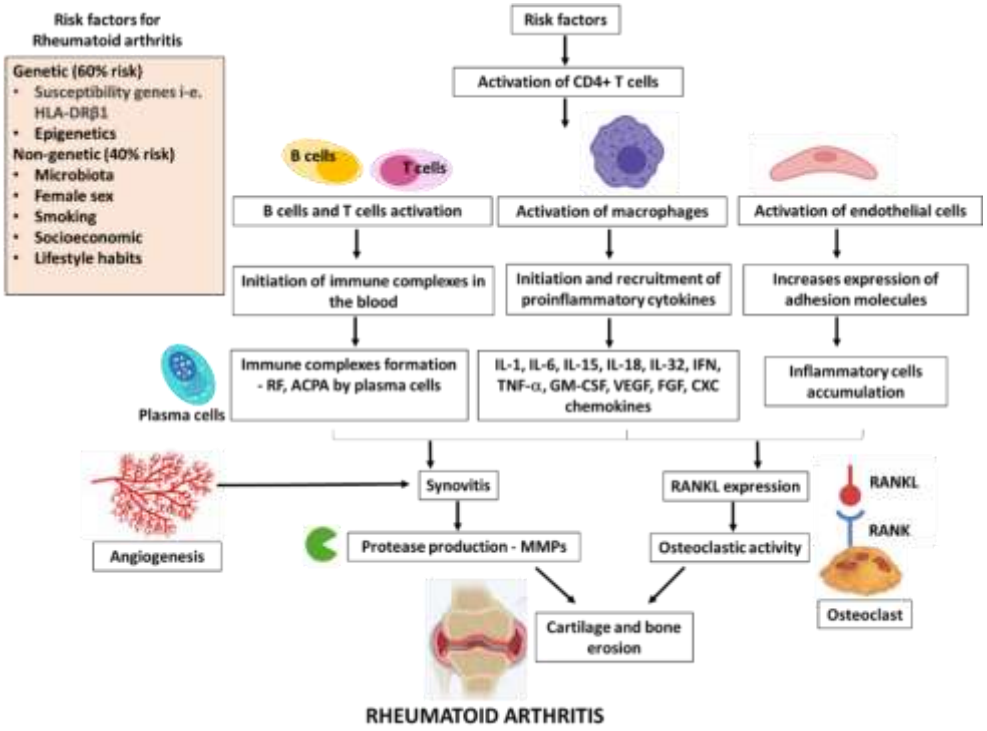

Figure 1.4: Pathophysiology of rheumatoid arthritis. This diagram summarises the multiple different cells, processes and mediators that contribute to the pathophysiology of RA. Various factors (top left side of figure) are involved in RA development that results in the activation of CD4+ T cells. These cells trigger macrophage, T and B cells, and endothelial cells activation, resulting in the secretion of pro-inflammatory cytokines, autoantibodies, and adhesion molecules which affect fibroblast, chondrocytes, and osteoclasts. Chondrocytes release MMP, while fibroblasts transform into FLS and produce pro-inflammatory cytokines, ultimately leading to the destruction of the extracellular matrix. Pro-inflammatory cytokines can also stimulate angiogenesis leading to pannus formation resulting in cartilage damage and bone destruction.

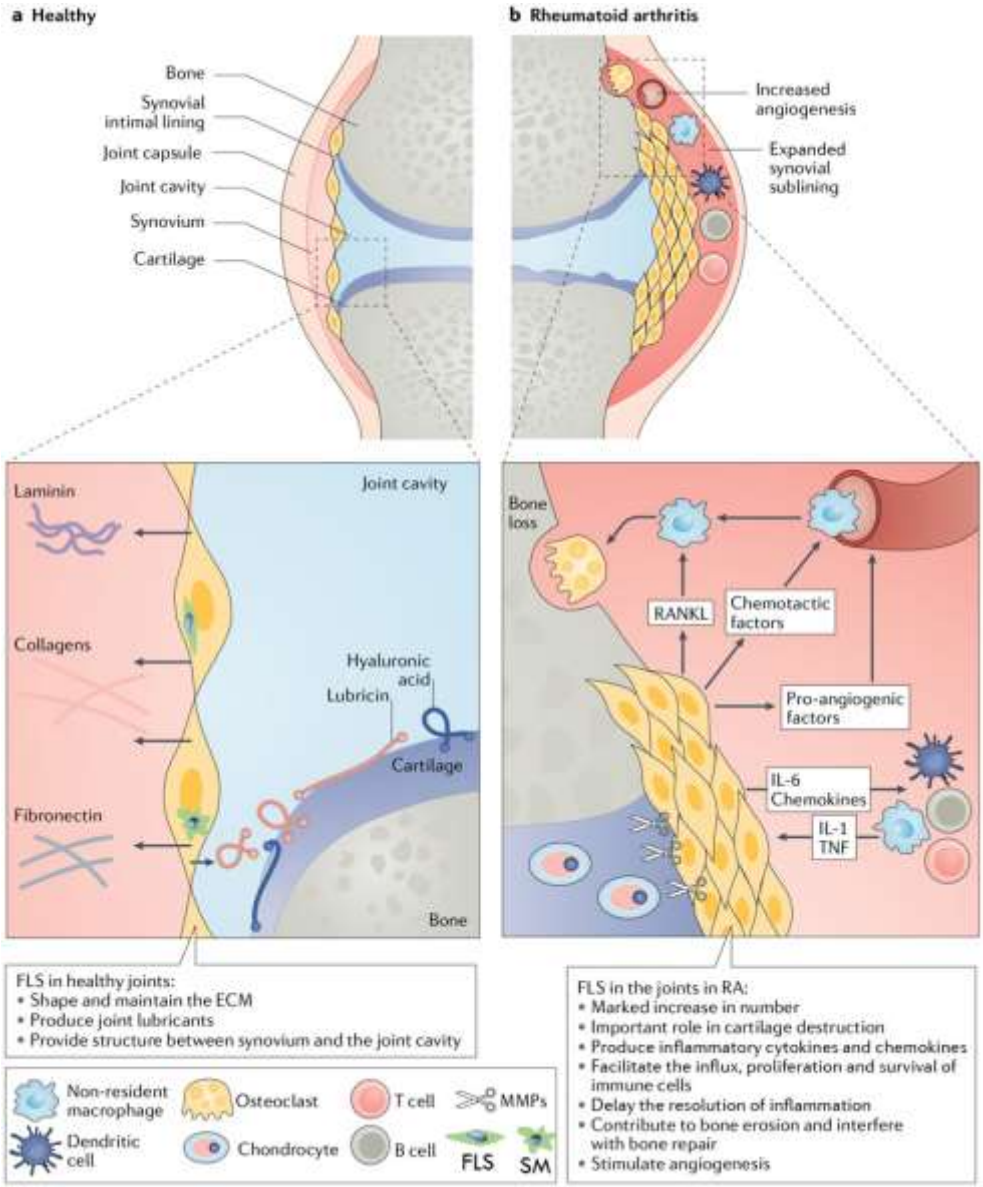

Figure 1.5: Comparison of healthy (left) versus arthritic joint (right). (a) Healthy joint (left) shows synovial intimal lining with thin layer (1-2 cells) of synoviocytes (Type A: tissue resident macrophages; Type B: Fibroblast-like synoviocytes (FLS). Synovial macrophages maintain intra-articular homeostasis engulfing foreign bodies in the joint cavity. Synovial FLS controls ECM composition via secretion of several matrix components such as hyaluronic acid, fibronectin, lubricin, laminin, and collagen (b) while in rheumatoid arthritis, there is expansion of synovial intimal lining and transformation into invasive pannus (also known as hyperplasia). Hyperplastic synovial cells express matrix metalloproteases (MMPs), chemokines (CXC-chemokine ligand 10), cytokines (IL-6), and pro-angiogenic factors (VEGF-A) which maintain joint inflammation and lead to cartilage and bone destruction (Nygaard & Firestein, 2020). FLS: Fibroblast-like synoviocytes, SM: Synovial macrophages (resident); ECM: extracellular matrix; RANK: Receptor activator of nuclear factor kappa beta, TNF: Tumour necrosis factor, IL1: Interleukin 1; IL6: Interleukin 6.

1.4 Risk factors

The exact cause of RA is still unknown. However, there are a number of factors that increase the risk of developing this disease. These factors include genetics, epigenetics, being female, and both socioeconomic and environmental factors. Some of the environmental risk factors include smoking, exposure to airborne agents such as silica and dust from inorganic and textile sources, air pollution, poor dietary habits including high consumption of red meat, sodium, and iron, infectious agents, vitamin D deficiency, obesity, and changes in the microbiota (Deane et al., 2017; Romao & Fonseca, 2021).

1.4.1 Genetics

Rheumatoid arthritis has a strong genetic component; having a family history increases the chances of developing it by around 60% (MacGregor et al., 2000). The HLA (human leukocyte antigens) class II family, which correspond to the major histocompatibility complex (MHC) in animals, have a strong association with RA (Gregersen et al., 1987). The disease related alleles contain a conserved sequence of five amino acid known as a shared epitope. The shared epitope hypothesis suggests that certain alleles are directly involved in the pathogenesis of RA by allowing incorrect autoantigen presentation to T cells, leading to T cell-mediated autoimmune responses (Gregersen et al., 1987; van der Helm-van Mil et al., 2005). Many gene loci associated with RA studies consistently reveal the presence of HLA-DRB1 alleles within the MHC complex on chromosome 6. HLA-DRB1 contributes nearly 30% of the whole genetic component involved in this disease (Deighton et al., 1989). HLA-DRB1 is present on APCs and plays a role in presenting pathogens to T cells to initiate immune antibody responses. In addition, other genetic risk factors with weaker associations (~5%) have been recognised, such as a PTPN22 (tyrosine-protein phosphatase nonreceptor type 22) gene polymorphism which is thought to be associated with lowering the threshold for T cell activation (Rieck et al., 2007; Stanford & Bottini, 2014; Jinyi Zhang et al., 2011) and hypercitrullination by interacting with the enzyme peptidyl arginine deiminase, and hence responsible for citrullination (Chang et al., 2015). The majority of associations are with alteration in molecules related to

immune and inflammatory pathways involved in RA such as STAT4 (signal transducer and activator of transcription 4) (Remmers et al., 2007), CTLA4 (cytotoxic T-lymphocyte associated protein 4) (Plenge et al., 2005), NF-kB (nuclear factor kappa B) (Spurlock et al., 2015), and IL-6 (Ferreira et al., 2013).

1.4.2 Epigenetics

Epigenetic modifications including DNA methylation and histone acetylation also promote inflammatory responses and might have a role in RA progression. DNA methylation is a crucial process that allows environmental factors to change cellular activity. For instance, people with ACPA-positive disease carrying the risk allele HLA-DRB1 who smoke, have higher DNA methylation levels compared to those without the risk allele. Non-smokers did not have a difference in methylation (Meng et al., 2017) indicating a potential gene – environment interaction that could increase the risk of developing ACPA positive RA. Posttranslational protein modifications such as citrullination of arginine residues, generate new epitopes and result in the formation of autoantibodies against autoantigens (e.g. ACPAs, IgG - RF, or autoantigens that cross-react with viral or bacterial viral antigens for example Epstein-Barr virus or *Prevotella* (Pianta et al., 2017; Tan & Smolen, 2016). These autoantibodies can break the immunological tolerance to form immune complexes that may activate complement which further increases inflammatory responses (Tan & Smolen, 2016). ACPAs alone can cause little inflammation but together with RF can promote a considerable inflammatory response. Rheumatoid factors also increase immune responses formed by ACPAs and amplify the inflammatory reactions produced by complement activation and immune complexes (Aletaha et al., 2015; Sokolove et al., 2014; Yoo et al., 2008).

1.4.3 Microbiota

Regarding the microbiome, periodontal disease is associated with an increased risk of developing RA. The link between periodontal disease and RA is thought to be partially facilitated by oral microbiota such as *Porphyromonas gingivalis* (Kharlamova et al., 2016) and *Aggregatibacter actinomycetemcomitans* (Konig et al., 2016). In addition to periodontal microbiota, the gut microbiota such as *Prevotella* species may have an important role in RA (Wegner et al., 2010). Data suggest that bacteria may

cause autoimmunity and inflammation via translocation from the gut to tissues (Manfredo Vieira et al., 2018). The link between environment, genetics, and disease is supported by the findings of homology in the sequence of HLA-DR molecules in RA patients with protein epitopes from bacterial species (*Prevotella* and other gut bacteria species) in RA (Pianta et al., 2017). Furthermore, the similarities between amino acid sequences of bacterial or viral proteins, and autoantigens have been described (Alam et al., 2014). Regarding the role of viruses, Epstein-Barr virus infection (Tan & Smolen, 2016) has been implicated in autoimmune diseases and RA (Tan & Smolen, 2016) and parvovirus B19 may also be implicated following a 2019 case study showing parvovirus mimicking RA (Alexander et al., 2019).

1.4.4 Sex

In general, RA affects women more than men (Favalli et al., 2019; Y.-J. Lin et al., 2020; S. Ngo, 2014) with 4-5 times higher incidence and prevalence rates (Kvien et al., 2006). The lifetime risk estimation of developing adult-onset RA in female is 3.6 percent while 1.7 percent in men (Crowson et al., 2011). In women, symptoms of RA appear most commonly in middle age or at menopause, while disease onset in men tends to be later. Men are also more likely to be RF positive and have increased ACPA titres (Alamanos et al., 2006).

The prevalence of RA is higher in women, which is linked to immune system stimulation by oestrogen. However, the role of hormonal factors in the pathogenesis and development of RA remains complex and controversial despite extensive research. Oestrogen can have both stimulatory and inhibitory effects (Cutolo et al., 2006), while androgens have inhibitory effects on the immune system. More specifically, oestrogen can have a range of effects on different immune cells based on serum concentration, reproductive phase or ovarian ageing stage such as reproductive, menopausal transition or post-menopausal, and oestrogen receptor (ER) expression (Straub, 2007). It has been proposed that the dichotomous effects (pro-inflammatory and anti-inflammatory) of oestrogens in several inflammatory conditions could be due the relative abundance of different oestrogen pro-inflammatory metabolites (Straub, 2007) in synovial cells from patients with RA (Schmidt et al., 2009).

Many cells of the immune system, for example B cells, natural killer cells, macrophages, $CD4^+$ (cytotoxic) and $CD8^+$ (helper) T cells, express oestrogen receptors (Ackerman, 2006; Bouman et al., 2005). High levels of oestrogenic show a strong stimulatory effect on these cells of immune system with the tendency towards producing autoimmune responses through the secretion of pro-inflammatory cytokines and stimulation of antibody production. Hence, these immuno-stimulatory effects of oestrogen contribute to increase female susceptibility to develop autoimmune diseases (Lockshin, 2001, 2005). In contrast, progesterone and androgens are considered natural immunosuppressors (Cutolo & Straub, 2020; Grimaldi, 2006; Hughes, 2012; Straub, 2007). These exert anti-inflammatory effects by downregulating immune-related genes and pathways implicated in RA such as inhibition of Th1 and Th17 differentiation, and human peripheral blood mononuclear cells (PBMC) activity (Sthoeger et al., 1988) which results in the reduction of IL-1, IL-6 and TNF-α (Gubbels Bupp & Jorgensen, 2018; Hughes, 2012; Lu et al., 2015).

On the other hand, pregnancy is associated with disease remission as well as decreased onset of RA in 75% of women (Krause & Makol, 2016; Lansink et al., 1993; Nelson & Ostensen, 1997; Silman et al., 1992) due to complex pregnancy-related hormonal and immunological alterations (Monika Ostensen & Villiger, 2007). The reduction of RA disease activity during pregnancy is due to an increase in oestrogen and progesterone levels which may play an indirect role in the induction of this beneficial type of immune regulation (Forger et al., 2008; Kahn & Baltimore, 2010; Masi et al., 1995; Nelson & Ostensen, 1997; Monica Ostensen, 1999; Whitacre, 2001). Moreover, during pregnancy, increased levels of oestrogen, cortisol, and vitamin D reduce pro-inflammatory cytokines such as IL-12 and TNF-α (Elenkov et al., 2001). However, disease flares are common after childbirth (Borba et al., 2019; Lansink et al., 1993; Nelson & Ostensen, 1997; Oka, 1953) and are also found in association with breastfeeding (Barrett et al., 2000). Prolactin was thought to be responsible for disease flare in breastfeeding but the data available so far on the prolactin role in human RA is conflicting and limited (M. W. Tang et al., 2017). Some studies conducted after the Barrett study (Barrett et al., 2000) show a consistent association of breastfeeding with a decreased risk of RA (Adab et al., 2014; H. Chen et al., 2015; Pikwer et al., 2008). Other large prospective cohort (Karlson et al., 2004; Salliot et al., 2021) and case-

control (Orellana et al., 2017) studies show no substantial link between breastfeeding and risk of RA, whereas an increased risk was identified in a single study by Berglin et al. (Berglin et al., 2010).

In menopause, the rapid decline in circulating oestrogens is linked with a spontaneous rise in pro-inflammatory cytokines e.g. IL-1β, IL-6, and TNF-α (O. Y. Kim et al., 2012; Mateen et al., 2016; Pfeilschifter et al., 2002).

In summary, sex hormones exert pleiotropic effects on the immune system. Although there are conflicting reports in the literature as discussed earlier, higher levels of oestrogen provide protection during pregnancy. Conversely, lower levels of oestrogen and/or progesterone following childbirth and during menopause commonly result in an increased risk and severity of RA (Cutolo & Gotelli, 2023; Raine & Giles, 2022).

1.5 Articular joint damage in rheumatoid arthritis

1.5.1 Synovial inflammation

Rheumatoid arthritis is a systemic disease, in which immune-mediated events occur both in joints and systemically in other sites such as primary lymphoid tissues and mucosal surfaces. The synovium is however the main site of pathology, where a variety of immunological events occur (Figure 1.5).

Two key pathogenetic changes are prominent in RA synovium. First, there is an increase in number and activation of both types of synoviocytes leading to the expansion of intimal lining (McInnes & Schett, 2011). Macrophage-like and fibroblast-like (FLS) synoviocytes are prominent sources of proteases and pro-inflammatory cytokines, such as IL-1, IL-6, and TN F and others are produced by macrophage-like synoviocytes. Production of small-molecule mediators such as prostaglandins and leukotrienes is stimulated by IL-6. These molecules are involved in the degradation of many components of ECM in the synovial joint (Bartok & Firestein, 2010). Fibroblast-like synoviocytes are thought to contribute to cartilage destruction and propagation of disease because of their potential to migrate from joint to joint via the blood stream (Lefevre et al., 2009). Angiogenesis, vascular cell adhesion molecule 1 (VCAM-1) and integrins are important mediators of FLS transmigration into the vascular system and

invasion into the cartilage (El-Gabalawy et al., 1996; Giancotti & Ruoslahti, 1999; Morales-Ducret et al., 1992; Muller-Ladner et al., 1997; Schedel et al., 2004).

Secondly, adaptive immune cells infiltrate into the synovial sublining such as CD4+ which activate B cells (as discussed earlier in section 1.3) (Ziff, 1974). Hence, these cells in addition to mast cells, antigen-presenting follicular dendritic cells, and macrophages play significant roles in the progression of inflammation (Orr et al., 2017).

Synovial hyperplasia is the hallmark of RA pathology. In RA, a large number of immune and inflammatory cells migrate into the synovium and the synovium proliferates and grows into a mass-like invasive tissue termed pannus (Figure 1.5). RA synovial fibroblasts are resistant to apoptosis and cause persistent inflammation of the synovium by interacting with immune and inflammatory cells. They also promote the formation of ectopic lymphoid follicles (I. Y. Choi et al., 2017). In addition, synovial fibroblasts produce inflammatory cytokines and MMPs, and directly invade articular cartilage and subchondral bone. In some respects, RA synovium is considered to show tumour-like features which are largely contributed by fibroblasts (Lefevre et al., 2009; You et al., 2018). Pannus exhibits neovascularisation which supports growth and invasion into adjacent cartilage and bone leading to joint damage (Fassbender, 1983).

1.5.2 Cartilage damage

Cartilage is a target tissue in RA. During the course of the disease, synovial cells particularly activated FLS, progressively destroy the cartilage (Bottini & Firestein, 2013; Huber et al., 2006). The mediators of cartilage destruction in RA include MMPs, a disintegrin-like and metalloproteinase with thrombospondin motifs-*4 & 5* (ADAMTS-4, ADAMTS-5) and cathepsins, which play a key role in inducing cartilage damage (Pap et al., 1999). In RA, these enzymes are present in the synovial fluid and can cause direct cartilage destruction due to their activation state and level (Yoshihara et al., 2000). However, many studies suggest that the inflamed synovial membrane's proximity to cartilage also plays a critical role in aggressive ingrowth and consequent matrix destruction (Pap et al., 2000). The mechanism by which cartilage damage facilitates attachment of synovial cells includes synovial hyperplasia and ECM

degradation. Fragments of ECM are released, which can bind to cell-surface molecules on synovial cells. In fact, fibronectin fragments from cartilage ECM have been found to promote the formation of synovial pannus (S. Shiozawa et al., 1992; Yasuda, 2006). Deletion of IL-1 genes prevents cartilage proteoglycan loss and reduces synovial adherence and damage in experimental models (Korb-Pap et al., 2012; Zwerina et al., 2007).

1.5.3 Bone erosion

Bone consists of four different cell types: osteoblasts, osteocytes, osteoclasts, and bone lining cells found in and around the osteoid matrix. The bony skeleton protects various other organs of the body by providing mechanical support. The bone ECM is an essential component of bone (Y. Fan et al., 2020; J. Wang et al., 2013; R. Zhou et al., 2021), which is secreted by osteoblasts cells into the extracellular space. ECM is composed of inorganic (40%) phosphate and calcium, predominantly in the form of hydroxyapatite ($Ca_{10}(PO_4)_6(OH)_2$) (Tavafoghi & Cerruti, 2016) and organic compounds (60%) including both collagen and non-collagenous materials.

Collagen is an important protein in bones, providing support and structure. The three types of collagen most responsible for this function are types I, III, and V. (M. Saito & Marumo, 2015). Type I collagen is the most abundant, making up 90% of the organic bone matrix (Varma et al., 2016). The remaining 10% of the matrix is made up of non-collagenous proteins, which can be divided into four groups: proteoglycans (Coulson-Thomas et al., 2015; Kalamajski et al., 2009; Moorehead et al., 2019), γ-carboxyglutamic acid containing proteins (Kaipatur et al., 2008; Mizokami et al., 2017; Wen et al., 2018), glycoproteins (A. Delany et al., 2000; A. M. Delany & Hankenson, 2009; Rosset & Bradshaw, 2016; Shi et al., 2017), and small integrin-binding ligand N-linked glycoproteins (SIBLINGs) (Jani et al., 2016; Marinovich et al., 2016; A. Singh et al., 2018; Zelenchuk et al., 2015). In bone, ECM regulates tissue elasticity, cell adhesion, proliferation, growth factor responses, differentiation, and bone function (X. Lin et al., 2020). Bone ECM undergoes constant remodelling due to changes in growth factors, receptors, and local pH levels to maintain tissue homeostasis (Bonnans et al., 2014; Mouw et al., 2014).

Bone homeostasis is maintained by a balance between osteoblasts and osteoclasts. This process ensures the bone eroded by osteoclasts is completely replaced by osteoblasts with fresh bone. The balance is tightly regulated by various growth factors, osteogenic cytokines, and hormones (Takayanagi, 2005). Fluctuation in this homeostatic equilibrium towards excessive osteoclast activity is associated with pathological disorders such as osteoporosis (P. Tang et al., 2014), and bone tumours (Maurizi & Rucci, 2018; Russo et al., 2022). Increased osteoclastic activity also contributes in the progression of RA (Allard-Chamard et al., 2020; Niu et al., 2022; Schett, 2007), OA (Bertuglia et al., 2016; Weber et al., 2019), and Paget's disease (Sabharwal et al., 2014).

In RA, bone erosion or focal articular bone loss is a common and characteristic feature which manifests early in the disease process (Scott, 2004). Erosions take place upon pannus invasion into subchondral and cortical bone, and the adjacent marrow spaces. Ultimately, trabecular bone is lost resulting in increased fracture risk (Joffe & Epstein, 1991; Sambrook, 2000). Bone erosion may develop early in the course of RA (K. P. Machold et al., 2002; Plant et al., 1998; DMFM Van der Heijde, 1995) sometimes within weeks after diagnosis, for example as seen in >10% of the patients as early as 8 weeks after the appearance of symptoms (K. P. Machold et al., 2002), and up to 60% have erosions after one year (K. Machold et al., 2007; Plant et al., 1998; Proudman et al., 2000; DMFM Van der Heijde, 1995). This indicates that, in some patients, the process of disease may start earlier than the onset of symptoms, which is supported by the evidence of autoantibodies presence long before the appearance of disease (Aho et al., 1985; Nielen et al., 2004; Rantapaa-Dahlqvist et al.). Development of bone erosions and joint damage progression in some early RA patients, even when ‘very early’ DMARD treatment was instituted, may indicate early determination of disease towards joint damage (Lard et al., 2001; Nell et al., 2004; van Aken et al., 2004). On the other hand, in some patients substantial joint damage despite early treatment with DMARDs is attributable to a lack of a good clinical response to treatment (K. Machold et al., 2007).

The understanding of mechanisms driving bone erosion are critical objectives in treating people with RA to prevent focal bone erosions.

1.5.3.1 Osteoclast formation in the inflamed joint in rheumatoid arthritis

Osteoclasts arise from cells of monocyte-macrophage lineage and are multinucleated cells normally found at the trabecula surface of cancellous bone. Osteoclast activity creates bone resorption in 'pits'. Pits may be repopulated by osteoblasts to form new bone matrix in remodelling. Osteoclasts attach to the bone matrix and mediate bone remodelling by creating a local acidic environment by secreting proteinases. During physiological bone remodelling, osteoclast-mediated bone loss is balanced by osteoblast-mediated bone formation.

During normal physiological bone remodelling, osteoclast differentiation and function is regulated by the receptor activator of NF-κB (RANK) ligand (RANKL) pathway. RANKL binds to its cognate receptor RANK expressed on osteoclast precursor cells, thereby promoting osteoclastogenesis. Osteoprotegerin (OPG) is a soluble decoy receptor for RANKL, preventing it from binding to RANK. This action of OPG acts as a vital negative regulator of osteoclastogenesis (Kong et al., 1999; Skoumal et al., 2005). Osteoclastogenesis also needs macrophage-colony stimulating factor (M-CSF) to stimulate osteoclast cellular precursors for differentiation into osteoclasts (Tsurukai et al., 2000). During physiologic bone remodelling, both RANKL and M-CSF are produced by cells of the osteoblast lineage (S. Tanaka et al., 1993).

The synovial membrane in RA contains numerous monocytes/macrophages, which can differentiate into osteoclasts on exposure to appropriate signals. Activated T cells and synovial fibroblast-like cells are the most important cells in the synovium providing essential signals for monocyte differentiation into osteoclasts. Synovial FLS express RANKL and therefore can drive osteoclast formation (Gravallese et al., 2000; Shigeyama et al., 2000). In addition, activated T lymphocytes producing IL-17, are potent stimulators of osteoclast formation (Sato et al., 2006). Pro-inflammatory cytokines such as TNFα, IL-1, IL-6, and IL-17 are abundant in RA synovium and regulate RANKL expression. Upregulation of RANKL is also observed in psoriatic arthritis, and in experimental models of arthritis (Gravallese et al., 2000; Ritchlin et al., 2003; Shigeyama et al., 2000; Stolina et al., 2005), demonstrating RANKL as an important factor for osteoclast formation in the joint. Therefore, there appears to be a

tight relationship between inflammatory cytokines, RANKL expression and osteoclast formation in the joint.

It has been shown that when inflamed synovial tissue comes into direct contact with the bone surface, terminally differentiated osteoclasts express the calcitonin receptor (CTR). This suggests that the final differentiation of osteoclasts may be dependent upon direct interaction with mineralized tissue. Late osteoclast differentiation markers such as tartrate-resistant acid phosphatase (TRAP), cathepsin K, and CTR are expressed in the synovium of RA. (Gravallese et al., 1998; Gravallese et al., 2000). TRAP is a marker for bone-resorbing osteoclasts as TRAP positive multinucleated osteoclasts secrete cytokines and various proteinases such as MMPs that lead to cartilage and bone damage (I. Adamopoulos et al., 2006; I. E. Adamopoulos et al., 2006; Delaissé et al., 2000; Tsuboi et al., 2003). In normal physiology, TRAP positive multinucleated cells in the growth plate, known as chondroclasts, play important roles in the process of replacing the hypertrophic chondrocyte zone with bone (Vu et al., 1998).

1.5.3.2 Osteoclasts and the cartilage damage in rheumatoid arthritis

As discussed earlier, the development of structural damage in RA is a complex process involving cartilage destruction, inflammation of the tendons near joints, and bone erosion. Articular cartilage includes both unmineralized cartilage, forming the surface of the joint, and mineralised cartilage which is present deep in articular cartilage and connects it to subchondral bone. Osteoclasts do not target or invade the unmineralized cartilage, as shown in samples from joint replacement surgery (Figure 1.6). The key players involved in cartilage degradation include degrading enzymes such as MMPs and the invasive properties of the synovial tissue (Pap et al., 2001). Osteoclasts in the pannus may have an important roles in the damage to mineralised articular cartilage in RA as TRAP positive mononuclear and multinucleated cells at the cartilage-synovial interface produce MMP-2 and MMP-9 (Tsuboi et al., 2003).

It is reasonable to suggest that mineralized cartilage is sensitive to bone resorption by osteoclasts because the most abundant ossification pathway, endochondral

ossification, involves the removal of mineralized cartilage and its remodelling into bone. Therefore, the mineralized cartilage may be a weak point in the joint which permits osteoclast invasion, contributing to cartilage surface damage. Tunnels resulting from osteoclast invasion can then be occupied by pannus containing high MMP and cytokine concentrations which cause rapid degradation. Thus, invasion into mineralized cartilage may allow synovial tissue to gain access to the bone marrow by breaking the thin subchondral bone barrier (Schett, 2007).

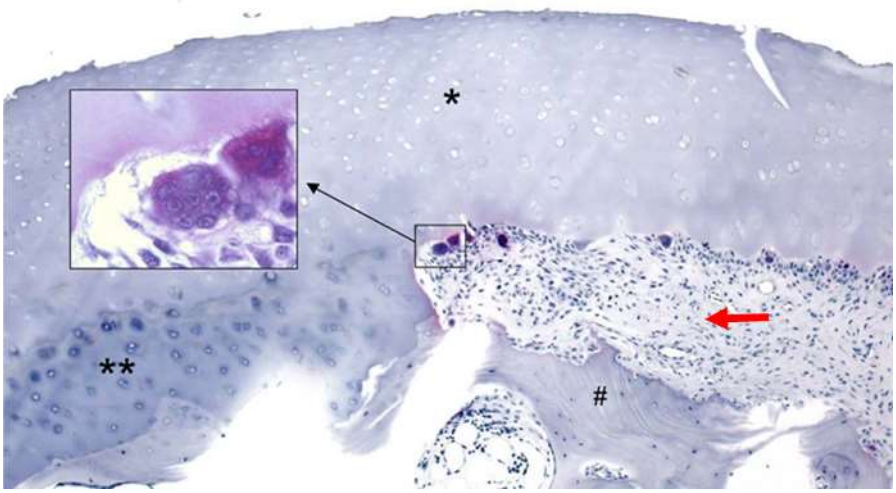

Figure 1.6: Mineralized surface cartilage erosion by osteoclasts in metacarpophalangeal joint section from a patient with RA. Arrow (red) shows the infiltration of synovial inflammatory into the mineralized cartilage (**), where it is accompanied by osteoclasts that erode the cartilage, whereas the unmineralized surface cartilage (*) looks intact. Additionally, the subchondral bone (#) displays resorption lacunae. Inset shows magnified boxed field including osteoclasts in 'pits' at the interface between the invading synovium and cartilage (Schett, 2007)

1.5.4 Subchondral fibrovascular tissue

Subchondral neovascularization and inflammation are well-known for their co-existence in RA (Appel et al., 2006; Bugatti et al., 2005). Subchondral bone marrow replacement by fibrovascular tissue (FVT) is a feature of both RA (Appel et al., 2006; Bromley et al., 1985; Bugatti et al., 2005) and OA (Bugatti et al., 2005; Milgram, 1983; D. A. Walsh et al., 2022). In RA, subchondral inflammatory infiltrates contain lymphocytes which produce MMPs and chemokines (Appel et al., 2006; Bugatti et al.,

2005), and promote osteoclastic activity (Bugatti et al., 2005; Kaneko et al., 2001; Lisignoli et al., 2007). Subchondral osteoclastic activity (D. A. Walsh et al., 2010) and angiogenesis are involved in the FVT replacement of SCB bone marrow in both experimental and human arthritis (P. Mapp et al., 2008). The blood vessels in subchondral bone marrow FVT invade articular cartilage by breaching the tide mark, and this is associated with cartilage damage and joint pain.

1.6 Classification and diagnosis of rheumatoid arthritis

The 2010 RA classification criteria were proposed by the American College of Rheumatology/European League Against Rheumatism (ACR/EULAR) to assist early diagnosis of RA (Aletaha et al., 2010; Radner et al., 2014). According to the classification, diagnosis of RA requires evidence of at least one clinically swollen joint and overall 6 points from a scoring system (Table 1.1) which is the indication of early RA.

UK National institute of Health and Care Excellence (NICE) guidelines recommend that any adult with suspected ‘persistent synovitis of unknown cause’ is referred urgently for investigation in case of any of the following exist; (a) the small joints of the hands or feet are involved (b) more than one joint is involved. It is important to identify the patients in the earlier stages of RA as soon as possible because early diagnosis and effective treatment prevents the joint damage progression in 90% of patients (Goekoop - Ruiterman et al., 2005).

Initial assessment for RA usually involves serologic testing for autoantibodies (RF and ACPAs) and acute phase reactants (APRs) such as plasma fibrinogen, serum C-reactive protein (CRP), platelet count, and ferritin (Arvidson et al., 2002; Beyan et al., 2003; Dessein et al., 2004; Mackiewicz et al., 1991; Yildirim et al., 2004) as well as joint examination for synovitis of unknown origin. UK NICE guidelines recommend blood tests for RF followed by measuring anti-cyclic citrullinated peptide antibody (ACCP) in the case of negative RF in suspected RA patients with persistent synovitis. The diagnosis may also include X-ray of hands and feet in these individuals. Follow-up includes evaluation of APRs, assessment of joint and disease activity, and evaluation of physical function using the Health Assessment Questionnaire (HAQ)

which also provides a baseline to measure the functional response to treatment (UK NICE guidelines).

Serological biomarkers and autoantibodies, such as ACPAs and RF, can be detected up to 10 years before disease onset in two-thirds of individuals. This enables the identification of patients at increased risk of developing RA. Hence, in addition to diagnosis, these serological markers can be used as a prognostic marker (Aletaha et al., 2015; Aletaha et al., 2010; Laurent et al., 2015; Nielen et al., 2004; Sokolove et al., 2014).

One of the most effective ways to assess the level of RA disease activity in both clinical trials and practical applications is by using a composite measure. Such measures can incorporate various metrics such as a disease activity score calculated using multiple joint counts (DAS28), a clinical disease activity index (CDAI), and the simplified disease activity index (SDAI), all of which are used to evaluate the extent of disease activity (Aletaha et al., 2005; Smolen et al., 2006; DMFM Van der Heijde et al., 1992). In the 1990s, composite measures of disease activity were established to reduce the error in measurements and improve the analysis/interpretation of clinical trials for the evaluation of new biological agents and disease-modifying anti-rheumatic drugs.

Table 1.1: 2010 EULAR/ACR classification criteria for RA.

Classification criteria	Point score
Joint involvement (0–5 points)	
1 large joint	0
2–10 large joints	1
1–3 small joints (large joints not counted)	2
4–10 small joints (large joints not counted)	3
>10 joints including at least one small joint	5
Serology (at least one test needed for classification; 0–3 points)	
Negative RF and negative ACPA	0
Low positive RF or low positive ACPA	2
High positive RF or high positive ACPA	3
Acute-phase reactants (at least one test needed for classification; 0–1 point)	
Normal CRP and normal ESR	0
Abnormal CRP or abnormal ESR	1
Duration of symptoms	
<6 weeks	0
≥6 weeks	1

Table 1.1: A score ≥6 = definite RA diagnosis. ACPA: anti-cyclic citrullinated protein antibody; RF: rheumatoid factor; ESR: erythrocyte sedimentation rate; CRP: C-reactive protein.

1.7 Treatment of rheumatoid arthritis

In the UK, and elsewhere, the goal for treating RA is to achieve disease remission, particularly in early RA, or low disease activity if remission is not attainable in established RA (termed ‘treat to target’ in UK NICE guidelines) (Aletaha et al., 2016). Disease remission is a state described by SDAI or CDAI which shows reduced/halted progression of joint damage with improved physical function (Aletaha & Smolen, 2011).

Treatment regimens for RA consist of various aspects such as educating patients about the disease for example offering written and verbal information to counter any misconceptions and improve understanding regarding the condition, management of the disease, and pharmacological and non-pharmacological management (UK NICE guidelines). Treatments are mostly tailored to a patient's needs and according to their general health which includes factors such as age, overall health, disease progression, occupation, the joints involved and compliance (J. Bullock et al., 2019).

1.7.1 Initial pharmacological management – DMARDs

Conventional disease-modifying antirheumatic drugs (cDMARDs) are the UK 1st line drugs (NICE) used for the treatment of RA to promote remission by reducing or stopping the development of joint destruction and deformity. NSAIDS are also used for pain control as concurrent treatment in RA (Crofford, 2013).

DMARDs can take from weeks to months to be effective and are considered as slow-acting medications. Hence, short-term bridging treatment with glucocorticoids (anti-inflammatory and immunosuppressant) is also considered for the short period of time in individuals starting new DMARD. This is intended to reduce symptoms while waiting for the new DMARD to start producing its effect (NICE guidelines). Methotrexate (MTX) is an effective cDMARD and the initial first-line immunosuppressive drug used in RA in the UK. MTX has fewer side effects than other cDMARDs, and has dosage flexibility (i.e. doses can be easily adjusted as required) (Tian & Cronstein, 2007). The initial dose is estimated to be well tolerated and then titrated up on the basis of therapeutic response (J. A. Singh et al., 2016; Smolen et al., 2010). Patients taking MTX require regular blood tests due to the possible side effects, for example bone marrow deterioration, liver damage and cirrhosis. Taking folic acid supplements can help to lower the risk of side effects associated with MTX. Leflunomide, sulfasalazine and hydroxychloroquine are additional first-line cDMARDs that can also be used in combination with MTX if low disease activity or remission is not achieved with one DMARD. There is substantial evidence to support the use of combination conventional synthetic DMARDs over MTX monotherapy (Daien et al., 2017; D. Liu et al., 2013; Smolen et al., 2018). All DMARDs have anti-inflammatory mechanisms of action, for example, hydroxychloroquine decreases the secretion of monocyte-derived pro-

inflammatory cytokines and can be used for long-term treatment of RA, with common side effects of skin, GI tract, and central nervous system problems. Patients on this medication require routine consultation with an ophthalmologist because this drug particularly affect eyes at higher doses (Silva et al., 2013). DMARDs can also reduce the risk of developing lymphoma associated with RA (Smolen et al., 2010).

1.7.2 Biological DMARDs

The marketed biologics or biological DMARDs (bDMARDs) include two IL-6 receptor targeting drugs, five TNF-targeting drugs, one selective T cell co-stimulatory modulator and one B cell antigen CD20-targeting antibody (Table 1.2). They are considered highly effective and safe drugs when used in combination with MTX for the treatment of RA refractory to conventional DMARDs (Smolen et al., 2020).

Some TNF-targeting drugs have been demonstrated to show high therapeutic effects in MTX-naive RA patients when administered in combination with MTX. Ten-year follow up studies have shown the effectiveness of Etanercept and adalimumab (bDMARDs) in retarding the joint damage progression with no major safety concerns regarding the long term use of these drugs (Keystone et al., 2014; Weinblatt et al., 2011). Monotherapy with sarilumab, an IL-6 receptor targeting drug, has been shown to be as effective as adalimumab monotherapy (anti -TNF) for MTX-refractory RA (Burmester et al., 2017).

On the other hand, biologics which target IL-17 or IL-12/IL-23 have failed to show efficacy in the treatment of RA. In addition, bDMARDs including mavrilimumab, an anti-GM-CSF antibody and IL-20, which target cytokines did not show superiority over TNF-targeting drugs (Senolt et al., 2015; Weinblatt et al., 2018). However, a different anti- GM-CSF antibody otilimab was observed to reduce disease activity scores and pain in addition to improvement in physical function in combination with MTX. These findings supported further investigation on the clinical development of otilimab in RA (Buckley, Simón-Campos et al. 2020). Recently, two phase III, double-blind randomised controlled trials showed that Otilimab has limited efficacy over the approved JAK inhibitor, tofacitinib (Xeljanz®) (Fleischmann, van der Heijde et al.

2023) and the anti-IL6 receptor antibody bDMARD, sarilumab (Kevzara®) (Taylor, Weinblatt et al. 2023).

Table 1.2: Disease modifying anti-rheumatic drugs (DMARDs) and targets.

Synthetic DMARDs	**Biological DMARDs**
Conventional synthetic DMARDs	**Biological originator DMARDs**
Unknown target: methotrexate, sulfasalazine, chloroquine, hydroxychloroquine**,** and gold salts *Known target*: dihydroorotate-dehydrogenase for leflunomide	• Tumour necrosis factor: adalimumab, certolizumab, etanercept, golimumab and infliximab • IL 6 receptor: tocilizumab and sarilumab • IL 6[a]: clazakizumab, olokizumab and sirukumab • CD80 and CD86 (involved in T cell co stimulation): abatacept • CD20 (expressed by B cells): rituximab
Targeted synthetic DMARDs	
• Janus kinase 1 (JAK1): filgotinib • Janus kinase 1 (JAK1) and JAK2: baricitinib • JAK1, JAK2 and JAK3: tofacitinib, Peficitinib, upadacitinib	

Table 1.2: DMARD nomenclature (Smolen et al., 2014). [a]Not yet approved or not further pursued (sirukumab). CD, cluster of differentiation.

Furthermore, combination drugs have been developed consisting of bispecific antibodies that are formed artificially on combinations of an Fc fragment and two Fab fragments and are capable of simultaneously recognising two or more types of antigens. ABT- 122, a bispecific antibody against IL-17 and TNF, did not show equivalent or superior efficacy to anti-TNF antibodies in MTX-refractory RA (Genovese et al., 2018). Another bispecific antibody Rozibafusp (AMG 570), a bispecific inhibitor of B Cell activating factor and inducible T cell co-stimulator ligand, has completed phase Ib clinical trial in RA (Abuqayyas et al., 2022).

1.7.3 Targeted synthetic DMARDs

Targeted synthetic DMARDs are orally administered compounds which have gathered increasing attention due to their effectiveness in RA treatment. These low molecular weight compounds are known as Janus kinase (JAK) inhibitors because of their mechanism of blocking Janus kinases, enzymes important in cytokine production within cells (O'Shea et al., 2013; Y. Tanaka, 2019; Y. Tanaka et al., 2012).

In 2012, tofacitinib was the first approved JAK inhibitor for the treatment of RA (Traynor, 2012). At present, baricitinib (Mayence & Vanden Eynde, 2019), peficitinib (Markham & Keam, 2019), upadacitinib (Duggan & Keam, 2019), and filgotinib (Dhillon & Keam, 2020) have been approved for the treatment of moderate to severe RA in USA, EU, and UK but most of these drugs are not considered to be cost-effective for UK requirements.

Phase III international clinical trials have demonstrated the effects of JAK inhibitors as more rapid and robust in MTX-naive RA patients, as well as in patients with insufficient responses to conventional synthetic DMARDs (csDMARDs) (MTX) or bDMARDs (TNF-targeting drugs) (Combe et al., 2021; Fleischmann et al., 2019; Nash et al., 2021; Y. Tanaka et al., 2019; P. C. Taylor et al., 2017; Désirée Van Der Heijde et al., 2013). Baricitinib and filgotinib are significantly more effective than adalimumab (Combe et al., 2021; P. C. Taylor et al., 2017), while upadacitinib was found more effective than abatacept and adalimumab (Fleischmann et al., 2019; Rubbert-Roth et al., 2020). Furthermore, preclinical studies *in vitro* demonstrated an osteoprotective effect of JAK inhibitors such as baricitinib, which increases mineralization by significantly increasing osteoblast function *in vitro* (Adam et al., 2020).

The short and long-term use of JAK inhibitors showed almost comparable efficacy to that of bDMARDs (Cohen et al., 2021; Conaghan et al., 2021; Nash et al., 2021). On the other hand, the incidence rates of CVD, infections, malignancies, and thrombosis remain constant over time for tofacitinib (Cohen et al., 2020). Opportunistic infection rates are slightly higher for JAK inhibitors, except for filgotinib (Nash et al., 2021; Y. Tanaka et al., 2022). Post-hoc investigation of the Phase IIIb/4 study (A3921133-Phase IIIb/4 randomized safety endpoint of Tofacitinib) was conducted by the

European Medicines Agency in order to review all JAK inhibitors recommended for inflammatory diseases. The higher risks for tofacitinib compared to TNF-α inhibitors, including major cardiovascular events, risks of malignancy and serious infection, are now considered to apply to all JAK inhibitors approved for chronic inflammatory disorders (DrugSafetyUpdate, 2023).

Thus, it is very important to conduct risk assessments for other JAK inhibitors. JAK inhibitors should be prescribed with careful consideration with adequate screening and monitoring for the patients of 65 years age or older, current, or past history of smoking, having risk factors for CVD, thrombosis, infection, malignancies. In addition lower dose should be considered in such patents where applicable (DrugSafetyUpdate, 2023).

1.7.4 Surgery

Surgery is the last option for the treatment at end stage RA after the failure of all nonsurgical approaches. In the 1990s, joint surgery reached a peak in California, with decreased rates observed in RA patients of 40 - 59 years of age in 2010, whereas increased rates of surgery in patients older than 60 years (Louie & Ward, 2010). In UK, the most recent analysis shows the overall 10 year incidence rates of for total knee replacement and total hip replacement are 7.0% and 5.2%, respectively (Hawley et al., 2020). This is nearly double than the previously reported incident rate in the general population in the UK (Culliford et al., 2012).

There are various different types of surgery such as tenosynovectomy (K. C. Chung & Pushman, 2011), radiosynovectomy (Knut, 2015), osteotomy (Puddu et al., 2010), joint fusion (Brooks & Hariharan, 2013) and the need of surgical treatment depends on the need of patient. Lastly, a total joint replacement (TJR) is the procedure to remove damaged joint and replace it with a plastic, metallic, or ceramic prosthesis. This can be done in the ankle, knee, hip, wrist, elbow, and shoulder (Pajarinen et al., 2014). Moreover, recent studies showed an excellent survivorship in patients with total knee replacement (TKR) (Cieremans et al., 2023; Shah et al., 2022).

1.7.5 Approaches for ‘difficult-to-treat’ RA

Regardless of numerous molecular target drugs available in market, multiple drug resistance still remains an important challenge in the treatment of RA. EULAR defines

difficult-to-treat RA on three criteria: (i) resistance to ≥2 bDMARDs or targeted synthetic DMARDs (tsDMARDs) with different mechanisms of action in RA patients who failed to respond on treatment with csDMARD; (ii) the presence of any of the following: (a) moderate disease activity or greater, (b) clinical signs and symptoms of active disease, (c) inability to taper glucocorticoids, (d) RA symptoms affecting the quality of life; and (iii) difficulty in the management of RA symptoms by rheumatologist and/or patient (G. Nagy et al., 2021). Based on the number of previously failed bDMARDs, the available bDMARDs are increasingly less effective with an increased refractory rate for bDMARDs in patients with difficult-to-treat RA. However, the JAK inhibitors such as filgotinib and upadacitinib, regardless of prior medications, may remain therapeutically effective (Genovese et al., 2018) and safe in difficult-to-treat RA patients (Burmester et al., 2023; Cohen et al., 2021; Winthrop et al., 2022). Thus, these inhibitors may provide an effective therapeutic treatment for RA if they are found effective and safe in actual clinical practice.

1.7.6 Development of new treatments for inflammatory arthritis

There is still a need to discover new therapeutic targets as well as drugs for the treatment of difficult-to-treat RA despite various already discovered molecular targeted drugs.

Despite many reviews suggesting anti-VEGF therapy as a possible treatment in OA and RA (Balogh et al., 2019; Hamilton et al., 2016; Kovacs et al., 2019; Le & Kwon, 2021; Moretti et al., 2022; Vadala et al., 2018), no VEGFR blockers, or anti-VEGF-A antibodies are in clinical trial or approved for RA or OA treatment. When used systemically, the most frequent and problematic adverse effect of VEGF-A blockade is hypertension, but other issues such as renal damage (Hayman et al., 2012; Mourad & Levy, 2011; X. Zhu et al., 2009; X. Zhu et al., 2007), and endocrine effects including adrenal insufficiency, hypothyroidism, and altered insulin sensitivity have also been identified (Cao, 2014; Y. Zhang et al., 2016).

The most recently approved new drugs for IA are the JAK inhibitors baricitinib, tofacitinib, and upadacitinib (as mentioned above in section 1.7.4) (Roskoski Jr, 2022).

Potential new drugs such as Olokizumab (humanized anti-IL-6 IgG4κ antibody) and Ozoralizumab (anti-TNF multivalent nanobody) (Ishiwatari-Ogata et al., 2022) are currently in Phase III and Phase II/III clinical trials, respectively. Co-administration of Olokizumab with MTX proved more effective than MTX alone with no unexpected safety findings, in RA patients who failed to respond to MTX and anti-TNF-α to attain low disease activity, which is the main therapeutic goal in these patients (Feist et al., 2022; Nasonov et al., 2022; Smolen et al., 2022). Similarly, administration of ozoralizumab with MTX in active RA significantly reduced signs and symptoms with no new safety indications and acceptable tolerability compared to other anti-TNF antibodies such as certolizumab, golimumab and adalimumab (Takeuchi et al., 2022).

In addition, there are other drugs currently in Phase I or II clinical trials for RA treatment (briefly discussed below) such as rozibafusp alfa (Abuqayyas et al., 2022), R-2487 (RISETherapeutics, 2023), novel CBD/hydroxychloroquine formulation IHL-675A (Incannex, 2023), peresolimab (Tuttle et al., 2023), and 2-HOBA (2-Hydroxybenzylamine acetate) (Rathmacher et al., 2023).

Rozibafusp alfa (NCT03156023) is a first-in-class bispecific antibody–peptide fusion, designed to inhibit simultaneously T cell activation and B cell maturation as well as aberrant communication between these cells which are associated with autoimmune disorders. A Phase Ib study showed good tolerability of ascending doses of rozibafusp alfa and improved the disease activity, especially at higher doses in RA active patients with no safety issues. These findings also provided the information regarding the dose selection and design of rozibafusp alfa in active SLE (Systemic lupus erythematosus) patient (Abuqayyas et al., 2022) which is currently in phase II clinical development (Bubb, 2024; Garces et al., 2023).

R-2487 (NCT05961592) is an investigational new drug from Rise therapeutics which is currently in Phase I clinical trial. It a synthetic targeted immune therapy to reset regulatory T cell deficiencies and immune balance to reduce inflammatory cytokines in patients with autoimmune disorders including RA. R-2487 has been proposed to "reverse disease development and progression by targeting the root cause of RA" (RISETherapeutics, 2023).

Incannex has started Phase II studies of IHL-675A, after a safe and well tolerated Phase I trial (ACTRN12622000289718). IHL-675A is a fixed dose combination of cannabidiol (CBD) and hydroxychloroquine (HCQ) for the treatment of pain and function in RA patients (Incannex, 2023).

Peresolimab is a monoclonal humanized IgG1 antibody that is designed to activate the endogenous programmed cell death protein 1 (PD1). PD1 is the immune checkpoint inhibitor and is involved in the inhibition of immune responses and promoting self-tolerance by stopping T cells from attacking the healthy cells. Hence, PD1 stimulation is proposed to be a new therapeutic strategy for autoimmune diseases. Phase IIa of this therapy demonstrated effectiveness in treating people with RA who had an inadequate response to prior DMARDs treatment (Tuttle et al., 2023).

2-HOBA is a natural product found in Himalayan Tartary buckwheat currently in Phase II trials to target the immunogenic, pro-inflammatory and proatherogenic effects of isolevuglandins (isoLGs) in RA patients (Rathmacher et al., 2023). Very recently a bi-specific antibody against VEGF and TNFα has shown efficacy in reducing inflammation and arthritis severity in an animal model of RA (N. Zhang et al., 2024).

Recent advances in possible pharmacological treatments for OA include a CLK/DYRK/Wnt inhibitor lorecivivint (CLK, CDC2-like kinases; DYRK, dual-specificity tyrosine-regulated kinases; Wnt, "Wingless-related integration site" family of growth factors) which reported good patient-reported outcomes in Phase 2b trial (Y Yazici et al., 2021). The Phase III trial was terminated by the Sponsor Biosplice Therapeutics in 2022 (NCT04931667) (Inc Biosplice Therapeutics, 2022). Recently, the phase III study was resumed and the results demonstrated the efficacy of multiple injections of lorecivivint in delaying structural progression and provision of symptomatic benefit in OA (Inc Biosplice Therapeutics, 2023). Based on this, a recent review has proposed lorecivivint as safe, reliable, and effective potential treatment for OA (Kou et al., 2023).

1.8 Rodent models of arthritis

Animal models of RA can be broadly classified into induced and spontaneous models. These models may be monoarthritic or polyarthritic models which affect one joint or

two/more joints, respectively. Polyarthritis is often a systemic response to a stimulus and is more severe than monoarthritis. Additionally, models of RA can mimic the disease using an autoimmune mechanism to induce inflammation, or the inflammation and pain can be modelled using a direct inflammatory stimulus in one or more joints is induced, without stimulating an autoimmune response. The latter models are useful for study of inflammatory and pain responses, but obviously cannot be used to infer anything about the mechanisms of disease induction or progression.

Induced models of autoimmune-induced models in mice include antigen-induced arthritis (AIA), collagen-induced arthritis (CIA), and collagen antibody-induced arthritis (CAIA). Similar models are also used in rats (Figure 1.7). Genetic (induced or inbred) models include HLA class II transgenic mice, SKG, IL-1RA$^{-/-}$, K/BxN, F759, and TNFα mice (Figure 1.7). These models can be useful to study different aspects of inflammatory arthritis such as breach of immune tolerance or T cell dependent disease. Most models have multiple joint involvement and may show some of the systemic effects of autoimmune-induced inflammatory responses (Benson et al., 2018).

As the main purpose of the original studies that supplied the tissues used in this thesis was to study inflammatory pain and histological joint effects, and because in the UK there is an expectation to use animal models that have the minimum impact on animal welfare while still modelling the features under study, we used a well-established, refined inflammatory monoarthritis induced by peri-articular subcutaneous injection of Complete Freund's Adjuvant (CFA). Inflammatory arthritis induced by CFA has been shown to replicate many features of RA joint inflammation, including synovitis, pannus formation and bone remodelling (Gauldie et al., 2004; Larson et al., 1986; Micheli et al., 2019; Paquet et al., 2010; Silva Rodrigues et al., 2018). Figure 1.8 shows the similarities and differences between the CFA-induced animal model and RA.

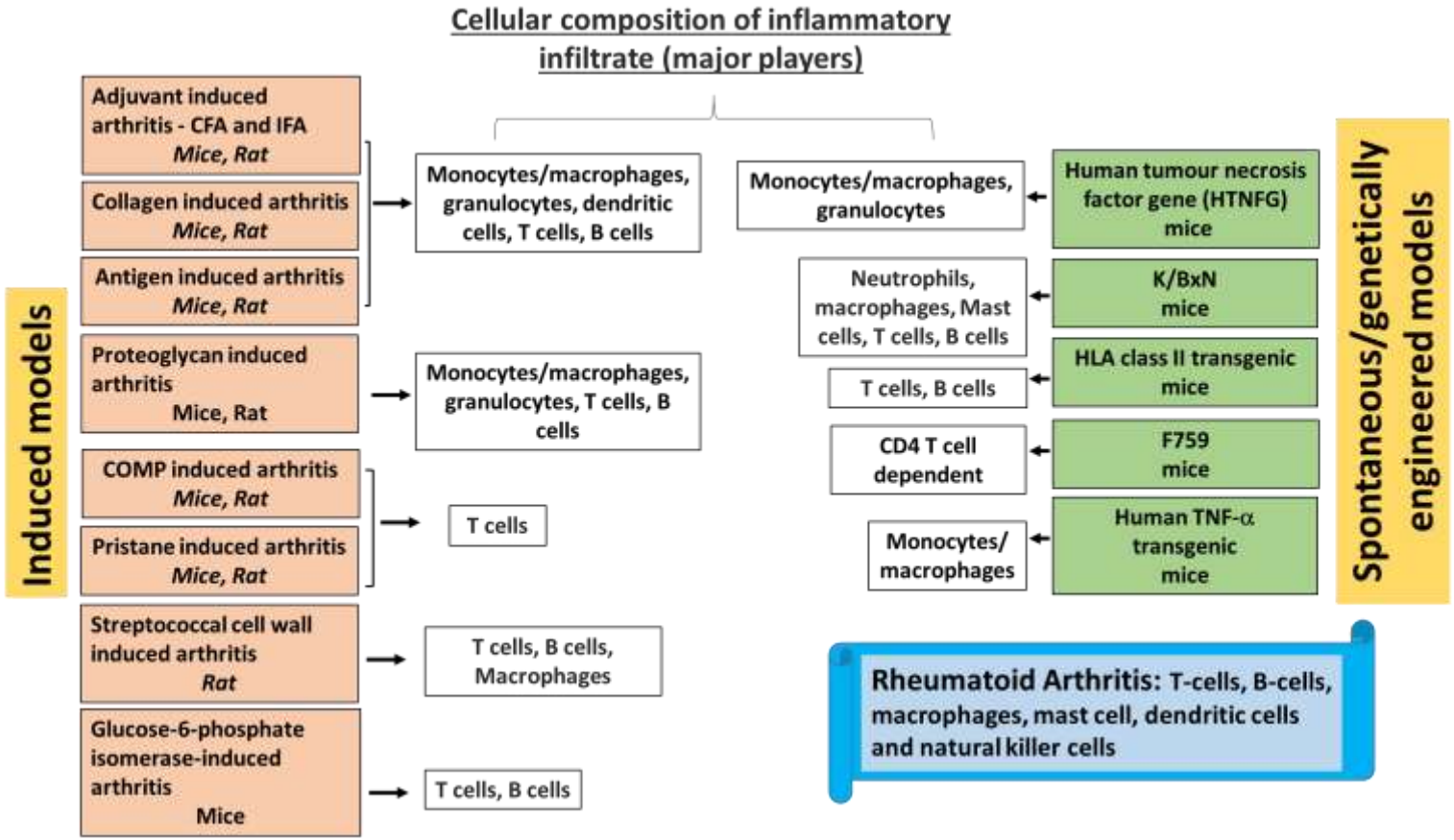

Figure 1.7: Experimental models of rheumatoid arthritis. Similarities between animal models and RA in terms of key inflammatory cells in the induction of IA in animals (Chidomere et al., 2023; S. Wang et al., 2023; L. Ye et al., 2021). CFA: Complete Freund's adjuvant; IFA: In complete Freund's adjuvant; HLA: human leukocyte antigens; CD4: cluster of differentiation 4; TNF: Tumour necrosis factor.

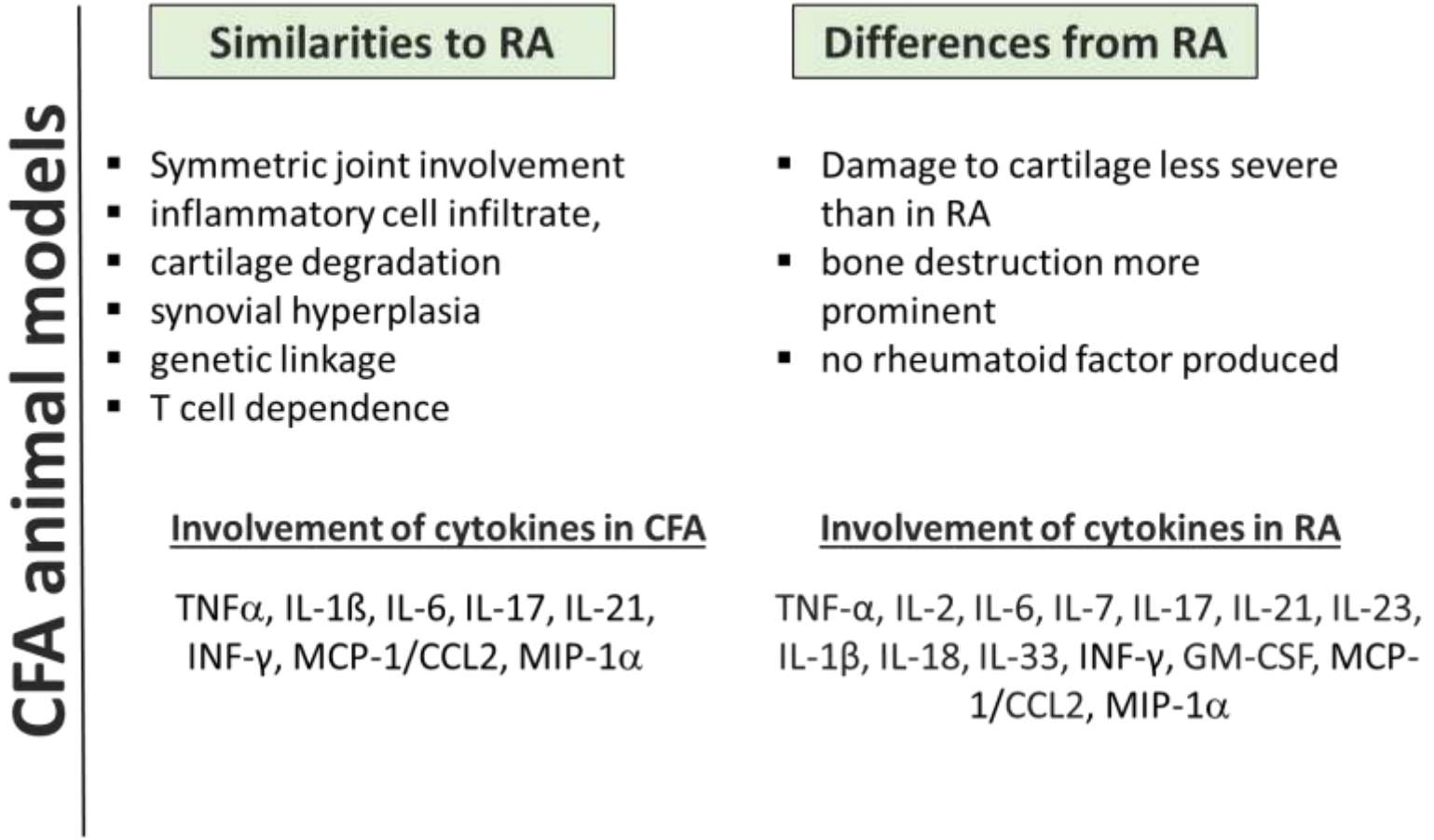

Figure 1.8: Similarities and differences between CFA animal model and rheumatoid arthritis and key cytokines in the pathogenesis of CFA- induced IA and RA (Bevaart et al., 2010; Kondo et al., 2021). TNF-α: Tumour necrosis factor: IL: Interleukin, INF-γ: Interferon gamma, MCP-1: Monocyte chemoattractant protein-1 - also known as Chemokine (CC-motif) ligand 2 (CCL2); MIP-1α; Macrophage inflammatory protein 1α; GM-CSF: granulocyte macrophage colony-stimulating factor.

1.9 Vascular endothelial growth factors

Before introducing the role of VEGF-A in pathogenesis of RA and importance of its inhibition, I will discuss the multiple VEGFs, their functions, receptors and signalling in biological systems.

VEGF belongs to a family of homodimeric proteins comprising of at least 6 members: VEGF-A, VEGF-B, VEGF-C, VEGF-D, VEGF-E, and Placental growth factor (PlGF) (discussed below) (Dakowicz et al., 2022).

1.9.1 VEGF-A

Vascular endothelial growth factor (VEGF-A, a.k.a VEGF) was originally defined as VPF (vascular permeability factor), first isolated by Senger et al. in 1983 (Senger et al., 1983). VEGF-A consists of a family of homodimeric 46–48 kD glycoproteins composed of two monomers of between 111 and 206 amino acids in length, generated from a single VEGF-A gene by alternative splicing (Figure 1.9) (see section 1.11.4 for more details). VEGF-A splice variants can bind to both VEGFR1 and 2 (Figure 1.10). VEGF-A is best known as a key mediator of angiogenesis (Ferrara, 1999; T. Matsumoto & Claesson-Welsh, 2001; Mentlein & Held-Feindt, 2003; Neufeld et al., 1999; Robinson & Stringer, 2001; R. O. Smith et al., 2020) and vascular permeability, and is highly expressed during embryogenesis (Carmeliet et al., 1996; Ferrara et al., 1996; Han et al., 2018). In adults VEGF-A is expressed in conditions of physiological angiogenesis such as during the menstrual cycle, wound healing, and tissue remodelling (Chintalgattu et al., 2003; Ferrara et al., 1996; Gerber et al., 1999; Reichardt & Tomaselli, 1991).

VEGF-A usually functions as a homodimer formed by two anti-parallel VEGF-A monomers which bind specifically to VEGFR1 and VEGFR2 on endothelial and other cell types. VEGF-A also has binding affinity for the co-receptors Neuropilin-1 **(**NP-1) and Neuropilin-2 (NP-2) (Hoeben et al., 2004).

VEGF-A is produced by multiple cell types such as macrophages (McLaren et al., 1996), fibroblasts (Pertovaara et al., 1994), endothelial cells (Namiki et al., 1995) , T cells (M. R. Freeman et al., 1995), and neutrophils (Taichman et al., 1997). VEGF-A is known as the most abundant VEGF that acts on endothelial cells and it plays key roles in endothelial cell proliferation, migration, and activation, as well as in promotion of vascular fenestration and increased permeability, and the induction of various genes involved in tissue remodelling. VEGF receptors (VEGFR) are expressed by many cell types including monocytes and specialized macrophages (Forstreuter et al., 2002), osteoblasts (Mayr-Wohlfart et al., 2002), and osteoarthritic, but not resting, chondrocytes (Enomoto et al., 2003; Pfander et al., 2001; Thomas Pufe et al., 2001). The effects of VEGF-A on monocytes, endothelial cells and osteoblasts have been reported by numerous studies (Forstreuter et al., 2002; Mayr-Wohlfart et al., 2002), but less is known about VEGF-A and VEGFR expression and responses in chondrocytes.

VEGF-A expression is regulated by various factors including growth factors, oxygen tension, and cytokines (Neufeld et al., 1999; Semenza, 2000, 2000). Hypoxia is a potent stimulus for increased VEGF-A expression (Sabi et al., 2022). VEGF-A is also found in malignant and inflammatory diseases (Le & Kwon, 2021). The understanding of VEGF-A has led to the development of new treatments in some diseases for instance cancer or retinopathy (Exonate, 2023; Hang et al., 2023; Moon et al., 2023; S. A. Patel et al., 2023). Currently, many drugs targeting VEGF-A pathways have been developed. These have limited clinical effectiveness in tumours, although they can prolong survival in most cancer patients (K. He et al., 2012; T. Qiu et al., 2018), but are highly effective in treatment of retinal diseases that feature angiogenesis, such as age-related macular degeneration (Enríquez-Fuentes et al., 2024). VEGF-A has been extensively investigated for anti-cancer therapeutics because it is produced by 60% of tumours (Bowler & Oltean, 2019). Bevacizumab was the first FDA approved humanized form of anti-VEGF antibody indicated in metastatic colon cancer (Ferrara et al., 2004). Though bevacizumab is usually well tolerated, it has some serious although infrequent toxic effects such as bleeding, hypertension, and arterial thromboembolism (Ferrara et al., 2004; Sandler et al., 2006; J. C. Yang et al., 2003). Ranibizumab, a humanised recombinant antibody fragment was effective after two

years treatment of age-related intraocular macular degeneration (Rosenfeld et al., 2006). Moreover, ramucirumab, a VEGFR2 inhibitor, Ziv-aflibercept, a combined VEGF-A, VEGF-B and PlGF inhibitor, and multiple VEGFR tyrosine kinase inhibitors (TKI's) are indicated for treating various cancers in combination with other therapies (Zirlik & Duyster, 2018). Faricimab, a joint VEGF-A and Ang-2 inhibitor, was effective as well as safe in phase II diabetic macular oedema trials (Nicolò et al., 2021). Despite the success of many anti-VEGF-A drugs, the major concerns about anti-VEGF-A therapies are the adverse effects particularly on systemic blood pressure. Adverse effects are significantly reduced by local administration due to the lower dose required, and the lack of exposure to other tissues/organs compared to systemic administration. Therefore, anti-VEGF therapy is a crucial suggestion for several disease studies such as arthritis (Le & Kwon, 2021). To date, no clinical trial data have been published on anti-VEGF therapies in arthritis.

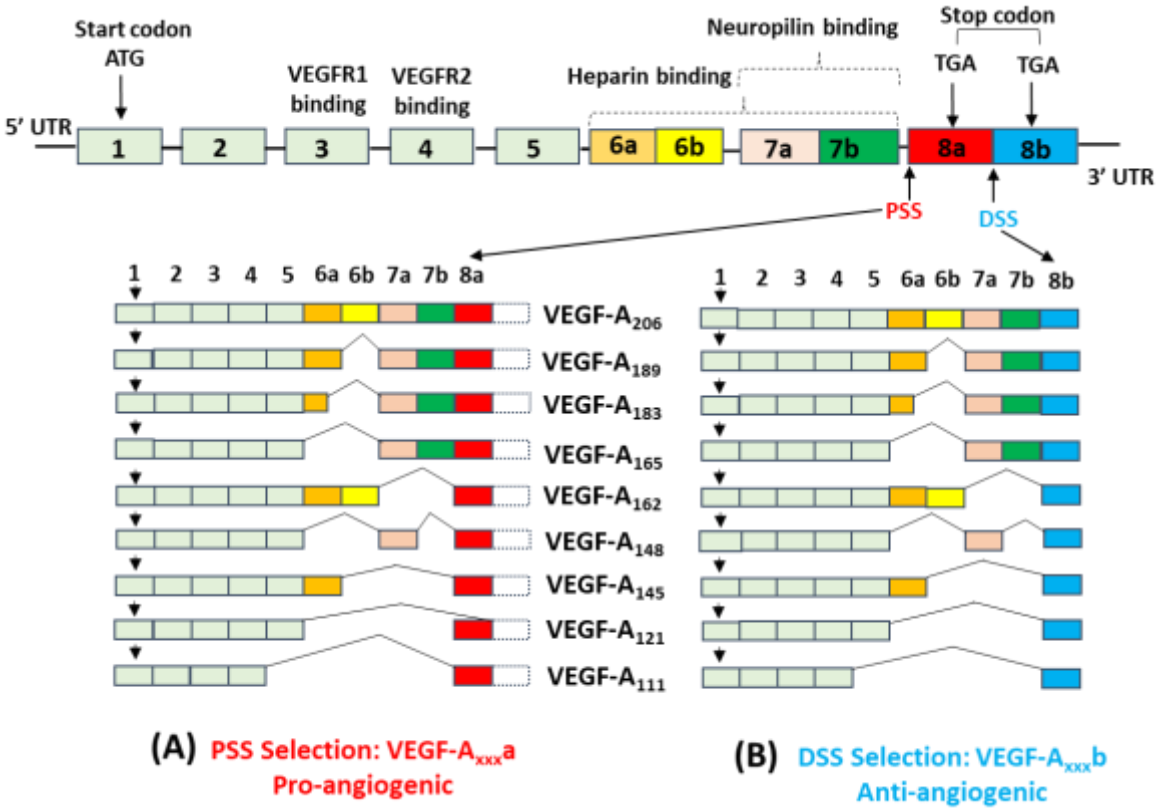

Figure 1.9: Splice variants of vascular endothelial growth factor A (VEGF-A). The VEGF-A pre-mRNA consists of eight exons, the arrow in exon 1 indicates the translational start. Inclusion or exclusion of exons gives rise to several isoforms of different lengths of amino acids. (A) Pro-angiogenic VEGF-A_{xxx}a isoforms are produced by selection of the exon 8 proximal splice site (B) whereas distal splice site at the exon 8 results in the formation of anti-angiogenic VEGF-A_{xxx}b family with the same number of amino acids but differ only in the C-terminus sequence. This family is functionally different (anti-angiogenic) from the VEGF-A_{xxx}a (angiogenic) isoform family. PSS: proximal splice site; DSS: distal splice site; UTR: untranslated region. Figure adapted from (Donaldson & Beazley-Long, 2016; Stevens & Oltean, 2019; White & Bix, 2023).

1.9.2 VEGF-B

Initial studies focussed on the role of VEGF-B in angiogenesis because VEGF-B shares 47% of its amino acid sequence with VEGF-A (Olofsson et al., 1996) but VEGF-B does not stimulate angiogenesis (Karpanen et al., 2008; Mould et al., 2005; F. Zhang et al., 2009).

Like VEGF-A, VEGF-B is alternatively spliced to generate two isoforms, VEGF-B_{167} and VEGF-B_{186}. These only bind to VEGFR1. VEGFR1 activation by VEGF-B has negligible effect in inducing blood vessel growth due to poor signalling (Grünewald et al., 2010; Otrock et al., 2007). Though VEGF-B was initially proposed to be capable of inducing endothelial cell growth, this was eventually attributed to heterodimer formation of VEGF-A and VEGF-B, and not a direct VEGF-B-mediated function (Bry et al., 2014). There is, however, evidence for an indirect role of VEGF-B in angiogenesis as high levels of VEGF-B can displace VEGF-A from VEGFR1, allowing greater VEGF-A binding to VEGFR2 promoting angiogenesis initiation (Kivelä et al., 2014). Despite a relatively poor understanding of the role of VEGF-B in angiogenesis, mice lacking a functional VEGF-B gene have impaired angiogenic responses, and smaller hearts as well as reduced capillary density (Abraham et al., 2000). Hence, VEGF-B is considered important for blood vessel survival (Guaiquil et al., 2014; X. Li et al., 2009; Yue et al., 2014; F. Zhang et al., 2009).

1.9.3 VEGF-C and VEGF-D

Both VEGF-C and D specifically bind to VEGFR3 expressed on lymphatic endothelial cells and stimulate lymphangiogenesis. VEGF-C and D have a much lower affinity for VEGFR2 than VEGF-A but can also activate angiogenesis to some extent (Alitalo & Carmeliet, 2002; Baldwin et al., 2005; Iyer & Acharya, 2011). Mature VEGF-C and VEGF-D are produced via proteolytic processing and unlike VEGF-A and VEGF-B there are no known VEGF-C and VEGF-D splice variants (Bui et al., 2016; Stacker et al., 1999).

1.9.4 Other VEGFs

Placental growth factor (PIGF) is principally found in placental tissues. Four isoforms, PIGF-1 – 4, are produced by alternative RNA splicing. The isoforms bind to VEGFR1, but not VEGFR2 and VEGFR3 (Figure 1.10) (Autiero et al., 2003; Otrock et al., 2007). Impaired angiogenesis and wound healing as well as inflammation are observed with PIGF knockout (Autiero et al., 2003; Carmeliet et al., 2001). On the other hand, upregulation of PIGF is related with pathological angiogenesis (Odorisio et al., 2002).

VEGF-E and VEGF-F gene are found in Para poxvirus, which infects goats, sheep and sometimes humans, and in the venom of some vipers (Trimereserus flavoviridis), respectively but are absent in humans. The VEGF-E amino acid sequence is <25% (Cebe-Suarez et al., 2008) and the VEGF-F ~50% identical to VEGF-A (Masabumi Shibuya, 2011). VEGF-E selectively binds to VEGFR2 not VEGFR1 to promote angiogenesis while VEGF-F binds tightly to VEGFR1 and weakly to VEGFR2 and results in vascular permeability but very weak cell proliferation (H. Takahashi et al., 2004).

1.9.5 VEGF receptors

1.9.5.1 VEGFR1

Human VEGFR1 is a ~180 kDa glycoprotein which comprises of 1312 amino acids. VEGFR1 expression is found in endothelial, epithelial, and immune cells and neural tissues. All isoforms of VEGF-A, VEGF-B and PIGF bind to VEGFR1 (Olofsson et al., 1998; J. E. Park et al., 1994) (Figure 1.10). The binding affinity of the most studied VEGF-A isoform VEGF-A_{165} to VEGFR1 is ~1 picomolar (pM) (Kd), which is higher than its affinity at VEGFR2 (10mM) (Mamer et al., 2020), whereas PIGF binds to VEGFR1 with~170 pM affinity (Kd) (Sawano et al., 1996; Shaik et al., 2020) (Figure 1.10).

Depending on alternative splicing, VEGFR1 is expressed as both soluble and membrane-bound forms. The membranous-bound and soluble forms of VEGFR1 can function as decoy receptors of VEGF-A, as shown by a study in which decreased

VEGFR1 expression in endothelial cells from infantile haemangioma tumours resulted in constitutive VEGFR2 activation and abnormal angiogenesis (Ferrara et al., 2003; Jinnin et al., 2008). Thus, VEGF-A binding to VEGFR1 can act as a negative regulator for VEGFR2 by reducing the local concentrations of VEGF-A leading to reduced VEGF-A binding to VEGFR2 (H. Takahashi & Shibuya, 2005). In contrast, other studies show that VEGFR1 can transduce mitogenic signals in a similar way to VEGFR2 in certain circumstances (Maru et al., 1998). For example, monocyte migration in response to VEGF- A depends on the tyrosine kinase domain of VEGFR1 rather than involvement of VEGFR2 (Barleon et al., 1996; Weddell et al., 2017).

1.9.5.2 VEGFR2

Human VEGFR2 is a ~200–230 kDa glycoprotein which contains 1337 amino acids. VEGFR2 has high binding affinity to VEGF-A, VEGF-C and VEGF-D. VEGFR2 is the main VEGF signalling receptor and is abundantly expressed in vascular and lymphatic endothelial cells. A soluble form of VEGFR2 (sVEGFR2) has been recognised in human plasma as well as in mouse (Ebos et al., 2004). The distinct function of sVEGFR2 is still unclear, even though higher plasma levels of sVEGFR2 were observed in association with the risk of breast cancer (H. Harris et al., 2016).

VEGF-A homodimers bind to IgD2 and IgD3 of VEGFR2 (Figure 1.10), which induces receptor dimerization, stable binding of neuropilin-1, trans-autophosphorylation of tyrosine residues (Tyr801, Try951, Try1175, and Try1214) and receptor activation, leading to the intracellular signalling cascade initiation (X. Wang et al., 2020). This results in stimulation of angiogenesis and vasculogenesis (Ferrara et al., 2003; X. Wang et al., 2020). VEGFR2 is the key receptor involved in the increased vessel permeability in response to VEGF-A (S. Koch & Claesson-Welsh, 2012; R. O. Smith et al., 2020) and acts as the major signal transducer for stimulation of angiogenesis through PLCγ-PKC-eNOS-NO, PLCγ-PKC-MAPK, SHB-FAK-paxillin, TSAd-Src-PI3K-Akt, NCK-p38-MAPKAPK2/3 and SHB-PI3K-Akt pathways (Masabumi Shibuya, 2011; Wong & Jin, 2005) (Figure 1.10).

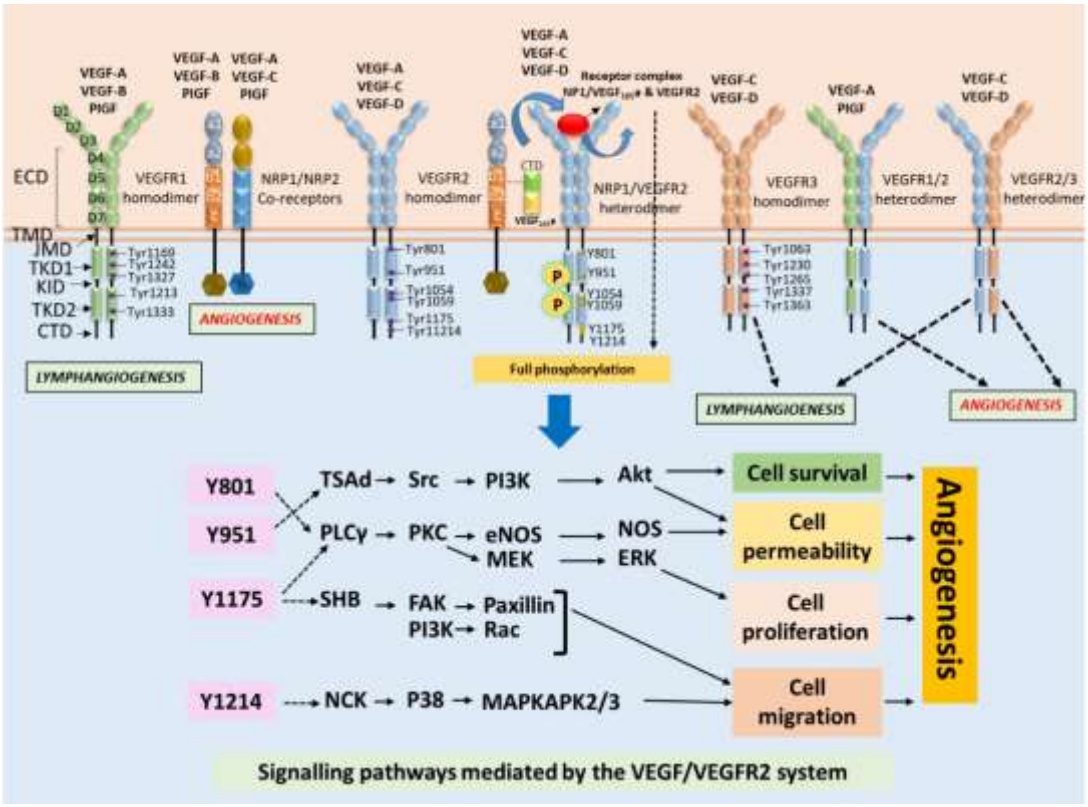

Figure 1.10: VEGF and its receptors with respective functions defined in endothelial cells. **Adapted from (Tota et al., 2023). All VEGFs bind to three tyrosine kinases receptors (RTKs); VEGFR1, VEGFR2, and VEGFR3. VEGF receptors have extracellular domain (ECD) including seven Ig-like subdomains (IgD1~7), transmembrane domain (TMD), and a cytoplasmic domain (CD). CD domain is further divided into two domains such as juxtamembrane domain (JMD) and a catalytic tyrosine kinas domain (TKD). TKD includes ATP binding domain (TKD1), phosphotransferase domain (TKD2) and kinase insert domain (KID), and a flexible C-terminal domain (CTD), and various functional sites. Upon ligand binding, VEGF receptors form homodimer and heterodimers. VEGFR1 form heterodimers with VEGFR2, whereas VEGFR3 forms a heterodimer with VEGFR2. VEGF-A binds to VEGFR1/2 homodimer and heterodimers; VEGF-B recognise VEGFR1 homodimer. VEGF-C and VEGF-D recognise VEGFR2, VEGFR3 homodimers and VEGFR2/3 heterodimer, whereas placental growth factor (PlGF) has binding affinity for VEGFR1 homodimers and VEGFR1/2 heterodimers. VEGFR1 and VEGFR2 play a key role in angiogenesis, while VEGFR3 is primarily involved in lymphangiogenesis. NRP1 and NRP2 are coreceptor for VEGFs. NRP1 plays important role in angiogenesis by formation of heterodimers with VEGFR2. NRP1 has a large extracellular domain comprised of a1/a2, b1/2 subunits, and a 'c' domain, and a small cytosolic domain. The C-terminal domain of VEGF-A_{165} encoded by exons 7th and 8th (yellow and green oblongs, respectively) binds to the extracellular domain (b1) of NRP1. Concomitant binding of the similar VEGF-A_{165} domain (red ovals) to VEGFR-2 lead to the formation of a receptor complex of NRP1 with VEGF-A_{165} and VEGFR-2 which results in enhanced intracellular signalling, required for optimal angiogenesis. KID: kinase insert domain; TKD1: Tyrosine kinas domain 1; TKD2: Tyrosine kinase domain 2; CTD, carboxy-terminal domain; ERK: extracellular signal-regulated kinase, PCLγ: Endothelial phospholipase Cγ; PKC: Protein kinase C; TSAd: T cell specific adaptor; Src: Proto-oncogene tyrosine-protein kinase Src (sarcoma); MEK: Mitogen-activated protein kinase; SHB: SH2 domain–containing scaffold protein; FAK: Focal adhesion kinase; PI3K: Phosphoinositide 3-kinase, Akt/PKB: protein kinase; NCK: non-catalytic**

region of tyrosine kinase; P38: mitogen-activated protein kinase; MAPKAPKS: Mitogen-Activated Protein Kinase-Activated Protein Kinases.

1.9.5.2.1 Modulation of VEGFR1/VEGFR2 signalling

VEGF receptors upon binding to ligands results in phosphorylation of certain receptor tyrosine residues, and this facilitates downstream mitogenic, chemotactic and pro-survival signals (Figure 1.10) (X. Wang et al., 2020). Each of these receptors has the chance to combine factors which belongs to VEGF family due to different selectivity and affinity (Zajkowska et al., 2018). VEGF-A binding affinity towards VEGFR2 is ~100 - 400 pM (Kd) which is 10 - 100-fold lower affinity compared to VEGFR1 (Sawano et al., 1996). On the other hand, VEGFR1 has tyrosine kinase activity at least 10-fold less than VEGFR2 in endothelial cells; hence, it can be argued that VEGFR2 homodimers are responsible for the major signal transduction upon VEGF-A binding (Facemire et al., 2009; Lopez-Garcia et al., 2018).

1.9.5.2.2 VEGFR2 homodimerization and VEGFR1/R2 heterodimerization

Although VEGFR2 homodimers are involved in functional regulation, VEGFR1 and VEGFR2 heterodimer formation has been identified in cell-free systems (Kendall et al., 1996) and in endothelial cell lines (Autiero et al., 2003; Cudmore et al., 2012; K. Huang et al., 2001; Kanno et al., 2000; Neagoe et al., 2005; Sarkar et al., 2022). According to a computational model of VEGF receptor subunit dimerization, it is speculated that heterodimerization is inevitable in cells that express both VEGFR1 and VEGFR2 subunits (Mac Gabhann & Popel, 2007). Moreover, it has been revealed that overabundance of one VEGF receptor subunit would lead to minimal homodimerization of the less abundant receptor subunit (Mac Gabhann & Popel, 2007). On the endothelial cell surface, VEGFR1 is identified to be up to 10 fold less abundant than VEGFR2 (Imoukhuede & Popel, 2011; M. I. Lin & Sessa, 2006). This suggests that homodimerization of VEGFR1 in endothelial cells may be relatively rare with the majority of VEGFR1 in endothelial cells existing in heterodimeric complexes with VEGFR2 which predominantly modulates VEGF activity (Cudmore et al., 2012). Thus, VEGFR1/R2 heterodimers regulate angiogenesis and maintain endothelial cell homeostasis by negatively regulating pro-angiogenic and proliferative function mediated by VEGFR2/R2 homodimers (M. Cai et al., 2017; Cudmore et al., 2012). The

functional roles of VEGFR heterodimers in an in-vivo setting are currently difficult to predict due to the unknown signal transduction properties (Uemura et al., 2021).

It is possible for heterodimers to have both stimulatory and inhibitory effects, which depend on the circumstances. However, it's still not clear how important receptor heterodimers are compared to homodimers. Understanding the molecular interactions between various VEGFs and VEGFR1 and VEGFR2 homodimerization/heterodimerization is crucial for interpreting experimental manipulations and clinical observations. Additionally, it's important to keep in mind that differences may exist between humans and animal models in terms of isoform prevalence, heterodimers in the VEGF receptor family, and immune cell subpopulations (Uemura et al., 2021).

VEGFR1/2 activation and signalling depend on various factors, including the availability of VEGFR ligands, the specific binding of ligands to VEGFR1 or VEGFR2 (Koch and Claesson-Welsh 2012), and the binding competition of VEGF-A, VEGF-B, and PlGF for VEGFRs and ECM binding sites (Koch and Claesson-Welsh 2012). The formation of heterodimers of VEGFR subtypes also plays a crucial role in the activation and signalling of VEGFR1/2.

Neuropilin-1 is the main co-receptor for VEGFR2 and is also expressed in endothelial cells, being involved in the regulation of VEGFR2 dependent angiogenesis. NP-1 is fundamentally important for the full phosphorylation and activation of VEGFR2 particularly by VEGF-A_{xxx}a splice variants (Figure 1.10). NP-1 enhances $VEGF_{165}$a binding to VEGFR2 as well as increasing its signal transduction up to 6-fold (Soker et al., 1998). These splice variants result in VEGFR2 phosphorylation at key tyrosine residues, receptor dimerization and binding to NP-1, and different downstream signalling leads to various cellular fates such as proliferation via RAF/MEK/ERK (T. Takahashi et al., 1999) and PLCγ (T. Takahashi et al., 2001), cell migration (Abu-Ghazaleh et al., 2001) and vascular permeability (X. L. Chen et al., 2012; Holmqvist et al., 2004) through focal adhesion kinase (FAK) and cell survival through protein kinase B (AKT)/phosphatidylinositol-4,5-bisphosphate 3-kinase (PI3K) (Gerber et al., 1998).

1.9.5.3 VEGFR3

Human VEGFR3 contains 1363 residues which produces a mature ~195 kDa glycoprotein heterodimer. VEGFR3 binds to VEGF-C and VEGF-D in lymphatic endothelial cells with high affinity and plays a vital role in regulation of lymphangiogenesis (Joukov et al., 1996; Mäkinen et al., 2001).

VEGFR2/3 heterodimers have been associated with angiogenesis and modulation of angiogenic sprouting (Nilsson et al., 2010). However, formation of VEGFR1 and VEGFR3 heterodimer is unlikely. VEGFR3 also exists as a soluble form (sVEGFR3) (H. Harris et al., 2016) expressed in corneal endothelial cells and have binding affinity to both VEGF-C and VEGF-D (Figure 1.10). Hence, sVEGFR3 act as a decoy receptor for both ligands and lead to anti-lymphangiogenic properties via blocking VEGFR3 signal transduction (N. Singh et al., 2013).

1.9.6 Biological activities of VEGFR1 and VEGFR2

1.9.6.1 Endothelial cells

Endothelial cells express both VEGFR1 and VEGFR2. Both receptors upon VEGF-A binding facilitate endothelial cells survival and increase permeability (Hudson et al., 2014). Even though VEGF-A/VEGFR2 are thought to mediate vascular permeability (Olsson et al., 2006; Peach et al., 2018), there is also evidence showing the role of PlGF/VEGFR1 and VEGF-A/PlGF heterodimers in vascular permeability (Cudmore et al., 2012; Ziche et al., 1997). But cell proliferation and vascular permeability induced by PlGF/VEGFR1 is weaker than those of VEGF-A/VEGFR2 (S. Koch & Claesson-Welsh, 2012; Olsson et al., 2006; Sawano et al., 1996) and seems to contribute about one tenth of the total signal compared to VEGFR2 due to a significant difference in the level of tyrosine kinase activity of the two VEGFRs.

1.9.6.2 Synoviocytes

VEGF and its receptors (VEGFR1 and VEGFR2) are expressed in normal synovial cells but higher expression is found in both OA and RA synoviocytes (Dimitrios Amanitis, 2022; De Bandt et al., 2003; Fava et al., 1994; M. Ikeda et al., 2000; S. Ryu

et al., 2006). VEGFR2 is also abundantly expressed in the RA synovial tissues compared to OA, whereas VEGFR1 expression is found constitutively in both RA and OA synovial tissues (M. Ikeda et al., 2000; Nagashima et al., 1995; J.-l. Zhou et al., 2009) see section 1.12.3 for more details.

1.9.6.3 Chondrocytes

Adult human articular cartilage does not express VEGF-A/VEGFR under most physiological conditions, though VEGF-A/VEGFR have important roles in neonatal endochondral bone development (Carlevaro et al., 2000; Moskowitz, 2007). VEGF-A and VEGFR expression have been observed in cartilage from donors with OA and RA in several studies (Enomoto et al., 2003; Pfander et al., 2001; Thomas Pufe et al., 2001; Shakibaei et al., 2003; J. O. Smith et al., 2003; Tsuchida et al., 2014) (see section 1.12.4 for more details).

1.10 Methods of investigation of VEGFR2 function

1.10.1 Pharmacological tools – brief introduction

There are many VEGFR inhibitors/blockers of several classes available, including small molecules (e.g. sorafenib (VEGFR2 & VEGFR3), sunitinib (which acts at all VEGFRs, plus other targets), lenvatinib, vandetanib, pazopanib, axitinib, cabozantinib, regorafenib, apatinib) and also humanised antibodies against VEGF-A such as bevacizumab (Avastin®), all of which are in use for treatment of various cancers. VEGFR inhibitors usually act by binding to the VEGF-A binding site or blocking the receptor tyrosine kinase (RTK) ATP-binding site, thus blocking ligand binding, tyrosine phosphorylation and receptor activation.

1.10.2 Alternative methods of receptor inhibition– gene knockout

Gene knockout (KO) has made a significant impact in understanding gene function. KO cells and KO mice have been frequently used for the analysis of physiological roles of specific molecules in mammalian cells as well as to discover novel therapeutic interventions for human diseases. CRISPR/Cas9 (Gaj et al., 2013; Gupta & Musunuru,

2014) and short interference RNA (siRNA) (Crooke et al., 2018; Fire et al., 1998) are well known genome editing or silencing systems, that have high efficiency, relatively easy design and implementation, and good cost/time effectiveness; however, sometimes these knockdown systems which can lead to inconclusive results because they may not completely suppress target gene expression.

1.10.3 Germ-line VEGF-A knockout is problematic.

VEGF-A (Ferrara et al., 1996),VEGFR2 (Shalaby et al., 1995; Yin et al., 1998) and VEGFR1 (Fong et al., 1995) germ-line knockouts are all embryonically lethal. As a result, inducible and/or tissue specific knockout models have to be used in genetic studies of VEGF-A/VEGFR2 functions.

A conditional knockout (cKO) is a suitable approach to study genes that difficult to investigate by standard techniques (Gu et al., 1994). In addition, cKO has an advantage over conventional gene KO with the deletion of a gene within germ cells, where knockout in the whole organism may produce complicated results or embryonic lethality (Jian Zhang et al., 2012). The embryonic KO studies showed that VEGF-A has haploinsufficiency, as a single copy of the VEGF-A gene in heterozygote mice was embryonically lethal, causing multiple defects in vasculature formation resulting in circulatory system dysfunction (Carmeliet et al., 1996; Ferrara et al., 1996; Ferrara & Kerbel, 2005). VEGFR1 and VEGFR2 homozygous null mutant mice were also embryonically lethal causing death due to blood vessel disorganization and lack of vascular system development or haematopoiesis, respectively (Fong et al., 1995; Shalaby et al., 1995).

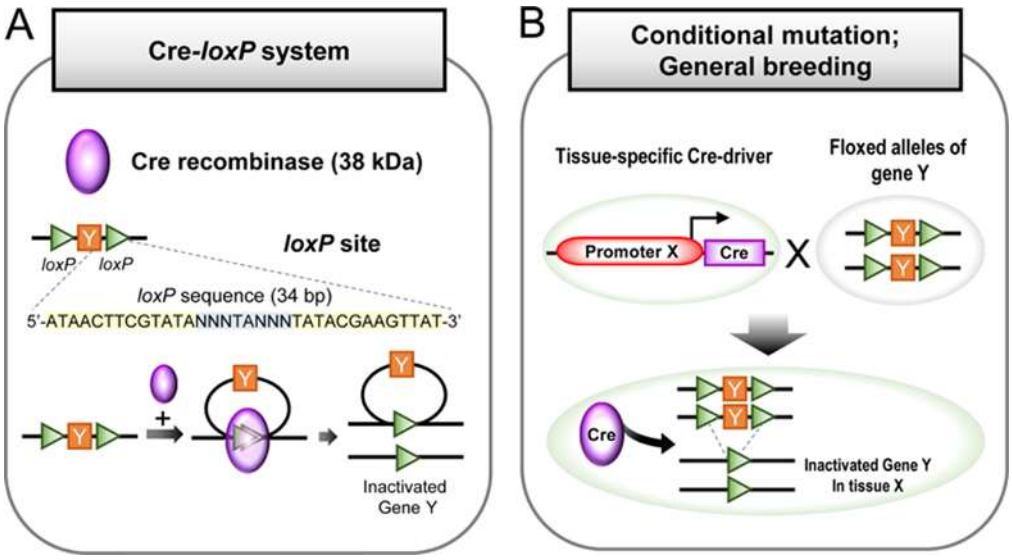

Figure 1.11: Diagrammatic illustration of mechanism involved in Cre-loxP system. (A) A summary of Cre-loxP system. Cre recombinase (38 kDa) identifies the loxP sites comprises of 34 bp DNA sequences. (B) Conditional knockout using Cre-loxP system in which one mouse must have a tissue-specific Cre driver gene and another mouse with alleles of interest gene Y containing loxP flanked (floxed). Floxed locus is excised by the Cre recombinases and leads to inactivation of the gene Y (H. Kim et al., 2018).

In the Cre-loxP system, two directly repeated loxP sites are recognised by a single Cre recombinase which excises the loxP flanked (floxed) DNA leading to the creation of two types of DNA (a) circular; (b); excised and inactivated gene Y (Figure 1.11). In addition to gene excision, the predominant mechanism used in Cre-LoxP system, it also induces the translocation and inversion of DNA between two loxP sites which depends on the location and orientation of loxP sites (Branda & Dymecki, 2004; Meinke et al., 2016; A. Nagy, 2000).

The generation of cKO in specific cell types can be achieved using the now well-defined Cre-LoxP system driven by an inducible promoter such as the oestrogen receptor (ER) to produce a timed gene knockout in specific cellular types or locations (Figure 1.12). This approach can thus overcome the difficulties described above for VEGF-A and VEGFR germ line knockout.

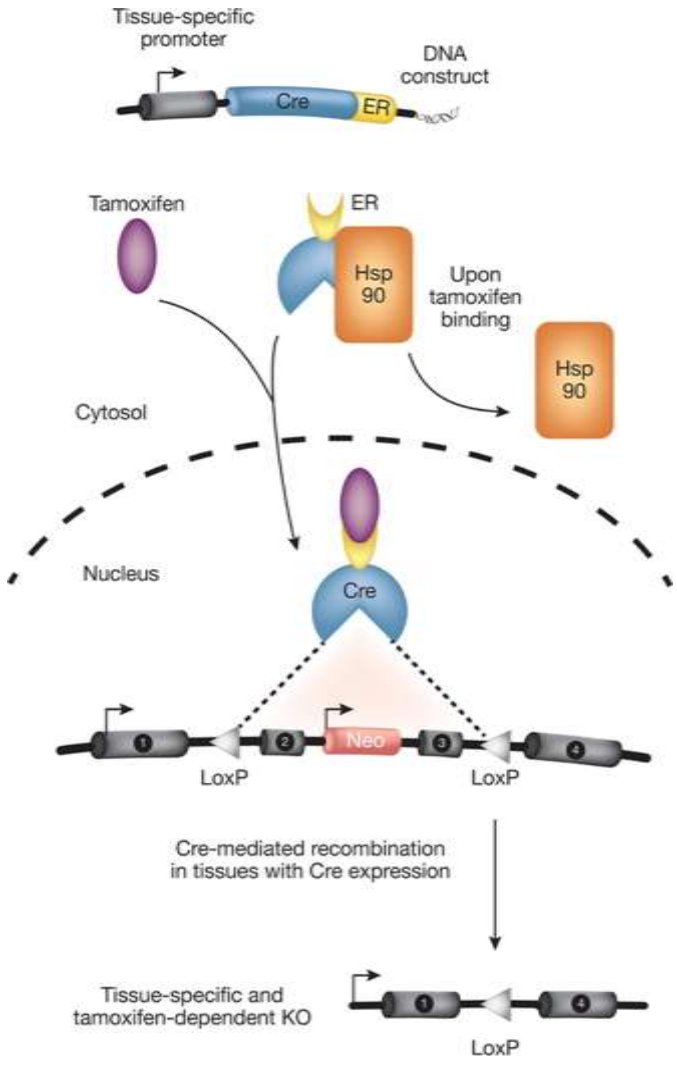

Figure 1.12: The Tamoxifen-inducible Cre-loxP system involves a modified oestrogen receptor (ER) fused with Cre recombinase, regulated by a promoter (tissue-specific). In its inactive state, the oestrogen receptor binds to heat shock protein 90 (Hsp90) and stays in the cytosol. However, upon administering tamoxifen to an animal, it binds to the ER, causing the Cre-ER protein to be released from Hsp90.This causes the CreER-tamoxifen complex to move into the nucleus, where it recombines the loxP-flanked (floxed) target gene, resulting in a gene knockout (Gunschmann et al., 2014).

1.11 Alternative splicing

The human genome comprises of an estimated 20,000 protein-coding genes (Salzberg, 2018), but many more than 20,000 proteins are produced in the body. More than 95% of pre-mRNAs can be alternatively spliced in mammals (Kornblihtt et al., 2013). Up to 40% of protein modifications result from alternative splicing and is thus considered one of the main processes that increase protein to gene ratio (Ponomarenko et al., 2016). Alternative splicing is a complex process which increases

the capacity of a restricted number of genes to generate multiple proteins by the formation of multiple mRNA products from a single pre-mRNA. Multiple proteins from a single transcript can, but do not always, have distinct structures or functions (Mthembu et al., 2017).

Alternative splicing is heavily controlled, like most biological processes. It's not surprising that mutations in splice factors, splice sites, or regulatory sequences have been described to contribute to numerous pathological processes or diseases. Moreover, in comparison with physiologic states, disease states are found to have strong associations with expression of abnormal proportions of splice isoforms or novel isoforms (Stevens & Oltean, 2016).

1.11.1 Mechanisms of alternative splicing

The process of alternative splicing of pre-mRNAs involves the inclusion/exclusion of whole exons or parts of exons/introns which leads to the formation of the mature mRNA transcript which is accordingly translated into protein (Matera & Wang, 2014). This process is achieved through a splicing reaction facilitated by the spliceosome, a large molecule composed of five small nuclear ribonucleoprotein particles (snRNPs) and over 100 associated accessory proteins (Coltri et al., 2019) .

In pre-mRNA transcripts, the spliceosome assembles at a conserved sequence at the exon-intron junction known as the splice site. During splicing, constituents of the spliceosome undergo two trans-esterification reactions involving a specific intronic sequence called the branch point, and the 5´ and 3´ splice sites to achieve splicing out of the intron. The major forms of alternative splicing include exon skipping or retention, intron retention, using alternative 3´ or 5´ splice sites in exons, and the inclusion or exclusion of mutually exclusive exons (Figure 1.13) (Stevens & Oltean, 2016).

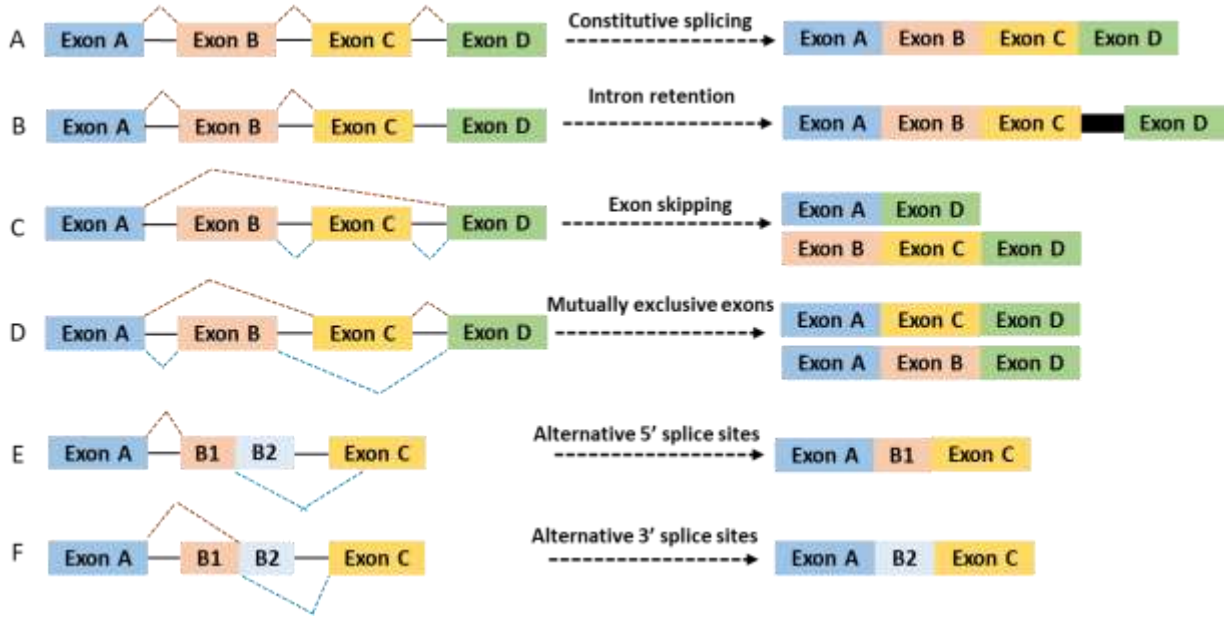

Figure 1.13: Pre mRNA transcript showing different alternative splicing mechanisms. Exons shown by different colours while black lines indicate introns, and dotted lines show where splicing events occur. (A) Constitutive splicing, with exons connected and introns removed. (B) Intron retention, which is the retention of an intron in this case between the last two exons. (C) Exon skipping, in this case two exons B and C are omitted from the final mRNA transcript. The number of skipped exons can vary. (D) Mutually exclusive exons: Either one or the other exon, but not both, is retained while other is spliced out. (E) Alternative 5' splice site selection, where a 5' splicing sequence in an alternative location is used, in this case within the final exon. (F) Alternative 3' splice site selection. In this case there is an alternative 3' splicing sequence at the beginning of exon B2 (blue dotted line). There is also a potential alternative 5' splice site indicated at the end of exon B1 (orange dotted line). Recreated from (Donaldson & Beazley-Long, 2016).

1.11.2 Control of Serine-Rich (SR) splice factor proteins

Alternative splicing is facilitated by the reversible phosphorylation and activation of splicing regulators from SR family (Pandit et al., 2008). These splicing factors are phosphorylated by two families of protein kinases - the Serine-Arginine-Rich protein kinases (SRPKs) and the CDC-like-kinases (CLKs). The process of SR protein binding to splicing regulating elements (SREs) is complex and is regulated via SR-protein activation through phosphorylation by these protein kinases. The CDC-like-kinases (CLKs1-4) have the ability to phosphorylate both Arg-Ser and Ser-Pro dipeptides, which are present in all SR proteins. On the other hand, SR-protein kinases (SRPK1-

3) only phosphorylate Arg-Ser dipeptides. SRSF1, SRSF2, and SRSF6 are some examples of splicing factors that regulate the choice of splice site by the spliceosome.

An established pathway for SRSF1-mediated alternative splicing involves phosphorylation of SRSF1 by SRPK1, which triggers SRSF1 binding to a transporting protein (Tr-SR). The resulting complex then moves to the nucleus. (Serrano et al., 2016) (Figure 1.14), where SRSF1 is stored in nuclear speckles. SRSF1 is subsequently hyper-phosphorylated by CLK1 which permits SRSF1 release from nuclear speckle storage, enabling SRSF1 to bind to splicing regulatory elements (SREs) on the pre-mRNA promoting the splicing reaction (Figure 1.14) (Naro & Sette, 2013).

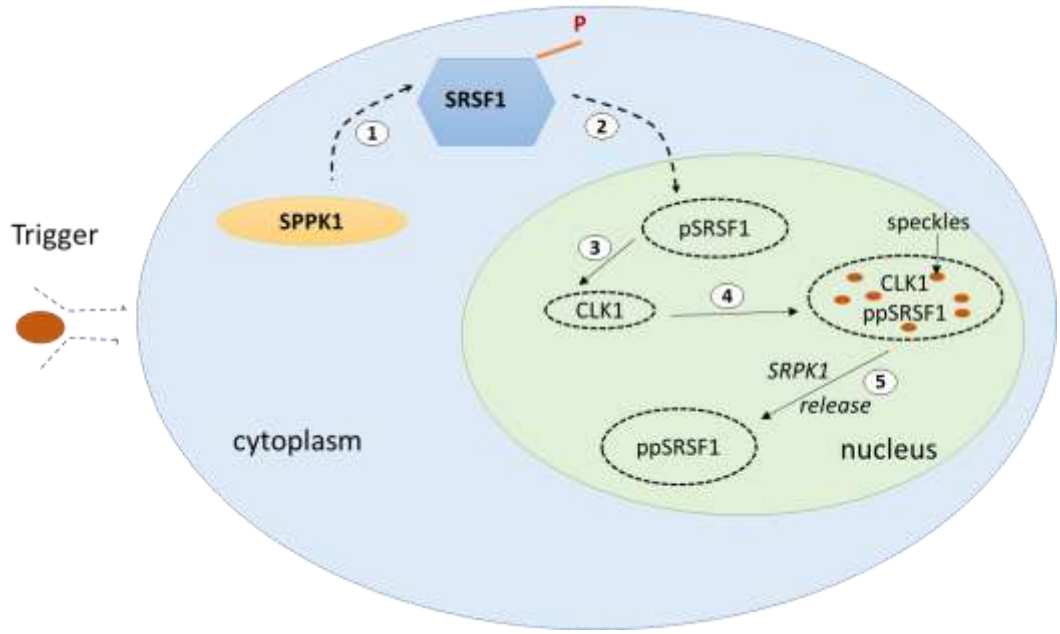

Figure 1.14: Diagrammatic representation of activation of SR proteins by CLK1/SRPK1 complexes. SR proteins are concentrated mostly in the cytoplasm in unstimulated cells. On cell stimulation, kinases such as SRPK1 are activated (1), and lead to phosphorylation of SR proteins causing them to move into the nucleus (2) where mostly they are held into nuclear speckles (3,4). SRSF1 is hyper-phosphorylated by CLK1 resulting in its release from the complex with CLK1 through SRPK1. This allows it to be released from speckles and interact with splicing regulatory elements (5). Adapted from (Aubol et al., 2021).

Dysregulation of SRPK1 as well as its downstream targets has been reported in many pathological processes such cancer, including colon, breast, prostate, pancreas, and lung cancer (D. Bates et al., 2015; L. Gong et al., 2016; Hayes et al., 2007; Odunsi et al., 2012). High expression of SRPK1 can result in hyper-phosphorylation of SRSF1

protein (da Silva et al., 2015), and consequently cause an increase in the transcription, alternative splicing and translation of downstream target proteins such as VEGF-A.

1.11.3 SRPK1-CLK1 interactions and nuclear localization of SRPK1

SRPKs are present in both the nucleus and cytoplasm, although their cytoplasmic functions are better understood. By phosphorylating SR proteins, SRPKs stimulate their transport from the cytoplasm to the nucleus (as discussed earlier) (Kataoka et al., 1999; Lai et al., 2001; C. Y. Yun et al., 2003). In contrast, CLKs are found only in the nucleus and have a nuclear localization signal in their N-termini. They play a crucial role in mobilizing SR proteins from nuclear speckles, where they are often held, to the active gene splicing sites, through Ser-Pro phosphorylation (Keshwani et al., 2015). According to this simple model, basal SR protein phosphorylation levels are produced by SRPKs in the cytoplasm, while CLKs increase nuclear phosphorylation of such protein in the nucleus for splicing regulation (Ding et al., 2006; Keshwani et al., 2015). Despite this, two persistent issues about the function of phosphorylation in alternative splicing remain unexplained. Firstly, elevated levels of CLK inhibit SR proteins activity in splice-site recognition, which is supposed to be enhanced by phosphorylation (Prasad et al., 1999). Secondly, both SRPKs and CLKs creates a possible competitive rather than cooperative relationship in the nucleus. It has been observed that the process of phosphorylation aids in the release of SR proteins with the help of SRPK. (Aubol et al., 2014; Koizumi et al., 1999), whereas CLK does not release fully phosphorylated SR proteins (Aubol et al., 2014). These findings suggest that some unknown release factor is required by CLKs to generate functional SR protein.

In relation to the presence of SRPKs and CLKs in the same compartment, a study conducted by Aubol et.al in 2016 sheds light on the distinctive function of SRPKs in the nucleus. The study showed that endogenous CLK1 and SRPK1 interact in the nucleus to form a complex and work together to phosphorylate substrates. Rather than acting competitively, the dual kinase complex acts symbiotically, with SRPK1 functioning as a release factor for CLK1, which in turn releases phosphorylated SR proteins to promote spliceosome assembly. These findings resolve some of the previous puzzles in the field. It explains that two protein kinases are needed to complete the phosphorylation cycle of their substrates, from binding to release. Further

studies have confirmed and expanded upon these findings (Aubol & Adams, 2022; Aubol et al., 2021; Aubol et al., 2016).

1.11.4 Alternative Splicing of VEGF-A

The VEGF-A gene consists of eight exons and seven introns (Ferrara et al., 2003) and VEGF-A pre-mRNA undergoes extensive alternative splicing which leads to a variety of isoforms. Several alternatively spliced isoforms of VEGF-A have been identified, including VEGF-A_{111}, VEGF-A_{121}, VEGF-A_{145}, VEGF-A_{148}, VEGF-A_{162}, VEGF-A_{165}, VEGF-A_{183}, VEGF-A_{189} and VEGF-A_{206} (Figure 1.9) (where the numbers represent the number of amino acids present in the isoform) (Arcondeguy et al., 2013; Peach et al., 2018; Shaik et al., 2020). VEGF-A_{121}, VEGF-A_{165}, and VEGF-A_{189} are the most abundant isoforms in most biological systems (Alvarez-Aznar et al., 2017).

In an additional layer of complexity, all these isoforms exist in two families (Figure 1.9 A, B) that only differ by 6 amino acids at the C-terminus. Many studies have only used N-terminal antibodies and so measurement of VEGF-A protein expression frequently has not distinguished between the two families (D. O. Bates et al., 2002). Almost 20 years ago, it was discovered that alternative splicing of exon 8 give rise to another family of VEGF-A isoforms termed VEGF-A_{xxx}b. These alternative splicing isoforms have the same overall number of amino acids as the VEGF-A_{xxx}a isoforms, but a six amino acid difference in the C terminus resulting from a distal alternative splice site at exon 8b (Figure 1.9B) (D. O. Bates et al., 2002). VEGF-A_{165}b, as opposed to VEGF-A_{165}a, is the most predominant isoform in most normal tissues (Harper & Bates, 2008) other than tissues with physiological angiogenesis such as reproductive organs (Alvarez-Aznar et al., 2017). Note: both before and after the discovery of VEGF-A_{xxx}b isoforms, many studies using VEGF-A_{165}a have referred to this as $VEGF_{165}$, or VEGF-A_{165}. In papers cited in this thesis, where the isoform is not clearly stated by the authors and there is no information on the source of the protein used, I have assumed that it is VEGF-A_{165}a, and I use the most common way to refer to it, as VEGF-A_{165}.

VEGF-A_{165}a is the most potent angiogenic isoform (Apte et al., 2019) that is involved in both physiological and pathological angiogenesis initiation and progression (Ferrara et al., 2003; Perez-Gutierrez & Ferrara, 2023). This isoform has been widely examined

for its expression, signalling, function, and roles in cancer. VEGF-A_{165}a is the most common VEGF-A isoform. It is known to fully activate VEGFR2-driven signalling responses, as shown by both *in vivo* and *in vitro* studies. Therefore, it is typically used as a benchmark ligand for investigating other VEGF-A isoforms (Catena et al., 2010; Cebe Suarez et al., 2006; Delcombel et al., 2013; Fearnley et al., 2015; Fearnley et al., 2016; Hervé et al., 2005; Kawamura et al., 2008; Krilleke et al., 2007; Q. Pan et al., 2007; Pang et al., 2017; Shiying et al., 2017; Woolard et al., 2004). Moreover, VEGF-A_{165}a has been found to induce the highest levels of phosphorylation of VEGFR2 (at the Y1175 residue) by AKT and ERK signalling (Fearnley et al., 2016). VEGF-A_{121}a appears to act as a partial agonist at VEGFR2 compared to VEGF-A_{165}a, (Cebe Suarez et al., 2006; Kawamura et al., 2008). VEGF-A_{121}a (Fearnley et al., 2014; Q. Pan et al., 2007; Shiying et al., 2017) and VEGF-A_{145}a (Kawamura et al., 2008) show reduced VEGFR2 phosphorylation in endothelial cells compared to VEGF-A_{165}a.

As a result of alternative splicing, VEGF-A isoforms differ in their molecular masses, bioavailability, and biological properties such as their binding affinity to heparin or heparin-sulphate proteoglycans (HSPG) on the cell surface and in the ECM (Figure 1.9), as well as in their binding to different VEGF receptors. The shortest isoforms VEGF-A_{111}a/b and VEGF-A_{121}a/b lack exons 6 and 7 and are freely diffusible (Houck et al., 1992; Krilleke et al., 2007; J. E. Park et al., 1993), whereas the longer isoforms VEGF-A_{145}a/b, VEGF-A_{189}a/b and VEGF-A_{206}a/b contain both exons 6a and 7, and therefore bind to heparin sulphate glycoproteins with high affinity (Houck et al., 1991; J. E. Park et al., 1993). These isoforms therefore have the lowest bioavailability (Mamer et al., 2020). The prototypical VEGF-A_{165}a has intermediate binding affinity to heparin proteoglycans and shows moderate to high bioavailability between the freely diffusible and bound isoforms (Houck et al., 1992) which contributes to its greater potency in inducing angiogenesis compared to the other isoforms (Robinson & Stringer, 2001).

Following the discovery of VEGF-A_{165}b (D. O. Bates et al., 2002) a new sub-family of VEGF-A_{xxx}b isoforms were identified (Figure 1.9B) (Harper & Bates, 2008). Since then, the anti-angiogenic and anti-migratory properties of VEGF-A_{xxx}b isoforms have been evaluated by several other publications, particularly the downregulation of VEGFR

signalling pathway leading to a decrease of tumour growth (E. Rennel et al., 2008; E. S. Rennel et al., 2008; Varey et al., 2008). These findings have been attained conducting *in vitro* study on proliferation and migration of endothelial cells along with *in vivo* studies on tumour volume of melanoma, colorectal cancers, renal cell carcinoma, and experimental choroidal neovascularization (Magnussen et al., 2010; E. Rennel et al., 2008; Woolard et al., 2004). Downregulation of $VEGF_{165}b$ expression cause metastatic melanoma while $VEGF_{165}b$ expression reduces metastasis (Pritchard-Jones et al., 2007). In addition, downregulation of VEGF-$A_{xxx}b$ expression also has been reported in various other cancers, Denys Drash syndrome, diabetic retinopathy, and retinal vein occlusion, and its upregulation in asthma and systemic sclerosis (D. O. Bates et al., 2013). The proportion between the pro- and the anti-angiogenic isoforms may be fundamental for the angiogenic balance, supporting exploration of VEGF-$A_{xxx}b$ anticancer properties (E. Rennel et al., 2008; E. S. Rennel et al., 2008; Varey et al., 2008) and as an efficient therapy of eye and other pathologies accompanying with exacerbated angiogenesis (Perrin et al., 2005).

All VEGF-$A_{xxx}a$ splice isoforms stimulate the tyrosine kinase activity of VEGFRs; for VEGFR2 this is mediated through VEGFR2 receptor dimerization and stabilisation of the receptor dimer with NP-1 (Figure 1.10) (Ballmer-Hofer et al., 2011). Interestingly, VEGF-$A_{165}b$ and VEGF-$A_{165}a$ have equal binding affinity to VEGFR2 but stimulate both phosphorylation of different tyrosine residues linked to VEGFR2/NP-1 heterodimerization patterns (Cebe Suarez et al., 2006; Kawamura et al., 2008) and distinct downstream signalling pathways (Cebe Suarez et al., 2006) in endothelial as well as other cell types (D. O. Bates et al., 2002; Kawamura et al., 2008; Magnussen et al., 2010).

VEGF-$A_{165}b$ isoforms compete with VEGF-$A_{165}a$ isoforms for VEGFR2 binding (Woolard et al., 2004) through different intra-cellular pathways (Beazley-Long et al., 2013) and only partially activate VEGFR2 as they do not stabilise NP-1 binding (Ballmer-Hofer et al., 2011; Kawamura et al., 2008) nor phosphorylate VEGFR2 at the key tyrosine residues such as Y1175. VEGF-$A_{165}b$ blocks the responses to VEGF-$A_{165}a$ such as vascularization in the rat mesentery, rabbit cornea, chorioallantoic membrane, the chicken embryo, and Xeno transplanted cancer cells in mice (D. O.

Bates et al., 2002; Cebe Suarez et al., 2006; Woolard et al., 2004). Conversely VEGF-A_{165}b binds weakly to heparan sulphate and does not interact with neuropilin-1, which leads to significantly weaker signalling output through VEGFR2 and results in lacking or strongly reduced ability to induce angiogenesis (Kawamura et al., 2008). This further shows the importance of binding to HSPG and NP-1 that is not only requisite for VEGF-A_{165}a deposition as well as storage on NP-1 expressing cells, and in the ECM, but also that these interactions have a direct effect on receptor signalling pathways.

Prior to the discovery of the alternatively spliced VEGF-A_{xxx}b family, and indeed still in recent publications studying VEGF-A contributions to pathology, the molecule was referred to as VEGF-A_{165} or $VEGF_{165}$. In the discussion of literature where authors did not distinguish the splicing families, I refer to VEGF-A_{165} and assume that in most cases this is the same as VEGF-A_{165}b.

1.11.5 Control of alternative splicing of VEGF-A isoforms

As outlined in section 1.11 – 1.11.4, there has been considerable research into the control of alternative splicing in exon 8 between families to generate VEGF-A_{xxx}a or VEGF-A_{xxx}b isoforms, and this is better understood than mechanisms of alternative splicing within VEGF-A splice variant families. Very few mechanisms of alternative splicing producing isoforms of different sizes *within* the VEGF-A_{xxx}a/b families (Figure 1.9) have been identified.

The inclusion of exon 6a to make the longer splice variants VEGF-A_{189} and VEGF-A_{206} depends on a complex of splicing factors, methyltransferase and chromatin modulator (Salton et al., 2014). VEGF-A_{165} and VEGF-A_{189} differ in that VEGF-A_{189} includes exon 6a but not 6b, whereas VEGF-A_{165} excludes both exons 6a and 6b (Figure 1.9). This is due to an exonic splicing silencer sequence in exon 6a, but how this is controlled to give either isoform is not yet understood (R. Wang et al., 2009).

Several factors are involved in the stimulation of alternative splicing of VEGF-A including hypoxia, and pH (Elias & Dias, 2008). Hypoxia is a major stimulus for both upregulation and alternative splicing of VEGF-A (Bowler & Oltean, 2019; Korbecki et

al., 2021), mediated by activation by hypoxia inducible factor-1 (HIF-1) (Staels et al., 2019; H. Takahashi & Shibuya, 2005). For example, there is evidence of a shift in expression to VEGF-A_{165}a and VEGF-A_{121}a in hypoxic conditions which has been detected in both human tumours and cancer cell lines, though the pattern of expression of these splice variants depends on the cancer type (Elias & Dias, 2008).

Acidic environments (~pH 5.5) have been observed to induce alternative splicing of VEGF-A that results in the predominant expression of $VEGF_{121}$a, followed by $VEGF_{165}$a, and slight increases in other variants such as $VEGF_{145}$a and $VEGF_{189}$a (Elias & Dias, 2008).

Loss of Wilms tumour suppressor-1 (WT1) activity promotes splicing of VEGF-A_{121} (Cunningham et al., 2013), whereas overexpression of WT1D isoform increases VEGF-A_{165} (Katuri et al., 2014). VEGF-A_{111} isoform expression is increased by DNA damage and genotoxic drugs (Danastas et al., 2015).

1.12 VEGF and arthritis

1.12.1 VEGF-A and VEGF receptors in arthritis

The first publications suggesting a role for VEGF in arthritis appeared in the late 1994, showing increased VEGF-A concentrations in synovial tissue and fluid from RA compared to OA patients (Fava et al., 1994; A. E. Koch, 1998; A. E. Koch et al., 1994; S. Lee et al., 2001; Yoo et al., 2008), and VEGF-A was shown to be induced in synoviocytes by inflammatory mediators (Ben-Av et al., 1995; J. Jackson et al., 1997). Serum and synovial VEGF-A as well as the levels of both VEGF receptors (VEGFR1 and 2) were also raised in RA patients rather than in OA patients (Harada, 1998; M. Ikeda et al., 2000; S. Lee et al., 2001; Ozgonenel et al., 2010; Sone et al., 2001), and VEGF-A serum levels of were associated with RA disease activity, predominantly with swollen joints (S. Lee et al., 2001).

VEGF and its receptors contribute to RA inflammation through several potential mechanisms (Figure 1.15).

(i) Increased angiogenesis caused by VEGF-A binding to VEGFR2 which leads to peripheral leukocyte recruitment to inflamed synovium. Hence, the developing burden of synoviocytes to supply the oxygen and nutrients essential for tissue metabolism is reduced (Falconer et al., 2018).

(ii) VEGF-A interaction with VEGFR1 (Flt1) may directly lead to the stimulation of cytokines and chemokines such as IL-6, IL-8, MCP-1, and TNF-α which results in chronic inflammation in joints (Murakami et al., 2006; Murakami & Shibuya, 2008).

(iii) Lastly, NP-1 can act as a survival factor to impede synoviocyte apoptosis upon binding with $VEGF_{165}$a through induction of expression of Bcl-2. Thus, $VEGF_{165}$a plays key role to regulate simultaneously synovial inflammation, hyperplasia, and angiogenesis in RA joints through NP1 actions (Yoo et al., 2008).

1.12.2 VEGF-A and angiogenesis in arthritis

Angiogenesis plays an important role in the development and progression of arthritis. Detailed reviews have been published on the angiogenesis process in arthritis (Eelen et al., 2020; Tahergorabi & Khazaei, 2012; D. Walsh, 1999). Angiogenesis is found in the synovium of arthritic joints and is closely related to chronic synovitis (Giatromanolaki et al., 2001). It has been shown that synovial angiogenesis and inflammation, being closely integrated processes, are contributing factors across the full range of disease severity, showing that they are not unique to early or late-stage disease (Malcolm Douglas Smith et al., 1997). In arthritis, vascular permeability is increased because of activated endothelial cells' detachment from their neighbouring cells. Endothelial cell migration and proliferation is stimulated by proteolytic enzymes such as MMPs, leading to the degradation of endothelial basement membrane (Bonnet & Walsh, 2005).

Several steps are involved in synovial angiogenesis, each of which is modulated by specific factors (Elshabrawy et al., 2015). The factors responsible for the increased endothelial cell proliferation are increased VEGF-A expression, vascular density, macrophage infiltration within the synovium, representing that synovial neovascularization may be largely driven by synovitis (L Haywood et al., 2003). The

process begins with hypoxia and induction of growth factors i-e. VEGF-A and fibroblast growth factor (FGF). These factors bind to their cognate receptors on endothelial cells and result in the production of proteolytic enzymes (Fraser et al., 2001). Subsequently, degradation of the basement membrane occurs by MMPs, leading to migration and further endothelial proliferation to form vascular tubules. Finally, pro-angiogenic factors such as Angiotensin-1 stabilize the blood vessels with subsequent incorporation of pericytes into the newly formed basement membrane to facilitate the blood flow process (MacDonald et al., 2018).

1.12.3 VEGF-A and synovial inflammation in arthritis

VEGF-A has been known for its significance in angiogenesis associated with both inflammation and malignancies (Szekanecz et al., 2009). Synovial macrophages and fibroblasts express VEGF-A protein and mRNA in RA joints. Moreover, cultured synovial cells secrete VEGF-A when stimulated by IL-1, IL-6, IL-17, IL-18, prostaglandin, TGF-*β* or hypoxic conditions (Yoo et al., 2008). These findings strongly suggest that inflammation and angiogenesis are closely related and that suppressing the angiogenic action of VEGF-A is likely to alleviate inflammation in RA. (Ferrara et al., 2003; A. E. Koch, 1998). However, angiogenesis can occur without inflammation, whereas chronic inflammation is always associated with angiogenesis (Bonnet & Walsh, 2005).

VEGF-A_{165} contributes to the production of TNF-α and IL-6 by PBMC and has a direct pro-inflammatory effect on the development of RA (Yoo et al., 2005). Additionally, synovial fluid monocytes from RA patients show a greater response to VEGF-A_{165}a stimulation compared to PBMC from healthy controls These findings indicate that VEGF-A_{165} is an important mediator of both angiogenesis and inflammation in RA joints, thereby establishing a crucial link between the two processes (Yoo et al., 2008).

Several inflammatory cell types are involved in establishment of a self-perpetuating cycle of autoimmunity thus retaining a mutually activating network in RA joints (Firestein, 2003). Endothelial cells are activated by VEGF-A_{165} to produce chemokines, such as MCP-1 and IL-8 (T.-H. Lee et al., 2002; Marumo et al., 1999). Monocytes are attracted by MCP-1 and IL-8, and they and synoviocytes both respond

to both VEGF-A_{165}, and endothelial cell contact by producing IL-6 and TNF-α. This results in a positive feedback loop, promoting further VEGF-A release from synoviocytes and macrophages, and enhancing endothelial cell-contact macrophage activation (Figure 1.15) (Yoo et al., 2008).

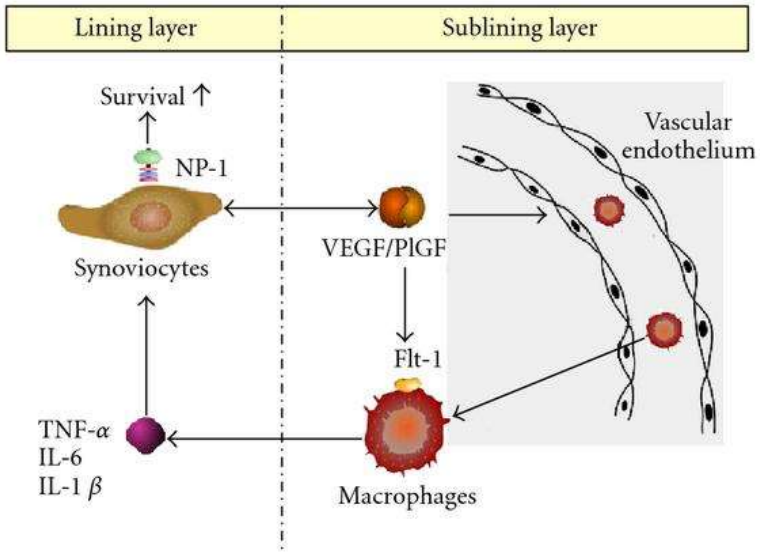

Figure 1.15: Diagrammatic illustration of progression of rheumatoid arthritis by VEGF-A. In RA, VEGF-A production by synoviocytes increases the permeability of vascular endothelial cells and leads to angiogenesis. This results in the influx of macrophages, which produce IL-6 and TNF-α when stimulated by VEGF-A/Flt-1 binding or by interacting with activated endothelial cells. These cytokines further enhance the production of VEGF-A by macrophages and synoviocytes, creating a self-perpetuating cycle of inflammation. Moreover, binding of VEGF-A to NP-1 prevents rheumatoid synoviocytes from experiencing apoptosis, resulting in synovial hyperplasia. Hyperplastic synoviocytes secrete more VEGF-A, which generates a positive feedback loop that promotes cell survival. Thus, VEGF-A controls joint hyperplasia, synovial inflammation, and angiogenesis in RA patient (Yoo et al., 2008).

1.12.4 VEGF-A, chondrocyte hypertrophy and bone erosion in arthritis

VEGF-A is required during the process of endochondral ossification, and in hypertrophic cartilage remodelling accompanied with angiogenesis and subsequent ossification (Carlevaro et al., 2000; Duan et al., 2015; Gerber et al., 1999; A. Horner et al., 1999; Nagao et al., 2017). Normal adult chondrocytes are devoid of both VEGF-A ligand and its receptors, but chondrocytes from RA cartilage produce higher VEGF-A levels (Onnheim et al., 2022), and express VEGFR1 and VEGFR2 (Enomoto et al.,

2003; Pfander et al., 2001; Thomas Pufe et al., 2001). Therefore, the expression of VEGF-A and VEGFR2 in chondrocytes appears linked with RA.

VEGFR2 in hypertrophic chondrocytes shows an autocrine activation mediated by VEGF-A (Carlevaro et al., 2000). VEGF-A produced by hypertrophic chondrocytes recruits endothelial cells and as a result induces blood vessel growth into cartilage. These blood vessels not only bring in nutrients but also recruit osteoblasts and chondroclasts in addition to promoting pro-apoptotic signal(s). Moreover, endothelial cell exposure to VEGF-A may further stimulate signalling cascades to produce proteinases, cytokines and other mediators that in turn affect chondrocytes, chondroclasts and osteoblasts (Carlevaro et al., 2000). A study conducted on immortalized VEGFR2 expressing chondrocytes *in vitro* showed that VEGF-A regulates the production of MMPs and MMP inhibitors, which are among the effectors of ECM remodelling. VEGF-A has the ability to stimulate MMP-1, MMP3, and specifically MMP-13 expression; however, it decreases tissue inhibitor of metalloproteinases 2 (TIMP-2). As a result, VEGF-A appears to be a further damaging factor involved in the progression of arthritis by enhancing cartilage destruction (Thomas Pufe et al., 2004).

Increased bone resorption is one of the characteristic features of inflammatory rheumatic diseases which leads to permanent bone remodelling and joint deformation. VEGF-A stimulates increased osteoclast activity and leads to bone resorption through its actions on VEGFR1 (Aldridge et al., 2005), and VEGFR2 signalling (Nakagawa et al., 2000; Q. Yang et al., 2008) which may be mediated by an interaction between VEGFR and RANKL (Aldridge et al., 2005). Taken together, the role of VEGF-A in immune cells, synovium, chondrocytes, bone cells and angiogenesis (Figure 1.16) appears to be a substantial factor that contributes to the pathogenesis of rheumatoid arthritis as well as other arthritic and rheumatic diseases.

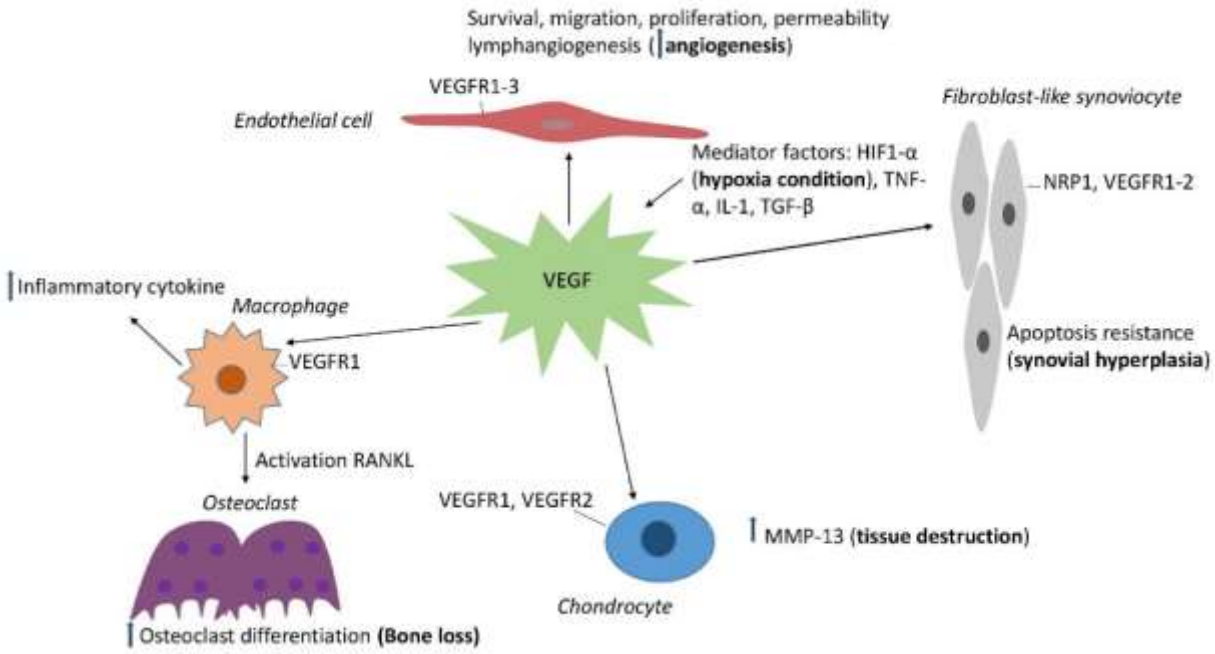

Figure 1.16: Illustration of the multiple roles of VEGF-A in the development and progression of joint damage in rheumatoid arthritis. Angiogenesis, a prominent feature of both RA and OA, is regulated by VEGF-A. VEGF-A and its receptors VEGFR1 and VEGFR2 are expressed in FLS, endothelial cells and are found in synovial fluid. VEGFR1 is also expressed in macrophages. VEGFR1, VEGFR2 and NRP1 activation lead to apoptotic resistance of synoviocytes and result in synovial hyperplasia. VEGF-A contributes to joint destruction and bone resorption by regulating the inflammatory process, with elevated cytokines, MMPs, and increased osteoclast differentiation (Le & Kwon, 2021).

1.12.5 VEGF-A splice variants in arthritis

VEGF-A exists in several isoforms within two families, and the expression of these isoforms is tissue dependent (T Pufe et al., 2001; Thomas Pufe et al., 2001, 2001). Some cell types express multiple VEGF-A splice forms form the same family for example VEGF-A_{121}, VEGF-A_{165}, VEGF-A_{189} and VEGF-A_{206} are all detected in human neonatal fibroblasts (Eckhart et al., 1999), while other cells or tissues such as synoviocytes (Thomas Pufe et al., 2001) or osteoarthritic cartilage (Thomas Pufe et al., 2001) express fewer splice isoforms. Hypertrophic chondrocytes express both VEGF-A_{121} and VEGF-A_{165}. Interestingly, the same VEGF splice forms (VEGF-A_{121} and VEGF-A_{165}) were also detected in synovial tissues of patients with RA (Thomas Pufe et al., 2001), whereas samples from OA cartilage and synovium expressed the splice forms VEGF-A_{121} and VEGF-A_{189} (Thomas Pufe et al., 2001) or only VEGF-A_{121}

(M. Ikeda et al., 2000) respectively. Recent work shows expression both VEGF-A_{165}a and VEGF-A_{165}b in human synovium from healthy post-mortem controls as well as RA and OA joints (D Amanitis et al., 2021).

1.13 Anti-VEGF treatment effects in inflammatory arthritis

VEGF-A plays such an important role in inflammation-related angiogenesis (as discussed earlier), VEGF-A inhibitors have been investigated in animal models with arthritis, as well as clinical oncology trials (A. E.-S. Abdel-Maged et al., 2018; A. E. Abdel-Maged et al., 2019; Hernandez et al., 2001; Kiselyov et al., 2007; A. E. Koch, 1998; A. E. Koch et al., 1994; Shams & Ianchulev, 2006; Masabumi Shibuya, 2008). Targeting VEGF-A is in the focus of cancer and inflammation research (Kiselyov et al., 2007; Naumov et al., 2008; Shams & Ianchulev, 2006) and VEGF-A-mediated neovascularization can be inhibited by using monoclonal antibodies to VEGF-A or VEGF receptors (VEGFR), soluble VEGF receptors, VEGF receptor tyrosine kinase inhibitors (RTKIs), VEGF-A splicing kinase inhibitors or inhibitors of VEGF-A, and VEGFR downstream signalling (S. T. Choi et al., 2009; Grosios et al., 2004; Holash et al., 2002; W.-U. Kim et al., 2007; Kiselyov et al., 2007; Lainer-Carr & Brahn, 2007; Manley et al., 2002; Masabumi Shibuya, 2008; Veale & Fearon, 2006) (Figure 1.17). Inhibition of VEGFR or VEGF-A has been effectively used *in vivo* to suppress synovial inflammation and pain in animal models (Beazley-Long et al., 2018; S. T. Choi et al., 2009; Grosios et al., 2004; Hamilton et al., 2016; W.-U. Kim et al., 2007; Lainer-Carr & Brahn, 2007; Ludin et al., 2013; Ma et al., 2023; Manley et al., 2002; Nagao et al., 2017).

Soluble VEGF receptor treatment that sequesters VEGF-A in collagen induced arthritis (CIA) showed a reduction in disease severity (Miotla et al., 2000). Other studies have also shown effectiveness of polyclonal anti-VEGF antibodies in the CIA model (Lu et al., 2000; Sone et al., 2001). VEGF-A inhibition using ranibizumab, an anti-VEGF-A antibody used in the treatment of wet age-related macular degeneration, reduced cartilage and bone destruction compared to MTX or tocilizumab (interleukin-6R antagonist) in rat adjuvant (CFA)-induced arthritis (A. E.-S. Abdel-Maged et al., 2018). Co-administration of the anti-VEGFR2 monoclonal antibody, Ramucirumab, and MTX

in an RA experimental model also had positive effects (A. E. Abdel-Maged et al., 2019). Hence, the small amount of evidence suggests that anti-VEGF-A mono- or combination therapy could be a potential treatment for IA.

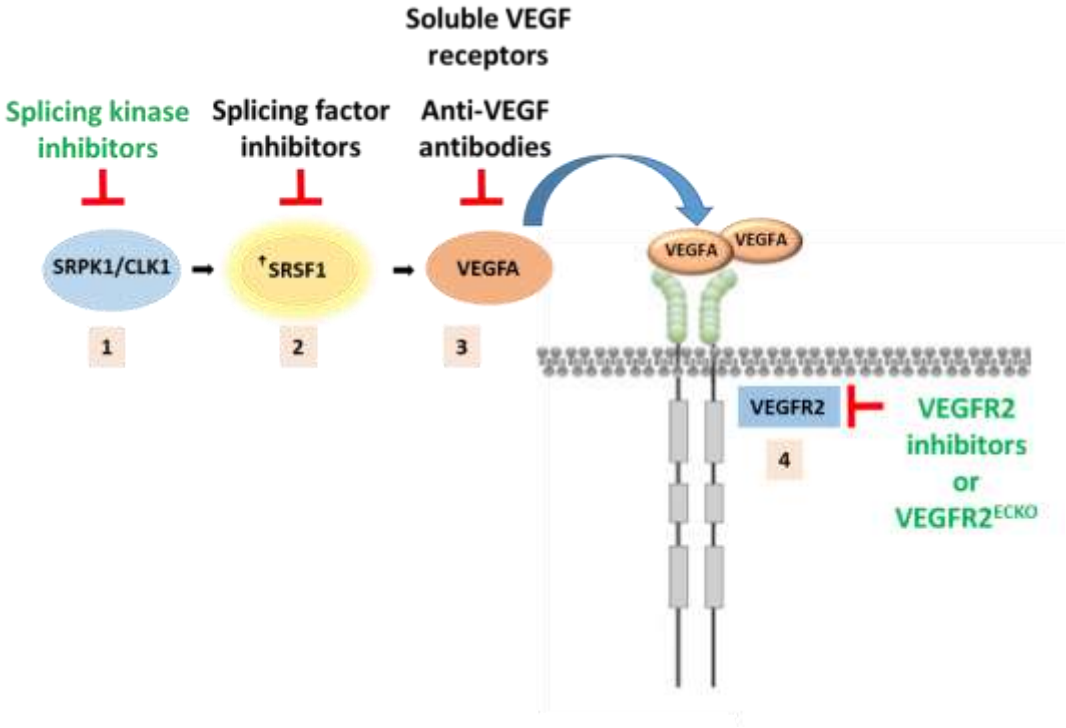

Figure 1.17: Different potential therapeutic approaches to target VEGF-A for treatment of arthritis including different methods to modulate VEGF-A actions. 1. Modulation of VEGF-A alternative splicing; 2. Block of splicing factor activation; 3. Neutralisation of VEGF-A with antibodies or soluble receptors; 4. VEGFR inhibition, blockade, or genetic manipulation (knockout or knockdown). The methods highlighted in green text have those used in this thesis.

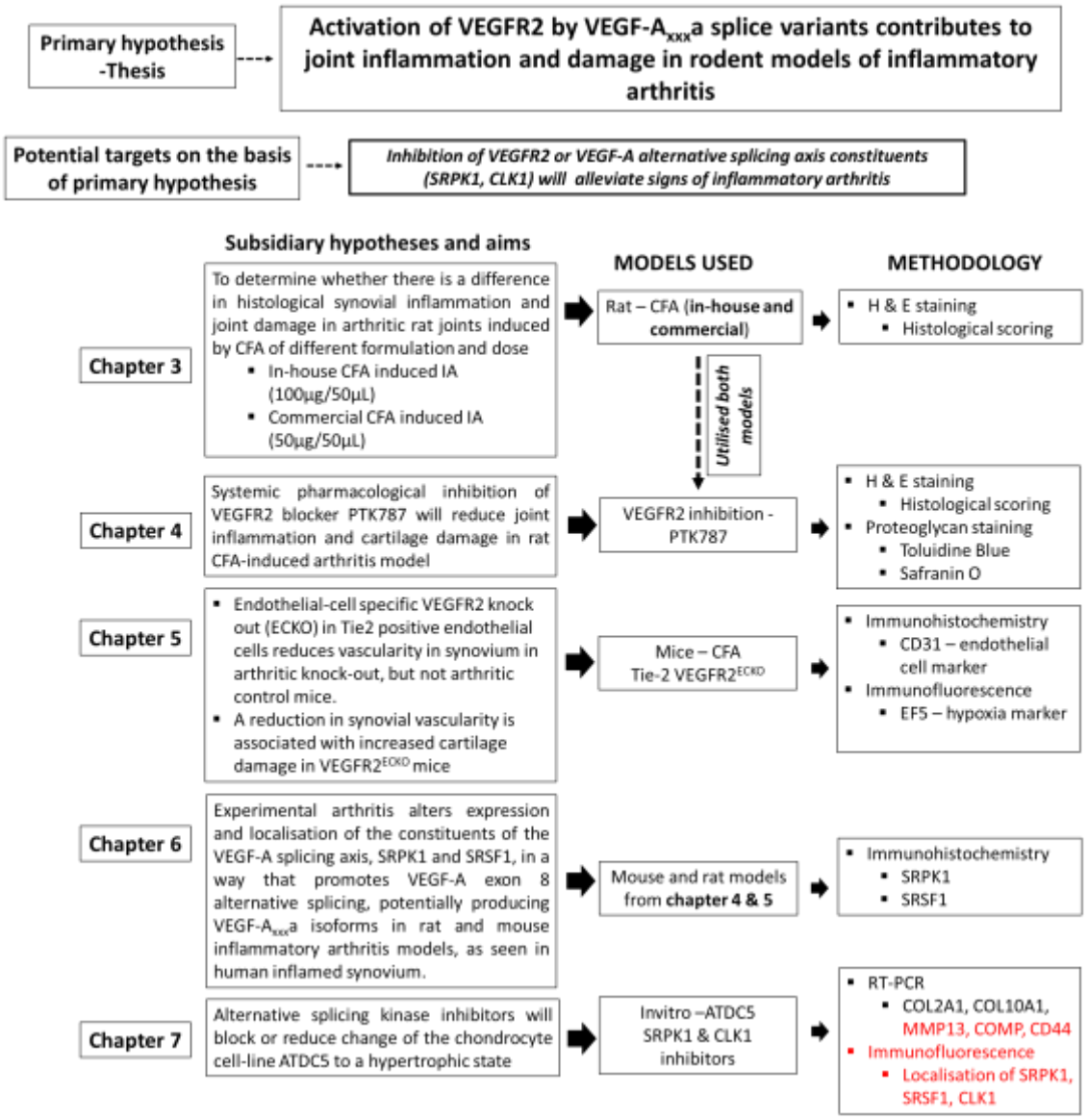

Figure 1.18: Schematic representation of the hypothesis, aims, models, and methods used in this thesis. The *in vivo* rat and mouse studies were conducted by Dr. Alexandra Durrant and Dr. Nicholas Beazley long, respectively. I used joints from these animals in the experiments described in this thesis. The experimental plans in red could not be conducted due to the impact of the COVID pandemic and time limitations.

Hypothesis

Overall hypothesis

Activation of VEGFR2 by VEGF-A_{xxx}a splice variants contributes to joint inflammation and damage in rodent models of inflammatory arthritis.

Subsidiary hypotheses

- Systemic pharmacological inhibition of the VEGFR2 blocker PTK787 will reduce joint inflammation and cartilage damage in rat CFA-induced arthritis model.
- Endothelial-cell specific VEGFR2 knock out (ECKO) in Tie2 positive endothelial cells reduces vascularity in synovium in arthritic knock-out, but not arthritic control mice.
- A reduction in synovial vascularity is associated with increased cartilage damage in $VEGFR2^{ECKO}$ mice.
- Experimental arthritis alters expression and localisation of the constituents of the VEGF-A splicing axis, SRPK1 and SRSF1, in a way that promotes VEGF-A exon 8 alternative splicing, potentially producing VEGF-A_{xxx}a isoforms in rat and mouse IA models, as seen in human inflamed synovium.
- Alternative splicing kinase inhibitors will block or reduce change of the chondrocyte cell-line ATDC5 to a hypertrophic state.

Thesis Aims

The aims of this thesis were to investigate;

- whether there is a difference in histological synovial inflammation and joint damage in arthritic rat joints induced by CFA of different formulation and dose
- the effect of pharmacological inhibition of VEGFR2 blocker PTK787 on synovial inflammation and cartilage damage in CFA arthritic rat joints.
- whether induction of Tie2-specific endothelial VEGFR2 knock-out affects blood vessel number/density in normal and/or arthritic mice, and whether this is related to cartilage damage.

- whether changes in SRPK1 and SRSF1 expression and localisation in synovium in mouse and rat arthritis models are similar to the changes seen in human arthritic synovium.
- the effect of IA and endothelial VEGFR2 inhibition/knockout on SRPK1 and SRSF1 expression and localisation in synovium in mouse and rat arthritis models.
- the effect of SRPK1 and CLK1 inhibitors on the morphology and COL2A1/COL10A1 expression by ATDC5 chondrocytes following change to a more hypertrophic state

2. MATERIALS AND METHODS

2.1 Introduction

This chapter includes the general methodology used for research work conducted throughout the PhD. Two inflammatory arthritis animal models (rat and mouse) and one *in vitro* study conducted on an immortalised chondrocyte-like cell line (ATDC5) were used in this thesis. Detailed methods are given in each chapter for more information.

2.2 Drug and adjuvant preparation

2.2.1 Complete Freund's adjuvant preparation

Complete Freund's Adjuvant (CFA, composed of heat-denatured mycobacterium tuberculosis suspended in mineral oil) was purchased from Sigma-Aldrich (1mg/mL, F5881) containing 1 mg/mL *mycobacterium tuberculosis* (M.tub.), heat killed and dried suspended in 85% paraffin oil / 15% mannide mono-oleate vehicle. 'In house' CFA was prepared by suspending heat denatured M.tub. (UK Ministry of Agriculture Fisheries and Food, now known as DEFRA, UK) in mineral oil (2mg/mL), sonicated for 1 hr and filtered (40μm pore size) (Kelly et al., 2007).

2.2.2 Pharmacological inhibitor preparation

Solutions of drugs inhibiting VEGFR-2 (PTK787, small molecule drug, AdooQ Bioscience USA) and TNF (Etanercept/ Enbrel®, Pfizer Ltd, anti-TNF antibody) were prepared in sterile PBS or saline - for PTK787 at 3.75mg/mL and Etanercept at 1.375mg/mL. Drugs or vehicle (PBS or saline) were administered by i.p. injection at 15mg/kg for PTK787 and 5.5mg/kg for Etanercept. Doses were determined on previous published studies showing efficacy on pain behaviour (Beazley-Long et al., 2018; Michael K Boettger et al., 2008).

2.3 *In vivo* procedures

2.3.1 *In vivo* animal experiments and tissue preparation

All animal procedures were approved by the University of Nottingham Animal Welfare and Ethical Review Group and conducted in accordance with the United Kingdom Animals (Scientific Procedures) Act 1986/Amendment Regulations 2012. The project licence was held by Professor Lucy Donaldson, and all licensed work was done by personal licence holders Drs Nicholas Beazley-Long (mice) and Alexandra Durrant (rats).

At the termination of the *in vivo* rat experiments, I was supplied with intact joints, which I then processed for histological analyses (section 2.5). For mouse experiments I was first supplied with some mounted and stained joint sections generated by Dr Beazley-Long for training and initial analyses and I later sectioned and processed additional joints for further investigations.

2.3.2 *In vivo* rat experimental hypotheses and design

The *in vivo* experiments in rats were conducted by Dr Alexandra Durrant to test the hypothesis that systemic block of VEGF receptor 2 and/or TNF-α would inhibit the spinal and/or dorsal root ganglia gliovascular/ neuroinflammatory response to IA in male rats. To test these hypotheses, two *in vivo* experiments were conducted by Dr Durrant with experimental groups and design as shown in Figure 2.1 and Table 2.1.

A secondary hypothesis in both experiments was that systemic block of VEGF receptor 2 and/or TNF-α would inhibit the *joint inflammation and damage* in IA in male rats. My work was done to address this secondary hypothesis.

Experiments were carried out on a total of 59 adult male Sprague Dawley rats (starting weight ≥175g) purchased from Charles River, UK. Animals were group housed (3-4 per cage) in individually ventilated cages and were maintained on a 12/12 light: dark cycle at 22^{o}C and 55% humidity, with *ad libitum* access to food and water. Male rats were used as the hormonal changes in the rat oestrus cycle can result in effects on pain signalling (Becker et al., 2005; Craft et al., 2004). It is now recommended that animal experiments include both sexes, and I recognise that this is a limitation in the studies presented in this thesis.

Table 2.1: Animal numbers and treatment groups from which joints were processed to compare histological features with different CFA formulations/doses and different drugs (Durrant, 2021).

***One animal was excluded from all analyses due to lack of CFA response (swelling).**

Study	Treatments	Study design	Number of animals
1	Anaesthetic control + Vehicle	Within/between subjects comparison of the effect of therapeutic pharmacological VEGFR and/or TNFα inhibition on histological arthritis.	6
	CFA (100µg) + Vehicle		6
	CFA + PTK787 (starting day 0)		6
	CFA + PTK787 (starting day 3)		6
	CFA + Etanercept		6
2	Anaesthetic control + Vehicle		6
	CFA (50µg) + Vehicle		6
	CFA + PTK787 (starting day 0)		6
	CFA + PTK787 (starting day 3)		6
	CFA + Etanercept		6
	CFA + PTK787 + Etanercept*		5

Sample sizes for these two studies were determined using sample size estimates from previous work done in the group, using GPower (Faul et al., 2007) and based on the primary hypothesis outcomes of increases in spinal gliovascular response. In these studies, the two control groups (anaesthetic + vehicle) were used to determine whether there were any differences in joint histological features between two different CFA preparations (Chapter 3) and the effect of VEGFR2 blockade on joint inflammation and damage (Chapter 4).

2.3.3 Induction of arthritis in rats

The surgical procedures on rats were done by Dr Durrant before I joined the lab. Anaesthesia was induced in rats with the inhalational anaesthetic isoflurane (Abbot Laboratories, Kent, UK), at 3% vapourised in oxygen, in an induction box. When the righting reflex was lost, rats were transferred to a heated mat to maintain body temperature and anaesthetic delivery continued through a non-rebreathable delivery system attached to a nose cone. Anaesthetic was extracted via a Fluo-vac system (Harvard Apparatus, Massachusetts, U.S.A) and active eradication system (Pioneer Kent U.K). Surgical anaesthesia was confirmed by the loss of the noxious paw withdrawal reflex.

The anterior surface of the 'knee' (tibio-femoral) joint was shaved with clippers, and the leg disinfected with 4% chlorhexidine gluconate surgical scrub (Hydrex®). With the right paw extended, the base of the patella was located and a 25-gauge 16mm needle inserted through the infrapatellar ligament into the joint, taking care not to insert the needle too far to avoid penetration of the posterior joint capsule and leakage. 50µl of 'in house' or commercial CFA containing either 50 or 100µg M.tub. was injected into the joint space. Control rats were anaesthetised, and knees shaved. After anaesthesia rats recovered in dedicated cages in a warm environment before returning to home cages. After recovery rats were transferred to individually ventilated cages and hind limb use and knee diameter measured as shown in Figure 2.1, and health monitoring carried out daily throughout the study by Dr Durrant (Durrant, 2021).

A

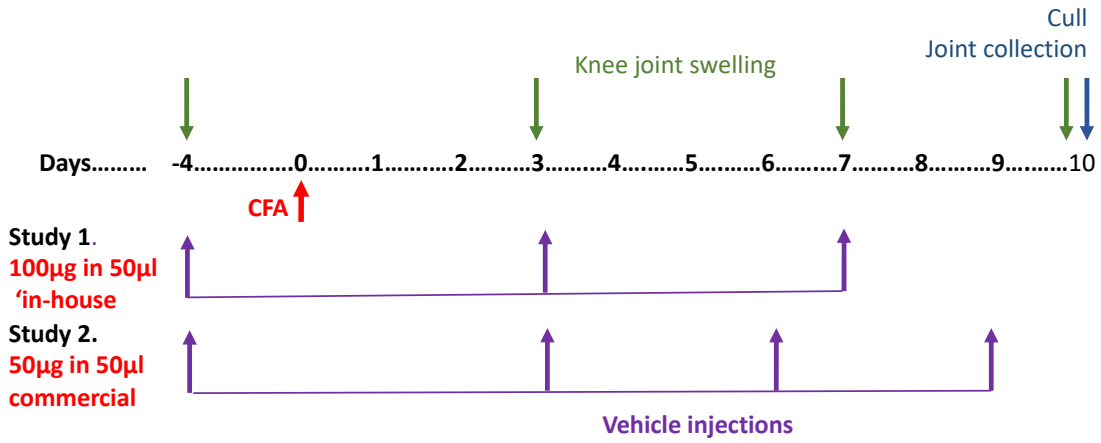

B

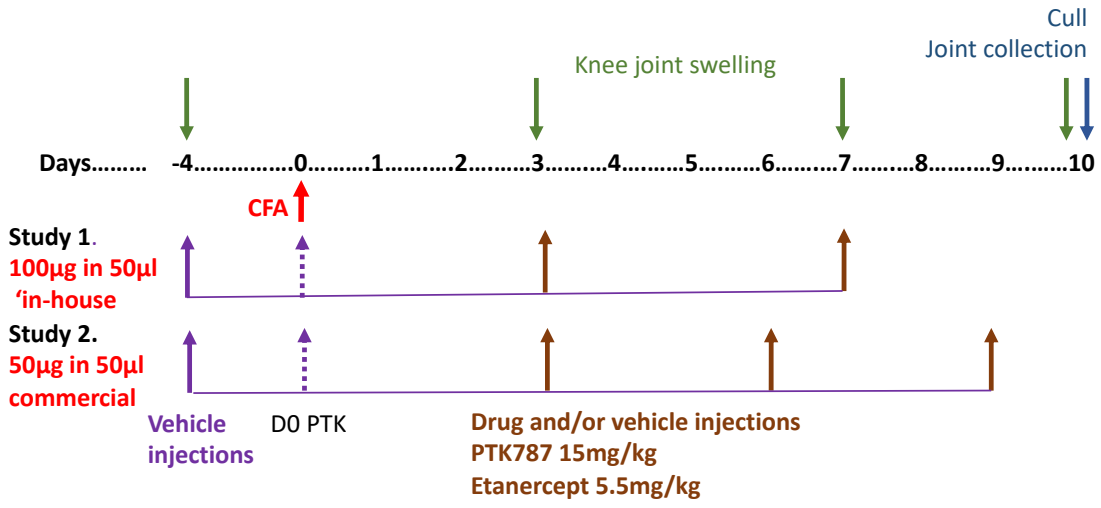

Figure 2.1: Experimental design and timelines for A. comparison of CFA preparations on joint inflammation and damage, and B. effects of CFA and VEGFR2 ± TNF-α blockers on joint inflammation and damage.

2.3.4 Drug administration in rats

Two different cohorts of rats followed a similar protocol, the main differences in studies being the CFA used and number of drug injections (Table 2.1, Figure 2.1). All animals were dosed intraperitoneally with vehicle for one week (2 injections, 3 days apart) before anaesthesia and CFA injection, to habituate them to the injection procedures, and then with PTK787, Etanercept, or PTK787+Etanercept (Table 2.1) as in the timelines in Figure 2.1. Drug injections were carried out at days 3, 6/7 and in the second study, day 9. In each study one additional group of animals received PTK787 from day 0 (CFA injection) which served as a positive control as this method had been previously reported to alter pain in rats (Beazley-Long et al., 2018). Animals were killed after 10 days of inflammation by intraperitoneal anaesthetic overdose and joints removed for further processing.

At the end of all experiments, rats were killed with an overdose of sodium pentobarbitone (intraperitoneal injection (i.p)., 60mg/kg body weight) and transcardially perfused with saline plus 1U heparin to prevent blood clotting, followed by perfusion with 4% paraformaldehyde in 0.1M phosphate buffer saline. Joints were removed and placed in 4% paraformaldehyde in PBS until processed for sectioning (section 2.4).

2.3.5 Inducible endothelial cell VEGFR2 knockout mice

A colony of tamoxifen-inducible endothelial cell-specific knockout mice was generated in 2015 by Dr Nicholas Beazley-Long. Mice homozygous for the VEGFR2 gene with floxP sites either side of exon 1 (vegfr2fl/fl) (Albuquerque et al., 2009) were crossed with Tie2Cre^{ERT2} mice [supplied from the European Mutant Mouse Archive EM:00715] (Forde et al., 2002) to enable oestrogen receptor-driven VEGFR2 knockout. Animals were bred for experimental purposes from double transgenic animals, and experiments described in this thesis were conducted on tissues from F3/F4 mice of both sexes. All mice used were confirmed as homozygous for the VEGFR2-loxP transgene (vegfr2fl/fl) and either heterozygous or wild-type for Tie2Cre^{ERT2}. Data on

the mice from which tissues are taken have been previously published (Beazley-Long et al 2018).

2.3.6 *In vivo* mouse experimental hypotheses and design

The *in vivo* experiments in mice were conducted by Dr Nicholas Beazley-Long to test the primary hypothesis that knock-out of endothelial VEGFR2 (VEGFR2^{ECKO}) would reduce spinal vascular endothelial cell and microglial activation, and hence activation of spinal VEGFR2 resulting in pain. VEGFR2^{ECKO} mice did show significantly reduced pain behaviours, but as VEGFR2 endothelial knock-out was not location-specific, these mice had significantly reduced endothelial cell numbers in other tissues as well as spinal cord (Beazley-Long et al 2018). My experiments were therefore designed to test the secondary hypothesis that VEGFR2^{ECKO} resulted in reduced synovial vascular endothelial cell and/or blood vessel number and therefore reduced joint inflammation and damage, leading to reduced pain behaviour.

Experiments were carried out on a total of 39 transgenic adult mice of both sexes (19 female, 20 male), derived from several litters and bred in house (starting weight ≥25g). Tissues came from the numbers of mice shown in each study, 30 animals in assessment of blood vessels density and cartilage damage (Chapter 5) and 19 for the assessment of hypoxia. Joint tissues from 26 of these mice were randomly selected for inclusion in the investigation of VEGF-A splicing axis (Chapter 6). Animals were group housed (2-4 per cage), with males and females housed separately in single-tier ventilated cages and were maintained on a 12/12 light: dark cycle at 22^{o}C and 55% humidity, with *ad libitum* access to food and water. Mice treated with tamoxifen were housed separately from vehicle-treated mice as tamoxifen is excreted in urine (Kisanga et al., 2005) which can lead to cross-contamination in the cage.

Sample sizes for the study was determined using sample size estimates from previous work done in the group, using GPower (Faul et al., 2007) and based on the primary hypothesis outcomes of changes in pain behaviour.

2.3.7 Induction of endothelial VEGFR2 knockout in mice

Tamoxifen (Sigma, T5648) was first dissolved in ethanol and then diluted in autoclaved sunflower oil (vehicle: 10% ethanol and 90% oil) (Acharya et al., 2011). Five daily

doses of vehicle or tamoxifen (1mg/100µL i/p.) were given to groups of Tie2Cre^{ERT2} negative (groups 1 & 2 tamoxifen) or Tie2Cre^{ERT2}-positive mice (groups 3&4 vehicle, 5&6 tamoxifen, Table 2.2, Figure 2.2). VEGFR2fl/fl-positive/Tie2Cre^{ERT2}-negative mice (groups 1&2) were included as controls for any potential effects of tamoxifen (sham (±Tam), and VEGFR2fl/fl x Tie2Cre^{ERT2} without tamoxifen (uninduced ±CFA) were the controls for any strain effect i.e. an effect of the genetic manipulation.

Table 2.2: Animal numbers and treatment groups from which joints were processed to compare histological features with and without endothelial VEGFR2 inducible knockout (Beazley-Long et al., 2018). * all animals underwent brief anaesthesia.

+ in column 3 denotes animals receiving CFA, therefore inflamed.

Genetic background	Treatments*	Groups	Number of animals	Study design
VEGFR2fl/fl (Tie2Cre^{ERT2} negative, genetic control)	Tam, no CFA	1. Sham (-)	5	Within/between subjects comparison of the effect of VEGFR2^{ECKO} on histological arthritis.
	Tam, CFA	2. Sham (+)	5	
VEGFR2fl/fl x Tie2Cre^{ERT2} (inducible knockout)	No Tam, no CFA	3. Uninduced (-)	5	
	No Tam, CFA	4. Uninduced (+)	5	
	Tam, no CFA	5. VEGFR2^{ECKO} (-)	5	
	Tam + CFA	6. VEGFR2^{ECKO} (+)	5	

2.3.8 Induction of arthritis in mice

Inflammatory arthritis was induced in mice as discussed below, up to the point of achieving surgical anaesthesia. Once areflexive surgical anaesthesia had been achieved, ankle (tibio-tarsal) joints were disinfected with 4% chlorhexidine gluconate surgical scrub (Hydrex®). Transgenic mice underwent two unilateral subcutaneous peri-articular injections each of 80µg CFA (in house) in 40µL mineral oil, on either side of the joint. Sham mice underwent limb preparation and anaesthesia with no injection. After anaesthesia mice recovered in dedicated cages in a warm environment before returning to home cages. After recovery mice were transferred to individually ventilated cages and joint swelling was measured throughout the duration of the study (Figure 2.2). Health monitoring carried out daily throughout the study by Dr Beazley-Long. At the end of the experiments, mice were killed using intraperitoneal pentobarbital overdose (60mg/kg), and joints collected and processed as for rat joints (section 2.4). At the end of experiments to determine joint hypoxia (Chapter 5), mice were terminally

anaesthetised as above and perfused fixed with 4% paraformaldehyde and tibio-talar joints removed for further processing (Section 5.2.2).

Figure 2.2: Timeline for genetic endothelial cell knockout in mouse.

2.4 Preparation and processing of mouse and rat joints

2.4.1 Decalcification of joint tissue

Hind limbs of mice and rat were collected, post-fixed and then skin and other soft tissues trimmed close to the tibio-tarsal (ankle) joint and tibio-femoral (knee) joint respectively in such a way to remove as much soft tissue as possible. Joints were decalcified in 10% EDTA buffer (10% EDTA, 0.01M Trisma base, 7.5% polyvinylpyrrolidone, 10% NaOH, Appendix Table A1) for three to four weeks until bone could be penetrated with a fine pin. EDTA buffer was changed 1 – 2 times per week and then joints were rinsed and embedded in paraffin (embedding was done in King's Mill hospital). Mouse ankle joints and rat knee joints were paraffin embedded in sagittal and coronal orientation respectively. Rat joints were treated in the same way but required a longer time, and more frequent changes of EDTA buffer to achieve complete decalcification.

2.4.2 Embedding and sectioning of joint tissue

After automated paraffin embedding (King's Mill hospital) with dehydration in graded ethanol (70%, 90%, 100%) over 2 hours, clearing in xylene, followed by wax infiltration, and embedding, 10 µm and 8µm sections were cut with a microtome for mice ankle and rat knee joints samples respectively and collected on poly-lysine coated slides (ThermoFisher Scientific UK). Mouse joints were orientated during embedding for sectioning in the sagittal plane to enable visualisation of the tibio-talar articulation from

the lateral aspect (Figure 2.3A), and rat tibio-femoral joints were oriented for sectioning in the coronal plane to enable visualisation of the joints from the anterior aspect (Figure 2.3B). After brief drying at room temperature, the slides were oven-dried at 59°C to fix the tissue on the slides.

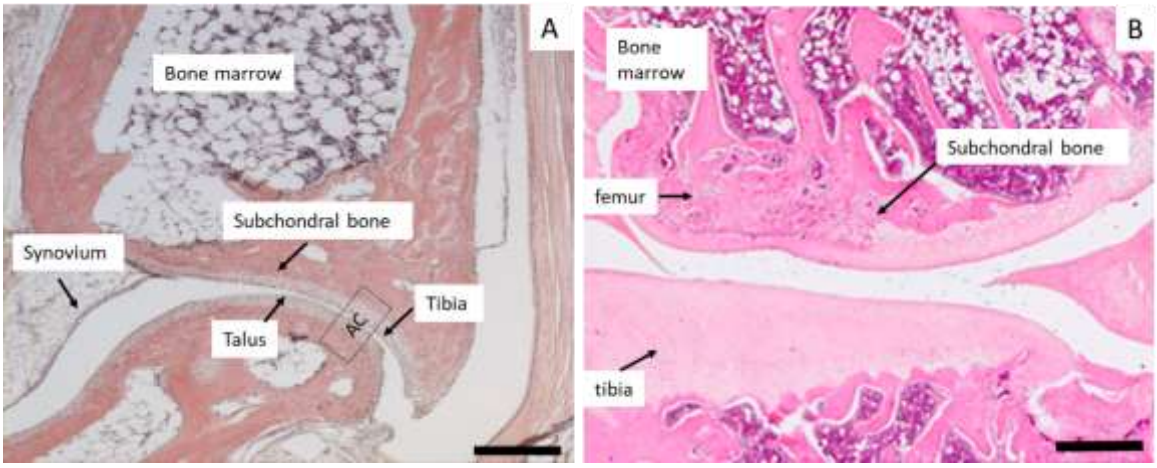

Figure 2.3. Mouse (left) and rat (right) joint sections and orientations. **(A) Sagittal section of mouse tibio-talar (ankle) joint and (B) of rat tibio-femoral (knee) joint. Scale bars 200µm. Labels show key structures in the joints, AC = articular cartilage**

2.5 Histological staining of rat joints

2.5.1 Histological staining methods

2.5.1.1 Haematoxylin and eosin (H&E) Staining

Haematoxylin and eosin (H&E) stain is a standard reference stain for cationic and anionic tissue components widely used for medical diagnosis and examination (Chan, 2014). It is a combination of two stains giving a clear distinction between the nucleus (stained blue with haematoxylin) and cytoplasm (stained pink by eosin). H&E staining was used for all histological scoring analysis in rat joints.

Paraffin embedded rat 'knee' joint sections (8µm) were dewaxed in xylene for 2 x 5 minutes. Descending methanol concentrations (100%, 70%, and 50%, 5 minutes each) were used to rehydrate the tissues followed by washing with distilled water for 1-5 minutes. The sections were then immersed in Mayer's haematoxylin (Sigma Aldrich: MHS32**)** for 15 minutes, and then washed in tap water. Afterwards, the sections were immersed briefly (20 seconds) in acid alcohol to define nuclei (1% HCl in 70% methanol). To remove any excess stain, the sections were rinsed with water

for three minutes. After that, they were stained with eosin (1%) solution for one minute, followed by another wash in tap water for one minute. Finally, the sections were dehydrated using increasing concentrations of methanol (50%, 70%, and 100%) and then treated with xylene. To complete the process, they were cover-slipped with DPX medium.

2.5.1.2. Toluidine blue and Safranin O Staining

The severity of disease in OA and RA tissue specimens has frequently been demonstrated by the intensity of glycosaminoglycan (GAG) and proteoglycan content in comparison with normal cartilage. Safranin O and toluidine blue are the cationic dyes which have been used routinely for this purpose (Rosenberg, 1971).

A. Toluidine blue staining protocol

Since its discovery by William Henry Perkin in 1856 toluidine blue has been used in various medical applications as well as being a histological stain (Sridharan & Shankar, 2012). Toluidine blue is a metachromatic cationic dye with high affinity for the sulphate groups of proteoglycans thus this staining visualizes the presence of proteoglycan content in a tissue (Vickers, 2017). It stains cell nuclei dark blue, cytoplasm light blue, and ECM, as in hyaline articular cartilage, pink or purple (Tyndall et al., 1998).

For staining, slides were de-waxed in xylene (2 x 5 minutes), rehydrated in graded methanol (100%, 70%, 50%), rinsed with tap water and staining in 0.04% toluidine blue (Sigma Aldrich:198161) for 8 minutes. Sections were rinsed again with tap water, dehydrated in graded methanol (50%, 70%, 100% for 5 minutes each), cleared in xylene (2 x 5 minutes) and cover-slipped with DPX.

B. Safranin O staining protocol

Safranin O/Fast Green is a standard stain used to assess cartilage damage in articular joints. The degree of pathological degradation of macromolecules in ECM of hyaline cartilage can be determined by evaluating the intensity of collagen and proteoglycan

staining (Alibegović et al., 2020). Safranin O stains cartilage red in proportion to its proteoglycan content and Fast Green stains bone green (Zorzi et al., 2015).

Following dewaxing in xylene (2 x 5minutes), sections were stained with Weigert's iron haematoxylin solution (1% haematoxylin (Sigma Aldrich: H3136), 45mM $FeCl_3$ (Sigma Aldrich:157740) in 50% acidified ethanol, Appendix Table A3), rinsed quickly with acid alcohol solution for no more than 20 seconds and washed for 3 minutes in running tap water. Sections were then stained with Fast Green (0.2% Fast Green in deionised water) for 5 minutes, followed by a brief dip in acetic acid (1% in distilled water) and stained with Safranin O (Sigma Alrich: S8884)/Fast Green (Sigma Alrich:F7258) (0.1% in distilled water) for 5 minutes followed by wash for 5 minutes with running tap water. All sections were dehydrated and cover slipped as above.

2.5.1.3. Masson's trichrome staining

Masson's trichrome staining (Abcam: ab150686) was used to identify collagen in bone marrow, as an indication of FVT formation (Bain et al., 2019; Bancroft & Gamble, 2008; Kuter et al., 2007). The sections were deparaffinised as above and further fixed for 15 minutes in preheated Bouin's Solution at 56°C. Sections were washed under running tap water until the water ran clear of yellow stain, then stained with Wiegert's iron haematoxylin solution for 5 minutes and washed again in running tap water for 5 minutes. Sections were then stained in Bieberich Scarlet-Acid fuchsin (Bierich scarlet 0.9%, acid fuchsin 0.1% in 1% acetic acid) for 5 minutes followed by rinsing in deionized water. The staining was differentiated in phosphomolybdic-phosphotungstic acid solution (Appendix Table A3) for 5 minutes transferred to aniline blue solution (2.4% aniline blue in 2% acetic acid) for 5 minutes, differentiated in 1% acetic acid for 2 minutes, and rinsed in deionised water, then rapidly dehydrated through alcohols, cleared in xylene, and mounted as described above.

2.6 Scoring of histological parameters of arthritis in rat joints

2.6.1 Histological scoring

Several different parameters of joint inflammation and damage were scored: physical cartilage damage and proteoglycan loss, degree of synovial inflammation, presence/

absence of pannus infiltration, appearance of FVT in bone marrow was assessed morphologically and bone marrow collagen fibre presence (Figure 2.4). H&E staining was used for initial histological/morphological scoring of cartilage damage, synovial inflammation, pannus infiltration and bone marrow FVT.

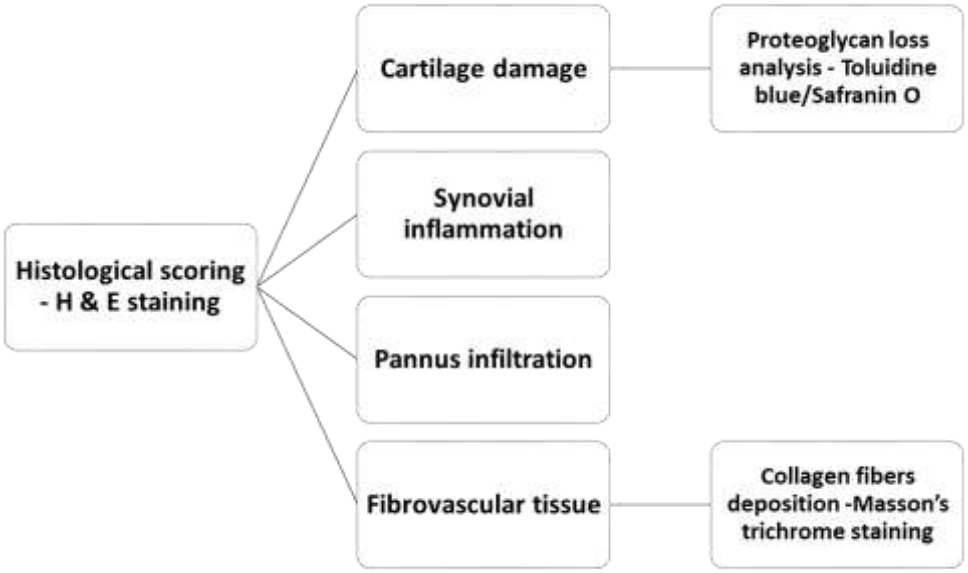

Figure 2.4: Histological scoring of joints. H&E stained sections were first scored for physical cartilage damage, synovial inflammation, and the presence or absence of pannus infiltration and FVT in bone marrow. The degree of FVT was also assessed by the degree of collagen fibre deposition in Masson's trichrome stained sections. Cartilage proteoglycan loss was assessed using Toluidine blue/Safranin O stained sections.

The scores were graded by examining three stained sections from different depths of sectioning for each joint using a Zeiss Axioscop-50 microscope (Carl Zeiss, Welwyn Garden City, UK) under 5x, 20x and 40x magnification. All sections were blinded during scoring, and only unblinded once all scoring was completed. Examples of scored features for each parameter are shown in Figures below, and the scoring system for each in the respective tables below the Figures.

Signs of physical/morphological cartilage damage were scored on changes in several parameters according to existing recognised systems (Armstrong et al., 2021; Z. Yan et al., 2015). These included cartilage surface smoothness, presence of empty lacunae showing chondrocyte loss, fibrillation of the cartilage surface, fissures in the

cartilage surface of varying degrees of penetration, and partial or full thickness loss of cartilage (Figure 2.5, Table 2.3).

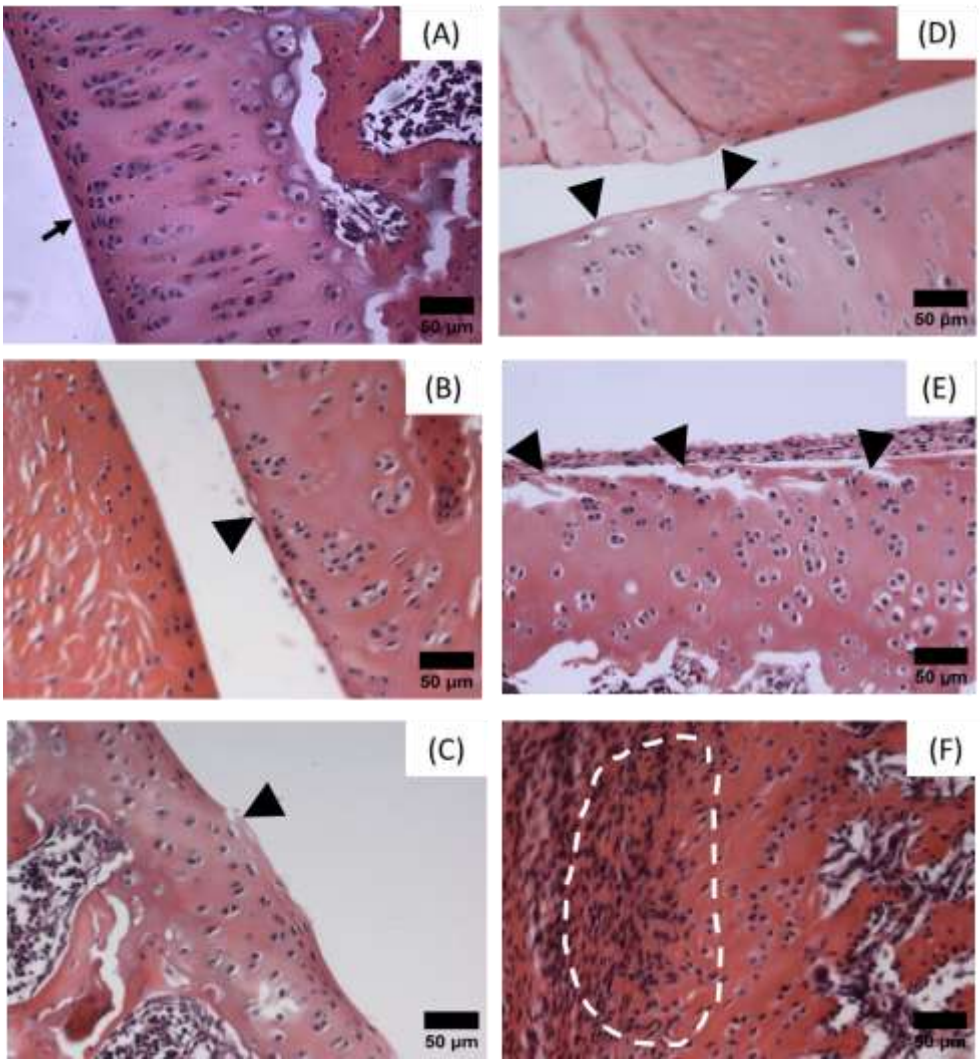

Figure 2.5: H&E staining in rat knee joint showing physical/morphological features used in cartilage damage scoring. (A) Normal. The arrow shows the normal cartilage surface. (B) Minimal surface damage only, Arrowhead shows a superficial wear. (C) Mild surface fibrillation (upper middle zone damage). Arrowhead shows mild surface tear. (D) Moderate damage - arrowheads show empty lacunae indicating damage into the midzone. (E) Splitting damage into cartilage deep zone that did not reach the tidemark. Arrows show splits. (F) Full thickness loss. Complete cartilage damage is shown by the dotted line where pannus infiltration occurs, and cartilage has been replaced/lost. Scale bar - 50µm for all images.

Table 2.3: Cartilage morphological damage scoring system.

Cartilage damage scoring	Description
0	Normal
1	Minimal surface damage only
2	Mild, upper middle zone
3	Moderate, well into mid-zone
4	Marked, into deep zone but not to tidemark
5	Full thickness degradation

Cartilage damage was also assessed by scoring of proteoglycan loss in cartilage, based on the degree / area of cartilage over which there was a loss of toluidine blue and/or Safranin O/Fast Green staining in cartilage (Gerwin et al., 2010) (Figures 2.6 & 2.7; Table 2.4).

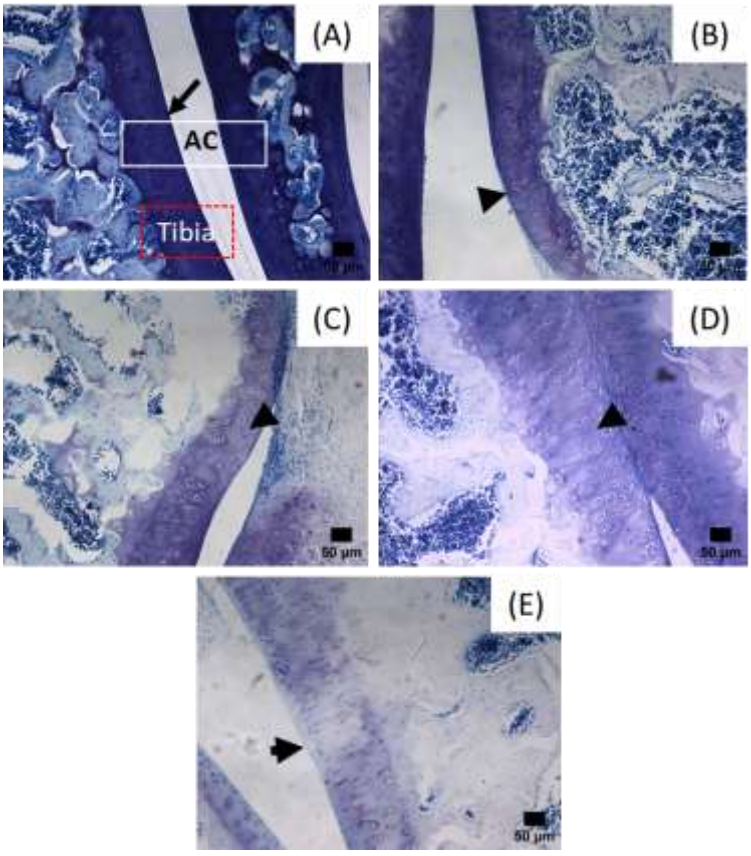

Figure 2.6: Toluidine blue staining in rat knee joint cartilage. (A) Normal proteoglycan content indicated by intense toluidine blue stain. (B) Mild proteoglycan loss showed 11–25% of cartilage damage indicated by loss in toluidine blue staining. (C) Moderate proteoglycan loss shown by 26–50% loss in toluidine blue staining. (D) Marked proteoglycan loss (51–75% reduction in toluidine blue staining) (E) Severe proteoglycan loss with greater than 75% toluidine blue reduction. Arrowheads show loss of toluidine blue in the tibia, whereas normal cartilage is indicated by an arrow. AC: articular cartilage. Scale bar, 50µm for all images.

Table 2.4: Cartilage damage scoring using toluidine blue and Safranin O staining for proteoglycan loss analysis.

Parameter	Grade	Toluidine blue staining	Safranin O staining
Cartilage degeneration score	0	No degeneration or loss	Normal proteoglycan staining
	1	Mild loss: 11–25% affected	Minimal loss (slight reduction) in superficial zone
	2	Moderate degeneration: 26–50% affected	Moderate loss (reduction) to mid zone
	3	Marked loss; 51–75% affected	Marked loss (reduction) in proteoglycan staining
	4	Severe loss; greater than 75% affected	Severe loss of proteoglycan staining

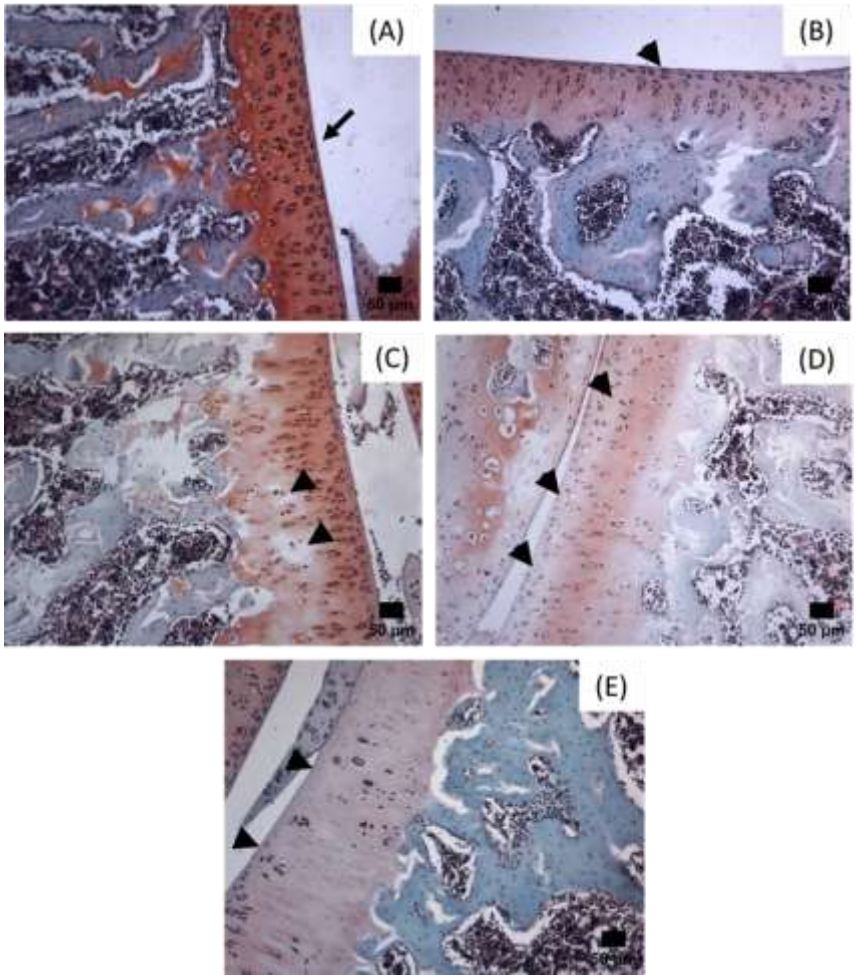

Figure 2.7: Safranin O staining in rat knee joint cartilage. (A) Normal proteoglycan staining. (B) Minimal proteoglycan loss (slight reduction SO stain in superficial zone. (C) Moderate proteoglycan loss into the mid zone. (D) Severe proteoglycan loss (E) Complete proteoglycan loss indicated by reduction of SO stain in the entire cartilage. Black arrow shows normal cartilage while arrow heads indicate areas of cartilage damage. Scale bar - 50µm for all images.

Synovial inflammation was scored on several features of inflammation including the thickness of the synovial lining/number of cellular layers, and infiltration/increased cellularity of the synovium and sub-synovial tissues (Figure 2.8, Table 2.5).

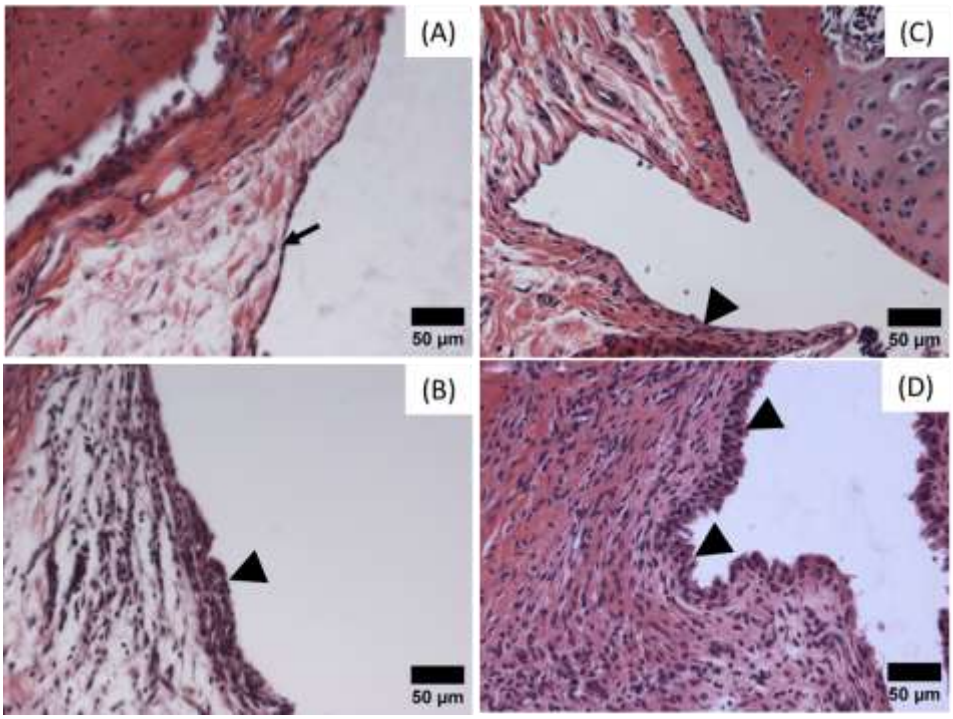

Figure 2.8: H&E staining in rat knee joint showing features identified in synovial inflammation scoring. (A) Normal with 1–2 layers of synovial lining cells. (B) Mild synovitis with increased number of lining cell layers (3–5 layers). (C) Moderate synovitis with further increased number of lining cell layers (6–8 layers). (D) Severe synovitis with greater increased number of lining cell layers (≥9 layers) and /or large increase in cellularity. Arrow indicating normal synovium while arrowheads show the inflamed synovium. Scale bar - 50µm for all images.

Table 2.5: Synovial inflammation scoring.

Synovial inflammation scoring	Description
0	Normal
1	Mild (lining 3- 5 layers)
2	Moderate (lining 6 – 8 layers or mild increase in cellularity
3	Severe (Lining > 9 cell layers and / or severe increase in cellularity)

Pannus (Figure 2.9) and the morphological FVT presence in bone marrow (Figure 2.10) were scored as either present or absent in H&E stained sections. Scoring for pannus was based on the appearance and thickness of the synovial lining, and any signs of infiltration of pannus into cartilage or bone.

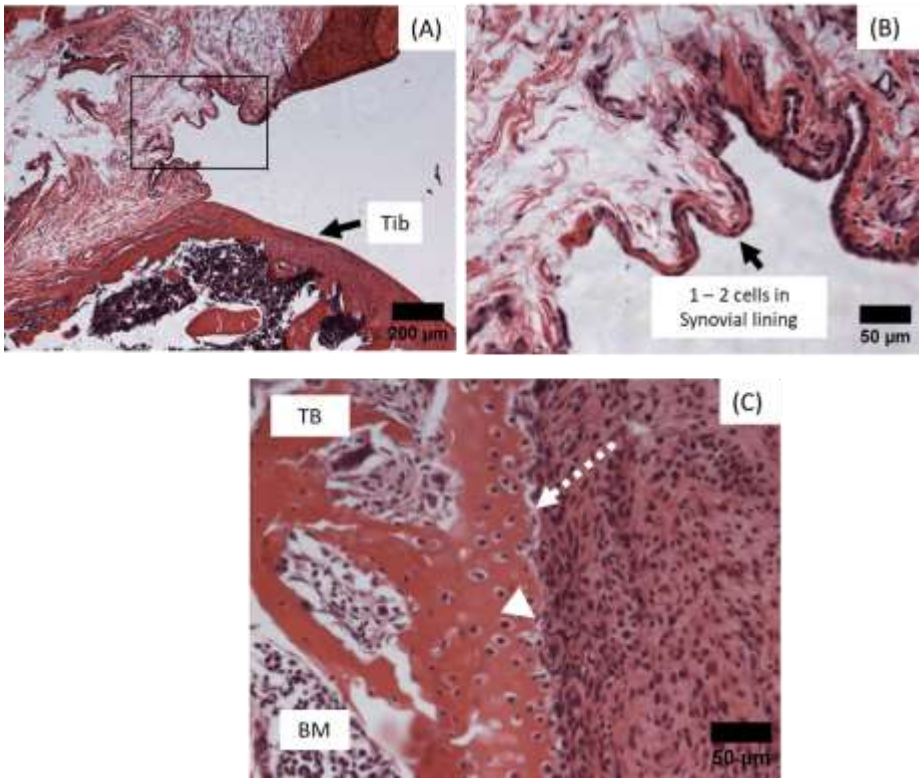

Figure 2.9. (A) Normal synovium, no pannus (B) Zoom image of A showing 1 – 2 cells in synovial lining, score 0. (C) Pannus infiltration into articular cartilage damaging the joint, score 1. Tib; tibia. BM; bone marrow, TB; trabecular bone. Dotted white arrow indicates pannus infiltration into articular cartilage, the white arrowhead shows the articulating cartilage/ joint. Scale bar - (A) 200 µm, (B & C) 50µm.

FVT scoring in H&E stained sections was based on the presence/absence of fibroblast proliferation and infiltration of inflammatory cells in the bone marrow (Figure 2.10), and analysis of Masson's trichrome stained sections, in which the degree of collagen deposition was assessed (Figure 2.11, Table 2.6).

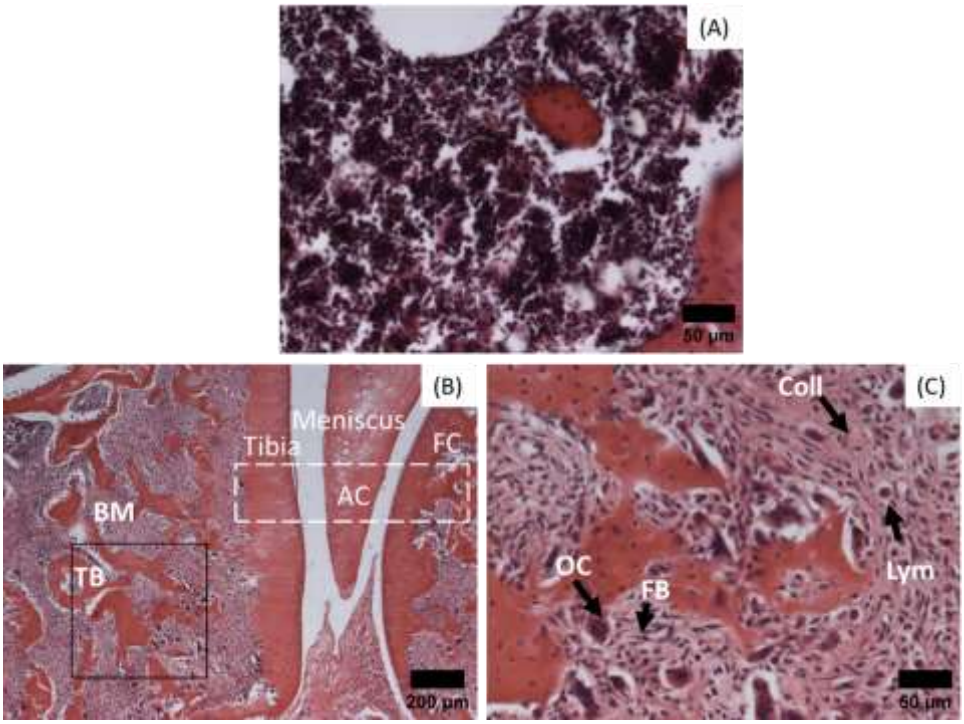

Figure 2.10: H&E staining in rat knee joint for FVT presence in bone marrow. (A) Normal bone marrow, score 0. (B) low power view of H&E stained inflamed joint; (C) zoom image of black box in B showing proliferation of fibroblasts, deposition of collagen, formation of thin-walled vascular channels, infiltration of macrophages, lymphocytes and plasma cells into bone marrow (score 1). Arrows indicate collagen fibres (Coll), osteoclast (OC), fibroblasts (FB), lymphocytes (Lym) in the bone marrow. White dotted box shows the articulating cartilage.

AC; articulating cartilage joint, TB; trabecular bone, BM; bone marrow, FC; femoral condyle. Scale bar – (A&C) 50µm, (B) 200µm.

Table 2.6: Bone marrow FVT based on collagen staining.

FVT score	Description
0	Normal, Perivascular collagen only
1	Focal paratrabecular or/and central collagen deposition without connecting meshwork
2	Paratrabecular or/and central deposition of collagen with focally connecting meshwork or generalized
3	Diffuse (complete) connecting meshwork of collagen

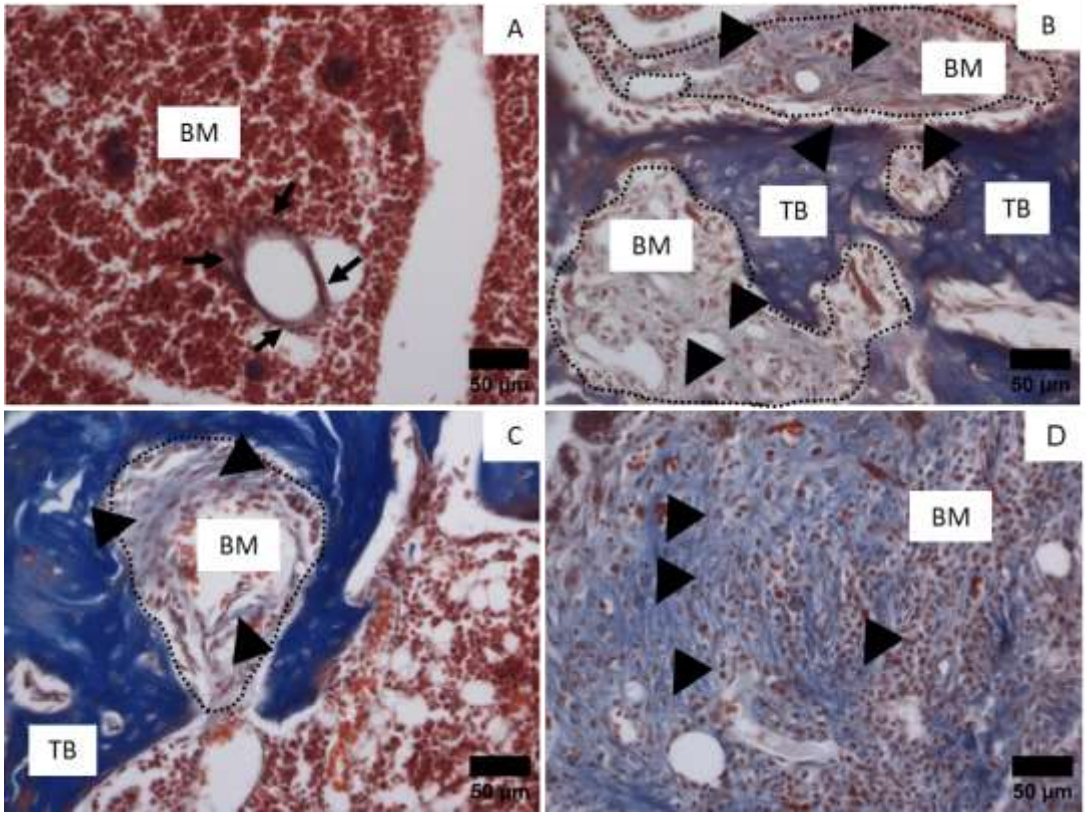

Figure 2.11: Collagen deposition scoring using Masson's trichrome staining. (A) Grade 0 corresponding to a normal bone marrow where there is only staining of the perivascular tissue (positive control) shown by arrows. (B) Grade 1 with a central collagen deposition without connecting meshwork; area with the dotted line and indicted by arrowheads. (C) Grade 2 shows presence of collagen fibres with central deposition which leads to a focally connecting meshwork shown by marked dotted area and arrowheads. (D) Grade 3 is the presentation of connecting meshwork of collagen shown in the whole image and indicted by arrowheads. TB: Trabecular bone; BM: Bone marrow. Scale bar - 50µm for all images.

2.7 Immunohistochemistry

Immunohistochemistry (IHC) is an important application for the detection of specific antigens in tissue sections ranging from amino acids and proteins by the utilization of monoclonal and polyclonal antibodies. It plays pivotal role in the diagnosis of diseases as well as in research laboratories (Brandtzaeg, 1998; Compton et al., 2015; Fukuvama et al., 1970; Garcia & Swerdlow, 2009; Guerrero et al., 2023; Imam, 1985; Oumarou Hama et al., 2022; Roskams, 2002; Terra et al., 2023; Truong & Shen, 2011; Yoon et al., 2020). Histological and histochemical methods are key tools in the analysis

of joint tissue samples for degenerative joint diseases in humans and in animal models (Schmitz et al., 2010).

Antibodies (Abs) are immunoglobulins formed by the humoral immune system by plasma cells for identification and neutralization of foreign antigens such as pathogenic bacteria and viruses. There are several types of antibodies including IgA, IgD, IgE IgG and IgM. Experimentally, the most used antibody is IgG which is composed of two light and two heavy chains joined by disulfide bonds (bridges) to form a "Y" shaped structure (Odell & Cook, 2013). Antibodies are further divided into two regions (1); a variable region and (2); a constant region (Figure 2.12).

The variable region includes fragment antigen binding (Fab) which is responsible for the antigenic specificity of an antibody, while the constant region of an antibody comprises a fragment crystallization (Fc) portion that binds cell surface receptors (Fc receptors) on the surface of circulating of immune cells. This binding is necessary to initiate an immune reaction (Figure 2.12).

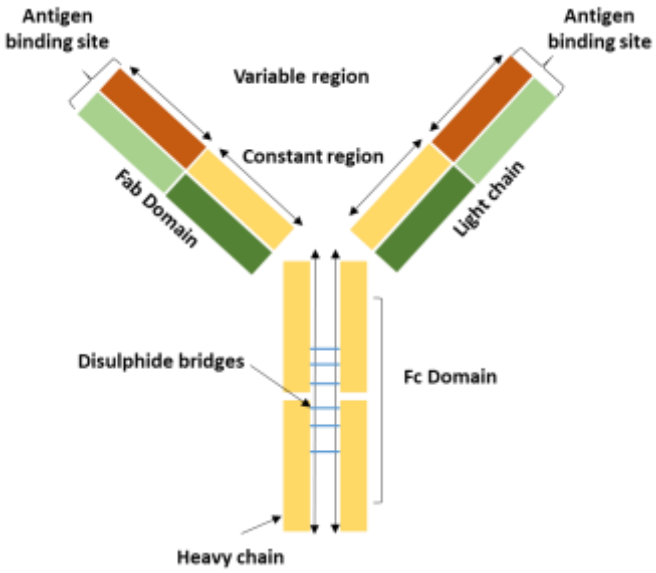

Figure 2.12: Diagrammatic representation of the "Y-shaped" structure of an IgG antibody molecule showing the light and heavy chains, disulphide bridges, Fab and Fc domains, and antigen binding sites.

Antibodies used in IHC are categorised in to two classes (a) monoclonal; (b) polyclonal. Kohler and Milstein were the first to describe the procedure used to produce monoclonal antibodies from an immunised animal (Köhler & Milstein, 1975). A monoclonal antibody secreting cell line is produced by hybridisation of the antibody producing lymphoid B cells with immortal myeloma cells to produce an immortalised antibody producing cell line, termed a hybridoma. Monoclonal antibodies produced in this way are a homogeneous population produced from a single B cell clone. They can bind with high specificity and affinity to a single epitope. This can be useful for the detection of a single member of a protein family and can distinguish proteins that may share a high percentage of amino acid identity. Polyclonal antibodies are acquired from experimental animals through repetitive stimulation of antigen. This produces a population of antibodies that recognize multiple epitopes in a single antigen which can give greater sensitivity but also potential for off-target or non-specific antibody binding.

Labelled secondary antibodies tagged with enzymes are usually used for the detection of the sites of interaction between the primary antibody and the target antigen. The avidin-biotin complex method labelled streptavidin biotin method (Figure 2.13), phosphatase anti-phosphatase method, polymer-based detection system are the commonly used detection systems (Hou et al., 2014), many of which also amplify the signal produced for more sensitive detection.

2.7.1 Indirect immunohistochemistry

There are two commonly utilized methods of IHC, known as direct and indirect methods. Irrespective of the specific method, the main purpose of this technique is the selective binding of the primary antibody with its specific target which can then be visualized with a chromogenic reaction catalysed by reporter enzymes for example Horseradish Peroxidase (HRP) or Alkaline Phosphatase (AP). In the case of direct IHC, the primary antibody is labelled directly with HRP or AP enzymes for detection of location (Figure 2.13A). The labelled primary antibody method is faster, less expensive and reduces the necessity for a secondary antibody and additional incubation phases for signal detection. However, indirect detection is usually the preferred strategy because of its higher sensitivity and amplified signal.

Indirect IHC is a technique that uses an unlabelled primary antibody to bind to the antigen of interest. The antigen is then detected by a secondary antibody that is raised against the host species of the primary antibody. The secondary antibody is conjugated or labelled to enable detection of the antigen. The secondary antibody is either bound directly to a chromogen, labelled with a fluorescent agent to produces a chromogen, or bound to a target such as biotin which can then bind to molecules with enzymatic activity such as HRP or AP. Use of several secondary antibodies that bind different epitopes of the primary antibodies can provide high flexibility in detection of a wide range of primary antibodies against different antigens in the same tissue or location.

There are several mechanisms used to amplify the signal generated in IHC such as peroxidase/anti-peroxidase (PAP), the Avidin-Biotin complex (ABC), Labelled Streptavidin Biotin (LSAB), or Polymer-based detection methods. However, the most used detection methods are peroxidase/anti-peroxidase (PAP) and the Avidin/Biotinylated enzyme complex (ABC). PAP detection depends on the formation of a peroxidase/anti-peroxidase complex (Figure 2.13B), which connects to the primary antibody through a secondary antibody and is the most extensively used method in diagnostic immunohistochemistry.

The ABC method is the most popular and widely used IHC detection method in experimental science and involves non-covalent interaction between avidin and biotin as an amplification step. Avidin is a large (67 - 68 kDa) tetrameric glycoprotein, found in the egg-whites of birds, amphibians, and reptiles, with enormously high affinity for a biotin molecule. Up to four biotin molecules can bind per avidin molecule. Biotin is a small vitamin (~244 Da) and act as an essential co-enzyme for mammalian carboxylases in the synthesis of fatty acids, gluconeogenesis, and metabolism of amino acids. Due to the moderate size of biotin, it easily conjugates with other macromolecules for example avidin without altering their activity. Its carboxylase activity is not needed in the ABC method.

The ABC method consist of a three-step detection technique that involves the binding of the primary antibody to the specific target antigen, and binding of the biotinylated

secondary antibody to the primary antibody. The secondary antibody, raised against the host species in which the primary antibody was raised, acts a link between the primary antibody and the ABC complex. Due to the binding properties of avidin and biotin, extensive enzyme/avidin/biotin complexes can form resulting in very strong signal amplification at the antigenic site (Figure 2.13C). The elevated enzyme:antibody ratio and high sensitivity makes the ABC detection system one of the most widely used techniques in both diagnostic and research fields.

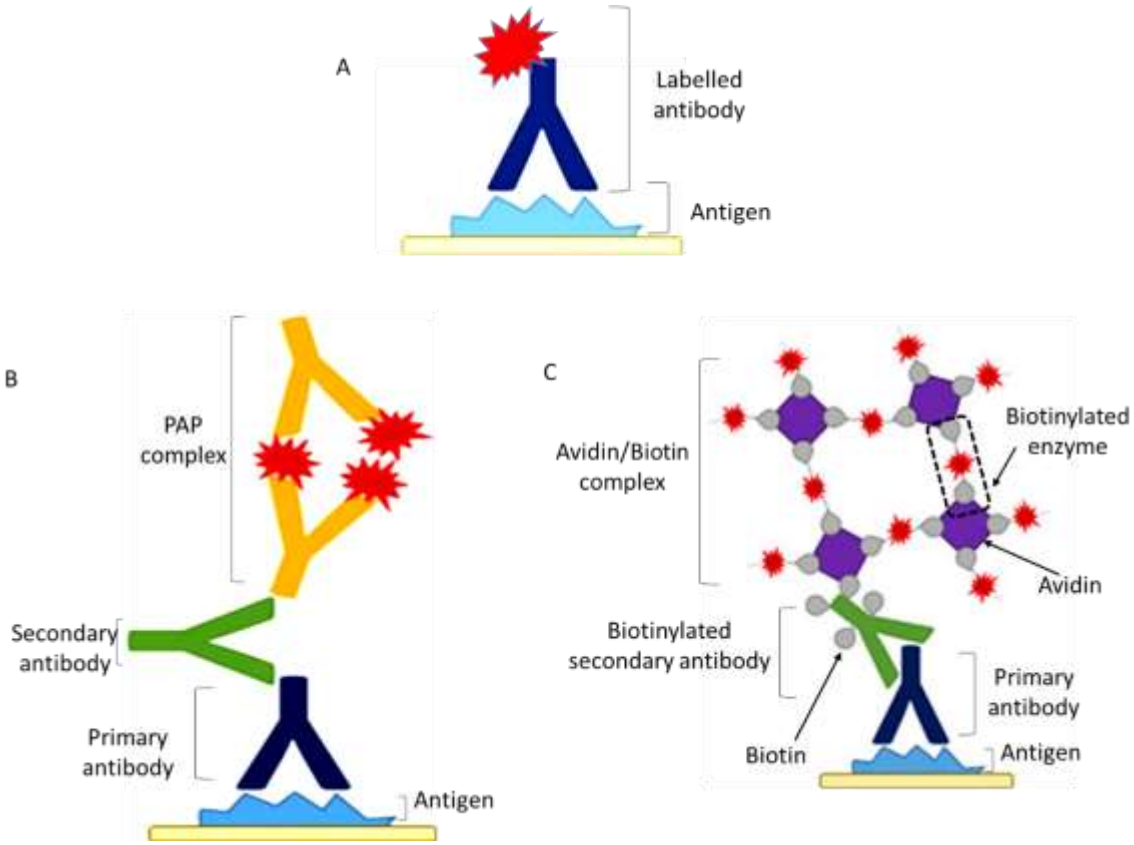

Figure 2.13: Schematic illustration (A) Direct IHC detection: the primary antibody is directly labelled with a chromogenic or fluorescent molecule. (B) PAP detection method involves the binding of an unlabelled primary antibody (dark blue) to the antigen of interest (light blue) on the cell surface (yellow matrix). The secondary antibody binds both the unlabelled primary antibody (dark blue) and the PAP complex (yellow), which produces a signal (red). (C) ABC detection method: Like the PAP method, the secondary antibody binds the unlabelled primary antibody (dark blue). The primary antibody is then recognised by a biotinylated secondary antibody (green). Subsequent incubation with avidin (purple) and the biotinylated-peroxidase enzyme (grey), ABC are formed. These amplify the signal and can be visualised using different chromogens, such as DAB. (Adapted: Enzo Life Sciences, Plymouth Meeting, PA, USA).

2.7.2 General indirect immunohistochemistry protocol and workflow

Existing protocols for different antibodies were performed to validate and optimise immunohistochemistry experiments to visualise CD31, SRPK1, and SRSF1 immunoreactivity. Details on the individual antibodies and reagents used are shown in Table 2.8 and 2.9, respectively. The master IHC protocol with original reagent concentrations can be seen in Figure 2.14 below, while the adjustments made for each antibody are discussed in the results chapters. Details on how each primary antibody was optimized in the master protocol and how non-specific staining was minimized can be found in section 2.7.3.

Different stages involved in IHC are illustrated in Table 2.7. The slides underwent de-waxing and rehydration through a process involving xylene and graded methanol (100%, 70%, and 50%), followed by a wash in Tris buffered saline (20 mM Tris, TBS, , 0.9% NaCl pH 7.4). Antigen retrieval was performed because the epitopes may be cross-linked and inaccessible after fixation making it difficult for antibody-binding. The cross-linked epitopes can be re-opened by pre-treatment with antigen retrieval reagents or procedures allowing antibody access to target antigens. Antigen retrieval was done using Tris-EDTA solution (10mMTris, 1mM EDTA, 0.05% Tween-20 buffer, pH9) solution at 65 - 80°C for 20 - 30 minutes. The slides were immersed in the buffer preheated to boiling point using a microwave. They were then placed in a closed box inside a water bath. The temperature of the water bath was adjusted depending on the antibodies used and how it affected the adhesion of the sections to the slides. The specific temperature for each antibody is shown in relevant chapter methods sections. After 20-30 minutes slides were left to cool in running tap water for 10 minutes. Tissues were then circled with a PAP pen to minimise the volume of reagents and avoid drying out the tissue. Blocking of endogenous peroxidase was done by incubating slides in 0.3% H_2O_2 for 20 - 30 minutes in a humid environment at room temperature, followed by TBS wash and incubation with a blocking solution (1.5 % NHS (normal horse serum) + 1% BSA (bovine serum albumin in TBS) in a humid environment at 4°C. The concentrations of H_2O_2 and NHS and BSA in blocking solution used were different for each antibody and are detailed in the results chapters. Blocking buffer was removed by aspiration, and sections were washed with TBS and incubated with the primary

antibodies diluted in blocking solution overnight at 4°C, and at concentrations specific to individual antibodies (Table 2.8). Sections were then washed with TBS before incubation with secondary antibodies diluted in blocking solution (1.5% NHS + 1% BSA, at the concentrations in Table 2.8) in a humid environment at room temperature. The sections were washed with Tris-buffered saline + 0.1% Tween 20 (TBST) before applying the ABC horseradish peroxidase kit (Table 2.9) for 30 minutes, followed by a TBST wash and 3,3'-diaminobenzidine (DAB) precipitation staining for 15 minutes. All incubations were performed at room temperature in a humid environment. After performing DAB staining, the slides were washed for 5 minutes in deionized water. Then, they were counterstained with haematoxylin for 10 seconds and washed again in water. This was done to prevent the staining from interfering with the DAB signal. The tissue was then dehydrated in graded methanol and cleared in xylene. Finally, the tissue was mounted with glass coverslips using DPX mountant (Sigma-Aldrich 44581).

Table 2.7: Stages involved in immunohistochemistry.

Tissue preparation	stages in the process	Analysis
specimen fixation and tissue processing	1. antigen retrieval 2. non-specific site block 3. endogenous peroxidase block 4. primary antibody incubation, and the employment of systems of detection, revealing and counterstaining and 5. slide mounting and storage	interpretation and quantification of the obtained expression

Table 2.8: List of antibodies, sources, and dilutions.

Antibodies	Working conc.	Catalogue no.	Details	Manufacturer
Anti-CD31 antibody 0.2mg/ml,	1:100	AF3628	CD31/ PECAM-1 Antibody (Goat IgG)	R&D, UK
Anti-EF5, ELK3-51 2mg/mL	75µg/mL	EF5-30A4	EF5 Hypoxia detection kit, Alexa Fluor488	ThermoFisher Scientific, UK
Anti-SRSF1 antibody 0.5mg/mL	1:100	32-4500	Mouse monoclonal anti- SRSF1 (96)	ThermoFisher Scientific, UK
Anti-SRPK1 antibody 0.2mg/mL	1:300	Ab90527	Rabbit polyclonal antiSRPK1	Abcam
anti-SRPK1 antibody 1mg/mL	1:200	SAB4502857	Rabbit polyclonal Anti SRPK1	Sigma Aldrich, UK
Secondary Donkey anti-Goat IgG 0.2mg/ml,	1:200	BAF109	Donkey anti-Goat IgG Secondary Ab (Biotinylated Ab)	R&D, UK
Secondary Goat anti-Rabbit 0.60mg/mL	1:100	656140	Goat anti-Rabbit IgG Secondary Ab (biotinylated Ab)	Invitrogen, UK
Secondary goat anti-mouse 1.3 mg/mL	1:100	31800	Goat anti-Mouse IgG Secondary Ab (Biotinylated Ab)	ThermoFisher Scientific, UK
M.O.M.® (Mouse on Mouse) Immunodetection Kit		BMK-2202	For blocking of mouse epitopes and detection of IgG primary antibodies on mouse tissue sections.	Vector laboratories

Table 2.9: Reagents used in immunohistochemistry.

Reagents	Working conc.	Catalogue no.	Details	Manufacturer
H_2O_2 (30%)	0.3%	2167633	Hydrogen peroxide solution	Sigma Aldrich, UK
BSA	1 -5%	A7906	Bovine serum albumin	Sigma Aldrich, UK
NHS 60mg/mL	1.5 -3%	135899	Normal horse serum	Jackson Immuno Research
EDTA	1mM	15697	Ethylene diamine tetra acetic acid	USB corporation, USA
Trizma Base	10mM	T6066	-	Sigma Life sciences, UK
ABC kit	-	PK-4000	Avidin-biotin complex/horseradish peroxidase standard kit	Vector Laboratories Ltd, UK
Tween 20	0.05%	P1379	-	Sigma Aldrich, UK
DAB	-	SK-4100	Peroxidase substrate kit	Vector Laboratories Ltd, UK
Haematoxylin	-	361075	Harris haematoxylin (mercury-free)	RAL-diagnostics, France
DPX mountant	-	STBGG996	Distyrene Plasticizer Xylene	Sigma Aldrich, UK

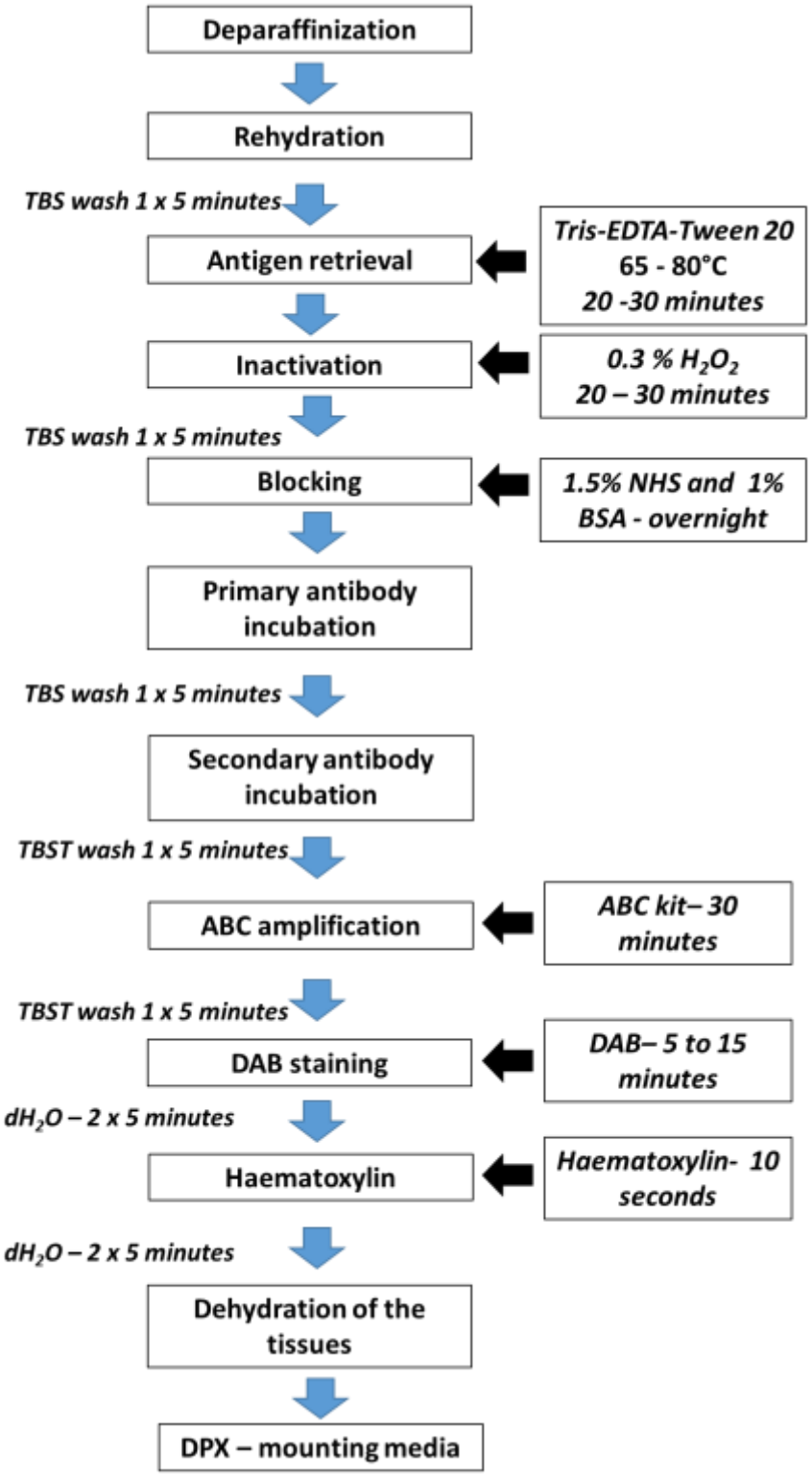

Figure 2.14: Flow diagram showing the master protocol for IHC. Adjustments and changes were made for specific antibodies as detailed in results chapters.

2.7.3 Optimisation of conditions in immunohistochemistry

The aim of IHC is to achieve specific staining and to minimise non-specific background staining. There are various conditions that influence the outcome and quality of IHC. The conditions which were changed to optimise the IHC protocols for different antigen targets were:

- antigen retrieval temperature,
- washing time,
- H_2O_2 concentration and incubation time,
- concentration and incubation time of NHS and BSA,
- Control for antibodies.
- Primary antibody and secondary antibody concentration.

A series of initial experiments were conducted changing a single parameter between the runs to optimise of conditions for IHC. The optimal concentration of primary antibody was unknown, so on first use antibodies were first used at several different dilutions (1:300, 1:200, 1:100), to give an idea of a suitable concentration. Simultaneously different antigen retrieval methods were explored using citrate buffer or Tris buffer (incubation for 20 mins at 90°C and 30mins at 75°C in either buffer).

A. Antigen retrieval

Antigen retrieval is crucial for IHC standardization to unmask binding epitopes for antibody in formaldehyde-based fixation due to the cross-linking of amino groups on end-to-end molecules, which limit antigen: antibody interactions (Fox et al., 1985). Various approaches can be used for antigen retrieval such as proteolytic/enzymatic or heat induced methods. In proteolytic-induced epitope retrieval (PIER), the retrieval is done using proteinases such as trypsin, proteinase K or pepsin for degradation of protein links which allows the interaction of primary antibody and antigen. The most used procedure is heat-induced epitope retrieval (HIER) which uses heat and buffers, for example Tris-EDTA pH 9 or citrate buffer pH 6, to break the protein-protein cross-linking. The samples are placed in either a basic or acidic buffer solution and incubated at high temperature (65 – 80^{o}C) either in a water-bath or microwave to promote

degradation protein cross-links. There are important factors to considering when using HIER in IHC, such as the chemical composition of the retrieval buffer, the use of different heating devices (e.g. water bath, heating plate, pressure cookers, autoclaves and microwave ovens), temperature and duration of heating. To optimise the protocols for antibodies used in this thesis, a variety of different combinations of these were tested to identify the best combination to retrieve the masked epitopes with maximum efficiency, to optimise IHC signal, while maintaining the tissue integrity. The two most common practices for heating use water-baths or microwave ovens. Previous use of microwave approaches in the lab had resulted in rapid boiling and evaporation of buffer solutions and poor temperature control (Dimitrios Amanitis, 2022), so I used water bath approaches for antigen retrieval. Further details on HIER protocols optimisation for specific investigations are in later chapters.

B. Non-specific IHC staining

Non-specific staining in IHC can occur when primary or secondary antibodies bind to unintended antigens, leading to high background staining and masking of the desired antigen signal. To reduce non-specific binding, a blocking solution can be used before incubating tissue samples with the primary antibody. Protein blocking reagents and serum are often used to prevent antibodies from binding to non-specifically to Fc receptors present on cell surfaces. However, serum used for blocking should be obtained from a different species than the primary antibody, as using serum from the same species may result in significant non-specific signal. To achieve optimal results, it is recommended to use a serum that matches the species in which the secondary antibody was raised. Either casein or BSA can be used to prevent non-specific binding of antibodies with no requirement of matching these reagents to the secondary antibody species. The most used protein blocking reagent is BSA.

When using serum for blocking, it is important to make sure that the serum comes from a different species than the primary antibody. This is because using serum from the same species could lead to significant non-specific signal. To get the best results possible, it is recommended to use serum from the same species in which the secondary antibody was raised.

High background or nonspecific staining may also appear because of endogenous peroxidase activity when using the HRP detection method. Endogenous peroxidases are found in tissues such as liver, kidney, and those containing red blood cells for example vascular tissue, or if tissues are not perfused to remove blood prior to removal. Endogenous peroxidase results in nonspecific staining because it reacts with H_2O_2 to reduce the 3, 3'-diaminobenzidine (DAB) substrate or any other peroxidase substrates. To analyse the endogenous peroxidase activity level, test tissues can be incubated with DAB before incubation with primary antibody. A blocking step is required if tissues have high levels of endogenous peroxidase, indicated by brown staining on DAB incubation. Tissue incubation in 0.3% H_2O_2 for 10 -15 minutes is considered adequate for blocking endogenous peroxidase activity. I used different concentrations of BSA as well as H_2O_2 for blocking non-specific antibodies binding and endogenous peroxidases activity, as discussed in detail in later chapters.

After incubating samples with primary and secondary antibodies, two main steps of IHC protocols can be used such as signal amplification and visualisation steps using ABC or alkaline phosphatase (AP) amplification followed by DAB visualisation. Both steps can cause non-specific staining. Biotin is present in many tissues so blocking nonspecific binding by this compound is required. Non-specific avidin/biotin staining can be reduced with pre-incubation of the tissue sections with avidin followed by biotin to block biotin binding sites on the avidin molecule, prior to incubation with the biotinylated secondary antibody.

As mentioned, HRP or AP enzymes can be biotinylated and used for visualisation of antigen: antibody complexes with enzymatic chromogenic reactions. Blocking endogenous peroxidase activity is described above. Blocking of endogenous AP is necessary when endogenous AP is present, which can be determined by incubating the tissue with 5-bromo-4-chloro-3-indoyl phosphate (BCIP) in combination with nitro blue tetrazolium (NBT), where an appearance of blue colour indicates the presence of endogenous AP. Levamisole (Ponder & Wilkinson, 1981) or 1% acetic acid are used to block endogenase AP. Levamisole is the equivalent to using H_2O_2 for blocking

endogenous peroxidase, and acetic acid is used in tissues where Levamisole is ineffective such as when blocking intestinal AP.

I used DAB staining to visualise all antigen: antibody complexes in IHC. In this technique the conjugated HRP oxidises DAB and result in the formation of a brown precipitate. These brown precipitates can be visualised via light microscopy. When tissues are incubated with DAB for a long time, it can result in decreased signal to noise ratio due to non-specific precipitation in the tissues and high background staining. To avoid this problem, I kept the duration of DAB incubation to 15 minutes. This was sufficient to enhance immunoreactivity and prevent any increase in non-specific staining, for further analysis.

C. Controls for IHC

The inclusion of appropriate controls is crucial for analysis of IHC results and confirmation of the specificity of the antibodies used (Burry, 2011). There are different types of controls used in IHC such as negative, positive and antibody isotype controls. All controls should be run in parallel with each experiment. Negative controls are important to exclude false positive staining. The most common negative control is omission of the primary antibody from the staining run with replacement with serum solution (NHS + BSA). This will confirm the specificity of the secondary antibody and identify any non-specific binding caused by the secondary antibody if present. There will be no staining if the secondary antibody is specific to the primary antibody, background staining may occur if the secondary antibody binds to alternative sites in the tissue. Secondary antibody may bind to charged groups in cells in fixed tissues, this can usually be prevented by the addition of BSA to the normal serum in blocking solution (Burry, 2011). If negative controls show positive staining this would indicate elevated levels of unspecific background staining or a lack of specificity of the antibody which can be avoided by optimising the conditions discussed above. A positive control, such as inclusion of a tissue sample known to express the target protein which should show positive staining in predicted locations should also be included in each experiment.

I routinely ran two controls for IHC staining, (a); the primary antibody was omitted and replaced with blocking solution (NHS + BSA) alone; (b) the secondary antibody was omitted, and only primary antibody was used. No signal with omission of the primary antibody indicates that non-specific binding is not caused by primary antibody but may be caused by the secondary antibody. To determine whether the primary antibody shows non-specific binding, an IgG isotype control can be used at the same concentration as the primary antibody under the same experimental conditions. Isotype controls are used only for monoclonal antibodies. An isotype control uses the same class and subtype as the primary antibody raised against the target of interest, e.g. an IgG, that does not bind specifically to a potential or known target. The purpose of including isotype control is to verify that the binding of the primary antibody is specific for the antigen, and there are no nonspecific interactions with Fc receptor proteins. I did not see any signal when primary antibodies were omitted, and most of my primary antibodies were polyclonal, so I did not use isotype controls.

There are further IHC controls such as negative tissue (a tissue known not to express the target protein), anti-body absorption and endogenous tissue background controls. Negative tissue controls can reveal false positive or nonspecific binding using tissues which do not express the protein of interest. An absorption control is performed to determine antibody specificity to the protein of interest, using prior incubation of the primary antibody at an antigen to antibody working dilution of 10:1 molar ratio. This pre-absorption technique should result in binding of protein to all available antibodies. The pre-absorbed antibody solution is then used in place of the primary antibody in the standard protocol and should result in no tissue staining as antibody binding sites are blocked and cannot binding to tissue epitopes. This control is not always possible to use, due to limitations in obtaining the necessary specific purified immunogens. It is a highly specific control for verification of specific primary antibody binding/staining.

Endogenous tissue background controls are performed because some tissues have inherent properties resulting in background staining (or natural fluorescence that can confound immunofluorescence) which can result in misinterpretation of results. One example is background staining resulting from endogenous tissue peroxidase described above. Tissues should be inspected, prior incubation with primary

antibodies, using bright field illumination (chromogenic labels) or fluorescence microscopy (for immunofluorescence) to ensure that there is no endogenous background.

Finally, optimisation included omission of both primary and secondary antibodies to determine whether the reagents used in the IHC caused non-specific staining. This allowed me to identify non-specific staining caused by the ABC / DAB kit reagents, which were then replaced.

2.8 SRPK1 and SRSF1 expression in rodent models of inflammatory arthritis

SRPK1 and SRSF1 expression was studied in rodent synovium using the general IHC protocol (SRPK1 as in section 2.7.2, Figure 2.14) with specific modifications detailed in Chapter 6, Table 6.1.

2.8.1. Mouse-on-mouse (M.O.M) immunohistochemistry method

When using antibodies generated in mouse to detect protein expression in mouse and sometimes rat tissues, there is a risk of high non-specific binding. The detection of anti-mouse antibodies in mouse tissues is very challenging because anti-mouse detection antibody cannot distinguish between the endogenous mouse immunoglobulins present in mouse tissue and a primary antibody produced in mouse and results in obscuring specific staining due to in high background staining. To block mouse endogenous immunoglobulins in a mouse tissue, M.O.M blocking solution is used which controls the background nonspecific staining. The only suitable, specific and available anti-SRSF1 antibody is raised in mouse, and so I optimised the mouse-on-mouse protocol for SRSF1 identification in synovium.

Table 2.10: Working solutions for M.O.M IHC protocol.

Solution	M.O.M. working solutions
1	➢ M.O.M. Mouse IgG Blocking Reagent: add 2 drops (90 µL) of M.O.M Blocking Reagent stock solution to 2.5 mL of PBS or TBS
2	➢ M.O.M. Diluent: add 600 µL of M.O.M. Protein Concentrate stock solution to 7.5 mL of PBS or TBS
3	➢ M.O.M. Biotinylated Anti-Mouse IgG Reagent: add 10 µL of M.O.M. Biotinylated Anti-Mouse IgG stock solution to 2.5 mL of M.O.M Diluent prepared above

2.8.1.2 Staining procedure

The M.O.M IHC protocol is similar to the general IHC method (section 2.7.2) apart from a few differences such as the use of specific M.O.M blocking reagents and an additional Avidin/Biotin blocking step. Paraffin embedded tissue sections were deparaffinised and hydrated by xylene and descending concentration of methanol (100%, 70% and 50%), respectively followed by washing with TBS. Antigen retrieval was done for 30 minutes using Tris-EDTA (pH9) solution to unmask antigen epitope, followed by washing with TBS for 10 minutes (2x). Avidin/Biotin blocking was performed using Avidin/Biotin Blocking Kit (SP-2001). Tissue sections were then incubated for 1 hour in working solution of prepared M.O.M. Mouse IgG blocking reagent and subsequently washed for 10 minutes (2x) in TBS followed by incubation for 5 minutes in working solution of prepared M.O.M. diluent. Primary antibody was diluted in M.O.M. diluent to the working concentration and applied on the tissues sections, after M.O.M. Diluent removed, for overnight followed by washes with TBS for 10 minutes (2x). Sections were incubated with working solution of prepared M.O.M. biotinylated anti-mouse IgG for 2 hours followed by TBS washes for 10 minutes (2x). Avidin/Biotin and DAB was used as detection system and visualise signal, respectively. Finally, the tissue was dehydrated in graded methanol and xylene and mounted with glass coverslips using DPX.

2.8.2 SRPK1 and SRSF1 fractional area of expression in inflamed rodent synovium

Following staining for SRPK1 and SRSF1, fractional area of expression in synovium was measured in three images taken per joint section – from two sections per animal from mice and one section per animal from rats. Images were captured using a Zeiss Axioskop-50 microscope (Carl Zeiss, Welwyn Garden City UK), a 3-CCD camera and KS300 imaging software (Zeiss). All slides were blinded to condition throughout image capture and analysis.

A custom macro in the KS300 software (housed in Prof. David Walsh's laboratory City Hospital Nottingham) was used for SRPK1 and SRSF1 fractional area calculation in synovium (Figure 2.15). The area was selected for analysis was based on hotspot regions having greater expression of staining (Figure 2.15A). The region of interest (ROI) was identified and highlighted (Figure 2.15B) to isolate the region of staining. The ROI was isolated (Figure 2.15 C&D), a threshold set to identify stained cells (Figure 2.15E) and background subtracted to identify only stained cells (Figure 2.16 F&G). Background levels for subtraction were set from negative control sections. Data were extracted from the software and held in Excel (Microsoft365). The total positive area and the total area of staining in cells were used to calculate fractional area of expression.

$$Fractional\ area\ expression = \frac{Total\ area\ of\ staining\ in\ cells}{Total\ positive\ area}$$

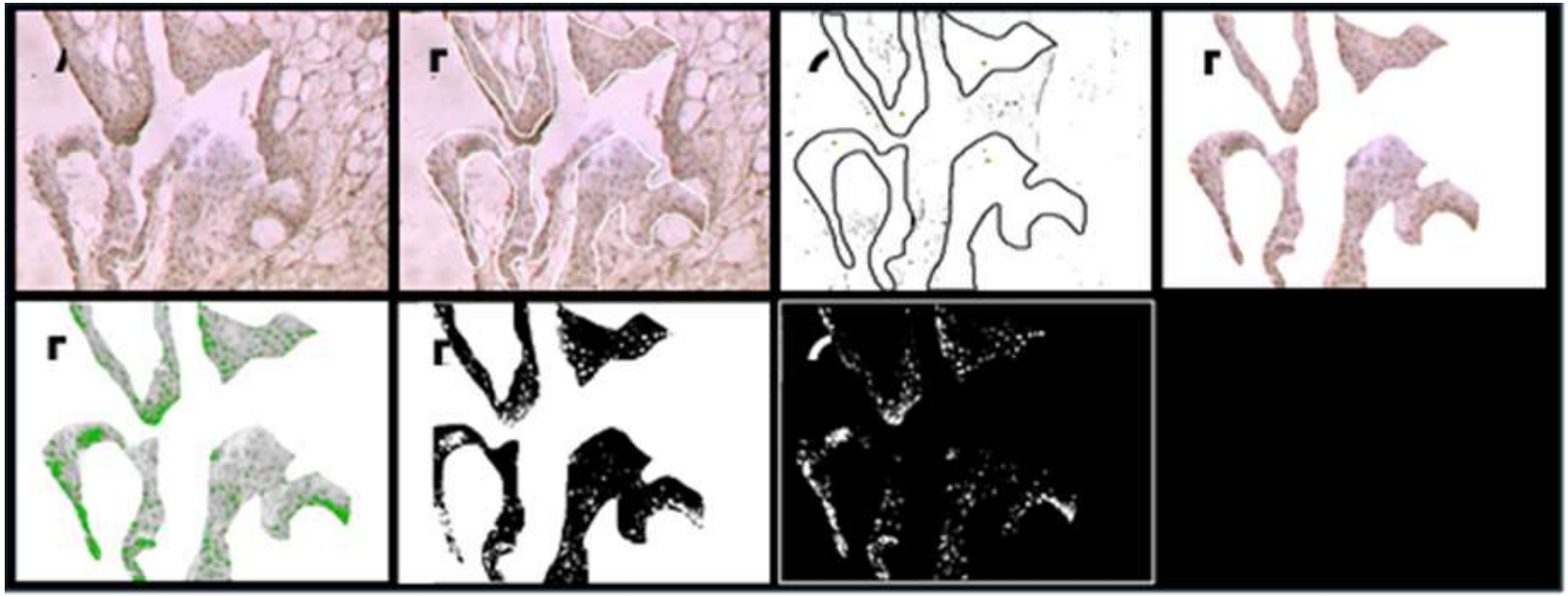

Figure 2.15: Method for quantification of % area of SRSF1 staining. (A) Photomicrograph showing the area of interest with synovial cells stained with SRSF1 antibody. (B) Areas of interest selected to separate the region of interest (ROI). (C) The ROI of SRSF1 staining was isolated and (D) background was removed to isolate the ROI. (E) Positive cellular staining identified and threshold set. (F). Background threshold set and positive cellular staining identified (G) Final image analysed for cellular SRSF1 staining and percentage area with staining calculated.

2.8.3 SRPK1 and SRSF1 expressing cells and nuclear localisation.

To calculate SRPK1 and SRSF1 nuclear localisation (NL) in synovium from the mice and rat (sham vs CFA inflamed), three images per section, two sections per animal from mice and one section per animal from rat, were captured from areas of hotspot staining using a light field Leica DM4000B microscope. To ensure consistency in the analysis, I selected three hotspot regions for quantification, taking into account that a maximum of three hotspots can be considered from uninflamed tissue in both mouse and rat tissues.

A. Identification of SRPK1 and SRSF1 positively stained cells

Positively stained cells were identified as those cells which had clear and distinct cytoplasmic and nuclear IHC staining compared to unstained areas and control sections.

B. Identification of SRPK1 and SRSF1 nuclear staining in cells

The evaluation of SRPK1/SRSF1 NL was done using ImageJ (Rueden et al., 2017). SRPK1 and SRSF1 activation was measured by the degree of NL of SRPK1 and SRSF1 compared to total number of cells with positive stained in synovium using ImageJ. The number of cells with strong nuclear staining was counted. Strong nuclear staining was defined as staining in more than 70% of the nuclei. The number of cells with strong nuclear staining was then divided by the total number of positive cells (cells with nuclear staining, cytoplasmic staining and cells having positive but less than 70% nuclear staining) in the surrounding area, to provide a ratio demonstrating the percentage of SRSF1 NL. Figure 2.16 shows the procedure for cell counting in normal (a) and inflamed synovium (b). Cell counter was used indicating total number marked as 1 (nuclear staining, cytoplasmic staining and cell having less than 70% of staining) and nuclear staining marked as 2.

$$Nuclear\ localisation = \frac{Total\ number\ of\ cells\ with\ nuclear\ stain\ only}{Total\ number\ of\ postive\ stained\ cell\ (nuclear + cytoplasmic)}$$

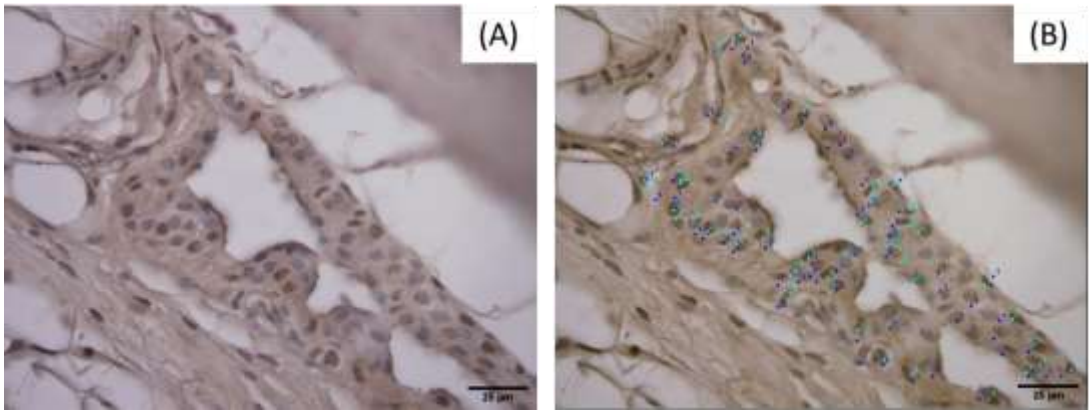

Figure 2.16: Fiji software - ImageJ used for the analysis of nuclear localisation of SRSF1 in (A) synovial cells including macrophages like synoviocytes and fibroblast like synoviocytes in tibiotalar mouse joint. (B) ImageJ quantification of stained cells in synovium. Blue dots indicate cells with positive cytoplasmic staining and cells with less than 70% of staining in the nucleus (nuclei show slightly blue with haematoxylin stain) while green dots show cells with strong brown nuclear staining. Scale bar = 25µm.

2.9. Statistical analyses

Data were extracted from images as described in results chapters. Statistical analysis of data used Student's t-tests or Mann-Whitey U tests for comparisons of two groups, and one way ANOVA followed by Dunnett's or Sidak's multiple comparison tests for comparison of three or more groups. Dunnett's tests were used for statistical comparisons with a single control, and Sidak's tests were used for selected multiple independent comparisons. Statistical p value < 0.05 was considered as significant.

3. COMPARISON OF DIFFERENT COMPLETE FREUND'S ADJUVANT FORMULATIONS ON RAT KNEE JOINT MODELS OF INFLAMMATORY ARTHRITIS

3.1 INTRODUCTION

Animal disease models have been established and used for many years to explore the mechanisms and pathogenesis of inflammatory arthritis as well as for testing of efficacy of therapeutic agents. Mice and rats are the most widely used animal species in the study of induced arthritis. Arthritis is induced in these species by several different methods such as direct injection of arthritogenic stimuli into the joint or systemically, or by means of joint destabilisation using surgical approaches (Fischer et al., 2017; Glasson et al., 2007).

Many different arthritogenic reagents have been used to induce acute or chronic inflammatory arthritis models. These include irritants, enzymes, and toxins such as carrageenan with or without kaolin, collagenase and distinct molecules that can directly stimulate an immune system response. Among the most widely used approaches to stimulate immune reactions are adjuvants, immunisation against collagen, or administration of autoreactive antibodies or sera (Bevaart et al., 2010; Sardar & Andersson, 2016).

Complete Freund's adjuvant consists of a suspension of heat-killed mycobacteria in mineral oil, usually *Mycobacterium tuberculosis* or *butyricum*, often with an emulsifying agent (Freund et al., 1947). For the induction of inflammatory arthritis in rats, CFA was originally administered systemically by injection at the tail base (Boyle et al., 2002) when it stimulates a multiarticular reaction, but more latterly it has been administered locally, in refined, usually single joint models (Butler et al., 1992; Chillingworth & Donaldson, 2003; Donaldson et al., 1993). CFA injection is hypothesised to trigger an immune reaction involving T lymphocytes and macrophages, due to structural similarities between Mycobacterium cell wall constituents and proteoglycans. This

results in T-cell-dependent destructive relapsing-remitting inflammatory articular disease, with pannus formation, and cartilage and bone damage (Barbosa et al., 2014; Hawkins et al., 2015; Kong et al., 1999; Pearson & Wood, 1959; Rainsford, 1982).

No animal model of rheumatoid or osteoarthritis is capable of fully replicating all human disease features. CFA-induced arthritis is one of the most common and widely accepted methods for modelling RA in rodents due to the similarities with the clinical features of human arthritis including joint swelling, lymphocyte infiltration, pannus invasion and cartilage degradation (Q. Guo et al., 2018; Kamal et al., 2021; Ren et al., 2019; Silverman et al., 1996). In refined CFA models, joint disease with inflammation and bone destruction typically develops rapidly, usually within 10 -14 days. The disease can continue in a relapsing-remitting pattern for weeks to months, and eventually results in joint deformity and ankylosis (Hawkins et al., 2015; Pearson & Wood, 1959; Rainsford, 1982), although this is reduced in the more refined monoarticular models (L. Bracht et al., 2012; Donaldson et al., 1993). Key cytokines and chemokines are also produced in rodent joints using CFA based models e.g. IFN-γ, IL-17 and TNF-α are expressed on macrophage stimulation, and levels of monocyte chemotactic protein-1, IL-4, IL-6, and TGF-ß are correlated with the severity of inflammation in the joint. There are also physiological, morphological and histological similarities such as bone and cartilage destruction, infiltration of T cells (Asquith et al., 2009), and pain (Fischer et al., 2017). While the CFA model may therefore have a disadvantage in the different time course of disease compared to human RA, it also has utility for study of many aspects of the disease process.

The degree and location of inflammation, joint damage, and duration of disease in the CFA model have been linked to various factors, such as the dose, constituents and route of CFA given (A. Bracht et al., 2016; Donaldson et al., 1993)**,** the rodent species (Chillingworth & Donaldson, 2003) and strain (Cannon et al., 1999)**.** While there has been comparison of the effects of different CFA doses on histological inflammation, to my knowledge there has been no direct comparison made between commercial CFA and in-house CFA. The latter has been routinely used in our group to enable induction of arthritis using a lower intra-articular injection volume to deliver the necessary dose to induce arthritis (Kelly et al., 2007) in mice, where higher concentrations of heat-

killed mycobacteria in the CFA may be required than are available in commercial preparations (Chillingworth & Donaldson, 2003).

My primary hypothesis for this thesis is that 'activation of VEGFR2 by VEGF-A_{xxx}a splice variants contributes to joint inflammation and damage in rodent models of inflammatory arthritis'. To address this hypothesis, I worked with other lab members who supplied me with joint tissues from *in vivo* studies in rats and mice conducted to investigate spinal gliovascular/neuroinflammatory mechanisms and pain consequent to peripheral arthritis (Beazley-Long et al., 2018; Durrant, 2021).

In rat experiments with a primary hypothesis that systemic block of VEGF receptor 2 and/or TNF-α would inhibit the nervous system gliovascular/neuroinflammatory response to inflammatory arthritis in male rats, I hypothesised that such pharmacological intervention would also affect synovitis and joint integrity/damage (Chapter 4), in view of the importance of VEGF-A in arthritis (Section 1.12). In the first *in vivo* study conducted by Dr Durrant, some animal welfare issues were raised which resulted in a second study where a lower dose of commercial CFA (50µg in 50µl) was used instead of 100µg in 50µl CFA made 'in house'. Dr Durrant's findings showed that inflamed knee joints injected with the 50µg commercial CFA had greater swelling than those injected with the 100µg 'in house' CFA, which was unexpected as most studies report a relationship between dose of CFA and joint swelling (Noh et al., 2021). As I planned to use the joints from these arthritic animals to determine any effects of systemic VEGFR2 and/or TNF-α blockade on joint histology, I first had to determine whether these two different doses of CFA resulted in equivalent features of arthritis.

Aim: to determine whether there is a difference in histological synovial inflammation and joint damage in arthritic rat joints induced by CFA of different formulation and dose.

Objective: to measure the histological changes in the inflamed joints from rats treated with two formulations and dose of CFA, in terms of cartilage damage, synovial inflammation, pannus infiltration and FVT formation and compare these between different CFA doses.

3.2. MATERIALS AND METHODS

3.2.1 Experimental design

The experimental design of the studies in which the effect of VEGFR2 and/or TNF-α block on features of arthritic joint histology was investigated used between subject comparisons (Chapter 4). To determine whether the two CFA formulations resulted in different joint histological changes, the data from the control group (anaesthetic control in which animals were briefly anaesthetised and knees shaved but no injection given) and the groups receiving CFA and drug vehicle (section 2.3.3) are presented in this chapter.

Detailed information on animal methods prior to the isolation of tissues, and for joint tissue processing and preparation for histology can be found in Chapter 2 General Methods (sections 2.3.2 – 2.3.4, 2.4 -2.6).

Table 3.1: Animal numbers and the two treatment groups from which joints were processed to compare histological features with different CFA formulations/doses (Durrant, 2021).

Study	Treatments	Study design	Number of animals
1	Anaesthetic control + Vehicle	Within/between subjects comparison of the effect of therapeutic pharmacological VEGF-R and/or TNFα inhibition on histological arthritis.	6
	CFA (100µg) + Vehicle		6
2	Anaesthetic control + Vehicle		6
	CFA (50µg) + Vehicle		6

The experiments were conducted by Dr Durrant as in the timeline shown in Figure 2.1 reproduced below for ease. Knee swelling was monitored throughout as a measure of the pro-inflammatory effect of CFA, which was apparent in all animals. Animals were habituated to intraperitoneal vehicle injections before CFA injection. Animals were killed 10 days after arthritis induction by anaesthetic overdose and perfusion-fixation

(section 2.3.4) and joints collected, post-fixed in 4% paraformaldehyde and embedded in paraffin (King's Mill hospital). Following sectioning and staining, the histological features of the joints were scored for cartilage damage, synovitis, pannus, and FVT.

Three sections from different depths were scored for each feature for each joint and the mean score for each animal used in the final analyses. The presence of pannus and FVT was scored as present (1) or absent (0), so the mean of the internal replicates was a value between 0 and 1. Full details on scoring methods are in Chapter 2 General Methods section 2.6.

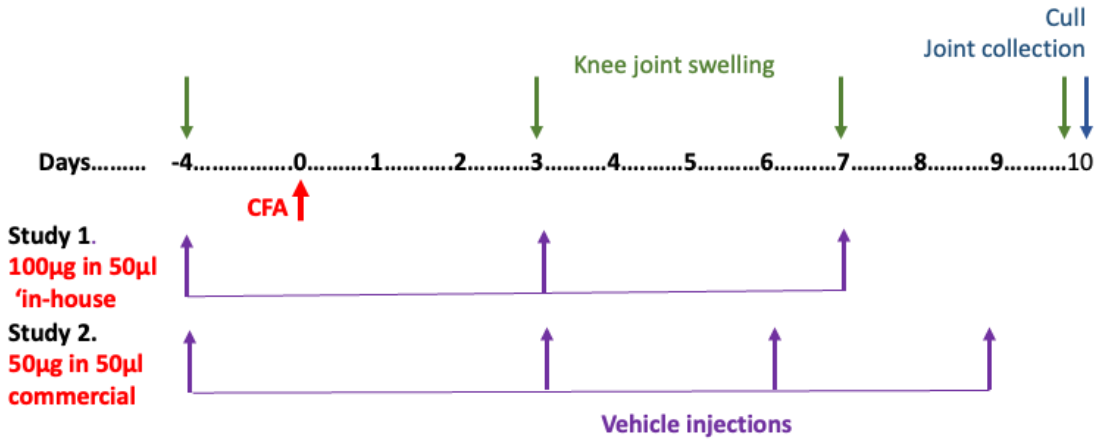

Figure 3.1: Experimental timeline of the two rat studies, partially reproduced from Chapter 2 for ease of reference, showing only the control groups that did not receive drugs. Both studies followed similar timelines, with monitoring of knee joint swelling (green arrows) before and after induction of arthritis with CFA (red arrow). At the end of the experiment, animals were killed with barbiturate anaesthetic overdose, joints removed and placed in 4% paraformaldehyde. Animals in both studies received intraperitoneal vehicle injections throughout (purple arrows) as they also serve as controls for the effects of VEGFR2 and TNF-α block (Chapter 4).

3.2.2 Statistical analysis:

One-way ANOVA was performed followed by Sidak's multiple comparison tests to compare histological scoring between in-house CFA and commercial CFA. A value of $p < 0.05$ was considered statistically significant.

3.3 RESULTS

Rats in the two anaesthetic control groups received exactly the same treatment. The histological scores for these two groups were not significantly different from each other for each histological component, so they were pooled for further analyses.

The cartilage damage that resulted from in-house CFA (100µg in 50µL) was only seen in half the animals (Figure 3.2A) and the mean damage score in this group was not significantly different from control animals. Commercial CFA (50µg in 50µL) resulted in cartilage damage in more animals than in-house CFA, and the mean score was significantly greater than in controls, but not significantly different to in-house CFA (control 0, in-house CFA 0.6±0.6 (mean ± SD), commercial CFA 0.8±0.8). Synovitis scores were significantly increased using both CFA formulations with equivalent mean values, but with less variability for commercial CFA (control 0.2 ± 0.5, in-house CFA 2.7±0.5), commercial CFA 2.9±0.1, Figure 3.2B). Pannus presence was significantly greater in CFA compared to controls and was slightly more variable using in house compared to commercial CFA (control 0, in-house CFA 0.9±0.3, commercial CFA 0.9±0.1, Figure 3.2C), as was the FVT in the bone marrow (control 0.03±0.1, in-house CFA 0.7±0.3, commercial CFA 0.9±0.1, Figure 3.2D). The mean value of all scores using commercial CFA was slightly but not significantly higher than in-house CFA despite the lower *M.tub*. dose. In addition, the data variability was lower in all scores for commercial CFA, except for cartilage damage.

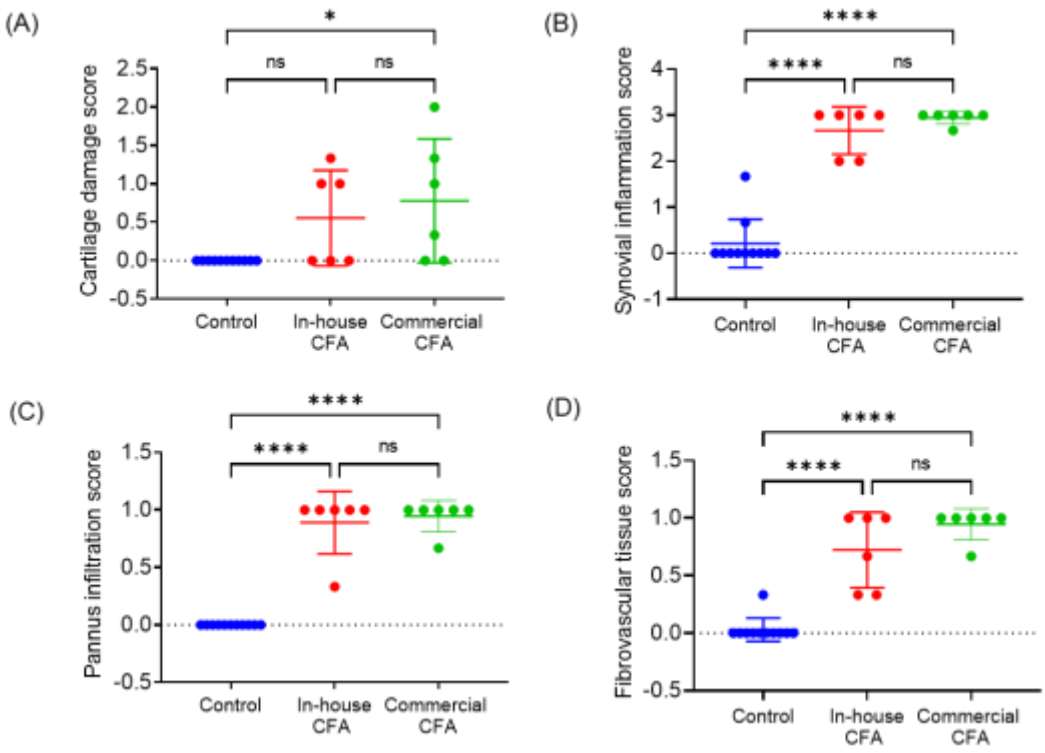

Figure 3.2: Histological scoring including cartilage damage, synovial inflammation, pannus infiltration and bone marrow FVT. Both CFA formulations produced equivalent histological changes, and there were no significant differences between in-house CFA (100ug in 50µL) and commercial CFA (50ug in 50µL) in all histological features. (A) Cartilage damage (F (2, 20) = 5.205) p=0.0151 (B) Synovial inflammation F (2, 20) = 93.50) p<0.0001 (C) Presence of pannus p=F (2, 20) = 104.4) p<0.0001 (D) Presence of FVT in bone marrow F (2, 20) = 52.68, p<0.0001. One way ANOVA followed by Sidak's multiple comparisons tests *p<0.05, ****p<0.0001.

3.4 DISCUSSION

The investigation aimed to determine any histopathological differences between two different formulations/doses of CFA used to induce inflammatory arthritis. Surprisingly, I found that the reduction in *M.tub* dose from 100µg to 50µg had no significant effect on any histological measure of arthritis (Figure 3.2), despite some (Donaldson et al 1993) but not all (Chillingworth et al 2003) previous reports suggesting that different doses of *M.tub* result in distinct differences in histological features. There have been very few more recent studies on the relationship between the arthritic stimulus and the resulting histopathology. Studies usually report the relationships between CFA dose and joint swelling, which is usually positive (Gomes et al., 2013; Lussier et al., 1984; Noh et al., 2021) but give little if any information on histopathological features (Cannon et al., 1999), and where histological changes are seen, these studies rarely report any quantitative analyses of histological differences (Cannon et al., 1999; Gomes et al., 2013; Lussier et al., 1984).

The rationale for using two models of CFA arthritis was due to animal welfare issues, but surprisingly the commercial, lower dose CFA caused significantly larger knee diameters than the higher dose in-house CFA (Durrant, 2021). My data show that this difference in swelling is not reflected in any difference in histopathological inflammation/damage in the joints.

The main differences between the two CFAs are the *M.tub* dose and the vehicle. The commercial CFA used contains the surfactant mannide monooleate which, when used in Freund's incomplete adjuvant without M.tub. is reported to induce an immune response (B. Berlin, 1962; B. S. Berlin & Wyman, 1971) and to boost the immune reaction when in an emulsion (Billiau & Matthys, 2001; van Doorn et al., 2016). Mineral oil alone, and other additives to incomplete Freund's adjuvant (IFA) can also cause inflammation (Kleinau et al., 1991). Considering this, the lack of difference in histology with a lower dose of M.tub could be due to the surfactant mannide monooleate (Kleinau et al., 1991) which is present in the commercial but not the 'in house' CFA, and could increase the level of inflammation from a lower M.tub dose to that equivalent of a higher dose.

Adjuvants result in more severe synovial joint destruction in both Freund's adjuvant arthritis (Whitehouse et al., 1974) and CIA (Larsson et al., 1990) compared to oil induced arthritis which is mild and limited (Donaldson et al 1993). This clearly shows that immune reactions induced by mycobacteria or collagen II add specific clinical features and augment arthritis above changes induced by oil (Kleinau et al., 1991).

While whole inactivated mycobacteria suspension has been used for many decades, it does result in variable histological effects which may be due to differences in actual dose when using a suspension. Similar arthritogenic responses can be achieved by replacement of inactivated mycobacteria with recombinant mycobacterial heat-shock protein 65 (MHSP65) which also causes lymphocyte infiltration, synovial inflammation, and cartilage erosion, probably through induction of TNF-α, IL-6 and IL-1β through the activation of Toll-like receptors (TLR)2 and TLR4 (L. Zhou et al., 2012). TLR2 causes antigen presentation cell activation and cytokine release and TLR4 is a key receptor in inflammatory responses (Wetzler, 2003). TLR2 and TLR4 are found in inflamed synovium in clinically active RA (Q.-Q. Huang et al., 2009). Thus, inactivated mycobacterium could be replaced by MHSP65 to potential yield a more reproducible model.

For animal welfare reasons, the use of a lower dose of commercial CFA was suggested as an approach to refine the model used; however, it resulted in increased joint swelling and, as I have shown, had similar effects on joint histology as the 'in-house' CFA. Moreover, use of the lower dose commercial CFA did not result in the primary physiological outcome measure under investigation, spinal reactive microgliosis, although the higher dose CFA did (Durrant, 2021). Spinal microglia are a vital players in mechanisms for arthritic (Hans-Georg Schaible et al., 2022) and neuropathic pain (Tsuda, 2016), and several already available agents that target microglia are being tested as possible analgesics (Haight et al., 2019). Thus, while the lower dose commercial CFA model may be useful for study of joint histological features, it is not associated with important spinal cord alterations that may contribute to pain. Use of higher M.tub doses therefore appears necessary to model both

histopathological features and central spinal mechanisms in rat inflammatory arthritis models (Beazley-Long et al., 2018).

Based on histological scoring, and the lack of significant differences between the arthritis models in the two studies, I subsequently used joints from rats from both studies for further investigation of the systemic inhibition of VEGFR2 on synovial inflammation and joint integrity.

3.5 CONCLUSION

The different doses/concentrations and formulation of CFA did not result in different degrees of histological arthritis in rats, but there was a greater range of scores using in-house CFA. This means that lower dose commercial CFA may be used to produce an equivalent and more consistent histological arthritis, showing both inflammation and cartilage damage after 10 days.

4. EFFECT OF VEGFR2 BLOCKER PTK787 (VATALANIB) ON SYNOVITIS AND JOINT INTEGRITY IN INFLAMMATORY ARTHRITIS

4.1 INTRODUCTION

Inflammation of the synovial membrane (synovitis) is an important contributor to the cartilage and bone damage in RA. Synovitis is caused by leucocyte infiltration in the synovial membrane, which is facilitated through several pathways, predominantly through endothelial cell activation in the synovial microvessels. This leads to an increase in the expression of pro-inflammatory cytokines, chemokines, and adhesion molecules (Szekanecz et al., 2009). The loss of the protective properties of the synovium alters the protein-binding features of the cartilage surface and promotes FLS adhesion and invasion. These processes result in cartilage surface destruction (McInnes & Schett, 2011) which is followed rapidly by bone erosion that affect 80% of untreated patients within 1 year after diagnosis (Daniel et al., 2010).

Cytokine production is central to the pathogenesis of RA (Remmers et al., 2007). TNF-α is considered the key inflammatory cytokine in RA (E. H. Choy & Panayi, 2001; Kokkonen et al., 2010; Tetta et al., 1990). It is produced by monocytes, macrophages, B-cells, T-cells (predominantly type 1 helper T cells (Th1)) and synovial fibroblasts (Horiuchi et al., 2010; Laurent et al., 2015). TNF-α plays a fundamental role in cartilage damage and bone erosion in RA through inflammatory cell recruitment (E. H. Choy & Panayi, 2001; S. R. Goldring, 2002; A. E. Koch et al., 1994; Pulik et al., 2023), and the activation of chemokines, including CCL5, CXCL10, CXCL8, (Bahlas et al., 2018), CXCL12 (H. R. Kim et al., 2014) and CXCL116 (Van Der Voort et al., 2005) and other pro-inflammatory and pro-angiogenic molecules such as VEGF-A (Giraudo et al., 1998), endothelial-cell adhesion molecules such as intercellular adhesion molecule (ICAM-I) (Feldmann, 1996; Hess et al., 2011), and MMPs (; Pulik et al., 2023; H.-J. Yun et al., 2008) (Figure 4.1).

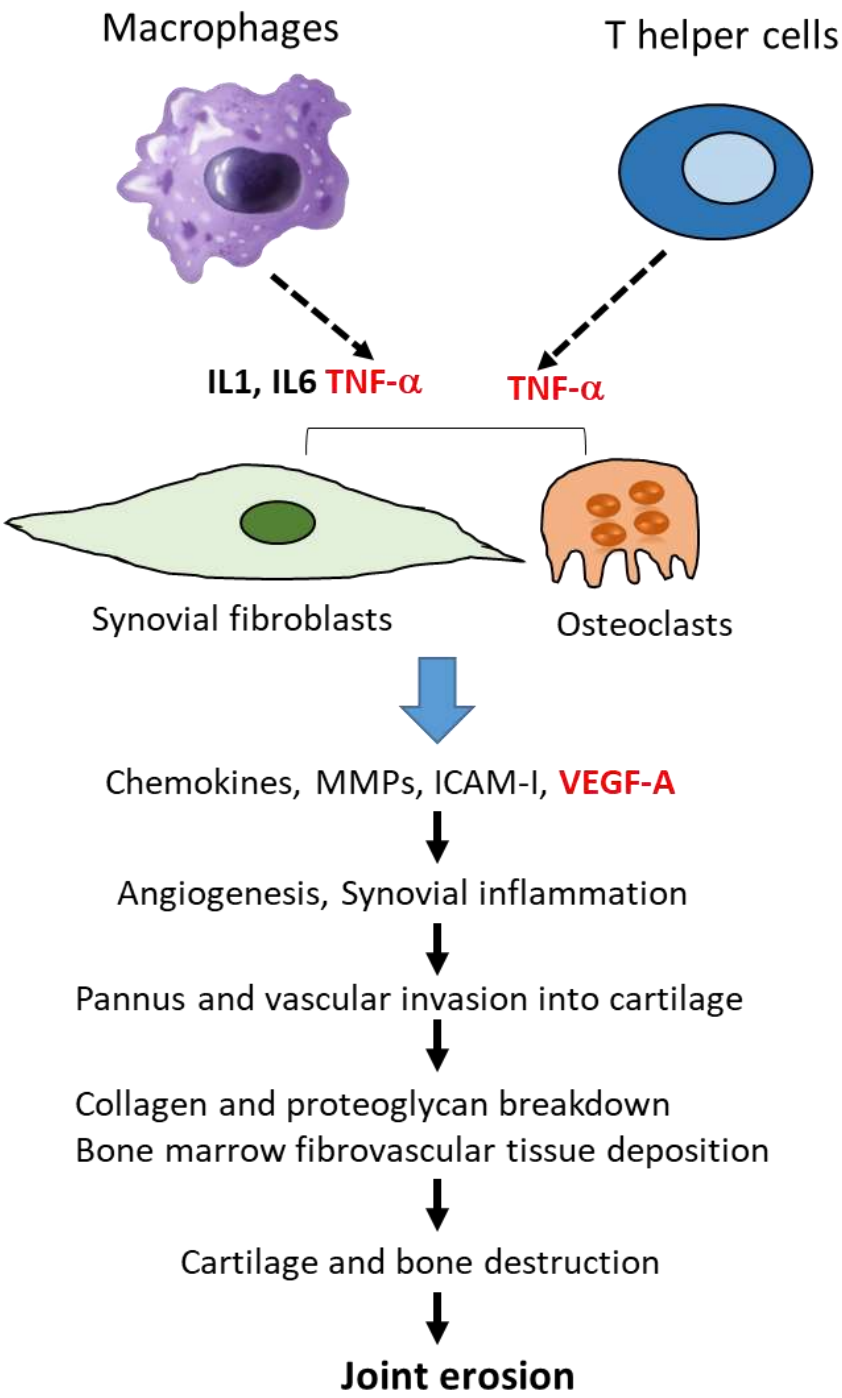

Figure 4.1: The role of TNF-α and VEGF-A in RA. In RA, TNF-α is secreted by T helper cells and macrophages. TNF-α activates synovial fibroblasts and promotes synovial hyperplasia, inflammation, and angiogenesis by the production of chemokines, cathepsins, adhesion molecules, MMPs and VEGF-A. All these factors cause the breakdown of proteoglycan and collagen followed by cartilage and bone destruction, and joint erosion. TNF-α also activates osteoclasts which induce synovial hyperplasia and angiogenesis in RA and results in joint destruction.

TNF-α drives expression of both endothelial VEGF-A_{165}a and adhesion molecules (Haraldsen et al., 1996; Radisavljevic et al., 2000) and is positively correlated with VEGF-A expression (Nowak et al., 2008). TNF-α plays a key role in endothelial proliferation and migration along with the formation of new blood vessels (Leibovich et al., 1987). Moreover, TNF-α promote angiogenesis indirectly by stimulating synovial fibroblasts and macrophages in the pannus to produce VEGF-A through its synergic effect with cytokines such as IL-1β and IL-17 (Harada, 1998; Honorati et al., 2006; A. E. Koch et al., 1994; Szekanecz & Koch, 2010).

Increased TNF-α expression was found in the serum of RA patients compared to controls (Nakahara et al., 2003). Etanercept is an approved anti-tumour necrosis factor (anti-TNF-α) biologic treatment which not only decreases the signs and symptoms of RA, but also delays the progression of radiographic damage (Haraoui & Bykerk, 2007). Etanercept was reported to significantly reduce the levels of VEGF-A in RA (Macías et al., 2005; Strunk et al., 2006). Etanercept reduced disease activity in adults and children with chronic rheumatoid arthritis who had insufficient response to other therapies (Lovell et al., 2000; Moreland et al., 1997; Moreland et al., 1999; Weinblatt et al., 1999); however, it was not effective in reducing VEGF-A levels (Knudsen et al., 2009). This suggests there is also TNF-independent VEGF-A expression in RA.

VEGF-A participates in synovitis and pannus formation in RA by promoting the formation of new blood vessels and enhancing vascular permeability (MacDonald et al., 2018). Pannus infiltration into the joint space further facilitates its invasion into the cartilage matrix (Matsui et al., 2009). VEGF-A stimulates a change to a catabolic pathway in articular cartilage tissue and chondrocyte hypertrophy through activation of MMPs and down-regulation of TIMPs (Fenwick et al., 1999; P. I. Mapp & Walsh, 2012) which eventually leads to cartilage destruction (Enomoto et al., 2003; Lotz, 2001; Thomas Pufe et al., 2004; Vuolteenaho et al., 2007). In addition to the increased VEGF-A expression in inflamed synovium and arthritic articular chondrocytes, vascular invasion of articular cartilage and increased osteochondral vascularity in arthritis are associated with subchondral bone marrow replacement by FVT expressing VEGF-A (D. A. Walsh et al., 2010) (see more details in section 1.5.4).

Targeting FVT formation is considered as a potential novel treatment approach that may reduce symptoms and modify structural progression in inflammatory arthritis (Appel et al., 2006; Bugatti et al., 2005).

Literature evidence shows a very strong relationship between VEGF-A and arthritis severity. Increased VEGF-A concentrations are found in both the synovial fluid and serum of RA patients compared to controls (Fava et al., 1994; Harada, 1998; A. E. Koch et al., 1994; S. Lee et al., 2001; Paleolog et al., 1998; Sakalyte et al., 2022). VEGF-A serum levels are directly related to the degree of joint damage/destructive lesions in radiographic studies (Ballara et al., 2001; Paleolog, 2002) and disease activity (Sone et al., 2001). The degree of synovial angiogenesis is associated with synovial VEGF-A expression, and VEGF-A and VEGFR2 expression in cartilage was also observed in association with vascular invasion at cartilage, consistent with angiogenesis (M. Ikeda et al., 2000). In addition, Qian, Xu et al. showed a direct correlation between the degree of arthritis and the expression of VEGF-A and VEGFR2 (J.-j. Qian et al., 2021).

As described in the Introduction, VEGF-A binds to multiple tyrosine kinase VEGF receptors, but with highest affinity to its cognate receptor, VEGFR2 (Lohela et al., 2009; M Shibuya, 2006). VEGF-A_{165}a isoform acts as a full agonist at VEGFR2 resulting in VEGFR2 dimerization, autophosphorylation, stabilisation of the VEGFR2 dimer with NP-1 and activation of intra-cellular signalling cascades (Ballmer-Hofer et al., 2011) (section 1.11.4 and 1.12.1 – chapter 1). These signalling cascades induce endothelial cells and synoviocytes proliferation, migration, and survival as well as increase neovascularization and vascular permeability (Holmes et al., 2007; Hong et al., 2017). Hence, it can be inferred that this particularly relates to VEGF-A_{xxx}a isoforms as these are known to promote angiogenesis and inflammation, which contribute to joint damage and pain. Angiogenesis, innervation, and inflammation are highly interconnected, and each may up-regulate the others (Bonnet & Walsh, 2005; J. R. Jackson et al., 1997). It has been speculated for many years that inhibition of angiogenesis and inflammation could reduce pain and retard joint damage in arthritis (Bonnet & Walsh, 2005; Lu et al., 2000; Semerano et al., 2016). All currently approved therapeutic anti-VEGF antibodies are targeted against the common N terminus and

thus block both VEGF-A_{xxx}a and VEGF-A_{xxx}b, and VEGFR blockers also inhibit actions of both isoform families at the receptors. VEGF-A blocking antibodies and low-molecular- weight VEGFR tyrosine kinase inhibitors (TKIs) are currently in experimental studies for multiple diseases, and despite the lack of isoform-specific block, anti-VEGF therapies using such strategies decrease the clinical severity score and joint destruction in collagen and antigen-induced models of arthritis (S. T. Choi et al., 2009; Mould et al., 2003).

I used rat knee joints collected from a study conducted by Dr. Durrant, in which rats with CFA-induced arthritis had been treated with PTK787 (Vatalanib) and/or Etanercept, to investigate the effect of VEGFR2 inhibition on synovial inflammation and joint integrity. PTK787/Vatalanib is a small molecule inhibitor with a broad spectrum multi-targeting of kinases, with some selectivity for VEGFRs, but which also inhibits c-kit, Flt3 and other kinases (Branca, 2005; Jain et al., 2006). PTK787 had significant activity against tumour growth and metastasis in pre-clinical studies (Traxler et al., 2001; Wood et al., 2000). The anti-arthritic effects of this receptor tyrosine kinase inhibitor are mediated by anti-angiogenic actions in a RA model and it also exerted analgesic actions in an acute inflammatory pain model (Grosios et al., 2004).

Hypothesis: systemic pharmacological inhibition of the VEGFR2 blocker PTK787 will reduce joint inflammation and cartilage damage in a rat CFA-induced arthritis model.

Aim: to determine the effect of pharmacological inhibition of VEGFR2 blocker PTK787 on synovial inflammation and cartilage damage in CFA arthritic rat joints.

Objective: to measure the histological changes in the inflamed joints from rats treated systemically with the pharmacological VEGFR2 blocker PTK787 and compare to vehicle treated inflamed rats.

4.2 MATERIALS AND METHODS

4.2.1 Experimental design

The experimental design of the studies in which the effect of VEGFR2 and/or TNF-α block on features of arthritic joint histology was investigated using between subject comparisons (Table 4.1).

Table 4.1: Animal numbers and treatment groups from which joints were processed to compare histological features with anti-VEGF-A and anti-TNF treatment (Durrant, 2021). *One animal was excluded from all analyses due to lack of CFA response (swelling).

Study	Treatments	Study design	Number of animals
1	Anaesthetic control (no CFA, no drug)	Between subjects comparison of the effect of therapeutic pharmacological VEGFR and/or TNF-α inhibition on histological arthritis.	6
	CFA (100µg/50µL) + vehicle		6
	CFA + PTK787 (from day 0 with CFA)		6
	CFA + PTK787 (from day 3)		6
	CFA + Etanercept (from day 3)		6
2.	Anaesthetic control (no CFA, no drug)		6
	CFA (50µg/50µL) + vehicle		6
	CFA + PTK787 (from day 0 with CFA)		6
	CFA + PTK787 (from day 3)		6
	CFA + Etanercept (from day 3)		6
	CFA + Etanercept + PTK787 (from day 3)		5

The primary differences in the design of these two studies was firstly the use of different CFA doses and preparations, and secondly that the animals in the second study received three drug injections rather than two (Figure 4.2). The different CFA preparations did not in themselves have different effects on inflammation and joint damage (Chapter 3), but the findings from each study are presented separately due to the different drug dosing regimen.

Detailed information on animal care and induction of inflammation can be found in Chapter 2 sections 2.3.3 and 2.3.4.

4.2.2 Drug dosing

Further details of drug preparation and dosing are in sections 2.2.2 and 2.3.4. Rats were dosed with the VEGFR2 selective blocker PTK787 (Vatanilib) at Day 0 and Etanercept as a positive control. Doses given were determined based on previous experiments (Beazley-Long et al., 2018; R. P. Hulse et al., 2016) and publications from other groups (Michael K Boettger et al., 2008; Michael Karl Boettger et al., 2010).

Briefly rats were habituated to intraperitoneal injections for one week before induction of CFA-arthritis in one 'knee' (tibio-femoral) joint under isoflurane anaesthesia (sections 2.3.3 and 2.3.4). Animals were then dosed intraperitoneally with timings as shown in Figure 4.2 and Table 4.1. Animals were killed 10 days after CFA injection by anaesthetic overdose, perfused with 4% paraformaldehyde, and joints isolated for processing, staining and analysis following further immersion fixation in 4% paraformaldehyde. Following decalcification (Section 2.4.1), paraffin embedding, sectioning (section 2.4.2) and staining (section 2.5), the histological features of the joints were scored for presence and degree of synovitis, cartilage damage, pannus, and FVT (section 2.6).

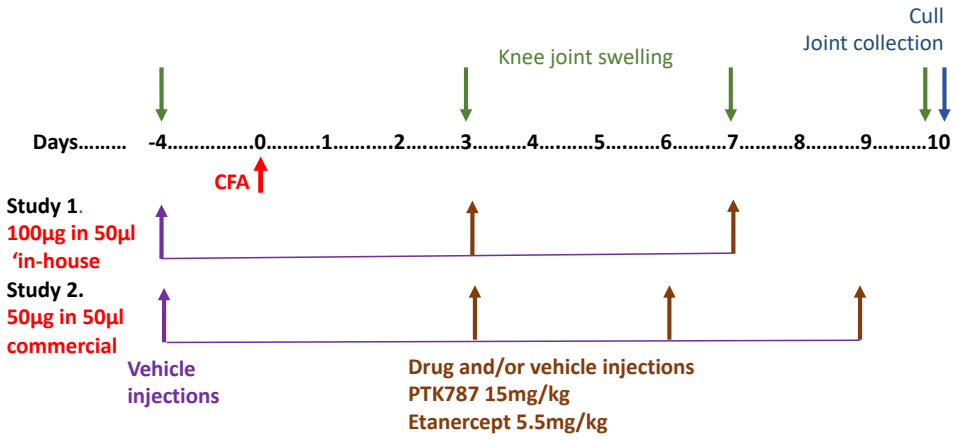

Figure 4.2: Experimental timelines for the two studies, in a partial reproduction from Chapter 2 for ease of reference, showing the timeline for therapeutic VEGFR2 or TNFα inhibition in the two study with different CFA doses (red). Timelines show days before and after arthritis induction on day zero (on dotted line), measurement of knee joint

diameter as indicator of swelling (green arrows), intra-articular CFA injections (red arrows), intraperitoneal vehicle and drug injections (purple and brown arrows) and tissue collection at the end of the experiments (blue arrow).

4.2.3 Histological features of inflammatory arthritis in the rat model

To quantify the histological features of IA in PTK787 and Etanercept treated rats, specific histopathological scoring systems were used for signs of physical cartilage damage, score range from 0 (normal) to 5 (full thickness degradation) (Table 2.3), synovial inflammation, score range 0 (normal) to 3 (severe) (Table 2.5), pannus infiltration, presence (1) or absence (0), FVT presence of a meshwork of connected collagen deposition in bone marrow (1), or absence (0). Proteoglycan loss in cartilage and collagen deposition in bone marrow were assessed using toluidine blue/Safranin O and intra-bone marrow collagen by Masson's trichrome staining, respectively. Where possible to score, proteoglycan loss was scored 0 (no loss) to 4 (severe loss) (Table 2.4), and collagen staining scored on 0 (normal) to 3 on the degree of staining (Table 2.6).

Scoring was done on at least 3 sections of each joint cut at different depths and a mean value for each joint calculated.

Note that the data shown in this chapter for the vehicle treated rats are the same as those used to compare the histological features of the two CFA doses, shown in Figure 3.2.

4.2.4 Data analysis

Data were analysed using one-way ANOVA followed by Dunnett's multiple comparison tests to compare the effects of drugs with vehicle. Comparisons were also made to the absolute control CFA to confirm the positive effect of CFA on joint histological features, i.e. the induction of inflammation. Statistical p value < 0.05 was considered as significant.

4.3 RESULTS

4.3.1 Histological features of inflammatory arthritis

Injection of CFA into the knee joint of rats resulted in varying degrees of synovitis, pannus formation and invasion, bone marrow FVT formation and cartilage damage, the latter assessed as either physical damage, or loss of proteoglycans assessed by toluidine blue or Safranin O/Fast Green staining.

4.3.1.1 Synovial inflammation (synovitis) and pannus

A. Synovitis

Synovitis was scored on the morphology of the synovium, primarily on thickness of synovial lining and the cellularity of the sub-synovium (Figure 2.8, Table 2.5). Commercial CFA resulted in significant consistent severe synovitis, whereas synovitis with in-house CFA was more variable across all groups (Figure 4.3), as already noted in the vehicle control groups in Chapter 3. Synovitis scores were significantly higher in all CFA groups compared to untreated controls (one-way ANOVA followed by Dunnett's multiple comparisons test, all groups ****$p<0.0001$ compared to uninflamed control).

None of the drug treatments (2 or 3 doses of PTK787 or PTK787 + Etanercept) had any significant effect on synovitis although there were slight non-significant reductions in synovitis scores observed after 2 doses of PTK787 or Etanercept treatment starting on day 3, using in-house CFA (Figure 4.3A control 0±0, CFA + vehicle 2.7±0.5, Day 0 PTK787 2.8±0.3, Day 3 PTK787 2.6±0.7, Day 3 Etanercept 2.1±1, $F (4, 24) = 17.66$). No effect was found in treatment groups compared to vehicle treated groups for the commercial CFA (Figure 4.3B control 0.4±0.7, CFA + vehicle 3±0.1, Day 0 PTK787 3±0, Day 3 PTK787 3±0, Day 3 Etanercept 3±0, Day 3 PTK787 + Etanercept 3±0.1, $F (5, 29) = 77.43$).

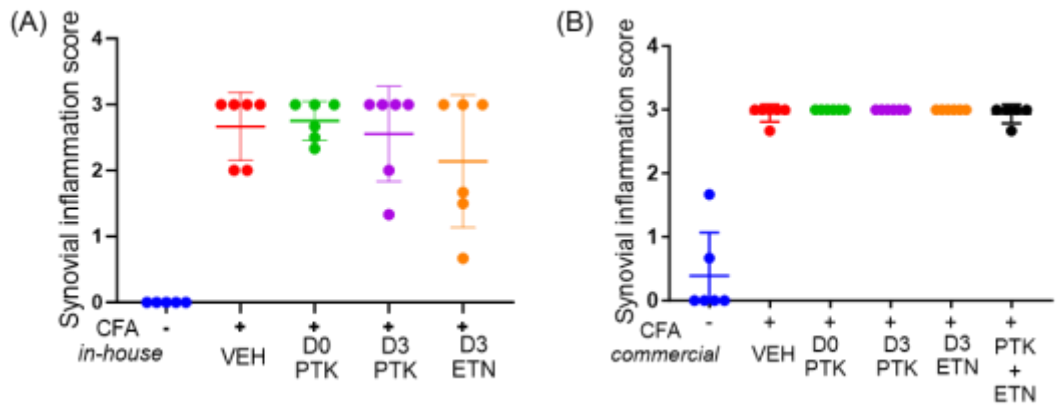

Figure 4.3: (A&B) Effect of PTK787 and/or Etanercept on synovial inflammation scoring in IA rat knee joints. Symbols (+ and -) indicate when animals have received CFA. There was no significant reduction in synovial inflammation with any treatment (PTK787 and/or Etanercept) compared to vehicle in either study (In-house CFA: drug groups left to right p=0.9980, p=0.9939, p=0.4136 respectively c.f vehicle. Commercial CFA: Commercial CFA: drug groups left to right p=0.9974, p=0.9974, p=0.9974, p=>0.9999 respectively cf. vehicle. One-way ANOVA followed by Dunnett's multiple comparisons test for all treatments vs vehicle. D0: Day 0, D3: Day 3, PTK: PTK787; ETN: Etanercept.

B. Pannus

Pannus score was based on the synovial tissue invasion into the subchondral bone and cartilage surface. Both in-house and commercial CFA caused significant pannus proliferation compared to uninflamed controls (one-way ANOVA followed by Dunnett's multiple comparison tests, vehicle and PTK groups all $p<0.001$, Etanercept group $p=0.02$). Neither 2 nor 3 doses of PTK787 or PTK + Etanercept showed any significant changes compared to vehicle in animals receiving either 2 doses of PTK (Figure 4.4A control 0±0, CFA + vehicle 0.9±0.3, Day 0 PTK787 0.9±0.2, Day 3 PTK787 0.8±0.3, Day 3 Etanercept 0.5±0.5, $F(3, 20) = 1.674$) or 3 doses of PTK (Figure 4.4B control = 0 ± 0, CFA + vehicle 1±,0.1, Day 0 PTK787 = 1 ± 0, Day 3 PTK787 1±0, Day 3 Etanercept 1±0, Day3 PTK787 + Etanercept 1±0, $F(4, 24) = 0.9517$).

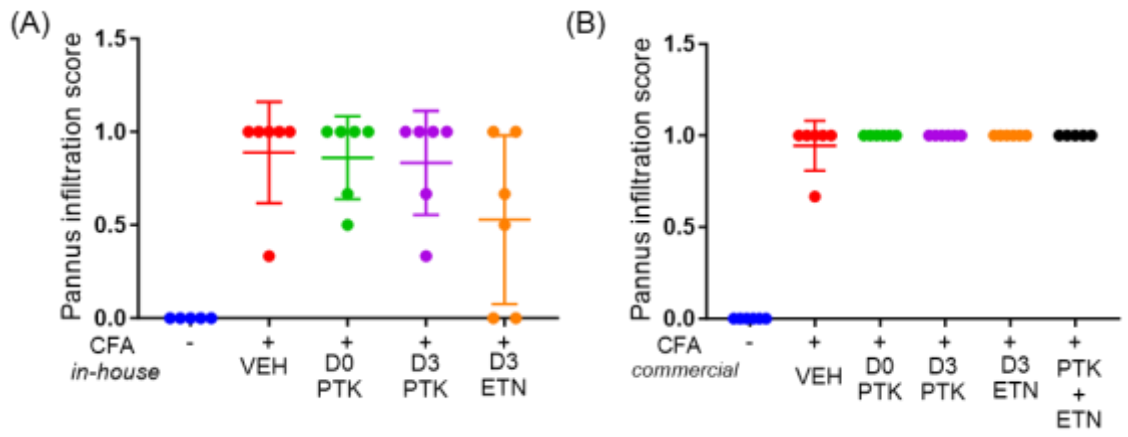

Figure 4.4: (A&B) Effect of PTK787 and/or Etanercept on pannus infiltration scores in IA rat knee joints. Symbols (+ and -) indicate when animals have received CFA injections. There was no significant effect of treatment (PTK787 and/or Etanercept) on pannus infiltration compared to vehicle either study (In-house CFA: drug groups left to right p=0.9975, p=0.9810, p=0.1527 respectively cf. vehicle, Commercial CFA: Commercial CFA: drug groups left to right p=0.3642, p=0.3642, p=0.3642, p=0.4049 respectively cf. vehicle). One-way ANOVA followed by Dunnett's multiple comparisons test for all treatments vs vehicle. D0: Day 0, D3: Day 3, PTK: PTK787; ETN: Etanercept.

4.3.1.2 Cartilage damage

Neither CFA formulation resulted in significant cartilage damage in all animals in all groups, compared to the uninflamed controls (Figure 4.5A, Figure 4.5B). In some groups where commercial CFA was used, and all groups treated with the in-house CFA there were animals in which there was no cartilage damage at all (Figure 4.5A&B). There were also no statistical differences between the cartilage damage in animals treated PTK787 or PTK787 + Etanercept and vehicle in either study irrespective of whether 2 or 3 doses of drugs were given.

Cartilage damage scores were, however, slightly lower using in-house CFA (Figure 4.5A) compared to the commercial CFA (Fig 4.5B in-house CFA control 0 ± 0, CFA + vehicle 0.6 ± 0.6, Day 0 PTK787 1.1±0.8, Day 3 PTK787 0.7±0.7, Day 3 Etanercept 0.4±0.4 (mean ± SD), $F(3, 20) = 1.150$). Commercial CFA control 0±0, CFA + vehicle 0.8±0.8, Day 0 PTK787 1.2±0.8, Day 3 PTK787 1.7±1.3, Day 3 Etanercept 1.6±1.3, Day 3 PTK787 + Etanercept 1.3±1.1) $F(4, 24) = 0.6432$).

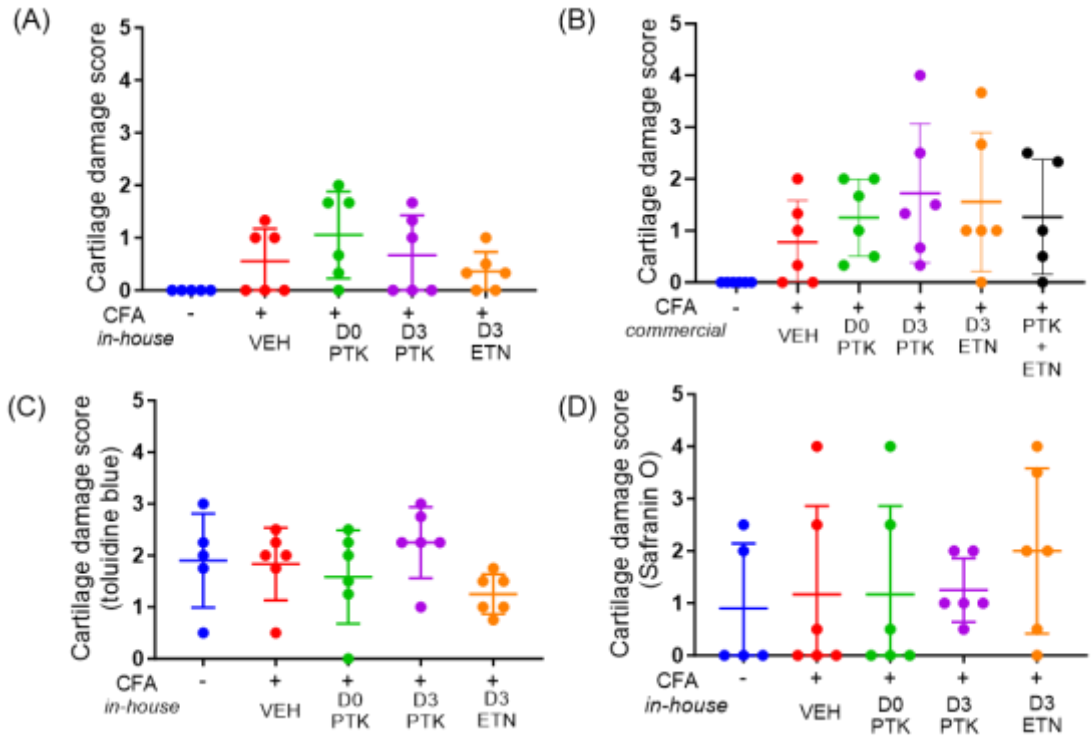

Figure 4.5: Effect of PTK787 and/or Etanercept on cartilage damage (A&B) and proteoglycan loss (C&D) in IA in rat knee joints. Symbols (+ and -) indicate when animals have received CFA injections.
(A&B) There were no significant differences in cartilage damage scores between groups treated with PTK787 and/or Etanercept compared with CFA + vehicle (In-house CFA: drug groups left to right p=0.4422, p=0.9834, p=0.9225p respectively cf. vehicle. Commercial CFA: Commercial CFA: drug groups left to right p=0.9176, p=0.4777, p=0.6529, p=0.9210 respectively cf. vehicle). (C&D) There was loss of both toluidine blue and Safranin O staining in control animals (Toluidine blue -CFA vs +CFA p=0.9998, Safranin O -CFA vs +CFA; p=0.9967). (C) There was no significant effect of treatment (PTK787 and/or Etanercept) on toluidine blue staining compared to vehicle (drug groups left to right p=0.8677, p=0.6071, p=0.3542 respectively cf. vehicle). (D) There was also no significant effect of treatment (PTK787 and/or Etanercept) on Safranin O staining compared to vehicle (drug groups left to right p>0.9999, p=0.9993, p=0.6435 respectively cf. vehicle). One-way ANOVA followed by Dunnett's multiple comparisons test for all treatments vs (+) vehicle. D0; Day 0, D3: Day 3, PTK; PTK787; ETN; Etanercept

Toluidine staining was used to determine cartilage damage in terms of proteoglycan (PG) loss (Figure 4.5 C&D). Staining was not fully effective in some of the animals in which in-house CFA was used, and many control (no CFA) joints showed unexpectedly low toluidine blue staining intensities (Figure 4.5C. control = 2 ± 0.7, CFA + vehicle = 1.9 ± 0.7, Day 0 PTK787 = 1.6 ± 0.9, Day 3 PTK787 = 2.2 ± 0.7, Day 3 Etanercept = 1.2 ± 0.4, F (3, 20) = 2.205, p=0.1190. Hence, Safranin O was used for

PG analysis in these sections. Only two control animals showed loss of safranin O staining, thus control vs inflamed joints had nearly equivalent mean values (control 1±1.7, CFA + vehicle 1.1±1.7, Day 0 PTK787 1.1±1.7, Day 3 PTK787 1.2±0.6, Day 3 Etanercept 2±1.6, F (3, 20) = 0.4566). There were no statistical differences in either toluidine blue or Safranin O staining between drug-treated animals and vehicle in either study irrespective of whether 2 or 3 doses of drugs were given.

Only the data from the in-house CFA groups are shown in Figures 4.5 C&D as none of the joint sections from animals in which commercial CFA (Figure 4.2) showed any toluidine blue staining. I attempted to use Safranin O/Fast Green as an alternative stain for proteoglycans in these sections as well, but this was also unsuccessful suggesting a problem with the tissue rather than the staining techniques.

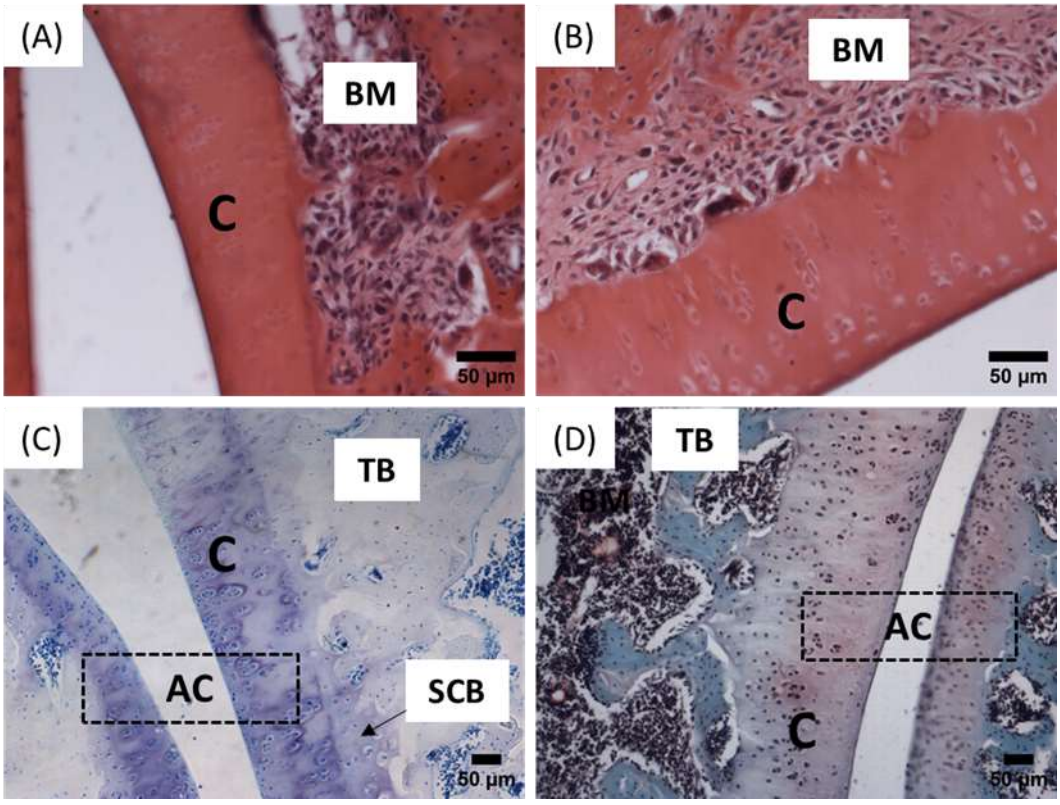

Figure 4.6: Rat knee joints stained with H&E (A & B), Toluidine blue (TB) (C) and Safranin O (SO) (D). H&E with complete absence of nuclear staining in cartilage. Proteoglycan staining by TB and SO also did not give desired staining in control cartilage. C: cartilage, AC: articular cartilage (shown by dotted box), TB: trabecular bone, SCB: subchondral bone, BM: bone marrow.

4.3.1.3 Bone marrow fibrovascular tissue

The presence of FVT was assessed as described in Chapter 2, using both presence/absence of morphological changes in the bone marrow (Figure 2.10) and the degree of bone marrow collagen deposition (Figure 2.11).

A. Morphological changes in bone marrow

Control uninflamed animals showed no FVT in bone marrow, as expected. All inflamed groups had varying degrees of FVT present in bone marrow. As with synovitis, cartilage damage and pannus, the degree and variability of bone marrow FVT score was related to the CFA used, being most variable when in-house CFA was used (Figure 4.7A. control = 0 ± 0, CFA + vehicle = 0.7 ± 0.3, Day 0 PTK787 = 0.7 ± 0.3, Day 3 PTK787 = 0.4 ± 0.4, Day 3 Etanercept = 0.66 ± 0.2, F (3, 20) = 1.274). compared to commercial CFA (Figure 4.7B. control = 0 ± 0.1, CFA + vehicle = 0.9 ± 0.14, Day 0 PTK787 = 0.9 ± 0.2, Day 3 PTK787 = 1.0 ± 0, Day 3 Etanercept = 1.0 ± 0, Day 3 PTK787 + Etanercept = 0.9 ± 0.1. F (4, 25) = 1.120). There were no statistically significant differences in FVT between drug and vehicle treated animals in either study.

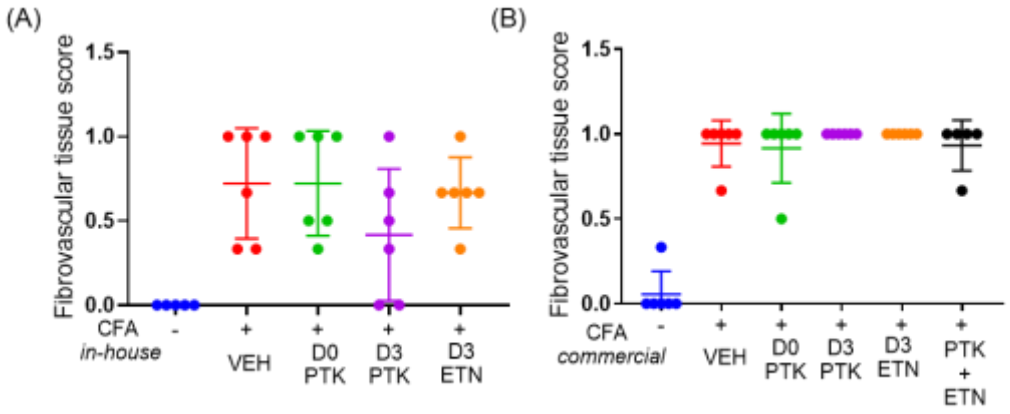

Figure 4.7: (A&B) Effect of PTK787 and/or Etanercept on histological scoring for bone marrow FVT in IA rat joint. Symbols (+ and -) indicate when animals have received CFA injections. There was no significant effect of treatment (PTK787 and/or Etanercept) on bone marrow FVT compared to vehicle either study (In-house CFA: drug groups left to right p>0.9999, p=0.2523, p=0.9807 respectively cf. vehicle. Commercial CFA: drug groups left to right p=0.9869, p=0.8657, p=0.8657, p=0.9997 respectively cf. vehicle. One-way ANOVA followed by Dunnett's multiple comparisons test for all treatments vs (+) vehicle. D0; Day 0, D3: Day 3, PTK: PTK787; ETN: Etanercept.

B. Collagen deposition scoring

Neither CFA preparation resulted in significantly increased bone marrow collagen deposition (BMCD) in treated groups compared to controls although in this measure commercial CFA resulted in greater variability in BMCD (Figure 4.8A in house: control = 0 ± 0, CFA + vehicle = 0.8 ± 1.3, Day 0 PTK787 = 0.3 ± 0.5, Day 3 PTK787 = 0.4 ± 0.9, Day 3 Etanercept = 0.3 ± 0.5, F (3, 19) = 0.4477); (Figure 4.8B Commercial: control 0.6 ± 0.9, CFA + vehicle = 1.8 ± 1.5, Day 0 PTK787 = 1.7 ± 1.4, Day 3 PTK787 = 1.6 ± 1.5, D3 Etanercept 0.8 ± 0.4, PTK787 + Etanercept 1.3 ± 1.3, F (4, 20) = 0.5076). Interestingly, two animals in the control group for commercial CFA + 3 drug doses showed BMCD, and these animals also had low level synovitis (Figure 4.3B) and PG loss (Figure 4.5D).

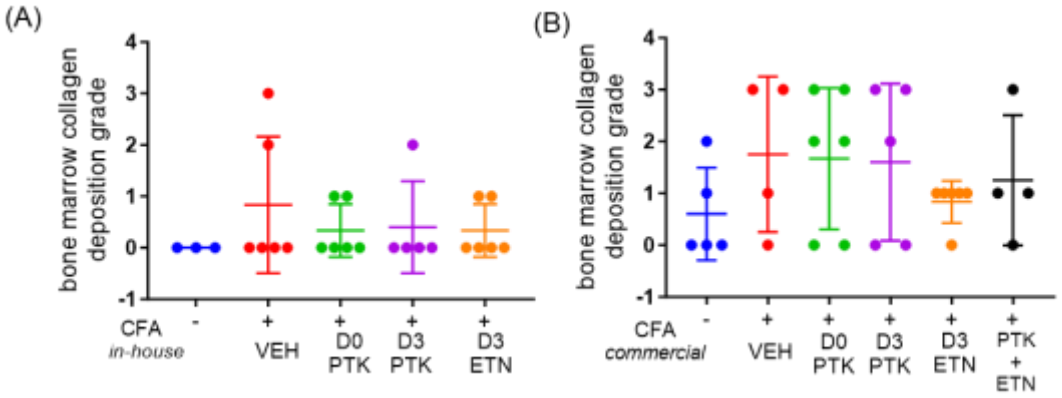

Figure 4.8: (A&B) Effect of PTK787 and/or Etanercept on bone marrow collagen deposition scoring in inflammatory arthritis rat knee joint. Symbols (+ and -) indicate when animals have received CFA injections. There was no significant effect of treatment (PTK787 and/or Etanercept) on BMCD compared to vehicle in either study (In-house CFA: drug groups left to right p=0.6468, p=0.7591, p=0.6468 respectively vs vehicle. Commercial CFA: drug groups left to right p=0.9999, p=0.9991, p=0.5975, p=0.9354 respectively cf. vehicle. One-way ANOVA followed by Dunnett's multiple comparisons test for all treatments vs (+) vehicle. D0 PTK787 – positive control, D3 PTK787, D3 Etanercept and PTK787 + Etanercept. VEH; vehicle, PTK; PTK787, ETN; Etanercept, D0; Day 0, D3; Day 3.

There was no statistically significant effect of either 2 or 3 doses of drugs on BMCD in any group compared to vehicle treated animals. In the commercial CFA group where BMCD scores were slightly higher, there was a slight non-significant reduction in both level and variability of BMCD score with 3 doses of PTK787 + Etanercept.

4.4 DISCUSSION

I used joints from two studies where rats with CFA-induced arthritis were treated with PTK787 (Figure 4.2) to test the hypothesis that systemic pharmacological inhibition of VEGFR2 would reduce joint inflammation and cartilage damage. The differences between these studies were that 1. different CFA preparations were used due to animal welfare issues (as discussed earlier), and 2. the animals that received commercial CFA also had one additional dose of PTK787 or PTK787 + Etanercept. In chapter 3 I showed that there were no statistically significant differences between the two studies in the model histopathology. Histopathological features were evaluated in both studies but although there were some small differences in the two studies, neither two nor three doses of PTK787 or PTK787 + Etanercept had an effect on synovitis, cartilage damage, or bone marrow FVT compared to vehicle. This lack of effect of PTK787 could result for several reasons: the dose and frequency of dosing; the half-life of the drug; the receptor targeted by the drug and the potential effects of VEGFR2 inhibition on other cell types in the joint.

Beazley-Long et al used the same dose of PTK787 (15mg/kg) in the CFA model in rats and showed that PTK787 was effective at reducing pain in this model (Beazley-Long et al., 2018). Despite this, the dose might be ineffective at reducing inflammation. Other studies have showed an analgesic effect of PTK787 at higher doses of 30 mg/kg i.p. (R. Hulse et al., 2014; R. P. Hulse et al., 2016), but anti-angiogenic and anti-oedema effects were only seen at higher oral doses (45mg/kg p.o) (Grosios et al., 2004). In the latter study, oral PTK787 exerted significant effects on histological arthritis scores at 45 mg/kg in collagen-induced arthritis, but not in BSA antigen-induced arthritis in mice (Grosios et al., 2004). It is possible that the dose of PTK787 in the studies presented here was not sufficient to have an effect on joint inflammation, although the bioavailability of small molecules in rodents is usually higher when they are delivered by intraperitoneal injection compared to oral administration (Al Shoyaib et al., 2020). It is also possible that the cellular mechanisms in the CFA model are not VEGFR2-depdendent. The short half-life of PTK787 (4–6 hours) (Gerstner et al., 2011; Thomas et al., 2005) could also affect the concentration of drug in the joint, as would the frequency of dosing and length of study time. It is therefore possible that although

this dose of PTK787 is effective for pain control in *in vivo* models (Beazley-Long et al., 2018), it was not present in sufficient quantity or time to affect joint structures at the dose, frequency and duration given. Therefore, different doses of PTK787 at higher concentration, frequency or alternative route of administration i-e intra-articular administration would be an option to determine the optimal concentration of PTK787, as administered in various pilot studies using VEGFR2 inhibitors as therapeutic strategy for OA and RA (Y.-Y. Chen et al., 2014; Ma et al., 2023; Nagao et al., 2017). Intra-articular injections appear to have some potential advantages, such as lower dose, increased bioavailability and minimal side effects if any, over systemic administration (C. H. Evans et al., 2014).

PTK787 inhibits all three VEGFRs (VEGFR1, VEGFR2 and VEGFR3) (Hess-Stumpp et al., 2005) but has up to 100-fold greater selectivity for VEGFR2 than VEGFR1. VEGFR1 and VEGFR2 are highly expressed on vascular endothelial cells (Eichmann et al., 1993; Jakeman et al., 1992; Kaipainen et al., 1993; Yamane et al., 1994) that regulate vascular permeability and angiogenesis (X. Wang et al., 2020) in normal development and pathological angiogenesis (Ferrara & Davis-Smyth, 1997; Giatromanolaki et al., 2001; Mustonen & Alitalo, 1995; Risau, 1997; Schroeder et al., 2013; Masabumi Shibuya, 2001; Masaubmi Shibuya, 2006). Both receptors are upregulated in synovial cells (Enomoto et al., 2003; Pfander et al., 2001; Thomas Pufe et al., 2001; Shakibaei et al., 2003; J. O. Smith et al., 2003; Tsuchida et al., 2014), chondrocytes and cartilage tissue in OA and RA (De Bandt et al., 2003; M. Ikeda et al., 2000; J.-l. Zhou et al., 2009).

There is evidence that VEGFR1 is more strongly correlated with animal IA model progression than VEGFR2 (De Bandt et al., 2003; Luttun et al., 2002; Murakami et al., 2006) which suggests that VEGFR1 may be more important in joint integrity. VEGFR1 inhibition attenuates synovial inflammation, and bone destruction in animal models of IA (Autiero et al., 2003; Harris Jr, 1990; Murakami et al., 2006). Therefore, a possible reason of PTK787 treatment showing no effects on joint histology could be that PTK787 inhibits VEGFR2 more effectively than VEGFR1. Although VEGF-A_{165}a has a high affinity at VEGFR1 (1pM), this receptor has much lower kinase activity than that

of VEGFR2 (Davis-Smyth et al., 1996; Ferrara & Davis-Smyth, 1997; Sawano et al., 1996; Seetharam et al., 1995). A limiting factor for a contribution of VEGFR1 signalling in the progress of inflammatory arthritis could therefore be the availability of VEGFR1 rather than that of VEGF-A ligand. VEGFR1 is also highly expressed in monocytes/macrophages (Barleon et al., 1996; Clauss et al., 1996; Sawano et al., 2001) and is important for the VEGF-A dependent tissue migration of these cells (Barleon et al., 1996; Hiratsuka et al., 1998; Sawano et al., 2001); there is reduced infiltration of inflammatory cells in an IA model in VEGFR*1 tk*–deficient *pX* mice (Murakami et al., 2006). It is possible that VEGFR1 could be important in joint integrity and PTK787 didn't affect my outcome measures because of its selectivity for VEGFR2 and that VEGFR1 is also important in mechanisms of IA joint damage.

Novel compounds are being considered for VEGFR2 and/or VEGFR1 inhibition for RA treatment. Recently, a new compound, a VEGFR2 inhibitor named ***compound 25*** has been synthesised as a prospective drug candidate for anti-angiogenic and anti-arthritic therapy. This compound potently inhibits VEGFR2 (IC_{50} = 19.8 nM), reducing phosphorylation of VEGFR2 in human umbilical vein endothelial cells in a dose dependant manner and inhibits capillary-like tube formation *in vitro*. It also fully inhibits platelet-derived growth factor receptor α **(**PDGFRα), and Aurora kinase B, and partially inhibits Tie2 and fibroblast growth factor receptor 1 (FGFR1) at 1µM concentration) (Y. Liu et al., 2022). Compound 25 reduced the severity and development of adjuvant-induced arthritis in rats by inhibiting synovial VEGFR2 phosphorylation, angiogenesis, pannus formation, cartilage damage and arthritic index (Q. Chen et al., 2023).

PTK787 did not show any significant effect on joint histology in IA. This is most likely due an insufficient concentration of the drug for full penetration into the joint to alleviate inflammatory arthritis damage, or the mode of administration used although i.p. injection usually gives good bioavailability, and increased perfusion in an inflamed joint would predict good penetration into arthritic tissues. It is also possible that it may have competing actions at different cell types in the joint, for example there was an indication that groups treated with PTK787 for longer might have slightly *more*

cartilage damage (Figure 4.5B). Alternative possible routes of administration such as intra-articular injection (Ma et al., 2023), or using a higher systemic dose may, however, show better effects in the treatment of IA.

Etanercept is effective in experimental IA arthritis models, for example therapeutic administration of Etanercept either every other day (Gözel et al., 2018), every 3-4 days (Michael K Boettger et al., 2008; X. Huang et al., 2019; H-G Schaible et al., 2010) or once a week (Lon et al., 2011) reduced arthritis score, swelling and inflammation in collagen-induced arthritis (CIA), but did not fully resolve histological inflammation. Single doses of Etanercept showed only modest effects, so multiple dosing was suggested to be necessary for a strong effect (Lon et al., 2011). In CFA-induced arthritis, a lower dose of Etanercept given every other day was also effective against thermal and mechanical hypersensitivity as well as swelling (Elsheemy et al., 2019; Inglis et al., 2005).

Etanercept was used here as a positive control and was expected to have an impact on IA score as the dosing regimens were comparable to previous studies, but surprisingly it did not. Etanercept has good penetration into arthritic tissue (X. Chen et al., 2015) so Etanercept should reach the site of inflammation provided the circulating concentration is sufficient. However, the half-life of Etanercept is 1.2–1.9 days in rats (Lon et al., 2011), so it is possible that the dosing regime in this study was not sufficient to have an effect on joint histology in IA .

Taken together, an increased concentration, possibly an alternative route of administration as well as longer duration of dosing of PTK787 and/or Etanercept, or inhibition of both VEGFR1 and VEGFR2 may show greater effectiveness on joint inflammation and cartilage damage in rodent IA.

4.5 CONCLUSION

Systemic inhibition of VEGFR2 over a short period of time did not reduce histological signs of cartilage damage, synovial inflammation, pannus infiltration and FVT in inflammatory arthritis in rats.

5. INDUCIBLE ENDOTHELIAL-CELL VEGFR2 KNOCKOUT CONTRIBUTES TO ARTICULAR CARTILAGE DAMAGE IN EXPERIMENTAL INFLAMMATORY ARTHRITIS

5.1 INTRODUCTION

Most research relating to angiogenesis in inflammation and arthritis has focused on the actions of VEGF-A/VEGFR2 on endothelial cells, and a blockade of angiogenesis has been frequently suggested as a possible therapeutic target in arthritis (Beazley-Long et al., 2018; Bonnet & Walsh, 2005; Q. Chen et al., 2023; D'Aura Swanson et al., 2009; Hamilton et al., 2016; Le & Kwon, 2021; MacDonald et al., 2018). Angiogenesis is accepted as a vital step in the development of arthritis, promoting synoviocyte proliferation, pannus formation and invasion, and immune cell recruitment to sites of inflammatory arthritis (Marrelli et al., 2011), as well as delivery of nutrients to an active inflammatory reaction. Angiogenesis drives initial synovial proliferation and expansion, and enhances cartilage and bone damage in later stages of IA (P. Taylor, 2005).

Increased angiogenesis is closely associated with an hypoxic environment within joints in RA (Akhavani et al., 2009; Hitchon et al., 2002; Konisti et al., 2012), and is facilitated by a number of pro-angiogenic factors, including growth factors, adhesion molecules and cytokines such as VEGF-A (see section 1.12 for more details) (De Bandt et al., 2000). VEGF-A induces angiogenesis through endothelial cell activation by VEGFR2, endothelial cell proliferation and migration *in vitro,* and stimulation of capillary formation in *in vivo* models of inflammation and angiogenesis (A. E. Koch et al., 1994; Szekanecz & Koch, 2010).

Systemic VEGFR2 blockade has been reported to reduce pain behaviours in inflammation/arthritis (Beazley-Long et al., 2018), as has endothelial-specific-VEGFR2 knockout (Tie2-VEGFR2^{ECKO}) in inflammatory arthritis in mice (Beazley-Long et al., 2018) but has more unpredictable effects on joint damage as discussed in Chapter 4.

Two VEGFR2-selective small molecules have been reported to be systemically effective in animal models of inflammatory arthritis, PTK787/ZK222584/Vatalanib and compound 25, as discussed in Chapter 4 (Q. Chen et al., 2023; Grosios et al., 2004). Intra-articular pharmacological VEGFR2 blockade is also reported to inhibit cartilage damage in rodent OA models (Ma et al., 2023), angiogenesis and swelling/oedema in mice CIA (Gözel et al., 2018; K. Qian et al., 2022), and cartilage and bone damage in rat adjuvant arthritis (Y. Gong et al., 2021; Z.-Z. Wang et al., 2020). Systemic treatment with agents that reduce VEGF-A expression (Talaat et al., 2015) or neutralise circulating VEGF-A (Miotla et al., 2000) also reduce joint damage in IA in rats and mice. Many of these small molecules are, however, not specific for VEGFR2 and may also interact with other effector molecules.

Genetic alteration is a more targeted alternative to such pharmacological methods for investigating the functions of specific molecules in physiological and pathological processes. Germ-line VEGFR2 knock-out is, however, embryonically lethal in heterozygotes, when even only one allele is lost, due to multiple defects in the formation of vascular structures (Section 1.10.3) (Shalaby et al., 1995). Genetic tools now enable more specific knockout, both in terms of cell type targeted and the time of gene knockout.

The Tie2-VEGFR2^{ECKO} colony was established in Nottingham in 2015 to investigate whether VEGFR2 block would affect pain in IA. The mice were used to test the primary hypothesis that altered VEGF-A/VEGFR2 mediated vascular responses in the *spinal cord* would affect arthritic pain behaviour. Induced Tie2-VEGFR2^{ECKO} mice have significantly reduced endothelial VEGFR2 protein expression in lung and spinal cord, a significant reduction in viable CD31+/Tie2+ cells and of VEGFR2 expression in these cells, and delayed onset and distant spread of pain in inflammatory CFA arthritis (Beazley-Long et al., 2018). It was, however, possible that changes in the joint vascular supply, and hence inflammatory response resulting from the VEGFR2 gene deletion, could also have contributed to the effect on pain.

Previous work in the lab had shown that Tie2-VEGFR2^{ECKO} had no significant effect on the histological features of synovitis and bone erosion (Figure 5.1, Nalvelnathan, Beazley-Long and Donaldson, unpublished), but had highly significant effects on

cartilage integrity only in arthritic Tie2-VEGFR2^{ECKO} mice (Figure 5.1B, (Vitterso et al., 2018). The potential cause of these differences was not known, but VEGFR2, therefore a study was designed with the hypothesis that Tie2-VEGFR2^{ECKO} arthritic mice would have reduced blood vessel number/density in mouse tibio-talar joint.

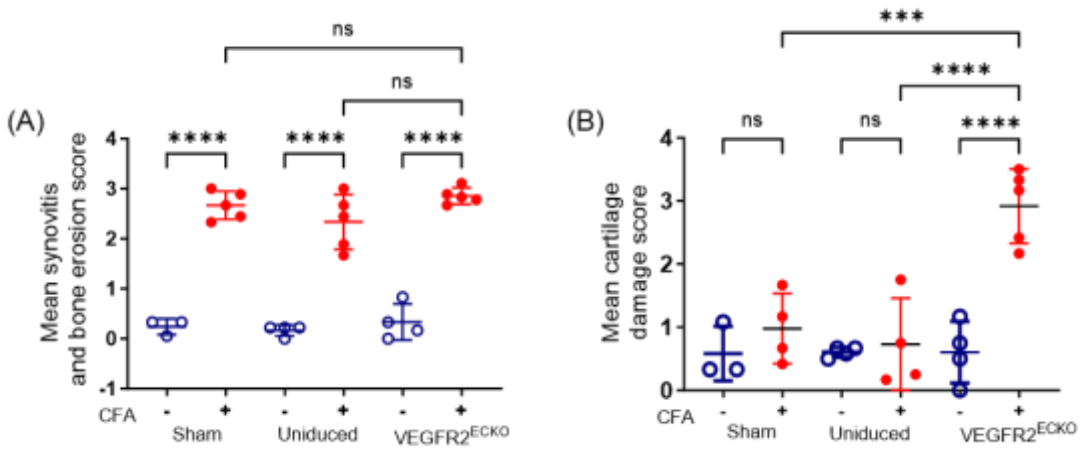

Figure 5.1: (A) CFA caused a significant and equivalent increase in the overall synovitis and bone erosion scores in all groups, control (VEGFR2fl/fl +ve/Tie2CreERT2 -ve), uninduced (VEGFR2fl/fl x Tie2Cre^{ERT2}, no tamoxifen) and induced Tie2- VEGFR2^{ECKO} mice. This shows that inducible endothelial-VEGFR2 knockout had no significant effect on histological signs of synovitis or bone erosion (Nalvelnathan J and Donaldson LF, unpublished). (B) Mean cartilage damage scores were significantly higher in induced Tie2- VEGFR2^{ECKO} mice than in all other groups, showing that loss of endothelial-VEGFR2 had significantly greater effect on cartilage damage than arthritis alone. ****p<0.0001, ***p= 0.0002. One-way ANOVA followed by Sidak's multiple comparisons test (see Supplementary data Table S1 and Figure S1) (Vitterso et al 2018, data shown provided by J Nalvelnathan and E Vitterso).

Inflamed joints are more hypoxic than normal joints (Sivakumar et al., 2008). Hypoxic synovium produces and releases several MMPs responsible for breakdown of collagen and gelatin in cartilage such as MMPs 2, 8 and 9, and thus results in damage. It has been hypothesised that the level of hypoxia drives the invasive, destructive nature of rheumatoid synovium (Akhavani et al., 2009). Cartilage is hypoxic under normal conditions (Lafont, 2010) and in addition, greater hypoxia in inflammation can result in chondrocyte death and cartilage damage (Zeng et al., 2022). Cartilage oxygen supply has long been thought to come predominantly from synovial fluid (Ito & Bishat, 1924; Strangeways, 1920; Y. Wang et al., 2013).

My primary thesis hypothesis was that 'activation of VEGFR2 by VEGF-A$_{xxx}$a splice variants contributes to joint inflammation and damage in rodent models of arthritis'. In

the experiments presented in this chapter I used joints from induced Tie2-VEGFR2 mice and controls to address the following primary hypotheses and aims.

Hypotheses:

1. Endothelial-cell specific VEGFR2 knock out (ECKO) in Tie2 positive endothelial-cells reduces vascularity in synovium in arthritic knock-out, but not arthritic control mice.

2. A reduction in synovial vascularity is associated with increased cartilage damage in VEGFR2^{ECKO} mice.

Aim: to determine whether induction of Tie2-specific endothelial-VEGFR2 knock-out affects blood vessel number/density in normal and/or arthritic mice, and whether this is related to cartilage damage.

Objective: to measure the blood vessel density in synovium in Tie2-VEGFR2^{ECKO} mice and controls, with and without inflammatory arthritis and determine the relationship with cartilage damage.

5.2 MATERIALS AND METHODS

5.2.1 Experimental design

The experimental design to test the hypothesis that tamoxifen-induced knockout of endothelial-VEGFR2 would affect synovial vascularity in IA in mice was investigated using between subjects comparisons (Table 5.1). Additional control groups were included to determine any effects of tamoxifen dosing (Sham) in VEGFR2 floxed mice, and the effect of genetic background without induction of the gene knockout (Uninduced). Experiments were conducted on F3/F4 mice of both sexes. All mice used were confirmed homozygous for the VEGFR2-loxP transgene (*vegfr2$^{fl/fl}$*) and either heterozygous or wild-type for Tie2CreER^{T2}. Symbols are used to show when animals also received CFA injections (+ and -). Tibio-talar joint ('ankle') tissues from Tie2-VEGFR2^{ECKO} mice were provided by Dr N Beazley-Long for experiments shown in this chapter (Figure 2.2), these came from six groups of mice with 5 -6 per group previously used in studies reported in Beazley-Long et al (2018).

Table 5.1: Experimental groups with numbers and treatments, from which joints were processed to compare histological features with and without CFA inflammation and endothelial-VEGFR2 inducible knockout (Beazley-Long et al., 2018).
*** all animals underwent brief anaesthesia to control for any effects.**

This Table contains the same information as Table 2.2, reproduced here for ease of understanding.

Genetic background	Treatments*	Groups	Number of animals
VEGFR2fl/fl (Tie2Cre^{ERT2} negative, genetic control)	Tam, no CFA	1. Sham (-)	6
	Tam, CFA	2. Sham (+)	5
VEGFR2fl/fl x Tie2Cre^{ERT2} (inducible knockout)	No Tam, no CFA	3. Uninduced (-)	5
	No Tam, CFA	4. Uninduced (+)	5
	Tam, no CFA	5. VEGFR2^{ECKO} (-)	5
	Tam + CFA	6. VEGFR2^{ECKO} (+)	5

5.2.2 Synovial blood vessel fractional area and density in mouse tibio-talar joints

5.2.2.1. CD31 immunohistochemical staining was used to stain the endothelial cell lining on blood vessels to investigate the effect of Tie2-VEGFR2^{ECKO} on the total area occupied by vessels (fractional area) and density of blood vessels in synovium and subsequently also in subchondral bone (section 5.31, 5.3.2). CD31 is an endothelial cell marker expressed in vascular development and is used for identification of newly formed and mature blood vessels (Lertkiatmongkol et al., 2016; J.-j. Qian et al., 2021).

Details on the general IHC methods and antibodies used in this thesis are in sections 2.7.1, Figure 2.14, and Table 2.8, 2.9).

The experiment for CD31 IHC was carried out as illustrated in Figure 2.15. All the sections were stained on the same day in two batches, with some modifications in the master IHC protocol. For instance, the time and temperature for antigen retrieval were increased from 20 minutes to 25 minutes and from 65°C to 70°C, respectively. The timing for inactivation by H_2O_2 was increased from 20 minutes to 25 minutes, and the concentration of BSA in blocking solution was increased from 1% to 2%. The methods used in processing of tissues, sectioning and blinding of sections are in section 2.4.

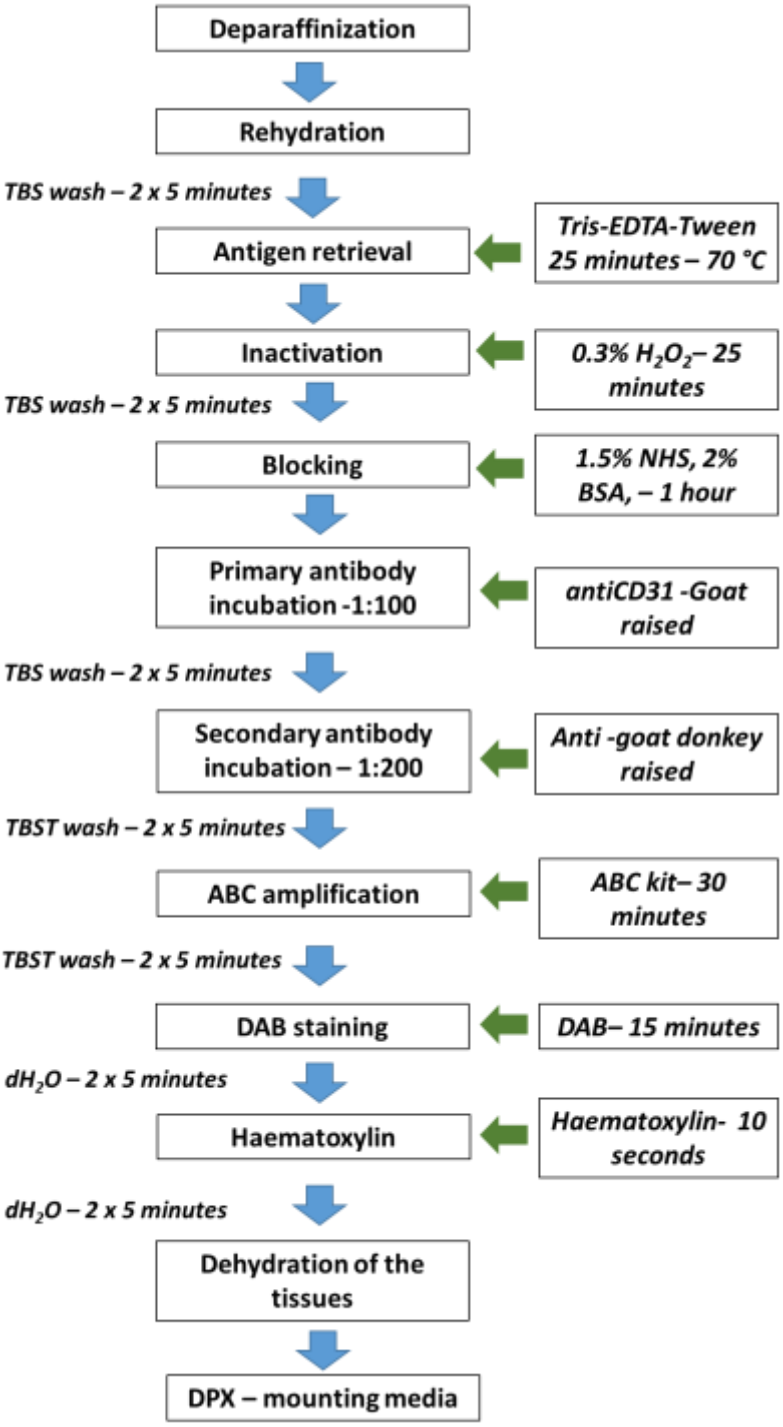

Figure 5.2: Flow diagram showing the protocol and adaptations used in CD31 IHC in mouse synovium.

Images were captured using a Zeiss Axioplan microscope located in SLIM (School of Life Sciences Imaging) with a 20x objective lens and analysed by using Fiji Imaging analysis software. Images were adjusted for colour balance to clearly visualize the

CD31 DAB staining in vessels. Hotspots of CD31 staining were identified in the synovium and subchondral bone and the area of vessels with positive expression measured. Blood vessel density in synovium was measured to a 100µm depth from the synovial surface (Figure 5.3A). The total area of the synovium was outlined as a region of interest (ROI) and measured (Figure 5.3B). The area of all individual CD31-positive blood vessels within the synovial ROI, excluding vessel lumens (Figures 5.3C &D) was also measured and the CD31-positive blood vessel area calculated using the equation below. Three images per section were measured and means for each joint was calculated (as discussed in section 2.3.3 - the reason of considering three hotspots/three images).

$$\%\ Synovial/SCB\ BVD = \frac{Mean\ area\ CD31\ positive\ blood\ vessels\ in\ synovium/SCB}{Mean\ area\ of\ synovium/SCB} X\ 100$$

The length of synovium, over which measurements were made, was also recorded was to verify that equivalent lengths of expanded synovium were studied (Figure 5.4).

During quantitation of synovial blood vessel density, observation of CD31 staining in blinded mouse joint sections suggested differences in blood vessel density in SCB. Subchondral bone blood vessel density was therefore calculated in a similar manner to synovium, over a length of 100 µm, and to an initial depth of 100µm from the cartilage/SCB junction. Vascular density was also calculated at a depth of 200-300µm from the cartilage/SCB junction for comparison with the more superficial SCB.

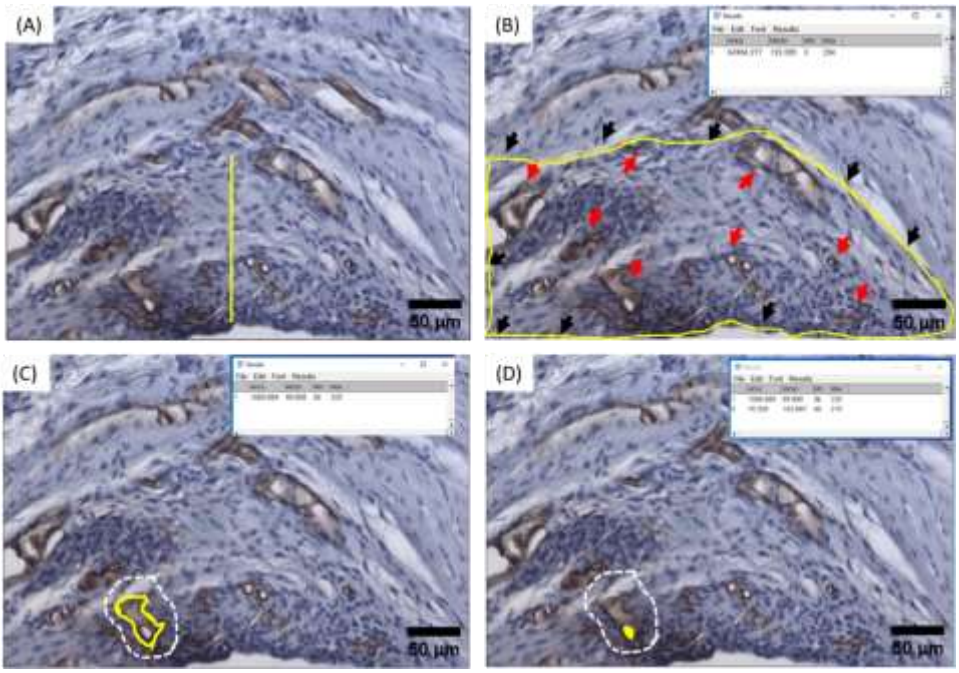

Figure 5.3: Determination of regions of interest (ROI) and vessel density in inflamed synovium in mice. Sections were stained for CD31 to identify vessels and H&E for morphology. Scale bars = 50µm. (A) Vertical yellow line shows 100µm depth from surface of synovium. (B) Yellow outline shows the area of synovium identified as the region of interest for measurement. Red arrows show vessels within the ROI, black arrows show the edges of the ROI. (C) White dotted lines outline an area containing a vessel, the area of which is outlined in yellow. (D) Vessel lumen area (shown in yellow) was also measured and subtracted from the vessel area in C. to determine total vascular area in the ROI.

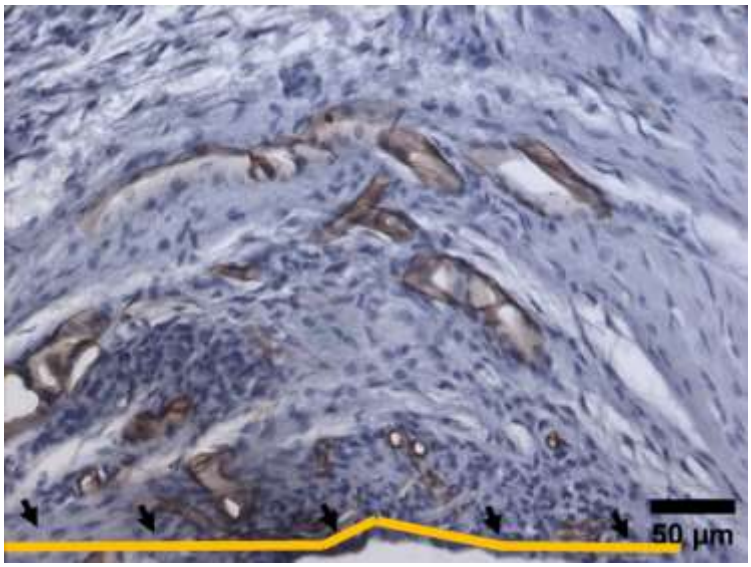

Figure 5.4: Measurement of length of region of interest in inflamed synovium in mice. Sections are stained for CD31 to identify vessels and H&E for morphology. Scale bars = 50µm. Straight horizontal line shows the length of synovium indicated by arrows.

5.2.3 Measurement of hypoxia in mouse joints

Based on the findings on cartilage damage (Figure 5.1B) and synovial vascularity in Tie2-VEGFR2^{ECKO} mice I hypothesised that VEGFR2 knockout may have increased the level of hypoxia in arthritic mice. A study was therefore designed to attempt to investigate the level of hypoxia in Tie2-VEGFR2^{ECKO} mouse joints.

A further 19 genetically modified mice of both sexes from multiple litters were included in this pilot study (Table 5.2). The same experimental groups were used as in the histology study (Vitterso et al., 2018), with 2 – 5 animals per group as shown in table 5.2, using the same experimental design and timeline as shown in Figure 2.2. Animals were housed in the same conditions as above and all licenced procedures including endothelial-VEGFR2 knockout were performed as described in section 2.3.7 by Dr Beazley-Long.

Table 5.2: Experimental groups with numbers and treatments, from which joints were processed to compare hypoxia with and without CFA inflammation and endothelial-VEGFR2 inducible knockout (Beazley-Long et al., 2018).

*** all animals underwent brief anaesthesia to control for any effects.**

Genetic background	Treatments*	Groups	Number of animals
VEGFR2fl/fl (Tie2Cre^{ERT2} negative, genetic control)	Tam, no CFA, no EF5	1. Sham (-)	2
	Tam, CFA, no EF5	2. Sham (+)	2
VEGFR2fl/fl x Tie2Cre^{ERT2} (inducible knockout)	No Tam, no CFA + EF5	3. Uninduced (-)	3
	No Tam, CFA +EF5	4. Uninduced (+)	4
	Tam, no CFA + EF5	5. VEGFR2^{ECKO} (-)	3
	Tam + CFA + EF5	6. VEGFR2^{ECKO} (+)	5

Inflammation was induced in 11 animals under brief anaesthesia using CFA injection, as described in section 2.3.8. In these animals, the dose of CFA was halved to 40µg on welfare grounds and based on advice of University of Nottingham Named Animal Welfare Officer.

At the end of the experiment, 14 days after induction of inflammation, mice were deeply anaesthetised with pentobarbital and the hypoxia-sensitive molecule EF5 ((2-(2-Nitro-1H-imidazol-1-yl)-N-(2,2,3,3,3-pentafluoropropyl) acetamide) was injected intravenously (60mg/kg) in all uninduced and VEGFR2^{ECKO} animals 30 minutes prior to perfuse-fixation with 4% paraformaldehyde. Sham animals were not injected with EF5 as negative controls. Tissues were collected and processed as discussed earlier in section 2.4.

5.2.4 IHC protocol for EF5 detection to identify hypoxic tissues.

EF5 is a lipophilic, uncharged molecule that allows very rapid, even tissue distribution that selectively binds to hypoxic cells forming adducts with cellular macromolecules. Binding is inversely proportional to oxygen partial pressure (Jenkins et al., 2000). The distribution of EF5 was used to detect the location of cellular adducts using immunofluorescence (IF). The IF protocol was similar to the IHC protocol (Figure. 5.2), but without an antigen retrieval step, and a different process for detection of the fluorescent probe.

Slides were rinsed in PBS/0.3% Tween-20 (PBS-Tween, 3 x 10 minutes incubations) after rehydration and blocked overnight in blocking solution (10% non-fat dry milk (Bio-Rad Cat. No.1706404) dissolved in PBS, 1.5% NHS, and 3% lipid free bovine serum albumin (Cat. No. 126575) at 4°C. Sections were incubated with the EF5 antibody-conjugate (Alexa Fluor® 488) at 75µg/mL in PBS/0.3% Tween-20/1.5% albumin solution at 4°C in a humid box for 6 hours followed by 5 x 10 minutes washes in PBS-Tween at room temperature in the dark, followed by mounting in Fluoroshield (Sigma Aldrich, F6182). Slides were stored in the dark at 4^{o}C until imaged using a Leica SPE confocal microscope.

5.2.5 Data extraction and analysis

All measurements and analyses were performed blinded to the experimental conditions of each histological section. Statistical analysis for comparisons between groups was carried out using one way ANOVA followed by Sidak's multiple comparisons test. Correlations between vascular density and cartilage damage were determined using Spearman's test. Statistical P value < 0.05 was considered as significant.

5.3 RESULTS

These experiments were designed to test the hypothesis that endothelial-specific VEGFR2 knock out in Tie-2 positive endothelial cells (Tie2-VEGF2^{ECKO}) would reduce the vascularity in synovium in arthritic but not in arthritic genetic/tamoxifen control mice. Loss of VEGFR2 in the Tie2-VEGFR2^{ECKO} mice would be expected to reduce VEGF-A-dependent angiogenesis and blood vessel formation normally seen in inflammation/synovitis, and through this action, result in the observed increase in cartilage damage seen in Tie2-VEGFR2^{ECKO} mice (Figure 5.1B).

5.3.1 Effect of Tie2-VEGFR2^{ECKO} on synovial vascularity

Blood vessels were evident in sections from all groups (Figure 5.5) and initial observation suggested there were higher numbers of blood vessels in sections from inflamed compared to uninflamed joints (Figure 5.5B, D, F compared to A,C, E).

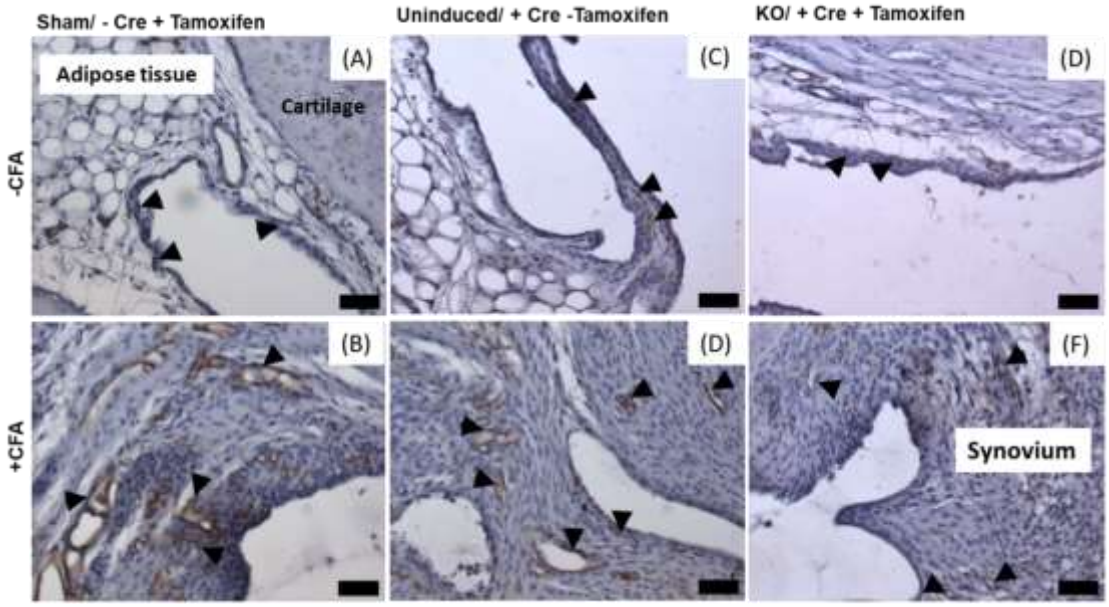

Figure 5.5: CD31 expression in synovial blood vessels in Tie2-VEGFR2^{ECKO} ± inflammation in mouse tibio-talar joint. (A & B) Sham animals (VEGFR2$^{fl/fl}$ Tie2Cre^{ERT} negative, + tamoxifen ± inflammation). (C & D) Uninduced animals (VEGFR2$^{fl/fl}$ Tie2Cre^{ERT}, no tamoxifen ± inflammation) (E & F) Induced animals (VEGFR2$^{fl/fl}$ Tie2Cre^{ERT} + tamoxifen ± inflammation). The appearance of brown CD31 staining was less in Tie2-VEGFR2^{ECKO} mouse joints with inflammation (F) compared to control mice with inflammation (B, D). Arrows indicate CD31 stained endothelial cells in blood vessels in synovium. Scale bar for all images - 50µm.

There were no differences in the mean synovial area in noninflamed joints between different groups (Figure 5.6A). There was an increase in synovial area in inflamed joints compared to controls ($F (5, 19) = 44.38$, ****$p<0.0001$) (Figure 5.6A), and, surprisingly, a significantly higher overall synovial area in inflamed Tie2-VEGFR2^{ECKO} joints compared to inflamed joints from both control groups. The length of synovial surface for each measured synovial segment was not different between the groups $F (5, 20) = 0.1948$, $p=0.9609$) (Figure 5.6B), and the depth in which vessels were quantitated (100µm) was the same in all sections, showing that similar areas of synovium were used in comparisons of total vascular number and vascular density (synovial length x 100µm depth).

The total area occupied by blood vessels (fractional area), not including vessel lumen in each ROI (Figure 5.6C) in synovium was measured to investigate differences in Tie2-VEGFR2^{ECKO} mice compared to controls (sham and uninduced animals with inflammation). There was a significant increase in the total area occupied by blood vessels in inflamed synovium in both sham and uninduced mice compared to non-inflamed mice (Figure 5.6C), as expected in synovitis (sham (-) 1001±915µm^2, sham (+) 2373±697µm^2, uninduced(-) 738±125µm^2, uninduced(+) 2265±313µm^2, mean vessel area±SD, $F (5, 20) = 6.450$, $p=0.0010$). There was no change in the total area of blood vessels in the same area of synovium in Tie2-VEGFR2^{ECKO} inflamed synovium (842±466, $p=0.9708$) in comparison to non-inflamed Tie2-VEGFR2^{ECKO} mice (1137±340). There was a significant reduction compared to the inflamed control groups, showing that knocking out endothelial-VEGFR2 in these animals reduced the total area occupied by blood vessels (fractional area) in inflamed synovium.

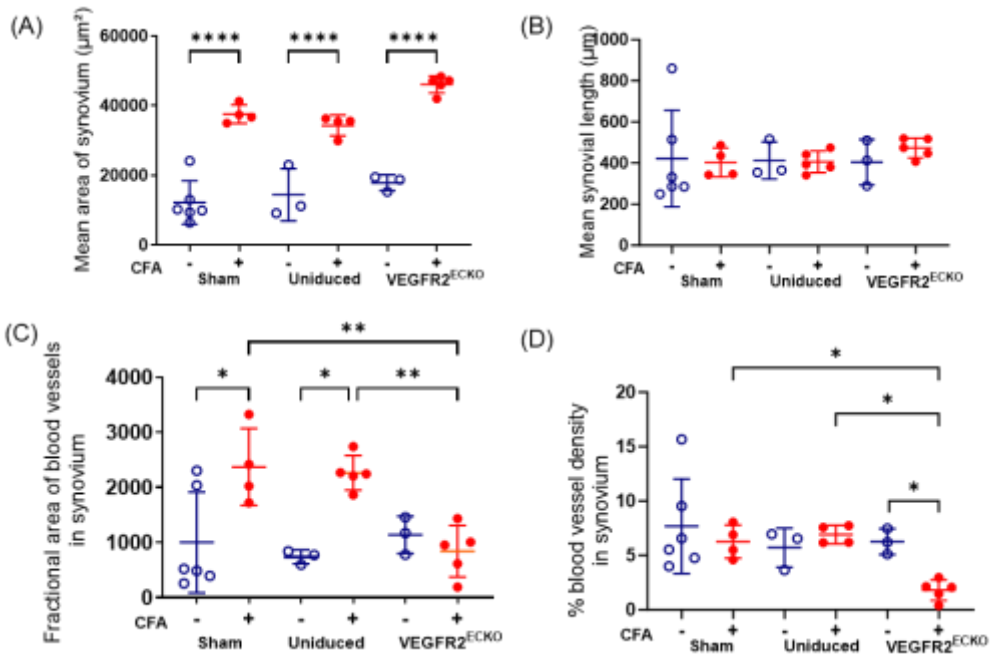

Figure 5.6: (A) Mean area of synovium of endothelial-VEGFR2 knockout mice. Symbols (+ and -) indicate when animals have received CFA injections. There was an expansion of synovium in CFA inflamed animals compared to their controls. (**p < 0.0001). The mean area of synovium in inflamed Tie2-VEGFR2^{ECKO} mice was significantly greater than in sham control (*p=0.04) and uninduced mice (**p=0.004). (B) Mean length of synovium was similar in all groups. (C) Fractional area of synovial blood vessels (total area occupied by blood vessels) was significantly higher in inflamed sham (+) (*p=0.0100) and uninduced (+) (*p=0.0114) animals compared to their non-inflamed controls, but not in Tie2-VEGFR2^{ECKO} mice (+). Tie2-VEGFR2^{ECKO} (+) mice had lower numbers of blood vessels than sham (+) (**p=0.0054) and uninduced (+) (**p=0.0062) mice. (D) % Synovial blood vessel density in endothelial-VEGFR2 knockout mice (+) decreased significantly as compared to VEGFR2^{ECKO} (-) (*p= 0.0357) as well as sham (+) (*p=0.023), and uninduced (+) (p=0.013). On-way ANOVA followed by Sidak's multiple comparisons tests. *p<0.05, **p<-0.01.**

All groups had similar blood vessel densities (Figure 5.6D) in inflamed and uninflamed joints, with mean vascular densities of 5-10% (sham (-) 7.7±4.4%, sham (+) 6.3±1.5%, uninduced (-) 5.7±1.8%, uninduced (+) 6.9±0.9%, Tie2-VEGFR2^{ECKO} (-) 5.9±1.2%, mean±SD). The mean blood vessel density in inflamed Tie2-VEGFR2^{ECKO} mice was significantly lower than the other inflamed control groups (1.8±0.9%), as hypothesized (Figures 5.5 B, D,F & 5.6D).These data show that the fractional area of blood vessels increased with the expansion synovium in most inflamed animals, maintaining synovial vascular density. The significantly higher synovial area with no change of blood vessel number in Tie2-VEGFR2^{ECKO} mice results in a reduced vascular density in Tie2-VEGFR2 knockout mice.

5.3.2 Effect of Tie2-VEGFR2^{ECKO} on subchondral bone vascularity

While analysing the blood vessel density in synovium, I also noted some sections in which there appeared to be fewer blood vessels in SCB. This led me to then evaluate blood vessel density in SCB. The aim of this was to determine whether Tie2-VEGFR2^{ECKO} affected SCB in normal and/or arthritic mice, and I determined this by measuring the blood vessel density in SCB in Tie2-VEGFR2^{ECKO} mice and controls, with and without IA, using the same sections and methods as described in sections 5.2.1 & 5.2.2. Vessel area was measured to a depth of 100um depth from the cartilage/SCB junction (Figure 5.7).

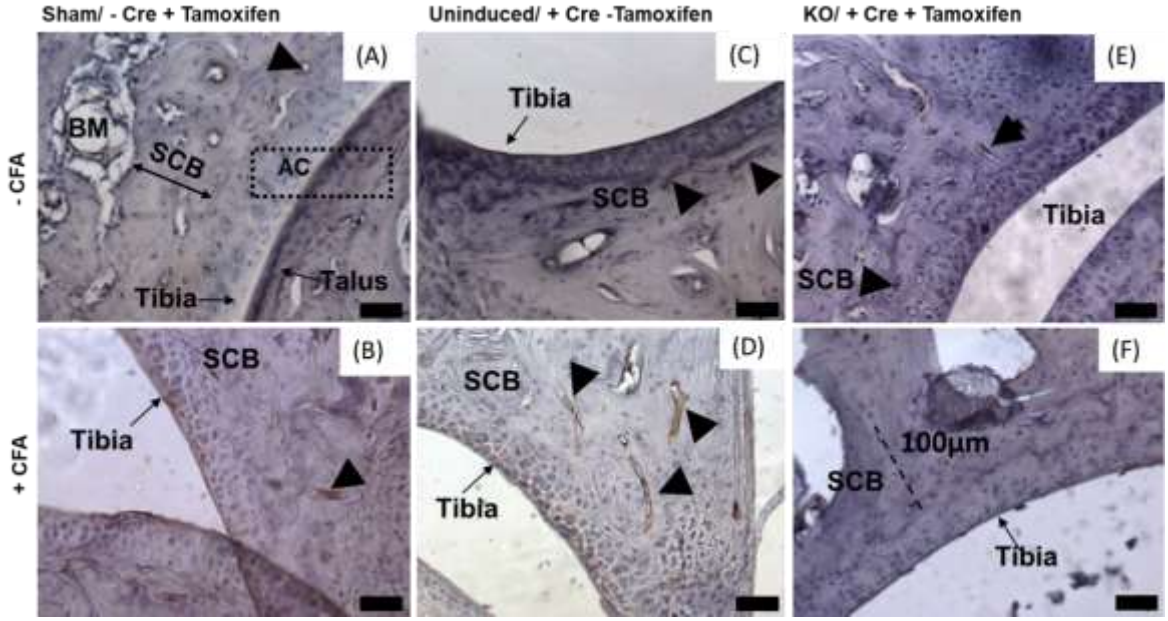

Figure 5.7: CD31 stained blood vessels in SCB in Tie2-VEGFR2ECKO ± inflammation in tibiotalar mouse joint. (A & B) Sham: VEGFR2$^{fl/fl}$ Tie2Cre^{ERT} negative, + tamoxifen ± inflammation (C & D) Uninduced: VEGFR2$^{fl/fl}$ Tie2Cre^{ER}, no tamoxifen ± inflammation (E & F) Induced: VEGFR2$^{fl/fl}$ Tie2Cre^{ERT}, + tamoxifen ± inflammation.
(A, B, C, D, E) There were blood vessels present in SCB from the cartilage/SCB junction to at least 100µm depth in all groups except in Tie2-VEGFR2^{ECKO} mice with inflammation (F) where there was a complete loss of blood vessels. Arrowheads indicate CD31 stained endothelial cells in blood vessels in SCB. White dotted lines starting from the cartilage/SCB junction show the depth of SCB considered for blood vessel density analysis. SCB: subchondral bone, BM: bone marrow, AC: articulating tibiotalar joint. Scale bar for all images = 50µm.

In the sham and uninduced groups (+ CFA), inflammation did not significantly affect the vascularity of SCB to a depth of 100µm although there was a lot of variability

between animals particularly in the uninduced (+ CFA) group (Figure 5.8A) with one animal having no SCB vessels in the measured area. There were no significant differences between the 4 control groups (sham (-) 2.7±0.6%, sham (+) 2.1±0.96%, uninduced (-) 2.2±1.1%, uninduced (+) 3±2.5%, Tie2-VEGFR2^{ECKO} (-) = 1.7 ± 1.0%, mean ± SD. Interestingly all inflamed Tie2-VEGFR2^{ECKO} mice had a complete absence of blood vessels in SCB from cartilage/SCB junction to 100um depth which was a significant reduction compared to other inflamed control groups (Figure 5.8A, Tie2-VEGFR2^{ECKO} (+) = 0 ± 0%, F(5,19)=3.296, p=0.026).

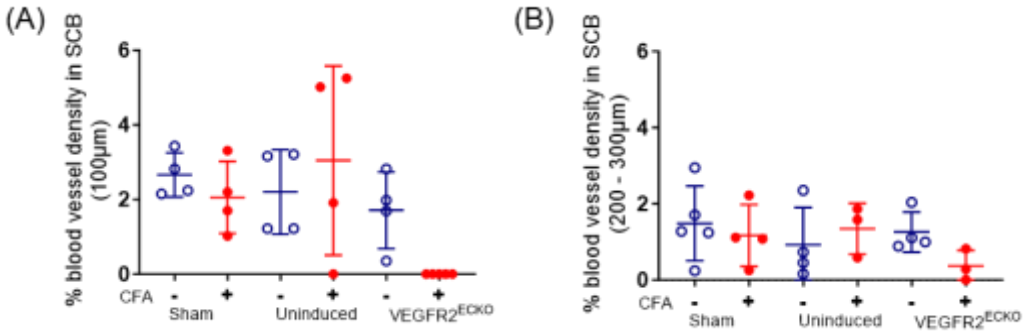

Figure 5.8: Blood vessel density in SCB 100µm length from tidemark. Symbols (+ and -) indicate when animals have received CFA injections. (A) Inflamed Tie2-VEGFR2^{ECKO} mice showed regression of blood vessels compared to inflamed control groups (p>0.05 cf. sham (+) and uninduced (+) groups. One-way ANOVA followed by Sidak's multiple comparisons tests (B) Blood vessel density in SCB 200 – 300µm from cartilage/SCB junction. There were no significant differences in subchondral bone blood vessel density in any groups (VEGFR^{ECKO} (+) p=0.0571 cf. VEGFR^{ECKO} (-).

I also investigated blood vessel density between 200 - 300 µm depth from the tidemark to determine whether this effect on blood vessels also affected those deeper in SCB (Figure 5.8B). At this depth there was no significant change found in blood vessel density (one way ANOVA F(5,17) = 0.87, p=0.52) between the 4 control groups (sham (±CFA) and uninduced (±CFA), similar to blood vessel density in 100µm depth, but a slight reduction was seen in VEGFR^{ECKO} (+) compared to all other groups (Sham (-) = 1.5±1%, sham (+) = 1.2±0.8%, uninduced (-) 0.9±1%, uninduced (+) 1.3 ± 0.7, Tie2-VEGFR2^{ECKO} (-) =1.2±0.5%, Tie2-VEGFR2^{ECKO} (+) = 0.4±0.4%).

5.3.3 The relationship between synovial/subchondral bone vascularity and cartilage damage

To investigate whether there was any relationship between synovial and SCB vascularity and cartilage damage, the correlation between blood vessel density (synovial and SCB) and cartilage damage score were determined (Figure 5.9). A moderate negative correlation was found between synovial/SCB blood vessel density and cartilage damage which supports my hypothesis that reduced synovial and SCB vascularity are associated with more severe cartilage damage.

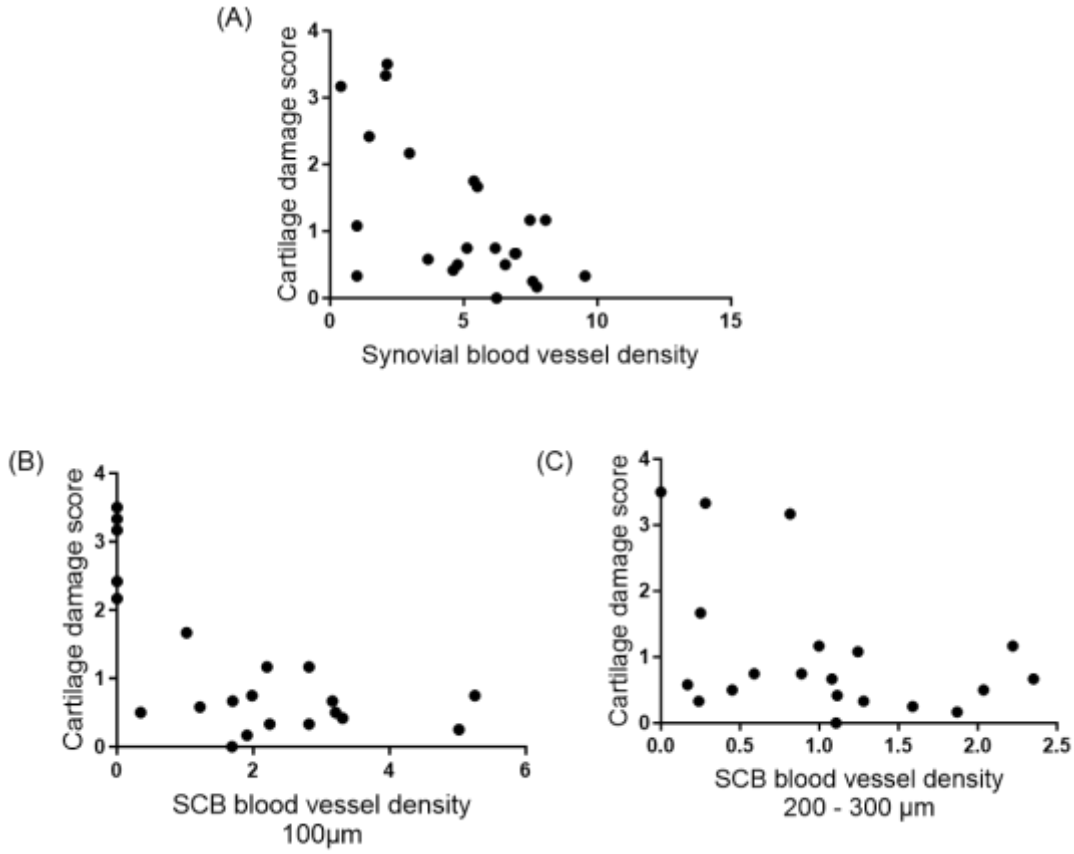

Figure 5.9: Synovial and subchondral bone vascularity is negatively correlated with cartilage damage in mouse tibio-talar joints in IA. There was a significant negative correlation between (A) synovial (r_s = - 0.5; p= 0.019) and (B) subchondral blood vessel density up to the depth of 100µm starting from the tidemark (r_s = - 0.6; p= 0.006), and cartilage damage. The correlation between cartilage damage and SCB blood vessel density up to the depth of 200 - 300µm from the cartilage/SCB junction (C) was not significant (r_s = - 0.4; p= 0.093). Two tailed Spearman's rank correlation.

After finding reduced blood vessel density in synovium and SCB Tie2-VEGFR2^{ECKO}, we designed a study to test the hypothesis that the reduction in vessel density in synovium and SCB in inflamed Tie2-VEGFR^{ECKO} mice might increase cartilage damage by increased hypoxia in inflamed joints. Joints from inflamed mice from all groups were imaged. Unfortunately, fluorescence was seen in negative control sections, in which no antibody against EF5 was used. As cartilage is normally hypoxic, I expected to see brighter fluorescence in this tissue than other tissues even in uninflamed controls. There were no obvious differences in the fluorescence staining between positive and negative controls (Figure 5.10), suggesting that there may be elevated levels background or auto-fluorescence. I was unfortunately unable to optimise the protocol for further analysis or get meaningful analyses from these joint sections with this technique.

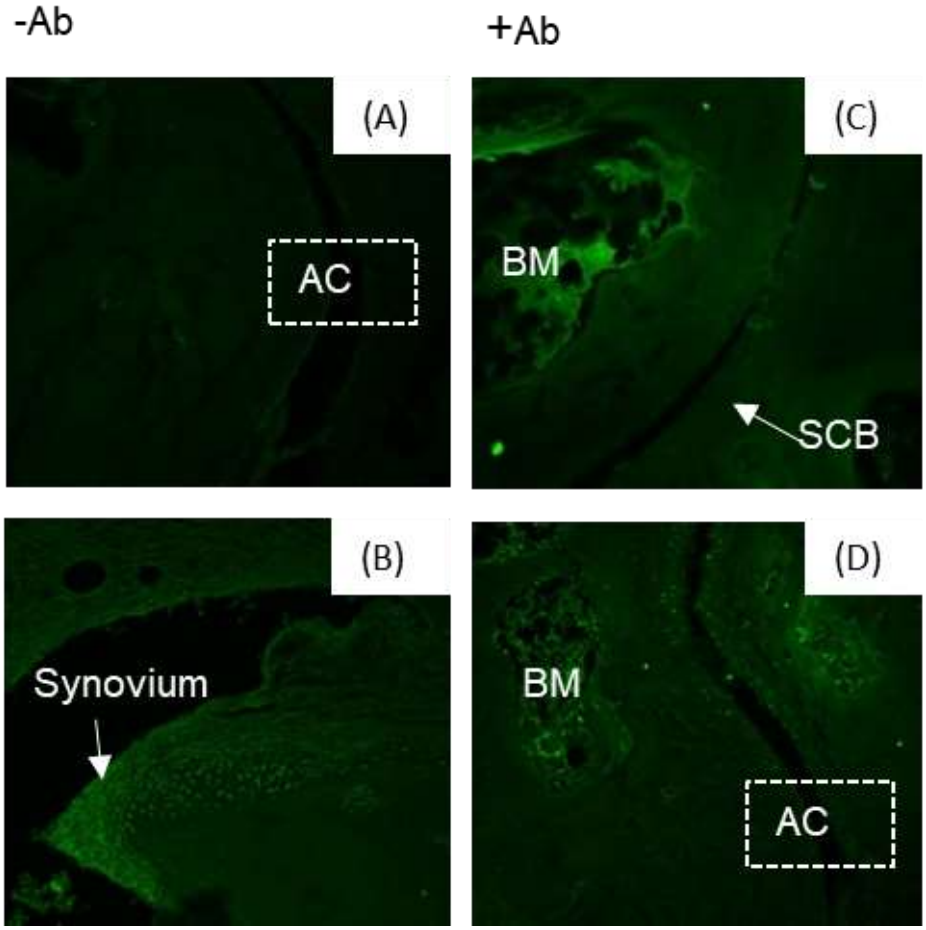

Figure 5.10: Optimisation of EF5 hypoxia antibody. Presence of EF5 fluorescence signal in randomly taken sections from EF5 injected inflamed mice (A, B) without primary anti-EF5 antibody, (C, D) with primary antibody. Arrows indicate synovium and SCB, while dotted box showing the articular cartilage. High background or autoflorescence was found which made it impossible to see any specific differences in staining between animals. S; Synovium, AC; articular cartilage, BM; bone marrow.

5.4 DISCUSSION

The initial study was designed to determine the effect of a reduction of endothelial-VEGFR2 on pain behaviour in mice, and then to verify whether Tie2-VEGFR2^{ECKO} effects on pain were mediated through an effect on synovial inflammation. Analysis of the effect of Tie2-VEGFR2^{ECKO} on joint inflammation showed little effect on synovitis but a detrimental effect on tibiotalar cartilage integrity during CFA-induced inflammation (Figure 5.1) (Vitterso et al., 2018). This unexpected finding led me to hypothesize that cartilage damage in Tie2-VEGFR2^{ECKO} mice might occur through altered synovial vascularity, which was evident in both synovium and superficial subchondral bone only in Tie2-VEGFR2^{ECKO} mice. In addition, the negative correlation between cartilage damage and synovial/superficial SCB blood vessel density further supports a relationship between the reduced synovial and subchondral vasculature density and cartilage integrity in IA in VEGFR2^{ECKO} mice. These findings suggest that endothelial-VEGFR2 in both synovial and superficial SCB may play a vital role in the maintenance of cartilage in IA.

5.4.1 Sources of cartilage nutrition

Extensive and old literature evidence indicate that deficiencies in the nutrition of cartilage could be one of the main reasons for this tissue's degeneration in arthritis (Grimshaw & Mason, 2000; H. A. Horner & Urban, 2001; A. R. Jackson & Gu, 2009; Razaq et al., 2003). Articular cartilage is an avascular tissue (A. R. Jackson & Gu, 2009) with little capability for self-repair, that is hypothesised to be nourished by two potential sources, synovial fluid and SCB vessels (Pörtner & Meenen, 2010).

Despite the close anatomical association between the tissues, the nutritional interaction between SCB and articular cartilage in synovial joints has not been the emphasis of broad research (Mansell et al., 2007) as the basal calcified cartilage zone at the osteochondral junction has been considered as an impermeable barrier to fluid and solute transport (Clark, 1990; M. A. R. Freeman, 1979). Although some still state that "The synovial fluid is the only source of nutrients for avascular, alymphatic, and aneural cartilage" (Semenistaja et al 2023), there is evidence for nutrition from both

sources (Kulkarni et al., 2021). More recent evidence does show that there is dynamic exchange of signals and communication taking place between cartilage and SCB (X. Wu et al., 2021; X. Zhou et al., 2020), and that small molecular weight solutes can penetrate calcified cartilage (Arkill & Winlove, 2008), suggesting that this interface is sufficiently permeable to contribute to cartilage support.

A. Synovium

The hypothesised synovial fluid contribution for nutrient supply to the articular cartilage is an old one. Synovial fluid derives from blood plasma and is concentrated as it filters through the synovium where molecules such as hyaluronan are secreted into the fluid providing lubrication (Tamer 2013). The cartilage surface can absorb fluid (Leidy, 1849 cited in (Malinin & Ouellette, 2000), such as synovial fluid, potentially providing sufficient nutrition to the articular cartilage (Virchow, 1867). Use of polymethacrylate bone cement at the osteochondral junction in fracture repair in sheep did not affect cartilage integrity (Goetzen et al., 2015). Depriving cartilage of nutrition from SCB, synovium, or both showed that, in the short term (8 weeks), synovial fluid derived nutrition is the prevailing source of nourishment for adult cartilage structure in rabbits (Wang, Wei et al. 2013) demostrating the importance of synovium to cartilage integrity. The predominant hypothesis is therefore that synovial fluid is the most significant route of nutrient supply to cartilage in mature animals (Hewitt & Stringer, 2008; HONNER & THOMPSON, 1971; Y. Wang et al., 2013) and that nutrition from SCB, even if it exists, is of little or no importance (Clark, 1990; HONNER & THOMPSON, 1971; McKibbin & Holdsworth, 1966; Y. Wang et al., 2013). The relative importance of nutrients supply to articular cartilage by diffusion either via synovial fluid or SCB is, however, arguable (Hewitt & Stringer, 2008), and the predominant concept that cartilage does not receive nutrition from underneath the SCB plate (Malinin & Ouellette, 2000) is open to reconsideration (X. Wu et al., 2021; X. Zhou et al., 2020).

B. Subchondral bone

My data showing a complete loss of blood vessels in SCB with greater cartilage damage suggested that subchondral vessels are important in cartilage nutrition. Subchondral bone is normally highly vascular, and highly innervated, and subchondral

blood vessels can extend into calcified cartilage through a networks of ‘canals’ in the SCB and calcified cartilage (Madry et al., 2010). In bovine articular tissues, SCB significantly affected chondrocyte survival in articular cartilage during explant culture (A. Amin et al., 2009). Excision of SCB from articular cartilage caused an increase in chondrocyte death at seven days exclusively in the cartilage superficial zone. The presence of SCB in the culture medium prevented the increase in chondrocyte death within the superficial zone. This is suggestive of some interaction and support for cartilage from SCB, even *in vitro*, although this cannot be attributed to SCB vessels under these conditions (A. Amin et al., 2009). Loss of SCB nutrition also caused significantly increased cartilage damage and chondrocyte apoptosis in slightly longer studies on rabbits by Wang and colleagues (12 versus 8 weeks), suggesting that chondrocyte survival may be influenced by an interaction between SCB and articular cartilage via soluble mediator(s) (Y. Wang et al., 2013).

Very few studies have been done on sources of cartilage nutrition in inflammatory or OA models. It is thought that increased metabolism in inflamed synovium reduces oxygen availability, also contributing to cartilage damage in both animal models and human OA (Zeng et al., 2022). As OA progresses, there is SCB remodelling and angiogenesis resulting from cross talk between cartilage and SCB (X. Zhou et al., 2020). Increased vascularization and microcracks development in cartilage and the SCB matrix allows the transfer of mediators between cartilage and subchondral bone (Burr & Radin, 2003; Lajeunesse & Reboul, 2003). Several biological factors, such as VEGF-A, TGF-ß, Cathepsin K, MMP13 and several others, produced by SCB and cartilage are involved in the communication of these two tissues (Konttinen et al., 2002; Moldovan et al., 1997; Nakase et al., 2000; Thomas Pufe et al., 2001).

VEGF-A plays an important role in cartilage and subchondral crosstalk in arthritis. As discussed earlier, in chapter 1, VEGF-A expression increases in the synovium (Dubuc, 2012; Giatromanolaki et al., 2003; L Haywood et al., 2003; J. Jackson et al., 1997; Yancopoulos et al., 2000), cartilage (Enomoto et al., 2003; Franses et al., 2010; Honorati et al., 2004; Pfander et al., 2001; Thomas Pufe et al., 2001; J. O. Smith et al., 2003; Tsuchida et al., 2014; D. A. Walsh et al., 2010) and SCB (Corrado et al., 2013; J.-E. Huh et al., 2010; Neve et al., 2013) in arthritis. Communication of VEG-A

between the cartilage, SCB, and bone marrow is potentially facilitated by vascular connections, channels formation and fissures between these tissues (Imhof et al., 1999; Lajeunesse & Reboul, 2003; Madry et al., 2010; Sokoloff, 1993). Vascular innervation into articular cartilage causes subchondral bone marrow replacement with FVT expressing VEGF-A (D. A. Walsh et al., 2010). On the other hand, osteoblasts and osteocytes in the subchondral bone led to increased VEGF-A expression which directly stimulates articular chondrocytes to secrete metalloproteinase and results in cartilage degeneration (Funck-Brentano et al., 2014; Moldovan et al., 1997).

Following VEGFR2 endothelial knockout, the vasculature in the synovium and SCB is unable to respond to the hypoxia, the vascular angiogenic response in inflammation is blocked and cartilage compromised by the increased hypoxia and loss of nutrients from both synovium and SCB. This suggests that there could be even ***greater*** hypoxia in cartilage due to compromised blood vessels in synovium and SCB in VEGFR2 endothelial knockout mouse joints. Although articular chondrocytes in avascular cartilage are well-adapted to low oxygen (2%-5% O_2) for survival (Gelse et al., 2008; S. Zhou et al., 2004), ***high*** hypoxia levels (≤1% O_2) are closely related with arthritic pathology (Hamada et al., 2008; Kennedy et al., 2011) due to alteration in transcription factors, chemokines, angiogenic growth factors and matrix-degrading enzymes (Gelse et al., 2008; L. Wu et al., 2012).

There are various experimental approaches for hypoxia investigation including direct and indirect methods in cell culture in the laboratory as well as tissues in animal. Direct methods involve detection of HIF proteins for example the immunolabeling of HIF-1α or HIF-2α (Ambrosetti et al., 2018; Gordan et al., 2008; K. E. Lee et al., 2016; F. Li et al., 2018) or downstream HIF-targets at protein and/or mRNA levels (Ambrosetti et al., 2018; Eisinger-Mathason et al., 2013). On the other hand, hypoxyprobes like EF5 can be used for the detection of *in vivo* tissue hypoxia (Eisinger-Mathason et al., 2013; K. E. Lee et al., 2016). This involves administration of exogenous 2-nitroimidazole probes, for instance pimonidazole or EF5 (2-(2-Nitro-1H-imidazol1-yl)-N-(2,2,3,3,3-pentafluoropropyl) acetamide), to animals which lead to formation of hypoxic adducts in tissues. These hypoxic adducts can be detected by immunolabeling with an antibody, such as Hypoxyprobe™ and ELK3-51 (Vermeer et al., 2020) for

pimonidazole and EF5, respectively, followed by the tissue fixation (S. M. Evans et al., 2007; S. M. Evans et al., 2001; F. Li et al., 2018; Varia et al., 1998; Vermeer et al., 2020).

Pimonidazole exists in two forms, very hydrophilic and lipophilic, which have a very complex biodistribution (C. J. Koch, 2008). In contrast, EF5 is lipophilic and uncharged which allows even and very rapid tissue distribution (C. J. Koch, 2008; C. J. Koch & Evans, 2015; Laughlin et al., 1996; Ziemer et al., 2003). Therefore, I attempted to use EF5 for hypoxia measurement (section 5.3.3) in damaged articular cartilage in inflamed Tie2-VEGFR^{ECKO} mouse joints to investigate whether an ***increased/ more severe*** hypoxic condition could be the possible reason for greater cartilage degradation. Unfortunately, the quantification of hypoxia measurement could not be completed due to background/autoflorescence.

Interference by autoflorescence is one of the major issues of fluorescence microscopy. Autoflorescence in formaldehyde-fixed, decalcified tissue paraffin embedded sections can be induced during the tissue processing techniques. It is often caused by precipitates formed during bone decalcification by excess aldehydes in tissues after fixation (Werner Baschong et al., 2001; W Baschong et al., 1997; Romijn et al., 1999). There are methods that can be used to reduce this, such as the use of ammonia-ethanol, or sodium borohydride, and Sudan Black B during the rehydration of deparaffinised sections. These remove precipitates and aldehydes. I did not attempt these techniques because there was also a question on whether EF5 was able to bind to already hypoxic tissues such as cartilage or its binding affinity requires certain tissue percentage of oxygen. A study shows that EF5 binds minimally at 10% oxygen with improvement of binding when the oxygen percentage drops to 1%, and a 10-fold stronger binding affinity was seen at oxygen concentration between 0.1% and 1% (Sperry et al., 2020). This study also indicates that severe hypoxia (≤1%) may be necessary for robust EF5 localization (C. Koch et al., 1995). Use of hypoxyprobes also depends on blood flow to the area, and lack of success in this approach may also be due to lack of EF5 access into cartilage, although this approach has been used previously to show cartilage hypoxia (Sperry et al., 2020).

An alternative approach to EF5 to investigate increased hypoxia in Tie2-VEGFR^{ECKO} mouse joints could have been to analyse the expression of factors known to be activated by increased hypoxia in cartilage. It is well described that when tissue's oxygen demand exceeds supply, this leads to the activation of a cascade of intracellular events that increases the expression of HIFs. Hypoxia-inducible factors are activated as an adaptive mechanism in reaction to the changes in oxygen tension (Imtiyaz & Simon, 2010) that allows cell survival in a hypoxic environment (A. L. Harris, 2002; Semenza, 1998), but in some cases these adaptive responses can result in the acceleration of disease progression (E. Ikeda, 2005) such as in pathogenesis of RA and OA.

Three HIF-α isoforms (HIF-1α, HIF-2α and HIF-3α) have been described and HIF-1α has been most extensively investigated (L. Fan et al., 2014). HIF-1α is detectable only in hypoxic milieu and is degraded rapidly under in normal oxygen conditions. HIF-1α is involved in cartilage homeostasis by maintaining chondrocyte phenotype, regulating autophagy and apoptosis, and inhibiting articular cartilage ECM degradation (S. Hu et al., 2020; Okada et al., 2020; L. Wu et al., 2012; F.-J. Zhang et al., 2015). HIF-1α expression is found both in normal and arthritic articular chondrocytes in human (Gelse et al., 2008). It plays a key role in inflammatory conditions by regulating VEGF-A to promote adaptation of chondrocytes to hypoxic environments (Y. Chen et al., 2019) in addition to ECM degradation inhibition (S. Hu et al., 2020) and increased ECM synthesis in articular cartilage (S. Hu et al., 2020; Kovacs et al., 2019; P. Wang et al., 2020).

HIF-2α is a key catabolic factor that is found predominantly in highly differentiated chondrocytes. HIF-2α expression increases in animal arthritis models and human OA and RA and mediates chondrocyte differentiation and hypertrophy contributing to degradation of cartilage. Moreover, HIF-2α is also involved in the initiation of blood vessel formation accompanied by increased expression of VEGF-A (Skuli et al., 2012) and upregulation of type X collagen and degenerative MMP enzymes, including MMP13 (Hirata et al., 2012; Y. H. Huh et al., 2015; Neefjes et al., 2020; J.-H. Ryu et al., 2014; T. Saito et al., 2010; Van der Kraan & Van den Berg, 2012; S. Yang et al., 2010; T. Ye et al., 2020). Hence, expression level of HIF-2α could be a potential

marker of a further hypoxic change in an already hypoxic cartilage environment in Tie2-VEGFR^{ECKO} mouse joints, as an alternative approach to EF5. I could not conduct this experiment as it would have required further animal studies, and due to the COVID19 pandemic and restrictions in labs and BSU this was not possible.

Together with the literature findings, my data show a negative relationship between synovial and superficial SCB vascularity and histological cartilage damage. This suggests that both SCB and synovial vasculatures contribute to cartilage nutrition, as compromise of vessels by VEGFR2 knockout in vascular endothelium in either, and particularly both locations, is associated with increased cartilage damage in inflamed joints.

5.5 CONCLUSIONS

Two main conclusions can be drawn from the data presented.

1- Endothelial-VEGFR2 knockout is detrimental to cartilage damage in IA.
2- Endothelial-VEGFR2 knockout reduces both synovial and superficial subchondral bone blood vessel density in IA.

This leads to the hypothesis that vessels in synovium and subchondral bone are important for maintenance of cartilage in IA.

These findings imply that VEGF-A$_{xxx}$a pro-angiogenic isoforms acting through VEGFR2 on endothelial cells are important in the synovial and subchondral vascular response to IA, with angiogenesis in these blood supplies playing a pivotal role in cartilage nutrient supply and maintenance of the cartilage milieu in IA. These data therefore do not support the proposal that inhibition of endothelial-VEGFR2 in joints would be a successful therapy to reduce destruction of joints in IA.

6. THE VEGF-A ALTERNATIVE SPLICING AXIS IN INFLAMMATORY ARTHRITIS IN RODENTS

6.1 INTRODUCTION

Alternative splicing plays a significant role in regulating gene expression and protein diversity but still its role in IA has received limited attention to date. There are very few studies which link alternative splicing events and clinical features of IA such as RA. Alternative splicing is a key step in the production of different VEGF-A isoforms and families (section 1.11, Figure 1.9), and there is very little published data on VEGF-A splice variant expression in either RA or OA.

In 1996, fibronectin splice variants were reported in synovial microvasculature (Elices et al., 1994; K. Shiozawa et al., 2001). Fibronectin variants including the 'extra domain A' (EDA, exon 22) promote adherence and migration of synoviocytes (Hino et al., 1996), and FN-EDA synovial levels are associated with joint damage (K. Shiozawa et al., 2001). Other alternatively spliced genes which are involved in cell metabolism and adhesion such as CD44 and MAP2K4 are also important in RA (Grisar et al., 2012; Shchetynsky et al., 2015). For instance, higher expression of specific variants of the signal transducing membrane receptor CD44 was reported in RA synovium compared with OA (Grisar et al., 2012) with more invasive synoviocytes (Wibulswas et al., 2002).

Different alternatively spliced isoforms within the VEGF family (Figure 1.9) are seen in IA and RA, but to date no association between production of VEGF-A_{xxx}a/b isoforms through alternative splicing in exon 8 has been reported. VEGF-A isoforms such as VEGF-A_{121} and VEGF-A_{165} were observed in RA synovium (Thomas Pufe et al., 2001), and both osteoarthritic and normal cartilage expresses VEGF-A_{189}, VEGF-A_{121} and VEGF-A_{165} (Enomoto et al., 2003; Fay et al., 2006; Thomas Pufe et al., 2001).

Chapter 1 outlined the current understanding of alternative splicing control of the VEGF-A family (section 1.11). Alternative splicing of VEGF-A pre-mRNA in exon 8 (section 1.11.2, 1.11.3) is regulated by SRPK1 via phosphorylation of SR proteins specifically SRSF1 (Giannakouros et al., 2011; Nowak et al., 2010; Z. Zhou & Fu,

2013). SRPK1 and other splicing kinases (DYRKs, CDKs, CLKs, MAPKs) and factors such as SRSF1 have been identified as potential therapeutic targets, particularly in oncology (Boni et al., 2020; Naro et al., 2021).

Dysregulated alternative splicing has been widely investigated in multiple cancers (Oltean & Bates, 2014; M. Patel et al., 2019) including colorectal (E. M. Amin et al., 2011; Hayes et al., 2007), kidney (Wagner et al., 2019), prostate (Mavrou et al., 2015), breast (Hayes et al., 2007; J.-C. Lin et al., 2014), melanoma (Gammons et al., 2014) and leukaemia (Siqueira et al., 2015; Tzelepis et al., 2018). It also contributes to pathogenesis in Alzheimer's disease and frontotemporal dementia (Hartmann et al., 2001; Nikom & Zheng, 2023), macular degeneration (Pujol-Lereis et al., 2018), arthritis (Aravilli et al., 2021), human papillomavirus infection (Basera et al., 2022), and atherosclerosis (Hasimbegovic et al., 2021).

The protein kinase SRPK1 acts to activate downstream splicing factors such as SRSF1 through phosphorylation, the key splicing factor to regulate alternative splicing of VEGF-A to produce pro-angiogenic VEGF-A_{xxx}a variants (Nowak et al., 2010). SRSF1 is also implicated in alternative splicing in autoimmune diseases (Cassidy et al., 2022) such as SLE (da Glória et al., 2014; Kono et al., 2018; Ramanujan et al., 2021) in which increased SRSF1 expression in T cells is associated with disease severity (Katsuyama et al., 2019). Furthermore, SRSF1 is overexpressed in many different cancer types such as prostate (Broggi et al., 2021), breast (Du et al., 2021), lung (Ezponda et al., 2010), colorectal (Sheng et al., 2017), and glioblastoma multiforme (GBM) (Barbagallo et al., 2021). Studies are now also showing that SRPK1 and SRSF1 alter VEGF-A splicing to affect angiogenesis in various cancers, renal cell carcinoma (X.-w. Pan et al., 2021), cholangiocarcinoma (Supradit et al., 2022), and squamous cell carcinoma (Biselli-Chicote et al., 2017).

Both VEGF-A and VEGFR2 are intimately involved in the pathogenesis of both RA and OA (Hamilton et al., 2016) as discussed in sections 1.12. In chapter 5, I showed that inducible endothelial cell knockout of VEGFR2 had a significantly detrimental effect on synovial and SCB blood vessels and cartilage damage in IA.

Many studies have shown an upregulation of total - (pan) - VEGF-A expression in inflammatory and degenerative arthritis in different cell and tissue types such as synoviocytes and chondrocytes (Franses et al., 2010; Fromm et al., 2019; Inoue et al., 2005; Xinying Zhang et al., 2016; Zupan et al., 2018). VEGF-A has also been identified as a candidate gene biomarker in arthritis in multiple bioinformatic analyses (A. Jiang et al., 2020; Z. Li et al., 2020; Xu et al., 2021; Yu et al., 2022). Despite progress in the understanding of RA pathogenesis and significant developments in RA treatment with biological therapy, some RA patients are refractory to biological disease-modifying anti-rheumatic drugs (DMARDs), and to the most recently developed small-molecule treatments, such as JAK inhibitors (P. C. Taylor et al., 2023). To address this issue, it is necessary to examine the presence and expression of target molecules in animal models for further investigation of new drugs, such as VEGF-A alternative splicing inhibitors (Dimitrios Amanitis, 2022).

A colleague in the laboratory showed that total VEGF-A expression was increased in inflamed human synovium and was positively correlated with the severity of synovitis, but VEGF-A_{165}b levels were unchanged (D Amanitis et al., 2020). This suggests that VEGF-A_{165}a isoforms are increased in inflamed human synovium. He also investigated the expression of the splicing kinase SRPK1 and activation of SRSF1 splicing factor (which control the VEGF-A splicing axis) in human RA and OA synovium. This showed for the first time that SRSF1 NL was increased in human inflamed synovium. Moreover, SRSF1 NL, indicating activation and also suggesting altered splicing to VEGF-A_{xxx}a isoforms, was highly correlated with the degree of synovitis (Dimitrios Amanitis, 2022). Splicing in favour of VEGF-A_{165}a will drive inflammation, as this isoform fully activates VEGFR2 to stimulate both angiogenesis (Section 1.11) and cartilage damage in animal models of arthritis (J.-j. Qian et al., 2021). In contrast, the alternatively spliced isoform VEGF-A_{165}b does not fully activate VEGFR2 (section 1.11). Prior to the study from our group, there were no reports on VEGF-A splice variant expression through alternative splicing in exon 8 in IA in either human tissue or animal models.

Animal models of arthritis continue to play an important part in pre-clinical research with the primary aim to translate these findings into clinical trials, taking research from

the “bench-to-bedside” (Chabner et al., 1998; Gibbs, 2000; Goldblatt & Lee, 2010; Saijo, 2002; Saijo et al., 2003; Woolf, 2008). Back-translation is the replication of human findings into animal models to verify that an animal model is valid for translational studies. I therefore investigated the expression of the key factors involved in VEGF-A exon 8 alternative splicing control, SRPK1 and SRSF1, to determine whether they were altered in IA in animal models.

Primary hypothesis: Experimental arthritis alters expression and localisation of the constituents of the VEGF-A splicing axis, SRPK1 and SRSF1, in a way that promotes VEGF-A exon 8 alternative splicing, potentially producing VEGF-A$_{xxx}$a isoforms in rat and mouse IA models, as seen in human inflamed synovium.

Aims:

1. to determine whether changes in SRPK1 and SRSF1 expression and localisation in synovium in mouse and rat arthritis models are similar to the changes seen in human arthritic synovium.
2. to determine the effect of inflammatory arthritis and endothelial-VEGFR2 inhibition/knockout on SRPK1 and SRSF1 expression and localisation in synovium in mouse and rat arthritis models.

Objectives:

1. to measure changes of expression of SRPK1 and SRSF1 in rat and mouse inflamed synovium in experimental arthritis models.
2. to compare the changes in the expression of SRPK1 and SRSF1 in rat and mouse experimental arthritis models to changes in human arthritic synovium.

As I used the tissues from the studies on arthritis in rats and mice to address this hypothesis, I also investigated the effect of VEGFR2 inhibition and endothelial-VEGFR2 knockout to determine whether inhibiting or blocking VEGFR2 had any effect on the expression of SRPK1 and SRSF1, or activation of SRSF1.

6.2 MATERIALS AND METHODS

6.2.1 Animal models

The tissues used to examine SRPK1 and SRSF1 expression in inflammation came from the rats (tibio-femoral joint) used in the PTK787 study (Chapter 4) and the mice (tibio-tarsal joint) used in the Tie2-VEGFR2 knockout and hypoxia studies (Chapter 5). In this chapter I only show the data from the rats using commercial CFA, as the histological changes were more consistent in these animals. Joints from rats were collected 10 days after CFA, and mouse joints 14 days after CFA. Details on animals and tissue preparation are in sections 2.3 and 2.4 respectively.

To examine the effect of VEGFR2 inhibition and endothelial-VEGFR2 knockout on splicing constituents I also used tissues from animals from these same studies treated with PTK787 (rats) and tamoxifen (mice).

6.2.2 IHC for SRPK1and SRSF1 expression in rat and mouse synovium

Immunohistochemical staining for SRPK1 and SRSF1 was done as described earlier (section 2.7.1, Figure 2.14), with changes to experimental conditions for SRPK1 in mouse, and SRPK1 and SRSF1 in rat as shown in Table 6.1. As the primary SRSF1 antibody was raised in mouse.

I optimised the 'mouse on mouse kit' for use in these tissues (Section 2.8.1 and Figure 6.1). The IHC was performed in two batches for mouse sections and three batches for rat sections for each antibody.

6.2.3. Quantification of SRPK1 and SRSF1 staining in rat and mouse synovium

SRPK1 and SRSF1 were analysed in rat and mouse synovium using measurement of fractional area (FA) of expression, and total number of cells with SRPK1/SRSF1 expression (cytoplasm and/or nucleus) and the number of cells with SRPK1 or SRSF1

NL, as discussed in detail in Chapter 2 sections 2.8.2 and 2.83. The following formulae (shown again from chapter 2 for convenience) were used for to calculate FA and NL. The area of synovium considered for fractional area expression and localisation was on the basis of hotspots regions. The images were analysed under 20x magnification using macro software while localisation measurements were analysed under 50x magnification (sections 2.8.2, and 2.83). To make sure that the equivalent area was quantified for both analysis (SRPK1/SRSF1), the whole area was considered under 20x magnification for FA expressions. On the other hand, the localisation was quantified in 100µm depth of inflamed synovium, whereas for sham (noninflamed) only synovium –excluding other tissue i-e adipose tissues- was analysed under 50x magnification.

$$Fractional\ area\ expression = \frac{Total\ area\ of\ staining\ in\ cells}{Total\ positive\ area}$$

$$= \frac{Nuclear\ localisation\ Total\ number\ of\ cells\ with\ nuclear\ stain\ only}{Total\ number\ of\ postive\ stained\ cells\ (nuclear + cytoplasmic)}$$

Table 6.1: Changes to the master IHC protocol during optimisation of conditions for SRPK1 in mouse and SRPK1/SRSF1 IHC in rat synovium.

	Antigen retrieval in Tris-EDTA-Tween 20	Inactivation H_2O_2	Blocking	Washes in TBS/TBST
SRPK1- IHC in mouse synovium	30 minutes @ 80°C	3% - 30 minutes	1.5% NHS, 5% BSA, – 1 hour	2 x 10 minutes
SRPK1- IHC in rat synovium	30 minutes @ 75°C	3% - 30 minutes	3% NHS, 5% BSA, – 1 hour	2 x 10 minutes
SRSF1 IHC in rat synovium	30 minutes @ 75°C	3% - 30 minutes	3% NHS, 5% BSA, – 1 hour	2 x 10 minutes

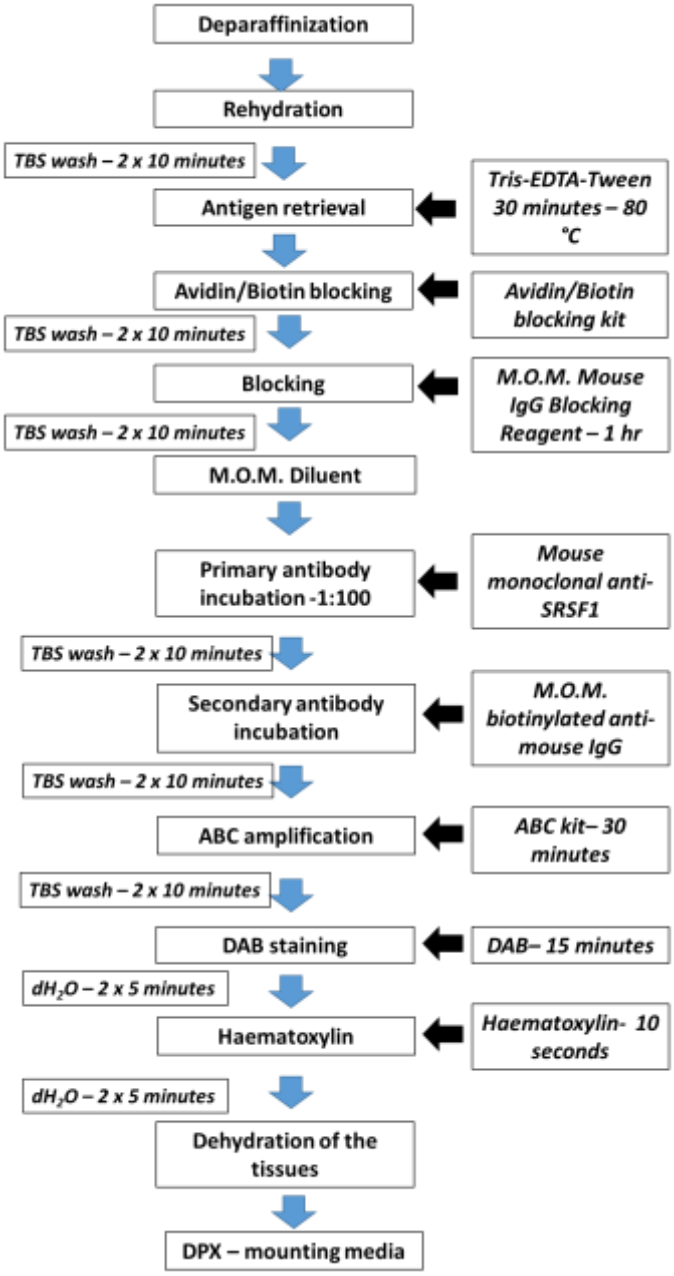

Figure 6.1: Flow diagram of SRSF1 immunohistochemistry in mouse synovium.

6.2.4. Data extraction and analysis

All measurements and analyses were performed blinded to the experimental conditions of each histological section. Statistical analysis was carried out using Mann-Whitney U tests and one way ANOVA followed by Dunnett's or Sidak's multiple

comparisons test for comparisons between two groups and more than three groups respectively. Statistical P value < 0.05 was considered as significant.

6.3 RESULTS

6.3.1 Expression of SRPK1 and SRSF1 in mouse and rat synovium

SRPK1 and SRSF1 expression was present in both mouse (Figure 6.2) and rat (Figure 6.3) normal and inflamed synovial cells.

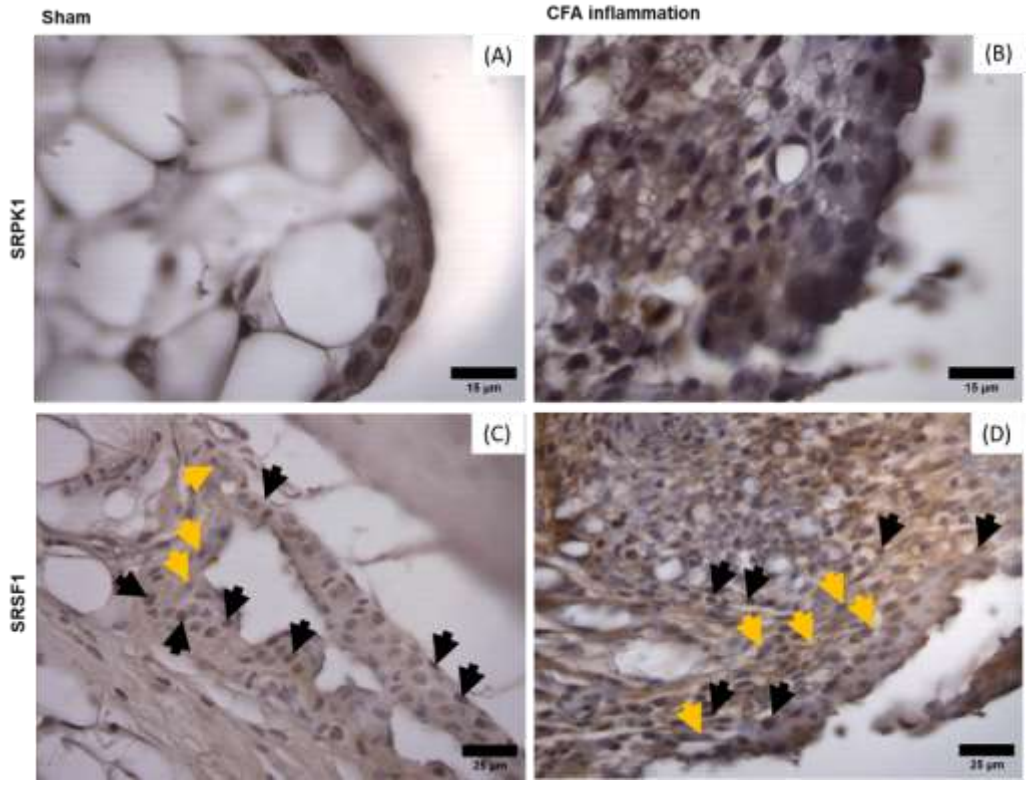

Figure 6.2: Synovial SRPK1 and SRSF1 nuclear localisation in mice. SRPK1 nuclear localisation (A) sham, (B) CFA inflamed. SRSF1 nuclear localisation (C) sham, (D) CFA inflamed. Black arrows indicate nuclear stained nuclei while yellow arrows show cytoplasmic stain in synoviocytes.

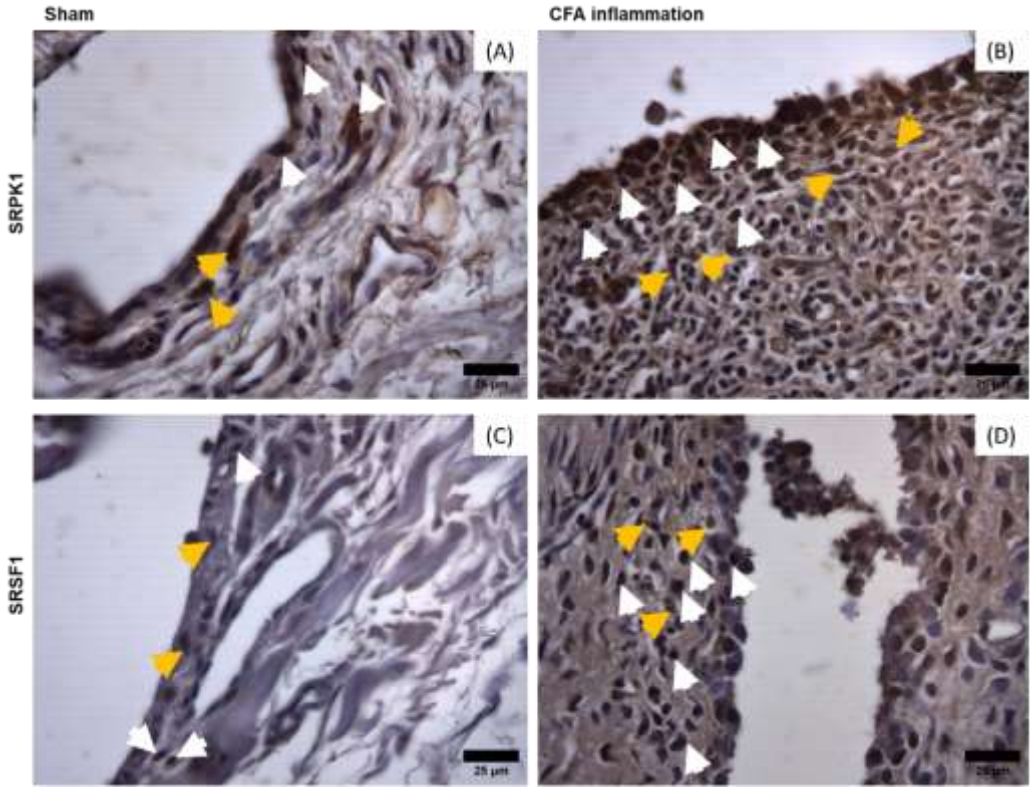

Figure 6.3: SRPK1 nuclear localisation (A) sham, (B) CFA inflamed in rat. SRSF1 nuclear localisation (C) sham, (D) CFA inflamed in rat. White arrows indicate nuclear stained nuclei while yellow arrows show cytoplasmic stain in synoviocytes. Inflammation was induced by commercial CFA (Section 2.3.3).

A. Effect of arthritis on synovial SRPK1 and SRSF1 fractional area expression in mice

Both SRPK1 and SRSF1 fractional area expression was observed in mouse synovium, with a non-significant reduction in CFA inflamed synovium compared to sham (Figure 6.4A. SRPK1: sham 0.23±0.03, inflamed synovium 0.14±0.1; (Figure 6.4B. SRSF1: sham 0.18±0.04, inflamed synovium 0.09±0.08).

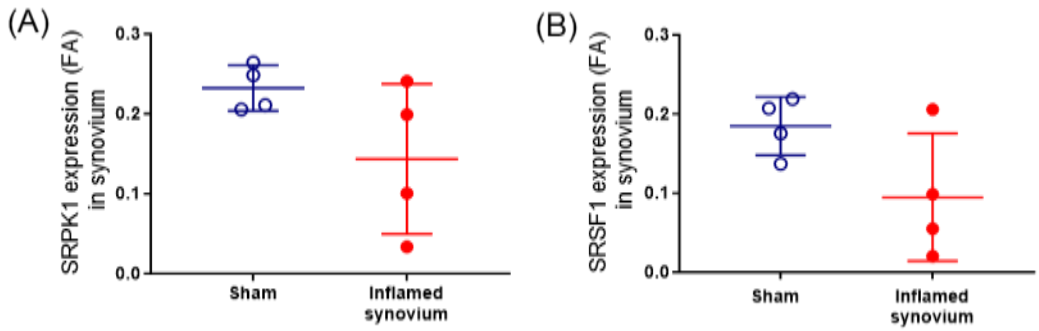

Figure 6.4: SRPK1 and SRSF1 fractional area expression in mouse tibio-tarsal inflammatory arthritis. There was a small, non-significant decrease in the of SRPK1 expression (p = 0.1143 cf. sham) (A) and SRSF1 expression (p=0.1143 cf. sham) (B) in inflamed synovium. Mann-Whitney U test.

B. Effect of arthritis on synovial SRPK1 and SRSF1 cellular expression and nuclear localisation in mice

There was no change in the absolute number of cells with SRPK1 NL in the total area of synovium (Figure 6.5A. sham 12±4.8, inflamed synovium 17±11.4, mean ± SD), but the absolute number of cells with SRSF1 NL was significantly increased in arthritis (Figure 6.5B. sham 18±4.2, inflamed synovium 36 ±7.9). The proportions of cells with SRPK1 and SRSF1 NL analysis did not change compared to sham (Figure 6.7C & D. SRPK1: sham 0.66±0.06, inflamed synovium 0.57±0.15; SRSF1: sham 0.74±0.04, inflamed synovium 0.71±0.10).

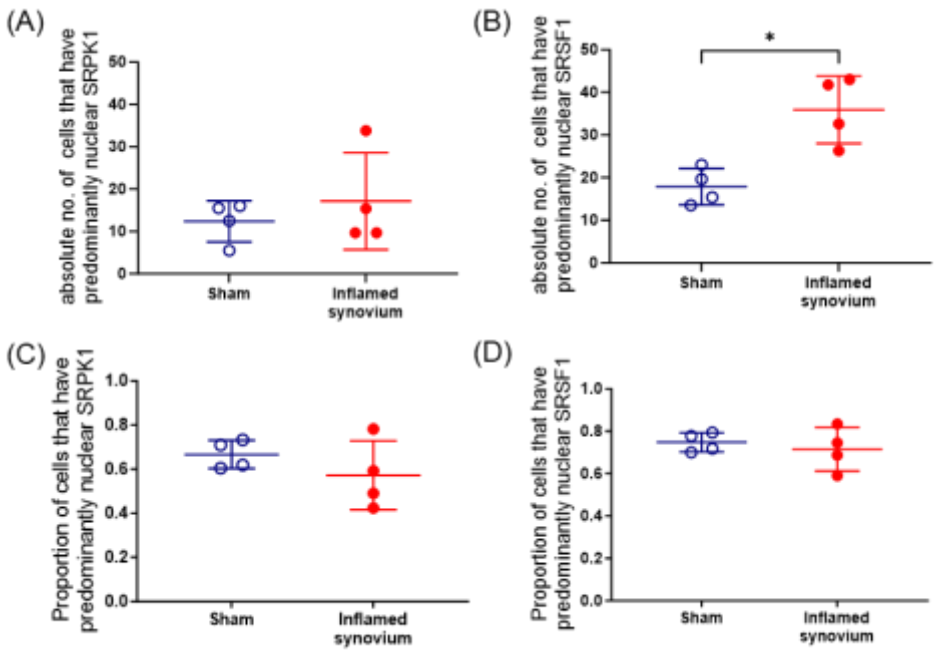

Figure 6.5: SRPK1 and SRSF1 synovial nuclear localisation in mouse tibio-tarsal joint inflammatory arthritis. (A) There was no change in the absolute cell numbers with NL SRPK1 (p>0.9999 cf. sham) but (B) there was a significant increase in absolute numbers of synoviocytes with SRSF1 NL (p= 0.0286 cf. sham). No changes in the proportions of synoviocytes with nuclear localisation of (C) SRPK1 (p>0.9999 cf. sham) or (D) SRSF1 p=0.1388 cf. sham). Mann-Whitney U test *p<0.05

C. Effect of arthritis on synovial SRPK1 and SRSF1 fractional area expression in rats

There was a slight increase, though not significant, in the mean values observed in SRPK1 FA expression but no change in SRSF1 FA expression in inflamed synovium as compared to sham (Figure 6.6A. SRPK1: sham = 0.2 ± 0.04, CFA inflamed = 0.3 ± 0.09; (Figure 6.6B. SRSF1: CFA inflamed: sham = 0.10 ± 0.08, CFA inflamed = 0.06 ± 0.02 (mean ± SD)).

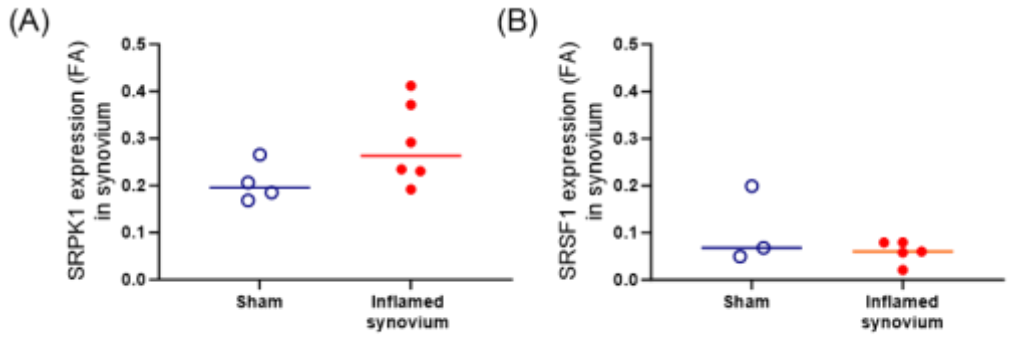

Figure 6.6: SRPK1 and SRSF1 fractional area expression in rat knee joint inflammatory arthritis. (A) There was a small, non-significant increase in the expression of SRPK1 expression, p=0.1143 cf. sham. (B) While no change in SRSF1 expression in inflamed synovium, p=0.7857 cf. sham. Mann-Whitney U test.

D. Effect of arthritis on synovial SRPK1 and SRSF1 cellular expression and nuclear localisation in rats

There was a significant increase in the absolute number of cells in the total area of synovium with NL of SRPK1 and SRSF1 (Figure 6.7A. SRPK1: sham = 17 ±11.5, inflamed synovium = 82 ± 29.3; (Figure 6.7B. SRSF1: sham = 25 ± 13.4, inflamed synovium = 109 ± 52.0). The proportion of cells with SRPK1 and SRSF1 NL analysis did not change compared to sham (Figure 6.7 C&D. SRPK1: sham = 0.7 ± 0.2, inflamed synovium = 0.7 ± 0.2; SRSF1: sham = 0.8 ± 0.1, inflamed synovium = 0.8 ± 0.2, mean ± SD.

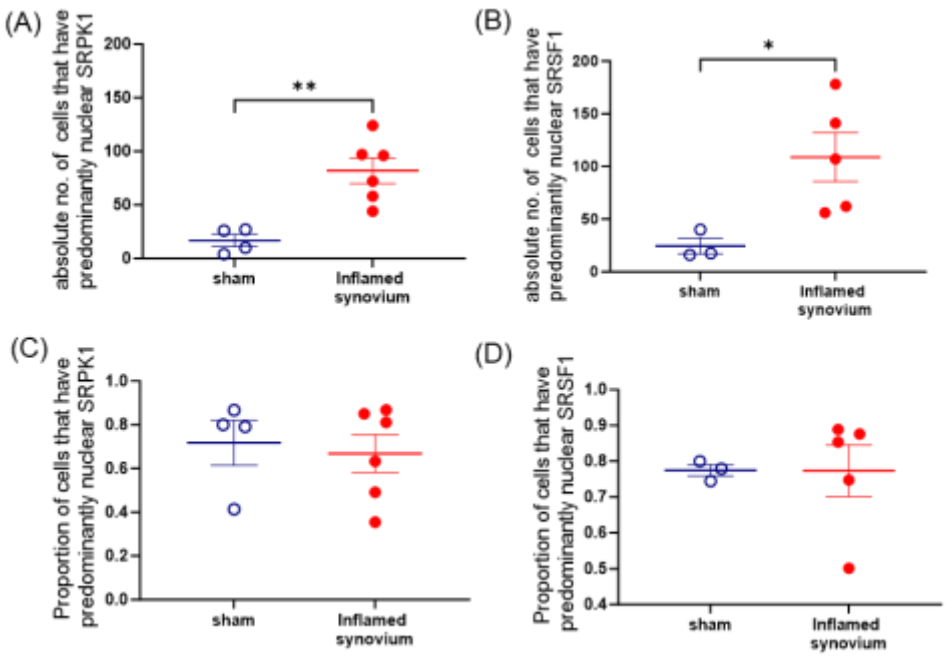

Figure 6.7: SRPK1 and SRSF1 nuclear localisation in rat knee joint inflammatory arthritis. A significant increase in absolute numbers of synoviocytes with NL of SRPK1 (p= 0.0032 c.f sham (A) and (B) SRSF1 p=0.0357 c.f sham, whereas no change was detected in the proportions of synoviocytes with nuclear localisation of (C) SRPK1, p>0.9999 c.f sham and (D) SRSF1, p=0.5714 c.f sham. Mann-Whitney U test *p<0.05, **p<0.01.

These results, taken together, show that IA in mice and rats did not fully recapitulate the human data but showed some effect on VEGF-A alternative splicing control molecules SRPK1 and SRSF1 in terms of increased SRPK1/SRSF1 cellular expression (absolute number of cells with nuclear SRSF/SRPK1 expression) in rat IA synovium, and activation of SRSF1 in mice.

6.3.2 Effect of VEGFR2 inhibition or endothelial knockout on VEGF-A splicing axis components in arthritis in rodents

A. Endothelial-VEGFR2 knockout effect on synovial SRPK1 and SRSF1 expression and localisation in arthritis in mice

In uninflamed mice, endothelial-VEGFR2 knockout ($VEGFR2^{ECKO}$) had no obvious effect on the absolute numbers of cells with SRPK1 NL (Sham (-) 12.3±4.9, uninduced (-) 9.3±5.2, $VEGFR2^{ECKO}$ (-) 10.5±2.4 Figure 6.8A blue symbols), but there was a significant increase in cells with SRSF1 NL in uninflamed $VEGFR2^{ECKO}$ mice

compared to both sham and uninduced mice (Sham (-) 18±4.3, uninduced (-) 15±3.1, VEGFR2^{ECKO} (-) 27.1±4.4, Figure 6.8B, blue symbols). In uninflamed mice, there was also no change in SRPK1 FA (sham (-) 0.23±0.02 ; uninduced (-) 0.21±0.04; VEGFR2^{ECKO} (-) 0.25±0.11), or SRSF1 fractional area (sham (-) 0.19±0.03 ; uninduced (-) 0.14±0.03, VEGFR2^{ECKO} (-) 0.14±0.08) (Figure 6.9 A&B blue symbols), and no effect on the proportions of cells with SRPK1 NL (sham (-) 0.7±0.06 ; uninduced (-) 0.53±0.10; VEGFR2^{ECKO} (-) 0.53±0.12) or SRSF1 NL (sham (-) 0.7±0.05 ; uninduced (-) 0.66±0.09; VEGFR2^{ECKO} (-) 0.77±0.09) (Figure 6.9 C&D blue symbols, Fig 6.9E).

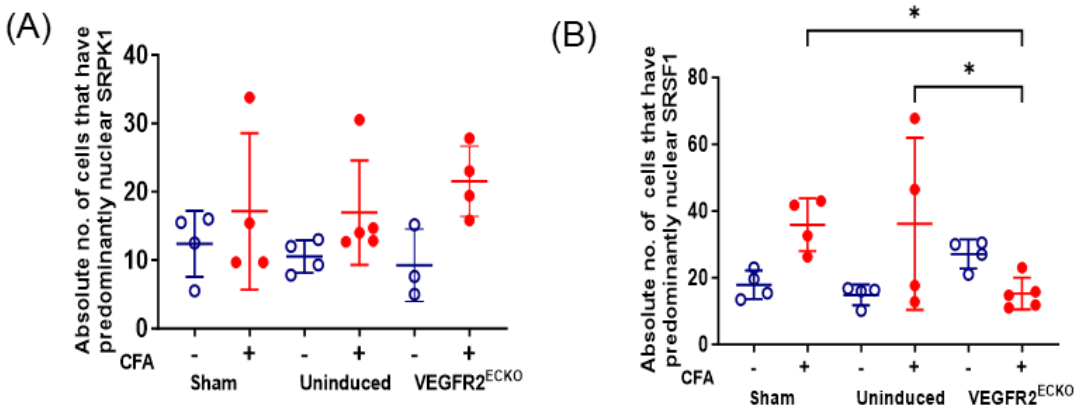

Figure 6.8: SRPK1 and SRSF1 nuclear localisation in mouse tibio-tarsal inflammatory arthritis. Symbols (+ and -) indicate when animals have received CFA injections. (A) There was no effect of the genetic background (uninduced (-) or tamoxifen (sham (-)) or VEGFR2^{ECKO} on absolute cell number with SRPK1 NL in mice without arthritis (A, blue symbols). There was a small insignificant increase in absolute number of cells SRPK1 NL in VEGFR^{2ECKO} mice with arthritis compared with other inflamed mice (p=0.9988 cf. (+) sham, p=0.5543 cf. (+) uninduced. On the other a significant reduction in the absolute number of cells with SRSF1 NL was observed in VEGFR2^{ECKO} mice with arthritis compared with other inflamed mice p=0.0263 c.f (+) sham, p=0.0245 cf. (+) uninduced (B). One way ANOVA followed by Sidak's multiple comparisons test. *p<0.05.

Comparing only inflamed mice in each group, VEGFR2^{ECKO} had no significant effect on absolute cell number with SRPK1 NL (Sham (+) 17±11.4, uninduced (+) 22±5.1, VEGFR2^{ECKO} (+) 17±7.6 Fig 6.8A red symbols); proportions of cells with SRPK1 NL (sham (+) 0.6±0.15; uninduced (+) 0.55±0.08; VEGFR2^{ECKO} (+) 0.49±0.11. Figure 6.9C); and SRPK1 FA (sham (+) 0.14±0.09; uninduced (+) 0.20±0.06, VEGFR2^{ECKO}

(+)= 0.14 ± 0.06), or SRSF1 FA (sham (+) 0.09±0.08; uninduced (+) 0.11±0.06, VEGFR2^{ECKO} (+) CFA 0.08±0.07. Figure 6.9 (A,B).

Inflamed VEGR2^{ECKO} mice had lower proportions of cells with SRSF1 NL (sham (+) 0.71±0.10 uninduced (+) 0.64±0.08; VEGFR2^{ECKO} (+) = 0.46 ± 0.15; VEGFR2^{ECKO} (-) 0.77±0.09) (Figure 6.9D red symbols, Figure 6.9F). When compared to uninflamed controls, arthritis increased the absolute number of cells with SRPK1 NL in VEGFR2^{ECKO} (+), although this was not statistically significant (Figure 6.8A, p=0.09). As shown in Figure 6.8 there were more cells with SRSF1 NL in both control groups, but fewer SRSF1 NL cells VEGFR2^{ECKO} + CFA mice (Fig 6.8B), in which was also a lower proportion of cells with SRSF1 NL compared to uninflamed VEGFR2^{ECKO} mice (Figure 6.9 D&F).

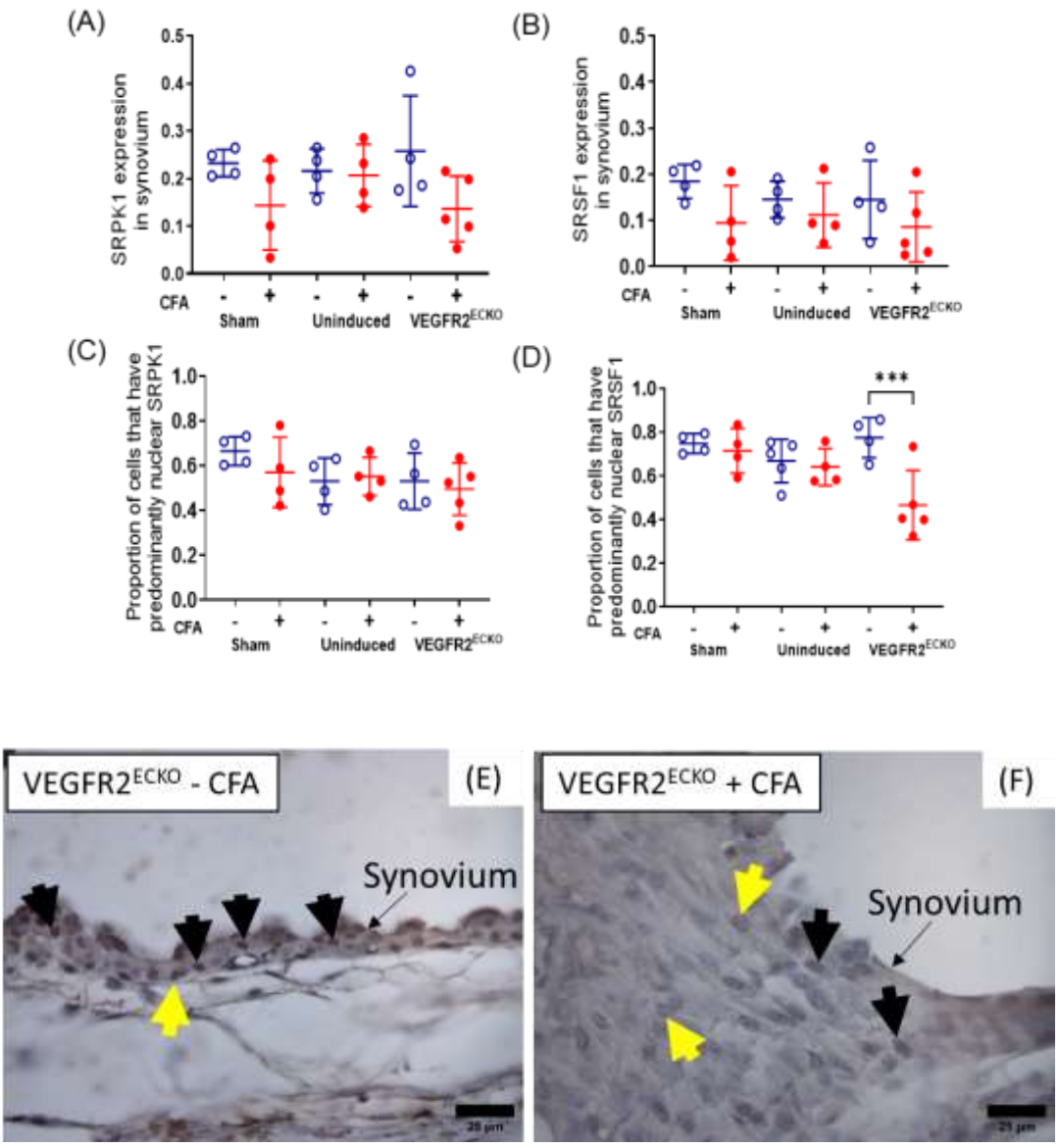

Figure 6.9: SRPK1/SRSF1 FA expression and nuclear localization in VEGFR2^{ECKO} inflammatory arthritis mice. Symbols (+ and -) indicate when animals have received CFA injections. There was no effect of either genetic manipulation (uninduced) or VEGFR2^{ECKO} on (A) SRPK1 FA, (B and E) SRSF1 FA, (C) SRPK1 NL or (D) SRSF1 NL in mice without arthritis (blue symbols). There were no significant changes in SRPK1 FA, SRSF1 FA or SRPK1 NL in mice with arthritis (red symbols). (D) VEGFR^{ECKO} significantly reduced SRSF1 NL in inflamed synovium compared to noninflamed VEGFR2^{ECKO}, uninduced and sham. One way ANOVA followed by Sidak's multiple comparisons test p=0.0006. (E, F) Photomicrographs of SRSF1 nuclear localisation in synoviocytes in VEGFR2^{ECKO} normal synovium (E) and inflamed synovium (F) in VEGFR2^{ECKO} mice. Black arrows indicating nuclear stained nuclei while yellow arrows showing cytoplasmic stain in synoviocytes. ***p<0.001

B. Effect of PTK787 on synovial SRPK1 and SRSF1 expression and localisation in arthritis in rats

Rats treated with PTK787 showed no change in either SRPK1 FA expression (inflamed: 0.3 ± 0.0, PTK787 treatment from day 0 (D0): 0.3 ± 0.1, PTK787 starting at day 3 (D3) 0.3 ± 0.1) or SRSF1 FA expression (inflamed 0.06±0.02, D0 0.07±0.03, D3 0.06±0.04) compared to the CFA inflamed group (Figure 6.10 A&B).

There were also no significant changes in either SRPK1 (inflamed 0.7±0.2, D0 0.6±0.1, D3 0.6±0.1) or SRSF1 NL in treated animals (inflamed 0.8±0.2, D0 0.7±0.1, D3 PTK787 0.7±0.1) compared to the inflamed groups (Figure 6.10 C&D) as well as SRPK1 absolute number (inflamed 81.83±29.34, D0 68.80±8.786, D3 95.60±33.93). However, there was a reduction in the number of cells with SRSF1 NL in treated groups than inflamed group, although this was not significant (inflamed 108.8±51.98, D0 65.67±19.38, D3 68.20±23.86) (Figure 6.11 A&B).

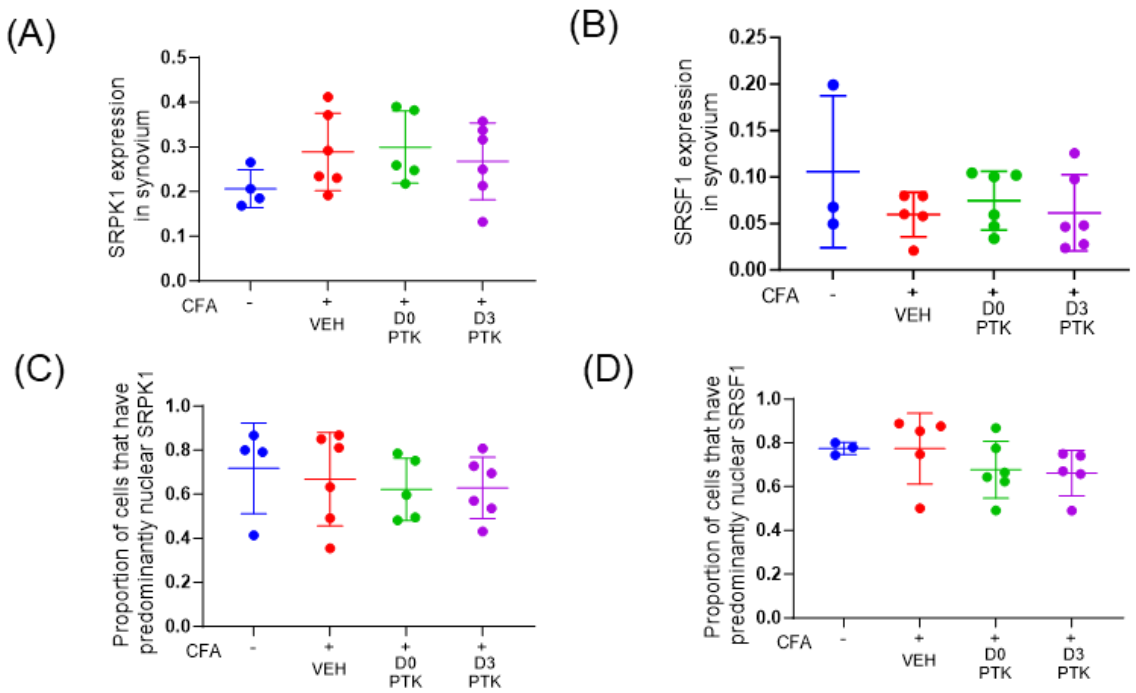

Figure 6.10: SRPK1 and SRSF1 FA expression and nuclear localisation with PTK787 VEGFR2 inhibition. Symbols (+ and -) indicate when animals have received CFA injections. No change was found in either (A) SRPK1 (D0 p=0.9689, D3 p=0.8776 respectively c.f inflamed, (B) SRSF1 fractional area (D0 p=0.6793, D3 p=0.9929 respectively c.f inflamed) or (C&D) nuclear localisation (SRPK1: D0 p=0.8687, D3 p=0.8885 c.f inflamed; (SRSF1: D0 p=0.4124, p=0.3423 c.f inflamed in PTK787 treated

rats compared to inflamed controls). One way ANOVA followed by Dunnett's multiple comparisons test. D0: Day 0, D3: Day 3, PTK: PTK787.

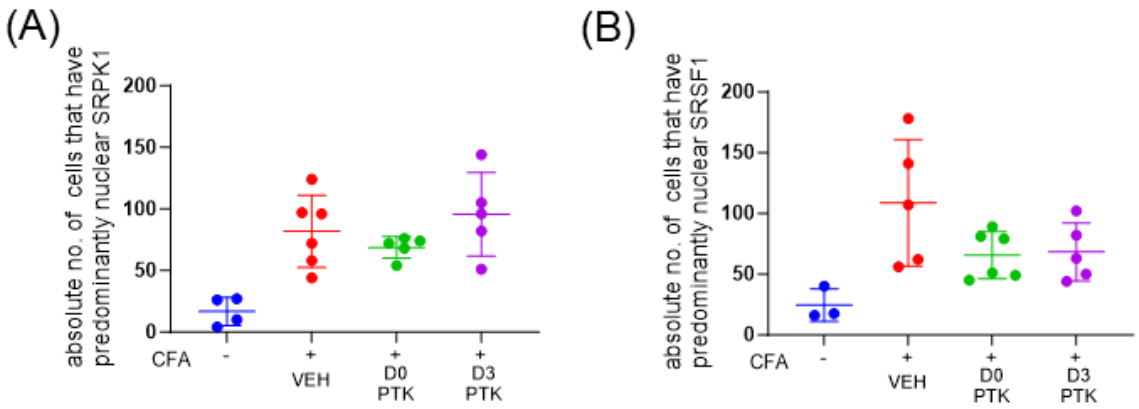

Figure 6.11 SRPK1 and SRSF1 cellular nuclear localisation in arthritic rats treated with VEGFR2 inhibitor. Symbols (+ and -) indicate when animals have received CFA injections. (A) No significant change was found in the numbers of cells with SRPK1 (D0 p=0.6478, D3 p=0.6182 c.f inflamed or (B) SRSF1 (D0 p=0.0978, D3 p=0.1396 c.f inflamed nuclear localisation in PTK787 treated rats, although there was a trend for lower numbers of cells with nuclear SRSF1 in PTK787 treated rats compared to arthritic vehicle treated controls. One way ANOVA followed by Dunnett's multiple comparisons test. D0; Day 0, D3: Day 3, PTK: PTK787.

These results show that endothelial-VEGFR2 knockout had significant effect on SRSF1 only in IA model in mice, whereas systemic inhibition of VEGFR2 by PTK787 did not show any effect on VEGF-A alternative splicing axis constituents in the joint.

6.4 DISCUSSION

6.4.1 Effect of inflammation on VEGF-A alternative splicing axis constituents

I hypothesised that I would see changes in the expression and localisation of the constituents of the VEGF-A splicing axis, SRPK1 and SRSF1 in these animal models of inflammatory arthritis similar to the results found in human synovitis where inflammation in human OA and RA synovium of duration > 5 years was associated with higher SRSF1 NL compared to controls (D Amanitis et al., 2020). I therefore compared expression patterns, including NL, of SRPK1 and SRSF1 in mouse and rat synovium in CFA-induced arthritis.

A. Changes in the components of the VEGF-A splicing axis in rodent inflammatory arthritis models (back translation).

Previous evidence suggested upregulation of expression of SRPK1 in highly proliferative or inflamed tissue (Yanfen Yao et al., 2021) or in conditions where angiogenesis is key factor such as tumours (E. M. Amin et al., 2011). Activation of SRPK1 is induced by TNF-α (Mavrou et al., 2015), which is a major contributor in the pathogenesis of both RA (Farrugia & Baron, 2016) and OA (Grunke & Schulze-Koops, 2006). SRPK1 is also activated by hypoxia (Jakubauskiene et al., 2015). However, SRPK1 function is not controlled by the alteration in the expression levels of SRPK1, but rather than the modification in the active state (Stevens & Oltean, 2016) which cannot be established by IHC experiments in paraffin fixed tissue (Dimitrios Amanitis, 2022). However, the NL of the downstream signalling target SRSF1 within the nucleus can be assessed as an indirect readout out SRPK1 activity (R. P. Hulse et al., 2016; Nowak et al., 2010; Oltean et al., 2012).

Contrary to the hypothesis, and in contrast to data in human synovium (D Amanitis et al., 2020), CFA inflammation in mice showed no significant change in the expression (SRPK1) and proportions of cells with NL (SRSF1) of splicing components in synovium

compared to controls. There was a significant increase in the absolute number of synoviocytes with SRSF1 NL. There were similar changes in rat CFA arthritis with an increased absolute cell number expressing SRPK1 and with SRSF1 NL.

Taken together, my data showed an increase in the total number of cells with SRSF1 NL in mouse synovium (Figure 6.5B), and in rats both SRPK1 and SRSF1 NL (Figure 6.7 A&B), despite no change in the proportion with increased NL. These changes may still indicate alteration in alternative splicing in these animal models. This could suggest a switch of protein expression towards the angiogenic isoforms i-e VEGF-A_{165}a. The current data is not enough to clearly show the VEGF-A_{165}a isoform expression which requires further investigation. Moreover, it was not possible to conduct experiments looking for VEGF-A_{165}a isoform analysis in mouse synovium for two reasons; 1. the VEGF-A_{xxx}a antibody needed to be purified and I was unable to get this at the time, and 2. due the nature of the antibody which is raised in mouse and is therefore difficult to use on rat and mouse tissue. Back-translation results from human tissue to animal models is necessary to validate such models for the study of common mechanisms such as changes in the VEGF-A alternative splicing axis.

While some similar changes in the splicing axis can be seen in these animal models compared to the human data, they do not replicate the human data. A possible explanation for this could be that SRPK1 and SRSF1 may not regulate VEGF-A splicing in rodents. However, there is evidence demonstrating a clear role for these proteins in rodent VEGF-A splicing (Jia et al., 2021; Xie et al., 2017). The most likely reason is the difference in duration of IA in rodents (10-14 days) and the human study (>5 years). Complete Freund's adjuvant is considered as a reliable model for inflammation in RA (Bhalekar et al., 2015; Chillingworth & Donaldson, 2003) as it has common features with the human condition e.g. joint swelling, cartilage degradation, bone resorption and loss of function, similar features as detected in human RA (Bevaart et al., 2010). The chronic state and duration of the disease may, however, result in different changes on the splicing axis in human than in the more acute rodent models. The synovium samples analysed for splicing axis from human RA; came from donors who had had diagnosed arthritis for more than five years, whereas the rodent IA models experienced arthritis for only 10 (rat) and 14 (mouse) days. Therefore, the

duration of the study is probably very important, increasing the timeline of inducing IA by CFA may provide an opportunity to replicate the human splicing axis findings. Literature shows that extended duration (> 3 weeks and up to 3 months) of IA in rat models induced by *M. tuberculosis* (CFA) produce a prolonged and persistent increase in inflammation (Donaldson et al., 1993; Nasuti et al., 2019; Pearson & Wood, 1959). Rat IA models might be better to use for splicing axis analysis because it would provide an opportunity to investigate the alterations in VEGF-A isoforms i-e VEGF-A_{xxx}a and VEGF-A_{xxx}b which is not possible in mouse tissue due to nature of the only isoform specific antibodies. In addition, there is also a possibility of the technique used, IHC, was not sensitive enough for the expected outcomes as explained later in section 6.4.2.1.

Rodent models have been used for decades to understand the pathophysiology of RA and to test various of anti-rheumatic drugs to slow down the disease progression (Hegen et al., 2008; Ismail et al., 2022). There are many rodent models of RA, and each has its own specific characteristics with the ability to replicate certain aspects of the disease (Bevaart et al., 2010; Hegen et al., 2008; Vincent et al., 2012; T. Zhao et al., 2022). There is no animal model of IA that can perfectly recapitulate all features of RA in humans. Differences between the rodent and human immune system (Mestas & Hughes, 2004; Zschaler et al., 2014) make it difficult for one animal model to translate or back-translate all events or changes from the rodent to human or human to rodent model, respectively. Neither species fully replicated the human findings, suggesting that this is not due to species. The most likely reason for the difference between the rodent models and the human data is the duration of disease.

6.4.2 Effect of VEGFR2 inhibition on control of VEGF-A alternative splicing

6.4.2.1 Effect of VEGFR2 knockout in mice on the VEGF-A splicing axis (SRPK1/SRSF1)

In the $VEGFR2^{ECKO}$ mice, loss of VEGFR2 was associated with reduction of vessels in synovium and superficial SCB. When VEGFR2 number is reduced, pro-angiogenic

VEGF-A isoforms would be unable to effectively stimulate angiogenesis. This would increase hypoxia, which is known to increase transcription of VEGF-A_{xxx}a isoforms through SRSF1 activation (Nowak et al., 2008). Pharmacological blockade of VEGFR2 would be predicted to have a similar effect, although in my studies I did not see a decrease in histological synovitis with PTK787 treatment. One aim of these studies was to determine whether inhibition or knockdown of VEGFR2 affected expression or activation of SRPK1 or SRSF1.

Surprisingly I found a significant reduction in NL of SRSF1 in the inflamed $VEGFR2^{ECKO}$ mice. This suggests that the reduced VEGFR2, and reduced angiogenesis could be the result of decreased phosphorylation and NL of SRSF1 in VEGFR2 KO IA, as increased SRSF1 NL leads to proximal splice site selection and VEGF-A_{xxx}a splicing. These isoforms have high affinity for VEGFR2 and induce angiogenesis (da Silva et al., 2015). I could not conduct the experiment for the analysis of the specific VEGF-A_{165}a and VEGF-A_{165}b isoforms in mouse synovium mostly due to the nature of the antibodies available, as these were raised in mouse, and also because the VEGF-A_{165}a antibody required further purification before use, and this was not possible during the Covid pandemic. Both *in vitro* and *in vivo* studies show that VEGF-A_{165}a acts as a *full agonist* for VEGFR2 driven signalling responses, by inducing full phosphorylation of VEGFR2 (Fearnley et al., 2016). My findings in mice support the conclusion that the knockdown of endothelial-VEGFR2 receptors in IA results in changes in splicing control mechanisms that should cause a decrease in angiogenic isoforms such as VEGF-A_{165}a and/or an increase in VEGF-A_{xxx}b anti-angiogenic isoforms. The combination of a change in splicing away from pro-angiogenic isoforms with a reduction of VEGFR2 would possibly explain the complete loss of blood vessels in SCB. There is no published evidence of an interaction between SRPK1/SRSF1 splicing mechanisms and VEGF receptors. VEGF-A is known to affect the splicing of VEGFR1 so it is possible that VEGFR2 signalling, and therefore loss of VEGFR2 signalling, may also control VEGF-A splicing (Abou Faycal et al., 2019).

Phosphorylation plays a highly important part in the cytoplasmic–nuclear trafficking and splicing function of SR proteins. Two main enzymes are involved in the post-translational modifications, SRPKs and CLKs, which target and phosphorylate RS

domains. Both enzymes have high binding affinity to SR proteins but possess different mechanisms for substrate recognition and product dissociation (J. C. K. Ngo et al., 2008).

SRPK1 is normally in the cytoplasm where it can phosphorylate SRSF1, which can then enter the nucleus where it sits in nuclear speckles. Further phosphorylation of SRSF1 by CLK1 releases the SRSF1 from the speckles. SRPK1 can also be phosphorylated, upon which it also enters the nucleus and accelerates CLK1 release by peeling away the N terminus from SRSF1 (Aubol et al., 2016). The high-affinity product complex of CLK1 and SRSF1 also provides a means for nuclear transport of CLK1 (George et al., 2019) (section 1.11.3 for more details).

It is possible that for some reason, SRSF1 was held in speckles in complex formation with CLK1 in the nucleus (Malhi et al., 2022). I found some evidence of SRSF1 in speckles in VEGFR2 mouse IA synovium. This gives an appearance of much nuclear lower staining (Figure 6.12) and so the reduced NL of SRSF1 I found might actually be lower release from speckles into nucleoplasm. This could be due to a lack of CLK1 activity to release SRSF1. Whether CLK1 is altered in this model of IA is not known, and there is no literature evidence on any functions of CLK1 in IA. CLK2 is implicated in OA and is one of the targets of the novel DMOAD lorecivivint.

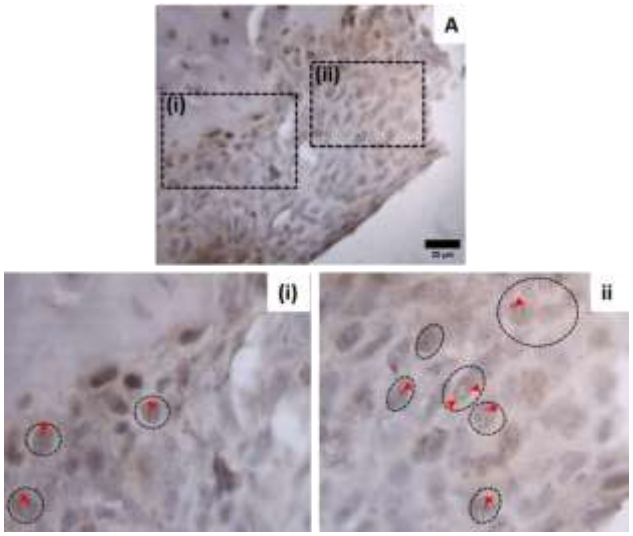

Figure 6.12: (A) SRSF1 expression in VEGFR2 IA synovium. (i and ii) Digital zoom images showing SRSF1 in nucleus as speckles shown by red arrow heads in encircled synoviocytes.

6.4.2.2 Effect of VEGFR2 inhibition in rats on the VEGF-A splicing axis (SRPK1/SRSF1)

In contrast to the effect of $VEGFR^{ECKO}$ there was no change in histological synovitis or cartilage damage, or VEGF-A splicing axis with PTK787 treatment in rats. This, together with the lack of effect of PTK787 on the histopathology, further support my conclusion that the dose of PTK787 in the joint may have been too low to have any effect on joint damage. As I conducted these studies on tissues supplied from experiments powered for other measures, the number of animals may have been too low to see effects in the histological variables.

6.4.2.3 Limitations

Immunohistochemistry to show NL of SRSF1 is a proxy marker of SRSF1 activation. Direct measurement of phosphorylation of SRSF1 by SRPK1 could be done using incubation of synoviocytes with and without an SRPK1 inhibitor, and western blotting, but this is not possible in tissue sections as there is no specific antibody against phospho-SRSF1. So the power of cellular localisation would be lost. Information on localisation of the different components of the splicing axis could help interpretation of the data through showing whether SRPK1 was in the nucleus, SRSF1 was mostly in speckles, or whether CLK1 was in speckles or nucleoplasm. The locations of these different components would be more easily seen using, fluorescence imaging in synovium and dual (SRPK1, SRSF1) or triple staining (SRPK1, SRSF1, and CLK1). Immunofluorescence in decalcified formaldehyde-fixed, paraffin-embedded tissue has not been successful in the lab, due to high levels of background or auto-fluorescence as described in chapter 5 section 5.4. Some of these limitations could be overcome using immunofluorescence to identify SRPK1 and SRSF1 subcellular locations in cultured primary synoviocytes (Malhi et al., 2022) activated by the inflammatory mediators involved in RA. The effect of SRSPK1 and SRSF1 inhibitors can also be investigated, however this approach does not take into account the effects in other joint tissues in IA which may also be involved.

6.5 CONCLUSION

This is the first time the VEGF-A alternatively splicing axis has been investigated in rodent IA models. The CFA model in rats and mice did not fully recapitulate the changes in the VEGF-A alternative splicing axis results observed in human RA in that there was no change in SRPK1 expression and an increase in the absolute number but not the proportion of cells in synovium with activated (nuclear localised) SRSF1. It is probable that this difference is due to the shorter duration of IA in these animal models compared to the human samples. Targeting VEGFR2 using an endothelial cell knockout approach resulted in a reduction in activation of SRSF1, which would also suggest a decrease in the mRNA expression of VEGF-A_{xxx}a isoforms and/ or increases in VEGF-A_{xxx}b isoforms. This leads to an additional hypothesis that inhibiting VEGF endothelial signalling cascade might control its own splicing in synoviocytes.

7. INVESTIGATING THE EFFECT OF SRPK1 AND CLK1 SPLICING KINASE INHIBITION ON CHONDROCYTE PHENOTYPE *IN VITRO*

7.1 INTRODUCTION

In Chapter 6 I showed the data I obtained on the number of synoviocytes with SRSF1 NL, showing that animal models do in some ways replicate the findings in human synovium. I was unable to follow up on the observations in Chapter 6 looking at VEGF-A splice variant expression, or at different times in animal models due to the Covid 2019 pandemic, problems with purification of the VEGF-A_{xxx}a specific antibody, and the closure of labs and the animal unit.

During my investigations into the splicing axis in rats and mice, I observed hypertrophic chondrocytes in CFA-induced IA (Figure 7.1A-C), and SRPK1 expression in chondrocytes (Fig 7.1D) in my histological sections. These observations led me to hypothesise that the SRPK1/SRSF1 splicing axis might be involved in chondrocyte hypertrophy. Chondrocyte hypertrophy is important in normal skeletal growth (Hallett et al., 2021), is present in both inflammatory and OA in humans and in models in mice (Kung et al., 2017; S. Park et al., 2021; Stahle-Backdahl et al., 1997), involves VEGF-A (Patil et al., 2012), and has been linked with OA progression (Fuerst et al., 2009; B. Li et al., 2021; Rim et al., 2020).

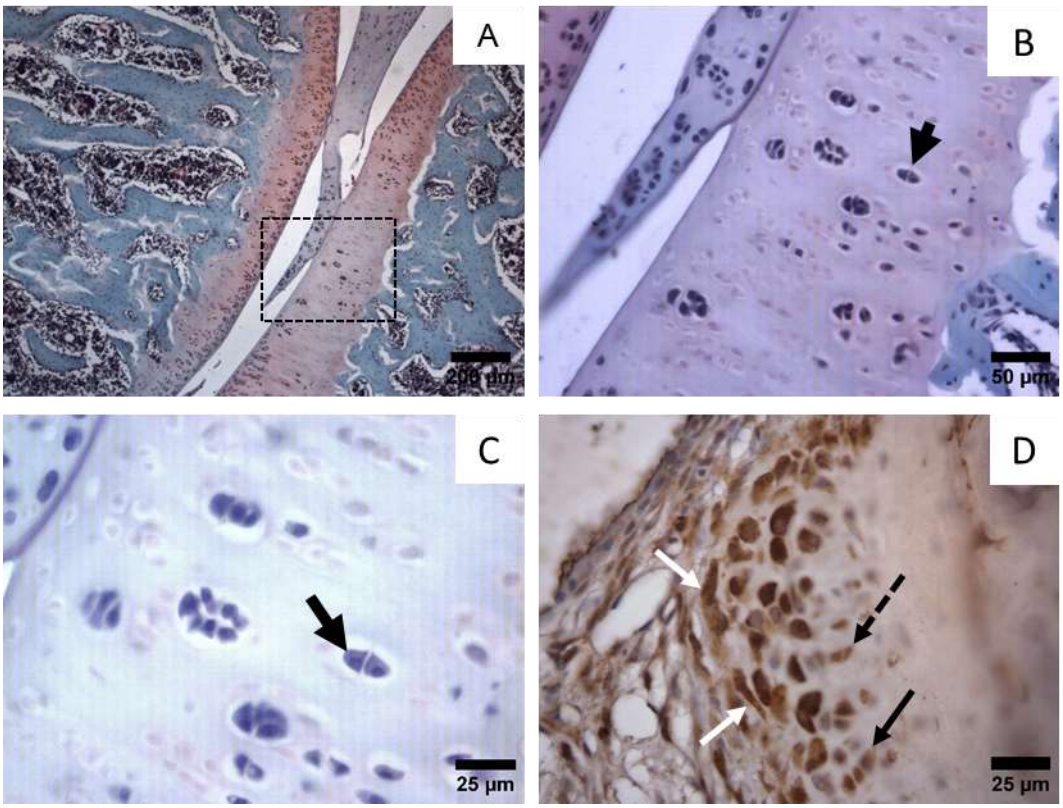

Figure 7.1: A-C Histological sections from rats with experimental inflammatory arthritis showing the presence of hypertrophic chondrocytes. (A) shows low power image, (B) and (C) show higher power images of the dotted box in A, arrows show hypertrophic chondrocytes. (D) Expression of SRPK1 in chondrocytes. Arrows show superficial (white arrows) and deeper (black) chondrocytes with SRPK1 positive staining, some of which also appear hypertrophic (black dotted arrow). Scale bars A=200µm, B=50µm, C & D = 25µm.

In both OA and RA, articular chondrocytes shift to a catabolic phenotype and become hypertrophic (Chou et al., 2020; Ji et al., 2019; C.-C. Tseng et al., 2020). There are several factors that can contribute to these changes, for example excessive mechanical load, age, trauma, and autoimmune disorders (Loeser, 2009; Rim et al., 2020; Van der Kraan & Van den Berg, 2012). Normal chondrocytes express SRY-box transcription factor (SOX9) (Q. Zhao et al., 1997) and type II collagen (COL2A1) (T Aigner & Stöve, 2003; Xin et al., 2015), the key constituent of the cartilage matrix which maintains physiological homeostasis (T Aigner & Stöve, 2003) (Figure 7.2). Hypertrophic chondrocytes are recognised by an enlarged size and upregulation of ECM-degrading proteases such as disintegrin, MMP13, and ADAMTS5, which induce chondrocyte death (Rim et al., 2020; Xia et al., 2014) and promote cartilage damage. VEGF-A is also upregulated in hypertrophic chondrocytes (Thomas Pufe et al., 2001).

Furthermore, hypertrophic chondrocytes enhance the calcification of the matrix by the production of Alkaline Phosphatase (ALPL) and increase hypertrophic-related genes expression, for example type X Collagen (COL10A1) (Thomas Aigner et al., 2006; Brew et al., 2010; Hoyland et al., 1991; Kirsch et al., 2000; O Pullig et al., 2000; Ripmeester et al., 2018; Klaus von der Mark et al., 1995; K Von der Mark et al., 1992; Walker et al., 1995) and Runt-related transcription factor 2 (RUNX2) (D. Yan et al., 2011).

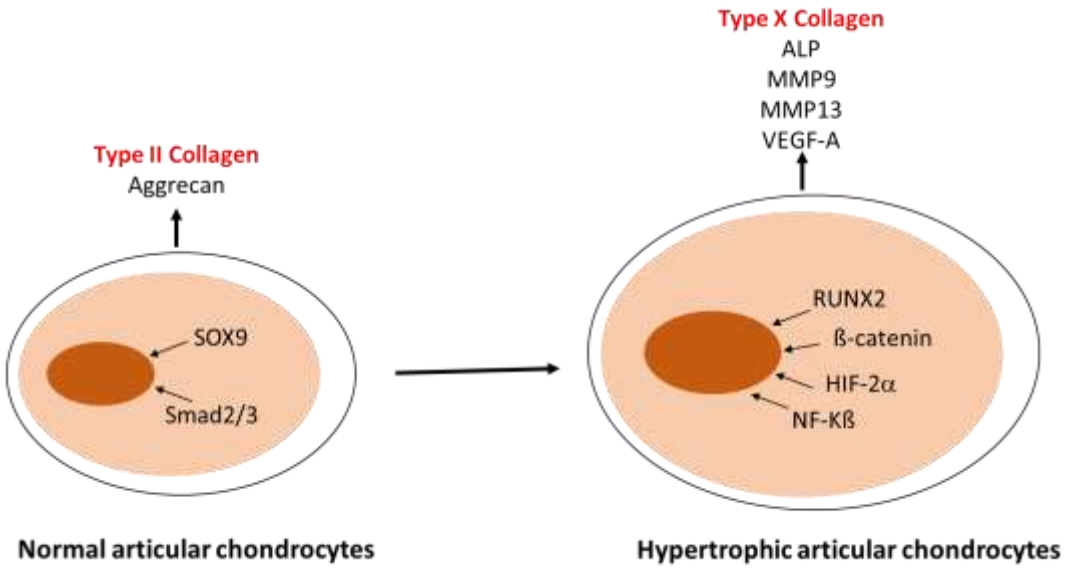

Figure 7.2: Diagrammatic representation of normal articular chondrocytes (left) compared to hypertrophic chondrocytes (right). Normal chondrocyte signalling that maintains chondrocytes homeostasis involves Sox9 and Smad2/3. These cells typically produce Type II collagen and aggrecans. The diagram on the right shows the signalling and transcriptional events that regulate chondrocyte hypertrophic-like modifications to differentiate a normal articular chondrocyte to a terminal differentiated chondrocyte and lead to tissue remodelling and calcification. These cells express Type X collagen, alkaline phosphatase (ALP), MMP9, MMP13 and VEGF-A. The collagens marked red were investigated in this chapter as markers for normal and hypertrophic chondrocytes analysis.

VEGF-A and all VEGFRs are highly expressed in OA and RA chondrocytes (Shakibaei et al., 2003; Shen et al., 2015), but VEGF-A is not expressed in normal chondrocytes. VEGFR-1 and 2 are the most extensively studied VEGF receptors in OA and RA pathogenesis. Hypertrophic chondrocytes produce VEGF-A during osteophyte formation leading to bone formation via vascular invasion into the cartilage matrix in an OA animal model (Hashimoto et al., 2002), and increased VEGF-A expression

correlated with increased osteochondral vascular density and chondropathy in human OA cartilage (Franses et al., 2010). Anti-angiogenic factors such as chondromodulin and troponin-C are downregulated in OA, and there is vascular invasion of cartilage promoted by VEGF-A (Chawla et al., 2022). There are no available data on expression of the VEGF-A_{165}a or VEGF-A_{165}b isoforms in cartilage under any conditions, but it is presumed that these actions come from the VEGF-A_{165}a isoforms as VEGF-A_{165}b isoforms have been known to be anti-angiogenic (Kikuchi et al., 2019). VEGF-A inhibition/block or neutralisation with antibodies such as bevacizumab has been suggested as a strategy to halt chondrocyte hypertrophy as this decreases Runx2, MMP13, and COL10A1 expression and protects cartilage from hypertrophic change (Xufang Zhang et al., 2016). However, no existing anti-VEGF-A treatments distinguish between the two isoform families, and small molecule VEGFR inhibitors have the same problem in that receptor block or inhibition affects receptor-mediated actions of both VEGF-A isoform families.

An alternative way to target VEGF-A pro-angiogenic activity, and potentially pro-hypertrophic actions is to alter VEGF-A splicing. As discussed earlier, two main enzymes, SRPKs and CLKs are involved in the post-translational modifications of SR proteins having high binding affinity towards RS domain but hold different mechanisms for recognition of substrate and dissociation of the product (Aubol & Adams, 2022; Aubol et al., 2021; J. C. K. Ngo et al., 2008). As I showed that SRPK1, one of the primary splicing kinases responsible for VEGF-A alternative splicing, is expressed in rodent chondrocytes, I was interested to target VEGF-A alternative splicing kinases such as SRPK1 and CLK1 to investigate the effect on hypertrophic changes in chondrocytes. Because of Covid constraints, I chose to use the ATDC5 cell line in these studies.

The ATDC5 cell line was initially isolated from differentiating teratocarcinoma AT805 stem cells (Atsumi et al., 1990) and has been used as a invitro model in over 300 studies to explore mechanisms of chondrocyte differentiation (Fujii et al., 1999; James et al., 2005; Mendes et al., 2012; Yamaura et al., 2012). ATDC5 cells are a reliable model of *in vitro* chondrocyte differentiation and mineralisation in which early-stage differentiation results in type II collagen expression (Col2A1) and formation of cartilage

nodules (Shukunami *et al.*, 1996). Hypertrophy and mineral deposition can be induced over three weeks with the addition of insulin to the culture medium (Shukunami et al., 1997). After the expansion of nodules, hypertrophic chondrocytes increase ALP activity and express type X (Col10A1) collagen gene, leading to matrix mineralization (Shukunami *et al.*, 1997; Shukunami *et al.*, 1996).

SRPK1 and CLK1, both kinase regulators of alternative splicing, are considered promising therapeutic tools for the treatment of diseases caused by alternative splicing dysregulation such as various human cancers, OA, RA and neurodegenerative, neuromuscular and neovascular eye disease (D Amanitis et al., 2021; Batson et al., 2017; Capra et al., 2006; Deshmukh et al., 2019; Dong et al., 2022; ElHady et al., 2023; C. He et al., 2022; Malhi et al., 2022; J. Tang et al., 2022; Tollervey et al., 2011; Waiker et al., 2014). Both SRPK1 and CLK1 inhibitors are currently in preclinical and clinical studies predominantly for neoplastic diseases (Araki et al., 2023; Naro et al., 2021; Nikas et al., 2019).

EXN-407, an SRPK1 inhibitor, is the product of Exonate Ltd (Exonate, 2022; Malhi et al., 2022) and has recently announced successful Phase Ib/II clinical trials (NCT04565756) in diabetic macular oedema (Exonate, 2023). SRPIN340, an SRPK1/2 dual inhibitor, inhibits tumour angiogenesis effectively and has been used experimentally to block growth in various types cancers (Gammons et al., 2014). SRPIN803 was developed after SRPIN340 and has potential applications as a topical treatment for ocular neovascularization in addition to anticancer effects (Czubaty & Piekiełko-Witkowska, 2017; Morooka et al., 2015).

Currently, there are five small molecule inhibitors in clinical testing that target the CLKs kinase family including SM04690, SM09419, CTX-712, SM08502 and SM04755. SM04690 (Lorecivivint, Adavivint), developed by Biosplice has shown anti-inflammatory and chondroprotective effects in animal models (Deshmukh et al., 2019; Seo et al., 2021) and is currently in Phase III clinical trials (NCT03928184) for OA.. It is a dual kinase inhibitor (CLK2/DYRK1A) which inhibits the SR protein phosphorylation predominantly at SRSF4, SRSF5, SRSF6 in human chondrocytes (Inc. Biosplice Therapeutics, 2021). It blocks pain and joint damage in animal models

of arthritis (Deshmukh et al., 2019) and has shown some efficacy in patient reported outcomes in clinical (Phase IIb) trials. This trial identified the optimal dose (Lorecivivint) for future studies (Y Yazici et al., 2021; Yusuf Yazici et al., 2020). Lorecivivint is not only a splicing kinase inhibitor, it also modulates the Wnt pathway. Wnt signalling is upregulated in arthritic joint tissues which drives chondrocyte hypertrophy, cartilage degradation, bone differentiation and inflammation (Luyten et al., 2009). Wnt downstream ß-catenin modulation suggests a promising method for homeostatic modulation of Wnt signalling and treatment of arthritis such as OA (Deshmukh et al., 2019). In addition, this compound has shown therapeutic potential for cancer treatment (Moroney et al., 2021; J. Tang et al., 2022). Other pan-CLK inhibitors developed by Biosplice include SM09419 and SM08502 which are in phase I clinical trial and proposed as treatment for haematological malignancies (H. Chung et al., 2019) and advanced solid tumours (Bossard et al., 2020; Tam et al., 2020), respectively. SM04755 (Biosplice) has completed phase 1 trial for tendinopathy with no published results (ClinicalTrials.gov NCT03229291). CTX-712 is a non-selective CLKs inhibitor owned by Chordia Therapeutics currently in phase I clinical study for the treatment of refractory and recurrent malignancies (Yoda et al., 2019).

There are several other CLK inhibitors such as 1,143,529 (Lee Walmsley et al., 2021), 1,104,962 (CaNDY) (Sonamoto et al., 2015), T-025 (Iwai et al., 2018), 970,757 (Sun et al., 2017), CLK2 CC-671 (D. Zhu et al., 2018), J-10688 (C. Li et al., 2018), TG-003 (Funnell et al., 2017; Mott et al., 2009) in preclinical studies for the treatment of various cancers and other diseases such as glioblastoma multiforme, cystic fibrosis, and influenza.

In the light of evidence in the literature, I used SPHINX31 and Griffin6 to explore any potential chondroprotective effect by the inhibition of SRPK1 and CLK1 respectively.

Primary hypothesis: Alternative splicing kinase inhibitors will block or reduce change of the chondrocyte cell-line ATDC5 to a hypertrophic state.

Aim: to determine the effect of SRPK1 and CLK1 inhibitors on the morphology and COL2A1/COL10A1 expression by ATDC5 chondrocytes following change to a more hypertrophic state.

Original objectives:

1. to determine changes in cell morphology and measure the expression of COL2A1, COL10A1, CD44, COMP and MMP13 expression in differentiated ATDC5 cells, and
2. to determine the effect on expression of these markers in ATDC5 cells treated with SRPK1 and CLK1 inhibitors.

7.2 MATERIALS AND METHODS

7.2.1 List of reagents/primers used

The detail of all reagents used in the experiment is given in table 7.1 – 7.3.

Table 7.1: List of reagents used in RNA extraction

Reagents	Purchased from
TRIzole	ThermoFisher Scientific , AM9738
PBS	Sigma-Aldrich, D8537
Chloroform	Fischer chemicals, C2432
Isopropanol	Sigma-Aldrich, 9500-1
Ethyl alcohol	Sigma-Aldrich, 459836
DEPC	Invitrogen, 10289104

Table 7.2: List of reagents used in cell culture

Reagents	Purchased from	Catalogue number
DMEM/F-12	ThermoFisher Scientific	11320033
MEM - α	ThermoFisher Scientific	12571063
PBS	Sigma-Aldrich	D8537
FBS	Sigma-Aldrich	F2442
Trypsin-EDTA	Sigma-Aldrich	T4049

Table 7.3: List of reagents used in RT-PCR

DNase treatment	Reverse transcription
RQ1 RNase – Free DNase (Promega, M6101: contents part no. M610A) RQ1 RNase – Free DNase 10X Reaction Buffer (Promega M6101: contents part no. M198A RQ1 DNase Stop Solution (Promega, M6101: contents part no. M199A RNase – Free water, ThermoFisher R0581 1.25ml (4 x 1.25ml)	Oligo – dT (Promega, C1101 contents part no. C110A - 500 µg/ml) Random Primers (500ng, Promega, C1181: content part no. C118A - 20µg) MMLV - RT (Promega, M1701: content part no.M170A - 10,000u) MMLV -RT Buffer (5X) Promega, M1701: content part no. M531A – 1ml DNTPs Promega, U1515 (10mM)
Amplification	**Visualisation**
▪ 2X Master mix (Promega M7501) ❖ Contains 50U/mL Taq DNA polymerase, 0.4mM dNTPs, 3Mm $MgCl_2$ cDNA Primers (forward and reverse 0.5µM each) ▪ H_2O	Agarose (Sigma, A9535) 0.5X TAE buffer (Tris base, glacial acetic acid, EDTA, Water) Ethidium bromide (Sigma, E1510) Loading dye (Bioline 5X) 50bp Ladder

7.2.2 ATDC5 storage conditions and expansion

7.2.2.1 General cell culture method

ATDC5 (ECACC 99072806) mouse chondro-progenitor cells AT805 were purchased at passage 5 (P5) from UK Health Security Agency (UKHSA) (supplied by European Collection of Authenticated Cell Cultures (ECACC). The cells were first stored in an isopropanol freezing container and later transferred to liquid nitrogen storage. ATDC5 were taken out from liquid nitrogen and expanded in DMEM/F12+ 5% FBS (Foetal Bovine Serum: SIGMA F2442- 500ml)) in a T25 (Corning) flask and their growth were monitored by regularly viewing under the microscope (Figure 7.3). The cells were placed in an incubator at a temperature of 37°C and an atmosphere composed of 5% CO2 and 95% O2, unless stated otherwise (Sanyo MCO-18AC). Cells were allowed to reach 80% confluence after which they were passaged. These cells reached maximum confluence (80%) by Day 3 (Figure 7.3) and were then split (P5 – P8) (Figure 7.4). Passages 8, 9 and 10 were used to freeze down the cells again to make stock (Figure 7.5).

1ml vial of ATDC5 cells P5 was removed from liquid nitrogen and added to 5ml of pre-warmed (heated to 37°C) growth media (DMEM/F12) in 50ml of falcon tube to centrifuge at 150G for 5 minutes to get a pellet of cells at bottom. All the media was removed leaving the pellet followed by the addition of 1ml of growth media. This media containing the cells was transferred to T25 flask and 8ml of growth media (DMEM/F12 + 5% FBS was added. Cells were incubated until they reached 80% confluence and then passaged.

To prepare for further experiments, the culture medium was removed from the T25 flask and washed twice with phosphate-buffered saline (PBS, D8537-500ml). After washing, the PBS was removed and replaced with 3ml of Trypsin-EDTA (1x) (containing 0.05% w/v Trypsin and 0.5mM EDTA - T4049, 100ml) in the same flask. The flask containing the cells was then placed in an incubator at 37°C with 5% CO2 /95% O2 for a maximum of two minutes. After quenching the Trypsin-EDTA solution with 3x ATDC5 growth medium (DMEM/F12) and centrifuging at 150G for 5 minutes in a 50ml falcon tube, the cell pellet was isolated. All the media was then removed

leaving the pellet and 1ml of media was added back to resuspend and count the cells using a Haemocytometer (Cat. No. 5610, Vetlab supplies UK). The ATDC5 cells were then split and seeded in a T75 flask at a 1:3 ratio (Figure 7.4).

7.2.2.2 Preparation and storage of cell stocks

Cell stocks were prepared following the general cell culture method up to the centrifugation phase (see section 7.2.2.1). The cells were collected in a Falcon tube (50ml) after trypsinisation and centrifugation. Cells were re-suspended in freezing medium that contained of 10% dimethyl-sulfoxide (DMSO) as cryo-preservant, ThermoFisher 20688), basal growth medium (DMEM/F12 + 20%FBS) and the number of cells count was $1x10^6$ cells/mL per cryo-vial (Nunc V7384). The cryo-vials containing cell aliquots were placed in a Mr Frosty isopropanol chamber (Sigma, SIGMA C1562) and left to freeze overnight at -80°C before being transferred to liquid nitrogen for storage.

When thawing cells from stocks, aliquots were quickly removed from liquid nitrogen and pre-warmed growth medium at 37°C was added in order to make up a final volume of 5ml. The cells were immediately centrifuged for 5 minutes at 150G to remove any excess DMSO content. The cells were then resuspended in 8 ml of media and transferred to a T75 flask.

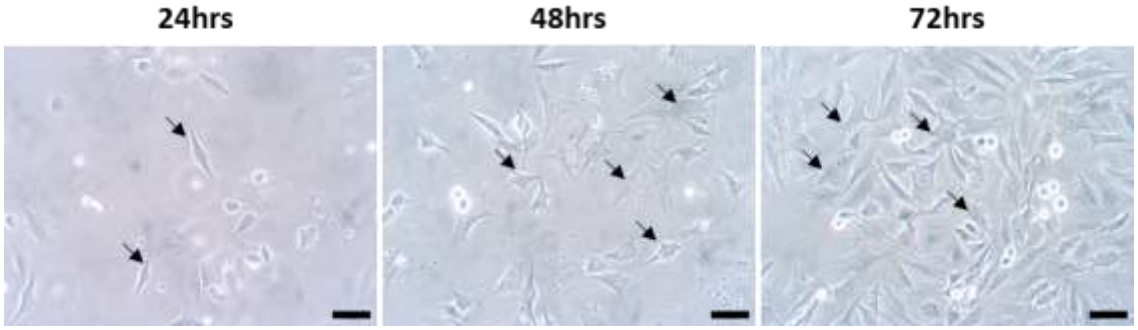

Figure 7.3: Images showing post seeding ATDC5 cells at 24hrs, 48hrs, and 72hrs. Arrows show the growing cells with initial spindle shape appearance changing to larger more rounded cells as time progresses. Images were taken with 20x magnification under light microscope. Scale bars = 25µm

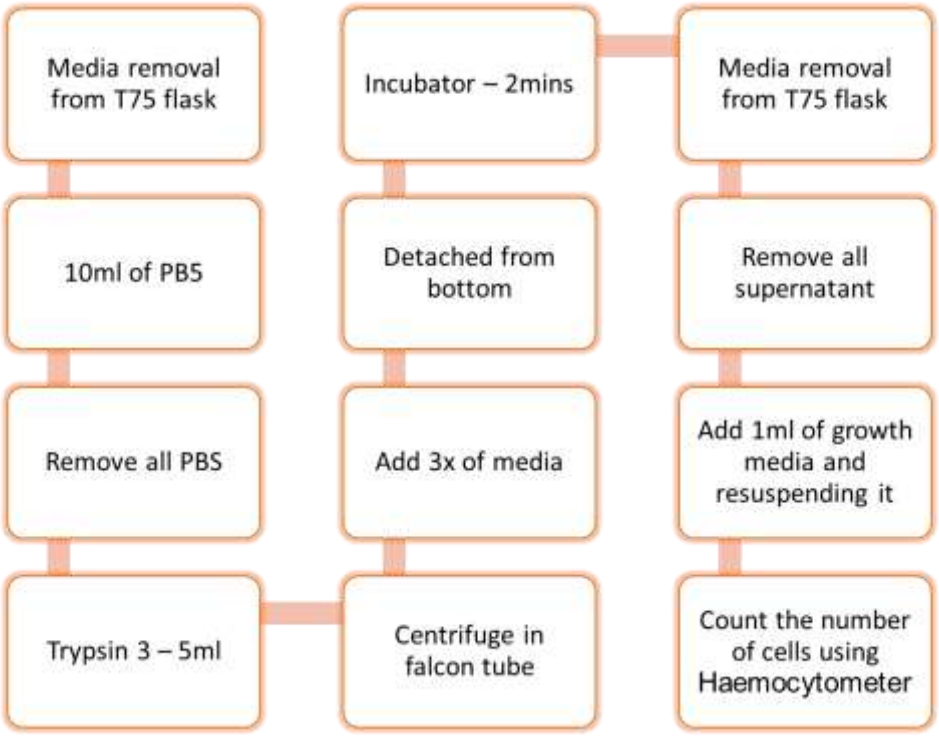

Figure 7.4: Flowchart showing process for splitting of ATDC5 cells.

7.2.3. Optimisation of the ATDC5 differentiation protocol

7.2.3.1 Cell culture for RNA extraction

ATDC5 cells were cultured in T75 and allowed to reach 80% confluence as discussed previously in section 7.2.2.1, followed by trypsinisation and centrifugation for 5 minutes at 150G to form a cell pellet. The pellet was resuspended in 1 mL of DMEM/F12 + 5 %FBS. The cells were counted using a haemocytometer, before seeding in six well plates at the cell density of 100,000 cells per well with 1 mL of media (DMEM/F12 1:1 + 5% FBS). The plates were incubated for 24 hours at 37°C at 5% CO_2 to attach to the wells and confluent to 80%. After reaching the confluency (80%), I replaced the media (DMEM/F12 + 5% FBS) with MEM - α (Minimum Essential Medium α) containing the differentiation promotor, ascorbic acid (50µg/mL), with added 5% FBS.

Ascorbic acid facilitates the synthesis of collagen matrix, which in turn reduces cell proliferation and promotes differentiation (Newton et al., 2012; Okita et al., 2023; Temu et al., 2010). ATDC5 cells cultured in ascorbic acid-containing MEM-α medium show

rapid spontaneous differentiation in reduced time ≤14days (Temu et al., 2010). I therefore decided to use the MEM- α + ascorbic acid protocol for speed and cost reasons, as well as ease of access to reagents during 2020-21. Many ATDC5 differentiation protocols have used high concentrations of insulin to induce differentiation (Hodax et al., 2019; Yongchang Yao et al., 2014), and others have investigated ways to simplify the method to increase the speed of differentiation and the rate of ECM mineralisation using inorganic phosphate ≥34 days (Newton et al., 2012; Okita et al., 2023; Temu et al., 2010) or ascorbic acid (Altaf et al., 2006).

The culture medium was replaced every other day and the cells were grown in this medium for 8, 12 and 21 days to optimise the experimental protocols (Figure 7.7). MEM - α (Minimum Essential Medium α) containing ascorbic acid (50µg/mL) was used for differentiation of ATDC5 cells. The duration used in the protocol was based previous studies on ATDC5 cell production of COL2A1 at day 8, detectable COL10A1 at day 12 (Hodax et al., 2019), and no COL2A1 and higher COL10A1 expression at day 21.

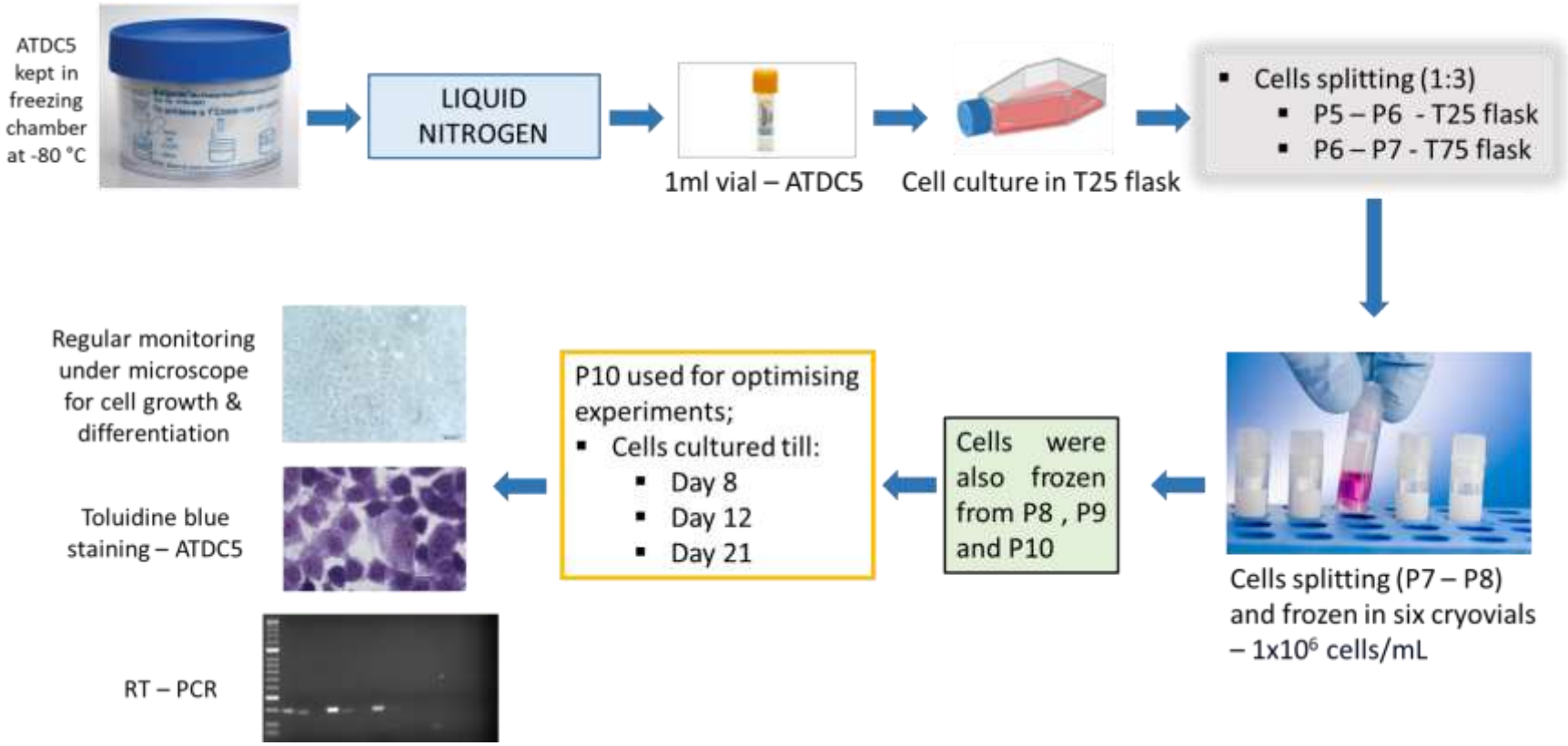

Figure 7.5: Diagram showing the procedure followed to culture the frozen ATDC5 cells bought from UK Health Security Agency (UKHSA) and utilization of these cells to optimise experimental protocols for designed study.

7.2.3.2 Morphological and phenotypic changes in ATDC5 cells

ATDC5 cells change morphology as they change phenotype (Figure 7.6). To assess these changes, cells were plated on coverslips in DMEM/F-12 with 5% FBS, allowed to reach confluence, and differentiated as in section 7.2.2 for 8, 12 or 21 days. Some were imaged without staining (Figure 7.7). Additional cells were stained with toluidine blue (Figure 7.8). For staining, all the growth media was removed and coverslips were rinse with PBS (2X). Subsequently, the cells were incubated with 4% formaldehyde for 15 minutes at room temperature for fixation and afterwards repeatedly washed with PBS in the culture hood. These coverslips were then stained with 1% toluidine blue for 30 seconds and washed with PBS, mounted on slides with DPX after a very brief rinse with 100% ethanol and images were taken using light microscope to see morphological changes (Figure 7.8).

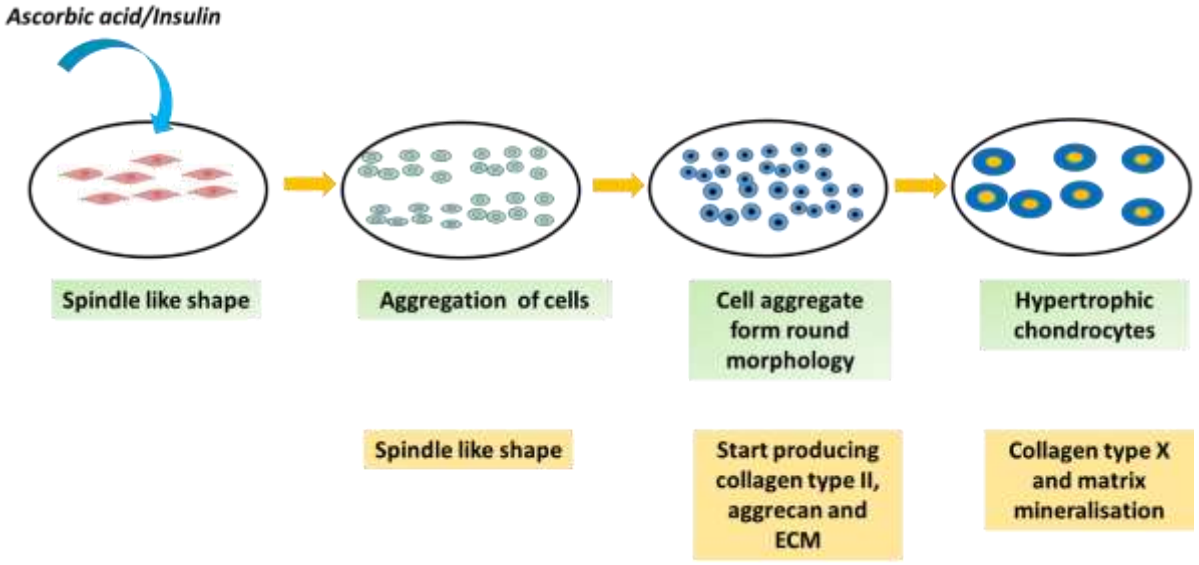

Figure 7.6: Schematic representation of phenotypic transition of ATDC5 cells to a hypertrophic state. Ascorbic acid or insulin induces differentiation of ATDC5 cells to induce first collagen II expression, then hypertrophic chondrocytes with collagen X expression. Recreated from figure published (Yongchang Yao & Wang, 2013).

At day 8 ATDC5 cells lose their spindle-like appearance and begin to aggregate (Figure 7.7, 7.8A&B), at day 12 cells are rounded and are beginning to show some ECM formation, with the appearance of some cells with a slight increase in size compared to normal pre-hypertrophic ATDC5 cells (Figure 7.7, 7.8 C&D) and at day 21 cells show a hypertrophic morphology, with drastically increased volume of cell, large cytoplasmic lacunae and matrix

vesicles, and condensed and fragmented nuclear chromatin (Figure 7.7, 7.8E&F) (Bruckner et al., 1989; Pazzaglia et al., 2020).

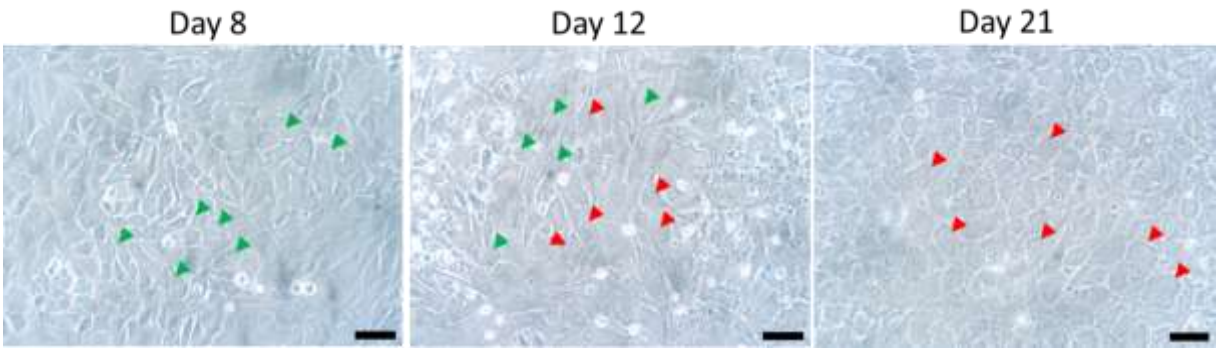

Figure: 7.7: ATDC5 cell differentiation at Day 8, 12 and 21 without staining (phase contrast microscopy). Green arrowheads; normal chondrocytes like cells, Red arrowheads; pre-hypertrophic/hypertrophic ATDC5 cells. Differentiation of ATDC5 cells into chondrocyte-like cells (green arrowheads) was observed at Day 8, Day 12 have much normal chondrocytes (green arrowheads) and also dedifferentiation into hypertrophy (red arrowheads) started at Day 12 (pre-hypertrophic) while hypertrophic chondrocytes are visible (red arrowheads) at Day 21. Images were taken with 20x magnification under light microscope. Scale bars = 25µm

7.2.4 RNA extraction

RNA extraction consists of steps from cell homogenisation, phase separation, RNA precipitation, RNA wash and re-dissolving of the RNA pellet (Figure 7.9). Following cell culture and differentiation, culture medium was removed, and cells were washed twice with 2mL of PBS. 1mL of TRI reagent (Trizol, ThermoFisher Scientific, AM9738) was added to each well to lyse the cells with the help of a cell scraper. The homogenous lysate was collected in a 1.5mL Eppendorf tube and incubated for 5 minutes at room temperature to dissociate nucleoprotein complexes. 200µL chloroform was added, shaken vigorously for 15 seconds, and incubated for 15 minutes at room temperature followed by centrifugation at 12000rpm for 15 minutes at 4°C. This gives 3 different phases; a pink organic lower phase containing proteins; (b) a white / grey interphase containing DNA), and (c) a colourless upper aqueous phase containing RNA. The upper aqueous phase was transferred to a fresh Eppendorf tube with addition of 500µL of isopropanol (Thermo-Fischer, 9500-1) and incubated for 10 minutes at room temperature. Afterwards, the sample was centrifuged at 12000rpm for 10 minutes at 4°C. The supernatant was removed and the RNA pellet was

washed in 75% ethanol (SIGMA 459836-1L) followed by centrifugation at 1000rpm at 4°C for 10 seconds. The ethanol was removed and the pellet briefly dried. RNA was dissolved in 20µL of DEPC treated (Invitrogen, 10289104) RNA-free water and stored at -20°C overnight for Nanodrop measurement the next day.

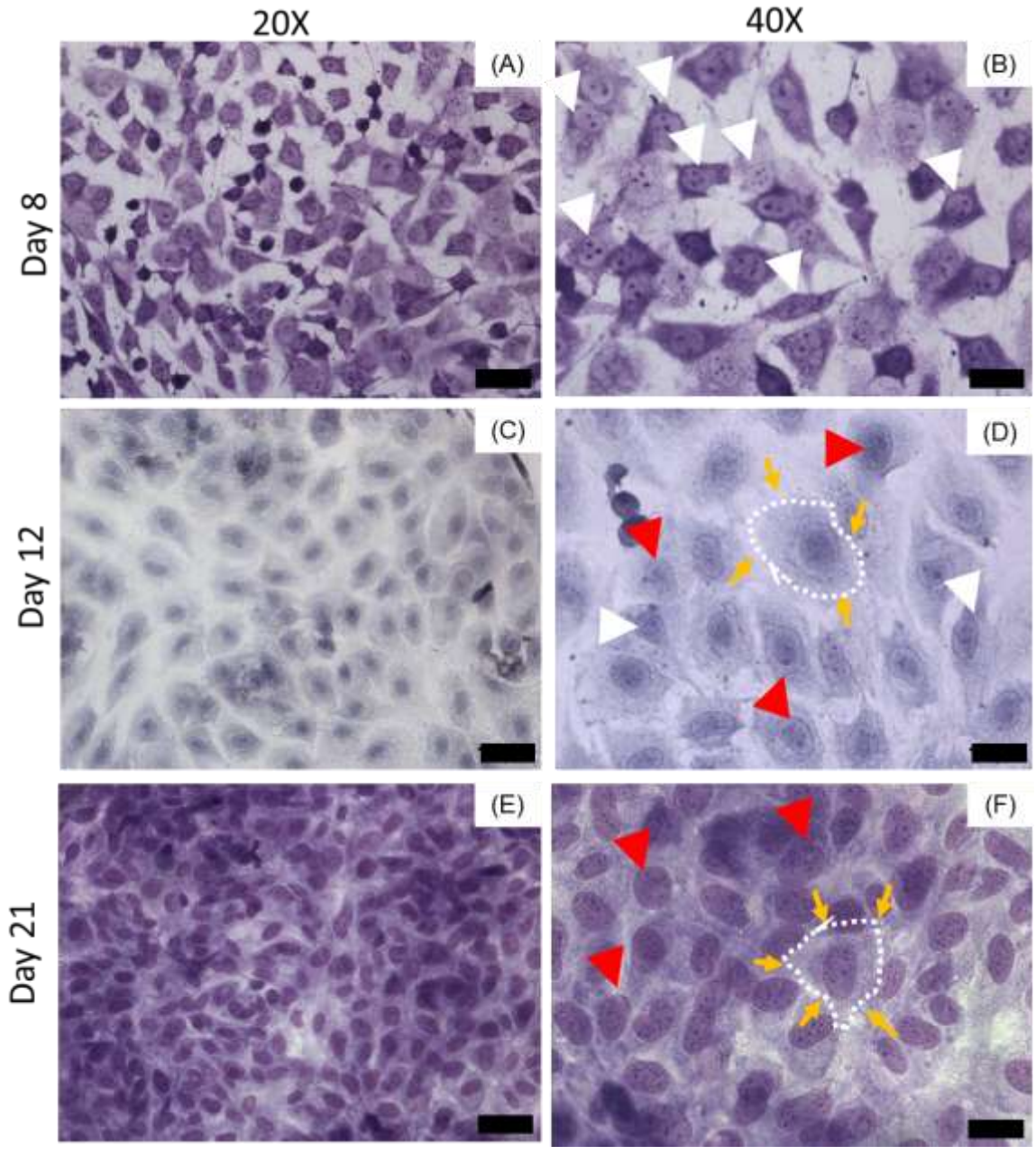

Figure: 7.8: ATDC5 cells were grown on cover slips and stained with 1% toluidine blue at 8, 12 and 21 days after addition of ascorbic acid. (A&B) At day 8 ATDC5 start differentiating to chondrocytes (white arrowheads) showing cellular aggregation. (C&D) Fully differentiated chondrocytes with loss of spindle appearance (white arrowheads) are obvious at Day 12 and initiation of hypertrophy is seen (red arrowheads). This phase is also referred as the pre-

hypertrophic phase where cells start transforming into hypertrophic chondrocyte-like cells while (E&F) hypertrophic chondrocytes can be seen at Day 21 (red arrowheads). Yellow arrows denote cells with visible large matrix vesicles in hypertrophic chondrocytes (D,F). Scale bars 50µm (A,C,E), 25µm (B,D,F).

The quality and concentration of the RNA were measured using a Nanodrop 2000 spectrophotometer (Thermo-Fisher). Total RNA content was measured by determining the ratio of absorbance at 260/230nm for RNA/proteins and purity was assessed by the ratio of absorbance at 260/280nm for RNA/DNA (Table 7.4). RNA was diluted to 1ng/µl in nuclease-free water to ensure equal input mass for experiments and stored at -80˚C.

Figure 7.9: Steps in the RNA extraction protocol using TRI reagent (Trizol).

Table 7.4: Nanodrop data of cDNA extracted from ATDC5 cells showing measurements of purity (absorbance ratios 260/280 and 260/230) and concentrations.

Date and T	Nucleic Acid	Unit	A260 (Abs)	A280 (Abs)	260/280	260/230	Sample Type
28/04/2021 1	1077.5	ng/µl	26.937	13.502	2	0.96	RNA
28/04/2021 1	3700	ng/µl	92.5	46.948	1.97	1.93	RNA
28/04/2021 1	10984.1	ng/µl	274.604	138.434	1.98	2.09	RNA

7.2.5 PCR amplification

Two-step RT-PCR involves two separate reactions which start with cDNA synthesis by reverse transcription (RT) followed by amplification of a portion of the resulting cDNA by PCR (Figure 7.10). The steps in RT-PCR are (a) reverse transcription; (b) amplification; (c) gel visualisation.

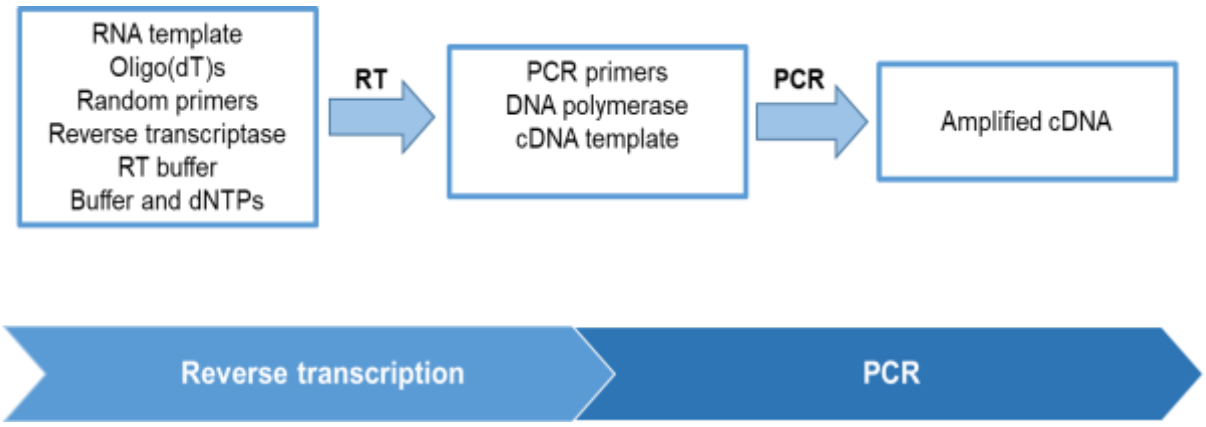

Figure 7.10: Flow diagram RT-PCR reaction.

7.2.5.1 cDNA synthesis by reverse transcription

A. DNase treatment

Complementary (c)DNA was synthesized using 1µg of RNA (section 7.2.4) dissolved in a total of 8µL nuclease free water (ThermoFisher R0581) in a 200µl PCR tube (Starlab, I1402-8100). If the RNA concentration was greater 1µg/µl in the initial samples, the final concentration was adjusted by addition of nuclease free water to ensure equal RNA input from each sample. On the other hand, when the total RNA was <1µg/ml, then the total RNA used in each reaction was the same as in the lowest yield sample.

The RNA sample underwent DNase treatment to eliminate any potential genomic DNA contamination. To achieve this, 1µL of RQ1 DNase (Promega, M6101:M610A) was added to a mixture containing 10mM HEPES, 50% v/v glycerol, 10mM CaCl2 and 10mM MgCl2. Additionally, 1µL of RQ1 DNase buffer (Promega M6101: M198A) was included in the mixture, which comprised of 400mM Tris-HCl, 100mM MgSO4 and 10mM CaCl2 [pH 8.0 at 25°C]. The final volume of the mixture was 10µL. The samples were incubated for 30 minutes at 37°C in a PTC-200 Thermocycler followed by the addition of 1µL RQ1 DNase stop solution (Promega, M6101:M199A) (20mM EGTA [pH 8.0 at 25°C]) to stop the DNase activity. Afterwards the sample was incubated for 10 minutes at 65°C and stored at -20 °C for immediate use or stored at -80ºC for later use. Repeat thawing should be avoided thus it is recommended to make small aliquots of the cDNA after the first thaw and then reverse-transcribed.

B. Reverse transcription

Reverse transcription was performed using 1µL (500ng) of Oligo-dT (Promega C1101:C110A - 500 µg/ml) that anneals to poly(A) tails of eukaryotic mRNAs. These are recommended with reverse transcriptase (RTs) and ideal for constructing cDNA libraries. 0.5 µL (500ng) random primers (Promega C1181:C118A - 20µg) were also added to the samples. Random primers or hexamers are short oligo-deoxyribonucleotides with random base sequences (usually [d(N)6]) that are typically used to prime single-stranded DNA or RNA for extension by DNA polymerases or reverse transcriptase. During cDNA generation, these hexamers randomly cover all regions of the RNA, resulting in a cDNA pool that contains cDNAs of various lengths. The RNA sample was incubated for 10minutes at 70°C followed by quenching on ice to prevent secondary conformation changes in RNA because of its highly dynamic nature to interact with binding partners. Stock solution of MMLV (Molony Murine Leukaemia Virus) reverse transcriptase RT buffer (Promega, M1701: content part no. M531A) (375mM KCl , 15mM $MgCl_2$, 250mM Tris-HCl, and 50mM DTT) was made with nuclease free water (NFW) and dNTPs (deoxyribonucleotides) (0.5Mm) (Promega, U1515) and 6.5µL added to each RNA sample. 1µl of MMLV-RT enzyme (Promega, M1701: content part no.M170A) was added to make up the final volume to 20µL. MMLV reverse transcriptase is an RNA-dependent DNA polymerase that uses single-stranded RNA as the template for first strand complementary DNA strand synthesis, using a hybridized primer such as oligo-dT or random primers. A negative control minus RT was used which contained all other constituents but no MMLV reverse transcriptase (1µL of nuclease free water was added to make up the final volume 20µL). Finally, all the samples were incubated in the PCR machine at 37°C for 60 minutes followed by incubation at 42°C for 30 minutes to allow for DNA polymerisation. After this, samples were incubated at 70°C for 10 minutes to inactivate the MMLV-RT, and finally stored at -20°C or -80°C depending on the interval between isolation and PCR experiment.

C. cDNA amplification

cDNA amplification was performed with target-specific forward and reverse primers (0.5µM each), using PCR master mix (Promega: final concentrations 25U/mL Taq DNA polymerase, 0.2mM dNTPs, 1.5mM $MgCl_2$). Aliquots of specific primer pair mixtures (1:1) were made to

avoid freeze thawing and diluted with nuclease-free water to a concentration of 10µM (Stock: 100µM: 10µM forward, 10µM reverse, 80µL nuclease free water). 1µL of primer mix was added to master mix to achieve a final primer concentration of 0.5µM for each primer. Finally, up to 2ng of cDNA was added to each tube, and nuclease-free water was added if necessary to reach a final reaction volume of 20µL. The negative controls contained all ingredients other than cDNA. Two negative controls were utilized in the experiment: (1) water control, which was used to identify DNA contamination of reagents. This was achieved by replacing the cDNA with water in the reaction mixture; (2) no RT (-RT) control, which was used to determine whether genomic contamination was present even after DNase treatment. The cDNA was amplified in 200 µl thin-walled tubes using a PTC-200 thermocycler under the general conditions shown in Figure 7.11 using specific primer sets shown in Table 7.5. Reactions were visualized by gel electrophoresis immediately or stored at 4°C overnight.

Figure 7.11: Generalised PCR steps and conditions.

Table 7.5: Primer sequences for RT-PCR targets

Target	Amplicon (bp)	Forward primer	Reverse primer
GAPDH	180	CAACTACATGGTTTAC ATGTTC	GCCAGTGGACTCCAC GAC
COL2A1	170	CTGCTGCTAATGTTCT TGAC	ACTGGAATCCCTTTAC TCTTT
COL10A1	143	ATCTTGCCGCATCTG TGTGT	CTCCTTTCTGCCCCTT TGGC

7.2.6 Optimisation of RT-PCR

My original aims were to study expression of multiple markers of chondrocyte state, specifically COL2A1, COL10A1, CD44, COMP and MMP13, but due to time and Covid-related restrictions I was only able to focus on COL2A1 (early differentiation marker) and COL10A1 (hypertrophy marker).

I used GAPDH as an internal control as these primers were already available in the lab. The classification of housekeeping genes comprises of genes which play a key role in the maintenance of basic cellular functions obligatory for the most of cells in their survival and normal functions (Eisenberg & Levanon, 2003). For normalization of gene expression, housekeeping genes have been used widely as reference genes for data derived from various experimental treatments and cell types by means of reverse-transcriptase polymerase chain reaction (RT-PCR). GAPDH is a basic regulatory enzyme, which participates in many cellular functions in addition to glycolysis such as DNA replication and repair, nuclear tRNA export, exocytosis, endocytosis, iron metabolism, cytoskeletal organization, carcinogenesis, and cell death (Colell et al., 2009; Sheokand et al., 2014).

RT-PCR conditions were optimised by varying reagents and PCR cycle conditions, such as the amount of input cDNA, denaturation time, and annealing temperature, for all primer pairs independently. Starting conditions for new primers were 3 min denaturation at 95^{o}C, followed by 35 cycles of 30s denaturation at 95^{o}C, 45s annealing at 50^{o}C, and 60s extension at 72^{o}C, followed by a final extension time of 10min at 72^{o}C, and incubation at 4^{o}C (Figure 7.11 & 7.12). Standard GAPDH cycle conditions were used which were as above but with annealing at 55^{o}C. Optimised cycle conditions and temperature are shown in Figure 7.10. Using 1ng input RNA I was able to show expression of both GAPDH and COL2A1, but not COL10A, so I increased input to 2ng which resulted in COL10A detection. Annealing temperatures for COL2A1 and COL10A were 59^{o}C and 55^{o}C, respectively. Expression of GAPDH and COL2A1 was seen in 2 of 3 plates (Figure 7.13) using the conditions above, but there was no expression of COL10A1. COL10A1 expression was detected when cDNA input was doubled (Figure 7.13). I then determined whether the expression of COL2A1 and COL10A changed at different times after ascorbic acid treatment, days 8, 12 and 21 (n=2/3).

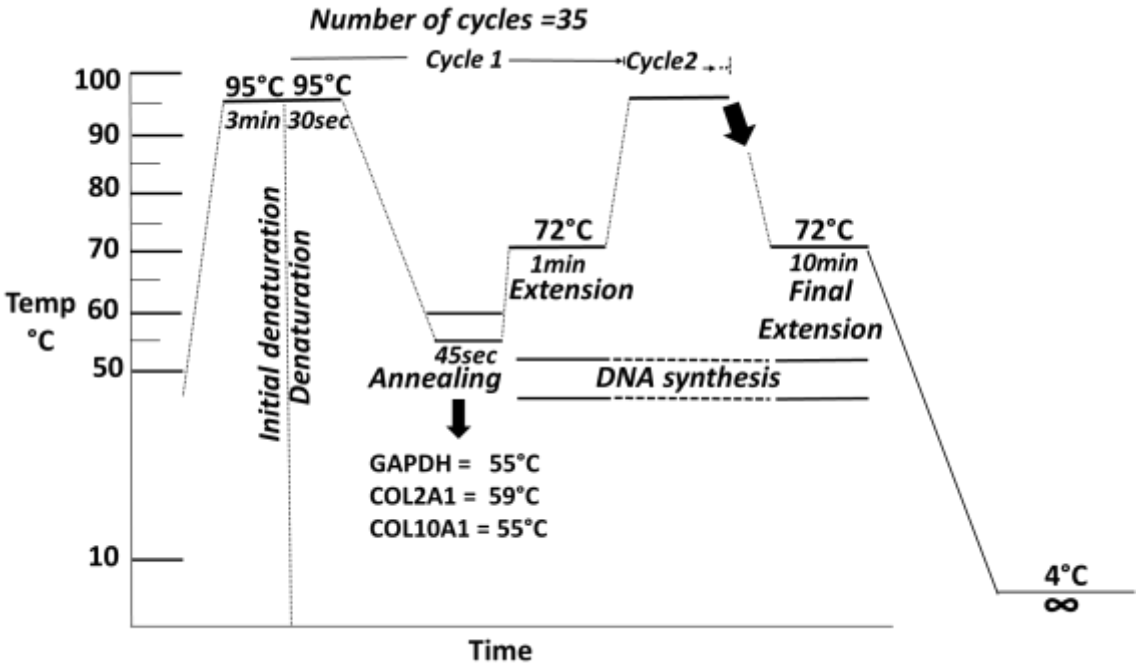

Figure 7.12: Cycle conditions for amplification of GAPDH, COL2A1 and COL10A1.

Table 7.6: Conditions used in RT-PCR for GAPDH, COL2A1 and COL10A1.

Primer	Conditions
GAPDH – Housekeeping gene	Denaturation: 95 °C 3 min Annealing: 55°C 45 sec Extension: 72 °C 1 min No. of cycles: 35
COL2A1	Denaturation: 95 °C 3 min Annealing: 59°C 45 sec Extension: 72 °C 1 min No. of cycles: 35
COL10A1	Denaturation: 95 °C 3 min Annealing: 55°C 45 sec Extension: 72 °C 1 min No. of cycles: 35

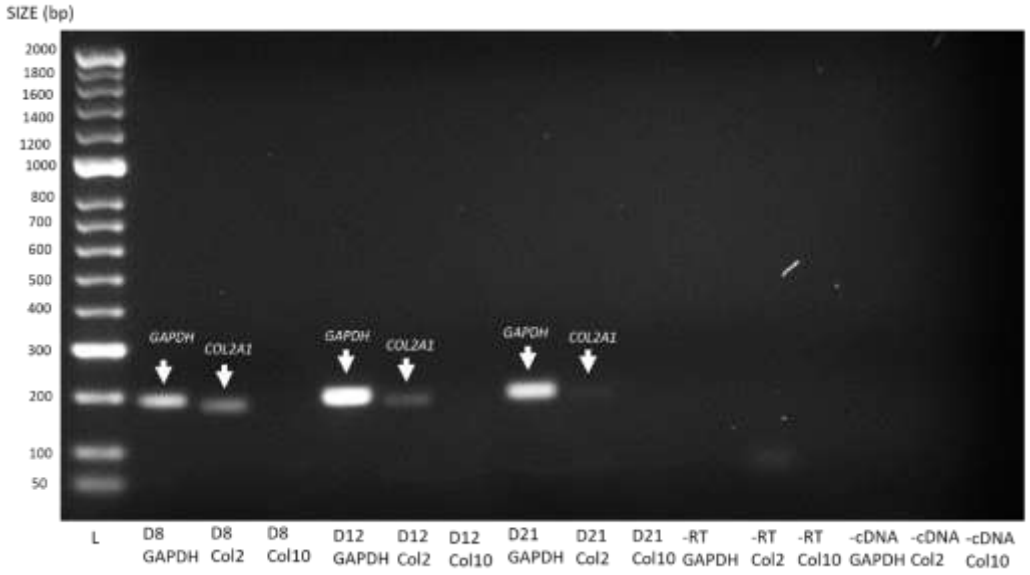

Figure 7.13: Optimisation of RT-PCR for GAPDH, COL2A1 and COL10A1 using 1ul of cDNA at concentration of 1ng/µl. PCR gel shows GAPDH (180bp) and COL2A (170bp) amplicons (arrows) in three ATDC5 samples cultured for 8, 12 and 21 days in differentiation medium. The COL10A1 amplicon (143bp) was not detected in any sample. -RT samples are negative controls for genomic DNA contamination, and -cDNA samples control for any DNA contamination introduced during reaction preparation.

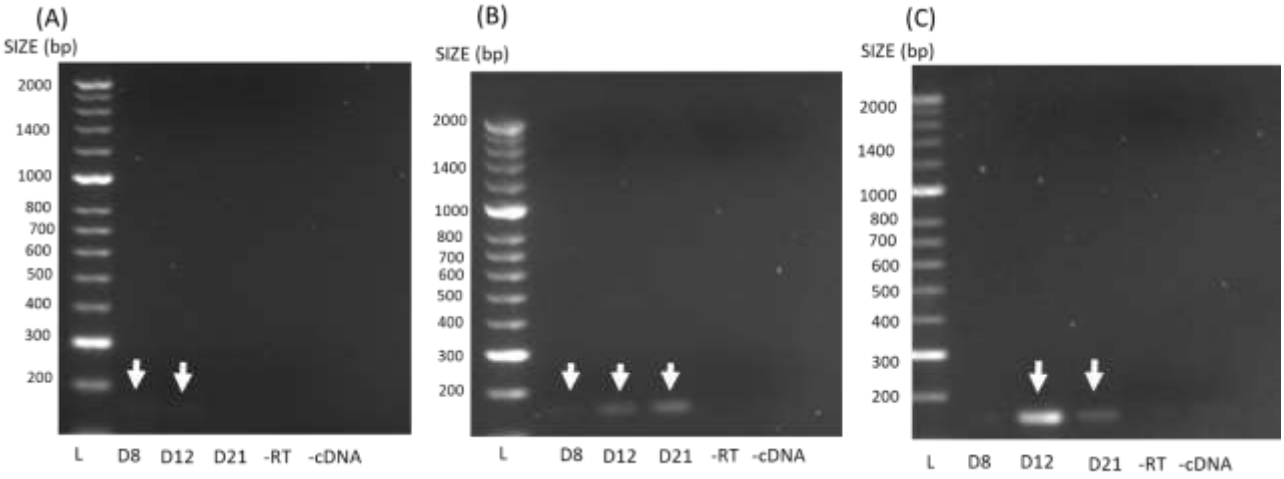

Figure 7.14: Optimisation of RT-PCR for COL10A1. (A) PCR gel shows barely visible COL10A1 amplicons (143bp) in two samples (arrows) using the cycle conditions in Table 7.6 and 1ng/µl input cDNA. (B) using the same cycle conditions but with 4ng/µl input cDNA, the COL10A1 amplicon (143bp) was detected in all samples. (C) 2ng/µl input cDNA showed COL10A1 at Day 12 and 21 samples. -RT samples are negative controls for genomic DNA contamination, and -cDNA samples control for any DNA contamination introduced during reaction preparation. L: Ladder; D8: Day 8; D12: Day12; D21: Day 21.

7.2.7 Treatment of ATDC5 cells with SRPK1 or CLK1 inhibitors

ATDC5 cells were passaged and plated at a total density of 2.5 x 10^4 cells/well in a 12-well plate (n = 4) (Figure 7.15) and cultured in DMEM/F-12 (Dulbecco's Modified Eagle Medium/Nutrient Mixture F-12) media with 5% FBS in 5%CO_2:95%O_2 at 37°C over 3-4 days until they reached confluence. Ascorbic acid (50µg/mL) was then added in MEM - α (Minimum Essential Medium α) with 5% FBS, to induce chondrogenesis. Media was changed every other day and cells cultured for a total of 21 days. Cells were also grown on coverslips (under the same conditions as above) for investigation of the effects of the treatments on cell morphology.

Alternative splicing inhibitors of SRPK1 (SPHINX31: 1µM and 5µM) or CLK1 (Griffin6: 1µM and 5µM) were dissolved in dimethyl-sulfoxide (DMSO 0.1% in PBS) and added to the growth media from day 1. Cells were exposed to inhibitor or DMSO vehicle (0.1%, equivalent to inhibitor treatment) for the whole 21 days (Figure 7.15), with fresh inhibitor added in each media change. SPHINX31 and Griffin 6 were kind gifts of Professor Jonathan Morris, University of New South Wales Australia. The concentrations used were based on IC_{50} values (Table 7.7) and data generated by Matthew N. Swift in which SPHINX31 and Griffin6 showed significant biological effects on primary rodent neurons at these concentrations (Swift, 2021).

Table 7.7: Novel splicing kinase Inhibitors' specificity and IC_{50} values (data kindly supplied by Prof Jonathan Morris).

Compound	IC50 SRPK1 (nM)	IC50 CLK1 (nM)	IC50 CLK2 (nM)	IC50 DYRK1A (nM)
SPHINX31	5.9	282	623	>1000
Griffin 6	199 ± 36	5.6 ± 1.1	3.9 ± 0.6	1400 ± 283

Light field images were taken of only the cells treated with the highest inhibitor concentrations from day 1 till day 21 for each repeat culture to monitor cell morphology changes. At day 21 cells were lysed using TRI-reagent and RNA extracted for PCR analysis as described in Section 7.2.3.1, 7.2.4 – 7.2.6.

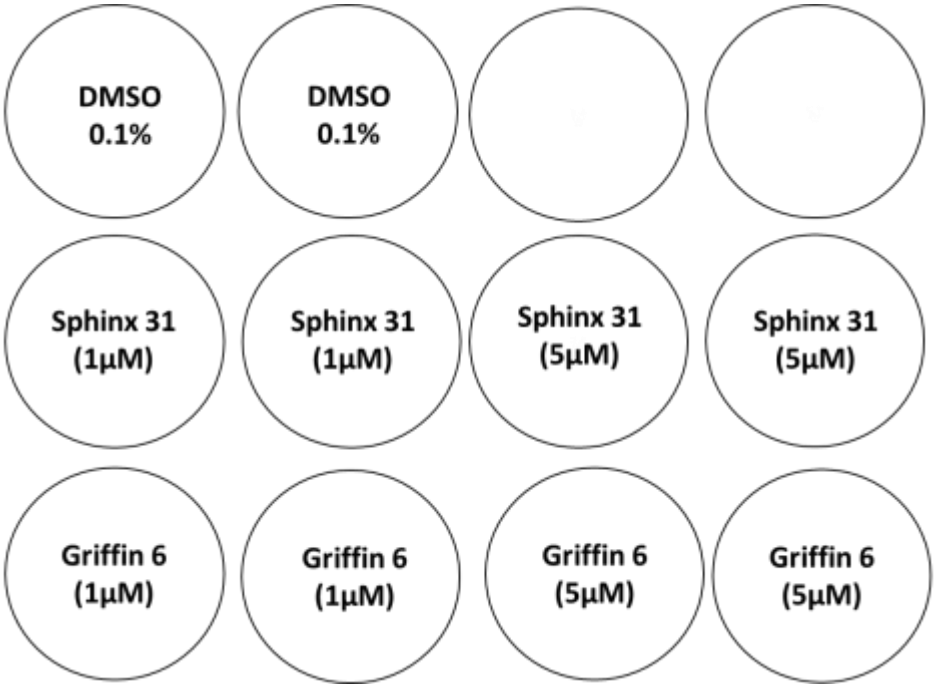

Figure 7.15. Illustration of the structure of each 12 well plate (n=4) containing treatments in duplicate for the RNA-extraction work.

7.2.8. Data extraction and statistical analysis

Raw data from PCR gel images was extracted using ImageJ (Figure 7.16). Gel images were loaded to ImageJ and the first visible band was marked by drawing a rectangular selection box. All the bands were then selected using the "Analyse-Gel" functions from ImageJ (Figure 7.16A) before selecting the "plot lanes" function. The "plot lanes" function generates a plot that displays peaks in the graph to represent the integrated density of fluorescence in each rectangle drawn. A straight line was drawn at the base of the peak connecting the bottom ends of the plotted lane (Figure 7.16B), using the line tool, to define the total area of the measured band and derive integrated image density (Figure 7.16C). Once all the peaks had been measured, using "Analyse-gels-Label peaks" function gave the percentage of maximum intensity (Figure 7.16D) which was then used for further analysis (see example of analysis shown in Figure 7.16E).

For COL2A1 and COL10A1 mRNA expression, ATDC5 cells were treated with two concentrations of SRPK1 inhibitor SPHINX31 and CLK1 inhibitor Griffin6 (1µM and 5µM). GAPDH was used as an internal loading control to normalise mRNA levels between the

samples. COL2A1 and COL10A1 expression was corrected against GAPDH expression in each sample (example of analysis shown in Figure 7.16E).

For data analysis, one-way ANOVA followed by Dunnett's multiple comparison tests was used to compare the effects of inhibitors with vehicle (DMSO). Statistical p value < 0.05 was considered as significant.

(A)

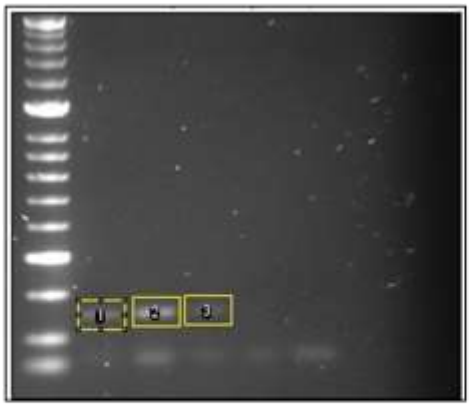

(B)

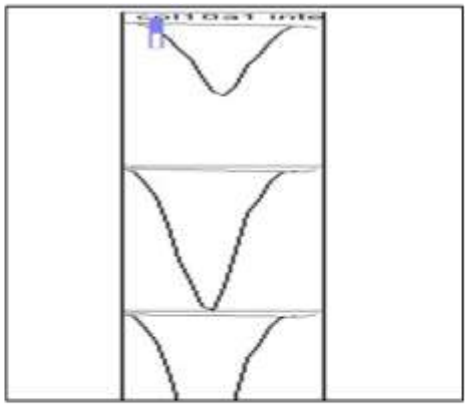

(C)

Results

File	Edit	Font	Re
	Area		
1	3030.548		
2	5971.841		
3	5872.305		

(D)

Results

File	Edit	Font	Results
	Area	Percent	
1	3030.548	20.374	
2	5971.841	40.148	
3	5872.305	39.478	

(E)

Example			
COL10A1 = gene of interest			
GAPDH = House keeping gene			
Normalization Formula = COL10A1/GAPDH			
COL10A1			
	Area	%	Normalization
1	3030.548	20.374	0.40748
2	5971.841	40.148	0.80296
3	5872.305	39.478	0.78956
GAPDH	Area	%	
1	8309.154	50	

Figure 7.16. Method showing generation of data from the PCR gel images using ImageJ. (A) Band selection (B,C,D) ImageJ-derived intensity peaks used to determine the area (rectangles in A) and percentage of area occupied by the band on the gel (E) Example of normalising the mRNA levels between the samples for further analysis.

7.3 RESULTS

I was able to optimise both the differentiation of ATDC5 cells (Figures 7.7 & 7.8) and PCR analysis of the differentiation of ATDC5 cells into chondrocyte-like cells and dedifferentiation to hypertrophic chondrocyte-like cells by the expression of COL2A1 and COL10A1 respectively (Figure 7.13 & 7.14).

7.3.1 Cell morphology changes during ATDC5 exposure to ascorbic acid over 21 days and the effect of SRPK1 and CLK1 splicing kinase inhibitors

Morphological examination of ATDC5 cells exposed to the ascorbic acid (50µg/mL) differentiation medium, either unstained or with toluidine blue staining showed obvious cellular changes up to 21 days (Figures 7.7 & 7.8). The ATDC5 cells transformation into hypertrophic chondrocytes can be seen from Day 1 to Day 21 in DMSO, SPHINX31 and Griffin6 treated cells (Figure 7.17). In DMSO-treated control cells, there was an initial spindle appearance, followed by cell aggregation, and rounder appearance as cells differentiate into chondrocyte-like cells with surrounding matrix. By day 12 cells were more organised with a rounder shape and were forming foci, with loss of spindle shape appearance as well as the appearance of some bigger cells (pre-hypertrophic). Compared to Day 8 and Day 12, by day 21 de-differentiation and hypertrophy was evident by an increase in the size of cells.

SRPK1 and CLK1 inhibition appeared to cause a slight reduction in cell proliferation and size of cells at Day 12, and 21 respectively compared with DMSO. There appeared to be fewer cells which maintained a spindle appearance at day 8, and fewer but larger and rounder cells at day 12 with SRPK1 inhibition (Figure 7.16). This suggests that SRPK1 inhibition might affect ATDC5 cell division and delay differentiation, although by day 21 the appearance of cells was very similar to controls. CLK1 inhibition also appeared to reduce cell proliferation, but resulted in more disorganised and spindle-like cells at day 8 than control or SRPK1 inhibition. SRPK1 inhibition appeared to reduce the number of dead/dying cells at days 8 and 12 than in control cultures (visible white dots in the images), but by day 21 there were no obvious differences in appearance between cells treated with either inhibitor.

I had originally planned to fix and stain cells with toluidine blue and analyse features of intracellular morphology, as well as determining NL of SRPK1 and SRSF1 in treated cells. Unfortunately due to time limitations I was unable to do these experiments, or perform quantitative analyses of cell morphology.

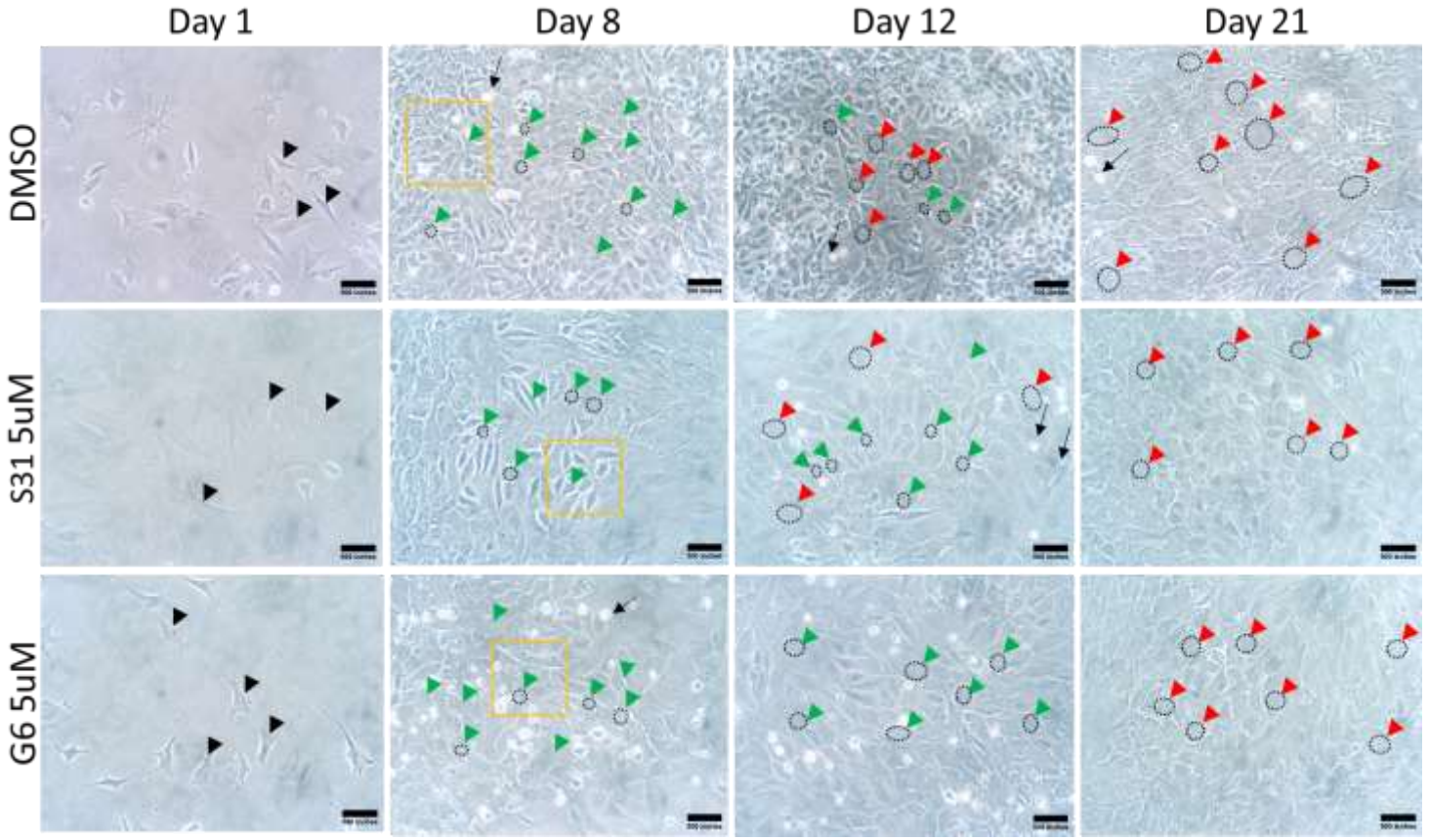

Figure 7.17: Comparison of ATDC5 cell morphology at different times after treatment with ascorbic acid plus vehicle (DMSO) (top row), 5μM SPHINX31 (middle row) or 5μM Griffin6. Green arrowheads: normal chondrocyte-like cells; red arrowheads: hypertrophic-like chondrocytes. Black arrowheads show baseline ATDC5 cell morphology, which transformed to spindle shape cells upon treatment with ascorbic acid (Day 8). Day 8 showed aggregation of cells and formation of some rounder cells which is the starting point of ATDC5 cell differentiation into chondrocyte-like cells (green arrowheads). At this phase formation of cartilage nodules through cellular condensation process can be observed indicated by the yellow square with high cell density and higher production of ECM. Day 12 cells showed more chondrocytes (green arrowheads) some with bigger size (red arrowheads) compared to cells at Day 8, while hypertrophic chondrocytes (red arrowheads) with larger size cells were clearly visible at day 21. Cells treated with S31 (5μM) and G6 (5μM) showed some differences in morphology at days 8 and 12, but were very similar to control cells at day 21. Black arrows show dead cells visible as white spots. S31: SPHINX31, G6: Griffin6. Scale bar =25μm.

7.3.2 Collagen expression during ATDC5 cell exposure to ascorbic acid over 21 days, and the effect of SRPK1 and CLK1 splicing kinase inhibitors

Upon investigation of COL2A1 and CO10A1 in ATDC5 cells differentiated with ascorbic acid, low COL2A1 expression was observed at the starting point of differentiation (differentiated ATDC5 cells; Day 8 mean ± SD: 0.6±0.01) and de-differentiation (pre-hypertrophic; Day 12 2.5±1.5) while no expression was detected in hypertrophic chondrocyte-like ATDC5 cells (Day 21 0±0). COL10A1 expression was also analysed at these time points. There was no COL10A1 expression seen at Day 8 (0±0), but higher expression was detected at pre-hypertrophic (Day 12 0.8±0.6) and hypertrophic stages (Day 21 0.8±0.02).

After successful differentiation and dedifferentiation of ATDC5 cells (Figure 7.18) COL2A1 and COL10A1 expression was investigated at day 21 in hypertrophic chondrocyte-like ATDC5 cells after treatment with alternative splicing kinase inhibitors of SRPK1 (S31) and CLK1 (G6). At day 21 cells treated with DMSO showed a very low expression of COL2A1 (mean ± SD: 0.3±0.5). Alternative splicing inhibitors had no effect on COL2A1 expression at either concentration (SPHINX31 @ 1µM: 0.1±0.1, SPHINX31@ 5µM: 0.1±0.3, Griffin 6 @ 1µM: 0.1±0.2, Griffin6 @ 5µM: 0.4±0.9.) (Figure 7.19 A,D,E).

There was a non-significant reduction in COL10A expression with both SRPK1 and CLK1 inhibition for 21 days (DMSO; mean SD = 1.4±2.2; SPHINX31 @ 1µM 0.3±0.2, SPHINX31 @ 5µM 0.7±0.5, Griffin 6 @ 1µM 0.4±0.5, Griffin6 @ 5µM 0.7±1.1) (Figure 7.19 B,F,G).

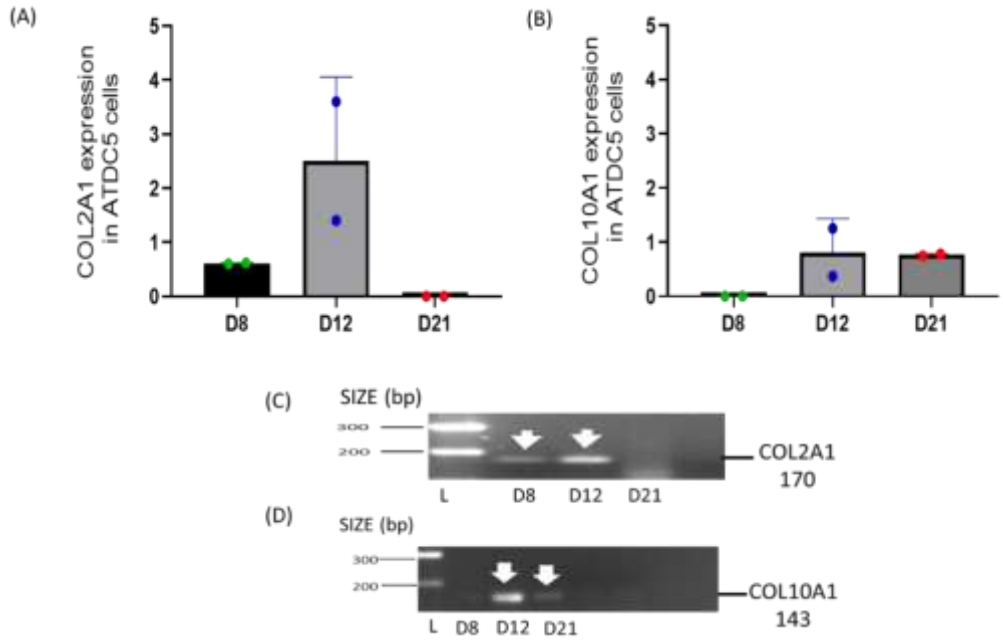

Figure 7.18: (A,B) COL2A1 and COL10A1 expression and (C,D) PCR amplicons in ascorbic acid (50µg/ml) treated ATDC5 cells at different time points (from optimisation data). COL2A1 was detected at days 8 and 12 with no expression seen at day 21. COL10A1 expression was found at all time-points with lower expression at day 8. n=2: NOTE: The reason for only n=2 is because this data is from the optimisation protocol. L: Ladder; D8: Day 8; D12: Day12; D21: Day 21.

SRPK1 (SPHINX31) and CLK1 (Griffin 6) inhibitor did not have any effect on COL2A1 or COL10A expression at either dose compared to control. Therefore, although I could demonstrate that ATDC5 cells changed morphology (Figure 7.7 & 7.8) and mRNA expression (Figure 7.18) over 21 days exposure to ascorbic acid, treatment with alternative splicing inhibitors SPHINX31 and Griffin6 had only a slight effect on cell morphology in terms of reduced proliferation and size of cells at Day 12 and 21 respectively, at the higher concentration (5µM) of both inhibitors.

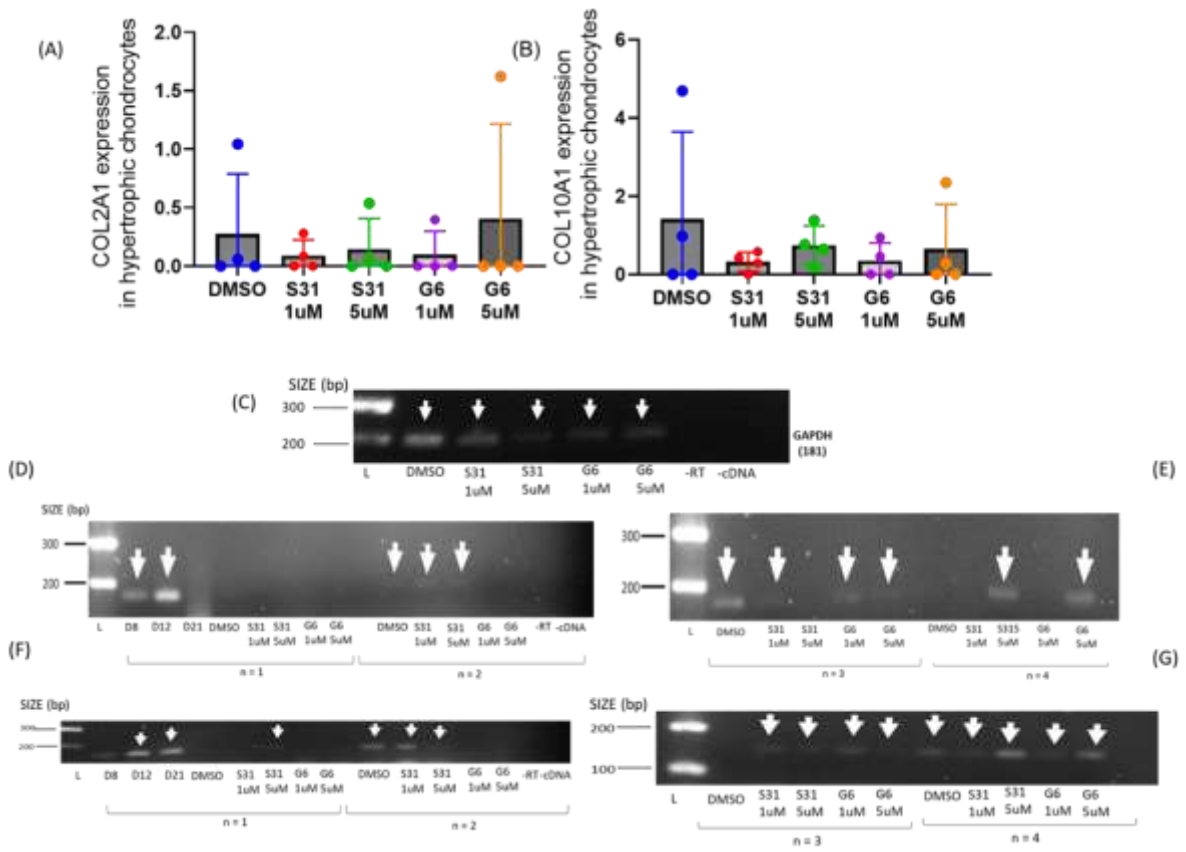

Figure 7.19: (A) COL2A1 and (B) COL10A1 expression in differentiated hypertrophic ATDC5 cells treated with SPHINX31 and Griffin6 (1μM and 5μM). There was no change in either (A) COL2A1 expression or (B) COL10A (B) in any treatment group. Representation of amplicon size of (C) GAPDH – housekeeping gene (181), (D,E) COL2A1 (170), (F,G) COL10A1 (143) in hypertrophic chondrocytes at day 21 in ATDC5 cells. Day 8, 12 and 21 samples were included as positive controls (D,E,F,G) which already showed COL2A1 and COL10A1 expression in optimising the protocol shown above in figure 7.13, 7.14, 7.18 S31: SPHINX31; G6: Griifin6;D8: Day 8; D12: Day12; D21: Day 21.

7.4 DISCUSSION

Though in most of the literature hypertrophic chondrocytes are described in association with OA (M. B. Goldring et al., 2016; Hwang & Kim, 2015; Utomo et al., 2016; Van der Kraan & Van den Berg, 2012), chondrocyte hypertrophy is also found in inflammatory arthritis, and, from my data, in rodent models of IA (Figure 7.1). Based on these observations, and of SRPK1 expression in chondrocytes in IA, I investigated the effects of SRPK1 and CLK1 inhibitors on differentiated ATDC5 cells with the ultimate aim to maintain normal chondrocyte phenotype or delay chondrocyte hypertrophy in ATDC5 cell line. The main experimental aims of this work were to determine changes in cell morphology and measure the expression of COL2A1, COL10A1, CD44, COMP and MMP13 expression in ATDC5 cells in different stages of differentiation/hypertrophy and determine the effects of SRPK1 and CLK1 inhibitors.

The findings of this study showed that the splicing kinase inhibitors did not significantly change either COL2A1 (Figure 7.19A) or COL10A1 expression (Figure 7.19B), in hypertrophic ATDC5 cells. There were slight reductions in expression of both at the end of the study, and indications of cellular morphology change and cell number at earlier stages of differentiation, which could indicate an effect that delayed differentiation. Due to time limitations, I could not generate samples at days 8 and 12 that would have given more meaningful data on possible earlier changes in collagen expression.

The lack of effect is probably not because the drug concentration used was too low. Both SPHINX31 and Griffin6 are potent, selective compounds with IC_{50} values for SRPK1 (S31) and CLK1 (G6) below 10nM (Table 7.7). Griffin6 is also a more potent CLK2 inhibitor than lorecivivint at this kinase (IC_{50}: lorecivivint = 7.8nM; G6 = 3.9nM). Dr Matt Swift used these compounds at the same concentrations as used in this thesis, to protect primary neurones against chemotherapy damage. Increasing the concentrations of these inhibitors above 5µM is unlikely to have a greater effect, and use of micromolar quantities would also be more likely to result in off-target effects e.g. on related kinases (see Table 7.7).

I used total collagen II and X as indicators of change, as Type II collagen is the major type found in mature articular cartilage, and Type 10 collagen is a network-forming collagen synthesised by hypertrophic chondrocytes. Lorecivivint, the Wnt/DYRK/CLK inhibitor reduced chondrocyte hypertrophy *in vitro*, so I tested whether SRPK1 or CLK1 inhibition could change expression of these key collagens. Very little is known about SRPK1 or CLK1 function in cartilage, so it is possible that collagens II and X are not affected by these kinases. Collagen II and X are both alternatively spliced (Savontaus et al., 1998). Collagen II has four alternatively spliced variants, COL2A, B, C and D and its alternative splicing is changed during chondrogenesis (McAlinden, 2014), and collagen X has at least two splice variants (Purkayastha et al., 2020). SRPK1 inhibition has recently been shown to reduce collagen I and III deposition in experimental lung fibrosis (Y. Qiu et al., 2020) but there are no published data on the control mechanisms of collagen II and X by splicing kinases or factors. With more time I could have looked at changes in mRNA expression of different collagen II and X variants with ATDC5 cell differentiation and hypertrophy and whether splicing kinase inhibition affected this.

My study originally also aimed to investigate MMP13, COMP and CD44 expression as additional indicators of chondrocyte phenotype, but due to time limitations these experiments were not possible. MMP13 (or collagenase-3) is a marker of hypertrophy frequently raised more than 40-fold in OA cartilage (Billinghurst et al., 1997; H. Li et al., 2017; Mitchell et al., 1996; Shlopov et al., 2000) and also produced by RA chondrocytes (Onnheim et al., 2022). Cartilage oligomeric matrix protein (COMP) is another marker of disease severity, also used to measure the effect of treatment (de Jong et al., 2008; Morozzi et al., 2007) in synovium in patients with RA as well as OA (S. Tseng et al., 2009). CD44 is a multi-structural cell-surface glycoprotein that can bind several types of ligands including HA, osteopontin (OPN), collagens, MMPs and proteoglycan-4 (PRG4) (Al-Sharif et al., 2015; Goodison et al., 1999), and is associated with progressive knee OA joint damage (F.-J. Zhang et al., 2013). Among the key markers mentioned above; CD44 is alternatively spliced, which might show change upon treatment with splicing kinase inhibitors even if the overall expression level remains unchanged (Herrlich et al., 1993; Latini et al., 2021; Mackay et al., 1994; Prochazka et al., 2014; H. Zhang et al., 2019).

There are other genes or proteins associated with chondrocyte hypertrophy that are highly expressed in OA cartilage than normal cartilage such as alkaline phosphatase (Goyal et al., 2010), VEGF-A_{121}, VEGF-A_{165}, and VEGF-A_{189} (Pfander et al., 2001), Runx2 (Orfanidou et al., 2009), osteocalcin (O Pullig et al., 2000), osteonectin (Goyal et al., 2010), osteopontin (Oliver Pullig et al., 2000), Indian Hedgehog (Tchetina et al., 2005), and beta-catenin (M. Zhu et al., 2009). Moreover, apoptosis can be considered as an additional chondrocyte hypertrophy marker in OA cartilage (Blanco et al., 1998) because hypertrophic chondrocytes in the growth plate were reported not only to express type X collagen, but also demonstrated to undergo apoptosis to make bone deposition possible (Zenmyo et al., 1996). Moreover, it is important to understand whether, and if so the mechanisms by which SRPK1 and CLK1 inhibitors could stabilize the functional activity of impaired chondrocytes in arthritis by reducing the expression or alternative splicing of key regulatory genes. For this, the different signalling pathways involved in the differentiation of chondrocytes can be further analysed. These signalling pathways are crucial for normal differentiation of chondrocyte and cartilage development that maintain the balance in matrix production and degradation.

There was high variability in expression of both collagens particularly in the DMSO control groups, probably somewhat due to the very low expression in most DMSO treated control cells. Use of one of the other markers of hypertrophy or concentrating on splice variant expression as mentioned above might be useful to address this. There is also a low number of samples in these experiments, meaning that the study probably had low power. Generation of samples at day 8 and 12 would have given more meaningful data on the changes in expression over time, and with cellular changes. Additionally I could have looked for protein expression of collagens and their splice variants or other key markers by western blotting, or IHC to link changes to cell morphology changes over time. Further morphological analysis would also have also provided a clear insight of the effects of the treatment on cell morphology or sub-cellular changes using toluidine blue staining (as above), or Alcian blue (Hodax et al., 2019; Nakatani et al., 2007; Yuan et al., 2022) or Alizarin red stains (Newton et al., 2012; Shukunami et al., 1997; van Eegher et al., 2021) for identification of GAGs (glycosaminoglycan) and calcium deposits, respectively.

7.5 CONCLUSION

These preliminary studies in ATDC5 cells do not give conclusive evidence that SRPK1 and CLK1 inhibition could be a novel therapeutic strategy in the treatment of cartilage changes in arthritis. There is further work required with these inhibitors, but as Griffin6 is a novel, potentially orally available compound, and is more potent against CLK1/2 than Lorecivivint, the DYRK/CLK inhibitor and disease modifying anti-osteoarthritis drug in phase III clinical trial, it is probably worth conducting more studies with this compound.

8.1 GENERAL DISCUSSION AND CONCLUSION

Synovial angiogenesis in arthritis is associated with cartilage and bone destruction in RA and OA (Lainer-Carr & Brahn, 2007; K. Qian et al., 2022; Szekanecz & Koch, 2008; Veale & Fearon, 2006). New blood vessel formation in the adult is usually a tightly regulated process which is activated during short periods of time, for instance in wound healing or in reproductive systems. The stimulators and inhibitors of angiogenesis exert positive and negative effects on the formation of blood vessels to keep the demands limited to the growing tissue requirement under normal physiological conditions (Figure 8.1A). On the other hand, this balance is lost in numerous pathological circumstances and can result in the production of an angiogenic phenotype. VEGF-A is an important main contributor to this process in both health and disease conditions (Carmeliet, 2003; Ferrara et al., 2003; Le & Kwon, 2021; Szekanecz & Koch, 2008). VEGF-A is strongly linked to both RA and OA (Le & Kwon, 2021; Murata et al., 2008), for example both serum and synovial fluid VEGF-A concentrations correlate well with the degree of arthritic disease activity such as the level of joint swelling (Sokolove & Lepus, 2013).

Inhibition of VEGF-A and its receptors have been widely explored in both arthritis and cancer research (A. E.-S. Abdel-Maged et al., 2018; A. E. Abdel-Maged et al., 2019; Q. Chen et al., 2023; Hernandez et al., 2001; Kiselyov et al., 2007; A. E. Koch, 1998; A. E. Koch et al., 1994; Le & Kwon, 2021; Shams & Ianchulev, 2006; Masabumi Shibuya, 2008). VEGF-A_{xxx}a isoforms drive angiogenesis, whereas VEGF-A_{165}b can reduce angiogenesis in multiple angiogenic pathologies such as retinal disease and tumorigenesis (Le & Kwon, 2021). VEGF-A_{165}a also promotes angiogenesis and pain in IA animal models (Beazley-Long et al., 2018; R. Hulse et al., 2014; R. P. Hulse, 2017; R. P. Hulse et al., 2015; R. P. Hulse et al., 2016), and VEGF-A level in human RA synovium strongly correlates with the degree of histological inflammation (D Amanitis et al., 2020).

The overall hypothesis tested in this thesis was that activation of VEGFR2 by VEGF-A_{xxx}a splice variants contributes to joint inflammation and damage in rodent models of inflammatory arthritis. I addressed this by looking at histological features of

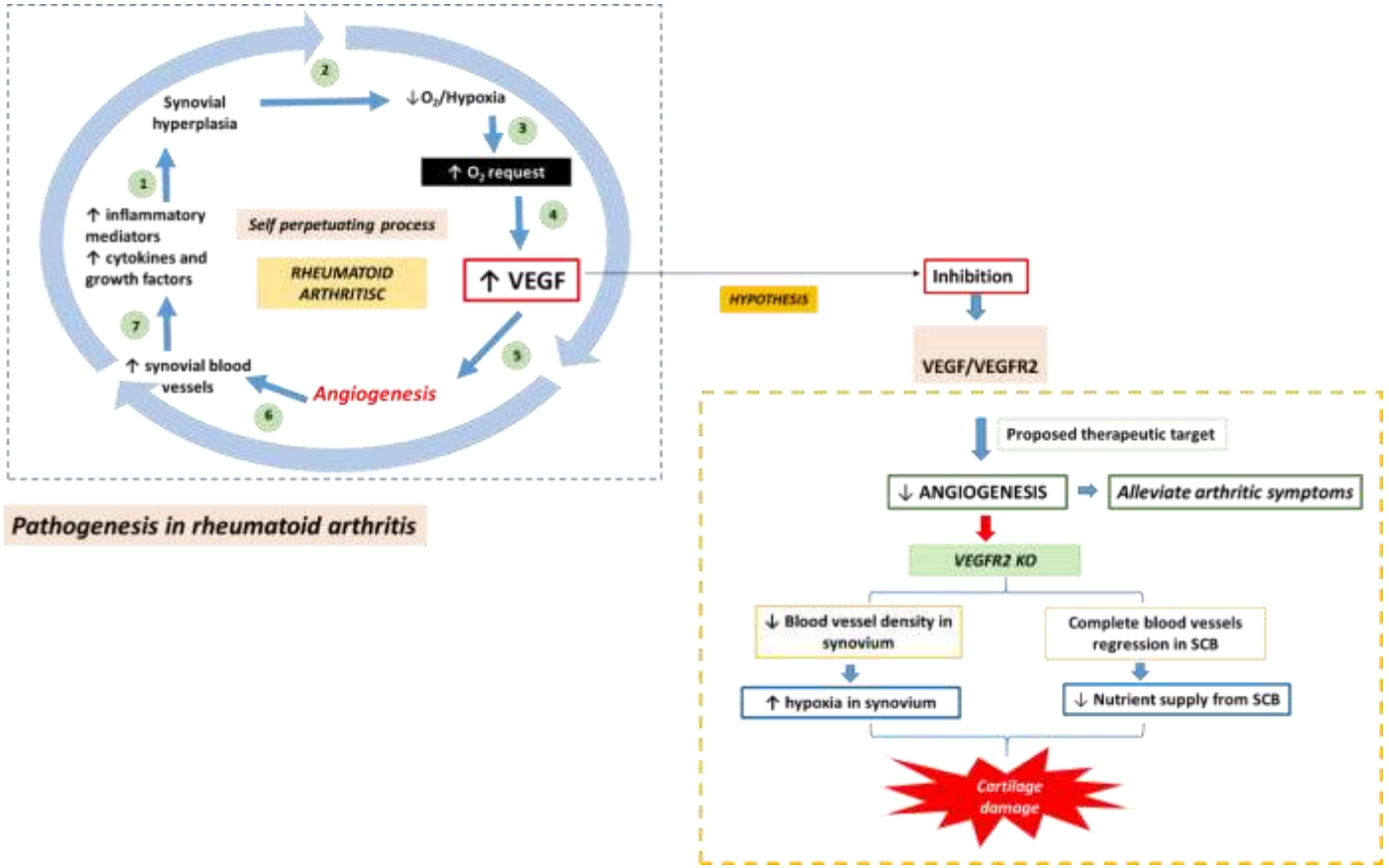

Figure 8.1: (A) Pathogenesis of rheumatoid arthritis. In RA, the inflammatory process initiates with the infiltration of inflammatory immune cells such as macrophages which secrete abundant chemokines, cytokines, and degrading enzymes, which lead to synovial hyperplasia. Synovial hyperplasia causes hypoxic environment which is the trigger that increases VEGF-A production which is mainly produced by rheumatoid synoviocytes. This stimulates angiogenesis and vascular permeability. Hence, more macrophages enter the synovium. These produce TNF-α and IL-6 which further enhance the capacity of macrophages and synoviocytes to secrete VEGF-A, and consequently create a self-perpetuating cycle of inflammation. VEGF-A is thus involved in the development of synovial inflammation, hyperplasia, and angiogenesis in the joints of RA. (B) Figure summarises the outcomes of my experiments in chapters 4, 5, 6 and 7 of blocking VEGFR2 on endothelial cells showing the proposed mechanisms through which VEGFR2 inhibition affects the cartilage integrity.

inflammation and joint damage in rat and mouse models of IA, using systemic pharmacological and cell-specific approaches to removing VEGFR2 activation. Prior to investigation of the hypothesis, I showed that two different doses of CFA in rats resulting in the same histological changes in the joints, meaning the results from two independent studies from which I obtained joint tissues were comparable.

I also used the animal models to back-translate observations from human synovium (Dimitrios Amanitis, 2022) into these models. I showed that there were only minor similarities between the mouse and rat models and human data. This was most likely due to the difference in time in the disease progression in the rodents compared to human.

In chapters 4, 5 and 6 I investigated various aspects of joint histology in rats and mice with IA, showing that

1. systemic VEGFR2 inhibition with PTK787 had no obvious effect on synovitis or joint damage and no change in the expression of key molecules involved in control of VEGF-A alternative splicing, and
2. VEGFR2 knockdown in endothelial cells resulted in a severe loss of blood vessels in superficial SCB and synovium, with increased cartilage damage but no change in the synovitis. In the same animals, expression of the splicing kinase SRPK1 and splicing factor SRSF1 showed some changes that indicate a possible change in VEGF-A splicing towards anti-angiogenic variants, VEGF-A_{xxx}b (Figure 8.2B).

These data led me to conclude that targeting *endothelial*-VEGFR2 would as hypothesised reduce blood vessel numbers in synovium and SCB but that this would be actually highly detrimental in IA as it could also cause cartilage damage. I also concluded that the potential effects of blocking endothelial-VEGFR2 might result in *decrease* in VEGF-A_{xxx}a isoforms as a result of an effect on VEGF-A splicing (Figure 8.2). These results therefore do not support the original hypothesis that blocking VEGF-A_{xxx}a isoforms acting at VEGFR2 would be beneficial and reduce inflammation and joint damage in IA.

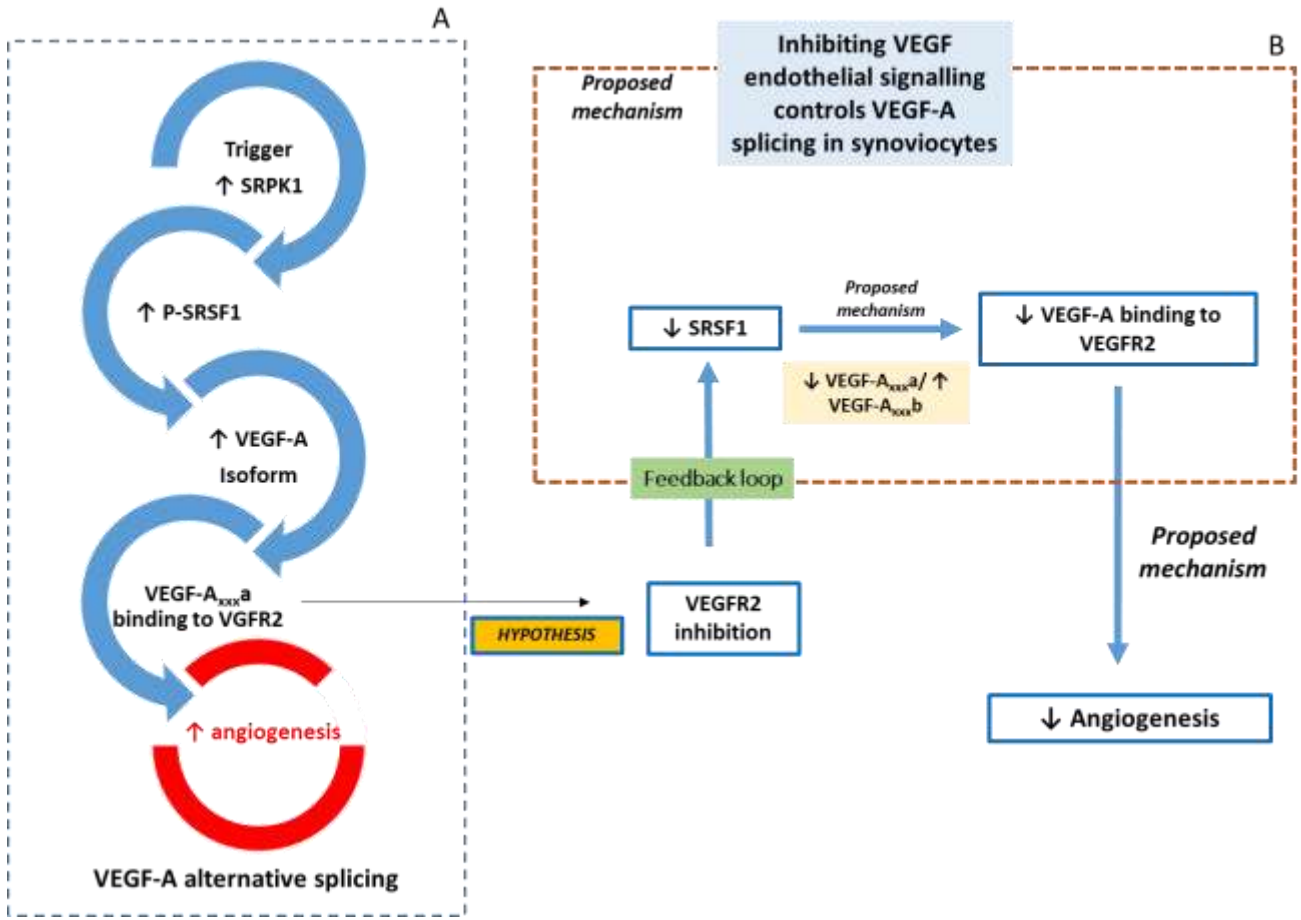

Figure 8.2: Left: Alternative splicing of VEGF-A. In unstimulated phase, SRPK1 and SRSF1 are concentrated mostly in the cytoplasm. (A) On stimulation, SRPK1 is activated which increases SRSF1 phosphorylation and results in stimulation of angiogenesis via increased binding of VEGF-A$_{xxx}$a isoforms to VEGFR2. (B) Flow diagram of possible VEGFR2 control of VEGF-A splicing. The mechanism(s) involved are not yet understood.

The lack of effect of systemic PTK787 is most likely due to the administered dose being too low to exert an effect, despite it being sufficient to affect pain behaviour (Durrant, 2021). In addition, while the animal models showed similarities in changes in splicing molecules, these may not be the same as seen in human synovium because of the differences in disease duration (10-14 days compared to >5 years).

Several studies have shown a beneficial effect of VEGFR inhibitors on histopathology, and this could be attributable to an action on other cell types or targets than VEGFR2, such as the VEGFR1 receptor which can also promote inflammatory responses and angiogenesis (Masabumi Shibuya, 2015). Other molecular targets of existing therapeutic VEGFR inhibitors are relevant because there are no FDA approved or experimental specific VEGFR2 small molecule inhibitor that can be used *in vivo* (X.-J. Liu et al., 2023). VEGFR2 inhibitors can have effects on multiple VEGFRs, platelet derived growth factor receptor, KIT (pazopanib, sunitinib), fibroblast growth factor receptor 1 and RET (sorafenib). These positive actions could have disguised a negative effect of VEGFR2 on endothelial cells, which is only seen when only endothelial VEGFR2 is specifically targeted. There are however certain important potential drawbacks of anti-VEGFR therapies, such as hypertension (Kamba & McDonald, 2007; Pandey et al., 2018), impaired healing of fractures (Beamer et al., 2010; Kamba & McDonald, 2007; Ogilvie et al., 2012; Yen et al., 2022), haemorrhage (Kamba & McDonald, 2007; Yoshimoto et al., 2021), and impaired wound healing (Bodnar, 2014; Kamba & McDonald, 2007).

In inflammatory conditions, upregulation of inflammatory mediators such as TNF-α, a key molecule in RA and other IA conditions activates SRPK1 and increases SRSF1 expression in the disease tissue (Giannakouros et al., 2011; Nowak et al., 2010; Z. Zhou & Fu, 2013). Increased SRPK1 levels are associated with abnormal splicing events such as atypical cell proliferation, migration and angiogenesis in various cancers; colon, pancreatic, prostate, lung, and breast (Hatcher et al., 2018), features also seen in RA synovium. Recent reports show that alternative splicing is altered in RA (Ibáñez-Costa et al., 2022), and although changes in SRPK1 or CLKs have not been reported in RA, the related splicing kinase DYRK1 is involved in driving the proliferation and invasion of synoviocytes in RA (X. Guo et al., 2018). DYRK1A

expression is also correlated with the degree of synovitis in RA and OA synovium (Dimitrios Amanitis, 2022).

In addition to control of $VEGF_{165}a$/$VEGF_{165}b$ alternative splicing, SRPK1 is also known to have other targets (Giannakouros et al., 2011) such as FAK, MAPK, PI3K-Akt and Wnt/ß catenin (N. Bullock & Oltean, 2017). This makes SRPK1 a potentially attractive target for RA treatment because many of these signalling pathways are also involved in the progression of RA, including JAK-STAT, SYK, Notch signalling, and the MAPK, FAK, Wnt and PI3K-AKT signalling pathways. The activation of MAPKs, FAK, Wnt/beta-catenin signalling causes cartilage matrix destruction mediated by MMPs (Kanai et al., 2020; Mengshol et al., 2000; Mon et al., 2006; Yuasa & Iwamoto, 2006). FAK is also involved in synovial fibroblast invasion, synovial angiogenesis (Infusino & Jacobson, 2012), T-cell activation (Wiemer et al., 2013), macrophage invasion regulation (Owen et al., 2007), neutrophil survival (Kasorn et al., 2009)[23], and osteoclast function (Y. Matsumoto et al., 2002). SRPK1 inhibitors could potentially target these signalling pathways (Figure 8.2) to alleviate RA symptoms. Although the CLK inhibitor Griffin6 did not show any effect on ATDC5 cells in vitro, it could still be considered for further investigation for local effects on joint integrity and pain in IA, as combined CLK/DYRK inhibition reduced inflammation and cytokine production (Deshmukh et al., 2019). There is a need for further work in this area.

It is possible that my observation of less nuclear localised SRSF1 in IA in VEGFR2 endothelial-specific knockout mice indicates a mechanism where loss of VEGFR2 signalling alters VEGF-A alternative splicing. How this happens is not clear as this has never been observed or reported before. Increased $VEGF\text{-}A_{xxx}b$ would be expected to reduce angiogenesis and synovitis as it blocks inflammation *in vivo* (Cromer et al., 2013), and leukocyte adhesion to endothelial cells (Desideri et al., 2019; Oltean et al., 2015) and synoviocytes *in vitro* (Dimitrios Amanitis, 2022).

There is strong literature evidence supporting a contribution of VEGF-A to inflammatory arthritis, demonstrating relationships between inflammation, pain, and splicing factors in RA synovium. There is also a growing recognition of the importance of alternative splicing to the pathology of RA. If the potential detrimental effects of VEGFR inhibition are also considered, the data presented in this thesis lead to the

conclusion that targeting VEGF-A splicing kinases SRPK1/CLK1 or use of VEGF-A_{165}b as protein therapy in IA could be ideal targets for RA treatment. This is because of their potential to rebalance the expression of VEGF-A isoforms without causing harmful effects on cell function as seen with VEGFR inhibition. It can be hypothesized that these treatments would alleviate inflammatory signs and symptoms without causing damage to cartilage/joint integrity.

..

9. List of potential future studies

1. The use of splicing kinase inhibitors i-e Griffin 6 (G6) alone or as adjuncts to already existing RA therapies: *in vitro* in human primary synoviocytes treated with TNF-α and *in vivo* IA animal models to investigate the effects of G6 on expression of inflammatory mediators, synovial inflammation, and joint damage, respectively.
2. RNA sequencing following splicing kinase inhibitor treatment in cells in vitro (e.g. synoviocytes) for the identification of alternative splicing targets of SRPK1 and CLK1, and effects of kinase inhibition on identified targets.
3. Investigation of the feedback mechanism (Figure 8.2) exploring the effect of VEGFR2 inhibition on SRSF1 nuclear localization in synoviocytes hypothesizing that stimulating synoviocytes with VEGF will increase SRSF1 NL and blocking the receptors by VEGFR2 inhibitors will block SRSF1 nuclear localization.
4. VEGFR knockout and the reduced activation of SRSF1 indicated by NL in synoviocytes suggests local signalling between synovial vasculature and synoviocytes that involves the control of alternative splicing in synoviocytes. Investigation of the mechanism through which synovial vascular endothelial cells communicate with synoviocytes, including knockdown of VEGFR2.
5. Study of expression of specific splice variants, including VEGF-A_{xxx}a and VEGF-A_{xxx}b isoforms in synovium to determine the effect of reduced SRSF1 NL on the expression of these isoforms (Figure 8.2).

APPENDIX

Reagents for and preparation of histology working solutions

Table A1: Decalcification buffer solution

EDTA Buffer Recipe	Concentration
Distilled water	1 L
Tris (Trizma) Base	1.34 g
10% w/v EDTA	100 g
NaOH (pellets)	10g
7.5% w/v polyvinylpyrolidone (PVP)	75 g

Table A2: Reagents used in Safranin O/ Fast Green staining

SNo	Reagent used	Lot number
1	Hematoxylin	1002755415
2	Anhydrous Ferric chloride	STBJ6683
3	Fast green FCF	SHBL4767
4	Safranin O	MKCG1165

Table A3: Preparation of Safranin O/Fast Green Working solution

Weigert's Iron Hematoxylin Solution:

Stock Solution A:
Hematoxylin ---------- 2 g
100% Alcohol ---------- 200 mL
Distilled water ---------- 10 mL

Stock Solution B:
2.9g of anhydrous Ferric chloride in water ---------- 10mL
Distilled water ---------- 190 mL
Hydrochloric acid, concentrated ---- 2mL

The Weigert's iron hematoxylin working solution was prepared by mixing equal volumes of stock solutions A and B.

Table A4: Reagents used in Masson's trichrome staining

Reagents	Catalog No.
Biebrich Scarlet-acid Fuchsin solution	Catalog No. HT151-250 mL Biebrich scarlet, 0.9%, acid fuchsin 0.1%, in acetic acid, 1.0%
Phosphotungstic acid solution	Catalog No. HT152-250 mL Phosphotungstic acid, 10%.
Phosphomolybdic acid solution,	Catalog No. HT153-250 mL Phosphomolybdic Acid, 10%
Aniline blue solution,	Catalog No. HT154-250 mL Aniline blue, 2.4% and acetic acid, 2%

The Masson's trichrome working solution was prepared by mixing 1 volume of phosphotungstic acid solution and 1 volume phosphomolybdic acid solution with 2 volumes of deionized water.

SUPPLEMENTARY DATA

Table S1: Histopathological scoring of cartilage

	Surface smoothness	Bleaching	Mean cartilage thickness
0	Smooth surface	No bleaching*	>45μm
1	Ragged surface on end of cartilage	Mild bleaching** in some regions	31-45μm
2	Cracks in surface	Mild bleaching widespread	16-30μm
3	Channels >50% through cartilage	Approximately 50% bleaching	1-15μm
4	Channel into bone marrow	>50% bleaching	<1μm

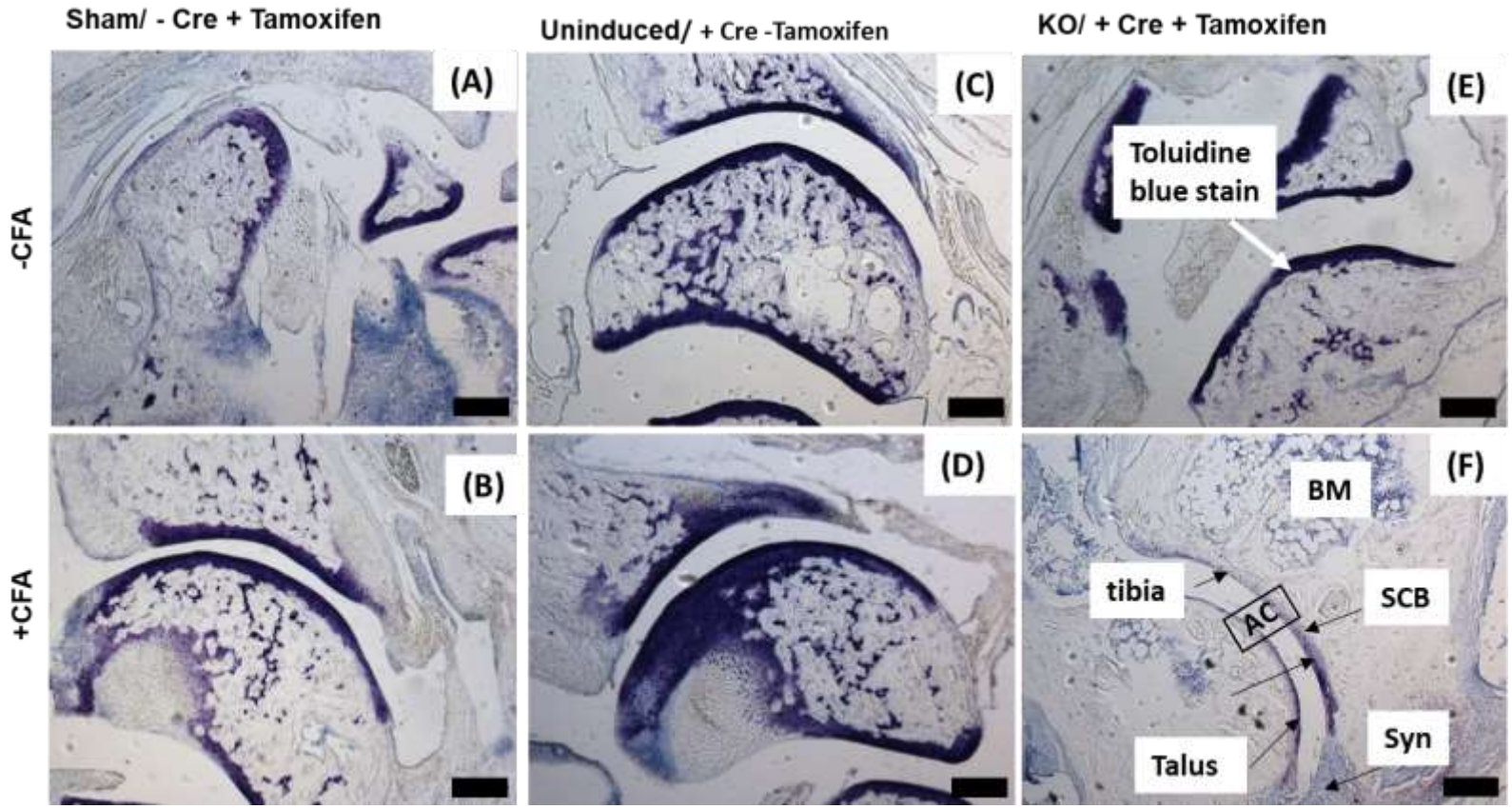

Figure S1: Effects of endothelial-VEGFR2 KO ± inflammation on histopathological features of inflammatory arthritis in mice. Toluidine blue staining of tibiotalar cartilage (purple) appeared reduced in the VEGFR2 KO mice compared with other groups, indicating a loss of proteoglycans, and altered cartilage integrity. Syn: Synovium; SCB: Subchondral bone; AC: Articulating cartilage; BM: Bone marrow. Scale bar 200µm.

10. REFERENCES

Abdel-Maged, A. E.-S., Gad, A. M., Abdel-Aziz, A. K., Aboulwafa, M. M., & Azab, S. S. (2018). Comparative study of anti-VEGF Ranibizumab and Interleukin-6 receptor antagonist Tocilizumab in Adjuvant-induced Arthritis. *Toxicology and Applied Pharmacology, 356*, 65-75.

Abdel-Maged, A. E., Gad, A. M., Wahdan, S. A., & Azab, S. S. (2019). Efficacy and safety of Ramucirumab and methotrexate co-therapy in rheumatoid arthritis experimental model: Involvement of angiogenic and immunomodulatory signaling. *Toxicology and Applied Pharmacology, 380*, 114702.

Abou Faycal, C., Gazzeri, S., & Eymin, B. (2019). A VEGF-A/SOX2/SRSF2 network controls VEGFR1 pre-mRNA alternative splicing in lung carcinoma cells. *Scientific reports, 9*(1), 336.

Abraham, D., Hofbauer, R., Schäfer, R., Blumer, R., Paulus, P., Miksovsky, A., Traxler, H., Kocher, A., & Aharinejad, S. (2000). Selective downregulation of VEGF-A165, VEGF-R1, and decreased capillary density in patients with dilative but not ischemic cardiomyopathy. *Circulation research, 87*(8), 644-647.

Abu-Ghazaleh, R., Kabir, J., Jia, H., Lobo, M., & Zachary, I. (2001). Src mediates stimulation by vascular endothelial growth factor of the phosphorylation of focal adhesion kinase at tyrosine 861, and migration and anti-apoptosis in endothelial cells. *Biochemical Journal, 360*(1), 255-264.

Abuqayyas, L., Cheng, L. E., Teixeira dos Santos, M., Sullivan, B. A., Ruiz-Santiago, N., Wang, H., Zhou, Y., Chindalore, V., Cohen, S., & Kivitz, A. J. (2022). Safety and Biological Activity of Rozibafusp alfa, a Bispecific Inhibitor of Inducible Costimulator Ligand and B Cell Activating Factor, in Patients With Rheumatoid Arthritis: Results of a Phase 1b, Randomized, Double-Blind, Placebo-Controlled, Multiple Ascending Dose Study. *ACR Open Rheumatology, 4*(10), 903-911.

Acharya, A., Baek, S. T., Banfi, S., Eskiocak, B., & Tallquist, M. D. (2011). Efficient inducible Cre-mediated recombination in Tcf21cell lineages in the heart and kidney. *Genesis, 49*(11), 870-877.

Ackerman, L. S. (2006). Sex hormones and the genesis of autoimmunity. *Archives of Dermatology, 142*(3), 371-376.

Adab, P., Jiang, C. Q., Rankin, E., Tsang, Y. W., Lam, T. H., Barlow, J., Thomas, G. N., Zhang, W. S., & Cheng, K. K. (2014). Breastfeeding practice, oral contraceptive use and risk of rheumatoid arthritis among Chinese women: the Guangzhou Biobank Cohort Study. *Rheumatology, 53*(5), 860-866.

Adam, S., Simon, N., Steffen, U., Andes, F. T., Scholtysek, C., Müller, D. I., Weidner, D., Andreev, D., Kleyer, A., & Culemann, S. (2020). JAK inhibition increases bone mass in steady-state conditions and ameliorates pathological bone loss by stimulating osteoblast function. *Science translational medicine, 12*(530), eaay4447.

Adamopoulos, I., Sabokbar, A., Wordsworth, B., Carr, A., Ferguson, D., & Athanasou, N. (2006). Synovial fluid macrophages are capable of osteoclast formation and resorption. *The Journal of Pathology: A Journal of the Pathological Society of Great Britain and Ireland, 208*(1), 35-43.

Adamopoulos, I. E., Danks, L., Itonaga, I., Locklin, R. M., Sabokbar, A., Ferguson, D. J., & Athanasou, N. A. (2006). Stimulation of osteoclast formation by inflammatory synovial fluid. *Virchows Archiv, 449*, 69-77.

Adams, R., Walsh, C., Veale, D., Bresnihan, B., FitzGerald, O., & Barry, M. (2010). Understanding the relationship between the EQ-5D, SF-6D, HAQ and disease activity in inflammatory arthritis. *Pharmacoeconomics, 28*(6), 477-487.

Agarwal, S. K. (2011). Core management principles in rheumatoid arthritis to help guide managed care professionals. *Journal of Managed Care Pharmacy, 17*(9 Supp B), S03-S08.

Agarwal, S. K., & Brenner, M. B. (2006). Role of adhesion molecules in synovial inflammation. *Current opinion in rheumatology, 18*(3), 268-276.

Aho, K., Palosuo, T., Raunio, V., Puska, P., Aromaa, A., & Salonen, J. (1985). When does rheumatoid disease start? *Arthritis & Rheumatism, 28*(5), 485-489.

Aigner, T., Fundel, K., Saas, J., Gebhard, P. M., Haag, J., Weiss, T., Zien, A., Obermayr, F., Zimmer, R., & Bartnik, E. (2006). Large-scale gene expression profiling reveals major pathogenetic pathways of cartilage degeneration in osteoarthritis. *Arthritis & Rheumatism: Official Journal of the American College of Rheumatology, 54*(11), 3533-3544.

Aigner, T., & Stöve, J. (2003). Collagens—major component of the physiological cartilage matrix, major target of cartilage degeneration, major tool in cartilage repair. *Advanced drug delivery reviews, 55*(12), 1569-1593.

Akhavani, M. A., Madden, L., Buysschaert, I., Sivakumar, B., Kang, N., & Paleolog, E. M. (2009). Hypoxia upregulates angiogenesis and synovial cell migration in rheumatoid arthritis. *Arthritis research & therapy, 11*(3), 1-11.

Al-Sharif, A., Jamal, M., Zhang, L. X., Larson, K., Schmidt, T. A., Jay, G. D., & Elsaid, K. A. (2015). Lubricin/proteoglycan 4 binding to CD44 receptor: a mechanism of the suppression of proinflammatory cytokine–induced synoviocyte proliferation by lubricin. *Arthritis & Rheumatology, 67*(6), 1503-1513.

Al Shoyaib, A., Archie, S. R., & Karamyan, V. T. (2020). Intraperitoneal route of drug administration: should it be used in experimental animal studies? *Pharmaceutical research, 37*, 1-17.

Alam, J., Kim, Y. C., & Choi, Y. (2014). Potential role of bacterial infection in autoimmune diseases: a new aspect of molecular mimicry. *Immune Network, 14*(1), 7-13.

Alamanos, Y., Voulgari, P. V., & Drosos, A. A. (2006). *Incidence and prevalence of rheumatoid arthritis, based on the 1987 American College of Rheumatology criteria: a systematic review.* Paper presented at the Seminars in arthritis and rheumatism.

Albuquerque, R. J., Hayashi, T., Cho, W. G., Kleinman, M. E., Dridi, S., Takeda, A., Baffi, J. Z., Yamada, K., Kaneko, H., & Green, M. G. (2009). Alternatively spliced vascular endothelial growth factor receptor-2 is an essential endogenous inhibitor of lymphatic vessel growth. *Nature medicine, 15*(9), 1023.

Aldridge, S., Lennard, T., Williams, J., & Birch, M. (2005). Vascular endothelial growth factor receptors in osteoclast differentiation and function. *Biochemical and biophysical research communications, 335*(3), 793-798.

Aletaha, D., Alasti, F., & Smolen, J. S. (2015). Rheumatoid factor, not antibodies against citrullinated proteins, is associated with baseline disease activity in rheumatoid arthritis clinical trials. *Arthritis research & therapy, 17*, 1-10.

Aletaha, D., Alasti, F., & Smolen, J. S. (2016). Optimisation of a treat-to-target approach in rheumatoid arthritis: strategies for the 3-month time point. *Annals of the rheumatic diseases, 75*(8), 1479-1485.

Aletaha, D., Nell, V. P., Stamm, T., Uffmann, M., Pflugbeil, S., Machold, K., & Smolen, J. S. (2005). Acute phase reactants add little to composite disease activity indices for rheumatoid arthritis: validation of a clinical activity score. *Arthritis research & therapy, 7*(4), 1-11.

Aletaha, D., Neogi, T., Silman, A. J., Funovits, J., Felson, D. T., Bingham III, C. O., Birnbaum, N. S., Burmester, G. R., Bykerk, V. P., & Cohen, M. D. (2010). 2010 rheumatoid arthritis classification criteria: an American College of Rheumatology/European League Against Rheumatism collaborative initiative. *Arthritis & Rheumatism, 62*(9), 2569-2581.

Aletaha, D., & Smolen, J. S. (2011). Joint damage in rheumatoid arthritis progresses in remission according to the Disease Activity Score in 28 joints and is driven by residual swollen joints. *Arthritis & Rheumatism, 63*(12), 3702-3711.

Aletaha, D., & Smolen, J. S. (2018). Diagnosis and management of rheumatoid arthritis: a review. *Jama, 320*(13), 1360-1372.

Alexander, V., Das, S., Mangan, A. S., & Iyadurai, R. (2019). Acute parvovirus B19 infection presenting as rheumatoid arthritis mimic. *Journal of family medicine and primary care, 8*(3), 1257.

Alibegović, A., Blagus, R., & Martinez, I. Z. (2020). Safranin O without fast green is the best staining method for testing the degradation of macromolecules in a cartilage extracellular matrix for the determination of the postmortem interval. *Forensic Science, Medicine and Pathology, 16*(2), 252-258.

Alitalo, K., & Carmeliet, P. (2002). Molecular mechanisms of lymphangiogenesis in health and disease. *Cancer cell, 1*(3), 219-227.

Allaire, S., Wolfe, F., Niu, J., & Lavalley, M. P. (2008). Contemporary prevalence and incidence of work disability associated with rheumatoid arthritis in the US. *Arthritis care & research, 59*(4), 474-480.

Allard-Chamard, H., Carrier, N., Dufort, P., Durand, M., de Brum-Fernandes, A., Boire, G., Komarova, S., Dixon, S., Harrison, R., & Manolson, M. (2020). Osteoclasts and their circulating precursors in rheumatoid arthritis: Relationships with disease activity and bone erosions. *Bone Reports, 12*, 100282.

Altaf, F., Hering, T., Kazmi, N., Yoo, J., & Johnstone, B. (2006). Ascorbate-enhanced chondrogenesis of ATDC5 cells. *Eur Cell Mater, 12*, 64-69.

Alvarez-Aznar, A., Muhl, L., & Gaengel, K. (2017). VEGF receptor tyrosine kinases: key regulators of vascular function. *Current topics in developmental biology, 123*, 433-482.

Amanitis, D. (2022). *Peripheral contributions to the development and maintenance of inflammation and pain in arthritis.* University of Nottingham,

Amanitis, D., Shahtaheri, S., Mcwilliams, D., Walsh, D., & Donaldson, L. (2021). Changes in the vascular endothelial growth factor a splicing axis in human synovium are related to arthritis pain. *Osteoarthritis and cartilage, 29*, S83.

Amanitis, D., Shahtaheri, S., Mcwilliams, D. D., Beazley-Long, N., Walsh, D., & Donaldson, L. (2020). AB0064 CHANGES IN THE VASCULAR ENDOTHELIAL GROWTH FACTOR A (VEGFA) SPLICING AXIS IN HUMAN SYNOVIUM ARE RELATED TO INFLAMMATION IN ARTHRITIS. In: BMJ Publishing Group Ltd.

Ambrosetti, D., Dufies, M., Dadone, B., Durand, M., Borchiellini, D., Amiel, J., Pouyssegur, J., Rioux-Leclercq, N., Pages, G., & Burel-Vandenbos, F. (2018). The two glycolytic markers GLUT1 and MCT1 correlate with tumor grade and survival in clear-cell renal cell carcinoma. *PloS one, 13*(2), e0193477.

Amin, A., Huntley, J., Simpson, A., & Hall, A. (2009). Chondrocyte survival in articular cartilage: the influence of subchondral bone in a bovine model. *The Journal of Bone & Joint Surgery British Volume, 91*(5), 691-699.

Amin, A., Huntley, J., Simpson, A., & Hall, A. (2009). Chondrocyte survival in articular cartilage: the influence of subchondral bone in a bovine model. *The Journal of bone and joint surgery. British volume, 91*(5), 691-699.

Amin, E. M., Oltean, S., Hua, J., Gammons, M. V., Hamdollah-Zadeh, M., Welsh, G. I., Cheung, M.-K., Ni, L., Kase, S., & Rennel, E. S. (2011). WT1 mutants reveal SRPK1 to be a downstream angiogenesis target by altering VEGF splicing. *Cancer cell, 20*(6), 768-780.

Appel, H., Kuhne, M., Spiekermann, S., Köhler, D., Zacher, J., Stein, H., Sieper, J., & Loddenkemper, C. (2006). Immunohistochemical analysis of hip arthritis in ankylosing spondylitis: evaluation of the bone–cartilage interface and subchondral bone marrow. *Arthritis & Rheumatism, 54*(6), 1805-1813.

Apte, R. S., Chen, D. S., & Ferrara, N. (2019). VEGF in signaling and disease: beyond discovery and development. *Cell, 176*(6), 1248-1264.

Araki, S., Ohori, M., & Yugami, M. (2023). Targeting pre-mRNA splicing in cancers: roles, inhibitors, and therapeutic opportunities. *Frontiers in Oncology, 13*, 1152087.

Aravilli, R. K., Vikram, S. L., & Kohila, V. (2021). The functional impact of alternative splicing and single nucleotide polymorphisms in rheumatoid arthritis. *Current Pharmaceutical Biotechnology, 22*(8), 1014-1029.

Arcondeguy, T., Lacazette, E., Millevoi, S., Prats, H., & Touriol, C. (2013). VEGF-A mRNA processing, stability and translation: a paradigm for intricate regulation of gene expression at the post-transcriptional level. *Nucleic acids research, 41*(17), 7997-8010.

Arkill, K., & Winlove, C. (2008). Solute transport in the deep and calcified zones of articular cartilage. *Osteoarthritis and cartilage, 16*(6), 708-714.

Armstrong, A. R., Carlson, C. S., Rendahl, A. K., & Loeser, R. F. (2021). Optimization of histologic grading schemes in spontaneous and surgically-induced murine models of osteoarthritis. *Osteoarthritis and cartilage, 29*(4), 536-546.

Arnett, F. C., Edworthy, S. M., Bloch, D. A., Mcshane, D. J., Fries, J. F., Cooper, N. S., Healey, L. A., Kaplan, S. R., Liang, M. H., & Luthra, H. S. (1988). The American Rheumatism Association 1987 revised criteria for the classification of rheumatoid arthritis. *Arthritis & Rheumatism: Official Journal of the American College of Rheumatology, 31*(3), 315-324.

Arvidson, N. G., Larsson, A., & Larsen, A. (2002). Disease activity in rheumatoid arthritis: fibrinogen is superior to the erythrocyte sedimentation rate. *Scandinavian journal of clinical and laboratory investigation, 62*(4), 315-319.

Asquith, D. L., Miller, A. M., McInnes, I. B., & Liew, F. Y. (2009). Animal models of rheumatoid arthritis. *European journal of immunology, 39*(8), 2040-2044.

Atsumi, T., Ikawa, Y., Miwa, Y., & Kimata, K. (1990). A chondrogenic cell line derived from a differentiating culture of AT805 teratocarcinoma cells. *Cell Differentiation and Development, 30*(2), 109-116.

Aubol, B. E., & Adams, J. A. (2022). SRPK1 regulates RNA binding in a pre-spliceosomal complex using a catalytic bypass mechanism. *The FEBS journal, 289*(23), 7428-7445.

Aubol, B. E., Plocinik, R. M., Keshwani, M. M., McGlone, M. L., Hagopian, J. C., Ghosh, G., Fu, X.-D., & Adams, J. A. (2014). N-terminus of the protein kinase CLK1 induces SR protein hyperphosphorylation. *Biochemical Journal, 462*(1), 143-152.

Aubol, B. E., Wozniak, J. M., Fattet, L., Gonzalez, D. J., & Adams, J. A. (2021). CLK1 reorganizes the splicing factor U1-70K for early spliceosomal protein assembly. *Proceedings of the National Academy of Sciences, 118*(14), e2018251118.

Aubol, B. E., Wu, G., Keshwani, M. M., Movassat, M., Fattet, L., Hertel, K. J., Fu, X.-D., & Adams, J. A. (2016). Release of SR proteins from CLK1 by SRPK1: a symbiotic kinase system for phosphorylation control of pre-mRNA splicing. *Molecular cell, 63*(2), 218-228.

Autiero, M., Luttun, A., Tjwa, M., & Carmeliet, P. (2003). Placental growth factor and its receptor, vascular endothelial growth factor receptor-1: novel targets for stimulation of ischemic tissue revascularization and inhibition of angiogenic and inflammatory disorders. *Journal of Thrombosis and Haemostasis, 1*(7), 1356-1370.

Autiero, M., Waltenberger, J., Communi, D., Kranz, A., Moons, L., Lambrechts, D., Kroll, J., Plaisance, S., De Mol, M., & Bono, F. (2003). Role of PlGF in the intra-and intermolecular cross talk between the VEGF receptors Flt1 and Flk1. *Nature medicine, 9*(7), 936-943.

Bahlas, S., Damiati, L., Dandachi, N., Sait, H., Alsefri, M., & Pushparaj, P. N. (2018). Rapid immunoprofiling of cytokines, chemokines and growth factors in patients with active rheumatoid arthritis using Luminex Multiple Analyte Profiling technology for precision medicine. *Clinical and experimental rheumatology, 37*(1), 112-119.

Bain, B. J., Clark, D. M., & Wilkins, B. S. (2019). *Bone marrow pathology*: John Wiley & Sons.

Baldwin, M. E., Halford, M. M., Roufail, S., Williams, R. A., Hibbs, M. L., Grail, D., Kubo, H., Stacker, S. A., & Achen, M. G. (2005). Vascular endothelial growth factor D is dispensable for development of the lymphatic system. *Molecular and cellular biology, 25*(6), 2441-2449.

Ballara, S., Taylor, P. C., Reusch, P., Marmé, D., Feldmann, M., Maini, R. N., & Paleolog, E. M. (2001). Raised serum vascular endothelial growth factor levels are associated with destructive change in inflammatory arthritis. *Arthritis & Rheumatism: Official Journal of the American College of Rheumatology, 44*(9), 2055-2064.

Ballmer-Hofer, K., Andersson, A. E., Ratcliffe, L. E., & Berger, P. (2011). Neuropilin-1 promotes VEGFR-2 trafficking through Rab11 vesicles thereby specifying signal output. *Blood, The Journal of the American Society of Hematology, 118*(3), 816-826.

Balogh, E., Biniecka, M., Fearon, U., Veale, D. J., & Szekanecz, Z. (2019). Angiogenesis in Inflammatory Arthritis. *The Israel Medical Association Journal: IMAJ, 21*(5), 345-352.

Bancroft, J. D., & Gamble, M. (2008). *Theory and practice of histological techniques*: Elsevier health sciences.

Barbagallo, D., Caponnetto, A., Barbagallo, C., Battaglia, R., Mirabella, F., Brex, D., Stella, M., Broggi, G., Altieri, R., & Certo, F. (2021). The GAUGAA motif is responsible for the binding between circSMARCA5 and SRSF1 and related downstream effects on glioblastoma multiforme cell migration and angiogenic potential. *International Journal of Molecular Sciences, 22*(4), 1678.

Barbosa, C. P., Ritter, A. M., Da Silva, L. G., Grespan, R., Cuman, R. K. N., Hernandes, L., & Bersani-Amado, C. A. (2014). Effects of simvastatin, ezetimibe, and their combination on histopathologic alterations caused by adjuvant-induced arthritis. *Inflammation, 37*, 1035-1043.

Barleon, B., Sozzani, S., Zhou, D., Weich, H. A., Mantovani, A., & Marme, D. (1996). Migration of human monocytes in response to vascular endothelial growth factor (VEGF) is mediated via the VEGF receptor flt-1.

Barrett, J. H., Brennan, P., Fiddler, M., & Silman, A. (2000). Breast-feeding and postpartum relapse in women with rheumatoid and inflammatory arthritis. *Arthritis & Rheumatism: Official Journal of the American College of Rheumatology, 43*(5), 1010-1015.

Bartok, B., & Firestein, G. S. (2010). Fibroblast-like synoviocytes: key effector cells in rheumatoid arthritis. *Immunological reviews, 233*(1), 233-255.

Baschong, W., Suetterlin, R., & Laeng, R. H. (2001). Control of autofluorescence of archival formaldehyde-fixed, paraffin-embedded tissue in confocal laser scanning microscopy (CLSM). *Journal of Histochemistry & Cytochemistry, 49*(12), 1565-1571.

Baschong, W., Sütterlin, R., & Aebi, U. (1997). Punch-wounded, fibroblast populated collagen matrices: a novel approach for studying cytoskeletal changes in three dimensions by confocal laser scanning microscopy. *European journal of cell biology, 72*(3), 189-201.

Basera, A., Hull, R., Demetriou, D., Bates, D. O., Kaufmann, A. M., Dlamini, Z., & Marima, R. (2022). Competing endogenous RNA (ceRNA) networks and splicing switches in cervical cancer: HPV oncogenesis, clinical significance and therapeutic opportunities. *Microorganisms, 10*(9), 1852.

Bates, D., Mavrou, A., Brakspear, K., Hamdollah-Zadeh, M., Damodaran, G., Babaei-Jadidi, R., Oxley, J., Gillatt, D., Ladomery, M., & Harper, S. (2015). Serine-arginine protein kinase 1 (SRPK1) inhibition as a potential novel targeted therapeutic strategy in prostate cancer.

Bates, D. O., Cui, T.-G., Doughty, J. M., Winkler, M., Sugiono, M., Shields, J. D., Peat, D., Gillatt, D., & Harper, S. J. (2002). VEGF165b, an inhibitory splice variant of vascular endothelial growth factor, is down-regulated in renal cell carcinoma. *Cancer research, 62*(14), 4123-4131.

Bates, D. O., Mavrou, A., Qiu, Y., Carter, J. G., Hamdollah-Zadeh, M., Barratt, S., Gammons, M. V., Millar, A. B., Salmon, A. H., & Oltean, S. (2013). Detection of VEGF-Axxxb isoforms in human tissues. *Plos one, 8*(7).

Batson, J., Toop, H. D., Redondo, C., Babaei-Jadidi, R., Chaikuad, A., Wearmouth, S. F., Gibbons, B., Allen, C., Tallant, C., & Zhang, J. (2017). Development of potent, selective SRPK1 inhibitors as potential topical therapeutics for neovascular eye disease. *ACS chemical biology, 12*(3), 825-832.

Beamer, B., Hettrich, C., & Lane, J. (2010). Vascular endothelial growth factor: an essential component of angiogenesis and fracture healing. *HSS Journal®, 6*(1), 85-94.

Beazley-Long, N., Hodge, D., Ashby, W. R., Bestall, S. M., Almahasneh, F., Durrant, A. M., Benest, A. V., Blackley, Z., Ballmer-Hofer, K., & Hirashima, M. (2018). VEGFR2 promotes central endothelial activation and the spread of pain in inflammatory arthritis. *Brain, behavior, and immunity, 74*, 49-67.

Beazley-Long, N., Hua, J., Jehle, T., Hulse, R. P., Dersch, R., Lehrling, C., Bevan, H., Qiu, Y., Lagrèze, W. A., & Wynick, D. (2013). VEGF-A165b is an endogenous

neuroprotective splice isoform of vascular endothelial growth factor A in vivo and in vitro. *The American journal of pathology, 183*(3), 918-929.

Beazley-Long, N., Moss, C. E., Ashby, W. R., Bestall, S. M., Almahasneh, F., Durrant, A. M., Benest, A. V., Blackley, Z., Ballmer-Hofer, K., & Hirashima, M. (2018). VEGFR2 promotes central endothelial activation and the spread of pain in inflammatory arthritis. *Brain, behavior, and immunity, 74*, 49-67.

Becker, J. B., Arnold, A. P., Berkley, K. J., Blaustein, J. D., Eckel, L. A., Hampson, E., Herman, J. P., Marts, S., Sadee, W., & Steiner, M. (2005). Strategies and methods for research on sex differences in brain and behavior. *Endocrinology, 146*(4), 1650-1673.

Ben-Av, P., Crofford, L. J., Wilder, R. L., & Hla, T. (1995). Induction of vascular endothelial growth factor expression in synovial fibroblasts by prostaglandin E and interleukin-1: a potential mechanism for inflammatory angiogenesis. *FEBS letters, 372*(1), 83-87.

Benson, R. A., McInnes, I. B., Garside, P., & Brewer, J. M. (2018). Model answers: rational application of murine models in arthritis research. *European journal of immunology, 48*(1), 32-38.

Berglin, E., Kokkonen, H., Einarsdottir, E., Ågren, Å., & Rantapää Dahlqvist, S. (2010). Influence of female hormonal factors, in relation to autoantibodies and genetic markers, on the development of rheumatoid arthritis in northern Sweden: a case–control study. *Scandinavian journal of rheumatology, 39*(6), 454-460.

Berlin, B. (1962). Tests for biologic safety of Arlacel A. *Annals of allergy, 20*, 472-479.

Berlin, B. S., & Wyman, R. (1971). Fractionation of Arlacel A. *Proceedings of the society for experimental biology and medicine, 136*(4), 1363-1368.

Bertuglia, A., Lacourt, M., Girard, C., Beauchamp, G., Richard, H., & Laverty, S. (2016). Osteoclasts are recruited to the subchondral bone in naturally occurring post-traumatic equine carpal osteoarthritis and may contribute to cartilage degradation. *Osteoarthritis and cartilage, 24*(3), 555-566.

Bevaart, L., Vervoordeldonk, M. J., & Tak, P. P. (2010). Evaluation of therapeutic targets in animal models of arthritis. *Arthritis Rheum, 62*(8), 2192-2205.

Bevaart, L., Vervoordeldonk, M. J., & Tak, P. P. (2010). Evaluation of therapeutic targets in animal models of arthritis: how does it relate to rheumatoid arthritis? *Arthritis & Rheumatism, 62*(8), 2192-2205.

Beyan, E., Beyan, C., Demirezer, A., Ertuğrul, E., & Uzuner, A. (2003). The relationship between serum ferritin levels and disease activity in systemic lupus erythematosus. *Scandinavian journal of rheumatology, 32*(4), 225-228.

Bhalekar, M. R., Upadhaya, P. G., Nalawade, S. D., Madgulkar, A. R., & Kshirsagar, S. J. (2015). Anti-rheumatic activity of chloroquine-SLN gel on wistar rats using complete freund's adjuvant (CFA) model. *Indian Journal of Rheumatology, 10*(2), 58-64.

Bhosale, A. M., & Richardson, J. B. (2008). Articular cartilage: structure, injuries and review of management. *British medical bulletin, 87*(1), 77-95.

Billiau, A., & Matthys, P. (2001). Modes of action of Freund's adjuvants in experimental models of autoimmune diseases. *Journal of leukocyte biology, 70*(6), 849-860.

Billinghurst, R. C., Dahlberg, L., Ionescu, M., Reiner, A., Bourne, R., Rorabeck, C., Mitchell, P., Hambor, J., Diekmann, O., & Tschesche, H. (1997). Enhanced cleavage of type II collagen by collagenases in osteoarthritic articular cartilage. *The Journal of clinical investigation, 99*(7), 1534-1545.

Biosplice Therapeutics, I. (2021). A Study Utilizing Patient-Reported and Radiographic Outcomes and Evaluating the Safety and Efficacy of Lorecivivint (SM04690) for the Treatment of Moderately to Severely Symptomatic Knee Osteoarthritis (STRIDES-X-ray). Retrieved from https://clinicaltrials.gov/study/NCT03928184

Biosplice Therapeutics, I. (2022). 3-year, Open-Label Study Evaluating Safety, Tolerability, and Efficacy of Lorecivivint in Subjects With Osteoarthritis of the Knee. (NCT04931667). Retrieved from https://clinicaltrials.gov/study/NCT04931667

Biosplice Therapeutics, I. (2023). Biosplice Presents Successful Structure and Pain Results from Completed Phase 3 Long-Term Extension Clinical Trial for Lorecivivint for the Treatment of Knee Osteoarthritis. Retrieved from https://www.biospace.com/article/releases/biosplice-presents-successful-structure-and-pain-results-from-completed-phase-3-long-term-extension-clinical-trial-for-lorecivivint-for-the-treatment-of-knee-osteoarthritis/

Biselli-Chicote, P. M., Biselli, J. M., Cunha, B. R., Castro, R., Maniglia, J. V., de Santi Neto, D., Tajara, E. H., de Góis Filho, J. F., Fukuyama, E. E., & Pavarino, É. C. (2017). Overexpression of antiangiogenic vascular endothelial growth factor isoform and splicing regulatory factors in oral, laryngeal and pharyngeal squamous cell carcinomas. *Asian Pacific journal of cancer prevention: APJCP, 18*(8), 2171.

Blanco, F. J., Guitian, R., Vázquez-Martul, E., de Toro, F. J., & Galdo, F. (1998). Osteoarthritis chondrocytes die by apoptosis: a possible pathway for osteoarthritis pathology. *Arthritis & Rheumatism: Official Journal of the American College of Rheumatology, 41*(2), 284-289.

Bodnar, R. J. (2014). Anti-angiogenic drugs: involvement in cutaneous side effects and wound-healing complication. *Advances in wound care, 3*(10), 635-646.

Boettger, M. K., Hensellek, S., Richter, F., Gajda, M., Stöckigt, R., von Banchet, G. S., Bräuer, R., & Schaible, H. G. (2008). Antinociceptive effects of tumor necrosis factor α neutralization in a rat model of antigen-induced arthritis: evidence of a neuronal target. *Arthritis & Rheumatism: Official Journal of the American College of Rheumatology, 58*(8), 2368-2378.

Boettger, M. K., Weber, K., Grossmann, D., Gajda, M., Bauer, R., Bär, K. J., Schulz, S., Voss, A., Geis, C., & Bräuer, R. (2010). Spinal tumor necrosis factor α neutralization reduces peripheral inflammation and hyperalgesia and suppresses autonomic responses in experimental arthritis: a role for spinal tumor necrosis factor α during induction and maintenance of peripheral inflammation. *Arthritis & Rheumatism, 62*(5), 1308-1318.

Boni, J., Rubio-Perez, C., López-Bigas, N., Fillat, C., & de la Luna, S. (2020). The DYRK family of kinases in cancer: molecular functions and therapeutic opportunities. *Cancers, 12*(8), 2106.

Bonnans, C., Chou, J., & Werb, Z. (2014). Remodelling the extracellular matrix in development and disease. *Nature reviews Molecular cell biology, 15*(12), 786-801.

Bonnet, C., & Walsh, D. (2005). Osteoarthritis, angiogenesis and inflammation. *Rheumatology, 44*(1), 7-16.

Borba, V. V., Zandman-Goddard, G., & Shoenfeld, Y. (2019). Exacerbations of autoimmune diseases during pregnancy and postpartum. *Best Practice & Research Clinical Endocrinology & Metabolism, 33*(6), 101321.

Bossard, C., Cruz, N., Chiu, K., Eastman, B., Mak, C. C., KC, S., Bucci, G., Stewart, J., Phalen, T. J., & Cha, S. (2020). SM08502, a novel, small-molecule CDC-like kinase (CLK) inhibitor, demonstrates strong antitumor effects and Wnt pathway inhibition

in castration-resistant prostate cancer (CRPC) models. *Cancer research, 80*(16_Supplement), 5691-5691.

Bottini, N., & Firestein, G. S. (2013). Duality of fibroblast-like synoviocytes in RA: passive responders and imprinted aggressors. *Nature Reviews Rheumatology, 9*(1), 24.

Bouman, A., Heineman, M. J., & Faas, M. M. (2005). Sex hormones and the immune response in humans. *Human reproduction update, 11*(4), 411-423.

Bowler, E., & Oltean, S. (2019). Alternative splicing in angiogenesis. *International Journal of Molecular Sciences, 20*(9), 2067.

Boyle, D. L., Moore, J., Yang, L., Sorkin, L. S., & Firestein, G. S. (2002). Spinal adenosine receptor activation inhibits inflammation and joint destruction in rat adjuvant-induced arthritis. *Arthritis & Rheumatism: Official Journal of the American College of Rheumatology, 46*(11), 3076-3082.

Bracht, A., Silveira, S. S., Castro-Ghizoni, C. V., Sá-Nakanishi, A. B., Oliveira, M. R. N., Bersani-Amado, C. A., Peralta, R. M., & Comar, J. F. (2016). Oxidative changes in the blood and serum albumin differentiate rats with monoarthritis and polyarthritis. *SpringerPlus, 5*(1), 1-14.

Bracht, L., Barbosa, C. P., Caparroz-Assef, S. M., Cuman, R. K. N., Ishii-Iwamoto, E. L., Bracht, A., & Bersani-Amado, C. A. (2012). Effects of simvastatin, atorvastatin, ezetimibe, and ezetimibe+ simvastatin combination on the inflammatory process and on the liver metabolic changes of arthritic rats. *Fundamental & clinical pharmacology, 26*(6), 722-734.

Branca, M. A. (2005). Multi-kinase inhibitors create buzz at ASCO. *Nature biotechnology, 23*(6), 639-640.

Branda, C. S., & Dymecki, S. M. (2004). Talking about a revolution: The impact of site-specific recombinases on genetic analyses in mice. *Developmental cell, 6*(1), 7-28.

Brandtzaeg, P. (1998). The increasing power of immunohistochemistry and immunocytochemistry. *Journal of immunological methods, 216*(1-2), 49-67.

Brennan, F., Jackson, A., Chantry, D., Maini, R., & Feldmann, M. (1989). Inhibitory effect of TNFα antibodies on synovial cell interleukin-1 production in rheumatoid arthritis. *The Lancet, 334*(8657), 244-247.

Brew, C. J., Clegg, P. D., Boot-Handford, R. P., Andrew, J., & Hardingham, T. (2010). Gene expression in human chondrocytes in late osteoarthritis is changed in both fibrillated and intact cartilage without evidence of generalised chondrocyte hypertrophy. *Annals of the rheumatic diseases, 69*(01), 234-240.

Broggi, G., Lo Giudice, A., Di Mauro, M., Asmundo, M. G., Pricoco, E., Piombino, E., Caltabiano, R., Morgia, G., & Russo, G. I. (2021). SRSF-1 and microvessel density immunohistochemical analysis by semi-automated tissue microarray in prostate cancer patients with diabetes (DIAMOND study). *The Prostate, 81*(12), 882-892.

Bromley, M., Bertfield, H., Evanson, J. M., & Woolley, D. E. (1985). Bidirectional erosion of cartilage in the rheumatoid knee joint. *Annals of the rheumatic diseases, 44*(10), 676-681.

Brooks, F., & Hariharan, K. (2013). The rheumatoid forefoot. *Current reviews in musculoskeletal medicine, 6*, 320-327.

Bruckner, P., Hörler, I., Mendler, M., Houze, Y., Winterhalter, K. H., Eich-Bender, S. G., & Spycher, M. A. (1989). Induction and prevention of chondrocyte hypertrophy in culture. *The Journal of cell biology, 109*(5), 2537-2545.

Bry, M., Kivelä, R., Leppänen, V.-M., & Alitalo, K. (2014). Vascular endothelial growth factor-B in physiology and disease. *Physiological reviews, 94*(3), 779-794.

Bubb, M. R. (2024). A Phase 2 Dose Ranging Study to Evaluate the Efficacy and Safety of AMG 570 in Subjects With Active Systemic Lupus Erythematosus (SLE) With Inadequate Response to Standard of Care (SOC) Therapy. Retrieved from https://ufhealth.org/clinical-trials/efficacy-and-safety-of-amg-570-in-subjects-with-active-sle

Buckwalter, J., & Mankin, H. (1997). Instructional course lectures, The American Academy of Orthopaedic Surgeons-articular Cartilage. Part I: Tissue design and chondrocyte-matrix interactions. *Jbjs, 79*(4), 600-611.

Bugatti, S., Caporali, R., Manzo, A., Vitolo, B., Pitzalis, C., & Montecucco, C. (2005). Involvement of subchondral bone marrow in rheumatoid arthritis: lymphoid neogenesis and in situ relationship to subchondral bone marrow osteoclast recruitment. *Arthritis & Rheumatism, 52*(11), 3448-3459.

Bui, H. M., Enis, D., Robciuc, M. R., Nurmi, H. J., Cohen, J., Chen, M., Yang, Y., Dhillon, V., Johnson, K., & Zhang, H. (2016). Proteolytic activation defines distinct lymphangiogenic mechanisms for VEGFC and VEGFD. *The Journal of clinical investigation, 126*(6), 2167-2180.

Bullock, J., Rizvi, S. A., Saleh, A. M., Ahmed, S. S., Do, D. P., Ansari, R. A., & Ahmed, J. (2019). Rheumatoid arthritis: a brief overview of the treatment. *Medical Principles and Practice, 27*(6), 501-507.

Bullock, N., & Oltean, S. (2017). The many faces of SRPK1. *The Journal of pathology, 241*(4), 437-440.

Burmester, G. R., Cohen, S. B., Winthrop, K. L., Nash, P., Irvine, A. D., Deodhar, A., Mysler, E., Tanaka, Y., Liu, J., & Lacerda, A. P. (2023). Safety profile of upadacitinib over 15 000 patient-years across rheumatoid arthritis, psoriatic arthritis, ankylosing spondylitis and atopic dermatitis. *RMD open, 9*(1), e002735.

Burmester, G. R., Lin, Y., Patel, R., Van Adelsberg, J., Mangan, E. K., Graham, N. M., Van Hoogstraten, H., Bauer, D., Vargas, J. I., & Lee, E. B. (2017). Efficacy and safety of sarilumab monotherapy versus adalimumab monotherapy for the treatment of patients with active rheumatoid arthritis (MONARCH): a randomised, double-blind, parallel-group phase III trial. *Annals of the rheumatic diseases, 76*(5), 840-847.

Burr, D. B., & Radin, E. L. (2003). Microfractures and microcracks in subchondral bone: are they relevant to osteoarthrosis? *Rheumatic Disease Clinics, 29*(4), 675-685.

Burry, R. W. (2011). Controls for immunocytochemistry: an update. *Journal of Histochemistry & Cytochemistry, 59*(1), 6-12.

Butler, S. H., Godefroy, F., Besson, J.-M., & Weil-Fugazza, J. (1992). A limited arthritic model for chronic pain studies in the rat. *Pain, 48*(1), 73-81.

Cai, M., Wang, K., Murdoch, C. E., Gu, Y., & Ahmed, A. (2017). Heterodimerisation between VEGFR-1 and VEGFR-2 and not the homodimers of VEGFR-1 inhibit VEGFR-2 activity. *Vascular Pharmacology, 88*, 11-20.

Cai, Y., Zhang, J., Liang, J., Xiao, M., Zhang, G., Jing, Z., Lv, L., Nan, K., & Dang, X. (2023). The burden of rheumatoid arthritis: findings from the 2019 global burden of diseases study and forecasts for 2030 by Bayesian age-period-cohort analysis. *Journal of Clinical Medicine, 12*(4), 1291.

Cannon, G., Openshaw, S., Clayton, F., Sawitzke, A., & Griffiths, M. (1999). *Adjuvant arthritis in rats: susceptibility to arthritis induced by Mycobacterium butyricum and Mycobacterium tuberculosis.* Paper presented at the Transplantation proceedings.

Cao, Y. (2014). VEGF-targeted cancer therapeutics—paradoxical effects in endocrine organs. *Nature reviews Endocrinology, 10*(9), 530-539.

Capra, M., Nuciforo, P. G., Confalonieri, S., Quarto, M., Bianchi, M., Nebuloni, M., Boldorini, R., Pallotti, F., Viale, G., & Gishizky, M. L. (2006). Frequent alterations in the expression of serine/threonine kinases in human cancers. *Cancer research, 66*(16), 8147-8154.

Carle, C., Degboe, Y., Ruyssen-Witrand, A., Arleevskaya, M. I., Clavel, C., & Renaudineau, Y. (2023). Characteristics of the (Auto) Reactive T Cells in Rheumatoid Arthritis According to the Immune Epitope Database. *International Journal of Molecular Sciences, 24*(5), 4296.

Carlevaro, M. F., Cermelli, S., Cancedda, R., & Cancedda, F. D. (2000). Vascular endothelial growth factor (VEGF) in cartilage neovascularization and chondrocyte differentiation: auto-paracrine role during endochondral bone formation. *J Cell Sci, 113*(1), 59-69.

Carlevaro, M. F., Cermelli, S., Cancedda, R., & Descalzi Cancedda, F. (2000). Vascular endothelial growth factor (VEGF) in cartilage neovascularization and chondrocyte differentiation: auto-paracrine role during endochondral bone formation. *Journal of cell science, 113*(1), 59-69.

Carmeliet, P. (2003). Angiogenesis in health and disease. *Nature medicine, 9*(6), 653-660.

Carmeliet, P., Ferreira, V., Breier, G., Pollefeyt, S., Kieckens, L., Gertsenstein, M., Fahrig, M., Vandenhoeck, A., Harpal, K., & Eberhardt, C. (1996). Abnormal blood vessel development and lethality in embryos lacking a single VEGF allele. *Nature, 380*(6573), 435-439.

Carmeliet, P., Moons, L., Luttun, A., Vincenti, V., Compernolle, V., De Mol, M., Wu, Y., Bono, F., Devy, L., & Beck, H. (2001). Synergism between vascular endothelial growth factor and placental growth factor contributes to angiogenesis and plasma extravasation in pathological conditions. *Nature medicine, 7*(5), 575-583.

Cassidy, M. F., Herbert, Z. T., & Moulton, V. R. (2022). Splicing factor SRSF1 controls distinct molecular programs in regulatory and effector T cells implicated in systemic autoimmune disease. *Molecular Immunology, 141*, 94-103.

Castaneda, S., Roman-Blas, J. A., Largo, R., & Herrero-Beaumont, G. (2012). Subchondral bone as a key target for osteoarthritis treatment. *Biochemical pharmacology, 83*(3), 315-323.

Castor, C. W. (1960). The microscopic structure of normal human synovial tissue. *Arthritis & Rheumatism: Official Journal of the American College of Rheumatology, 3*(2), 140-151.

Catena, R., Larzabal, L., Larrayoz, M., Molina, E., Hermida, J., Agorreta, J., Montes, R., Pio, R., Montuenga, L. M., & Calvo, A. (2010). VEGF 121 b and VEGF 165 b are weakly angiogenic isoforms of VEGF-A. *Molecular cancer, 9*, 1-14.

Catrina, A. I., Joshua, V., Klareskog, L., & Malmström, V. (2016). Mechanisms involved in triggering rheumatoid arthritis. *Immunological reviews, 269*(1), 162-174.

Cebe-Suarez, S., Grünewald, F. S., Jaussi, R., Li, X., Claesson-Welsh, L., Spillmann, D., Mercer, A. A., Prota, A. E., & Ballmer-Hofer, K. (2008). Orf virus VEGF-E NZ2 promotes paracellular NRP-1/VEGFR-2 coreceptor assembly via the peptide RPPR. *The FASEB journal, 22*(8), 3078-3086.

Cebe Suarez, S., Pieren, M., Cariolato, L., Arn, S., Hoffmann, U., Bogucki, A., Manlius, C., Wood, J., & Ballmer-Hofer, K. (2006). A VEGF-A splice variant defective for heparan

sulfate and neuropilin-1 binding shows attenuated signaling through VEGFR-2. *Cellular and Molecular Life Sciences CMLS, 63*, 2067-2077.

Chabner, B. A., Boral, A. L., & Multani, P. (1998). Translational research: walking the bridge between idea and cure—seventeenth Bruce F. Cain Memorial Award lecture. *Cancer research, 58*(19), 4211-4216.

Chan, J. K. (2014). The wonderful colors of the hematoxylin–eosin stain in diagnostic surgical pathology. *International journal of surgical pathology, 22*(1), 12-32.

Chang, H. H., Dwivedi, N., Nicholas, A. P., & Ho, I. C. (2015). The W620 polymorphism in PTPN22 disrupts its interaction with peptidylarginine deiminase type 4 and enhances citrullination and NETosis. *Arthritis & Rheumatology, 67*(9), 2323-2334.

Chawla, S., Mainardi, A., Majumder, N., Dönges, L., Kumar, B., Occhetta, P., Martin, I., Egloff, C., Ghosh, S., & Bandyopadhyay, A. (2022). Chondrocyte hypertrophy in osteoarthritis: mechanistic studies and models for the identification of new therapeutic strategies. *Cells, 11*(24), 4034.

Chen, H., Wang, J., Zhou, W., Yin, H., & Wang, M. (2015). Breastfeeding and risk of rheumatoid arthritis: a systematic review and metaanalysis. *The Journal of rheumatology, 42*(9), 1563-1569.

Chen, Q., Chen, Z., Li, F., Zha, H., He, W., Jiang, F., Wei, J., Xu, J., Li, R., & Cai, L. (2023). Discovery of highly potent and selective VEGFR2 kinase inhibitors for the treatment of rheumatoid arthritis. *European Journal of Medicinal Chemistry, 257*, 115456.

Chen, X., DuBois, D. C., Almon, R. R., & Jusko, W. J. (2015). Biodistribution of etanercept to tissues and sites of inflammation in arthritic rats. *Drug Metabolism and Disposition, 43*(6), 898-907.

Chen, X. L., Nam, J.-O., Jean, C., Lawson, C., Walsh, C. T., Goka, E., Lim, S.-T., Tomar, A., Tancioni, I., & Uryu, S. (2012). VEGF-induced vascular permeability is mediated by FAK. *Developmental cell, 22*(1), 146-157.

Chen, Y.-Y., Brown, N. J., Jones, R., Lewis, C. E., Mujamammi, A. H., Muthana, M., Seed, M. P., & Barker, M. D. (2014). A peptide derived from TIMP-3 inhibits multiple angiogenic growth factor receptors and tumour growth and inflammatory arthritis in mice. *Angiogenesis, 17*, 207-219.

Chen, Y., Zhao, B., Zhu, Y., Zhao, H., & Ma, C. (2019). HIF-1-VEGF-Notch mediates angiogenesis in temporomandibular joint osteoarthritis. *American journal of translational research, 11*(5), 2969.

Chidomere, C. I., Wahid, M., Kemble, S., Chadwick, C., Thomas, R., Hardy, R. S., McGettrick, H. M., & Naylor, A. J. (2023). Bench to Bedside: Modelling Inflammatory Arthritis. *Discovery Immunology, 2*(1), kyac010.

Chillingworth, N. L., & Donaldson, L. F. (2003). Characterisation of a Freund's complete adjuvant-induced model of chronic arthritis in mice. *Journal of neuroscience methods, 128*(1-2), 45-52.

Chintalgattu, V., Nair, D. M., & Katwa, L. C. (2003). Cardiac myofibroblasts: a novel source of vascular endothelial growth factor (VEGF) and its receptors Flt-1 and KDR. *Journal of molecular and cellular cardiology, 35*(3), 277-286.

Choi, I. Y., Karpus, O. N., Turner, J. D., Hardie, D., Marshall, J. L., de Hair, M. J., Maijer, K. I., Tak, P. P., Raza, K., & Hamann, J. (2017). Stromal cell markers are differentially expressed in the synovial tissue of patients with early arthritis. *PloS one, 12*(8), e0182751.

Choi, S. T., Kim, J. H., Seok, J.-Y., Park, Y.-B., & Lee, S.-K. (2009). Therapeutic effect of anti-vascular endothelial growth factor receptor I antibody in the established collagen-induced arthritis mouse model. *Clinical rheumatology, 28*, 333-337.

Choi, S. T., Kim, J. H., Seok, J.-Y., Park, Y.-B., & Lee, S.-K. (2009). Therapeutic effect of anti-vascular endothelial growth factor receptor I antibody in the established collagen-induced arthritis mouse model. *Clinical rheumatology, 28*(3), 333-337.

Chopra, A., & Abdel-Nasser, A. (2008). Epidemiology of rheumatic musculoskeletal disorders in the developing world. *Best Practice & Research Clinical Rheumatology, 22*(4), 583-604.

Chou, C.-H., Jain, V., Gibson, J., Attarian, D. E., Haraden, C. A., Yohn, C. B., Laberge, R.-M., Gregory, S., & Kraus, V. B. (2020). Synovial cell cross-talk with cartilage plays a major role in the pathogenesis of osteoarthritis. *Scientific Reports, 10*(1), 1-14.

Choy, E. (2012). Understanding the dynamics: pathways involved in the pathogenesis of rheumatoid arthritis. *Rheumatology, 51*(suppl_5), v3-v11.

Choy, E., Ganeshalingam, K., Semb, A. G., Szekanecz, Z., & Nurmohamed, M. (2014). Cardiovascular risk in rheumatoid arthritis: recent advances in the understanding of the pivotal role of inflammation, risk predictors and the impact of treatment. *Rheumatology, 53*(12), 2143-2154.

Choy, E. H., & Panayi, G. S. (2001). Cytokine pathways and joint inflammation in rheumatoid arthritis. *New England journal of medicine, 344*(12), 907-916.

Chuang, C. Y., Lord, M. S., Melrose, J., Rees, M. D., Knox, S. M., Freeman, C., Iozzo, R. V., & Whitelock, J. M. (2010). Heparan sulfate-dependent signaling of fibroblast growth factor 18 by chondrocyte-derived perlecan. *Biochemistry, 49*(26), 5524-5532.

Chung, H., Creger, E., Sitts, L., Chiu, K., Mak, C.-C., Sunil, K., Tam, B., Bucci, G., Stewart, J., & Phalen, T. (2019). Sm09419, a novel, small-molecule cdc-like kinase (clk) inhibitor, demonstrates strong inhibition of the wnt signaling pathway and antitumor effects in mantle cell lymphoma models. *Blood, 134*, 4059.

Chung, K. C., & Pushman, A. G. (2011). Current concepts in the management of the rheumatoid hand. *The Journal of hand surgery, 36*(4), 736-747.

Cieremans, D., Shah, A., Slover, J., Schwarzkopf, R., & Meftah, M. (2023). Trends in Complications and Outcomes in Patients Aged 65 Years and Younger Undergoing Total Hip Arthroplasty: Data From the American Joint Replacement Registry. *JAAOS Global Research & Reviews, 7*(3).

Clark, J. M. (1990). The structure of vascular channels in the subchondral plate. *Journal of anatomy, 171*, 105.

Clauss, M., Weich, H., Breier, G., Knies, U., Röckl, W., Waltenberger, J., & Risau, W. (1996). The vascular endothelial growth factor receptor Flt-1 mediates biological activities: implications for a functional role of placenta growth factor in monocyte activation and chemotaxis. *Journal of Biological Chemistry, 271*(30), 17629-17634.

Cohen, S. B., Tanaka, Y., Mariette, X., Curtis, J. R., Lee, E. B., Nash, P., Winthrop, K. L., Charles-Schoeman, C., Wang, L., & Chen, C. (2020). Long-term safety of tofacitinib up to 9.5 years: a comprehensive integrated analysis of the rheumatoid arthritis clinical development programme. *RMD open, 6*(3), e001395.

Cohen, S. B., Van Vollenhoven, R. F., Winthrop, K. L., Zerbini, C. A., Tanaka, Y., Bessette, L., Zhang, Y., Khan, N., Hendrickson, B., & Enejosa, J. V. (2021). Safety profile of upadacitinib in rheumatoid arthritis: integrated analysis from the SELECT phase III clinical programme. *Annals of the rheumatic diseases, 80*(3), 304-311.

Colell, A., Green, D., & Ricci, J. (2009). Novel roles for GAPDH in cell death and carcinogenesis. *Cell Death & Differentiation, 16*(12), 1573-1581.

Coltri, P. P., dos Santos, M. G., & da Silva, G. H. (2019). Splicing and cancer: Challenges and opportunities. *Wiley Interdisciplinary Reviews: RNA, 10*(3), e1527.

Combe, B., Kivitz, A., Tanaka, Y., van der Heijde, D., Simon, J. A., Baraf, H. S., Kumar, U., Matzkies, F., Bartok, B., & Ye, L. (2021). Filgotinib versus placebo or adalimumab in patients with rheumatoid arthritis and inadequate response to methotrexate: a phase III randomised clinical trial. *Annals of the rheumatic diseases, 80*(7), 848-858.

Compton, L. A., Murphy, G. F., & Lian, C. G. (2015). Diagnostic immunohistochemistry in cutaneous neoplasia: an update. *Dermatopathology, 2*(1), 15-42.

Conaghan, P. G., Mysler, E., Tanaka, Y., Da Silva-Tillmann, B., Shaw, T., Liu, J., Ferguson, R., Enejosa, J. V., Cohen, S., & Nash, P. (2021). Upadacitinib in rheumatoid arthritis: a benefit–risk assessment across a Phase III program. *Drug Safety, 44*, 515-530.

Corrado, A., Neve, A., & Cantatore, F. P. (2013). Expression of vascular endothelial growth factor in normal, osteoarthritic and osteoporotic osteoblasts. *Clinical and experimental medicine, 13*, 81-84.

Coulson-Thomas, Y. M., Coulson-Thomas, V. J., Norton, A. L., Gesteira, T. F., Cavalheiro, R. P., Meneghetti, M. C. Z., Martins, J. R., Dixon, R. A., & Nader, H. B. (2015). The identification of proteoglycans and glycosaminoglycans in archaeological human bones and teeth. *Plos one, 10*(6), e0131105.

Craft, R. M., Mogil, J. S., & Aloisi, A. M. (2004). Sex differences in pain and analgesia: the role of gonadal hormones. *European Journal of Pain, 8*(5), 397-411.

Crofford, L. J. (2013). Use of NSAIDs in treating patients with arthritis. *Arthritis research & therapy, 15*, 1-10.

Cromer, W. E., Ganta, C. V., Patel, M., Traylor, J., Kevil, C. G., Alexander, J. S., & Mathis, J. M. (2013). VEGF-A isoform modulation in an preclinical TNBS model of ulcerative colitis: protective effects of a VEGF164b therapy. *Journal of Translational Medicine, 11*(1), 1-12.

Crooke, S. T., Witztum, J. L., Bennett, C. F., & Baker, B. F. (2018). RNA-targeted therapeutics. *Cell metabolism, 27*(4), 714-739.

Cross, M., Smith, E., Hoy, D., Carmona, L., Wolfe, F., Vos, T., Williams, B., Gabriel, S., Lassere, M., & Johns, N. (2014). The global burden of rheumatoid arthritis: estimates from the global burden of disease 2010 study. *Annals of the rheumatic diseases, 73*(7), 1316-1322.

Crowson, C. S., Matteson, E. L., Myasoedova, E., Michet, C. J., Ernste, F. C., Warrington, K. J., Davis III, J. M., Hunder, G. G., Therneau, T. M., & Gabriel, S. E. (2011). The lifetime risk of adult-onset rheumatoid arthritis and other inflammatory autoimmune rheumatic diseases. *Arthritis & Rheumatism, 63*(3), 633-639.

Cudmore, M. J., Hewett, P. W., Ahmad, S., Wang, K.-Q., Cai, M., Al-Ani, B., Fujisawa, T., Ma, B., Sissaoui, S., & Ramma, W. (2012). The role of heterodimerization between VEGFR-1 and VEGFR-2 in the regulation of endothelial cell homeostasis. *Nature communications, 3*(1), 972.

Culliford, D., Maskell, J., Kiran, A., Judge, A., Javaid, M., Cooper, C., & Arden, N. (2012). The lifetime risk of total hip and knee arthroplasty: results from the UK general practice research database. *Osteoarthritis and cartilage, 20*(6), 519-524.

Cunningham, T. J., Palumbo, I., Grosso, M., Slater, N., & Miles, C. G. (2013). WT1 regulates murine hematopoiesis via maintenance of VEGF isoform ratio. *Blood, The Journal of the American Society of Hematology, 122*(2), 188-192.

Cutolo, M., & Gotelli, E. (2023). Complex role of ooestrogens in the risk and severity of rheumatoid arthritis in menopause. *RMD open, 9*(2).

Cutolo, M., & Straub, R. H. (2020). Sex steroids and autoimmune rheumatic diseases: state of the art. *Nature Reviews Rheumatology, 16*(11), 628-644.

Cutolo, M., Sulli, A., Capellino, S., Villaggio, B., Montagna, P., Pizzorni, C., Paolino, S., Seriolo, B., Felli, L., & Straub, R. H. (2006). Anti-TNF and sex hormones. *Annals of the New York Academy of Sciences, 1069*(1), 391-400.

Czubaty, A., & Piekiełko-Witkowska, A. (2017). Protein kinases that phosphorylate splicing factors: Roles in cancer development, progression and possible therapeutic options. *The international journal of biochemistry & cell biology, 91*, 102-115.

D'Aura Swanson, C., Paniagua, R. T., Lindstrom, T. M., & Robinson, W. H. (2009). Tyrosine kinases as targets for the treatment of rheumatoid arthritis. *Nature Reviews Rheumatology, 5*(6), 317-324.

da Glória, V. G., Martins de Araújo, M., Mafalda Santos, A., Leal, R., de Almeida, S. F., Carmo, A. M., & Moreira, A. (2014). T cell activation regulates CD6 alternative splicing by transcription dynamics and SRSF1. *The Journal of Immunology, 193*(1), 391-399.

da Silva, M. R., Moreira, G. A., da Silva, G., Anderson, R., de Almeida Alves Barbosa, É., Pais Siqueira, R., Teixera, R. R., Almeida, M. R., Silva Júnior, A., & Fietto, J. L. R. (2015). Splicing regulators and their roles in cancer biology and therapy. *BioMed research international, 2015*.

da Silva, M. R., Moreira, G. A., Goncalves da Silva, R. A., de Almeida Alves Barbosa, É., Pais Siqueira, R., Teixera, R. R., Almeida, M. R., Silva Júnior, A., Fietto, J. L. R., & Bressan, G. C. (2015). Splicing regulators and their roles in cancer biology and therapy. *BioMed research international, 2015*.

Daien, C. I., Charlotte, H., Combe, B., & Landewe, R. (2017). Non-pharmacological and pharmacological interventions in patients with early arthritis: a systematic literature review informing the 2016 update of EULAR recommendations for the management of early arthritis. *RMD open, 3*(1), e000404.

Dakowicz, D., Zajkowska, M., & Mroczko, B. (2022). Relationship between VEGF family members, their receptors and cell death in the neoplastic transformation of colorectal cancer. *International Journal of Molecular Sciences, 23*(6), 3375.

Danastas, K., Combes, V., Lindsay, L. A., Grau, G. E., Thompson, M. B., & Murphy, C. R. (2015). VEGF111: new insights in tissue invasion. *Frontiers in Physiology, 6*, 2.

Daniel, A., Tuhina, N., Alan, J. S. A., Julia, F., Felson, D. T., Bingham, C., Birnbaum, N., Burmester, G., Bykerk, V., & Cohen, M. (2010). rheumatoid arthritis classification criteria: an American College of Rheumatology/European League Against Rheumatism collaborative initiative. *Arthritis Rheum, 62*(9), 2569-2581.

Darrah, E., & Andrade, F. (2018). Rheumatoid arthritis and citrullination. *Current opinion in rheumatology, 30*(1), 72.

Davis-Smyth, T., Chen, H., Park, J., Presta, L. G., & Ferrara, N. (1996). The second immunoglobulin-like domain of the VEGF tyrosine kinase receptor Flt-1 determines ligand binding and may initiate a signal transduction cascade. *The EMBO journal, 15*(18), 4919-4927.

Dayer, J.-M., & Choy, E. (2010). Therapeutic targets in rheumatoid arthritis: the interleukin-6 receptor. *Rheumatology, 49*(1), 15-24.

De Bandt, M., Ben Mahdi, M. H., Ollivier, V., Grossin, M., Dupuis, M., Gaudry, M., Bohlen, P., Lipson, K. E., Rice, A., & Wu, Y. (2003). Blockade of vascular endothelial growth factor receptor I (VEGF-RI), but not VEGF-RII, suppresses joint destruction in the K/BxN model of rheumatoid arthritis. *The Journal of Immunology, 171*(9), 4853-4859.

De Bandt, M., Grossin, M., Weber, A. J., Chopin, M., Elbim, C., Pla, M., Gougerot-Pocidalo, M. A., & Gaudry, M. (2000). Suppression of arthritis and protection from bone destruction by treatment with TNP-470/AGM-1470 in a transgenic mouse model of rheumatoid arthritis. *Arthritis & Rheumatism: Official Journal of the American College of Rheumatology, 43*(9), 2056-2063.

De Hair, M., Van De Sande, M., Ramwadhdoebe, T., Hansson, M., Landewé, R., Van Der Leij, C., Maas, M., Serre, G., Van Schaardenburg, D., & Klareskog, L. (2014). Features of the synovium of individuals at risk of developing rheumatoid arthritis: implications for understanding preclinical rheumatoid arthritis. *Arthritis & Rheumatology, 66*(3), 513-522.

de Jong, Z., Munneke, M., Vilim, V., Zwinderman, A., Kroon, H., Ronday, H., Lems, W., Dijkmans, B., Breedveld, F., & Vliet Vlieland, T. (2008). Value of serum cartilage oligomeric matrix protein as a prognostic marker of large-joint damage in rheumatoid arthritis—data from the RAPIT study. *Rheumatology, 47*(6), 868-871.

Deane, K. D., Demoruelle, M. K., Kelmenson, L. B., Kuhn, K. A., Norris, J. M., & Holers, V. M. (2017). Genetic and environmental risk factors for rheumatoid arthritis. *Best Practice & Research Clinical Rheumatology, 31*(1), 3-18.

Deighton, C., Walker, D., Griffiths, I., & Roberts, D. (1989). The contribution of H LA to rheumatoid arthritis. *Clinical genetics, 36*(3), 178-182.

Delaissé, J.-M., Engsig, M. T., Everts, V., del Carmen Ovejero, M., Ferreras, M., Lund, L., Vu, T. H., Werb, Z., Winding, B., & Lochter, A. (2000). Proteinases in bone resorption: obvious and less obvious roles. *Clinica Chimica Acta, 291*(2), 223-234.

Delany, A., Amling, M., Priemel, M., Howe, C., Baron, R., & Canalis, E. (2000). Osteopenia and decreased bone formation in osteonectin-deficient mice. *The Journal of clinical investigation, 105*(7), 915-923.

Delany, A. M., & Hankenson, K. D. (2009). Thrombospondin-2 and SPARC/osteonectin are critical regulators of bone remodeling. *Journal of cell communication and signaling, 3*, 227-238.

Delcombel, R., Janssen, L., Vassy, R., Gammons, M., Haddad, O., Richard, B., Letourneur, D., Bates, D., Hendricks, C., & Waltenberger, J. (2013). New prospects in the roles of the C-terminal domains of VEGF-A and their cooperation for ligand binding, cellular signaling and vessels formation. *Angiogenesis, 16*, 353-371.

Deshmukh, V., O'Green, A., Bossard, C., Seo, T., Lamangan, L., Ibanez, M., Ghias, A., Lai, C., Do, L., & Cho, S. (2019). Modulation of the Wnt pathway through inhibition of CLK2 and DYRK1A by lorecivivint as a novel, potentially disease-modifying approach for knee osteoarthritis treatment. *Osteoarthritis and cartilage, 27*(9), 1347-1360.

Desideri, S., Onions, K. L., Baker, S. L., Gamez, M., El Hegni E Hussien, H., Russell, A., Satchell, S. C., & Foster, R. R. (2019). Endothelial glycocalyx restoration by growth factors in diabetic nephropathy. *Biorheology, 56*(2-3), 163-179.

Dessein, P. H., Joffe, B. I., & Stanwix, A. E. (2004). High sensitivity C-reactive protein as a disease activity marker in rheumatoid arthritis. *The Journal of rheumatology, 31*(6), 1095-1097.

Dhillon, S., & Keam, S. J. (2020). Filgotinib: first approval. *Drugs, 80*, 1987-1997.

Ding, J.-H., Zhong, X.-Y., Hagopian, J. C., Cruz, M. M., Ghosh, G., Feramisco, J., Adams, J. A., & Fu, X.-D. (2006). Regulated cellular partitioning of SR protein-specific kinases in mammalian cells. *Molecular biology of the cell, 17*(2), 876-885.

Donaldson, L. F., & Beazley-Long, N. (2016). Alternative RNA splicing: contribution to pain and potential therapeutic strategy. *Drug discovery today, 21*(11), 1787-1798.

Donaldson, L. F., Seckl, J. R., & McQueen, D. S. (1993). A discrete adjuvant-induced monoarthritis in the rat: effects of adjuvant dose. *Journal of neuroscience methods, 49*(1-2), 5-10.

Dong, Z., Chang, X., Xie, L., Wang, Y., & Hou, Y. (2022). Increased expression of SRPK1 (serine/arginine-rich protein-specific kinase 1) is associated with progression and unfavorable prognosis in cervical squamous cell carcinoma. *Bioengineered, 13*(3), 6100-6112.

DrugSafetyUpdate. (2023). Janus kinase (JAK) inhibitors: new measures to reduce risks of major cardiovascular events, malignancy, venous thromboembolism, serious infections and increased mortality. *Drug Safety Update volume 16, issue 9: April 2023: 2.* Retrieved from https://www.gov.uk/drug-safety-update/janus-kinase-jak-inhibitors-new-measures-to-reduce-risks-of-major-cardiovascular-events-malignancy-venous-thromboembolism-serious-infections-and-increased-mortality

Du, J.-X., Luo, Y.-H., Zhang, S.-J., Wang, B., Chen, C., Zhu, G.-Q., Zhu, P., Cai, C.-Z., Wan, J.-L., & Cai, J.-L. (2021). Splicing factor SRSF1 promotes breast cancer progression via oncogenic splice switching of PTPMT1. *Journal of Experimental & Clinical Cancer Research, 40*(1), 1-19.

Duan, X., Murata, Y., Liu, Y., Nicolae, C., Olsen, B. R., & Berendsen, A. D. (2015). Vegfa regulates perichondrial vascularity and osteoblast differentiation in bone development. *Development, 142*(11), 1984-1991.

Dubuc, L. C. M.-H. M. (2012). J.-E. Montell E. Vergés J. Munaut C. et al., Characterization of synovial angiogenesis in osteoarthritis patients and its modulation by chondroitin sulfate. *Arthritis Res. Ther, 14*(2), R58.

Duggan, S., & Keam, S. J. (2019). Upadacitinib: first approval. *Drugs, 79*(16), 1819-1828.

Durrant, A. M. (2021). *Investigating the roles of the gliovasculature and neuroinflammation on secondary pain in peripheral inflammation.* University of Nottingham,

Ebos, J. M., Bocci, G., Man, S., Thorpe, P. E., Hicklin, D. J., Zhou, D., Jia, X., & Kerbel, R. S. (2004). A naturally occurring soluble form of vascular endothelial growth factor receptor 2 detected in mouse and human plasma. *Molecular cancer research, 2*(6), 315-326.

Eckhart, L., Ban, J., Ballaun, C., Weninger, W., & Tschachler, E. (1999). Reverse transcription-polymerase chain reaction products of alternatively spliced mRNAs form DNA heteroduplexes and heteroduplex complexes. *Journal of Biological Chemistry, 274*(5), 2613-2615.

Eelen, G., Treps, L., Li, X., & Carmeliet, P. (2020). Basic and therapeutic aspects of angiogenesis updated. *Circulation research, 127*(2), 310-329.

Eichmann, A., Marcelle, C., Bréant, C., & Le Douarin, N. M. (1993). Two molecules related to the VEGF receptor are expressed in early endothelial cells during avian embryonic development. *Mechanisms of development, 42*(1-2), 33-48.

Eisenberg, E., & Levanon, E. Y. (2003). Human housekeeping genes are compact. *TRENDS in Genetics, 19*(7), 362-365.

Eisinger-Mathason, T. K., Zhang, M., Qiu, Q., Skuli, N., Nakazawa, M. S., Karakasheva, T., Mucaj, V., Shay, J. E., Stangenberg, L., & Sadri, N. (2013). Hypoxia-dependent modification of collagen networks promotes sarcoma metastasis. *Cancer discovery, 3*(10), 1190-1205.

El-Gabalawy, H., Canvin, J., Ma, G. M., Van der Vieren, M., Hoffman, P., Gallatin, M., & Wilkins, J. (1996). Synovial distribution of αd/CD18, a novel leukointegrin. Comparison with other integrins and their ligands. *Arthritis & Rheumatism, 39*(11), 1913-1921.

Elenkov, I. J., Wilder, R. L., Bakalov, V. K., Link, A. A., Dimitrov, M. A., Fisher, S., Crane, M., Kanik, K. S., & Chrousos, G. P. (2001). IL-12, TNF-α, and hormonal changes during late pregnancy and early postpartum: implications for autoimmune disease activity during these times. *The Journal of Clinical Endocrinology & Metabolism, 86*(10), 4933-4938.

ElHady, A. K., El-Gamil, D. S., Abadi, A. H., Abdel-Halim, M., & Engel, M. (2023). An overview of cdc2-like kinase 1 (Clk1) inhibitors and their therapeutic indications. *Medicinal research reviews, 43*(2), 343-398.

Elias, A. P., & Dias, S. (2008). Microenvironment changes (in pH) affect VEGF alternative splicing. *Cancer Microenvironment, 1*, 131-139.

Elices, M. J., Tsai, V., Strahl, D., Goel, A., Tollefson, V., Arrhenius, T., Wayner, E., Gaeta, F., Fikes, J., & Firestein, G. (1994). Expression and functional significance of alternatively spliced CS1 fibronectin in rheumatoid arthritis microvasculature. *The Journal of clinical investigation, 93*(1), 405-416.

Elshabrawy, H. A., Chen, Z., Volin, M. V., Ravella, S., Virupannavar, S., & Shahrara, S. (2015). The pathogenic role of angiogenesis in rheumatoid arthritis. *Angiogenesis, 18*(4), 433-448.

Elsheemy, M. S., Hasanin, A. H., Mansour, A., Mehrez, S. I., & Abdel-Bary, M. (2019). Etanercept improved anemia and decreased hepcidin gene expression in a rat model of rheumatoid arthritis. *Biomedicine & Pharmacotherapy, 112*, 108740.

Enomoto, H., Inoki, I., Komiya, K., Shiomi, T., Ikeda, E., Obata, K.-i., Matsumoto, H., Toyama, Y., & Okada, Y. (2003). Vascular endothelial growth factor isoforms and their receptors are expressed in human osteoarthritic cartilage. *The American journal of pathology, 162*(1), 171-181.

Enríquez-Fuentes, J. E., Oribio-Quinto, C., Pascual-Santiago, M. A., Alarcón-García, A., & Fernández-Vigo, J. (2024). Long-term results of treatment of neovascular age-related macular degeneration using antiangiogenic drugs: A review of the literature. *Archivos de la Sociedad Española de Oftalmología (English Edition)*.

Evans, C. H., Kraus, V. B., & Setton, L. A. (2014). Progress in intra-articular therapy. *Nature Reviews Rheumatology, 10*(1), 11-22.

Evans, S. M., Du, K. L., Chalian, A. A., Mick, R., Zhang, P. J., Hahn, S. M., Quon, H., Lustig, R., Weinstein, G. S., & Koch, C. J. (2007). Patterns and levels of hypoxia in head and neck squamous cell carcinomas and their relationship to patient outcome. *International Journal of Radiation Oncology* Biology* Physics, 69*(4), 1024-1031.

Evans, S. M., Hahn, S. M., Magarelli, D. P., & Koch, C. J. (2001). Hypoxic heterogeneity in human tumors: EF5 binding, vasculature, necrosis, and proliferation. *American journal of clinical oncology, 24*(5), 467-472.

Exonate. (2022). Phase 1b/2 – A Randomised, Single-Blind, Placebo Controlled, Multiple Dose, Dose Escalation Study to Evaluate the Safety and Tolerability of EXN407 in subjects with Centre Involved Diabetic Macular Oedema secondary to Diabetes Mellitus. Retrieved from https://www.lei.org.au/research/clinical-trials/exonate-pq-110-001/

Exonate. (2023). Exonate announces successful completion of Phase Ib/IIa trial in diabetic macular oedema. Retrieved from https://www.exonate.com/updates/exonate-announces-successful-completion-phase-ibii/

Ezponda, T., Pajares, M. J., Agorreta, J., Echeveste, J. I., López-Picazo, J. M., Torre, W., Pio, R., & Montuenga, L. M. (2010). The Oncoprotein SF2/ASF Promotes Non–Small Cell Lung Cancer Survival by Enhancing Survivin Expression. *Clinical Cancer Research, 16*(16), 4113-4125.

Facemire, C. S., Nixon, A. B., Griffiths, R., Hurwitz, H., & Coffman, T. M. (2009). Vascular endothelial growth factor receptor 2 controls blood pressure by regulating nitric oxide synthase expression. *Hypertension, 54*(3), 652-658.

Falconer, J., Murphy, A. N., Young, S. P., Clark, A. R., Tiziani, S., Guma, M., & Buckley, C. D. (2018). Synovial cell metabolism and chronic inflammation in rheumatoid arthritis. *Arthritis & Rheumatology, 70*(7), 984-999.

Fan, L., Li, J., Yu, Z., Dang, X., & Wang, K. (2014). The hypoxia-inducible factor pathway, prolyl hydroxylase domain protein inhibitors, and their roles in bone repair and regeneration. *BioMed research international, 2014*.

Fan, Y., Jalali, A., Chen, A., Zhao, X., Liu, S., Teli, M., Guo, Y., Li, F., Li, J., & Siegel, A. (2020). Skeletal loading regulates breast cancer-associated osteolysis in a loading intensity-dependent fashion. *Bone research, 8*(1), 9.

Farrugia, M., & Baron, B. (2016). The role of TNF-α in rheumatoid arthritis: A focus on regulatory T cells. *Journal of clinical and translational research, 2*(3), 84.

Fassbender, H. G. (1983). Histomorphological basis of articular cartilage destruction in rheumatoid arthritis. *Collagen and related research, 3*(2), 141-155.

Faul, F., Erdfelder, E., Lang, A.-G., & Buchner, A. (2007). G* Power 3: A flexible statistical power analysis program for the social, behavioral, and biomedical sciences. *Behavior research methods, 39*(2), 175-191.

Fautrel, B., & Guillemin, F. (2002). Cost of illness studies in rheumatic diseases. *Current opinion in rheumatology, 14*(2), 121-126.

Fava, R. A., Olsen, N. J., Spencer-Green, G., Yeo, K.-T., Yeo, T.-K., Berse, B., Jackman, R. W., Senger, D. R., Dvorak, H. F., & Brown, L. F. (1994). Vascular permeability factor/endothelial growth factor (VPF/VEGF): accumulation and expression in human synovial fluids and rheumatoid synovial tissue. *The Journal of experimental medicine, 180*(1), 341-346.

Favalli, E. G., Biggioggero, M., Crotti, C., Becciolini, A., Raimondo, M. G., & Meroni, P. L. (2019). Sex and management of rheumatoid arthritis. *Clinical reviews in allergy & immunology, 56*, 333-345.

Fay, J., Varoga, D., Wruck, C. J., Kurz, B., Goldring, M. B., & Pufe, T. (2006). Reactive oxygen species induce expression of vascular endothelial growth factor in chondrocytes and human articular cartilage explants. *Arthritis research & therapy, 8*(6), 1-8.

Fearnley, G. W., Bruns, A. F., Wheatcroft, S. B., & Ponnambalam, S. (2015). VEGF-A isoform-specific regulation of calcium ion flux, transcriptional activation and endothelial cell migration. *Biology open, 4*(6), 731-742.

Fearnley, G. W., Odell, A. F., Latham, A. M., Mughal, N. A., Bruns, A. F., Burgoyne, N. J., Homer-Vanniasinkam, S., Zachary, I. C., Hollstein, M. C., & Wheatcroft, S. B. (2014). VEGF-A isoforms differentially regulate ATF-2–dependent VCAM-1 gene expression and endothelial–leukocyte interactions. *Molecular biology of the cell, 25*(16), 2509-2521.

Fearnley, G. W., Smith, G. A., Abdul-Zani, I., Yuldasheva, N., Mughal, N. A., Homer-Vanniasinkam, S., Kearney, M. T., Zachary, I. C., Tomlinson, D. C., & Harrison, M. A. (2016). VEGF-A isoforms program differential VEGFR2 signal transduction, trafficking and proteolysis. *Biology open, 5*(5), 571-583.

Feist, E., Fatenejad, S., Grishin, S., Korneva, E., Luggen, M. E., Nasonov, E., Samsonov, M., Smolen, J. S., & Fleischmann, R. M. (2022). Olokizumab, a monoclonal antibody against interleukin-6, in combination with methotrexate in patients with rheumatoid arthritis inadequately controlled by tumour necrosis factor inhibitor therapy: efficacy and safety results of a randomised controlled phase III study. *Annals of the rheumatic diseases, 81*(12), 1661-1668.

Feldmann, M. (1996). Brennan, FM, and Maini, RN Rheumatoid Arthritis. *Cell, 85*, 1277-1289.

Fenwick, S., Gregg, P., & Rooney, P. (1999). Osteoarthritic cartilage loses its ability to remain avascular. *Osteoarthritis and cartilage, 7*(5), 441-452.

Ferrara, N. (1999). Molecular and biological properties of vascular endothelial growth factor. *Journal of molecular medicine, 77*, 527-543.

Ferrara, N., Carver-Moore, K., Chen, H., Dowd, M., Lu, L., O'Shea, K. S., Powell-Braxton, L., Hillan, K. J., & Moore, M. W. (1996). Heterozygous embryonic lethality induced by targeted inactivation of the VEGF gene. *Nature, 380*(6573), 439-442.

Ferrara, N., & Davis-Smyth, T. (1997). The biology of vascular endothelial growth factor. *Endocrine reviews, 18*(1), 4-25.

Ferrara, N., Gerber, H.-P., & LeCouter, J. (2003). The biology of VEGF and its receptors. *Nature medicine, 9*(6), 669-676.

Ferrara, N., Hillan, K. J., Gerber, H.-P., & Novotny, W. (2004). Discovery and development of bevacizumab, an anti-VEGF antibody for treating cancer. *Nature reviews Drug discovery, 3*(5), 391-400.

Ferrara, N., & Kerbel, R. S. (2005). Angiogenesis as a therapeutic target. *Nature, 438*(7070), 967-974.

Ferreira, R. C., Freitag, D. F., Cutler, A. J., Howson, J. M., Rainbow, D. B., Smyth, D. J., Kaptoge, S., Clarke, P., Boreham, C., & Coulson, R. M. (2013). Functional IL6R 358Ala allele impairs classical IL-6 receptor signaling and influences risk of diverse inflammatory diseases. *PLoS genetics, 9*(4), e1003444.

Fire, A., Xu, S., Montgomery, M. K., Kostas, S. A., Driver, S. E., & Mello, C. C. (1998). Potent and specific genetic interference by double-stranded RNA in Caenorhabditis elegans. *Nature, 391*(6669), 806-811.

Firestein, G. S. (2003). Evolving concepts of rheumatoid arthritis. *Nature, 423*(6937), 356-361.

Fischer, B. D., Adeyemo, A., O'Leary, M. E., & Bottaro, A. (2017). Animal models of rheumatoid pain: experimental systems and insights. *Arthritis research & therapy, 19*(1), 1-9.

Fleischmann, R., Pangan, A. L., Song, I. H., Mysler, E., Bessette, L., Peterfy, C., Durez, P., Ostor, A. J., Li, Y., & Zhou, Y. (2019). Upadacitinib versus placebo or adalimumab in patients with rheumatoid arthritis and an inadequate response to methotrexate: results of a phase III, double-blind, randomized controlled trial. *Arthritis & Rheumatology, 71*(11), 1788-1800.

Fong, G.-H., Rossant, J., Gertsenstein, M., & Breitman, M. L. (1995). Role of the Flt-1 receptor tyrosine kinase in regulating the assembly of vascular endothelium. *Nature, 376*(6535), 66-70.

Forde, A., Constien, R., Gröne, H. J., Hämmerling, G., & Arnold, B. (2002). Temporal Cre-mediated recombination exclusively in endothelial cells using Tie2 regulatory elements. *Genesis, 33*(4), 191-197.

Forger, F., Marcoli, N., Gadola, S., Möller, B., Villiger, P. M., & Østensen, M. (2008). Pregnancy induces numerical and functional changes of CD4+ CD25high regulatory T cells in patients with rheumatoid arthritis. *Annals of the rheumatic diseases, 67*(7), 984-990.

Forstreuter, F., Lucius, R., & Mentlein, R. (2002). Vascular endothelial growth factor induces chemotaxis and proliferation of microglial cells. *Journal of neuroimmunology, 132*(1-2), 93-98.

Fox, C. H., Johnson, F. B., Whiting, J., & Roller, P. P. (1985). Formaldehyde fixation. *Journal of Histochemistry & Cytochemistry, 33*(8), 845-853.

Franses, R., McWilliams, D., Mapp, P., & Walsh, D. (2010). Osteochondral angiogenesis and increased protease inhibitor expression in OA. *Osteoarthritis and cartilage, 18*(4), 563-571.

Fraser, A., Fearon, U., Reece, R., Emery, P., & Veale, D. J. (2001). Matrix metalloproteinase 9, apoptosis, and vascular morphology in early arthritis. *Arthritis & Rheumatism: Official Journal of the American College of Rheumatology, 44*(9), 2024-2028.

Freeman, M. A. R. (1979). *Adult articular cartilage*: Pitman Medical.

Freeman, M. R., Schneck, F. X., Gagnon, M. L., Corless, C., Soker, S., Niknejad, K., Peoples, G. E., & Klagsbrun, M. (1995). Peripheral blood T lymphocytes and lymphocytes infiltrating human cancers express vascular endothelial growth factor: a potential role for T cells in angiogenesis. *Cancer research, 55*(18), 4140-4145.

Freund, J., Stern, E., & Pisani, T. (1947). Isoallergic encephalomyelitis and radiculitis in guinea pigs after one injection of brain and mycobacteria in water-in-oil emulsion. *The Journal of Immunology, 57*(2), 179-194.

Fromm, S., Cunningham, C., Dunne, M., Veale, D., Fearon, U., & Wade, S. (2019). Enhanced angiogenic function in response to fibroblasts from psoriatic arthritis synovium compared to rheumatoid arthritis. *Arthritis research & therapy, 21*(1), 1-11.

Fuerst, M., Bertrand, J., Lammers, L., Dreier, R., Echtermeyer, F., Nitschke, Y., Rutsch, F., Schäfer, F., Niggemeyer, O., & Steinhagen, J. (2009). Calcification of articular cartilage in human osteoarthritis. *Arthritis & Rheumatism, 60*(9), 2694-2703.

Fujii, M., Takeda, K., Imamura, T., Aoki, H., Sampath, T. K., Enomoto, S., Kawabata, M., Kato, M., Ichijo, H., & Miyazono, K. (1999). Roles of bone morphogenetic protein type I receptors and Smad proteins in osteoblast and chondroblast differentiation. *Molecular biology of the cell, 10*(11), 3801-3813.

Fukuvama, K., Douglas, S. D., Tuffanelli, D. L., & Epstein, W. L. (1970). Immunohistochemical method for localization of antibodies in cutaneous disease. *American Journal of Clinical Pathology, 54*(3), 410-418.

Funck-Brentano, T., Bouaziz, W., Marty, C., Geoffroy, V., Hay, E., & Cohen-Solal, M. (2014). Dkk-1–Mediated inhibition of Wnt signaling in bone ameliorates osteoarthritis in mice. *Arthritis & Rheumatology, 66*(11), 3028-3039.

Funnell, T., Tasaki, S., Oloumi, A., Araki, S., Kong, E., Yap, D., Nakayama, Y., Hughes, C. S., Cheng, S.-W. G., & Tozaki, H. (2017). CLK-dependent exon recognition and conjoined gene formation revealed with a novel small molecule inhibitor. *Nature communications, 8*(1), 7.

Gaj, T., Gersbach, C. A., & Barbas III, C. F. (2013). ZFN, TALEN, and CRISPR/Cas-based methods for genome engineering. *Trends in biotechnology, 31*(7), 397-405.

Gammons, M., Lucas, R., Dean, R., Coupland, S., Oltean, S., & Bates, D. (2014). Targeting SRPK1 to control VEGF-mediated tumour angiogenesis in metastatic melanoma. *British journal of cancer, 111*(3), 477-485.

Garces, S., Karis, E., Merrill, J. T., Askanase, A. D., Kalunian, K., Mo, M., & Milmont, C. E. (2023). Improving resource utilisation in SLE drug development through innovative trial design. *Lupus Science & Medicine, 10*(2).

Garcia, C. F., & Swerdlow, S. H. (2009). Best practices in contemporary diagnostic immunohistochemistry: panel approach to hematolymphoid proliferations. *Archives of pathology & laboratory medicine, 133*(5), 756-765.

Gauldie, S. D., McQueen, D. S., Clarke, C. J., & Chessell, I. P. (2004). A robust model of adjuvant-induced chronic unilateral arthritis in two mouse strains. *Journal of neuroscience methods, 139*(2), 281-291.

Gelse, K., Pfander, D., Obier, S., Knaup, K. X., Wiesener, M., Hennig, F. F., & Swoboda, B. (2008). Role of hypoxia-inducible factor 1alpha in the integrity of articular cartilage in murine knee joints. *Arthritis research & therapy, 10*(5), 1-12.

Genovese, M. C., Fleischmann, R., Combe, B., Hall, S., Rubbert-Roth, A., Zhang, Y., Zhou, Y., Mohamed, M.-E. F., Meerwein, S., & Pangan, A. L. (2018). Safety and efficacy of upadacitinib in patients with active rheumatoid arthritis refractory to biologic disease-modifying anti-rheumatic drugs (SELECT-BEYOND): a double-blind, randomised controlled phase 3 trial. *The Lancet, 391*(10139), 2513-2524.

Genovese, M. C., Weinblatt, M. E., Aelion, J. A., Mansikka, H. T., Peloso, P. M., Chen, K., Li, Y., Othman, A. A., Khatri, A., & Khan, N. S. (2018). ABT-122, a bispecific dual variable domain immunoglobulin targeting tumor necrosis factor and interleukin-17a, in patients with rheumatoid arthritis with an inadequate response to methotrexate: a randomized, double-blind study. *Arthritis & Rheumatology, 70*(11), 1710-1720.

George, A., Aubol, B. E., Fattet, L., & Adams, J. A. (2019). Disordered protein interactions for an ordered cellular transition: Cdc2-like kinase 1 is transported to the nucleus via its Ser–Arg protein substrate. *Journal of Biological Chemistry, 294*(24), 9631-9641.

Gerber, H.-P., McMurtrey, A., Kowalski, J., Yan, M., Keyt, B. A., Dixit, V., & Ferrara, N. (1998). Vascular endothelial growth factor regulates endothelial cell survival through the phosphatidylinositol 3′-kinase/Akt signal transduction pathway: requirement for Flk-1/KDR activation. *Journal of Biological Chemistry, 273*(46), 30336-30343.

Gerber, H.-P., Vu, T. H., Ryan, A. M., Kowalski, J., Werb, Z., & Ferrara, N. (1999). VEGF couples hypertrophic cartilage remodeling, ossification and angiogenesis during endochondral bone formation. *Nature medicine, 5*(6), 623-628.

Gerstner, E. R., Eichler, A. F., Plotkin, S. R., Drappatz, J., Doyle, C. L., Xu, L., Duda, D. G., Wen, P. Y., Jain, R. K., & Batchelor, T. T. (2011). Phase I trial with biomarker studies of vatalanib (PTK787) in patients with newly diagnosed glioblastoma treated with enzyme inducing anti-epileptic drugs and standard radiation and temozolomide. *Journal of neuro-oncology, 103*(2), 325-332.

Gerwin, N., Bendele, A., Glasson, S., & Carlson, C. (2010). The OARSI histopathology initiative–recommendations for histological assessments of osteoarthritis in the rat. *Osteoarthritis and cartilage, 18*, S24-S34.

Giancotti, F. G., & Ruoslahti, E. (1999). Integrin signaling. *Science, 285*(5430), 1028-1033.

Giannakouros, T., Nikolakaki, E., Mylonis, I., & Georgatsou, E. (2011). Serine-arginine protein kinases: a small protein kinase family with a large cellular presence. *The FEBS journal, 278*(4), 570-586.

Giatromanolaki, A., Sivridis, E., Athanassou, N., Zois, E., Thorpe, P. E., Brekken, R. A., Gatter, K. C., Harris, A. L., Koukourakis, I. M., & Koukourakis, M. I. (2001). The angiogenic pathway 'vascular endothelial growth factor/flk-1 (KDR)-receptor'in rheumatoid arthritis and osteoarthritis. *The Journal of Pathology: A Journal of the Pathological Society of Great Britain and Ireland, 194*(1), 101-108.

Giatromanolaki, A., Sivridis, E., Maltezos, E., Athanassou, N., Papazoglou, D., Gatter, K. C., Harris, A. L., & Koukourakis, M. I. (2003). Upregulated hypoxia inducible factor-1α and-2α pathway in rheumatoid arthritis and osteoarthritis. *Arthritis Res Ther, 5*(4), 1-9.

Gibbs, J. B. (2000). Mechanism-based target identification and drug discovery in cancer research. *Science, 287*(5460), 1969-1973.

Gibofsky, A. (2014). Epidemiology, pathophysiology, and diagnosis of rheumatoid arthritis: A Synopsis. *The American Journal of managed care, 20*(7 Suppl), S128-135.

Giraudo, E., Primo, L., Audero, E., Gerber, H.-P., Koolwijk, P., Soker, S., Klagsbrun, M., Ferrara, N., & Bussolino, F. (1998). Tumor necrosis factor-α regulates expression of vascular endothelial growth factor receptor-2 and of its co-receptor neuropilin-1 in human vascular endothelial cells. *Journal of Biological Chemistry, 273*(34), 22128-22135.

Glasson, S., Blanchet, T., & Morris, E. (2007). The surgical destabilization of the medial meniscus (DMM) model of osteoarthritis in the 129/SvEv mouse. *Osteoarthritis and Cartilage, 15*(9), 1061-1069.

Goekoop-Ruiterman, Y. d., de Vries-Bouwstra, J., Allaart, C., Van Zeben, D., Kerstens, P., Hazes, J., Zwinderman, A., Ronday, H., Han, K., & Westedt, M. (2005). Clinical and radiographic outcomes of four different treatment strategies in patients with early rheumatoid arthritis (the BeSt study): a randomized, controlled trial. *Arthritis & Rheumatism, 52*(11), 3381-3390.

Goetzen, M., Hofmann-Fliri, L., Arens, D., Zeiter, S., Stadelmann, V., Nehrbass, D., Richards, R. G., & Blauth, M. (2015). Does metaphyseal cement augmentation in fracture management influence the adjacent subchondral bone and joint cartilage?: an in vivo study in sheep stifle joints. *Medicine, 94*(3).

Goldblatt, E. M., & Lee, W.-H. (2010). From bench to bedside: the growing use of translational research in cancer medicine. *American Journal of Translational Research, 2*(1), 1.

Goldring, M. B., Dayer, J.-M., & Goldring, S. R. (2016). Osteoarthritis and the Immune System. In *Osteoimmunology* (pp. 257-269): Elsevier.

Goldring, M. B., & Goldring, S. R. (2010). Articular cartilage and subchondral bone in the pathogenesis of osteoarthritis. *Annals of the New York academy of Sciences, 1192*(1), 230-237.

Goldring, S. R. (2002). Pathogenesis of bone erosions in rheumatoid arthritis. *Current opinion in rheumatology, 14*(4), 406-410.

Goldring, S. R. (2012). Alterations in periarticular bone and cross talk between subchondral bone and articular cartilage in osteoarthritis. *Therapeutic advances in musculoskeletal disease, 4*(4), 249-258.

Gomes, R. P., Bressan, E., Silva, T. M. d., Gevaerd, M. d. S., Tonussi, C. R., & Domenech, S. C. (2013). Standardization of an experimental model suitable for studies on the effect of exercise on arthritis. *Einstein (São Paulo), 11*, 76-82.

Gong, L., Song, J., Lin, X., Wei, F., Zhang, C., Wang, Z., Zhu, J., Wu, S., Chen, Y., & Liang, J. (2016). Serine-arginine protein kinase 1 promotes a cancer stem cell-like phenotype through activation of Wnt/β-catenin signalling in NSCLC. *The Journal of pathology, 240*(2), 184-196.

Gong, Y., Huang, T., Yu, Q., Liu, B., Wang, J., Wang, Z., & Huang, X. (2021). Sorafenib suppresses proliferation rate of fibroblast-like synoviocytes through the arrest of cell cycle in experimental adjuvant arthritis. *Journal of Pharmacy and Pharmacology, 73*(1), 32-39.

Goodison, S., Urquidi, V., & Tarin, D. (1999). CD44 cell adhesion molecules. *Molecular Pathology, 52*(4), 189.

Gordan, J. D., Lal, P., Dondeti, V. R., Letrero, R., Parekh, K. N., Oquendo, C. E., Greenberg, R. A., Flaherty, K. T., Rathmell, W. K., & Keith, B. (2008). HIF-α effects on c-Myc distinguish two subtypes of sporadic VHL-deficient clear cell renal carcinoma. *Cancer cell, 14*(6), 435-446.

Goyal, N., Gupta, M., Joshi, K., & Nagi, O. N. (2010). Immunohistochemical analysis of ageing and osteoarthritic articular cartilage. *Journal of molecular histology, 41*(4), 193-197.

Gözel, N., Çakirer, M., Karataş, A., Tuzcu, M., Özdemir, F. A., Dağli, A. F., Şahin, K., & Koca, S. S. (2018). Sorafenib reveals anti-arthritic potentials in collagen induced experimental arthritis model. *Archives of Rheumatology, 33*(3), 309.

Gravallese, E. M., Harada, Y., Wang, J.-T., Gorn, A. H., Thornhill, T. S., & Goldring, S. R. (1998). Identification of cell types responsible for bone resorption in rheumatoid arthritis and juvenile rheumatoid arthritis. *The American journal of pathology, 152*(4), 943.

Gravallese, E. M., Manning, C., Tsay, A., Naito, A., Pan, C., Amento, E., & Goldring, S. R. (2000). Synovial tissue in rheumatoid arthritis is a source of osteoclast differentiation factor. *Arthritis & Rheumatism: Official Journal of the American College of Rheumatology, 43*(2), 250-258.

Gregersen, P. K., Silver, J., & Winchester, R. J. (1987). The shared epitope hypothesis. An approach to understanding the molecular genetics of susceptibility to rheumatoid arthritis. *Arthritis & Rheumatism: Official Journal of the American College of Rheumatology, 30*(11), 1205-1213.

Grimaldi, C. M. (2006). Sex and systemic lupus erythematosus: the role of the sex hormones oestrogen and prolactin on the regulation of autoreactive B cells. *Current opinion in rheumatology, 18*(5), 456-461.

Grimshaw, M., & Mason, R. (2000). Bovine articular chondrocyte function in vitro depends upon oxygen tension. *Osteoarthritis and cartilage, 8*(5), 386-392.

Grisar, J., Munk, M., Steiner, C., Amoyo-Minar, L., Tohidast-Akrad, M., Zenz, P., Steiner, G., & Smolen, J. (2012). Expression patterns of CD44 and CD44 splice variants in patients with rheumatoid arthritis. *Clinical and Experimental Rheumatology-Incl Supplements, 30*(1), 64.

Grosios, K., Wood, J., Esser, R., Raychaudhuri, A., & Dawson, J. (2004). Angiogenesis inhibition by the novel VEGF receptor tyrosine kinase inhibitor, PTK787/ZK222584, causes significant anti-arthritic effects in models of rheumatoid arthritis. *Inflammation Research, 53*(4), 133-142.

Grosios, K., Wood, J., Esser, R., Raychaudhuri, A., & Dawson, J. (2004). Angiogenesis inhibition by the novel VEGF receptor tyrosine kinase inhibitor, PTK787/ZK222584, causes significant anti-arthritic effects in models of rheumatoid arthritis. *Inflammation Research, 53*, 133-142.

Grünewald, F. S., Prota, A. E., Giese, A., & Ballmer-Hofer, K. (2010). Structure–function analysis of VEGF receptor activation and the role of coreceptors in angiogenic signaling. *Biochimica et Biophysica Acta (BBA)-Proteins and Proteomics, 1804*(3), 567-580.

Grunke, M., & Schulze-Koops, H. (2006). Successful treatment of inflammatory knee osteoarthritis with tumour necrosis factor blockade. *Annals of the rheumatic diseases, 65*(4), 555-556.

Gu, H., Marth, J. D., Orban, P. C., Mossmann, H., & Rajewsky, K. (1994). Deletion of a DNA polymerase β gene segment in T cells using cell type-specific gene targeting. *Science, 265*(5168), 103-106.

Guaiquil, V. H., Pan, Z., Karagianni, N., Fukuoka, S., Alegre, G., & Rosenblatt, M. I. (2014). VEGF-B selectively regenerates injured peripheral neurons and restores sensory and trophic functions. *Proceedings of the National Academy of Sciences, 111*(48), 17272-17277.

Guan, Y., You, H., Cai, J., Zhang, Q., Yan, S., & You, R. (2020). Physically crosslinked silk fibroin/hyaluronic acid scaffolds. *Carbohydrate polymers, 239*, 116232.

Gubbels Bupp, M. R., & Jorgensen, T. N. (2018). Androgen-induced immunosuppression. *Frontiers in Immunology, 9*, 794.

Guerrero, J., Rojas, J. A. B., & Ballesteros, G. E. B. (2023). Immunohistochemistry in oral and maxillofacial pathology: The role and rational use of antibodies in the diagnosis of surgical lesions. *Revista Estomatología, 31*(1).

Gunschmann, C., Chiticariu, E., Garg, B., Hiz, M. M., Mostmans, Y., Wehner, M., & Scharfenberger, L. (2014). Transgenic mouse technology in skin biology: inducible gene knockout in mice. *The Journal of investigative dermatology, 134*(7), e22.

Guo, Q., Wang, Y., Xu, D., Nossent, J., Pavlos, N. J., & Xu, J. (2018). Rheumatoid arthritis: pathological mechanisms and modern pharmacologic therapies. *Bone research, 6*(1), 15.

Guo, X., Zhang, D., Zhang, X., Jiang, J., Xue, P., Wu, C., Zhang, J., Jin, G., Huang, Z., & Yang, J. (2018). Dyrk1A promotes the proliferation, migration and invasion of fibroblast-like synoviocytes in rheumatoid arthritis via down-regulating Spry2 and activating the ERK MAPK pathway. *Tissue and Cell, 55*, 63-70.

Gupta, R. M., & Musunuru, K. (2014). Expanding the genetic editing tool kit: ZFNs, TALENs, and CRISPR-Cas9. *The Journal of clinical investigation, 124*(10), 4154-4161.

Haight, E. S., Forman, T. E., Cordonnier, S. A., James, M. L., & Tawfik, V. L. (2019). Microglial modulation as a target for chronic pain: from the bench to the bedside and back. *Anesthesia and analgesia, 128*(4), 737.

Hallett, S. A., Ono, W., & Ono, N. (2021). The hypertrophic chondrocyte: To be or not to be. *Histology and histopathology, 36*(10), 1021.

Hamada, T., Torikai, M., Kuwazuru, A., Tanaka, M., Horai, N., Fukuda, T., Yamada, S., Nagayama, S., Hashiguchi, K., & Sunahara, N. (2008). Extracellular high mobility group box chromosomal protein 1 is a coupling factor for hypoxia and inflammation in arthritis. *Arthritis & Rheumatism, 58*(9), 2675-2685.

Hamilton, J. L., Nagao, M., Levine, B. R., Chen, D., Olsen, B. R., & Im, H. J. (2016). Targeting VEGF and its receptors for the treatment of osteoarthritis and associated pain. *Journal of Bone and Mineral Research, 31*(5), 911-924.

Han, S., Tan, C., Ding, J., Wang, J., Ma'ayan, A., & Gouon-Evans, V. (2018). Endothelial cells instruct liver specification of embryonic stem cell-derived endoderm through endothelial VEGFR2 signaling and endoderm epigenetic modifications. *Stem Cell Research, 30*, 163-170.

Hang, A., Feldman, S., Amin, A. P., Ochoa, J. A. R., & Park, S. S. (2023). Intravitreal Anti-Vascular Endothelial Growth Factor Therapies for Retinal Disorders. *Pharmaceuticals, 16*(8), 1140.

Harada, K. M., Hiroshi Yoshida, Shotaro Sakisaka, Eitaro Taniguchi, Takumi Kawaguchi, Mamoru Ariyoshi, Tomohisa Saiki, Masaharu Sakamoto, Kensei Nagata, Michio Sata, Katsuhiko Matsuo, Kyuichi Tanikawa, Masaru. (1998). Vascular endothelial growth factor in patients with rheumatoid arthritis. *Scandinavian journal of rheumatology, 27*(5), 377-380.

Haraldsen, G., Kvale, D., Lien, B., Farstad, I. N., & Brandtzaeg, P. (1996). Cytokine-regulated expression of E-selectin, intercellular adhesion molecule-1 (ICAM-1), and vascular cell adhesion molecule-1 (VCAM-1) in human microvascular endothelial cells. *Journal of immunology (Baltimore, Md.: 1950), 156*(7), 2558-2565.

Haraoui, B., & Bykerk, V. (2007). Etanercept in the treatment of rheumatoid arthritis. *Therapeutics and clinical risk management, 3*(1), 99.

Harper, S. J., & Bates, D. O. (2008). VEGF-A splicing: the key to anti-angiogenic therapeutics? *Nature Reviews Cancer, 8*(11), 880-887.

Harris, A. L. (2002). Hypoxia—a key regulatory factor in tumour growth. *Nature Reviews Cancer, 2*(1), 38-47.

Harris, H., Wolk, A., Larsson, A., Vasson, M.-P., & Basu, S. (2016). Soluble vascular endothelial growth factor receptors 2 (sVEGFR-2) and 3 (sVEGFR-3) and breast cancer risk in the Swedish Mammography Cohort. *International Journal of Molecular Epidemiology and Genetics, 7*(1), 81.

Harris Jr, E. D. (1990). Rheumatoid arthritis: pathophysiology and implications for therapy. *New England journal of medicine, 322*(18), 1277-1289.

Hartmann, A. M., Rujescu, D., Giannakouros, T., Nikolakaki, E., Goedert, M., Mandelkow, E.-M., Gao, Q. S., Andreadis, A., & Stamm, S. (2001). Regulation of alternative splicing of human tau exon 10 by phosphorylation of splicing factors. *Molecular and Cellular Neuroscience, 18*(1), 80-90.

Hashimoto, S., Creighton-Achermann, L., Takahashi, K., Amiel, D., Coutts, R., & Lotz, M. (2002). Development and regulation of osteophyte formation during experimental osteoarthritis. *Osteoarthritis and cartilage, 10*(3), 180-187.

Hasimbegovic, E., Schweiger, V., Kastner, N., Spannbauer, A., Traxler, D., Lukovic, D., Gyöngyösi, M., & Mester-Tonczar, J. (2021). Alternative splicing in cardiovascular disease—a survey of recent findings. *Genes, 12*(9), 1457.

Hatcher, J. M., Wu, G., Zeng, C., Zhu, J., Meng, F., Patel, S., Wang, W., Ficarro, S. B., Leggett, A. L., & Powell, C. E. (2018). SRPKIN-1: a covalent SRPK1/2 inhibitor that potently converts VEGF from pro-angiogenic to anti-angiogenic isoform. *Cell chemical biology, 25*(4), 460-470. e466.

Hawkins, P., Armstrong, R., Boden, T., Garside, P., Knight, K., Lilley, E., Seed, M., Wilkinson, M., & Williams, R. O. (2015). Applying refinement to the use of mice and rats in rheumatoid arthritis research. *Inflammopharmacology, 23*, 131-150.

Hawley, S., Edwards, C. J., Arden, N. K., Delmestri, A., Cooper, C., Judge, A., & Prieto-Alhambra, D. (2020). *Descriptive epidemiology of hip and knee replacement in rheumatoid arthritis: an analysis of UK electronic medical records.* Paper presented at the Seminars in Arthritis and Rheumatism.

Hayes, G. M., Carrigan, P. E., & Miller, L. J. (2007). Serine-arginine protein kinase 1 overexpression is associated with tumorigenic imbalance in mitogen-activated protein kinase pathways in breast, colonic, and pancreatic carcinomas. *Cancer research, 67*(5), 2072-2080.

Hayman, S. R., Leung, N., Grande, J. P., & Garovic, V. D. (2012). VEGF inhibition, hypertension, and renal toxicity. *Current oncology reports, 14*, 285-294.

Haywood, L., McWilliams, D., Pearson, C., Gill, S., Ganesan, A., Wilson, D., & Walsh, D. (2003). Inflammation and angiogenesis in osteoarthritis. *Arthritis & Rheumatism: Official Journal of the American College of Rheumatology, 48*(8), 2173-2177.

Haywood, L., & Walsh, D. (2001). Vasculature of the normal and arthritic synovial joint. *Histology and histopathology, 16*(1), 277-284.

He, C., Liu, B., Wang, H.-Y., Wu, L., Zhao, G., Huang, C., Liu, Y., Shan, B., & Liu, L. (2022). Inhibition of SRPK1, a key splicing regulator, exhibits antitumor and chemotherapeutic-sensitizing effects on extranodal NK/T-cell lymphoma cells. *BMC cancer, 22*(1), 1-13.

He, K., Cui, B., Li, G., Wang, H., Jin, K., & Teng, L. (2012). The effect of anti-VEGF drugs (bevacizumab and aflibercept) on the survival of patients with metastatic colorectal cancer (mCRC). *OncoTargets and therapy*, 59-65.

Hegen, M., Keith, J. C., Collins, M., & Nickerson-Nutter, C. L. (2008). Utility of animal models for identification of potential therapeutics for rheumatoid arthritis. *Annals of the rheumatic diseases, 67*(11), 1505-1515.

Hernandez, G. L., Volpert, O. V., Íñiguez, M. A., Lorenzo, E., Martínez-Martínez, S., Grau, R., Fresno, M., & Redondo, J. M. (2001). Selective inhibition of vascular endothelial growth factor–mediated angiogenesis by cyclosporin A: roles of the nuclear factor of activated T cells and cyclooxygenase 2. *The Journal of experimental medicine, 193*(5), 607-620.

Herrlich, P., Zoller, M., Pals, S. T., & Ponta, H. (1993). CD44 splice variants: metastases meet lymphocytes. *Immunology today, 14*(8), 395-399.

Hervé, M.-A., Buteau-Lozano, H., Mourah, S., Calvo, F., & Perrot-Applanat, M. (2005). VEGF189 stimulates endothelial cells proliferation and migration in vitro and up-

regulates the expression of Flk-1/KDR mRNA. *Experimental cell research, 309*(1), 24-31.

Hess-Stumpp, H., Haberey, M., & Thierauch, K. H. (2005). PTK 787/ZK 222584, a tyrosine kinase inhibitor of all known VEGF receptors, represses tumor growth with high efficacy. *Chembiochem, 6*(3), 550-557.

Hess, A., Axmann, R., Rech, J., Finzel, S., Heindl, C., Kreitz, S., Sergeeva, M., Saake, M., Garcia, M., & Kollias, G. (2011). Blockade of TNF-α rapidly inhibits pain responses in the central nervous system. *Proceedings of the National Academy of Sciences, 108*(9), 3731-3736.

Hewitt, K. M., & Stringer, M. D. (2008). Correlation between the surface area of synovial membrane and the surface area of articular cartilage in synovial joints of the mouse and human. *Surgical and Radiologic Anatomy, 30*(8), 645-651.

Hewitt, K. M., & Stringer, M. D. (2008). Correlation between the surface area of synovial membrane and the surface area of articular cartilage in synovial joints of the mouse and human. *Surgical and Radiologic Anatomy, 30*, 645-651.

Hino, K., Maeda, T., Sekiguchi, K., Shiozawa, K., Hirano, H., Sakashita, E., & Shiozawa, S. (1996). Adherence of synovial cells on EDA-containing fibronectin. *Arthritis & Rheumatism: Official Journal of the American College of Rheumatology, 39*(10), 1685-1692.

Hirata, M., Kugimiya, F., Fukai, A., Saito, T., Yano, F., Ikeda, T., Mabuchi, A., Sapkota, B. R., Akune, T., & Nishida, N. (2012). C/EBPβ and RUNX2 cooperate to degrade cartilage with MMP-13 as the target and HIF-2α as the inducer in chondrocytes. *Human molecular genetics, 21*(5), 1111-1123.

Hiratsuka, S., Minowa, O., Kuno, J., Noda, T., & Shibuya, M. (1998). Flt-1 lacking the tyrosine kinase domain is sufficient for normal development and angiogenesis in mice. *Proceedings of the National Academy of Sciences, 95*(16), 9349-9354.

Hitchon, C., Wong, K., Ma, G., Reed, J., Lyttle, D., & El-Gabalawy, H. (2002). Hypoxia-induced production of stromal cell–derived factor 1 (CXCL12) and vascular endothelial growth factor by synovial fibroblasts. *Arthritis & Rheumatism, 46*(10), 2587-2597.

Hochberg, M. C., Johnston, S. S., & John, A. K. (2008). The incidence and prevalence of extra-articular and systemic manifestations in a cohort of newly-diagnosed patients with rheumatoid arthritis between 1999 and 2006. *Current medical research and opinion, 24*(2), 469-480.

Hodax, J. K., Quintos, J. B., Gruppuso, P. A., Chen, Q., Desai, S., & Jayasuriya, C. T. (2019). Aggrecan is required for chondrocyte differentiation in ATDC5 chondroprogenitor cells. *PloS one, 14*(6), e0218399.

Hoeben, A., Landuyt, B., Highley, M. S., Wildiers, H., Van Oosterom, A. T., & De Bruijn, E. A. (2004). Vascular endothelial growth factor and angiogenesis. *Pharmacological reviews, 56*(4), 549-580.

Holash, J., Davis, S., Papadopoulos, N., Croll, S. D., Ho, L., Russell, M., Boland, P., Leidich, R., Hylton, D., & Burova, E. (2002). VEGF-Trap: a VEGF blocker with potent antitumor effects. *Proceedings of the National Academy of Sciences, 99*(17), 11393-11398.

Holmes, K., Roberts, O. L., Thomas, A. M., & Cross, M. J. (2007). Vascular endothelial growth factor receptor-2: structure, function, intracellular signalling and therapeutic inhibition. *Cellular signalling, 19*(10), 2003-2012.

Holmqvist, K., Cross, M. J., Rolny, C., Hägerkvist, R., Rahimi, N., Matsumoto, T., Claesson-Welsh, L., & Welsh, M. (2004). The adaptor protein shb binds to tyrosine 1175 in vascular endothelial growth factor (VEGF) receptor-2 and regulates VEGF-dependent cellular migration. *Journal of Biological Chemistry, 279*(21), 22267-22275.

Hong, B.-K., You, S., Yoo, S.-A., Park, D., Hwang, D., Cho, C.-S., & Kim, W.-U. (2017). MicroRNA-143 and-145 modulate the phenotype of synovial fibroblasts in rheumatoid arthritis. *Experimental & Molecular Medicine, 49*(8), e363-e363.

HONNER, R., & THOMPSON, R. C. (1971). The Nutritional Pathways of Articular Cartilage: AN AUTORADIOGRAPHIC STUDY IN RABBITS USING: 35: S INJECTED INTRAVENOUSLY. *JBJS, 53*(4), 742-748.

Honorati, M. C., Cattini, L., & Facchini, A. (2004). IL-17, IL-1β and TNF-α stimulate VEGF production by dedifferentiated chondrocytes. *Osteoarthritis and cartilage, 12*(9), 683-691.

Honorati, M. C., Neri, S., Cattini, L., & Facchini, A. (2006). Interleukin-17, a regulator of angiogenic factor release by synovial fibroblasts. *Osteoarthritis and cartilage, 14*(4), 345-352.

Horiuchi, T., Mitoma, H., Harashima, S.-i., Tsukamoto, H., & Shimoda, T. (2010). Transmembrane TNF-α: structure, function and interaction with anti-TNF agents. *Rheumatology, 49*(7), 1215-1228.

Horner, A., Bishop, N., Bord, S., Beeton, C., Kelsall, A., Coleman, N., & Compston, J. (1999). Immunolocalisation of vascular endothelial growth factor (VEGF) in human neonatal growth plate cartilage. *The Journal of Anatomy, 194*(4), 519-524.

Horner, H. A., & Urban, J. P. (2001). 2001 Volvo Award Winner in Basic Science Studies: effect of nutrient supply on the viability of cells from the nucleus pulposus of the intervertebral disc. *Spine, 26*(23), 2543-2549.

Hou, L., Tang, Y., Xu, M., Gao, Z., & Tang, D. (2014). Tyramine-based enzymatic conjugate repeats for ultrasensitive immunoassay accompanying tyramine signal amplification with enzymatic biocatalytic precipitation. *Analytical chemistry, 86*(16), 8352-8358.

Houck, K. A., Ferrara, N., Winer, J., Cachianes, G., Li, B., & Leung, D. W. (1991). The vascular endothelial growth factor family: identification of a fourth molecular species and characterization of alternative splicing of RNA. *Molecular endocrinology, 5*(12), 1806-1814.

Houck, K. A., Leung, D., Rowland, A., Winer, J., & Ferrara, N. (1992). Dual regulation of vascular endothelial growth factor bioavailability by genetic and proteolytic mechanisms. *Journal of Biological Chemistry, 267*(36), 26031-26037.

Hoyland, J. A., Thomas, J., Donn, R., Marriott, A., Ayad, S., Boot-Handford, R., Grant, M., & Freemont, A. (1991). Distribution of type X collagen mRNA in normal and osteoarthritic human cartilage. *Bone and mineral, 15*(2), 151-163.

Hu, S., Zhang, C., Ni, L., Huang, C., Chen, D., Shi, K., Jin, H., Zhang, K., Li, Y., & Xie, L. (2020). Stabilization of HIF-1α alleviates osteoarthritis via enhancing mitophagy. *Cell Death & Disease, 11*(6), 481.

Hu, X.-X., Wu, Y.-j., Zhang, J., & Wei, W. (2019). T-cells interact with B cells, dendritic cells, and fibroblast-like synoviocytes as hub-like key cells in rheumatoid arthritis. *International immunopharmacology, 70*, 428-434.

Huang, K., Andersson, C., Roomans, G. M., Ito, N., & Claesson-Welsh, L. (2001). Signaling properties of VEGF receptor-1 and-2 homo-and heterodimers. *The international journal of biochemistry & cell biology, 33*(4), 315-324.

Huang, Q.-Q., Sobkoviak, R., Jockheck-Clark, A. R., Shi, B., Mandelin, A. M., Tak, P. P., Haines, G. K., Nicchitta, C. V., & Pope, R. M. (2009). Heat shock protein 96 is elevated in rheumatoid arthritis and activates macrophages primarily via TLR2 signaling. *The Journal of Immunology, 182*(8), 4965-4973.

Huang, X., He, Y., Han, J., Zhuang, J., He, J., & Sun, E. (2019). Not only anti-inflammation, etanercept abrogates collagen-induced arthritis by inhibiting dendritic cell migration and maturation. *Central European Journal of Immunology, 44*(3), 237-245.

Huber, L., Distler, O., Tarner, I., Gay, R., Gay, S., & Pap, T. (2006). Synovial fibroblasts: key players in rheumatoid arthritis. *Rheumatology, 45*(6), 669-675.

Hudson, N., Powner, M. B., Sarker, M. H., Burgoyne, T., Campbell, M., Ockrim, Z. K., Martinelli, R., Futter, C. E., Grant, M. B., & Fraser, P. A. (2014). Differential apicobasal VEGF signaling at vascular blood-neural barriers. *Developmental cell, 30*(5), 541-552.

Hughes, G. C. (2012). Progesterone and autoimmune disease. *Autoimmunity reviews, 11*(6-7), A502-A514.

Huh, J.-E., Seo, D.-M., Baek, Y.-H., Choi, D.-Y., Park, D.-S., & Lee, J.-D. (2010). Biphasic positive effect of formononetin on metabolic activity of human normal and osteoarthritic subchondral osteoblasts. *International immunopharmacology, 10*(4), 500-507.

Huh, Y. H., Lee, G., Song, W.-H., Koh, J.-T., & Ryu, J.-H. (2015). Crosstalk between FLS and chondrocytes is regulated by HIF-2α-mediated cytokines in arthritis. *Experimental & Molecular Medicine, 47*(12), e197-e197.

Hulse, R., Beazley-Long, N., Hua, J., Kennedy, H., Prager, J., Bevan, H., Qiu, Y., Fernandes, E., Gammons, M., & Ballmer-Hofer, K. (2014). Regulation of alternative VEGF-A mRNA splicing is a therapeutic target for analgesia. *Neurobiology of disease, 71*, 245-259.

Hulse, R. P. (2017). Role of VEGF-A in chronic pain. *Oncotarget, 8*(7), 10775.

Hulse, R. P., Beazley-Long, N., Ved, N., Bestall, S. M., Riaz, H., Singhal, P., Ballmer Hofer, K., Harper, S. J., Bates, D. O., & Donaldson, L. F. (2015). Vascular endothelial growth factor-A165b prevents diabetic neuropathic pain and sensory neuronal degeneration. *Clinical science, 129*(8), 741-756.

Hulse, R. P., Drake, R. A., Bates, D. O., & Donaldson, L. F. (2016). The control of alternative splicing by SRSF1 in myelinated afferents contributes to the development of neuropathic pain. *Neurobiology of disease, 96*, 186-200.

Hwang, H. S., & Kim, H. A. (2015). Chondrocyte apoptosis in the pathogenesis of osteoarthritis. *International Journal of Molecular Sciences, 16*(11), 26035-26054.

Ibáñez-Costa, A., Perez-Sanchez, C., Patiño-Trives, A. M., Luque-Tevar, M., Font, P., de la Rosa, I. A., Roman-Rodriguez, C., Abalos-Aguilera, M. C., Conde, C., & Gonzalez, A. (2022). Splicing machinery is impaired in rheumatoid arthritis, associated with disease activity and modulated by anti-TNF therapy. *Annals of the rheumatic diseases, 81*(1), 56-67.

Ikeda, E. (2005). Cellular response to tissue hypoxia and its involvement in disease progression. *Pathology international, 55*(10), 603-610.

Ikeda, M., Hosoda, Y., Hirose, S., Okada, Y., & Ikeda, E. (2000). Expression of vascular endothelial growth factor isoforms and their receptors Flt-1, KDR, and neuropilin-1 in synovial tissues of rheumatoid arthritis. *The Journal of pathology, 191*(4), 426-433.

Imam, A. (1985). Application of immunohistochemical methods in the diagnosis of malignant disease. *Cancer Investigation, 3*(4), 339-359.

Imhof, H., Breitenseher, M., Kainberger, F., Rand, T., & Trattnig, S. (1999). Importance of subchondral bone to articular cartilage in health and disease. *Topics in magnetic resonance imaging, 10*(3), 180.

Imoukhuede, P., & Popel, A. S. (2011). Quantification and cell-to-cell variation of vascular endothelial growth factor receptors. *Experimental cell research, 317*(7), 955-965.

Imtiyaz, H. Z., & Simon, M. C. (2010). Hypoxia-inducible factors as essential regulators of inflammation. *Diverse Effects of Hypoxia on Tumor Progression*, 105-120.

Incannex. (2023). Phase II clinical trial of a novel cannabinoid combination product (IHL-675A) for treatment of rheumatoid arthritis. Retrieved from https://www.incannex.com/

Infusino, G. A., & Jacobson, J. R. (2012). Endothelial FAK as a therapeutic target in disease. *Microvascular research, 83*(1), 89-96.

Inglis, J. J., Nissim, A., Lees, D. M., Hunt, S. P., Chernajovsky, Y., & Kidd, B. L. (2005). The differential contribution of tumour necrosis factor to thermal and mechanical hyperalgesia during chronic inflammation. *Arthritis research & therapy, 7*(4), 1-10.

Inoue, K., Masuko-Hongo, K., Okamoto, M., & Nishioka, K. (2005). Induction of vascular endothelial growth factor and matrix metalloproteinase-3 (stromelysin) by interleukin-1 in human articular chondrocytes and synoviocytes. *Rheumatology international, 26*, 93-98.

Ishikawa, Y., & Terao, C. (2020). The impact of cigarette smoking on risk of rheumatoid arthritis: a narrative review. *Cells, 9*(2), 475.

Ishiwatari-Ogata, C., Kyuuma, M., Ogata, H., Yamakawa, M., Iwata, K., Ochi, M., Hori, M., Miyata, N., & Fujii, Y. (2022). Ozoralizumab, a humanized anti-TNFα NANOBODY® compound, exhibits efficacy not only at the onset of arthritis in a human TNF transgenic mouse but also during secondary failure of administration of an anti-TNFα IgG. *Frontiers in Immunology, 13*, 853008.

Ismail, C. A. N., Tan, D. C., Khir, N. A. M., & Shafin, N. (2022). A Review on Complete Freund's Adjuvant-Induced Arthritic Rat Model: Factors Leading to its Success. *IIUM Medical Journal Malaysia, 21*(4).

Ito, L. K., & Bishat, M. (1924). NUTRITION OF ARTICULAR CARTILAGE 31. *British Journal of Surgery: BJS., 12*, 31.

Iwai, K., Yaguchi, M., Nishimura, K., Yamamoto, Y., Tamura, T., Nakata, D., Dairiki, R., Kawakita, Y., Mizojiri, R., & Ito, Y. (2018). Anti-tumor efficacy of a novel CLK inhibitor via targeting RNA splicing and MYC-dependent vulnerability. *EMBO molecular medicine, 10*(6), e8289.

Iyer, S., & Acharya, K. R. (2011). Tying the knot: The cystine signature and molecular-recognition processes of the vascular endothelial growth factor family of angiogenic cytokines. *The FEBS journal, 278*(22), 4304-4322.

Jackson, A. R., & Gu, W. Y. (2009). Transport properties of cartilaginous tissues. *Current Rheumatology Reviews, 5*(1), 40-50.

Jackson, J., Minton, J., Ho, M., Wei, N., & Winkler, J. (1997). Expression of vascular endothelial growth factor in synovial fibroblasts is induced by hypoxia and interleukin 1beta. *The Journal of rheumatology, 24*(7), 1253-1259.

Jackson, J. R., Seed, M. P., Kircher, C. H., Willoughby, D. A., & Winkler, J. D. (1997). The codependence of angiogenesis and chronic inflammation. *The FASEB journal, 11*(6), 457-465.

Jain, R. K., Duda, D. G., Clark, J. W., & Loeffler, J. S. (2006). Lessons from phase III clinical trials on anti-VEGF therapy for cancer. *Nature clinical practice Oncology, 3*(1), 24-40.

Jakeman, L. B., Winer, J., Bennett, G., Altar, C., & Ferrara, N. (1992). Binding sites for vascular endothelial growth factor are localized on endothelial cells in adult rat tissues. *The Journal of clinical investigation, 89*(1), 244-253.

Jakubauskiene, E., Vilys, L., Makino, Y., Poellinger, L., & Kanopka, A. (2015). Increased serine-arginine (SR) protein phosphorylation changes pre-mRNA splicing in hypoxia. *Journal of Biological Chemistry, 290*(29), 18079-18089.

James, C. G., Appleton, C. T. G., Ulici, V., Underhill, T. M., & Beier, F. (2005). Microarray analyses of gene expression during chondrocyte differentiation identifies novel regulators of hypertrophy. *Molecular biology of the cell, 16*(11), 5316-5333.

Jani, P. H., Gibson, M. P., Liu, C., Zhang, H., Wang, X., Lu, Y., & Qin, C. (2016). Transgenic expression of Dspp partially rescued the long bone defects of Dmp1-null mice. *Matrix Biology, 52*, 95-112.

Jay, G. D., Britt, D. E., & Cha, C. J. (2000). Lubricin is a product of megakaryocyte stimulating factor gene expression by human synovial fibroblasts. *The Journal of rheumatology, 27*(3), 594-600.

Jenkins, W. T., Evans, S. M., & Koch, C. J. (2000). Hypoxia and necrosis in rat 9L glioma and Morris 7777 hepatoma tumors: comparative measurements using EF5 binding and the Eppendorf needle electrode. *International Journal of Radiation Oncology* Biology* Physics, 46*(4), 1005-1017.

Ji, Q., Zheng, Y., Zhang, G., Hu, Y., Fan, X., Hou, Y., Wen, L., Li, L., Xu, Y., & Wang, Y. (2019). Single-cell RNA-seq analysis reveals the progression of human osteoarthritis. *Annals of the rheumatic diseases, 78*(1), 100-110.

Jia, T., Jacquet, T., Dalonneau, F., Coudert, P., Vaganay, E., Exbrayat-Héritier, C., Vollaire, J., Josserand, V., Ruggiero, F., & Coll, J.-L. (2021). FGF-2 promotes angiogenesis through a SRSF1/SRSF3/SRPK1-dependent axis that controls VEGFR1 splicing in endothelial cells. *BMC biology, 19*, 1-26.

Jiang, A., Xu, P., Zhao, Z., Tan, Q., Sun, S., Song, C., & Leng, H. (2020). Identification of candidate genetic markers and a novel 4-genes diagnostic model in osteoarthritis through integrating multiple microarray data. *Combinatorial Chemistry & High Throughput Screening, 23*(8), 805-813.

Jiang, Q., Yang, G., Liu, Q., Wang, S., & Cui, D. (2021). Function and role of regulatory T cells in rheumatoid arthritis. *Frontiers in Immunology, 12*, 626193.

Jinnin, M., Medici, D., Park, L., Limaye, N., Liu, Y., Boscolo, E., Bischoff, J., Vikkula, M., Boye, E., & Olsen, B. R. (2008). Suppressed NFAT-dependent VEGFR1 expression and constitutive VEGFR2 signaling in infantile hemangioma. *Nature medicine, 14*(11), 1236-1246.

Joffe, I., & Epstein, S. (1991). *Osteoporosis associated with rheumatoid arthritis: pathogenesis and management.* Paper presented at the Seminars in arthritis and rheumatism.

Joukov, V., Pajusola, K., Kaipainen, A., Chilov, D., Lahtinen, I., Kukk, E., Saksela, O., Kalkkinen, N., & Alitalo, K. (1996). A novel vascular endothelial growth factor, VEGF-C, is a ligand for the Flt4 (VEGFR-3) and KDR (VEGFR-2) receptor tyrosine kinases. *The EMBO journal, 15*(2), 290-298.

Kahn, D. A., & Baltimore, D. (2010). Pregnancy induces a fetal antigen-specific maternal T regulatory cell response that contributes to tolerance. *Proceedings of the National Academy of Sciences, 107*(20), 9299-9304.

Kaipainen, A., Korhonen, J., Pajusola, K., Aprelikova, O., Persico, M., Terman, B., & Alitalo, K. (1993). The related FLT4, FLT1, and KDR receptor tyrosine kinases show distinct expression patterns in human fetal endothelial cells. *The Journal of experimental medicine, 178*(6), 2077-2088.

Kaipatur, N., Murshed, M., & McKee, M. (2008). Matrix Gla protein inhibition of tooth mineralization. *Journal of dental research, 87*(9), 839-844.

Kalamajski, S., Aspberg, A., Lindblom, K., Heinegård, D., & Oldberg, Å. (2009). Asporin competes with decorin for collagen binding, binds calcium and promotes osteoblast collagen mineralization. *Biochemical Journal, 423*(1), 53-59.

Kamal, R. M., Sabry, M. M., Aly, Z. Y., & Hifnawy, M. S. (2021). Phytochemical and in-vivo anti-arthritic significance of Aloe thraskii Baker in combined therapy with methotrexate in adjuvant-induced arthritis in rats. *Molecules, 26*(12), 3660.

Kamba, T., & McDonald, D. (2007). Mechanisms of adverse effects of anti-VEGF therapy for cancer. *British journal of cancer, 96*(12), 1788-1795.

Kanai, T., Kondo, N., Okada, M., Sano, H., Okumura, G., Kijima, Y., Ogose, A., Kawashima, H., & Endo, N. (2020). The JNK pathway represents a novel target in the treatment of rheumatoid arthritis through the suppression of MMP-3. *Journal of Orthopaedic Surgery and Research, 15*(1), 1-10.

Kaneko, M., Tomita, T., Nakase, T., Ohsawa, Y., Seki, H., Takeuchi, E., Takano, H., Shi, K., Takahi, K., & Kominami, E. (2001). Expression of proteinases and inflammatory cytokines in subchondral bone regions in the destructive joint of rheumatoid arthritis. *Rheumatology, 40*(3), 247-255.

Kanno, S., Oda, N., Abe, M., Terai, Y., Ito, M., Shitara, K., Tabayashi, K., Shibuya, M., & Sato, Y. (2000). Roles of two VEGF receptors, Flt-1 and KDR, in the signal transduction of VEGF effects in human vascular endothelial cells. *Oncogene, 19*(17), 2138-2146.

Karlson, E. W., Mandl, L. A., Hankinson, S. E., & Grodstein, F. (2004). Do breast-feeding and other reproductive factors influence future risk of rheumatoid arthritis?: Results from the Nurses' Health Study. *Arthritis & Rheumatism, 50*(11), 3458-3467.

Karmakar, S., Kay, J., & Gravallese, E. M. (2010). Bone damage in rheumatoid arthritis: mechanistic insights and approaches to prevention. *Rheumatic Disease Clinics, 36*(2), 385-404.

Karpanen, T., Bry, M., Ollila, H. M., Seppänen-Laakso, T., Liimatta, E., Leskinen, H., Kivelä, R., Helkamaa, T., Merentie, M., & Jeltsch, M. (2008). Overexpression of vascular endothelial growth factor-B in mouse heart alters cardiac lipid metabolism and induces myocardial hypertrophy. *Circulation research, 103*(9), 1018-1026.

Kasorn, A., Alcaide, P., Jia, Y., Subramanian, K. K., Sarraj, B., Li, Y., Loison, F., Hattori, H., Silberstein, L. E., & Luscinskas, W. F. (2009). Focal adhesion kinase regulates pathogen-killing capability and life span of neutrophils via mediating both adhesion-dependent and-independent cellular signals. *The Journal of Immunology, 183*(2), 1032-1043.

Kataoka, N., Bachorik, J. L., & Dreyfuss, G. (1999). Transportin-SR, a nuclear import receptor for SR proteins. *The Journal of cell biology, 145*(6), 1145-1152.

Katsuyama, T., Li, H., Comte, D., Tsokos, G. C., & Moulton, V. R. (2019). Splicing factor SRSF1 controls T cell hyperactivity and systemic autoimmunity. *The Journal of clinical investigation, 129*(12), 5411-5423.

Katuri, V., Gerber, S., Qiu, X., McCarty, G., Goldstein, S. D., Hammers, H., Montgomery, E., Chen, A. R., & Loeb, D. M. (2014). WT1 regulates angiogenesis in Ewing Sarcoma. *Oncotarget, 5*(9), 2436.

Kawamura, H., Li, X., Harper, S. J., Bates, D. O., & Claesson-Welsh, L. (2008). Vascular endothelial growth factor (VEGF)-A165b is a weak in vitro agonist for VEGF receptor-2 due to lack of coreceptor binding and deficient regulation of kinase activity. *Cancer research, 68*(12), 4683-4692.

Kelly, S., Dunham, J. P., & Donaldson, L. F. (2007). Sensory nerves have altered function contralateral to a monoarthritis and may contribute to the symmetrical spread of inflammation. *European Journal of Neuroscience, 26*(4), 935-942.

Kendall, R. L., Wang, G., & Thomas, K. A. (1996). Identification of a natural soluble form of the vascular endothelial growth factor receptor, FLT-1, and its heterodimerization with KDR. *Biochemical and biophysical research communications, 226*(2), 324-328.

Kennedy, A., Ng, C. T., Chang, T. C., Biniecka, M., O'Sullivan, J. N., Heffernan, E., Fearon, U., & Veale, D. J. (2011). Tumor necrosis factor blocking therapy alters joint inflammation and hypoxia. *Arthritis & Rheumatism, 63*(4), 923-932.

Keshwani, M. M., Aubol, B. E., Fattet, L., Ma, C.-T., Qiu, J., Jennings, P. A., Fu, X.-D., & Adams, J. A. (2015). Conserved proline-directed phosphorylation regulates SR protein conformation and splicing function. *Biochemical Journal, 466*(2), 311-322.

Keystone, E. C., Breedveld, F. C., van der Heijde, D., Landewé, R., Florentinus, S., Arulmani, U., Liu, S., Kupper, H., & Kavanaugh, A. (2014). Longterm effect of delaying combination therapy with tumor necrosis factor inhibitor in patients with aggressive early rheumatoid arthritis: 10-year efficacy and safety of adalimumab from the randomized controlled PREMIER trial with open-label extension. *The Journal of rheumatology, 41*(1), 5-14.

Kharlamova, N., Jiang, X., Sherina, N., Potempa, B., Israelsson, L., Quirke, A. M., Eriksson, K., Yucel-Lindberg, T., Venables, P. J., & Potempa, J. (2016). Antibodies to Porphyromonas gingivalis indicate interaction between oral infection, smoking, and risk genes in rheumatoid arthritis etiology. *Arthritis & Rheumatology, 68*(3), 604-613.

Kikuchi, R., Stevens, M., Harada, K., Oltean, S., & Murohara, T. (2019). Anti-angiogenic isoform of vascular endothelial growth factor-A in cardiovascular and renal disease. *Advances in clinical chemistry, 88*, 1-33.

Kim, H., Kim, M., Im, S.-K., & Fang, S. (2018). Mouse Cre-LoxP system: general principles to determine tissue-specific roles of target genes. *Laboratory animal research, 34*(4), 147-159.

Kim, H. R., Kim, K. W., Kim, B. M., Jung, H. G., Cho, M. L., & Lee, S. H. (2014). Reciprocal activation of CD4+ T cells and synovial fibroblasts by stromal cell–derived factor 1 promotes RANKL expression and osteoclastogenesis in rheumatoid arthritis. *Arthritis & Rheumatology, 66*(3), 538-548.

Kim, O. Y., Chae, J. S., Paik, J. K., Seo, H. S., Jang, Y., Cavaillon, J.-M., & Lee, J. H. (2012). Effects of aging and menopause on serum interleukin-6 levels and

peripheral blood mononuclear cell cytokine production in healthy nonobese women. *Age, 34*, 415-425.

Kim, W.-U., Kwok, S.-K., Hong, K.-H., Yoo, S.-A., Kong, J.-S., Choe, J., & Cho, C.-S. (2007). Soluble Fas ligand inhibits angiogenesis in rheumatoid arthritis. *Arthritis research & therapy, 9*(2), 1-9.

Kirsch, T., Swoboda, B., & Nah, H.-D. (2000). Activation of annexin II and V expression, terminal differentiation, mineralization and apoptosis in human osteoarthritic cartilage. *Osteoarthritis and cartilage, 8*(4), 294-302.

Kisanga, E. R., Mellgren, G., & Lien, E. A. (2005). Excretion of hydroxylated metabolites of tamoxifen in human bile and urine. *Anticancer research, 25*(6C), 4487-4492.

Kiselyov, A., Balakin, K. V., & Tkachenko, S. E. (2007). VEGF/VEGFR signalling as a target for inhibiting angiogenesis. *Expert opinion on investigational drugs, 16*(1), 83-107.

Kivelä, R., Bry, M., Robciuc, M. R., Räsänen, M., Taavitsainen, M., Silvola, J. M., Saraste, A., Hulmi, J. J., Anisimov, A., & Mäyränpää, M. I. (2014). VEGF-B-induced vascular growth leads to metabolic reprogramming and ischemia resistance in the heart. *EMBO molecular medicine, 6*(3), 307-321.

Kleinau, S., Erlandsson, H., Holmdahl, R., & Klareskog, L. (1991). Adjuvant oils induce arthritis in the DA rat. I. Characterization of the disease and evidence for an immunological involvement. *Journal of autoimmunity, 4*(6), 871-880.

Knudsen, L. S., Hetland, M. L., Johansen, J. S., Skjødt, H., Peters, N. D., Colic, A., Grau, K., Nielsen, H. J., & Østergaard, M. (2009). Changes in plasma IL-6, plasma VEGF and serum YKL-40 during treatment with etanercept and methotrexate or etanercept alone in patients with active rheumatoid arthritis despite methotrexate therapy. In: SAGE Publications Sage UK: London, England.

Knut, L. (2015). Radiosynovectomy in the therapeutic management of arthritis. *World Journal of Nuclear Medicine, 14*(01), 10-15.

Koch, A. E. (1998). Angiogenesis: implications for rheumatoid arthritis. *Arthritis & Rheumatism: Official Journal of the American College of Rheumatology, 41*(6), 951-962.

Koch, A. E., Harlow, L. A., Haines, G. K., Amento, E. P., Unemori, E. N., Wong, W. L., Pope, R. M., & Ferrara, N. (1994). Vascular endothelial growth factor. A cytokine modulating endothelial function in rheumatoid arthritis. *The Journal of Immunology, 152*(8), 4149-4156.

Koch, A. E., Harlow, L. A., Haines, G. K., Amento, E. P., Unemori, E. N., Wong, W. L., Pope, R. M., & Ferrara, N. (1994). Vascular endothelial growth factor. A cytokine modulating endothelial function in rheumatoid arthritis. *Journal of immunology (Baltimore, Md.: 1950), 152*(8), 4149-4156.

Koch, C., Evans, S., & Lord, E. (1995). Oxygen dependence of cellular uptake of EF5 [2-(2-nitro-1H-imidazol-1-yl)-N-(2, 2, 3, 3, 3-pentafluoropropyl) a cet amide]: analysis of drug adducts by fluorescent antibodies vs bound radioactivity. *British journal of cancer, 72*(4), 869-874.

Koch, C. J. (2008). Importance of antibody concentration in the assessment of cellular hypoxia by flow cytometry: EF5 and pimonidazole. *Radiation research, 169*(6), 677-688.

Koch, C. J., & Evans, S. M. (2015). *Optimizing hypoxia detection and treatment strategies.* Paper presented at the Seminars in nuclear medicine.

Koch, S., & Claesson-Welsh, L. (2012). Signal transduction by vascular endothelial growth factor receptors. *Cold Spring Harbor perspectives in medicine, 2*(7).

Köhler, G., & Milstein, C. (1975). Continuous cultures of fused cells secreting antibody of predefined specificity. *Nature, 256*(5517), 495-497.

Koizumi, J., Okamoto, Y., Onogi, H., Mayeda, A., Krainer, A. R., & Hagiwara, M. (1999). The subcellular localization of SF2/ASF is regulated by direct interaction with SR protein kinases (SRPKs). *Journal of Biological Chemistry, 274*(16), 11125-11131.

Kokkonen, H., Söderström, I., Rocklöv, J., Hallmans, G., Lejon, K., & Rantapää Dahlqvist, S. (2010). Up-regulation of cytokines and chemokines predates the onset of rheumatoid arthritis. *Arthritis & Rheumatism: Official Journal of the American College of Rheumatology, 62*(2), 383-391.

Komatsu, N., & Takayanagi, H. (2022). Mechanisms of joint destruction in rheumatoid arthritis—immune cell–fibroblast–bone interactions. *Nature Reviews Rheumatology, 18*(7), 415-429.

Kondo, N., Kuroda, T., & Kobayashi, D. (2021). Cytokine networks in the pathogenesis of rheumatoid arthritis. *International Journal of Molecular Sciences, 22*(20), 10922.

Kong, Y.-Y., Feige, U., Sarosi, I., Bolon, B., Tafuri, A., Morony, S., Capparelli, C., Li, J., Elliott, R., & McCabe, S. (1999). Activated T cells regulate bone loss and joint destruction in adjuvant arthritis through osteoprotegerin ligand. *Nature, 402*(6759), 304-309.

Kong, Y.-Y., Yoshida, H., Sarosi, I., Tan, H.-L., Timms, E., Capparelli, C., Morony, S., Oliveira-dos-Santos, A. J., Van, G., & Itie, A. (1999). OPGL is a key regulator of osteoclastogenesis, lymphocyte development and lymph-node organogenesis. *Nature, 397*(6717), 315-323.

Konig, M. F., Abusleme, L., Reinholdt, J., Palmer, R. J., Teles, R. P., Sampson, K., Rosen, A., Nigrovic, P. A., Sokolove, J., & Giles, J. T. (2016). Aggregatibacter actinomycetemcomitans–induced hypercitrullination links periodontal infection to autoimmunity in rheumatoid arthritis. *Science translational medicine, 8*(369), 369ra176-369ra176.

Konisti, S., Kiriakidis, S., & Paleolog, E. M. (2012). Hypoxia—a key regulator of angiogenesis and inflammation in rheumatoid arthritis. *Nature Reviews Rheumatology, 8*(3), 153-162.

Kono, M., Kurita, T., Yasuda, S., Kono, M., Fujieda, Y., Bohgaki, T., Katsuyama, T., Tsokos, G. C., Moulton, V. R., & Atsumi, T. (2018). Decreased expression of serine/arginine-rich splicing factor 1 in T Cells From patients with active systemic lupus erythematosus accounts for reduced expression of RasGRP1 and DNA methyltransferase 1. *Arthritis & Rheumatology, 70*(12), 2046-2056.

Konttinen, Y. T., Mandelin, J., Li, T. F., Salo, J., Lassus, J., Liljeström, M., Hukkanen, M., Takagi, M., Virtanen, I., & Santavirta, S. (2002). Acidic cysteine endoproteinase cathepsin K in the degeneration of the superficial articular hyaline cartilage in osteoarthritis. *Arthritis & Rheumatism: Official Journal of the American College of Rheumatology, 46*(4), 953-960.

Korb-Pap, A., Stratis, A., Mühlenberg, K., Niederreiter, B., Hayer, S., Echtermeyer, F., Stange, R., Zwerina, J., Pap, T., & Pavenstädt, H. (2012). Early structural changes in cartilage and bone are required for the attachment and invasion of inflamed synovial tissue during destructive inflammatory arthritis. *Annals of the rheumatic diseases, 71*(6), 1004-1011.

Korbecki, J., Simińska, D., Gąssowska-Dobrowolska, M., Listos, J., Gutowska, I., Chlubek, D., & Baranowska-Bosiacka, I. (2021). Chronic and cycling hypoxia: drivers of cancer chronic inflammation through HIF-1 and NF-κB activation: a review of the

molecular mechanisms. *International Journal of Molecular Sciences, 22*(19), 10701.

Kornblihtt, A. R., Schor, I. E., Alló, M., Dujardin, G., Petrillo, E., & Muñoz, M. J. (2013). Alternative splicing: a pivotal step between eukaryotic transcription and translation. *Nature reviews Molecular cell biology, 14*(3), 153-165.

Kou, H., Qing, Z., Zhao, G., Sun, X., Zhi, L., Wang, J., Chen, X., Guo, H., Zhang, R., & Ma, J. (2023). Effect of lorecivivint on osteoarthritis: A systematic review and meta-analysis. *Heliyon*.

Kovacs, B., Vajda, E., & Nagy, E. E. (2019). Regulatory effects and interactions of the Wnt and OPG-RANKL-RANK signaling at the bone-cartilage interface in osteoarthritis. *International Journal of Molecular Sciences, 20*(18), 4653.

Koziel, L., Kunath, M., Kelly, O. G., & Vortkamp, A. (2004). Ext1-dependent heparan sulfate regulates the range of Ihh signaling during endochondral ossification. *Developmental cell, 6*(6), 801-813.

Krause, M. L., & Makol, A. (2016). Management of rheumatoid arthritis during pregnancy: challenges and solutions. *Open access rheumatology: research and reviews*, 23-36.

Krilleke, D., DeErkenez, A., Schubert, W., Giri, I., Robinson, G. S., Ng, Y.-S., & Shima, D. T. (2007). Molecular mapping and functional characterization of the VEGF164 heparin-binding domain. *Journal of Biological Chemistry, 282*(38), 28045-28056.

Kulkarni, P., Martson, A., Vidya, R., Chitnavis, S., & Harsulkar, A. (2021). Pathophysiological landscape of osteoarthritis. *Advances in clinical chemistry, 100*, 37-90.

Kung, L., Zaki, S., Ravi, V., Rowley, L., Smith, M., Bell, K., Bateman, J., & Little, C. (2017). Utility of circulating serum miRNAs as biomarkers of early cartilage degeneration in animal models of post-traumatic osteoarthritis and inflammatory arthritis. *Osteoarthritis and cartilage, 25*(3), 426-434.

Kurz, B., Lange, T., Voelker, M., Hart, M. L., & Rolauffs, B. (2023). Articular Cartilage—From Basic Science Structural Imaging to Non-Invasive Clinical Quantitative Molecular Functional Information for AI Classification and Prediction. *International Journal of Molecular Sciences, 24*(19), 14974.

Kuter, D. J., Bain, B., Mufti, G., Bagg, A., & Hasserjian, R. P. (2007). Bone marrow fibrosis: pathophysiology and clinical significance of increased bone marrow stromal fibres. *British journal of haematology, 139*(3), 351-362.

Kvien, T. K., Uhlig, T., Ødegård, S., & Heiberg, M. S. (2006). Epidemiological aspects of rheumatoid arthritis: the sex ratio. *Annals of the New York academy of Sciences, 1069*(1), 212-222.

Lafont, J. E. (2010). Lack of oxygen in articular cartilage: consequences for chondrocyte biology. *International journal of experimental pathology, 91*(2), 99-106.

Lai, M.-C., Lin, R.-I., & Tarn, W.-Y. (2001). Transportin-SR2 mediates nuclear import of phosphorylated SR proteins. *Proceedings of the National Academy of Sciences, 98*(18), 10154-10159.

Lainer-Carr, D., & Brahn, E. (2007). Angiogenesis inhibition as a therapeutic approach for inflammatory synovitis. *Nature clinical practice Rheumatology, 3*(8), 434-442.

Lajeunesse, D., & Reboul, P. (2003). Subchondral bone in osteoarthritis: a biologic link with articular cartilage leading to abnormal remodeling. *Current opinion in rheumatology, 15*(5), 628-633.

Lansink, M., De Boer, A., Dijkmans, B., Vandenbroucke, J., & Hazes, J. (1993). The onset of rheumatoid arthritis in relation to pregnancy and childbirth. *Clinical and experimental rheumatology, 11*(2), 171-174.

Lard, L. R., Visser, H., Speyer, I., vander Horst-Bruinsma, I. E., Zwinderman, A. H., Breedveld, F. C., & Hazes, J. M. (2001). Early versus delayed treatment in patients with recent-onset rheumatoid arthritis: comparison of two cohorts who received different treatment strategies. *The American journal of medicine, 111*(6), 446-451.

Larson, A. A., Brown, D. R., El-Atrash, S., & Walser, M. M. (1986). Pain threshold changes in adjuvant-induced inflammation: a possible model of chronic pain in the mouse. *Pharmacology Biochemistry and Behavior, 24*(1), 49-53.

Larsson, P., Kleinau, S., Holmdahl, R., & Klareskog, L. (1990). Homologous type ii collagen—induced arthritis in rats. *Arthritis & Rheumatism: Official Journal of the American College of Rheumatology, 33*(5), 693-701.

Latini, A., Novelli, L., Ceccarelli, F., Barbati, C., Perricone, C., De Benedittis, G., Conti, F., Novelli, G., Ciccacci, C., & Borgiani, P. (2021). mRNA expression analysis confirms CD44 splicing impairment in systemic lupus erythematosus patients. *Lupus, 30*(7), 1086-1093.

Laughlin, K., Evans, S., Jenkins, W., Tracy, M., Chan, C., Lord, E., & Koch, C. (1996). Biodistribution of the nitroimidazole EF5 (2-[2-nitro-1H-imidazol-1-yl]-N-(2, 2, 3, 3, 3-pentafluoropropyl) acetamide) in mice bearing subcutaneous EMT6 tumors. *Journal of Pharmacology and Experimental Therapeutics, 277*(2), 1049-1057.

Laurent, L., Anquetil, F., Clavel, C., Ndongo-Thiam, N., Offer, G., Miossec, P., Pasquali, J.-L., Sebbag, M., & Serre, G. (2015). IgM rheumatoid factor amplifies the inflammatory response of macrophages induced by the rheumatoid arthritis-specific immune complexes containing anticitrullinated protein antibodies. *Annals of the rheumatic diseases, 74*(7), 1425-1431.

Le, T. H. V., & Kwon, S.-M. (2021). Vascular endothelial growth factor biology and its potential as a therapeutic target in rheumatic diseases. *International Journal of Molecular Sciences, 22*(10), 5387.

Lee, K. E., Spata, M., Bayne, L. J., Buza, E. L., Durham, A. C., Allman, D., Vonderheide, R. H., & Simon, M. C. (2016). Hif1a deletion reveals pro-neoplastic function of B cells in pancreatic neoplasia. *Cancer discovery, 6*(3), 256-269.

Lee, S., Joo, Y., Kim, W., Min, D., Min, J., Park, S., Cho, C., & Kim, H. (2001). Vascular endothelial growth factor levels in the serum and synovial fluid of patients with rheumatoid arthritis. *Clinical and experimental rheumatology, 19*(3), 321-324.

Lee, T.-H., Avraham, H., Lee, S.-H., & Avraham, S. (2002). Vascular endothelial growth factor modulates neutrophil transendothelial migration via up-regulation of interleukin-8 in human brain microvascular endothelial cells. *Journal of Biological Chemistry, 277*(12), 10445-10451.

Lee Walmsley, D., Murray, J. B., Dokurno, P., Massey, A. J., Benwell, K., Fiumana, A., Foloppe, N., Ray, S., Smith, J., & Surgenor, A. E. (2021). Fragment-derived selective inhibitors of dual-specificity kinases DYRK1A and DYRK1B. *Journal of Medicinal Chemistry, 64*(13), 8971-8991.

Lefevre, S., Knedla, A., Tennie, C., Kampmann, A., Wunrau, C., Dinser, R., Korb, A., Schnäker, E.-M., Tarner, I. H., & Robbins, P. D. (2009). Synovial fibroblasts spread rheumatoid arthritis to unaffected joints. *Nature medicine, 15*(12), 1414-1420.

Leibovich, S. J., Polverini, P. J., Shepard, H. M., Wiseman, D. M., Shively, V., & Nuseir, N. (1987). Macrophage-induced angiogenesis is mediated by tumour necrosis factor-α. *Nature, 329*(6140), 630-632.

Lertkiatmongkol, P., Liao, D., Mei, H., Hu, Y., & Newman, P. J. (2016). Endothelial functions of PECAM-1 (CD31). *Current opinion in hematology, 23*(3), 253.

Li, B., Guan, G., Mei, L., Jiao, K., & Li, H. (2021). Pathological mechanism of chondrocytes and the surrounding environment during osteoarthritis of temporomandibular joint. *Journal of cellular and molecular medicine, 25*(11), 4902-4911.

Li, C., Xu, L.-j., Lian, W.-w., Pang, X.-c., Jia, H., Liu, A.-l., & Du, G.-h. (2018). Anti-influenza effect and action mechanisms of the chemical constituent gallocatechin-7-gallate from Pithecellobium clypearia Benth. *Acta Pharmacologica Sinica, 39*(12), 1913-1922.

Li, F., Lee, K. E., & Simon, M. C. (2018). Detection of hypoxia and HIF in paraffin-embedded tumor tissues. *Hypoxia: Methods and Protocols*, 277-282.

Li, G., Yin, J., Gao, J., Cheng, T. S., Pavlos, N. J., Zhang, C., & Zheng, M. H. (2013). Subchondral bone in osteoarthritis: insight into risk factors and microstructural changes. *Arthritis research & therapy, 15*, 1-12.

Li, H., Wang, D., Yuan, Y., & Min, J. (2017). New insights on the MMP-13 regulatory network in the pathogenesis of early osteoarthritis. *Arthritis research & therapy, 19*(1), 248.

Li, X., Lee, C., Tang, Z., Zhang, F., Arjunan, P., Li, Y., Hou, X., Kumar, A., & Dong, L. (2009). VEGF-B: a survival, or an angiogenic factor? *Cell adhesion & migration, 3*(4), 322-327.

Li, Z., Xu, M., Li, R., Zhu, Z., Liu, Y., Du, Z., Zhang, G., & Song, Y. (2020). Identification of biomarkers associated with synovitis in rheumatoid arthritis by bioinformatics analyses. *Bioscience Reports, 40*(9), BSR20201713.

Lin, J.-C., Lin, C.-Y., Tarn, W.-Y., & Li, F.-Y. (2014). Elevated SRPK1 lessens apoptosis in breast cancer cells through RBM4-regulated splicing events. *Rna, 20*(10), 1621-1631.

Lin, M. I., & Sessa, W. C. (2006). Vascular endothelial growth factor signaling to endothelial nitric oxide synthase: more than a FLeeTing moment. *Circulation research, 99*(7), 666-668.

Lin, X., Patil, S., Gao, Y.-G., & Qian, A. (2020). The bone extracellular matrix in bone formation and regeneration. *Frontiers in pharmacology, 11*, 757.

Lin, Y.-J., Anzaghe, M., & Schülke, S. (2020). Update on the pathomechanism, diagnosis, and treatment options for rheumatoid arthritis. *Cells, 9*(4), 880.

Lisignoli, G., Piacentini, A., Cristino, S., Grassi, F., Cavallo, C., Cattini, L., Tonnarelli, B., Manferdini, C., & Facchini, A. (2007). CCL20 chemokine induces both osteoblast proliferation and osteoclast differentiation: Increased levels of CCL20 are expressed in subchondral bone tissue of rheumatoid arthritis patients. *Journal of cellular physiology, 210*(3), 798-806.

Liu, D., Ahmet, A., Ward, L., Krishnamoorthy, P., Mandelcorn, E. D., Leigh, R., Brown, J. P., Cohen, A., & Kim, H. (2013). A practical guide to the monitoring and management of the complications of systemic corticosteroid therapy. *Allergy, Asthma & Clinical Immunology, 9*, 1-25.

Liu, X.-J., Zhao, H.-C., Hou, S.-J., Zhang, H.-J., Cheng, L., Yuan, S., Zhang, L.-R., Song, J., Zhang, S.-Y., & Chen, S.-W. (2023). Recent development of multi-target VEGFR-2 inhibitors for the cancer therapy. *Bioorganic Chemistry*, 106425.

Liu, Y., Li, Y., Wang, Y., Lin, C., Zhang, D., Chen, J., Ouyang, L., Wu, F., Zhang, J., & Chen, L. (2022). Recent progress on vascular endothelial growth factor receptor

inhibitors with dual targeting capabilities for tumor therapy. *Journal of Hematology & Oncology, 15*(1), 1-28.

Lockshin, M. D. (2001). Invited review: sex ratio and rheumatic disease. *Journal of Applied Physiology, 91*(5), 2366-2373.

Lockshin, M. D. (2005). Sex differences in autoimmune disease. *Handbook of systemic autoimmune diseases, 4*, 3-10.

Loeser, R. F. (2009). Aging and osteoarthritis: the role of chondrocyte senescence and aging changes in the cartilage matrix. *Osteoarthritis and cartilage, 17*(8), 971-979.

Lohela, M., Bry, M., Tammela, T., & Alitalo, K. (2009). VEGFs and receptors involved in angiogenesis versus lymphangiogenesis. *Current opinion in cell biology, 21*(2), 154-165.

Lon, H.-K., Liu, D., Zhang, Q., DuBois, D. C., Almon, R. R., & Jusko, W. J. (2011). Pharmacokinetic-pharmacodynamic disease progression model for effect of etanercept in Lewis rats with collagen-induced arthritis. *Pharmaceutical research, 28*, 1622-1630.

Lon, H.-K., Liu, D., Zhang, Q., DuBois, D. C., Almon, R. R., & Jusko, W. J. (2011). Pharmacokinetic-pharmacodynamic disease progression model for effect of etanercept in Lewis rats with collagen-induced arthritis. *Pharmaceutical research, 28*(7), 1622-1630.

Lopez-Garcia, M., Nowicka, M., Bendtsen, C., Lythe, G., Ponnambalam, S., & Molina-París, C. (2018). Quantifying the phosphorylation timescales of receptor–ligand complexes: a Markovian matrix-analytic approach. *Open biology, 8*(9), 180126.

Lotz, M. (2001). Cytokines in cartilage injury and repair. *Clinical Orthopaedics and Related Research (1976-2007), 391*, S108-S115.

Louie, G. H., & Ward, M. M. (2010). Changes in the rates of joint surgery among patients with rheumatoid arthritis in California, 1983–2007. *Annals of the rheumatic diseases, 69*(5), 868-871.

Lovell, D. J., Giannini, E. H., Reiff, A., Cawkwell, G. D., Silverman, E. D., Nocton, J. J., Stein, L. D., Gedalia, A., Ilowite, N. T., & Wallace, C. A. (2000). Etanercept in children with polyarticular juvenile rheumatoid arthritis. *New England journal of medicine, 342*(11), 763-769.

Lu, J., Kasama, T., Kobayashi, K., Yoda, Y., Shiozawa, F., Hanyuda, M., Negishi, M., Ide, H., & Adachi, M. (2000). Vascular endothelial growth factor expression and regulation of murine collagen-induced arthritis. *The Journal of Immunology, 164*(11), 5922-5927.

Lu, J., Reese, J., Zhou, Y., & Hirsch, E. (2015). Progesterone-induced activation of membrane-bound progesterone receptors in murine macrophage cells. *The Journal of endocrinology, 224*(2), 183.

Ludin, A., Sela, J., Schroeder, A., Samuni, Y., Nitzan, D., & Amir, G. (2013). Injection of vascular endothelial growth factor into knee joints induces osteoarthritis in mice. *Osteoarthritis and cartilage, 21*(3), 491-497.

Lussier, A., De Medicis, R., & Tetreault, L. (1984). Adjuvant arthritis: influence of the adjuvant volume and composition on the established arthritis. *International journal of tissue reactions, 6*(2), 105-110.

Luttun, A., Tjwa, M., Moons, L., Wu, Y., Angelillo-Scherrer, A., Liao, F., Nagy, J. A., Hooper, A., Priller, J., & De Klerck, B. (2002). Revascularization of ischemic tissues by PlGF treatment, and inhibition of tumor angiogenesis, arthritis and atherosclerosis by anti-Flt1. *Nature medicine, 8*(8), 831-840.

Luyten, F. P., Tylzanowski, P., & Lories, R. J. (2009). Wnt signaling and osteoarthritis. *Bone, 44*(4), 522-527.

Lyons, T. J., McClure, S. F., Stoddart, R. W., & McClure, J. (2006). The normal human chondro-osseous junctional region: evidence for contact of uncalcified cartilage with subchondral bone and marrow spaces. *BMC musculoskeletal disorders, 7*(1), 1-8.

Ma, K., Singh, G., Wang, J., InSug, O., Votta-Velis, G., Bruce, B., Anbazhagan, A. N., van Wijnen, A. J., & Im, H.-J. (2023). Targeting Vascular Endothelial Growth Factor Receptors as a Therapeutic Strategy for Osteoarthritis and Associated Pain. *International Journal of Biological Sciences, 19*(2), 675.

Mac Gabhann, F., & Popel, A. S. (2007). Dimerization of VEGF receptors and implications for signal transduction: a computational study. *Biophysical chemistry, 128*(2-3), 125.

MacDonald, I. J., Liu, S.-C., Su, C.-M., Wang, Y.-H., Tsai, C.-H., & Tang, C.-H. (2018). Implications of angiogenesis involvement in arthritis. *International Journal of Molecular Sciences, 19*(7), 2012.

MacGregor, A. J., Snieder, H., Rigby, A. S., Koskenvuo, M., Kaprio, J., Aho, K., & Silman, A. J. (2000). Characterizing the quantitative genetic contribution to rheumatoid arthritis using data from twins. *Arthritis & Rheumatism: Official Journal of the American College of Rheumatology, 43*(1), 30-37.

Machold, K., Stamm, T., Nell, V., Pflugbeil, S., Aletaha, D., Steiner, G., Uffmann, M., & Smolen, J. (2007). Very recent onset rheumatoid arthritis: clinical and serological patient characteristics associated with radiographic progression over the first years of disease. *Rheumatology, 46*(2), 342-349.

Machold, K. P., Stamm, T. A., Eberl, G. J., Nell, V. K., Dunky, A., Uffmann, M., & Smolen, J. S. (2002). Very recent onset arthritis--clinical, laboratory, and radiological findings during the first year of disease. *The Journal of rheumatology, 29*(11), 2278-2287.

Macías, I., García-Pérez, S., Ruiz-Tudela, M., Medina, F., Chozas, N., & Girón-González, J. A. (2005). Modification of pro-and antiinflammatory cytokines and vascular-related molecules by tumor necrosis factor-a blockade in patients with rheumatoid arthritis. *The Journal of rheumatology, 32*(11), 2102-2108.

Mackay, C. R., Terpe, H.-J., Stauder, R., Marston, W. L., Stark, H., & Günthert, U. (1994). Expression and modulation of CD44 variant isoforms in humans. *The Journal of cell biology, 124*(1), 71-82.

Mackiewicz, A., Speroff, T., Ganapathi, M. K., & Kushner, I. (1991). Effects of cytokine combinations on acute phase protein production in two human hepatoma cell lines. *Journal of immunology (Baltimore, Md.: 1950), 146*(9), 3032-3037.

Madry, H., van Dijk, C. N., & Mueller-Gerbl, M. (2010). The basic science of the subchondral bone. *Knee Surgery, Sports Traumatology, Arthroscopy, 18*, 419-433.

Magnussen, A. L., Rennel, E. S., Hua, J., Bevan, H. S., Long, N. B., Lehrling, C., Gammons, M., Floege, J., Harper, S. J., & Agostini, H. T. (2010). VEGF-A165b is cytoprotective and antiangiogenic in the retina. *Investigative ophthalmology & visual science, 51*(8), 4273-4281.

Mäkinen, T., Veikkola, T., Mustjoki, S., Karpanen, T., Catimel, B., Nice, E. C., Wise, L., Mercer, A., Kowalski, H., & Kerjaschki, D. (2001). Isolated lymphatic endothelial cells transduce growth, survival and migratory signals via the VEGF-C/D receptor VEGFR-3. *The EMBO journal, 20*(17), 4762-4773.

Malhi, N. K., Allen, C. L., Stewart, E., Horton, K. L., Riu, F., Batson, J., Amoaku, W., Morris, J. C., Arkill, K. P., & Bates, D. O. (2022). Serine-arginine-rich protein kinase-1 inhibition for the treatment of diabetic retinopathy. *American Journal of Physiology-Heart and Circulatory Physiology, 322*(6), H1014-H1027.

Malinin, T., & Ouellette, E. (2000). Articular cartilage nutrition is mediated by subchondral bone: a long-term autograft study in baboons. *Osteoarthritis and cartilage, 8*(6), 483-491.

Mamer, S. B., Wittenkeller, A., & Imoukhuede, P. (2020). VEGF-A splice variants bind VEGFRs with differential affinities. *Scientific reports, 10*(1), 14413.

Manfredo Vieira, S., Hiltensperger, M., Kumar, V., Zegarra-Ruiz, D., Dehner, C., Khan, N., Costa, F., Tiniakou, E., Greiling, T., & Ruff, W. (2018). Translocation of a gut pathobiont drives autoimmunity in mice and humans. *Science, 359*(6380), 1156-1161.

Manley, P. W., Martiny-Baron, G., Schlaeppi, J.-M., & Wood, J. M. (2002). Therapies directed at vascular endothelial growth factor. *Expert opinion on investigational drugs, 11*(12), 1715-1736.

Mansell, J. P., Collins, C., & Bailey, A. J. (2007). Bone, not cartilage, should be the major focus in osteoarthritis. *Nature clinical practice Rheumatology, 3*(6), 306-307.

Mapp, P., Avery, P., McWilliams, D., Bowyer, J., Day, C., Moores, S., Webster, R., & Walsh, D. (2008). Angiogenesis in two animal models of osteoarthritis. *Osteoarthritis and cartilage, 16*(1), 61-69.

Mapp, P. I., & Walsh, D. A. (2012). Mechanisms and targets of angiogenesis and nerve growth in osteoarthritis. *Nature Reviews Rheumatology, 8*(7), 390-398.

Marinovich, R., Soenjaya, Y., Wallace, G. Q., Zuskov, A., Dunkman, A., Foster, B. L., Ao, M., Bartman, K., Lam, V., & Rizkalla, A. (2016). The role of bone sialoprotein in the tendon–bone insertion. *Matrix Biology, 52*, 325-338.

Markham, A., & Keam, S. J. (2019). Camrelizumab: first global approval. *Drugs, 79*(12), 1355-1361.

Maroudas, A., Wachtel, E., Grushko, G., Katz, E., & Weinberg, P. (1991). The effect of osmotic and mechanical pressures on water partitioning in articular cartilage. *Biochimica et Biophysica Acta (BBA)-General Subjects, 1073*(2), 285-294.

Marrelli, A., Cipriani, P., Liakouli, V., Carubbi, F., Perricone, C., Perricone, R., & Giacomelli, R. (2011). Angiogenesis in rheumatoid arthritis: a disease specific process or a common response to chronic inflammation? *Autoimmunity reviews, 10*(10), 595-598.

Maru, Y., Yamaguchi, S., & Shibuya, M. (1998). Flt-1, a receptor for vascular endothelial growth factor, has transforming and morphogenic potentials. *Oncogene, 16*(20), 2585-2595.

Marumo, T., Schini-Kerth, V. B., & Busse, R. (1999). Vascular endothelial growth factor activates nuclear factor-kappaB and induces monocyte chemoattractant protein-1 in bovine retinal endothelial cells. *Diabetes, 48*(5), 1131-1137.

Masi, A. T., Feigenbaum, S. L., & Chatterton, R. T. (1995). *Hormonal and pregnancy relationships to rheumatoid arthritis: convergent effects with immunologic and microvascular systems.* Paper presented at the Seminars in arthritis and rheumatism.

Mateen, S., Zafar, A., Moin, S., Khan, A. Q., & Zubair, S. (2016). Understanding the role of cytokines in the pathogenesis of rheumatoid arthritis. *Clinica Chimica Acta, 455*, 161-171.

Matera, A. G., & Wang, Z. (2014). A day in the life of the spliceosome. *Nature reviews Molecular cell biology, 15*(2), 108-121.

Matsui, T., Nakata, N., Nagai, S., Nakatani, A., Takahashi, M., Momose, T., Ohtomo, K., & Koyasu, S. (2009). Inflammatory cytokines and hypoxia contribute to 18F-FDG uptake by cells involved in pannus formation in rheumatoid arthritis. *Journal of Nuclear Medicine, 50*(6), 920-926.

Matsumoto, T., & Claesson-Welsh, L. (2001). VEGF receptor signal transduction. *Sci. Stke, 2001*(112), re21-re21.

Matsumoto, Y., Tanaka, K., Hirata, G., Hanada, M., Matsuda, S., Shuto, T., & Iwamoto, Y. (2002). Possible involvement of the vascular endothelial growth factor-Flt-1-focal adhesion kinase pathway in chemotaxis and the cell proliferation of osteoclast precursor cells in arthritic joints. *The Journal of Immunology, 168*(11), 5824-5831.

Maurizi, A., & Rucci, N. (2018). The osteoclast in bone metastasis: player and target. *Cancers, 10*(7), 218.

Mavrou, A., Brakspear, K., Hamdollah-Zadeh, M., Damodaran, G., Babaei-Jadidi, R., Oxley, J., Gillatt, D. A., Ladomery, M. R., Harper, S. J., & Bates, D. O. (2015). Serine–arginine protein kinase 1 (SRPK1) inhibition as a potential novel targeted therapeutic strategy in prostate cancer. *Oncogene, 34*(33), 4311-4319.

Mayence, A., & Vanden Eynde, J. J. (2019). Baricitinib: a 2018 novel FDA-approved small molecule inhibiting janus kinases. *Pharmaceuticals, 12*(1), 37.

Mayr-Wohlfart, U., Waltenberger, J., Hausser, H., Kessler, S., Günther, K.-P., Dehio, C., Puhl, W., & Brenner, R. (2002). Vascular endothelial growth factor stimulates chemotactic migration of primary human osteoblasts. *Bone, 30*(3), 472-477.

McAlinden, A. (2014). Alternative splicing of type II procollagen: IIB or not IIB? *Connective Tissue Research, 55*(3), 165-176.

McInnes, I. B., & Schett, G. (2011). The pathogenesis of rheumatoid arthritis. *New England journal of medicine, 365*(23), 2205-2219.

McKibbin, B., & Holdsworth, F. (1966). The nutrition of immature joint cartilage in the lamb. *The Journal of bone and joint surgery. British volume, 48*(4), 793-803.

McLaren, J., Prentice, A., Charnock-Jones, D., Millican, S., Müller, K., Sharkey, A., & Smith, S. (1996). Vascular endothelial growth factor is produced by peritoneal fluid macrophages in endometriosis and is regulated by ovarian steroids. *The Journal of clinical investigation, 98*(2), 482-489.

Meinke, G., Bohm, A., Hauber, J., Pisabarro, M. T., & Buchholz, F. (2016). Cre recombinase and other tyrosine recombinases. *Chemical reviews, 116*(20), 12785-12820.

Mendes, A. C., Baran, E. T., Pereira, R. C., Azevedo, H. S., & Reis, R. L. (2012). Encapsulation and survival of a chondrocyte cell line within xanthan gum derivative. *Macromolecular bioscience, 12*(3), 350-359.

Meng, W., Zhu, Z., Jiang, X., Too, C. L., Uebe, S., Jagodic, M., Kockum, I., Murad, S., Ferrucci, L., & Alfredsson, L. (2017). DNA methylation mediates genotype and smoking interaction in the development of anti-citrullinated peptide antibody-positive rheumatoid arthritis. *Arthritis research & therapy, 19*(1), 1-10.

Mengshol, J. A., Vincenti, M. P., Coon, C. I., Barchowsky, A., & Brinckerhoff, C. E. (2000). Interleukin-1 induction of collagenase 3 (matrix metalloproteinase 13) gene expression in chondrocytes requires p38, c-Jun N-terminal kinase, and nuclear factor κB: differential regulation of collagenase 1 and collagenase 3. *Arthritis & Rheumatism: Official Journal of the American College of Rheumatology, 43*(4), 801-811.

Mentlein, R., & Held-Feindt, J. (2003). Angiogenesis factors in gliomas: a new key to tumour therapy? *Naturwissenschaften, 90*, 385-394.

Mestas, J., & Hughes, C. C. (2004). Of mice and not men: differences between mouse and human immunology. *The Journal of Immunology, 172*(5), 2731-2738.

Micheli, L., Bozdag, M., Akgul, O., Carta, F., Guccione, C., Bergonzi, M. C., Bilia, A. R., Cinci, L., Lucarini, E., & Parisio, C. (2019). Pain relieving effect of-NSAIDs-CAIs hybrid molecules: systemic and intra-articular treatments against rheumatoid arthritis. *International Journal of Molecular Sciences, 20*(8), 1923.

Milgram, J. W. (1983). Morphologic Alterations of the Subchondrall Bone in Advanced Degenerative Arthritis. *Clinical Orthopaedics and Related Research (1976-2007), 173*, 293-312.

Miotla, J., Maciewicz, R., Kendrew, J., Feldmann, M., & Paleolog, E. (2000). Treatment with soluble VEGF receptor reduces disease severity in murine collagen-induced arthritis. *Laboratory investigation, 80*(8), 1195-1205.

Mitchell, P. G., Magna, H. A., Reeves, L. M., Lopresti-Morrow, L. L., Yocum, S. A., Rosner, P. J., Geoghegan, K. F., & Hambor, J. E. (1996). Cloning, expression, and type II collagenolytic activity of matrix metalloproteinase-13 from human osteoarthritic cartilage. *The Journal of clinical investigation, 97*(3), 761-768.

Mizokami, A., Kawakubo-Yasukochi, T., & Hirata, M. (2017). Osteocalcin and its endocrine functions. *Biochemical pharmacology, 132*, 1-8.

Moldovan, F., Pelletier, J. P., Hambor, J., Cloutier, J. M., & Martel-Pelletier, J. (1997). Collagenase-3 (matrix metalloprotease 13) is preferentially localized in the deep layer of human arthritic cartilage in situ. In vitro mimicking effect by transforming growth factor β. *Arthritis & Rheumatism: Official Journal of the American College of Rheumatology, 40*(9), 1653-1661.

Mon, N. N., Ito, S., Senga, T., & Hamaguchi, M. (2006). FAK signaling in neoplastic disorders: a linkage between inflammation and cancer. *Annals of the New York Academy of Sciences, 1086*(1), 199-212.

Moon, B.-H., Kim, Y., & Kim, S.-Y. (2023). Twenty years of anti-vascular endothelial growth factor therapeutics in neovascular age-related macular degeneration treatment. *International Journal of Molecular Sciences, 24*(16), 13004.

Moorehead, C., Prudnikova, K., & Marcolongo, M. (2019). The regulatory effects of proteoglycans on collagen fibrillogenesis and morphology investigated using biomimetic proteoglycans. *Journal of Structural Biology, 206*(2), 204-215.

Morales-Ducret, J., Wayner, E., Elices, M., Alvaro-Gracia, J., Zvaifler, N., & Firestein, G. (1992). Alpha 4/beta 1 integrin (VLA-4) ligands in arthritis. Vascular cell adhesion molecule-1 expression in synovium and on fibroblast-like synoviocytes. *The Journal of Immunology, 149*(4), 1424-1431.

Moreland, L. W., Baumgartner, S. W., Schiff, M. H., Tindall, E. A., Fleischmann, R. M., Weaver, A. L., Ettlinger, R. E., Cohen, S., Koopman, W. J., & Mohler, K. (1997). Treatment of rheumatoid arthritis with a recombinant human tumor necrosis factor receptor (p75)–Fc fusion protein. *New England journal of medicine, 337*(3), 141-147.

Moreland, L. W., Schiff, M. H., Baumgartner, S. W., Tindall, E. A., Fleischmann, R. M., Bulpitt, K. J., Weaver, A. L., Keystone, E. C., Furst, D. E., & Mease, P. J. (1999). Etanercept therapy in rheumatoid arthritis: a randomized, controlled trial. *Annals of internal medicine, 130*(6), 478-486.

Moretti, L., Bizzoca, D., Geronimo, A., Moretti, F. L., Monaco, E., Solarino, G., & Moretti, B. (2022). Towards Precision Medicine for Osteoarthritis: Focus on the Synovial Fluid Proteome. *International Journal of Molecular Sciences, 23*(17), 9731.

Moroney, M. R., Woodruff, E., Qamar, L., Bradford, A. P., Wolsky, R., Bitler, B. G., & Corr, B. R. (2021). Inhibiting Wnt/beta-catenin in CTNNB1-mutated endometrial cancer. *Molecular carcinogenesis, 60*(8), 511-523.

Morooka, S., Hoshina, M., Kii, I., Okabe, T., Kojima, H., Inoue, N., Okuno, Y., Denawa, M., Yoshida, S., & Fukuhara, J. (2015). Identification of a dual inhibitor of SRPK1 and CK2 that attenuates pathological angiogenesis of macular degeneration in mice. *Molecular pharmacology, 88*(2), 316-325.

Morozzi, G., Fabbroni, M., Bellisai, F., Pucci, G., & Galeazzi, M. (2007). Cartilage oligomeric matrix protein level in rheumatic diseases: potential use as a marker for measuring articular cartilage damage and/or the therapeutic efficacy of treatments. *Annals of the New York Academy of Sciences, 1108*(1), 398-407.

Moskowitz, R. W. (2007). *Osteoarthritis: diagnosis and medical/surgical management*: Lippincott Williams & Wilkins.

Mott, B. T., Tanega, C., Shen, M., Maloney, D. J., Shinn, P., Leister, W., Marugan, J. J., Inglese, J., Austin, C. P., & Misteli, T. (2009). Evaluation of substituted 6-arylquinazolin-4-amines as potent and selective inhibitors of cdc2-like kinases (Clk). *Bioorganic & medicinal chemistry letters, 19*(23), 6700-6705.

Mould, A. W., Greco, S. A., Cahill, M. M., Tonks, I. D., Bellomo, D., Patterson, C., Zournazi, A., Nash, A., Scotney, P., & Hayward, N. K. (2005). Transgenic overexpression of vascular endothelial growth factor-B isoforms by endothelial cells potentiates postnatal vessel growth in vivo and in vitro. *Circulation research, 97*(6), e60-e70.

Mould, A. W., Tonks, I. D., Cahill, M. M., Pettit, A. R., Thomas, R., Hayward, N. K., & Kay, G. F. (2003). Vegfb gene knockout mice display reduced pathology and synovial angiogenesis in both antigen-induced and collagen-induced models of arthritis. *Arthritis & Rheumatism: Official Journal of the American College of Rheumatology, 48*(9), 2660-2669.

Mourad, J.-J., & Levy, B. I. (2011). Mechanisms of antiangiogenic-induced arterial hypertension. *Current hypertension reports, 13*, 289-293.

Mouw, J. K., Ou, G., & Weaver, V. M. (2014). Extracellular matrix assembly: a multiscale deconstruction. *Nature reviews Molecular cell biology, 15*(12), 771-785.

Mthembu, N. N., Mbita, Z., Hull, R., & Dlamini, Z. (2017). Abnormalities in alternative splicing of angiogenesis-related genes and their role in HIV-related cancers. *HIV/AIDS (Auckland, NZ), 9*, 77.

Muller-Ladner, U., Elices, M., Kriegsmann, J., Strahl, D., Gay, R., Firestein, G., & Gay, S. (1997). Alternatively spliced CS-1 fibronectin isoform and its receptor VLA-4 in rheumatoid arthritis synovium. *The Journal of rheumatology, 24*(10), 1873-1880.

Murakami, M., Iwai, S., Hiratsuka, S., Yamauchi, M., Nakamura, K., Iwakura, Y., & Shibuya, M. (2006). Signaling of vascular endothelial growth factor receptor-1 tyrosine kinase promotes rheumatoid arthritis through activation of monocytes/macrophages. *Blood, 108*(6), 1849-1856.

Murakami, M., & Shibuya, M. (2008). Involvement of vascular endothelial growth factorreceptor-1 in rheumatoid arthritis. *Inflammation and Regeneration, 28*(2), 78-85.

Murata, M., Yudoh, K., & Masuko, K. (2008). The potential role of vascular endothelial growth factor (VEGF) in cartilage: how the angiogenic factor could be involved in the pathogenesis of osteoarthritis? *Osteoarthritis and cartilage, 16*(3), 279-286.

Mustonen, T., & Alitalo, K. (1995). Endothelial receptor tyrosine kinases involved in angiogenesis. *The Journal of cell biology, 129*(4), 895-898.

Myasoedova, E., Crowson, C. S., Kremers, H. M., Therneau, T. M., & Gabriel, S. E. (2010). Is the incidence of rheumatoid arthritis rising?: results from Olmsted County, Minnesota, 1955–2007. *Arthritis & Rheumatism, 62*(6), 1576-1582.

Nagao, M., Hamilton, J. L., Kc, R., Berendsen, A. D., Duan, X., Cheong, C. W., Li, X., Im, H.-J., & Olsen, B. R. (2017). Vascular endothelial growth factor in cartilage development and osteoarthritis. *Scientific reports, 7*(1), 13027.

Nagashima, M., Yoshino, S., Ishiwata, T., & Asano, G. (1995). Role of vascular endothelial growth factor in angiogenesis of rheumatoid arthritis. *The Journal of rheumatology, 22*(9), 1624-1630.

Nagy, A. (2000). Cre recombinase: the universal reagent for genome tailoring. *genesis, 26*(2), 99-109.

Nagy, G., Roodenrijs, N. M., Welsing, P. M., Kedves, M., Hamar, A., Van Der Goes, M. C., Kent, A., Bakkers, M., Blaas, E., & Senolt, L. (2021). EULAR definition of difficult-to-treat rheumatoid arthritis. *Annals of the rheumatic diseases, 80*(1), 31-35.

Nakagawa, M., Kaneda, T., Arakawa, T., Morita, S., Sato, T., Yomada, T., Hanada, K., Kumegawa, M., & Hakeda, Y. (2000). Vascular endothelial growth factor (VEGF) directly enhances osteoclastic bone resorption and survival of mature osteoclasts. *FEBS letters, 473*(2), 161-164.

Nakahara, H., Song, J., Sugimoto, M., Hagihara, K., Kishimoto, T., Yoshizaki, K., & Nishimoto, N. (2003). Anti–interleukin-6 receptor antibody therapy reduces vascular endothelial growth factor production in rheumatoid arthritis. *Arthritis & Rheumatism: Official Journal of the American College of Rheumatology, 48*(6), 1521-1529.

Nakase, T., Kaneko, M., Tomita, T., Myoui, A., Ariga, K., Sugamoto, K., Uchiyama, Y., Ochi, T., & Yoshikawa, H. (2000). Immunohistochemical detection of cathepsin D, K, and L in the process of endochondral ossification in the human. *Histochemistry and cell biology, 114*, 21-27.

Nakatani, S., Mano, H., Im, R., Shimizu, J., & Wada, M. (2007). Glucosamine regulates differentiation of a chondrogenic cell line, ATDC5. *Biological and Pharmaceutical Bulletin, 30*(3), 433-438.

Namiki, A., Brogi, E., Kearney, M., Kim, E. A., Wu, T., Couffinhal, T., Varticovski, L., & Isner, J. M. (1995). Hypoxia Induces Vascular Endothelial Growth Factor in Cultured Human Endothelial Cells (∗). *Journal of Biological Chemistry, 270*(52), 31189-31195.

Naro, C., Bielli, P., & Sette, C. (2021). Oncogenic dysregulation of pre-mRNA processing by protein kinases: challenges and therapeutic opportunities. *The FEBS journal, 288*(21), 6250-6272.

Naro, C., & Sette, C. (2013). Phosphorylation-mediated regulation of alternative splicing in cancer. *International journal of cell biology, 2013*.

Nash, P., Kerschbaumer, A., Dörner, T., Dougados, M., Fleischmann, R. M., Geissler, K., McInnes, I., Pope, J. E., Van Der Heijde, D., & Stoffer-Marx, M. (2021). Points to consider for the treatment of immune-mediated inflammatory diseases with Janus

kinase inhibitors: a consensus statement. *Annals of the rheumatic diseases, 80*(1), 71-87.

Nasonov, E., Fatenejad, S., Feist, E., Ivanova, M., Korneva, E., Krechikova, D. G., Maslyanskiy, A. L., Samsonov, M., Stoilov, R., & Zonova, E. V. (2022). Olokizumab, a monoclonal antibody against interleukin 6, in combination with methotrexate in patients with rheumatoid arthritis inadequately controlled by methotrexate: efficacy and safety results of a randomised controlled phase III study. *Annals of the rheumatic diseases, 81*(4), 469-479.

Nasuti, C., Fedeli, D., Bordoni, L., Piangerelli, M., Servili, M., Selvaggini, R., & Gabbianelli, R. (2019). Anti-inflammatory, anti-arthritic and anti-nociceptive activities of Nigella sativa oil in a rat model of arthritis. *Antioxidants, 8*(9), 342.

Naumov, G. N., Folkman, J., Straume, O., & Akslen, L. A. (2008). Tumor-vascular interactions and tumor dormancy. *Apmis, 116*(7-8), 569-585.

Neagoe, P.-E., Lemieux, C., & Sirois, M. G. (2005). Vascular endothelial growth factor (VEGF)-A165-induced prostacyclin synthesis requires the activation of VEGF receptor-1 and-2 heterodimer. *Journal of Biological Chemistry, 280*(11), 9904-9912.

Neefjes, M., van Caam, A. P., & van der Kraan, P. M. (2020). Transcription factors in cartilage homeostasis and osteoarthritis. *Biology, 9*(9), 290.

Nell, V., Machold, K., Eberl, G., Stamm, T., Uffmann, M., & Smolen, J. (2004). Benefit of very early referral and very early therapy with disease-modifying anti-rheumatic drugs in patients with early rheumatoid arthritis. *Rheumatology, 43*(7), 906-914.

Nelson, J. L., & Ostensen, M. (1997). Pregnancy and rheumatoid arthritis. *Rheumatic Disease Clinics of North America, 23*(1), 195-212.

Neufeld, G., Cohen, T., Gengrinovitch, S., & Poltorak, Z. (1999). Vascular endothelial growth factor (VEGF) and its receptors. *The FASEB journal, 13*(1), 9-22.

Neve, A., Cantatore, F. P., Corrado, A., Gaudio, A., Ruggieri, S., & Ribatti, D. (2013). In vitro and in vivo angiogenic activity of osteoarthritic and osteoporotic osteoblasts is modulated by VEGF and vitamin D3 treatment. *Regulatory peptides, 184*, 81-84.

Newton, P., Staines, K. A., Spevak, L., Boskey, A., Teixeira, C., Macrae, V., Canfield, A., & Farquharson, C. (2012). Chondrogenic ATDC5 cells: an optimised model for rapid and physiological matrix mineralisation. *International journal of molecular medicine, 30*(5), 1187-1193.

Ngo, J. C. K., Giang, K., Chakrabarti, S., Ma, C.-T., Huynh, N., Hagopian, J. C., Dorrestein, P. C., Fu, X.-D., Adams, J. A., & Ghosh, G. (2008). A sliding docking interaction is essential for sequential and processive phosphorylation of an SR protein by SRPK1. *Molecular cell, 29*(5), 563-576.

Ngo, S. (2014). Steyn fJ. *McCombe PA Gender differences in autoimmune disease. front Neuroendocrinol, 35*(3), 347-369.

NHSUK. (2022). Arthritis. Retrieved from https://www.nhs.uk/conditions/arthritis/

Nicolò, M., Ferro Desideri, L., Vagge, A., & Traverso, C. E. (2021). Faricimab: an investigational agent targeting the Tie-2/angiopoietin pathway and VEGF-A for the treatment of retinal diseases. *Expert opinion on investigational drugs, 30*(3), 193-200.

Nielen, M. M., van Schaardenburg, D., Reesink, H. W., Van de Stadt, R. J., van der Horst-Bruinsma, I. E., de Koning, M. H., Habibuw, M. R., Vandenbroucke, J. P., & Dijkmans, B. A. (2004). Specific autoantibodies precede the symptoms of rheumatoid arthritis: a study of serial measurements in blood donors. *Arthritis &*

Rheumatism: Official Journal of the American College of Rheumatology, 50(2), 380-386.

Nikas, I. P., Themistocleous, S. C., Paschou, S. A., Tsamis, K. I., & Ryu, H. S. (2019). Serine-arginine protein kinase 1 (SRPK1) as a prognostic factor and potential therapeutic target in cancer: current evidence and future perspectives. *Cells, 9*(1), 19.

Nikom, D., & Zheng, S. (2023). Alternative splicing in neurodegenerative disease and the promise of RNA therapies. *Nature Reviews Neuroscience*, 1-17.

Nilsson, I., Bahram, F., Li, X., Gualandi, L., Koch, S., Jarvius, M., Söderberg, O., Anisimov, A., Kholová, I., & Pytowski, B. (2010). VEGF receptor 2/-3 heterodimers detected in situ by proximity ligation on angiogenic sprouts. *The EMBO journal, 29*(8), 1377-1388.

Niu, Q., Gao, J., Wang, L., Liu, J., & Zhang, L. (2022). Regulation of differentiation and generation of osteoclasts in rheumatoid arthritis. *Frontiers in Immunology, 13*, 1034050.

Noh, A. S. M., Chuan, T. D., Khir, N. A. M., Zin, A. A. M., Ghazali, A. K., Long, I., Ab Aziz, C. B., & Ismail, C. A. N. (2021). Effects of different doses of complete Freund's adjuvant on nociceptive behaviour and inflammatory parameters in polyarthritic rat model mimicking rheumatoid arthritis. *Plos one, 16*(12), e0260423.

Nowak, D. G., Amin, E. M., Rennel, E. S., Hoareau-Aveilla, C., Gammons, M., Damodoran, G., Hagiwara, M., Harper, S. J., Woolard, J., & Ladomery, M. R. (2010). Regulation of vascular endothelial growth factor (VEGF) splicing from pro-angiogenic to anti-angiogenic isoforms: a novel therapeutic strategy for angiogenesis. *Journal of Biological Chemistry, 285*(8), 5532-5540.

Nowak, D. G., Woolard, J., Amin, E. M., Konopatskaya, O., Saleem, M. A., Churchill, A. J., Ladomery, M. R., Harper, S. J., & Bates, D. O. (2008). Expression of pro-and anti-angiogenic isoforms of VEGF is differentially regulated by splicing and growth factors. *Journal of cell science, 121*(20), 3487-3495.

Nygaard, G., & Firestein, G. S. (2020). Restoring synovial homeostasis in rheumatoid arthritis by targeting fibroblast-like synoviocytes. *Nature Reviews Rheumatology, 16*(6), 316-333.

O'Shea, J. J., Kontzias, A., Yamaoka, K., Tanaka, Y., & Laurence, A. (2013). Janus kinase inhibitors in autoimmune diseases. *Annals of the rheumatic diseases, 72*(suppl 2), ii111-ii115.

Odell, I. D., & Cook, D. (2013). Immunofluorescence techniques. *The Journal of investigative dermatology, 133*(1), e4.

Odorisio, T., Schietroma, C., Zaccaria, M. L., Cianfarani, F., Tiveron, C., Tatangelo, L., Failla, C. M., & Zambruno, G. (2002). Mice overexpressing placenta growth factor exhibit increased vascularization and vessel permeability. *Journal of cell science, 115*(12), 2559-2567.

Odunsi, K., Mhawech-Fauceglia, P., Andrews, C., Beck, A., Amuwo, O., Lele, S., Black, J. D., & Huang, R.-Y. (2012). Elevated expression of the serine-arginine protein kinase 1 gene in ovarian cancer and its role in Cisplatin cytotoxicity in vitro. *PloS one, 7*(12).

Ogilvie, C. M., Lu, C., Marcucio, R., Lee, M., Thompson, Z., Hu, D., Helms, J. A., & Miclau, T. (2012). Vascular endothelial growth factor improves bone repair in a murine nonunion model. *The Iowa orthopaedic journal, 32*, 90.

Oka, M. (1953). Effect of pregnancy on the onset and course of rheumatoid arthritis. *Annals of the rheumatic diseases, 12*(3), 227.

Okada, K., Mori, D., Makii, Y., Nakamoto, H., Murahashi, Y., Yano, F., Chang, S. H., Taniguchi, Y., Kobayashi, H., & Semba, H. (2020). Hypoxia-inducible factor-1 alpha maintains mouse articular cartilage through suppression of NF-κB signaling. *Scientific reports, 10*(1), 5425.

Okita, K., Hikiji, H., Koga, A., Nagai-Yoshioka, Y., Yamasaki, R., Mitsugi, S., Fujii, W., & Ariyoshi, W. (2023). Ascorbic acid enhances chondrocyte differentiation of ATDC5 by accelerating insulin receptor signaling. *Cell Biology International, 47*(10), 1737-1748.

Olofsson, B., Korpelainen, E., Pepper, M. S., Mandriota, S. J., Aase, K., Kumar, V., Gunji, Y., Jeltsch, M. M., Shibuya, M., & Alitalo, K. (1998). Vascular endothelial growth factor B (VEGF-B) binds to VEGF receptor-1 and regulates plasminogen activator activity in endothelial cells. *Proceedings of the National Academy of Sciences, 95*(20), 11709-11714.

Olofsson, B., Pajusola, K., Kaipainen, A., Von Euler, G., Joukov, V., Saksela, O., Orpana, A., Pettersson, R. F., Alitalo, K., & Eriksson, U. (1996). Vascular endothelial growth factor B, a novel growth factor for endothelial cells. *Proceedings of the National Academy of Sciences, 93*(6), 2576-2581.

Olsson, A.-K., Dimberg, A., Kreuger, J., & Claesson-Welsh, L. (2006). VEGF receptor signalling? In control of vascular function. *Nature reviews Molecular cell biology, 7*(5), 359-371.

Oltean, S., & Bates, D. O. (2014). Hallmarks of alternative splicing in cancer. *Oncogene, 33*(46), 5311-5318.

Oltean, S., Gammons, M., Hulse, R., Hamdollah-Zadeh, M., Mavrou, A., Donaldson, L., Salmon, A. H., Harper, S. J., Ladomery, M. R., & Bates, D. O. (2012). SRPK1 inhibition in vivo: modulation of VEGF splicing and potential treatment for multiple diseases. *Biochemical Society Transactions, 40*(4), 831-835.

Oltean, S., Qiu, Y., Ferguson, J. K., Stevens, M., Neal, C., Russell, A., Kaura, A., Arkill, K. P., Harris, K., & Symonds, C. (2015). Vascular endothelial growth factor-A165b is protective and restores endothelial glycocalyx in diabetic nephropathy. *Journal of the American Society of Nephrology: JASN, 26*(8), 1889.

Onnheim, K., Huang, S., Holmertz, A. S., Andersson, S., Lönnblom, E., Jonsson, C., Holmdahl, R., & Gjertsson, I. (2022). Rheumatoid arthritis chondrocytes produce increased levels of pro-inflammatory proteins. *Osteoarthritis and Cartilage Open, 4*(1), 100235.

Orellana, C., Saevarsdottir, S., Klareskog, L., Karlson, E. W., Alfredsson, L., & Bengtsson, C. (2017). Oral contraceptives, breastfeeding and the risk of developing rheumatoid arthritis: results from the Swedish EIRA study. *Annals of the rheumatic diseases, 76*(11), 1845-1852.

Orfanidou, T., Iliopoulos, D., Malizos, K. N., & Tsezou, A. (2009). Involvement of SOX-9 and FGF-23 in RUNX-2 regulation in osteoarthritic chondrocytes. *Journal of cellular and molecular medicine, 13*(9b), 3186-3194.

Orr, C., Vieira-Sousa, E., Boyle, D. L., Buch, M. H., Buckley, C. D., Cañete, J. D., Catrina, A. I., Choy, E. H., Emery, P., & Fearon, U. (2017). Synovial tissue research: a state-of-the-art review. *Nature Reviews Rheumatology, 13*(8), 463-475.

Ostensen, M. (1999). Sex hormones and pregnancy in rheumatoid arthritis and systemic lupus erythematosus. *Annals of the New York Academy of Sciences, 876*(1), 131-144.

Ostensen, M., & Villiger, P. M. (2007). *The remission of rheumatoid arthritis during pregnancy.* Paper presented at the Seminars in immunopathology.

Otrock, Z. K., Makarem, J. A., & Shamseddine, A. I. (2007). Vascular endothelial growth factor family of ligands and receptors. *Blood Cells, Molecules, and Diseases, 38*(3), 258-268.

Oumarou Hama, H., Aboudharam, G., Barbieri, R., Lepidi, H., & Drancourt, M. (2022). Immunohistochemical diagnosis of human infectious diseases: a review. *Diagnostic Pathology, 17*(1), 1-15.

Owen, K. A., Pixley, F. J., Thomas, K. S., Vicente-Manzanares, M., Ray, B. J., Horwitz, A. F., Parsons, J. T., Beggs, H. E., Stanley, E. R., & Bouton, A. H. (2007). Regulation of lamellipodial persistence, adhesion turnover, and motility in macrophages by focal adhesion kinase. *The Journal of cell biology, 179*(6), 1275-1287.

Ozgonenel, L., Cetin, E., Tutun, S., Tonbaklar, P., Aral, H., & Guvenen, G. (2010). The relation of serum vascular endothelial growth factor level with disease duration and activity in patients with rheumatoid arthritis. *Clinical rheumatology, 29*, 473-477.

Pajarinen, J., Lin, T.-H., Sato, T., Yao, Z., & Goodman, S. (2014). Interaction of materials and biology in total joint replacement–successes, challenges and future directions. *Journal of Materials Chemistry B, 2*(41), 7094-7108.

Paleolog, E. M. (2002). Angiogenesis in rheumatoid arthritis. *Arthritis research & therapy, 4*(3), 1-10.

Paleolog, E. M., Young, S., Stark, A. C., McCloskey, R. V., Feldmann, M., & Maini, R. N. (1998). Modulation of angiogenic vascular endothelial growth factor by tumor necrosis factor α and interleukin-1 in rheumatoid arthritis. *Arthritis & Rheumatism, 41*(7), 1258-1265.

Pan, Q., Chathery, Y., Wu, Y., Rathore, N., Tong, R. K., Peale, F., Bagri, A., Tessier-Lavigne, M., Koch, A. W., & Watts, R. J. (2007). Neuropilin-1 binds to VEGF121 and regulates endothelial cell migration and sprouting. *Journal of Biological Chemistry, 282*(33), 24049-24056.

Pan, X.-w., Xu, D., Chen, W.-j., Chen, J.-x., Chen, W.-j., Ye, J.-q., Gan, S.-s., Zhou, W., Song, X., & Shi, L. (2021). USP39 promotes malignant proliferation and angiogenesis of renal cell carcinoma by inhibiting VEGF-A 165b alternative splicing via regulating SRSF1 and SRPK1. *Cancer Cell International, 21*, 1-16.

Pandey, A. K., Singhi, E. K., Arroyo, J. P., Ikizler, T. A., Gould, E. R., Brown, J., Beckman, J. A., Harrison, D. G., & Moslehi, J. (2018). Mechanisms of VEGF (vascular endothelial growth factor) inhibitor–associated hypertension and vascular disease. *Hypertension, 71*(2), e1-e8.

Pandit, S., Wang, D., & Fu, X.-D. (2008). Functional integration of transcriptional and RNA processing machineries. *Current opinion in cell biology, 20*(3), 260-265.

Pang, V., Bates, D. O., & Leach, L. (2017). Regulation of human feto-placental endothelial barrier integrity by vascular endothelial growth factors: competitive interplay between VEGF-A165a, VEGF-A165b, PIGF and VE-cadherin. *Clinical science, 131*(23), 2763-2775.

Pap, T., Aupperle, K. R., Gay, S., Firestein, G. S., & Gay, R. E. (2001). Invasiveness of synovial fibroblasts is regulated by p53 in the SCID mouse in vivo model of cartilage invasion. *Arthritis & Rheumatism, 44*(3), 676-681.

Pap, T., & Korb-Pap, A. (2015). Cartilage damage in osteoarthritis and rheumatoid arthritis—two unequal siblings. *Nature Reviews Rheumatology, 11*(10), 606.

Pap, T., Müller-Ladner, U., Gay, R. E., & Gay, S. (2000). Fibroblast biology: role of synovial fibroblasts in the pathogenesis of rheumatoid arthritis. *Arthritis research & therapy, 2*(5), 361.

Pap, T., Shigeyama, Y., Kuchen, S., Fernihough, J., Simmen, B., Gay, R., Billingham, M., & Gay, S. (1999). EXPRESSION OF MEMBRANE-TYPE MATRIX METALLO PROTEINASES (MT-MMP), MMP-2 AND MMP-13 IN THE RHEUMATOID ARTHRITIS (RA) SYNOVIUM. *Arthritis & Rheumatism, 42*(9).

Paquet, J., Maskali, F., Poussier, S., Scala Bertola, J., Pinzano, A., Grossin, L., Netter, P., Olivier, P., & Gillet, P. (2010). Evaluation of a rat knee mono-arthritis using microPET. *Bio-Medical Materials and Engineering, 20*(3-4), 195-202.

Park, J. E., Chen, H. H., Winer, J., Houck, K. A., & Ferrara, N. (1994). Placenta growth factor. Potentiation of vascular endothelial growth factor bioactivity, in vitro and in vivo, and high affinity binding to Flt-1 but not to Flk-1/KDR. *Journal of Biological Chemistry, 269*(41), 25646-25654.

Park, J. E., Keller, G.-A., & Ferrara, N. (1993). The vascular endothelial growth factor (VEGF) isoforms: differential deposition into the subepithelial extracellular matrix and bioactivity of extracellular matrix-bound VEGF. *Molecular biology of the cell, 4*(12), 1317-1326.

Park, S., Bello, A., Arai, Y., Ahn, J., Kim, D., Cha, K.-Y., Baek, I., Park, H., & Lee, S.-H. (2021). Functional duality of chondrocyte hypertrophy and biomedical application trends in osteoarthritis. *Pharmaceutics, 13*(08), 1139.

Patel, M., Sachidanandan, M., & Adnan, M. (2019). Serine arginine protein kinase 1 (SRPK1): a moonlighting protein with theranostic ability in cancer prevention. *Molecular biology reports, 46*(1), 1487-1497.

Patel, S. A., Nilsson, M. B., Le, X., Cascone, T., Jain, R. K., & Heymach, J. V. (2023). Molecular mechanisms and future implications of VEGF/VEGFR in cancer therapy. *Clinical Cancer Research, 29*(1), 30-39.

Patil, A., Sable, R., & Kothari, R. (2012). Occurrence, biochemical profile of vascular endothelial growth factor (VEGF) isoforms and their functions in endochondral ossification. *Journal of cellular physiology, 227*(4), 1298-1308.

Pazzaglia, U. E., Reguzzoni, M., Casati, L., Sibilia, V., Zarattini, G., & Raspanti, M. (2020). New morphological evidence of the 'fate'of growth plate hypertrophic chondrocytes in the general context of endochondral ossification. *Journal of anatomy, 236*(2), 305-316.

Peach, C. J., Mignone, V. W., Arruda, M. A., Alcobia, D. C., Hill, S. J., Kilpatrick, L. E., & Woolard, J. (2018). Molecular pharmacology of VEGF-A isoforms: binding and signalling at VEGFR2. *International journal of molecular sciences, 19*(4), 1264.

Pearson, C. M., & Wood, F. D. (1959). Studies of polyarthritis and other lesions induced in rats by injection of mycobacterial adjuvant. I. General clinical and pathologic characteristics and some modifying factors. *Arthritis & Rheumatism: Official Journal of the American College of Rheumatology, 2*(5), 440-459.

Perez-Gutierrez, L., & Ferrara, N. (2023). Biology and therapeutic targeting of vascular endothelial growth factor A. *Nature reviews Molecular cell biology, 24*(11), 816-834.

Perrin, R., Konopatskaya, O., Qiu, Y., Harper, S., Bates, D., & Churchill, A. (2005). Diabetic retinopathy is associated with a switch in splicing from anti-to pro-angiogenic isoforms of vascular endothelial growth factor. *Diabetologia, 48*(11), 2422-2427.

Pertovaara, L., Kaipainen, A., Mustonen, T., Orpana, A., Ferrara, N., Saksela, O., & Alitalo, K. (1994). Vascular endothelial growth factor is induced in response to transforming growth factor-beta in fibroblastic and epithelial cells. *Journal of Biological Chemistry, 269*(9), 6271-6274.

Pfander, D., Körtje, D., Zimmermann, R., Weseloh, G., Kirsch, T., Gesslein, M., Cramer, T., & Swoboda, B. (2001). Vascular endothelial growth factor in articular cartilage of healthy and osteoarthritic human knee joints. *Annals of the rheumatic diseases, 60*(11), 1070-1073.

Pfeilschifter, J., Köditz, R., Pfohl, M., & Schatz, H. (2002). Changes in proinflammatory cytokine activity after menopause. *Endocrine reviews, 23*(1), 90-119.

Pianta, A., Arvikar, S. L., Strle, K., Drouin, E. E., Wang, Q., Costello, C. E., & Steere, A. C. (2017). Two rheumatoid arthritis–specific autoantigens correlate microbial immunity with autoimmune responses in joints. *The Journal of clinical investigation, 127*(8), 2946-2956.

Pikwer, M., Bergström, U., Nilsson, J.-Å., Jacobsson, L., Berglund, G., & Turesson, C. (2008). Breast-feeding, but not oral contraceptives, is associated with a reduced risk of rheumatoid arthritis. *Annals of the rheumatic diseases*.

Pisetsky, D. S., & Ward, M. M. (2012). Advances in the treatment of inflammatory arthritis. *Best Practice & Research Clinical Rheumatology, 26*(2), 251-261.

Plant, M. J., Jones, P. W., Saklatvala, J., Ollier, W., & Dawes, P. T. (1998). Patterns of radiological progression in early rheumatoid arthritis: results of an 8 year prospective study. *The Journal of rheumatology, 25*(3), 417-426.

Plenge, R. M., Padyukov, L., Remmers, E. F., Purcell, S., Lee, A. T., Karlson, E. W., Wolfe, F., Kastner, D. L., Alfredsson, L., & Altshuler, D. (2005). Replication of putative candidate-gene associations with rheumatoid arthritis in> 4,000 samples from North America and Sweden: association of susceptibility with PTPN22, CTLA4, and PADI4. *The American Journal of Human Genetics, 77*(6), 1044-1060.

Pollard, L., Choy, E., & Scott, D. (2005). The consequences of rheumatoid arthritis: quality of life measures in the individual patient. *Clinical and experimental rheumatology, 23*(5), S43.

Ponder, B., & Wilkinson, M. (1981). Inhibition of endogenous tissue alkaline phosphatase with the use of alkaline phosphatase conjugates in immunohistochemistry. *Journal of Histochemistry & Cytochemistry, 29*(8), 981-984.

Ponomarenko, E. A., Poverennaya, E. V., Ilgisonis, E. V., Pyatnitskiy, M. A., Kopylov, A. T., Zgoda, V. G., Lisitsa, A. V., & Archakov, A. I. (2016). The size of the human proteome: The width and depth. *International journal of analytical chemistry, 2016*.

Pörtner, R., & Meenen, N. (2010). Technological aspects of regenerative medicine and tissue engineering of articular cartilage. *Handchirurgie, Mikrochirurgie, plastische Chirurgie: Organ der Deutschsprachigen Arbeitsgemeinschaft fur Handchirurgie: Organ der Deutschsprachigen Arbeitsgemeinschaft fur Mikrochirurgie der Peripheren Nerven und Gefasse: Organ der V.. 42*(6), 329-336.

Prasad, J., Colwill, K., Pawson, T., & Manley, J. L. (1999). The protein kinase Clk/Sty directly modulates SR protein activity: both hyper-and hypophosphorylation inhibit splicing. *Molecular and cellular biology, 19*(10), 6991-7000.

Pritchard-Jones, R., Dunn, D., Qiu, Y., Varey, A., Orlando, A., Rigby, H., Harper, S., & Bates, D. (2007). Expression of VEGFxxxb, the inhibitory isoforms of VEGF, in malignant melanoma. *British journal of cancer, 97*(2), 223-230.

Prochazka, L., Tesarik, R., & Turanek, J. (2014). Regulation of alternative splicing of CD44 in cancer. *Cellular signalling, 26*(10), 2234-2239.

Proudman, S., Conaghan, P., Richardson, C., Griffiths, B., Green, M., McGonagle, D., Wakefield, R., Reece, R., Miles, S., & Adebajo, A. (2000). Treatment of poor-prognosis early rheumatoid arthritis: a randomized study of treatment with methotrexate, cyclosporin A, and intraarticular corticosteroids compared with sulfasalazine alone. *Arthritis & Rheumatism: Official Journal of the American College of Rheumatology, 43*(8), 1809-1819.

Puddu, G., Cipolla, M., Cerullo, G., Franco, V., & Giannì, E. (2010). Which osteotomy for a valgus knee? *International orthopaedics, 34*, 239-247.

Pufe, T., Harde, V., Petersen, W., Goldring, M. B., Tillmann, B., & Mentlein, R. (2004). Vascular endothelial growth factor (VEGF) induces matrix metalloproteinase expression in immortalized chondrocytes. *The Journal of pathology, 202*(3), 367-374.

Pufe, T., Petersen, W., Tillmann, B., & Mentlein, R. (2001). Detection of the vascular endothelial growth factor in fetal, degenerative and normal human tendons. *Virchows Arch, 439*, 355-359.

Pufe, T., Petersen, W., Tillmann, B., & Mentlein, R. (2001). Splice variants VEGF121 and VEGF165 of the angiogenic peptide vascular endothelial cell growth factor are expressed in the synovial tissue of patients with rheumatoid arthritis. *The Journal of rheumatology, 28*(7), 1482-1485.

Pufe, T., Petersen, W., Tillmann, B., & Mentlein, R. (2001). The splice variants VEGF121 and VEGF189 of the angiogenic peptide vascular endothelial growth factor are expressed in osteoarthritic cartilage. *Arthritis & Rheumatism: Official Journal of the American College of Rheumatology, 44*(5), 1082-1088.

Pujol-Lereis, L. M., Liebisch, G., Schick, T., Lin, Y., Grassmann, F., Uchida, K., Zipfel, P. F., Fauser, S., Skerka, C., & Weber, B. H. (2018). Evaluation of serum sphingolipids and the influence of genetic risk factors in age-related macular degeneration. *PloS one, 13*(8), e0200739.

Pulik, L., Legosz, P., & Motyl, G. (2023). Matrix metalloproteinases in rheumatoid arthritis and osteoarthritis: a state of the art review. *Reumatologia, 61*(3), 191.

Pullig, O., Weseloh, G., Gauer, S., & Swoboda, B. (2000). Osteopontin is expressed by adult human osteoarthritic chondrocytes: protein and mRNA analysis of normal and osteoarthritic cartilage. *Matrix Biology, 19*(3), 245-255.

Pullig, O., Weseloh, G., Ronneberger, D.-L., Käkönen, S.-M., & Swoboda, B. (2000). Chondrocyte differentiation in human osteoarthritis: expression of osteocalcin in normal and osteoarthritic cartilage and bone. *Calcified tissue international, 67*(3), 230-240.

Purkayastha, B., Chan, E., Ravillah, D., Ravi, L., Gupta, R., Canto, M., Wang, J., Shaheen, N., Willis, J., & Chak, A. (2020). Genome-scale analysis identifies novel transcript-variants in esophageal adenocarcinoma. *Cellular and Molecular Gastroenterology and Hepatology, 10*(3), 652.

Qian, J.-j., Xu, Q., Xu, W.-m., Cai, R., & Huang, G.-c. (2021). Expression of VEGF-A signaling pathway in cartilage of ACLT-induced osteoarthritis mouse model. *Journal of Orthopaedic Surgery and Research, 16*(1), 1-8.

Qian, K., Zheng, X.-X., Wang, C., Huang, W.-G., Liu, X.-B., Xu, S.-D., Liu, D.-K., Liu, M.-Y., & Lin, C.-S. (2022). β-Sitosterol inhibits rheumatoid synovial angiogenesis through suppressing VEGF signaling pathway. *Frontiers in pharmacology, 12*, 816477.

Qiu, T., Chen, W., Li, P., Sun, J., Gu, Y., & Chen, X. (2018). Subsequent anti-VEGF therapy after first-line anti-EGFR therapy improved overall survival of patients with metastatic colorectal cancer. *OncoTargets and therapy*, 465-471.

Qiu, Y., Wang, Z., Zhang, X., Huang, P., Zhang, W., Zhang, K., Wang, S., He, L., Guo, Y., & Xiang, A. (2020). A long-acting isomer of Ac-SDKP attenuates pulmonary fibrosis through SRPK1-mediated PI3K/AKT and Smad2 pathway inhibition. *IUBMB life, 72*(12), 2611-2626.

Radisavljevic, Z., Avraham, H., & Avraham, S. (2000). Vascular endothelial growth factor up-regulates ICAM-1 expression via the phosphatidylinositol 3 OH-kinase/AKT/nitric oxide pathway and modulates migration of brain microvascular endothelial cells. *Journal of Biological Chemistry, 275*(27), 20770-20774.

Radner, H., Neogi, T., Smolen, J. S., & Aletaha, D. (2014). Performance of the 2010 ACR/EULAR classification criteria for rheumatoid arthritis: a systematic literature review. *Annals of the rheumatic diseases, 73*(1), 114-123.

Raine, C., & Giles, I. (2022). What is the impact of sex hormones on the pathogenesis of rheumatoid arthritis? *Frontiers in Medicine, 9*, 909879.

Rainsford, K. (1982). Adjuvant polyarthritis in rats: is this a satisfactory model for screening anti-arthritic drugs? *Agents and actions, 12*, 452-458.

Raja, R., Chapman, P. T., O'DONNELL, J. L., Ipenburg, J., Frampton, C., Hurst, M., & Stamp, L. K. (2012). Comparison of the 2010 American College of Rheumatology/European League Against Rheumatism and the 1987 American Rheumatism Association classification criteria for rheumatoid arthritis in an early arthritis cohort in New Zealand. *The Journal of rheumatology, 39*(11), 2098-2103.

Ramanujan, S. A., Cravens, E. N., Krishfield, S. M., Kyttaris, V. C., & Moulton, V. R. (2021). Oestrogen-Induced hsa-miR-10b-5p Is Elevated in T Cells From Patients With Systemic Lupus Erythematosus and Down-Regulates Serine/Arginine-Rich Splicing Factor 1. *Arthritis & Rheumatology, 73*(11), 2052-2058.

Rantapaa-Dahlqvist, S., de Jong, B., Berglin, E., Hallmans, G., & Wadell, G. S. H., Sundin, U., and van Venrooij, WJ (2003) Antibodies against cyclic citrullinated peptide and IgA rheumatoid factor predict the development of rheumatoid arthritis. *Arthritis Rheum, 48*, 2741-2749.

Rathmacher, J. A., Fuller Jr, J. C., Abumrad, N. N., & Flynn, C. R. (2023). Inflammation Biomarker Response to Oral 2-Hydroxybenzylamine (2-HOBA) Acetate in Healthy Humans. *Inflammation*, 1-10.

Raychaudhuri, S., Sandor, C., Stahl, E. A., Freudenberg, J., Lee, H.-S., Jia, X., Alfredsson, L., Padyukov, L., Klareskog, L., & Worthington, J. (2012). Five amino acids in three HLA proteins explain most of the association between MHC and seropositive rheumatoid arthritis. *Nature genetics, 44*(3), 291-296.

Razaq, S., Wilkins, R. J., & Urban, J. P. (2003). The effect of extracellular pH on matrix turnover by cells of the bovine nucleus pulposus. *European Spine Journal, 12*(4), 341-349.

Redlich, K., & Smolen, J. S. (2012). Inflammatory bone loss: pathogenesis and therapeutic intervention. *Nature reviews Drug discovery, 11*(3), 234-250.

Reichardt, L. F., & Tomaselli, K. J. (1991). Extracellular matrix molecules and their receptors: functions in neural development. *Annual review of neuroscience, 14*(1), 531-570.

Remmers, E. F., Plenge, R. M., Lee, A. T., Graham, R. R., Hom, G., Behrens, T. W., De Bakker, P. I., Le, J. M., Lee, H.-S., & Batliwalla, F. (2007). STAT4 and the risk of

rheumatoid arthritis and systemic lupus erythematosus. *New England journal of medicine, 357*(10), 977-986.

Ren, S.-X., Zhang, B., Lin, Y., Ma, D.-S., & Li, H. (2019). Mechanistic evaluation of anti-arthritic activity of β-methylphenylalanine in experimental rats. *Biomedicine & pharmacotherapy, 113*, 108730.

Rennel, E., Waine, E., Guan, H., Schüler, Y., Leenders, W., Woolard, J., Sugiono, M., Gillatt, D., Kleinerman, E. S., & Bates, D. (2008). The endogenous anti-angiogenic VEGF isoform, VEGF 165 b inhibits human tumour growth in mice. *British journal of cancer, 98*(7), 1250-1257.

Rennel, E., Waine, E., Harper, S., Guan, H., Schüler, Y., Leenders, W., Woolard, J., Sugiono, M., Gillatt, D., & Kleinerman, E. (2008). The endogenous anti-angiogenic VEGF isoform, $VEGF_{165}b$ inhibits human tumour growth in mice.

Rennel, E. S., Hamdollah-Zadeh, M. A., Wheatley, E. R., Magnussen, A., Schüler, Y., Kelly, S. P., Finucane, C., Ellison, D., Cebe-Suarez, S., & Ballmer-Hofer, K. (2008). Recombinant human VEGF165b protein is an effective anti-cancer agent in mice. *European Journal of Cancer, 44*(13), 1883-1894.

Rhee, D. K., Marcelino, J., Baker, M., Gong, Y., Smits, P., Lefebvre, V., Jay, G. D., Stewart, M., Wang, H., & Warman, M. L. (2005). The secreted glycoprotein lubricin protects cartilage surfaces and inhibits synovial cell overgrowth. *The Journal of clinical investigation, 115*(3), 622-631.

Rieck, M., Arechiga, A., Onengut-Gumuscu, S., Greenbaum, C., Concannon, P., & Buckner, J. H. (2007). Genetic variation in PTPN22 corresponds to altered function of T and B lymphocytes. *The Journal of Immunology, 179*(7), 4704-4710.

Rim, Y. A., Nam, Y., & Ju, J. H. (2020). The role of chondrocyte hypertrophy and senescence in osteoarthritis initiation and progression. *International Journal of Molecular Sciences, 21*(7), 2358.

Ripmeester, E. G., Timur, U. T., Caron, M. M., & Welting, T. J. (2018). Recent insights into the contribution of the changing hypertrophic chondrocyte phenotype in the development and progression of osteoarthritis. *Frontiers in bioengineering and biotechnology, 6*, 18.

Risau, W. (1997). Mechanisms of angiogenesis. *Nature, 386*(6626), 671-674.

RISETherapeutics. (2023). FDA Clears Rise Therapeutics' IND Application to Initiate a Phase 1 Clinical Study of Its Novel Oral Immunotherapy for the Treatment of Rheumatoid Arthritis. Retrieved from https://www.risetherapeutics.com/news/65-fda-ind-announcement-2487

Ritchlin, C. T., Haas-Smith, S. A., Li, P., Hicks, D. G., & Schwarz, E. M. (2003). Mechanisms of TNF-α–and RANKL-mediated osteoclastogenesis and bone resorption in psoriatic arthritis. *The Journal of clinical investigation, 111*(6), 821-831.

Robinson, C. J., & Stringer, S. E. (2001). The splice variants of vascular endothelial growth factor (VEGF) and their receptors. *Journal of cell science, 114*(5), 853-865.

Romao, V. C., & Fonseca, J. E. (2021). Etiology and risk factors for rheumatoid arthritis: a state-of-the-art review. *Frontiers in Medicine, 8*, 689698.

Romijn, H. J., van Uum, J. F., Breedijk, I., Emmering, J., Radu, I., & Pool, C. W. (1999). Double immunolabeling of neuropeptides in the human hypothalamus as analyzed by confocal laser scanning fluorescence microscopy. *Journal of Histochemistry & Cytochemistry, 47*(2), 229-235.

Rosenberg, L. (1971). Chemical basis for the histological use of safranin O in the study of articular cartilage. *JBJS, 53*(1), 69-82.

Rosenfeld, P. J., Brown, D. M., Heier, J. S., Boyer, D. S., Kaiser, P. K., Chung, C. Y., & Kim, R. Y. (2006). Ranibizumab for neovascular age-related macular degeneration. *New England journal of medicine, 355*(14), 1419-1431.

Roskams, T. (2002). The role of immunohistochemistry in diagnosis. *Clinics in liver disease, 6*(2), 571-589.

Roskoski Jr, R. (2022). Properties of FDA-approved small molecule protein kinase inhibitors: A 2023 update. *Pharmacological research*, 106552.

Rosset, E. M., & Bradshaw, A. D. (2016). SPARC/osteonectin in mineralized tissue. *Matrix Biology, 52*, 78-87.

Rubbert-Roth, A., Enejosa, J., Pangan, A. L., Haraoui, B., Rischmueller, M., Khan, N., Zhang, Y., Martin, N., & Xavier, R. M. (2020). Trial of upadacitinib or abatacept in rheumatoid arthritis. *New England Journal of Medicine, 383*(16), 1511-1521.

Rudwaleit, M., & Taylor, W. J. (2010). Classification criteria for psoriatic arthritis and ankylosing spondylitis/axial spondyloarthritis. *Best Practice & Research Clinical Rheumatology, 24*(5), 589-604.

Rueden, C. T., Schindelin, J., Hiner, M. C., DeZonia, B. E., Walter, A. E., Arena, E. T., & Eliceiri, K. W. (2017). ImageJ2: ImageJ for the next generation of scientific image data. *BMC bioinformatics, 18*, 1-26.

Russo, S., Scotto di Carlo, F., & Gianfrancesco, F. (2022). The osteoclast traces the route to bone tumors and metastases. *Frontiers in Cell and Developmental Biology, 10*, 886305.

Ryu, J.-H., Chae, C.-S., Kwak, J.-S., Oh, H., Shin, Y., Huh, Y. H., Lee, C.-G., Park, Y.-W., Chun, C.-H., & Kim, Y.-M. (2014). Hypoxia-inducible factor-2α is an essential catabolic regulator of inflammatory rheumatoid arthritis. *PLoS biology, 12*(6), e1001881.

Ryu, S., Lee, J., & Kim, S. (2006). IL-17 increased the production of vascular endothelial growth factor in rheumatoid arthritis synoviocytes. *Clinical rheumatology, 25*, 16-20.

Sabharwal, R., Gupta, S., Sepolia, S., Panigrahi, R., Mohanty, S., Subudhi, S. K., & Kumar, M. (2014). An insight in to paget's disease of bone. *Nigerian Journal of Surgery, 20*(1), 9-15.

Sabi, E. M., Singh, A., Althafar, Z. M., Behl, T., Sehgal, A., Singh, S., Sharma, N., Bhatia, S., Al-Harrasi, A., & Alqahtani, H. M. (2022). Elucidating the role of hypoxia-inducible factor in rheumatoid arthritis. *Inflammopharmacology, 30*(3), 737-748.

Saijo, N. (2002). Translational study in cancer research. *Internal medicine, 41*(10), 770-773.

Saijo, N., Nishio, K., & Tamura, T. (2003). Translational and clinical studies of target-based cancer therapy. *International Journal of Clinical Oncology, 8*, 187-192.

Saito, M., & Marumo, K. (2015). Effects of collagen crosslinking on bone material properties in health and disease. *Calcified tissue international, 97*, 242-261.

Saito, T., Fukai, A., Mabuchi, A., Ikeda, T., Yano, F., Ohba, S., Nishida, N., Akune, T., Yoshimura, N., & Nakagawa, T. (2010). Transcriptional regulation of endochondral ossification by HIF-2α during skeletal growth and osteoarthritis development. *Nature medicine, 16*(6), 678-686.

Sakalyte, R., Bagdonaite, L., Stropuviene, S., Naktinyte, S., & Venalis, A. (2022). VEGF profile in early undifferentiated arthritis cohort. *Medicina, 58*(6), 833.

Salliot, C., Nguyen, Y., Gusto, G., Gelot, A., Gambaretti, J., Mariette, X., Boutron-Ruault, M.-C., & Seror, R. (2021). Female hormonal exposures and risk of rheumatoid arthritis in the French E3N-EPIC cohort study. *Rheumatology, 60*(10), 4790-4800.

Salton, M., Voss, T. C., & Misteli, T. (2014). Identification by high-throughput imaging of the histone methyltransferase EHMT2 as an epigenetic regulator of VEGFA alternative splicing. *Nucleic acids research, 42*(22), 13662-13673.

Salzberg, S. L. (2018). Open questions: How many genes do we have? *BMC biology, 16*(1), 1-3.

Sambrook, P. N. (2000). The skeleton in rheumatoid arthritis: common mechanisms for bone erosion and osteoporosis? In (Vol. 27, pp. 2541-2542).

Sandler, A., Gray, R., Perry, M. C., Brahmer, J., Schiller, J. H., Dowlati, A., Lilenbaum, R., & Johnson, D. H. (2006). Paclitaxel–carboplatin alone or with bevacizumab for non–small-cell lung cancer. *New England journal of medicine, 355*(24), 2542-2550.

Sangha, O. (2000). Epidemiology of rheumatic diseases. *Rheumatology, 39*(suppl_2), 3-12.

Sardar, S., & Andersson, Å. (2016). Old and new therapeutics for rheumatoid arthritis: in vivo models and drug development. *Immunopharmacology and immunotoxicology, 38*(1), 2-13.

Sarkar, J., Luo, Y., Zhou, Q., Ivakhnitskaia, E., Lara, D., Katz, E., Sun, M. G., Guaiquil, V., & Rosenblatt, M. (2022). VEGF receptor heterodimers and homodimers are differentially expressed in neuronal and endothelial cell types. *PloS one, 17*(7), e0269818.

Sato, K., Suematsu, A., Okamoto, K., Yamaguchi, A., Morishita, Y., Kadono, Y., Tanaka, S., Kodama, T., Akira, S., & Iwakura, Y. (2006). Th17 functions as an osteoclastogenic helper T cell subset that links T cell activation and bone destruction. *The Journal of experimental medicine, 203*(12), 2673-2682.

Savontaus, M., Ihanamäki, T., Perälä, M., Metsäranta, M., Sandberg-Lall, M., & Vuorio, E. (1998). Expression of type II and IX collagen isoforms during normal and pathological cartilage and eye development. *Histochemistry and cell biology, 110*, 149-159.

Sawano, A., Iwai, S., Sakurai, Y., Ito, M., Shitara, K., Nakahata, T., & Shibuya, M. (2001). Flt-1, vascular endothelial growth factor receptor 1, is a novel cell surface marker for the lineage of monocyte-macrophages in humans. *Blood, The Journal of the American Society of Hematology, 97*(3), 785-791.

Sawano, A., Takahashi, T., Yamaguchi, S., Aonuma, M., & Shibuya, M. (1996). Flt-1 but not KDR/Flk-1 tyrosine kinase is a receptor for placenta growth factor, which is related to vascular endothelial growth factor. *Cell growth & differentiation: the molecular biology journal of the American Association for Cancer Research, 7*(2), 213-221.

Scanzello, C. R. (2022). Synovial Structure and Physiology in Health and Disease. In *Synovial Fluid Analysis and The Evaluation of Patients With Arthritis* (pp. 5-19): Springer.

Schaible, H. G., König, C., & Ebersberger, A. (2022). Spinal pain processing in arthritis: Neuron and glia (inter) actions. *Journal of Neurochemistry*.

Schaible, H. G., Von Banchet, G. S., Boettger, M., Bräuer, R., Gajda, M., Richter, F., Hensellek, S., Brenn, D., & Natura, G. (2010). The role of proinflammatory cytokines in the generation and maintenance of joint pain. *Annals of the New York Academy of Sciences, 1193*(1), 60-69.

Schedel, J., Wenglén, C., Distler, O., Müller-Ladner, U., Schölmerich, J., Heinegård, D., & Krenn, V. (2004). Differential adherence of osteoarthritis and rheumatoid arthritis synovial fibroblasts to cartilage and bone matrix proteins and its implication for osteoarthritis pathogenesis. *Scandinavian journal of immunology, 60*(5), 514-523.

Schett, G. (2007). Cells of the synovium in rheumatoid arthritis. Osteoclasts. *Arthritis research & therapy, 9*, 1-6.

Schmitz, N., Laverty, S., Kraus, V., & Aigner, T. (2010). Basic methods in histopathology of joint tissues. *Osteoarthritis and Cartilage, 18*, S113-S116.

Schroeder, M., Viezens, L., Fuhrhop, I., Rüther, W., Schaefer, C., Schwarzloh, B., Algenstaedt, P., Fink, B., & Hansen-Algenstaedt, N. (2013). Angiogenic growth factors in rheumatoid arthritis. *Rheumatology international, 33*, 523-527.

Scott, D. L. (2004). Radiological progression in established rheumatoid arthritis. *The Journal of Rheumatology Supplement, 69*, 55-65.

Seetharam, L., Gotoh, N., Maru, Y., Neufeld, G., Yamaguchi, S., & Shibuya, M. (1995). A unique signal transduction from FLT tyrosine kinase, a receptor for vascular endothelial growth factor VEGF. *Oncogene, 10*(1), 135-147.

Semenza, G. L. (1998). Hypoxia-inducible factor 1: master regulator of O2 homeostasis. *Current opinion in genetics & development, 8*(5), 588-594.

Semenza, G. L. (2000). HIF-1: mediator of physiological and pathophysiological responses to hypoxia. *Journal of applied physiology, 88*(4), 1474-1480.

Semenza, G. L. (2000). HIF-1: using two hands to flip the angiogenic switch. *Cancer and Metastasis Reviews, 19*, 59-65.

Semerano, L., Duvallet, E., Belmellat, N., Marival, N., Schall, N., Monteil, M., Grouard-Vogel, G., Bernier, E., Lecouvey, M., & Hlawaty, H. (2016). Targeting VEGF-A with a vaccine decreases inflammation and joint destruction in experimental arthritis. *Angiogenesis, 19*, 39-52.

Senger, D. R., Galli, S. J., Dvorak, A. M., Perruzzi, C. A., Harvey, V. S., & Dvorak, H. F. (1983). Tumor cells secrete a vascular permeability factor that promotes accumulation of ascites fluid. *Science, 219*(4587), 983-985.

Senolt, L., Leszczynski, P., Dokoupilová, E., Göthberg, M., Valencia, X., Hansen, B. B., & Canete, J. D. (2015). Efficacy and Safety of Anti–Interleukin-20 Monoclonal Antibody in Patients With Rheumatoid Arthritis: A Randomized Phase IIa Trial. *Arthritis & Rheumatology, 67*(6), 1438-1448.

Seo, T., Deshmukh, V., & Yazici, Y. (2021). Lorecivivint (SM04690), an intra-articular, small-molecule CLK/DYRK1A inhibitor that modulates the WNT pathway, as a potential treatment for meniscal injuries. *Osteoarthritis and cartilage, 29*, S101-S102.

Serrano, P., Aubol, B. E., Keshwani, M. M., Forli, S., Ma, C.-T., Dutta, S. K., Geralt, M., Wüthrich, K., & Adams, J. A. (2016). Directional phosphorylation and nuclear transport of the splicing factor SRSF1 is regulated by an RNA recognition motif. *Journal of molecular biology, 428*(11), 2430-2445.

Shah, A., Cieremans, D., Slover, J., Schwarzkopf, R., & Meftah, M. (2022). Trends in Complications and Outcomes in Patients Aged 65 Years and Younger Undergoing Total Knee Arthroplasty: Data from the American Joint Replacement Registry. *JAAOS Global Research & Reviews, 6*(6).

Shaik, F., Cuthbert, G. A., Homer-Vanniasinkam, S., Muench, S. P., Ponnambalam, S., & Harrison, M. A. (2020). Structural basis for vascular endothelial growth factor

receptor activation and implications for disease therapy. *Biomolecules, 10*(12), 1673.

Shakibaei, M., Schulze-Tanzil, G., Mobasheri, A., Beichler, T., Dressler, J., & Schwab, W. (2003). Expression of the vegf receptor-3 in osteoarthritic chondrocytes: Stimulation by interleukin-1β and association with β1-integrins. *Histochemistry and cell biology, 120*(3), 235-241.

Shakibaei, M., Schulze-Tanzil, G., Mobasheri, A., Beichler, T., Dressler, J., & Schwab, W. (2003). Expression of the VEGF receptor-3 in osteoarthritic chondrocytes: stimulation by interleukin-1β and association with β 1-integrins. *Histochemistry and cell biology, 120*(3), 235-241.

Shalaby, F., Rossant, J., Yamaguchi, T. P., Gertsenstein, M., Wu, X.-F., Breitman, M. L., & Schuh, A. C. (1995). Failure of blood-island formation and vasculogenesis in Flk-1-deficient mice. *Nature, 376*(6535), 62-66.

Shams, N., & Ianchulev, T. (2006). Role of vascular endothelial growth factor in ocular angiogenesis. *Ophthalmology Clinics of North America, 19*(3), 335-344.

Shchetynsky, K., Protsyuk, D., Ronninger, M., Diaz-Gallo, L.-M., Klareskog, L., & Padyukov, L. (2015). Gene–gene interaction and RNA splicing profiles of MAP2K4 gene in rheumatoid arthritis. *Clinical Immunology, 158*(1), 19-28.

Shen, P., Jiao, Z., Zheng, J. S., Xu, W. F., Zhang, S. Y., Qin, A., & Yang, C. (2015). Injecting vascular endothelial growth factor into the temporomandibular joint induces osteoarthritis in mice. *Scientific reports, 5*(1), 1-11.

Sheng, J., Zhao, J., Xu, Q., Wang, L., Zhang, W., & Zhang, Y. (2017). Bioinformatics analysis of SRSF1-controlled gene networks in colorectal cancer. *Oncology letters, 14*(5), 5393-5399.

Sheokand, N., Malhotra, H., Kumar, S., Tillu, V. A., Chauhan, A. S., Raje, C. I., & Raje, M. (2014). Moonlighting cell-surface GAPDH recruits apotransferrin to effect iron egress from mammalian cells. *Journal of cell science, 127*(19), 4279-4291.

Sherwood, J., Bertrand, J., Nalesso, G., Poulet, B., Pitsillides, A., Brandolini, L., Karystinou, A., De Bari, C., Luyten, F. P., & Pitzalis, C. (2015). A homeostatic function of CXCR2 signalling in articular cartilage. *Annals of the rheumatic diseases, 74*(12), 2207-2215.

Shi, G.-X., Zheng, X.-F., Zhu, C., Li, B., Wang, Y.-R., Jiang, S.-D., & Jiang, L.-S. (2017). Evidence of the role of R-Spondin 1 and its receptor Lgr4 in the transmission of mechanical stimuli to biological signals for bone formation. *International journal of molecular sciences, 18*(3), 564.

Shibuya, M. (2001). Structure and function of VEGF/VEGF-receptor system involved in angiogenesis. *Cell structure and function, 26*(1), 25-35.

Shibuya, M. (2006). Claesson-Welsh L. *Signal transduction by VEGF receptors in regulation of angiogenesis and lymphangiogenesis. Exp Cell Res, 312*(5), 549Â560.

Shibuya, M. (2006). Vascular endothelial growth factor receptor-1 (VEGFR-1/Flt-1): a dual regulator for angiogenesis. *Angiogenesis, 9*(4), 225-230.

Shibuya, M. (2008). Vascular endothelial growth factor-dependent and-independent regulation of angiogenesis. *BMB reports, 41*(4), 278-286.

Shibuya, M. (2011). Vascular endothelial growth factor (VEGF) and its receptor (VEGFR) signaling in angiogenesis: a crucial target for anti-and pro-angiogenic therapies. *Genes & cancer, 2*(12), 1097-1105.

Shibuya, M. (2015). VEGF-VEGFR system as a target for suppressing inflammation and other diseases. *Endocrine, Metabolic & Immune Disorders-Drug Targets (Formerly Current Drug Targets-Immune, Endocrine & Metabolic Disorders), 15*(2), 135-144.

Shigeyama, Y., Pap, T., Kunzler, P., Simmen, B. R., Gay, R. E., & Gay, S. (2000). Expression of osteoclast differentiation factor in rheumatoid arthritis. *Arthritis & Rheumatism: Official Journal of the American College of Rheumatology, 43*(11), 2523-2530.

Shiozawa, K., Hino, K., & Shiozawa, S. (2001). Alternatively spliced EDA-containing fibronectin in synovial fluid as a predictor of rheumatoid joint destruction. *Rheumatology, 40*(7), 739-742.

Shiozawa, S., Yoshihara, R., Kuroki, Y., Fujita, T., Shiozawa, K., & Imura, S. (1992). Pathogenic importance of fibronectin in the superficial region of articular cartilage as a local factor for the induction of pannus extension on rheumatoid articular cartilage. *Annals of the rheumatic diseases, 51*(7), 869-873.

Shiying, W., Boyun, S., Jianye, Y., Wanjun, Z., Ping, T., Jiang, L., & Hongyi, H. (2017). The different effects of VEGFA121 and VEGFA165 on regulating angiogenesis depend on phosphorylation sites of VEGFR2. *Inflammatory Bowel Diseases, 23*(4), 603-616.

Shlopov, B. V., Gumanovskaya, M. L., & Hasty, K. A. (2000). Autocrine regulation of collagenase 3 (matrix metalloproteinase 13) during osteoarthritis. *Arthritis & Rheumatism: Official Journal of the American College of Rheumatology, 43*(1), 195-205.

Shukunami, C., Ishizeki, K., Atsumi, T., Ohta, Y., Suzuki, F., & Hiraki, Y. (1997). Cellular hypertrophy and calcification of embryonal carcinoma-derived chondrogenic cell line ATDC5 in vitro. *Journal of Bone and Mineral Research, 12*(8), 1174-1188.

Silman, A., Kay, A., & Brennan, P. (1992). Timing of pregnancy in relation to the onset of rheumatoid arthritis. *Arthritis & Rheumatism: Official Journal of the American College of Rheumatology, 35*(2), 152-155.

Silva, J. C. d., Mariz, H. A., Rocha Júnior, L. F. d., Oliveira, P. S. S. d., Dantas, A. T., Duarte, A. L. B. P., Pitta, I. d. R., Galdino, S. L., & Pitta, M. G. d. R. (2013). Hydroxychloroquine decreases Th17-related cytokines in systemic lupus erythematosus and rheumatoid arthritis patients. *Clinics, 68*, 766-771.

Silva Rodrigues, J. F., Santos Silva e Silva Figueiredo, C., França Muniz, T., de Aquino, A. F. S., Neuza da Silva Nina, L., Fialho Sousa, N. C., Nascimento da Silva, L. C., De Souza, B. G. G. F., da Penha-Silva, T. A., & Abreu-Silva, A. L. (2018). Sulforaphane Modulates Joint Inflammation in a Murine Model of Complete Freund's Adjuvant-Induced Mono-Arthritis. *Molecules, 23*(5), 988.

Silverman, A. B., Reinherz, H. Z., & Giaconia, R. M. (1996). The long-term sequelae of child and adolescent abuse: A longitudinal community study. *Child abuse & neglect, 20*(8), 709-723.

Singh, A., Gill, G., Kaur, H., Amhmed, M., & Jakhu, H. (2018). Role of osteopontin in bone remodeling and orthodontic tooth movement: a review. *Progress in orthodontics, 19*(1), 1-8.

Singh, J. A., Saag, K. G., Bridges Jr, S. L., Akl, E. A., Bannuru, R. R., Sullivan, M. C., Vaysbrot, E., McNaughton, C., Osani, M., & Shmerling, R. H. (2016). 2015 American College of Rheumatology guideline for the treatment of rheumatoid arthritis. *Arthritis & Rheumatology, 68*(1), 1-26.

Singh, N., Tiem, M., Watkins, R., Cho, Y. K., Wang, Y., Olsen, T., Uehara, H., Mamalis, C., Luo, L., & Oakey, Z. (2013). Soluble vascular endothelial growth factor receptor 3

is essential for corneal alymphaticity. *Blood, The Journal of the American Society of Hematology, 121*(20), 4242-4249.

Siqueira, R. P., Barbosa, É. d. A. A., Polêto, M. D., Righetto, G. L., Seraphim, T. V., Salgado, R. L., Ferreira, J. G., Barros, M. V. d. A., de Oliveira, L. L., & Laranjeira, A. B. A. (2015). Potential antileukemia effect and structural analyses of SRPK inhibition by N-(2-(piperidin-1-yl)-5-(trifluoromethyl) phenyl) isonicotinamide (SRPIN340). *PloS one, 10*(8), e0134882.

Sivakumar, B., Akhavani, M. A., Winlove, C. P., Taylor, P. C., Paleolog, E. M., & Kang, N. (2008). Synovial hypoxia as a cause of tendon rupture in rheumatoid arthritis. *The Journal of hand surgery, 33*(1), 49-58.

Skoumal, M., Kolarz, G., Haberhauer, G., Woloszczuk, W., Hawa, G., & Klingler, A. (2005). Osteoprotegerin and the receptor activator of NF-kappa B ligand in the serum and synovial fluid. A comparison of patients with longstanding rheumatoid arthritis and osteoarthritis. *Rheumatology international, 26*(1), 63-69.

Skuli, N., Majmundar, A. J., Krock, B. L., Mesquita, R. C., Mathew, L. K., Quinn, Z. L., Runge, A., Liu, L., Kim, M. N., & Liang, J. (2012). Endothelial HIF-2α regulates murine pathological angiogenesis and revascularization processes. *The Journal of clinical investigation, 122*(4), 1427-1443.

Smith, J. O., Oreffo, R. O., Clarke, N. M., & Roach, H. I. (2003). Changes in the antiangiogenic properties of articular cartilage in osteoarthritis. *Journal of Orthopaedic Science, 8*, 849-857.

Smith, M. D. (2011). The normal synovium. *The open rheumatology journal, 5*(1).

Smith, M. D., Barg, E., Weedon, H., Papengelis, V., Smeets, T., Tak, P., Kraan, M., Coleman, M., & Ahern, M. (2003). Microarchitecture and protective mechanisms in synovial tissue from clinically and arthroscopically normal knee joints. *Annals of the rheumatic diseases, 62*(4), 303-307.

Smith, M. D., Triantafillou, S., Parker, A., Youssef, P., & Coleman, M. (1997). Synovial membrane inflammation and cytokine production in patients with early osteoarthritis. *The Journal of rheumatology, 24*(2), 365-371.

Smith, R. O., Ninchoji, T., Gordon, E., André, H., Dejana, E., Vestweber, D., Kvanta, A., & Claesson-Welsh, L. (2020). Vascular permeability in retinopathy is regulated by VEGFR2 Y949 signaling to VE-cadherin. *Elife, 9*, e54056.

Smolen, J. S., Aletaha, D., Barton, A., Burmester, G. R., & Emery, P. (2018). Gary S. Firestein6, Arthur Kavanaugh6, Iain B. McInnes7, Daniel H. Solomon8, Vibeke Strand9 and Kazuhiko Yamamoto10 Abstract| Rheumatoid arthritis (RA) is a chronic, inflammatory, autoimmune disease that primarily affects the joints and is associated with autoantibodies that target various molecules including.

Smolen, J. S., Aletaha, D., Bijlsma, J. W., Breedveld, F. C., Boumpas, D., Burmester, G., Combe, B., Cutolo, M., de Wit, M., & Dougados, M. (2010). Treating rheumatoid arthritis to target: recommendations of an international task force. *Annals of the rheumatic diseases, 69*(4), 631-637.

Smolen, J. S., Feist, E., Fatenejad, S., Grishin, S. A., Korneva, E. V., Nasonov, E. L., Samsonov, M. Y., & Fleischmann, R. M. (2022). Olokizumab versus placebo or adalimumab in rheumatoid arthritis. *New England journal of medicine, 387*(8), 715-726.

Smolen, J. S., Landewé, R., Breedveld, F. C., Dougados, M., Emery, P., Gaujoux-Viala, C., Gorter, S., Knevel, R., Nam, J., & Schoels, M. (2010). EULAR recommendations for the management of rheumatoid arthritis with synthetic and biological disease-modifying antirheumatic drugs. *Annals of the rheumatic diseases, 69*(6), 964-975.

Smolen, J. S., Landewé, R. B., Bijlsma, J. W., Burmester, G. R., Dougados, M., Kerschbaumer, A., McInnes, I. B., Sepriano, A., Van Vollenhoven, R. F., & De Wit, M. (2020). EULAR recommendations for the management of rheumatoid arthritis with synthetic and biological disease-modifying antirheumatic drugs: 2019 update. *Annals of the rheumatic diseases, 79*(6), 685-699.

Smolen, J. S., van der Heijde, D., Machold, K. P., Aletaha, D., & Landewé, R. (2014). Proposal for a new nomenclature of disease-modifying antirheumatic drugs. *Annals of the rheumatic diseases, 73*(1), 3-5.

Smolen, J. S., Van Der Heijde, D. M., St. Clair, E. W., Emery, P., Bathon, J. M., Keystone, E., Maini, R. N., Kalden, J. R., Schiff, M., & Baker, D. (2006). Predictors of joint damage in patients with early rheumatoid arthritis treated with high-dose methotrexate with or without concomitant infliximab: results from the ASPIRE trial. *Arthritis & Rheumatism, 54*(3), 702-710.

Soker, S., Takashima, S., Miao, H. Q., Neufeld, G., & Klagsbrun, M. (1998). Neuropilin-1 is expressed by endothelial and tumor cells as an isoform-specific receptor for vascular endothelial growth factor. *Cell, 92*(6), 735-745.

Sokoloff, L. (1993). Microcracks in the calcified layer of articular cartilage. *Archives of pathology & laboratory medicine, 117*(2), 191-195.

Sokolove, J., Johnson, D. S., Lahey, L. J., Wagner, C. A., Cheng, D., Thiele, G. M., Michaud, K., Sayles, H., Reimold, A. M., & Caplan, L. (2014). Rheumatoid factor as a potentiator of anti–citrullinated protein antibody–mediated inflammation in rheumatoid arthritis. *Arthritis & Rheumatology, 66*(4), 813-821.

Sonamoto, R., Kii, I., Koike, Y., Sumida, Y., Kato-Sumida, T., Okuno, Y., Hosoya, T., & Hagiwara, M. (2015). Identification of a DYRK1A Inhibitor that Induces Degradation of the Target Kinase using Co-chaperone CDC37 fused with Luciferase nanoKAZ. *Scientific reports, 5*(1), 12728.

Sone, H., Kawakami, Y., Sakauchi, M., Nakamura, Y., Takahashi, A., Shimano, H., Okuda, Y., Segawa, T., Suzuki, H., & Yamada, N. (2001). Neutralization of vascular endothelial growth factor prevents collagen-induced arthritis and ameliorates established disease in mice. *Biochemical and biophysical research communications, 281*(2), 562-568.

Sone, H., Sakauchi, M., Takahashi, A., Suzuki, H., Inoue, N., Iida, K., Shimano, H., Toyoshima, H., Kawakami, Y., & Okuda, Y. (2001). Elevated levels of vascular endothelial growth factor in the sera of patients with rheumatoid arthritis correlation with disease activity. *Life sciences, 69*(16), 1861-1869.

Sophia Fox, A. J., Bedi, A., & Rodeo, S. A. (2009). The basic science of articular cartilage: structure, composition, and function. *Sports health, 1*(6), 461-468.

Sperry, M. M., Yu, Y. H., Kartha, S., Ghimire, P., Welch, R. L., Winkelstein, B. A., & Granquist, E. J. (2020). Intra-articular etanercept attenuates pain and hypoxia from TMJ loading in the rat. *Journal of Orthopaedic Research®, 38*(6), 1316-1326.

Sprott, H., & Fleck, C. (2023). Hyaluronic Acid in Rheumatology. *Pharmaceutics, 15*(9), 2247.

Spurlock, C. F., Tossberg, J. T., Olsen, N. J., & Aune, T. M. (2015). Cutting edge: chronic NF-κB activation in CD4+ T cells in rheumatoid arthritis is genetically determined by HLA risk alleles. *The Journal of Immunology, 195*(3), 791-795.

Sridharan, G., & Shankar, A. A. (2012). Toluidine blue: A review of its chemistry and clinical utility. *Journal of oral and maxillofacial pathology: JOMFP, 16*(2), 251.

Stacker, S. A., Stenvers, K., Caesar, C., Vitali, A., Domagala, T., Nice, E., Roufail, S., Simpson, R. J., Moritz, R., & Karpanen, T. (1999). Biosynthesis of vascular endothelial growth factor-D involves proteolytic processing which generates non-covalent homodimers. *Journal of Biological Chemistry, 274*(45), 32127-32136.

Staels, W., Heremans, Y., Heimberg, H., & De Leu, N. (2019). VEGF-A and blood vessels: a beta cell perspective. *Diabetologia, 62*, 1961-1968.

Stahle-Backdahl, M., Sandstedt, B., Bruce, K., Lindahl, A., Jiménez, M. G., Vega, J. A., & López-Otín, C. (1997). Collagenase-3 (MMP-13) is expressed during human fetal ossification and re-expressed in postnatal bone remodeling and in rheumatoid arthritis. *Laboratory investigation; a journal of technical methods and pathology, 76*(5), 717-728.

Stanford, S. M., & Bottini, N. (2014). PTPN22: the archetypal non-HLA autoimmunity gene. *Nature Reviews Rheumatology, 10*(10), 602-611.

Stevens, M., & Oltean, S. (2016). Alternative splicing in CKD. *Journal of the American Society of Nephrology, 27*(6), 1596-1603.

Stevens, M., & Oltean, S. (2019). Modulation of receptor tyrosine kinase activity through alternative splicing of ligands and receptors in the VEGF-A/VEGFR axis. *Cells, 8*(4), 288.

Sthoeger, Z., Chiorazzi, N., & Lahita, R. (1988). Regulation of the immune response by sex hormones. I. In vitro effects of estradiol and testosterone on pokeweed mitogen-induced human B cell differentiation. *Journal of immunology (Baltimore, Md.: 1950), 141*(1), 91-98.

Stolina, M., Adamu, S., Ominsky, M., Dwyer, D., Asuncion, F., Geng, Z., Middleton, S., Brown, H., Pretorius, J., & Schett, G. (2005). RANKL is a marker and mediator of local and systemic bone loss in two rat models of inflammatory arthritis. *Journal of Bone and Mineral Research, 20*(10), 1756-1765.

Strangeways, T. (1920). Observations on the nutrition of articular cartilage. *British medical journal, 1*(3098), 661.

Straub, R. H. (2007). The complex role of oestrogens in inflammation. *Endocrine reviews, 28*(5), 521-574.

Strunk, J., Bundke, E., & Lange, U. (2006). Anti-TNF-α antibody infliximab and glucocorticoids reduce serum vascular endothelial growth factor levels in patients with rheumatoid arthritis: a pilot study. *Rheumatology international, 26*, 252-256.

Sun, Q.-Z., Lin, G.-F., Li, L.-L., Jin, X.-T., Huang, L.-Y., Zhang, G., Yang, W., Chen, K., Xiang, R., & Chen, C. (2017). Discovery of potent and selective inhibitors of cdc2-like kinase 1 (clk1) as a new class of autophagy inducers. *Journal of Medicinal Chemistry, 60*(14), 6337-6352.

Supradit, K., Boonsri, B., Duangdara, J., Thitiphatphuvanon, T., Suriyonplengsaeng, C., Kangsamaksin, T., Janvilisri, T., Tohtong, R., Yacqub-Usman, K., & Grabowska, A. M. (2022). Inhibition of serine/arginine-rich protein kinase-1 (SRPK1) prevents cholangiocarcinoma cells induced angiogenesis. *Toxicology in Vitro, 82*, 105385.

Suri, S., & Walsh, D. A. (2012). Osteochondral alterations in osteoarthritis. *Bone, 51*(2), 204-211.

Swift, M. N. (2021). *Targeting alternative splicing as a novel approach to chemotherapy induced peripheral neuropathy.* University of Nottingham,

Szekanecz, Z., Besenyei, T., Paragh, G., & Koch, A. E. (2009). Angiogenesis in rheumatoid arthritis. *Autoimmunity, 42*(7), 563-573.

Szekanecz, Z., & Koch, A. E. (2008). Vascular involvement in rheumatic diseases:'vascular rheumatology'. *Arthritis research & therapy, 10*, 1-10.

Szekanecz, Z., & Koch, A. E. (2010). VEGF as an activity marker in rheumatoid arthritis. *International Journal of Clinical Rheumatology, 5*(3), 287-290.

Szekanecz, Z., Pakozdi, A., Szentpetery, A., Besenyei, T., & Koch, A. E. (2009). Chemokines and angiogenesis in rheumatoid arthritis. *Frontiers in bioscience (Elite edition), 1*, 44.

Tahergorabi, Z., & Khazaei, M. (2012). A review on angiogenesis and its assays. *Iranian journal of basic medical sciences, 15*(6), 1110.

Taichman, N. S., Young, S., Cruchley, A. T., Taylor, P., & Paleolog, E. (1997). Human neutrophils secrete vascular endothelial growth factor. *Journal of leukocyte biology, 62*(3), 397-400.

Takahashi, H., Hattori, S., Iwamatsu, A., Takizawa, H., & Shibuya, M. (2004). A novel snake venom vascular endothelial growth factor (VEGF) predominantly induces vascular permeability through preferential signaling via VEGF receptor-1. *Journal of Biological Chemistry, 279*(44), 46304-46314.

Takahashi, H., & Shibuya, M. (2005). The vascular endothelial growth factor (VEGF)/VEGF receptor system and its role under physiological and pathological conditions. *Clinical science, 109*(3), 227-241.

Takahashi, T., Ueno, H., & Shibuya, M. (1999). VEGF activates protein kinase C-dependent, but Ras-independent Raf-MEK-MAP kinase pathway for DNA synthesis in primary endothelial cells. *Oncogene, 18*(13), 2221-2230.

Takahashi, T., Yamaguchi, S., Chida, K., & Shibuya, M. (2001). A single autophosphorylation site on KDR/Flk-1 is essential for VEGF-A-dependent activation of PLC-γ and DNA synthesis in vascular endothelial cells. *The EMBO journal, 20*(11), 2768-2778.

Takayanagi, H. (2005). Mechanistic insight into osteoclast differentiation in osteoimmunology. *Journal of molecular medicine, 83*, 170-179.

Takeuchi, T., Kawanishi, M., Nakanishi, M., Yamasaki, H., & Tanaka, Y. (2022). Phase II/III results of a trial of anti–tumor necrosis factor multivalent NANOBODY compound ozoralizumab in patients with rheumatoid arthritis. *Arthritis & Rheumatology, 74*(11), 1776-1785.

Talaat, R. M., Abo-El-Atta, A. S., Farou, S. M., & El-Dosoky, K. I. (2015). Therapeutic effect of dimethyl dimethoxy biphenyl dicarboxylate on collagen-induced arthritis in rats. *Chinese journal of integrative medicine, 21*, 846-854.

Tam, B. Y., Chiu, K., Chung, H., Bossard, C., Nguyen, J. D., Creger, E., Eastman, B. W., Mak, C. C., Ibanez, M., & Ghias, A. (2020). The CLK inhibitor SM08502 induces anti-tumor activity and reduces Wnt pathway gene expression in gastrointestinal cancer models. *Cancer Letters, 473*, 186-197.

Tan, E. M., & Smolen, J. S. (2016). Historical observations contributing insights on etiopathogenesis of rheumatoid arthritis and role of rheumatoid factor. *Journal of experimental medicine, 213*(10), 1937-1950.

Tanaka, S., Takahashi, N., Udagawa, N., Tamura, T., Akatsu, T., Stanley, E. R., Kurokawa, T., & Suda, T. (1993). Macrophage colony-stimulating factor is indispensable for both proliferation and differentiation of osteoclast progenitors. *The Journal of clinical investigation, 91*(1), 257-263.

Tanaka, Y. (2019). The JAK inhibitors: do they bring a paradigm shift for the management of rheumatic diseases? In (Vol. 58, pp. i1-i3): Oxford University Press.

Tanaka, Y., Kavanaugh, A., Wicklund, J., & McInnes, I. B. (2022). Filgotinib, a novel JAK1-preferential inhibitor for the treatment of rheumatoid arthritis: an overview from clinical trials. *Modern rheumatology, 32*(1), 1-11.

Tanaka, Y., Maeshima, Y., & Yamaoka, K. (2012). In vitro and in vivo analysis of a JAK inhibitor in rheumatoid arthritis. *Annals of the rheumatic diseases, 71*(Suppl 2), i70-i74.

Tanaka, Y., Takeuchi, T., Tanaka, S., Kawakami, A., Iwasaki, M., Song, Y. W., Chen, Y.-H., Wei, J. C.-C., Lee, S.-H., & Rokuda, M. (2019). Efficacy and safety of peficitinib (ASP015K) in patients with rheumatoid arthritis and an inadequate response to conventional DMARDs: a randomised, double-blind, placebo-controlled phase III trial (RAJ3). *Annals of the rheumatic diseases, 78*(10), 1320-1332.

Tang, J., Xie, Y., Huang, J., Zhang, L., Jiang, W., Li, Z., & Bian, J. (2022). A critical update on the strategies towards small molecule inhibitors targeting Serine/arginine-rich (SR) proteins and Serine/arginine-rich proteins related kinases in alternative splicing. *Bioorganic & Medicinal Chemistry*, 116921.

Tang, M. W., Garcia, S., Gerlag, D. M., Tak, P. P., & Reedquist, K. A. (2017). Insight into the endocrine system and the immune system: a review of the inflammatory role of prolactin in rheumatoid arthritis and psoriatic arthritis. *Frontiers in Immunology, 8*, 720.

Tang, P., Xiong, Q., Ge, W., & Zhang, L. (2014). The role of microRNAs in osteoclasts and osteoporosis. *RNA biology, 11*(11), 1355-1363.

Tardito, S., Martinelli, G., Soldano, S., Paolino, S., Pacini, G., Patane, M., Alessandri, E., Smith, V., & Cutolo, M. (2019). Macrophage M1/M2 polarization and rheumatoid arthritis: a systematic review. *Autoimmunity reviews, 18*(11), 102397.

Tavafoghi, M., & Cerruti, M. (2016). The role of amino acids in hydroxyapatite mineralization. *Journal of The Royal Society Interface, 13*(123), 20160462.

Taylor, P. (2005). Serum vascular markers and vascular imaging in assessment of rheumatoid arthritis disease activity and response to therapy. *Rheumatology, 44*(6), 721-728.

Taylor, P. C., Keystone, E. C., Van Der Heijde, D., Weinblatt, M. E., del Carmen Morales, L., Reyes Gonzaga, J., Yakushin, S., Ishii, T., Emoto, K., & Beattie, S. (2017). Baricitinib versus placebo or adalimumab in rheumatoid arthritis. *New England Journal of Medicine, 376*(7), 652-662.

Taylor, P. C., Weinblatt, M. E., McInnes, I. B., Atsumi, T., Strand, V., Takeuchi, T., Bracher, M., Brooks, D., Davies, J., & Goode, C. (2023). Anti-GM-CSF otilimab versus sarilumab or placebo in patients with rheumatoid arthritis and inadequate response to targeted therapies: a phase III randomised trial (contRAst 3). *Annals of the rheumatic diseases, 82*(12), 1527-1537.

Tchetina, E. V., Squires, G., & Poole, A. R. (2005). Increased type II collagen degradation and very early focal cartilage degeneration is associated with upregulation of chondrocyte differentiation related genes in early human articular cartilage lesions. *The Journal of rheumatology, 32*(5), 876-886.

Temu, T. M., Wu, K.-Y., Gruppuso, P. A., & Phornphutkul, C. (2010). The mechanism of ascorbic acid-induced differentiation of ATDC5 chondrogenic cells. *American Journal of Physiology-Endocrinology and Metabolism, 299*(2), E325-E334.

Terra, S. A., de Arruda Lourenção, P. L. T., & Rodrigues, M. A. M. (2023). PTEN Immunohistochemistry: A New Approach for Diagnosis of Intestinal Neuronal Dysplasia Type B. *Archives of pathology & laboratory medicine, 147*(5), 577-583.

Tetta, C., Camussi, G., Modena, V., Di Vittorio, C., & Baglioni, C. (1990). Tumour necrosis factor in serum and synovial fluid of patients with active and severe rheumatoid arthritis. *Annals of the rheumatic diseases, 49*(9), 665-667.

Thomas, A. L., Morgan, B., Horsfield, M. A., Higginson, A., Kay, A., Lee, L., Masson, E., Puccio-Pick, M., Laurent, D., & Steward, W. P. (2005). Phase I study of the safety, tolerability, pharmacokinetics, and pharmacodynamics of PTK787/ZK 222584 administered twice daily in patients with advanced cancer. *Journal of clinical oncology, 23*(18), 4162-4171.

Tian, H., & Cronstein, B. N. (2007). Understanding the mechanisms of action of methotrexate. *Bull NYU Hosp Jt Dis, 65*(3), 168-173.

Tobisawa, Y., Fujita, N., Yamamoto, H., Ohyama, C., Irie, F., & Yamaguchi, Y. (2021). The cell surface hyaluronidase TMEM2 is essential for systemic hyaluronan catabolism and turnover. *Journal of Biological Chemistry, 297*(5).

Tollervey, J. R., Wang, Z., Hortobágyi, T., Witten, J. T., Zarnack, K., Kayikci, M., Clark, T. A., Schweitzer, A. C., Rot, G., & Curk, T. (2011). Analysis of alternative splicing associated with aging and neurodegeneration in the human brain. *Genome research, 21*(10), 1572-1582.

Torzilli, P. (1985). Influence of cartilage conformation on its equilibrium water partition. *Journal of orthopaedic research, 3*(4), 473-483.

Tota, M., Łacwik, J., Laska, J., Sędek, Ł., & Gomułka, K. (2023). The Role of Eosinophil-Derived Neurotoxin and Vascular Endothelial Growth Factor in the Pathogenesis of Eosinophilic Asthma. *Cells, 12*(9), 1326.

Traxler, P., Bold, G., Buchdunger, E., Caravatti, G., Furet, P., Manley, P., O'Reilly, T., Wood, J., & Zimmermann, J. (2001). Tyrosine kinase inhibitors: from rational design to clinical trials. *Medicinal research reviews, 21*(6), 499-512.

Traynor, K. (2012). FDA approves tofacitinib for rheumatoid arthritis. *American Journal of Health-System Pharmacy, 69*(24), 2120-2121.

Truong, L. D., & Shen, S. S. (2011). Immunohistochemical diagnosis of renal neoplasms. *Archives of pathology & laboratory medicine, 135*(1), 92-109.

Tseng, C.-C., Chen, Y.-J., Chang, W.-A., Tsai, W.-C., Ou, T.-T., Wu, C.-C., Sung, W.-Y., Yen, J.-H., & Kuo, P.-L. (2020). Dual role of chondrocytes in rheumatoid arthritis: the chicken and the egg. *International Journal of Molecular Sciences, 21*(3), 1071.

Tseng, S., Reddi, A. H., & Di Cesare, P. E. (2009). Cartilage oligomeric matrix protein (COMP): a biomarker of arthritis. *Biomarker insights, 4*, BMI. S645.

Tsuboi, H., Matsui, Y., Hayashida, K., Yamane, S., Maeda-Tanimura, M., Nampei, A., Hashimoto, J., Suzuki, R., Yoshikawa, H., & Ochi, T. (2003). Tartrate resistant acid phosphatase (TRAP) positive cells in rheumatoid synovium may induce the destruction of articular cartilage. *Annals of the rheumatic diseases, 62*(3), 196-203.

Tsuchida, A., Beekhuizen, M., Hart, M. C., Radstake, T., & Dhert, W. (2014). DB 25 Saris, GJ van Osch, and LB Creemers,"Cytokine profiles in the joint depend on 26 pathology, but are different between synovial fluid, cartilage tissue and cultured chon-27 drocytes,". *Arthritis research & therapy, 16*(5), 441.

Tsuchida, A., Beekhuizen, M., MC't Hart, T., Radstake, W., Dhert, D., Saris, G., & van Osch, L. (2014). Creemers, Cytokine profiles in the joint depend on pathology, but are different between synovial fluid, cartilage tissue and cultured chondrocytes. *Arthritis Res. Ther, 16*(5).

Tsuda, M. (2016). Microglia in the spinal cord and neuropathic pain. *Journal of diabetes investigation, 7*(1), 17-26.

Tsurukai, T., Udagawa, N., Matsuzaki, K., Takahashi, N., & Suda, T. (2000). Roles of macrophage-colony stimulating factor and osteoclast differentiation factor in osteoclastogenesis. *Journal of bone and mineral metabolism, 18*(4), 177-184.

Tuttle, J., Drescher, E., Simón-Campos, J. A., Emery, P., Greenwald, M., Kivitz, A., Rha, H., Yachi, P., Kiley, C., & Nirula, A. (2023). A Phase 2 Trial of Peresolimab for Adults with Rheumatoid Arthritis. *New England journal of medicine, 388*(20), 1853-1862.

Tyndall, D. A., Ludlow, J. B., Platin, E., & Nair, M. (1998). A comparison of Kodak Ektaspeed Plus film and the Siemens Sidexis digital imaging system for caries detection using receiver operating characteristic analysis. *Oral Surgery, Oral Medicine, Oral Pathology, Oral Radiology, and Endodontology, 85*(1), 113-118.

Tzelepis, K., De Braekeleer, E., Aspris, D., Barbieri, I., Vijayabaskar, M., Liu, W.-H., Gozdecka, M., Metzakopian, E., Toop, H. D., & Dudek, M. (2018). SRPK1 maintains acute myeloid leukemia through effects on isoform usage of epigenetic regulators including BRD4. *Nature communications, 9*(1), 1-13.

Uemura, A., Fruttiger, M., d'Amore, P. A., De Falco, S., Joussen, A. M., Sennlaub, F., Brunck, L. R., Johnson, K. T., Lambrou, G. N., & Rittenhouse, K. D. (2021). VEGFR1 signaling in retinal angiogenesis and microinflammation. *Progress in Retinal and Eye Research, 84*, 100954.

Utomo, L., Bastiaansen-Jenniskens, Y. M., Verhaar, J. A., & van Osch, G. J. (2016). Cartilage inflammation and degeneration is enhanced by pro-inflammatory (M1) macrophages in vitro, but not inhibited directly by anti-inflammatory (M2) macrophages. *Osteoarthritis and cartilage, 24*(12), 2162-2170.

Vadala, G., Russo, F., Musumeci, M., Giacalone, A., Papalia, R., & Denaro, V. (2018). Targeting VEGF-A in cartilage repair and regeneration: state of the art and perspectives. *J Biol Regul Homeost Agents, 32*(6 Suppl 1), 217-224.

Valcarcel, J., García, M. R., Varela, U. R., & Vázquez, J. A. (2020). Hyaluronic acid of tailored molecular weight by enzymatic and acid depolymerization. *International journal of biological macromolecules, 145*, 788-794.

van Aken, J., Lard, L., le Cessie, S., Hazes, J., Breedveld, F., & Huizinga, T. (2004). Radiological outcome after four years of early versus delayed treatment strategy in patients with recent onset rheumatoid arthritis. *Annals of the rheumatic diseases, 63*(3), 274-279.

Van der Heijde, D. (1995). Joint erosions and patients with early rheumatoid arthritis. *Rheumatology, 34*(suppl_2), 74-78.

Van Der Heijde, D., Tanaka, Y., Fleischmann, R., Keystone, E., Kremer, J., Zerbini, C., Cardiel, M. H., Cohen, S., Nash, P., & Song, Y. W. (2013). Tofacitinib (CP-690,550) in patients with rheumatoid arthritis receiving methotrexate: twelve-month data from a twenty-four–month phase III randomized radiographic study. *Arthritis & Rheumatism, 65*(3), 559-570.

Van der Heijde, D., Van Riel, P., Van Leeuwen, M., Van't Hof, M., Van Rijswijk, M., & Van de Putte, L. (1992). Prognostic factors for radiographic damage and physical disability in early rheumatoid arthritis. A prospective follow-up study of 147 patients. *Rheumatology, 31*(8), 519-525.

van der Helm-van Mil, A. H., Huizinga, T. W., Schreuder, G. M. T., Breedveld, F. C., de Vries, R. R., & Toes, R. E. (2005). An independent role of protective HLA class II alleles in rheumatoid arthritis severity and susceptibility. *Arthritis & Rheumatism, 52*(9), 2637-2644.

Van der Kraan, P., & Van den Berg, W. (2012). Chondrocyte hypertrophy and osteoarthritis: role in initiation and progression of cartilage degeneration? *Osteoarthritis and cartilage, 20*(3), 223-232.

Van der Linden, M., Knevel, R., Huizinga, T., & van der Helm-van Mil, A. M. (2011). Classification of rheumatoid arthritis: comparison of the 1987 American College of Rheumatology criteria and the 2010 American College of Rheumatology/European League Against Rheumatism criteria. *Arthritis & Rheumatism, 63*(1), 37-42.

Van Der Voort, R., Van Lieshout, A. W., Toonen, L. W., Slöetjes, A. W., Van Den Berg, W. B., Figdor, C. G., Radstake, T. R., & Adema, G. J. (2005). Elevated CXCL16 expression by synovial macrophages recruits memory T cells into rheumatoid joints. *Arthritis & Rheumatism, 52*(5), 1381-1391.

van Doorn, E., Liu, H., Huckriede, A., & Hak, E. (2016). Safety and tolerability evaluation of the use of Montanide ISA™ 51 as vaccine adjuvant: a systematic review. *Human vaccines & immunotherapeutics, 12*(1), 159-169.

van Eegher, S., Perez-Lozano, M.-L., Toillon, I., Valour, D., Pigenet, A., Citadelle, D., Bourrier, C., Courtade-Gaïani, S., Grégoire, L., & Cléret, D. (2021). The differentiation of prehypertrophic into hypertrophic chondrocytes drives an OA-remodeling program and IL-34 expression. *Osteoarthritis and cartilage, 29*(2), 257-268.

Van Nies, J., Krabben, A., Schoones, J., Huizinga, T., Kloppenburg, M., & Van Der Helm-Van Mil, A. (2014). What is the evidence for the presence of a therapeutic window of opportunity in rheumatoid arthritis? A systematic literature review. *Annals of the rheumatic diseases, 73*(5), 861-870.

Varey, A., Rennel, E., Qiu, Y., Bevan, H., Perrin, R., Raffy, S., Dixon, A., Paraskeva, C., Zaccheo, O., & Hassan, A. (2008). VEGF 165 b, an antiangiogenic VEGF-A isoform, binds and inhibits bevacizumab treatment in experimental colorectal carcinoma: balance of pro-and antiangiogenic VEGF-A isoforms has implications for therapy. *British journal of cancer, 98*(8), 1366-1379.

Varia, M. A., Calkins-Adams, D. P., Rinker, L. H., Kennedy, A. S., Novotny, D. B., Fowler Jr, W. C., & Raleigh, J. A. (1998). Pimonidazole: a novel hypoxia marker for complementary study of tumor hypoxia and cell proliferation in cervical carcinoma. *Gynecologic oncology, 71*(2), 270-277.

Veale, D. J., & Fearon, U. (2006). Inhibition of angiogenic pathways in rheumatoid arthritis: potential for therapeutic targeting. *Best Practice & Research Clinical Rheumatology, 20*(5), 941-947.

Vermeer, J. A., Ient, J., Markelc, B., Kaeppler, J., Barbeau, L. M., Groot, A. J., Muschel, R. J., & Vooijs, M. A. (2020). A lineage-tracing tool to map the fate of hypoxic tumour cells. *Disease models & mechanisms, 13*(7), dmm044768.

VERSUSARTHRITIS. (2023). What is rheumatoid arthritis? Retrieved from https://versusarthritis.org/about-arthritis/conditions/rheumatoid-arthritis/

Vickers, N. J. (2017). Animal communication: when i'm calling you, will you answer too? *Current biology, 27*(14), R713-R715.

Vincent, T. L., Williams, R. O., Maciewicz, R., Silman, A., Garside, P., & Group, A. R. U. a. M. W. (2012). Mapping pathogenesis of arthritis through small animal models. *Rheumatology, 51*(11), 1931-1941.

Virchow, R. (1867). *Die krankhaften Geschwülste: dreissig Vorlesungen gehalten während des Wintersemesters 1862-1863 an der Universität zu Berlin* (Vol. 4): A. Hirschwald.

Vitterso, E. D., Beazley-Long, N., & Donaldson, L. (2018). *Endothelial VEGFR2 KO during CFA induced inflammation is detrimental to murine tibiotalar cartilage integrity*. The Physiological Society 'Microvascular & Endothelial Physiology', (Europhysiology 2018 (London, UK) (2018) Proc Physiol Soc 41, PCA341). London, UK.

Volkov, M., van Schie, K. A., & van der Woude, D. (2020). Autoantibodies and B Cells: The ABC of rheumatoid arthritis pathophysiology. *Immunological reviews, 294*(1), 148-163.

von der Mark, K., Frischholz, S., Aigner, T., Beier, F., Belke, J., Erdmann, S., & Burkhardt, H. (1995). Upregulation of type X collagen expression in osteoarthritic cartilage. *Acta Orthopaedica Scandinavica, 66*(sup266), 125-129.

Von der Mark, K., Kirsch, T., Nerlich, A., Kuss, A., Weseloh, G., Glückert, K., & Stöss, H. (1992). Type X collagen synthesis in human osteoarthritic cartilage. Indication of chondrocyte hypertrophy. *Arthritis & Rheumatism: Official Journal of the American College of Rheumatology, 35*(7), 806-811.

Vos, T., Lim, S. S., Abbafati, C., Abbas, K. M., Abbasi, M., Abbasifard, M., Abbasi-Kangevari, M., Abbastabar, H., Abd-Allah, F., & Abdelalim, A. (2020). Global burden of 369 diseases and injuries in 204 countries and territories, 1990–2019: a systematic analysis for the Global Burden of Disease Study 2019. *The Lancet, 396*(10258), 1204-1222.

Vu, T. H., Shipley, J. M., Bergers, G., Berger, J. E., Helms, J. A., Hanahan, D., Shapiro, S. D., Senior, R. M., & Werb, Z. (1998). MMP-9/gelatinase B is a key regulator of growth plate angiogenesis and apoptosis of hypertrophic chondrocytes. *Cell, 93*(3), 411-422.

Vuolteenaho, K., Moilanen, T., Knowles, R., & Moilanen, E. (2007). The role of nitric oxide in osteoarthritis. *Scandinavian journal of rheumatology, 36*(4), 247-258.

Wagner, K.-D., El Maï, M., Ladomery, M., Belali, T., Leccia, N., Michiels, J.-F., & Wagner, N. (2019). Altered VEGF splicing isoform balance in tumor endothelium involves activation of splicing factors Srpk1 and Srsf1 by the Wilms' tumor suppressor Wt1. *Cells, 8*(1), 41.

Waiker, D. K., Karthikeyan, C., Poongavanam, V., Kongsted, J., Lozach, O., Meijer, L., & Trivedi, P. (2014). Synthesis, biological evaluation and molecular modelling studies of 4-anilinoquinazoline derivatives as protein kinase inhibitors. *Bioorganic & Medicinal Chemistry, 22*(6), 1909-1915.

Walker, G. D., Fischer, M., Gannon, J., Thompson Jr, R. C., & Oegema Jr, T. R. (1995). Expression of type-X collagen in osteoarthritis. *Journal of orthopaedic research, 13*(1), 4-12.

Wallach, D. (2016). *The cybernetics of TNF: Old views and newer ones.* Paper presented at the Seminars in Cell & Developmental Biology.

Walsh, D. (1999). Angiogenesis and arthritis. *Rheumatology (Oxford, England), 38*(2), 103-112.

Walsh, D. A., McWilliams, D. F., Turley, M. J., Dixon, M. R., Fransès, R. E., Mapp, P. I., & Wilson, D. (2010). Angiogenesis and nerve growth factor at the osteochondral junction in rheumatoid arthritis and osteoarthritis. *Rheumatology, 49*(10), 1852-1861.

Walsh, D. A., Sofat, N., Guermazi, A., & Hunter, D. J. (2022). Osteoarthritis bone marrow lesions. *Osteoarthritis and cartilage*.

Wang, J., Zhou, B., Parkinson, I., Thomas, C. D. L., Clement, J. G., Fazzalari, N., & Guo, X. E. (2013). Trabecular plate loss and deteriorating elastic modulus of femoral trabecular bone in intertrochanteric hip fractures. *Bone research, 1*(1), 346-354.

Wang, P., Zhu, P., Liu, R., Meng, Q., & Li, S. (2020). Baicalin promotes extracellular matrix synthesis in chondrocytes via the activation of hypoxia-inducible factor-1α. *Experimental and Therapeutic Medicine, 20*(6), 1-1.

Wang, R., Crystal, R. G., & Hackett, N. R. (2009). Identification of an exonic splicing silencer in exon 6A of the human VEGF gene. *BMC molecular biology, 10*, 1-11.

Wang, S., Zhou, Y., Huang, J., Li, H., Pang, H., Niu, D., Li, G., Wang, F., Zhou, Z., & Liu, Z. (2023). Advances in experimental models of rheumatoid arthritis. *European journal of immunology, 53*(1), 2249962.

Wang, X., Bove, A. M., Simone, G., & Ma, B. (2020). Molecular bases of VEGFR-2-mediated physiological function and pathological role. *Frontiers in Cell and Developmental Biology, 8*, 599281.

Wang, Y., Wei, L., Zeng, L., He, D., & Wei, X. (2013). Nutrition and degeneration of articular cartilage. *Knee Surgery, Sports Traumatology, Arthroscopy, 21*(8), 1751-1762.

Wang, Y., Wei, L., Zeng, L., He, D., & Wei, X. (2013). Nutrition and degeneration of articular cartilage. *Knee Surgery, Sports Traumatology, Arthroscopy, 21*, 1751-1762.

Wang, Z.-Z., Huang, T.-Y., Gong, Y.-F., Zhang, X.-M., & Huang, X.-Y. (2020). Effects of sorafenib on fibroblast-like synoviocyte apoptosis in rats with adjuvant arthritis. *International immunopharmacology, 83*, 106418.

Weber, A., Chan, P. M. B., & Wen, C. (2019). Do immune cells lead the way in subchondral bone disturbance in osteoarthritis? *Progress in biophysics and molecular biology, 148*, 21-31.

Weddell, J. C., Chen, S., & Imoukhuede, P. (2017). VEGFR1 promotes cell migration and proliferation through PLCγ and PI3K pathways. *NPJ systems biology and applications, 4*(1), 1.

Wegner, N., Wait, R., Sroka, A., Eick, S., Nguyen, K. A., Lundberg, K., Kinloch, A., Culshaw, S., Potempa, J., & Venables, P. J. (2010). Peptidylarginine deiminase from Porphyromonas gingivalis citrullinates human fibrinogen and α-enolase: Implications for autoimmunity in rheumatoid arthritis. *Arthritis & Rheumatism, 62*(9), 2662-2672.

Weinblatt, M. E., Bathon, J. M., Kremer, J. M., Fleischmann, R. M., Schiff, M. H., Martin, R. W., Baumgartner, S. W., Park, G. S., Mancini, E. L., & Genovese, M. C. (2011). Safety and efficacy of etanercept beyond 10 years of therapy in North American patients with early and longstanding rheumatoid arthritis. *Arthritis care & research, 63*(3), 373-382.

Weinblatt, M. E., Kremer, J. M., Bankhurst, A. D., Bulpitt, K. J., Fleischmann, R. M., Fox, R. I., Jackson, C. G., Lange, M., & Burge, D. J. (1999). A trial of etanercept, a recombinant tumor necrosis factor receptor: Fc fusion protein, in patients with rheumatoid arthritis receiving methotrexate. *New England journal of medicine, 340*(4), 253-259.

Weinblatt, M. E., McInnes, I. B., Kremer, J. M., Miranda, P., Vencovsky, J., Guo, X., White, W. I., Ryan, P. C., Godwood, A., & Albulescu, M. (2018). A randomized phase II b study of mavrilimumab and golimumab in rheumatoid arthritis. *Arthritis & Rheumatology, 70*(1), 49-59.

Wen, L., Chen, J., Duan, L., & Li, S. (2018). Vitamin K-dependent proteins involved in bone and cardiovascular health. *Molecular medicine reports, 18*(1), 3-15.

Wetzler, L. M. (2003). The role of Toll-like receptor 2 in microbial disease and immunity. *Vaccine, 21*, S55-S60.

Weyand, C. M., Hicok, K. C., Conn, D. L., & Goronzy, J. J. (1992). The influence of HLA-DRB1 genes on disease severity in rheumatoid arthritis. *Annals of internal medicine, 117*(10), 801-806.

Whitacre, C. C. (2001). Sex differences in autoimmune disease. *Nature immunology, 2*(9), 777-780.

White, A. L., & Bix, G. J. (2023). VEGFA Isoforms as Pro-Angiogenic Therapeutics for Cerebrovascular Diseases. *Biomolecules, 13*(4), 702.

Whitehouse, M., Orr, K., Beck, F. W., & Pearson, C. (1974). Freund's adjuvants: relationship of arthritogenicity and adjuvanticity in rats to vehicle composition. *Immunology, 27*(2), 311.

Wibulswas, A., Croft, D., Pitsillides, A. A., Bacarese-Hamilton, I., McIntyre, P., Genot, E., & Kramer, I. M. (2002). Influence of epitopes CD44v3 and CD44v6 in the invasive behavior of fibroblast-like synoviocytes derived from rheumatoid arthritic joints. *Arthritis & Rheumatism, 46*(8), 2059-2064.

Wiemer, A. J., Wernimont, S. A., Cung, T.-d., Bennin, D. A., Beggs, H. E., & Huttenlocher, A. (2013). The focal adhesion kinase inhibitor PF-562,271 impairs primary CD4+ T cell activation. *Biochemical pharmacology, 86*(6), 770-781.

Willemze, A., Trouw, L. A., Toes, R. E., & Huizinga, T. W. (2012). The influence of ACPA status and characteristics on the course of RA. *Nature Reviews Rheumatology, 8*(3), 144-152.

Winthrop, K. L., Tanaka, Y., Takeuchi, T., Kivitz, A., Matzkies, F., Genovese, M. C., Jiang, D., Chen, K., Bartok, B., & Jahreis, A. (2022). Integrated safety analysis of filgotinib in patients with moderately to severely active rheumatoid arthritis receiving treatment over a median of 1.6 years. *Annals of the rheumatic diseases, 81*(2), 184-192.

Wong, C., & Jin, Z.-G. (2005). Protein kinase C-dependent protein kinase D activation modulates ERK signal pathway and endothelial cell proliferation by vascular endothelial growth factor. *Journal of Biological Chemistry, 280*(39), 33262-33269.

Wood, J. M., Bold, G., Buchdunger, E., Cozens, R., Ferrari, S., Frei, J. r., Hofmann, F., Mestan, J. r., Mett, H., & O'Reilly, T. (2000). PTK787/ZK 222584, a novel and potent inhibitor of vascular endothelial growth factor receptor tyrosine kinases, impairs vascular endothelial growth factor-induced responses and tumor growth after oral administration. *Cancer research, 60*(8), 2178-2189.

Woolard, J., Wang, W.-Y., Bevan, H. S., Qiu, Y., Morbidelli, L., Pritchard-Jones, R. O., Cui, T.-G., Sugiono, M., Waine, E., & Perrin, R. (2004). VEGF165b, an inhibitory vascular endothelial growth factor splice variant: mechanism of action, in vivo effect on angiogenesis and endogenous protein expression. *Cancer research, 64*(21), 7822-7835.

Woolf, S. H. (2008). The meaning of translational research and why it matters. *Jama, 299*(2), 211-213.

Woolley, D. E., & Tetlow, L. C. (1997). Observations on the microenvironmental nature of cartilage degradation in rheumatoid arthritis. *Annals of the rheumatic diseases, 56*(3), 151-161.

Wu, G. T., Kam, J., & Bloom, J. D. (2023). Hyaluronic Acid Basics and Rheology. *Clinics in Plastic Surgery, 50*(3), 391-398.

Wu, L., Huang, X., Li, L., Huang, H., Xu, R., & Luyten, W. (2012). Insights on biology and pathology of HIF-1α/-2α, TGFα/BMP, Wnt/β-catenin, and NF-κB pathways in osteoarthritis. *Current pharmaceutical design, 18*(22), 3293-3312.

Wu, X., Crawford, R., Xiao, Y., Mao, X., & Prasadam, I. (2021). Osteoarthritic subchondral bone release exosomes that promote cartilage degeneration. *Cells, 10*(2), 251.

Xia, B., Chen, D., Zhang, J., Hu, S., Jin, H., & Tong, P. (2014). Osteoarthritis pathogenesis: a review of molecular mechanisms. *Calcified tissue international, 95*(6), 495-505.

Xie, N., Chen, M., Dai, R., Zhang, Y., Zhao, H., Song, Z., Zhang, L., Li, Z., Feng, Y., & Gao, H. (2017). SRSF1 promotes vascular smooth muscle cell proliferation through a Δ133p53/EGR1/KLF5 pathway. *Nature communications, 8*(1), 16016.

Xin, W., Heilig, J., Paulsson, M., & Zaucke, F. (2015). Collagen II regulates chondroycte integrin expression profile and differentiation. *Connective Tissue Research, 56*(4), 307-314.

Xu, J., Zhang, M.-Y., Jiao, W., Hu, C.-Q., Wu, D.-B., Yu, J.-H., & Chen, G.-X. (2021). Identification of candidate genes related to synovial macrophages in rheumatoid arthritis by bioinformatics analysis. *International Journal of General Medicine*, 7687-7697.

Yamane, A., Seetharam, L., Yamaguchi, S., Gotoh, N., Takahashi, T., Neufeld, G., & Shibuya, M. (1994). A new communication system between hepatocytes and sinusoidal endothelial cells in liver through vascular endothelial growth factor and Flt tyrosine kinase receptor family (Flt-1 and KDR/Flk-1). *Oncogene, 9*(9), 2683-2690.

Yamaura, K., Akiyama, S., & Ueno, K. (2012). Increased expression of the histamine H4 receptor subtype in hypertrophic differentiation of chondrogenic ATDC5 cells. *Journal of cellular biochemistry, 113*(3), 1054-1060.

Yan, D., Chen, D., Cool, S. M., Van Wijnen, A. J., Mikecz, K., Murphy, G., & Im, H.-J. (2011). Fibroblast growth factor receptor 1 is principally responsible for fibroblast growth factor 2-induced catabolic activities in human articular chondrocytes. *Arthritis research & therapy, 13*, 1-13.

Yan, Z., Xiong, J., Zhao, C., Qin, C., & He, C. (2015). Decreasing cartilage damage in a rat model of osteoarthritis by intra-articular injection of deoxycholic acid. *International journal of clinical and experimental medicine, 8*(6), 9038.

Yancopoulos, G. D., Davis, S., Gale, N. W., Rudge, J. S., Wiegand, S. J., & Holash, J. (2000). Vascular-specific growth factors and blood vessel formation. *Nature, 407*(6801), 242-248.

Yang, J. C., Haworth, L., Sherry, R. M., Hwu, P., Schwartzentruber, D. J., Topalian, S. L., Steinberg, S. M., Chen, H. X., & Rosenberg, S. A. (2003). A randomized trial of bevacizumab, an anti–vascular endothelial growth factor antibody, for metastatic renal cancer. *New England journal of medicine, 349*(5), 427-434.

Yang, Q., McHugh, K. P., Patntirapong, S., Gu, X., Wunderlich, L., & Hauschka, P. V. (2008). VEGF enhancement of osteoclast survival and bone resorption involves VEGF receptor-2 signaling and β3-integrin. *Matrix Biology, 27*(7), 589-599.

Yang, S., Kim, J., Ryu, J.-H., Oh, H., Chun, C.-H., Kim, B. J., Min, B. H., & Chun, J.-S. (2010). Hypoxia-inducible factor-2α is a catabolic regulator of osteoarthritic cartilage destruction. *Nature medicine, 16*(6), 687-693.

Yao, Y., Wang, H., Xi, X., Sun, W., Ge, J., & Li, P. (2021). miR-150 and SRPK1 regulate AKT3 expression to participate in LPS-induced inflammatory response. *Innate Immunity, 27*(4), 343-350.

Yao, Y., & Wang, Y. (2013). ATDC5: an excellent in vitro model cell line for skeletal development. *Journal of cellular biochemistry, 114*(6), 1223-1229.

Yao, Y., Zhai, Z., & Wang, Y. (2014). Evaluation of insulin medium or chondrogenic medium on proliferation and chondrogenesis of ATDC5 cells. *BioMed research international, 2014*.

Yap, H.-Y., Tee, S. Z.-Y., Wong, M. M.-T., Chow, S.-K., Peh, S.-C., & Teow, S.-Y. (2018). Pathogenic role of immune cells in rheumatoid arthritis: implications in clinical treatment and biomarker development. *Cells, 7*(10), 161.

Yasuda, T. (2006). Cartilage destruction by matrix degradation products. *Modern rheumatology, 16*(4), 197-205.

Yazici, Y., McAlindon, T., Gibofsky, A., Lane, N., Lattermann, C., Skrepnik, N., Swearingen, C., Simsek, I., Ghandehari, H., & DiFrancesco, A. (2021). A Phase 2b randomized trial of lorecivivint, a novel intra-articular CLK2/DYRK1A inhibitor and Wnt pathway modulator for knee osteoarthritis. *Osteoarthritis and cartilage, 29*(5), 654-666.

Yazici, Y., McAlindon, T. E., Gibofsky, A., Lane, N. E., Clauw, D., Jones, M., Bergfeld, J., Swearingen, C. J., DiFrancesco, A., & Simsek, I. (2020). Lorecivivint, a novel Intraarticular CDC-like kinase 2 and dual-specificity tyrosine phosphorylation-regulated kinase 1A inhibitor and Wnt pathway modulator for the treatment of knee osteoarthritis: a phase II randomized trial. *Arthritis & Rheumatology, 72*(10), 1694-1706.

Ye, L., Mingyue, H., Feng, Z., Zongshun, D., Ying, X., Xiong, C., & Liang, L. (2021). Systematic review of robust experimental models of rheumatoid arthritis for basic research. *Digital Chinese Medicine, 4*(4), 262-272.

Ye, T., He, F., Lu, L., Miao, H., Sun, D., Zhang, M., Yang, H., Zhang, J., Qiu, J., & Zhao, H. (2020). The effect of ooestrogen on mandibular condylar cartilage via hypoxia-inducible factor-2α during osteoarthritis development. *Bone, 130*, 115123.

Yen, J.-H., Chio, W.-T., Chuang, C.-J., Yang, H.-L., & Huang, S.-T. (2022). Improved Wound Healing by Naringin Associated with MMP and the VEGF Pathway. *Molecules, 27*(5), 1695.

Yildirim, K., Karatay, S., Melikoglu, M. A., Gureser, G., Ugur, M., & Senel, K. (2004). Associations between acute phase reactant levels and disease activity score (DAS28) in patients with rheumatoid arthritis. *Annals of Clinical & Laboratory Science, 34*(4), 423-426.

Yin, L.-Y., Wu, Y., Ballinger, C. A., & Patterson, C. (1998). Genomic structure of the human KDR/flk-1 gene. *Mammalian genome, 9*(5), 408-410.

Yoda, A., Morishita, D., Mizutani, A., Satoh, Y., Ochi, Y., Nannya, Y., Makishima, H., Miyake, H., & Ogawa, S. (2019). CTX-712, a Novel Clk inhibitor targeting myeloid neoplasms with SRSF2 mutation. *Blood, 134*, 404.

Yoo, S.-A., Bae, D.-G., Ryoo, J.-W., Kim, H.-R., Park, G.-S., Cho, C.-S., Chae, C.-B., & Kim, W.-U. (2005). Arginine-rich anti-vascular endothelial growth factor (anti-VEGF) hexapeptide inhibits collagen-induced arthritis and VEGF-stimulated productions of TNF-α and IL-6 by human monocytes. *The Journal of Immunology, 174*(9), 5846-5855.

Yoo, S.-A., Kwok, S.-K., & Kim, W.-U. (2008). Proinflammatory role of vascular endothelial growth factor in the pathogenesis of rheumatoid arthritis: prospects for therapeutic intervention. *Mediators of inflammation, 2008*.

Yoon, S. B., Moon, S.-H., Kim, J. H., Song, T. J., & Kim, M.-H. (2020). The use of immunohistochemistry for IgG4 in the diagnosis of autoimmune pancreatitis: a systematic review and meta-analysis. *Pancreatology, 20*(8), 1611-1619.

Yoshihara, Y., Nakamura, H., Obata, K. i., Yamada, H., Hayakawa, T., Fujikawa, K., & Okada, Y. (2000). Matrix metalloproteinases and tissue inhibitors of metalloproteinases in synovial fluids from patients with rheumatoid arthritis or osteoarthritis. *Annals of the rheumatic diseases, 59*(6), 455-461.

Yoshimoto, M., Takeda, N., Yoshimoto, T., & Matsumoto, S. (2021). Hypertensive cerebral hemorrhage with undetectable plasma vascular endothelial growth factor levels in a patient receiving intravitreal injection of aflibercept for bilateral diabetic macular edema: a case report. *Journal of Medical Case Reports, 15*(1), 1-9.

You, S., Koh, J. H., Leng, L., Kim, W. U., & Bucala, R. (2018). The Tumor-like phenotype of rheumatoid synovium: Molecular profiling and prospects for precision medicine. *Arthritis & Rheumatology, 70*(5), 637-652.

Young, A., Koduri, G., Batley, M., Kulinskaya, E., Gough, A., Norton, S., & Dixey, J. (2007). Mortality in rheumatoid arthritis. Increased in the early course of disease, in ischaemic heart disease and in pulmonary fibrosis. *Rheumatology, 46*(2), 350-357.

Yu, F., Hu, G., Li, L., Yu, B., & Liu, R. (2022). Identification of key candidate genes and biological pathways in the synovial tissue of patients with rheumatoid arthritis. *Experimental and Therapeutic Medicine, 23*(6), 1-16.

Yuan, Z., Liu, S., Song, W., Liu, Y., Bi, G., Xie, R., & Ren, L. (2022). Galactose Enhances Chondrogenic Differentiation of ATDC5 and Cartilage Matrix Formation by Chondrocytes. *Frontiers in Molecular Biosciences, 9*, 850778.

Yuasa, T., & Iwamoto, M. E. (2006). Mechanism of cartilage matrix remodeling by Wnt. *Clinical Calcium, 16*(6), 1034-1039.

Yue, X., Hariri, D. J., Caballero, B., Zhang, S., Bartlett, M. J., Kaut, O., Mount, D. W., Wüllner, U., Sherman, S. J., & Falk, T. (2014). Comparative study of the neurotrophic effects elicited by VEGF-B and GDNF in preclinical in vivo models of Parkinson's disease. *Neuroscience, 258*, 385-400.

Yun, C. Y., Velazquez-Dones, A. L., Lyman, S. K., & Fu, X.-D. (2003). Phosphorylation-dependent and-independent nuclear import of RS domain-containing splicing factors and regulators. *Journal of Biological Chemistry, 278*(20), 18050-18055.

Yun, H.-J., Yoo, W.-H., Han, M.-K., Lee, Y.-R., Kim, J.-S., & Lee, S.-I. (2008). Epigallocatechin-3-gallate suppresses TNF-α-induced production of MMP-1 and-3 in rheumatoid arthritis synovial fibroblasts. *Rheumatology international, 29*, 23-29.

Zajkowska, M., Lubowicka, E., Szmitkowski, M., & Ławicki, S. (2018). Czynniki z rodziny VEGF oraz ich receptory w diagnostyce raka piersi. *Diagn. Lab, 54*, 105-112.

Zelenchuk, L. V., Hedge, A.-M., & Rowe, P. S. (2015). Age dependent regulation of bone-mass and renal function by the MEPE ASARM-motif. *Bone, 79*, 131-142.

Zeng, C.-Y., Wang, X.-F., & Hua, F.-Z. (2022). HIF-1α in osteoarthritis: from pathogenesis to therapeutic implications. *Frontiers in pharmacology, 13*, 927126.

Zenmyo, M., KOMIYA, S., KAWABATA, R., SASAGURI, Y., INOUE, A., & MORIMATSU, M. (1996). Morphological and biochemical evidence for apoptosis in the terminal hypertrophic chondrocytes of the growth plate. *The Journal of pathology, 180*(4), 430-433.

Zhang, F.-J., Luo, W., Gao, S.-G., Su, D.-Z., Li, Y.-S., Zeng, C., & Lei, G.-H. (2013). Expression of CD44 in articular cartilage is associated with disease severity in knee osteoarthritis. *Modern rheumatology, 23*(6), 1186-1191.

Zhang, F.-J., Luo, W., & Lei, G.-H. (2015). Role of HIF-1α and HIF-2α in osteoarthritis. *Joint bone spine, 82*(3), 144-147.

Zhang, F., Tang, Z., Hou, X., Lennartsson, J., Li, Y., Koch, A. W., Scotney, P., Lee, C., Arjunan, P., & Dong, L. (2009). VEGF-B is dispensable for blood vessel growth but critical for their survival, and VEGF-B targeting inhibits pathological angiogenesis. *Proceedings of the National Academy of Sciences, 106*(15), 6152-6157.

Zhang, H., Brown, R. L., Wei, Y., Zhao, P., Liu, S., Liu, X., Deng, Y., Hu, X., Zhang, J., & Gao, X. D. (2019). CD44 splice isoform switching determines breast cancer stem cell state. *Genes & development, 33*(3-4), 166-179.

Zhang, J., Zahir, N., Jiang, Q., Miliotis, H., Heyraud, S., Meng, X., Dong, B., Xie, G., Qiu, F., & Hao, Z. (2011). The autoimmune disease–associated PTPN22 variant promotes calpain-mediated Lyp/Pep degradation associated with lymphocyte and dendritic cell hyperresponsiveness. *Nature genetics, 43*(9), 902-907.

Zhang, J., Zhao, J., Jiang, W.-j., Shan, X.-w., Yang, X.-m., & Gao, J.-g. (2012). Conditional gene manipulation: Cre-ating a new biological era. *Journal of Zhejiang University Science B, 13*(7), 511-524.

Zhang, N., Zheng, N., Luo, D., Lin, J., Lin, D., Lu, Y., Lai, W., Bian, Y., Wang, H., & Ye, J. (2024). A novel single domain bispecific antibody targeting VEGF and TNF-α ameliorates rheumatoid arthritis. *International immunopharmacology, 126*, 111240.

Zhang, X., Crawford, R., & Xiao, Y. (2016). Inhibition of vascular endothelial growth factor with shRNA in chondrocytes ameliorates osteoarthritis. *Journal of molecular medicine, 94*(7), 787-798.

Zhang, X., Yuan, Z., & Cui, S. (2016). Identifying candidate genes involved in osteoarthritis through bioinformatics analysis. *Clin Exp Rheumatol, 34*(2), 282-290.

Zhang, Y., Yang, Y., Hosaka, K., Huang, G., Zang, J., Chen, F., Zhang, Y., Samani, N. J., & Cao, Y. (2016). Endocrine vasculatures are preferable targets of an antitumor ineffective low dose of anti-VEGF therapy. *Proceedings of the National Academy of Sciences, 113*(15), 4158-4163.

Zhao, Q., Eberspaecher, H., Lefebvre, V., & de Crombrugghe, B. (1997). Parallel expression of Sox9 and Col2a1 in cells undergoing chondrogenesis. *Developmental dynamics: an official publication of the American Association of Anatomists, 209*(4), 377-386.

Zhao, T., Xie, Z., Xi, Y., Liu, L., Li, Z., & Qin, D. (2022). How to model rheumatoid arthritis in animals: from rodents to non-human primates. *Frontiers in Immunology, 13*, 887460.

Zhou, J.-l., Liu, S.-q., Qiu, B., Hu, Q.-j., Ming, J.-h., & Peng, H. (2009). Effects of hyaluronan on vascular endothelial growth factor and receptor-2 expression in a rabbit osteoarthritis model. *Journal of Orthopaedic Science, 14*(3), 313-319.

Zhou, L., Yu, Y., Chen, L., Zhang, P., Wu, X., Zhang, Y., Yang, M., Di, J., Jiang, H., & Wang, L. (2012). Recombinant mycobacterial HSP65 in combination with incomplete Freund's adjuvant induced rat arthritis comparable with that induced by complete Freund's adjuvant. *Journal of immunological methods, 386*(1-2), 78-84.

Zhou, R., Guo, Q., Xiao, Y., Guo, Q., Huang, Y., Li, C., & Luo, X. (2021). Endocrine role of bone in the regulation of energy metabolism. *Bone research, 9*(1), 25.

Zhou, S., Cui, Z., & Urban, J. P. (2004). Factors influencing the oxygen concentration gradient from the synovial surface of articular cartilage to the cartilage–bone interface: a modeling study. *Arthritis & Rheumatism, 50*(12), 3915-3924.

Zhou, X., Cao, H., Yuan, Y., & Wu, W. (2020). Biochemical signals mediate the crosstalk between cartilage and bone in osteoarthritis. *BioMed research international, 2020*.

Zhou, Z., & Fu, X.-D. (2013). Regulation of splicing by SR proteins and SR protein-specific kinases. *Chromosoma, 122*, 191-207.

Zhu, D., Xu, S., Deyanat-Yazdi, G., Peng, S. X., Barnes, L. A., Narla, R. K., Tran, T., Mikolon, D., Ning, Y., & Shi, T. (2018). Synthetic lethal strategy identifies a potent and selective TTK and CLK1/2 inhibitor for treatment of triple-negative breast cancer with a compromised G1–S checkpoint. *Molecular cancer therapeutics, 17*(8), 1727-1738.

Zhu, M., Tang, D., Wu, Q., Hao, S., Chen, M., Xie, C., Rosier, R. N., O'Keefe, R. J., Zuscik, M., & Chen, D. (2009). Activation of β-catenin signaling in articular chondrocytes leads to osteoarthritis-like phenotype in adult β-catenin conditional activation mice. *Journal of Bone and Mineral Research, 24*(1), 12-21.

Zhu, X., Stergiopoulos, K., & Wu, S. (2009). Risk of hypertension and renal dysfunction with an angiogenesis inhibitor sunitinib: systematic review and meta-analysis. *Acta oncologica, 48*(1), 9-17.

Zhu, X., Wu, S., Dahut, W. L., & Parikh, C. R. (2007). Risks of proteinuria and hypertension with bevacizumab, an antibody against vascular endothelial growth factor: systematic review and meta-analysis. *American Journal of Kidney Diseases, 49*(2), 186-193.

Ziche, M., Maglione, D., Ribatti, D., Morbidelli, L., Lago, C. T., Battisti, M., Paoletti, I., Barra, A., Tucci, M., & Parise, G. (1997). Placenta growth factor-1 is chemotactic, mitogenic, and angiogenic. *Laboratory investigation; a journal of technical methods and pathology, 76*(4), 517-531.

Ziemer, L., Evans, S., Kachur, A., Shuman, A., Cardi, C., Jenkins, W., Karp, J., Alavi, A., Dolbier, W., & Koch, C. (2003). Noninvasive imaging of tumor hypoxia in rats using the 2-nitroimidazole 18 F-EF5. *European journal of nuclear medicine and molecular imaging, 30*, 259-266.

Ziff, M. (1974). Relation of cellular infiltration of rheumatoid synovial membrane to its immune response. *Arthritis & Rheumatism: Official Journal of the American College of Rheumatology, 17*(3), 313-319.

Zirlik, K., & Duyster, J. (2018). Anti-angiogenics: current situation and future perspectives. *Oncology research and treatment, 41*(4), 166-171.

Zorzi, A. R., Amstalden, E. M., Plepis, A. M. G., Martins, V. C., Ferretti, M., Antonioli, E., Duarte, A. S., Luzo, A., & Miranda, J. B. (2015). Effect of human adipose tissue mesenchymal stem cells on the regeneration of ovine articular cartilage. *International Journal of Molecular Sciences, 16*(11), 26813-26831.

Zschaler, J., Schlorke, D., & Arnhold, J. (2014). Differences in innate immune response between man and mouse. *Critical Reviews™ in Immunology, 34*(5).

Zupan, J., Vrtačnik, P., Cör, A., Haring, G., Weryha, G., Visvikis-Siest, S., & Marc, J. (2018). VEGF-A is associated with early degenerative changes in cartilage and subchondral bone. *Growth factors, 36*(5-6), 263-273.

Zwerina, J., Redlich, K., Polzer, K., Joosten, L., Krönke, G., Distler, J., Hess, A., Pundt, N., Pap, T., & Hoffmann, O. (2007). TNF-induced structural joint damage is mediated by IL-1. *Proceedings of the National Academy of Sciences, 104*(28), 11742-11747.